

Fernando P.S. Guastaldi
Bhushan Mahadik *Editors*

Bone Tissue Engineering

Bench to Bedside Using 3D Printing

 Springer

Bone Tissue Engineering

Fernando P. S. Guastaldi • Bhushan Mahadik
Editors

Bone Tissue Engineering

Bench to Bedside Using 3D Printing

 Springer

Editors

Fernando P. S. Guastaldi
Boston, MA, USA

Bhushan Mahadik
College Park, MD, USA

ISBN 978-3-030-92013-5 ISBN 978-3-030-92014-2 (eBook)
<https://doi.org/10.1007/978-3-030-92014-2>

© Springer Nature Switzerland AG 2022

This work is subject to copyright. All rights are reserved by the Publisher, whether the whole or part of the material is concerned, specifically the rights of translation, reprinting, reuse of illustrations, recitation, broadcasting, reproduction on microfilms or in any other physical way, and transmission or information storage and retrieval, electronic adaptation, computer software, or by similar or dissimilar methodology now known or hereafter developed.

The use of general descriptive names, registered names, trademarks, service marks, etc. in this publication does not imply, even in the absence of a specific statement, that such names are exempt from the relevant protective laws and regulations and therefore free for general use.

The publisher, the authors and the editors are safe to assume that the advice and information in this book are believed to be true and accurate at the date of publication. Neither the publisher nor the authors or the editors give a warranty, expressed or implied, with respect to the material contained herein or for any errors or omissions that may have been made. The publisher remains neutral with regard to jurisdictional claims in published maps and institutional affiliations.

This Springer imprint is published by the registered company Springer Nature Switzerland AG
The registered company address is: Gewerbestrasse 11, 6330 Cham, Switzerland

Foreword

Bone tissue engineering is a science that spans nearly all of human history and, as such, is punctuated with important moments. From prehistoric gold cranioplasty plates found in Incan ruins, to the identification of bone morphogenetic proteins in the 1970s, up until the modern-day advancements in synthetic materials and cell phenotyping, scientists have been striving to harness the natural regenerative capacity of bone tissue. Despite this long history, there is still much room for innovation and improvement. Due to its highly organized, hierarchical structure, researchers have been longing for new means to fabricate bone tissue scaffolds with precise control over nano- and microarchitecture. In addition, the structural importance of bone combined with the irregularity of many defects has emphasized a need for patient-specific constructs that can be rapidly produced on-site. Recent advances in the availability and accessibility of 3D printers to researchers, particularly in regard to adapting them for biomedical applications, have provided the potential answer for both of these needs. With the rapid rise of 3D printing as a biofabrication method, this ancient field seems ripe for yet another leap forward in innovation and clinical outcomes.

In this textbook, *Bone Tissue Engineering: Bench to Bedside Using 3D Printing*, editors Dr. Fernando Guastaldi and Dr. Bhushan Mahadik use their combined expertise to present the current state of the art in applying 3D printing methods to bone tissue engineering, as well as what future research may have in store. The first four chapters establish a foundational knowledge of the current state of orthopedics and 3D printing technology. Chapter “Introduction” of this book introduces readers to the current gold standard in bone repair, such as autografts and allografts, as well as recent clinical trials in cell-based strategies. Chapter “Basic Bone Biology” discusses the anatomy and physiology of bone tissue, establishing an understanding of the underlying biology necessary for the reader to thoroughly study the subsequent chapters. In particular, the hierarchical structure of bone and the role these structural relationships play in bone remodeling and homeostasis are examined. Chapter “Biomaterial Design Principles to Accelerate Bone Tissue Engineering” introduces the design considerations of biomaterials applied to bone tissue engineering. A wide range of polymers, metals, and ceramics have been used to engineer bone tissue,

and so common strategies among these materials to induce bone regeneration are discussed, as well as emerging fabrication methods such as 3D printing. Chapter “Additive Manufacturing Technologies for Bone Tissue Engineering” introduces the various 3D printing technologies that have been applied to bone tissue engineering. 3D printing encompasses a range of modalities, such as extrusion printing, inkjet printing, and photolithography. Each of these modalities has different strengths and weaknesses that influence its success in fabricating bone constructs, which is discussed in this chapter.

Chapters “3D Printing for Oral and Maxillofacial Regeneration” through “Bone Grafting in the Regenerative Reconstruction of Critical-Size Long Bone Segmental Defects” examine the application of 3D printing in several different subfields of bone tissue engineering. Chapter “3D Printing for Oral and Maxillofacial Regeneration” presents the current use of 3D printing for oral and maxillofacial bone tissue engineering. Due to the cosmetic nature of many of these injuries, 3D printed bone tissue presents great potential for improving clinical outcomes through patient-specific treatments. Next, chapter “Printing for Orthopedic Joint Tissue Engineering” discusses osteochondral joint tissue, including the complicated challenge of regenerating both cartilage and bone. Cartilage defects and current strategies from a surgical perspective are discussed at length, and the chapter concludes with a discussion of cartilage tissue engineering. Chapter “3D Printing in Pediatric Orthopedics” examines applying 3D printing technologies towards pediatric orthopedic practice. By transforming MRI and CT scans into sliced print files, clinicians are able to print patient-specific surgical models for presurgical planning, as well as specialized instruments and implants. Finally, chapter “Bone Grafting in the Regenerative Reconstruction of Critical-Size Long Bone Segmental Defects” discusses recent advances in engineering long-bone segmental defects, including the development of improved allograft techniques as well as synthetic bone grafts.

Chapters “3D Bioprinting and Nanotechnology for Bone Tissue Engineering” through “Strategies for 3D Printing of Vascularized Bone” introduce emerging technologies that can be accompanied with 3D printing to improve engineering outcomes. Chapter “3D Bioprinting and Nanotechnology for Bone Tissue Engineering” discusses the combination of 3D printing and nanotechnology to fabricate materials that are more biomimetic of native bone tissue. Since bone tissue has a highly organized hierarchical structure down to the nanoscale, modification of nanoscale surface roughness or chemistries can increase the success of bone engineering techniques. Chapter “Bioreactors and Scale-Up in Bone Tissue Engineering” examines the importance of bioreactors in bone tissue engineering. Flow-perfusion bioreactors not only improve osteoinduction via flow-derived shear forces but are necessary to sustain cell growth in clinically sized constructs for critical-sized defects. Along similar lines, chapter “Strategies for 3D Printing of Vascularized Bone” discusses the complex challenge of vascularizing engineered bone tissue. Native bone tissue is highly vascularized which plays an important role in bone maintenance and remodeling. This chapter discusses techniques currently employed to best recapitulate this complex network.

Finally, chapters “Development of Additive Manufacturing-Based Medical Products for Clinical Translation and Marketing” and “Future Direction and Challenges” discuss clinical translation of 3D printed bone tissue engineering constructs, including considerations for meeting regulatory requirements, and future directions of the field, respectively. As a whole, this text represents a complete examination on the current state of bone tissue engineering, particularly as 3D printing emerges as a significant fabrication method. Drs. Guastaldi and Mahadik have done an excellent job compiling the expertise of the field and providing this resource for readers who hope to gain insight into new developments in this exciting field, and we hope the readers enjoy.

Department of Bioengineering
Rice University Houston, TX, USA

Adam M. Navara
Antonios G. Mikos

Preface

Since the advent of tissue engineering in the 1980s, bone has been a primary target for tissue regeneration. This field has seen some fantastic developments to assist patients in need of bone-related clinical interventions, but we are still far away from regenerating fully functional bone tissue. The hope and promise of tissue engineering to rebuild this complex organ has been mirrored on the rapidly evolving field of 3D printing that allows us to fabricate complex structures in a systematic manner. With this in mind, we are pleased to introduce the first book that offers a comprehensive overview of the state of the art, current challenges, and strategies to reconstruct large bone defects employing 3D printing technology.

This book is intended to be a concise handbook regarding 3D printing for bone tissue engineering, covering different 3D printing technologies that can be applied for bioengineering bone, the aspects of basic bone biology critical for clinical translation, the progress made in the field of regenerative medicine for the reconstruction of large bone defects, and tissue engineering platforms to investigate the bone niche microenvironment. Commercialization, legal and regulatory considerations are also discussed to help translate bone tissue engineered constructs and 3D printing-based products to the marketplace and the clinic. Although significant progress has been achieved over the past 2–3 decades, challenges that still exist and approaches to address them are discussed. This book can be read as a whole entity that provides an overall perspective on 3D printing in bone tissue engineering. Readers can also refer to select chapters that cater to specific topics without needing information from the preceding chapters.

This book is intended for scientists and researchers interested in learning more about the state-of-the-art progress made employing different 3D printing technologies for bone tissue engineering. This includes but is not limited to students (undergraduate, graduate) and postdoctoral researchers, professors who can assign this as a handbook for quick background studies to capture salient features of this field, scientists across academia and industry as a reference guide for their research, clinicians (dentistry and medicine), and professionals in the biomedical engineering, medical devices, tissue engineering, and biomaterial fields.

We wish to thank all the distinguished and expert contributors for their enthusiastic participation in this endeavor. We contacted the authors during the particularly challenging times of the COVID-19 global pandemic in 2020 and were heartened by their support. It was with utmost kindness and grace that they accepted our invitation and agreed to multiple chapter revisions, despite what we can only describe as being in unprecedented times. Finally, we sincerely thank the Springer staff for their support, patience, understanding, and encouragement while we compiled this book over almost 2 years. Their contribution to this academic venture is extremely appreciated.

We understand that the fields of tissue engineering and 3D printing are advancing rapidly with exciting new discoveries made regularly. It will be our sincere goal to keep the contents updated to reflect latest advances in the following editions of this book. We hope that this book serves as a guide and perhaps a source of inspiration to continue pushing scientific boundaries every day.

Boston, MA, USA
College Park, MD, USA
October 1, 2021

Fernando P. S. Guastaldi
Bhushan Mahadik

Contents

Introduction	1
Kevin C. Lee and Sidney B. Eising	
Basic Bone Biology	13
Matthew R. Allen, Corinne E. Metzger, Jaimo Ahn, and Kurt D. Hankenson	
Biomaterial Design Principles to Accelerate Bone Tissue Engineering . . .	37
Marley J. Dewey and Brendan A. C. Harley	
Additive Manufacturing Technologies for Bone Tissue Engineering	71
Joshua Copus, Sang Jin Lee, James J. Yoo, and Anthony Atala	
3D Printing for Oral and Maxillofacial Regeneration	93
Fernando Pozzi Semeghini Guastaldi, Toru Takusagawa, Joao L. G. C. Monteiro, Yan (Helen) He, Qingsong (Adam) Ye, and Maria J. Troulis	
3D Printing for Orthopedic Joint Tissue Engineering	121
Michael S. Rocca, Matthew Kolevar, Jocelyn Wu, and Jonathan D. Packer	
3D Printing in Pediatric Orthopedics	149
Anirejuoritse Bafor, Jayanthi Parthasarathy, and Christopher A. Iobst	
Bone Grafting in the Regenerative Reconstruction of Critical-Size Long Bone Segmental Defects	165
Xiaowen Xu and Jie Song	
3D Bioprinting and Nanotechnology for Bone Tissue Engineering	193
Robert Choe, Erfan Jabari, Bhushan Mahadik, and John Fisher	
Bioreactors and Scale-Up in Bone Tissue Engineering	225
Shannon Theresa McLoughlin, Bhushan Mahadik, and John Fisher	
Strategies for 3D Printing of Vascularized Bone	249
Favour Obuseh, Christina Jones, and Eric M. Brey	

**Development of Additive Manufacturing-Based Medical Products
for Clinical Translation and Marketing** 267
Johnny Lam, Brian J. Kwee, Laura M. Ricles, and Kyung E. Sung

Future Direction and Challenges 293
Nina Tandon and Sarindr Bhumiratana

Index 309

About the Editors

Fernando P. S. Guastaldi is an Assistant Professor of Oral and Maxillofacial Surgery at Harvard School of Dental Medicine (HSDM) and Director of the Skeletal Biology Research Center (SBRC), Department of Oral and Maxillofacial Surgery (OMFS), Massachusetts General Hospital (MGH). He completed his DDS (2006) at the Dental School of Ribeirão Preto (Brazil). He is Specialist in OMFS (2010), and he completed his MSc (2010) and PhD (2013) in OMFS at the Dental School of Araçatuba (UNESP/Brazil). He was a Visiting Scholar (2012) at the Department of Biomaterials and Biomimetics at New York University College of Dentistry (NYUCD). He completed two Postdoctoral Research Fellowships, the first at the Dental School of Araraquara (UNESP/Brazil) (2014–2017) and the second at MGH/HSDM (2017–2019) focused on bone regeneration of swine mandible critical-sized defects by leveraging principles of tissue engineering and 3D printing. Dr. Guastaldi has research publications and book chapters in the field of bone regeneration, maxillofacial reconstruction, and temporomandibular joint (TMJ) regeneration.

Bhushan Mahadik is the Assistant Director for the NIH/NIBIB Center for Engineering Complex Tissues (CECT) at the University of Maryland. He completed his BS (2008) at the University of California, Berkeley, in chemical engineering and his MS (2010) and PhD (2014) at the University of Illinois at Urbana Champaign (UIUC) in chemical and biomolecular engineering. His PhD and postdoctoral research at UIUC focused on engineering the hematopoietic stem cell niche within the bone marrow by leveraging principles of biomaterial design and microfluidic platforms. He joined the University of Maryland in 2017 where he helped build the research, collaborative, administrative, and strategic growth of CECT as a leading resource for the 3D printing and fabrication of engineered tissues. Dr. Mahadik has several research publications in the field of tissue engineering and regenerative medicine.

Introduction



Kevin C. Lee and Sidney B. Eisig

Soft and hard tissue defects due to trauma, pathology, and congenital anomalies can be daunting reconstructive challenges for the surgeon and patient. The goals of surgery, after removing disease, are to restore and maintain form, function, and esthetics while limiting donor site morbidity. However, it is particularly difficult to restore the precise anatomy in large three-dimensional defects of the craniofacial skeleton and soft tissue (Fig. 1a–e). The microvascular free fibula graft is currently the workhorse for reconstruction of large mandibular and maxillary defects. Unfortunately, this frequently requires a tracheostomy, an intensive care unit admission, is associated with donor site morbidity, and may not adequately restore anatomy and function. The much smaller defect seen in the deficient dental alveolus requiring dental implants following tooth loss can also be problematic. It has long been hoped that tissue engineering solutions will provide better patient outcomes with shorter hospital stays and improved quality of life.

The goal of tissue engineering is to create implantable biologically active scaffolds that can function as viable tissues. The groundwork for modern tissue engineering dates to the late 1970s when the first successful applications were used to improve skin grafting techniques [1]. At that time, scientists at Harvard University developed a novel method for harvesting, culturing, and growing patient-derived keratinocytes for extensive cutaneous burn injuries [2]. Early products had limited clinical utility because they were thin, fragile, and lacked dermal elements. Composite skin products were subsequently developed to include dermal fibroblasts in a collagen framework. These tissue-engineered skin substitutes demonstrated the feasibility of culturing and repurposing autogenous cells; however, they ultimately

K. C. Lee · S. B. Eisig (✉)

Division of Oral and Maxillofacial Surgery, New York Presbyterian/Columbia University Irving Medical Center, New York City, NY, USA

Section of Hospital Dentistry, New York-Presbyterian/Columbia University Irving Medical Center, Columbia University College of Dental Medicine, New York City, NY, USA

e-mail: sbe2002@cumc.columbia.edu



Fig. 1 Examples of challenging defects. (a) Mandibular marginal resection defect. (b) Alveolar and nasal floor defect in a cleft patient. (c) Orbital floor tumor requiring resection and reconstruction. (d) Dentoalveolar defect following tooth fracture and infection. (e) Soft and hard tissue defect following a hemimandibulectomy, radical neck dissection and floor of mouth resection prior to the introduction of microvascular free flap reconstruction

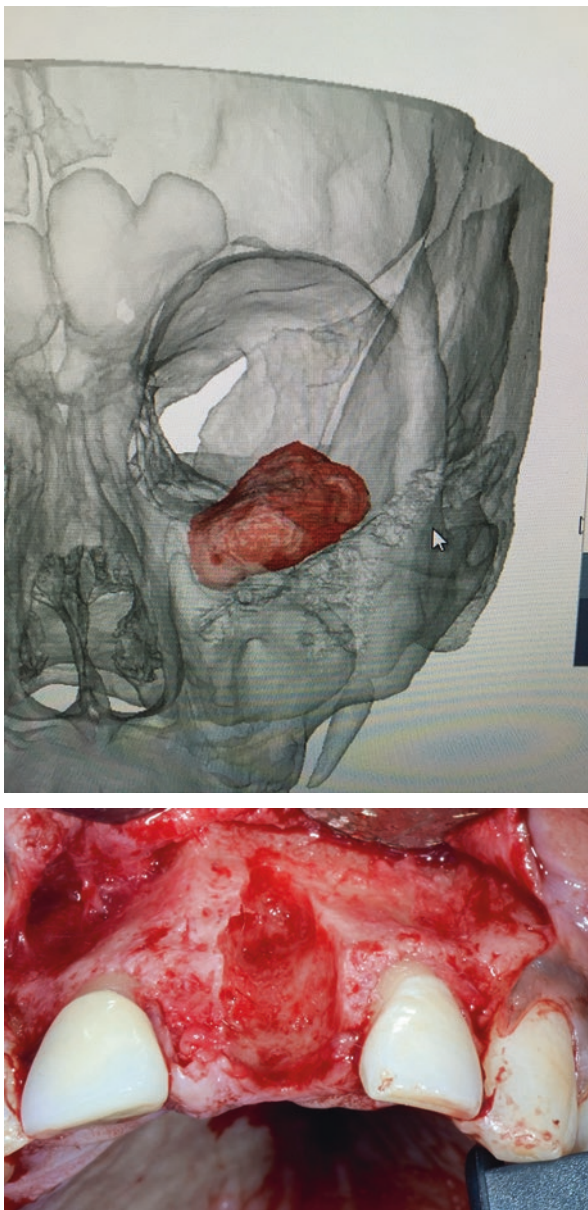


Fig. 1.1 (continued)

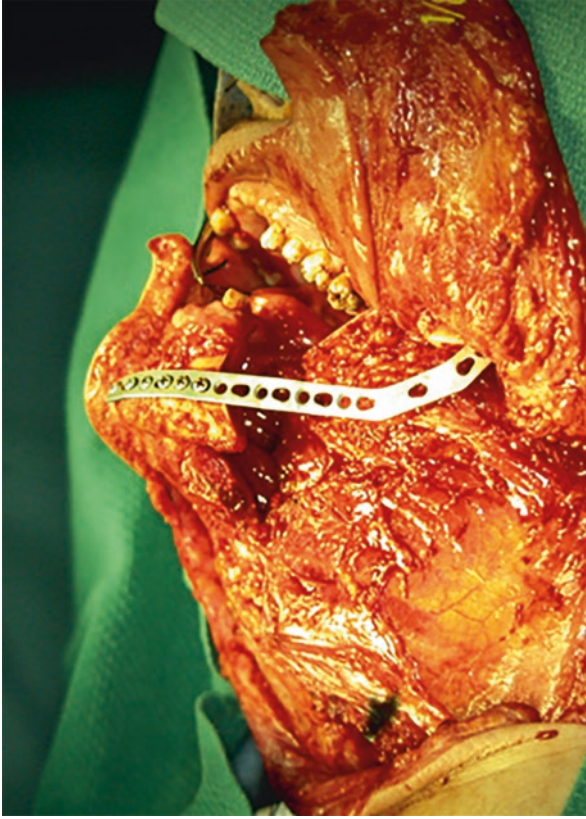


Fig. 1.1 (continued)

lacked a practical application. Today, decellularized dermal matrices are the preferred graft material given their “off-the-shelf” availability and their excellent ability to integrate, recruit host cells, and regenerate full-thickness skin defects. In the early 1990s, interest turned to regenerating other human organs. Cartilage attracted researchers given its poor proliferative capacity and the wide application of tissue-engineered cartilage to both traumatic and degenerative joint injuries [3]. Media publicity and public enthusiasm drove a rapid expansion in the field of tissue engineering between 1990 and 2000. At its peak, there were 73 companies with a combined annual research and development budget excess of \$580 million [4]. Ultimately, investor expectations were unrealistic and the field experienced precipitous drop in funding following the bursting of the dot-com bubble and the notable failures of multiple promising trials [5]. Over the last 20 years, there has been a progressive recovery of interest in regenerative medicine. Today, oral and maxillofacial surgeons are increasingly adding platelet-rich plasma (PRP) and fibrin (PRF) products to their office-based procedures.

The management of osteochondral defects has continued to remain both a clinical and biomedical challenge [6]. Autografts are presently the gold standard for reconstructing critical-sized skeletal defects; however, these materials are only available in limited supply and are often associated with significant patient morbidity. When harvesting calvarial bone and costochondral grafts, there is always the fear of penetrating into adjacent potential spaces. The fibula free flap is the workhorse flap in mandibular reconstruction, but flap harvest weakens the motor function of the foot. Long-term concerns also exist regarding ankle stability. Donor sites themselves may necessitate additional procedures to address lost tissue. The osteocutaneous radial forearm free flap generally requires a split thickness skin graft for coverage and a load-bearing plate to support the remnant radial bone. Particularly with craniofacial defects, complex geometric patterns may require extensive intraoperative carving and reshaping. Obtaining an accurate fit in this manner is often difficult or impossible, and any imperfections in the underlying substructure can compromise esthetics and function. Although the vascularized scapular free flap can mimic the curvature of native maxilla, the nonuniform shape poses a barrier to future dental implant placement. With more extensive central midface defects, there are few satisfactory options for restoring form and function outside of allogeneic face transplant. In these cases, bony reconstruction may be abandoned altogether in exchange for a soft tissue coverage flap. These and other shortcomings associated with autogenous bony reconstruction have spurred efforts to seek out other potential sources of patient-specific tissue (Fig. 2).

Reliance on autografts has progressively decreased as providers are increasingly interested in using synthetic bone substitutes [7, 8]. Unfortunately, the current forms of synthetic and allogeneic bone lack osteogenic and osteoinductive properties. The success of these techniques relies entirely on host substitution which can often be delayed or limited particularly with massive grafts. The quality of the recipient wound bed exerts a major influence on graft success and is prone to a combination of intrinsic and extrinsic influences. The failure of bone grafts among cigarette smokers and diabetics is well-documented in the dental implant literature. With respect to extrinsic factors, perioperative radiation following tumor surgery reduces the successful incorporation of allogeneic bone blocks [9]. Similarly, when treating patients with medication-related osteonecrosis of the jaw, we would rarely consider placing a nonvital bone graft alone into a segmental defect. In these unfavorable scenarios, some providers elect to defer bony reconstruction or graft the gap with autogenous bone or vascularized bone flaps to gain additional osteogenic support. Another limitation of acellular grafts is that they persist for months as foreign bodies given their slow incorporation rates. Unlike osteomyelitis, which can be managed with prolonged antibiotics, the infection of a nonvital graft typically necessitates surgical explanation. It is important to note that for cadaveric and bovine-derived grafts, despite manufacturing standards, there still remains the rare possibility of transmitting unknown pathogens even after donor screening and graft processing [10]. Given all the drawbacks, current bone substitutes are far from ideal.

In general, successful tissue engineering must satisfy four fundamental requirements, namely there must be a scaffold, a source of regenerative stem cells, a form

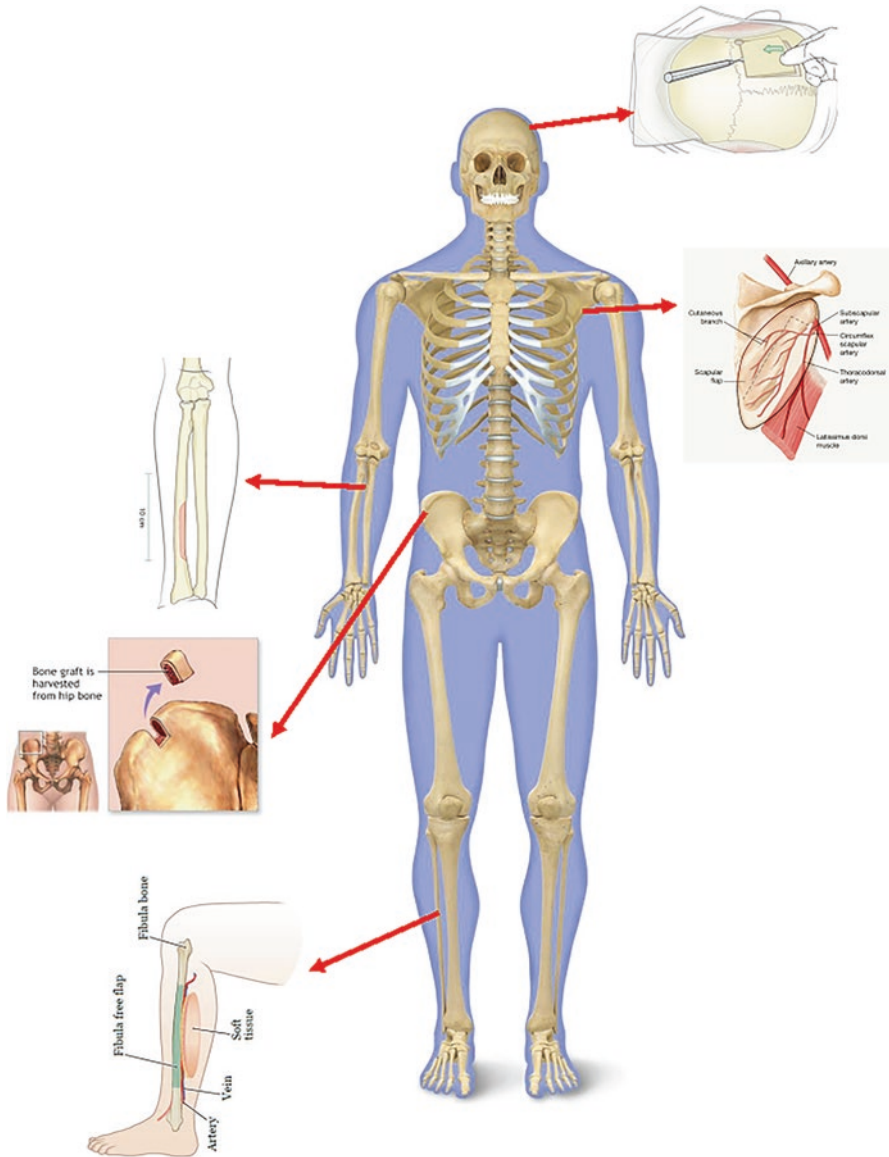


Fig. 2 The location of common bony autografts and free flaps

of signaling to promote cellular migration and differentiation, and sufficient vascularization to meet nutritional demands and remove cellular waste [11]. Innovative research seeks to creatively address these demands. Smart biomaterial scaffolds can respond to internal or external stimuli [12]. The controlled-delivery of drugs and bioactive factors over space and time adjusts to the needs of stem cells.

Immune-sensitive smart scaffolds can also dampen the host foreign body response against synthetic biomaterials. The advent of adjunct technologies, such as 3-dimensional rapid prototyping, has helped boost the precision by which researchers are able to work [13]. At our institution, we have leveraged this technology to address the challenging morphology of the ramus-condyle unit [14] (Fig. 3). Anatomically shaped frameworks can be milled or printed from traditional scaffold materials, and therefore they do not compromise structure or integrity. In many cases, customized frameworks can be deposited layer-by-layer to create spatial separation between different microenvironments [15]. These multilayered constructs can be designed to permit a more even distribution of vascularization zones which is important when creating large bulks of tissue.

Despite improvements and refinements to bone tissue engineering techniques, few studies have managed to translate their findings into clinical trials. Nearly all bone regenerative products on the market utilize only a single-component of either scaffold or growth factor [16]. Currently, recombinant human bone morphogenetic protein-2 carried on an acellular collagen sponge (rhBMP-2/ACS) is the only FDA-approved system that combines both bioactive signaling with scaffolding. There are multiple challenges facing the commercial viability of bone tissue engineering. A variety of biomaterials, preparations, and delivery methods have been proposed to

Fig. 3 Anatomically precise grafts can be designed using bioengineering principles. This is an example of a ramus/condyle unit engineered using autologous adipose derived stem cells with a bovine scaffold placed in a bioreactor. The graft is on the left



achieve in situ regeneration. Unfortunately, the heterogeneous methods of different research groups have precluded the cooperative development of a standard regenerative protocol. As with all therapeutics, the upfront costs of conducting trials and obtaining regulatory approval require tremendous financial support. Multi-component systems, such as rhBMP-2/ACS, are extremely difficult to bring to market given the many combinations of independent factors that require testing. There is also a practical challenge in obtaining regulatory approval within the window of intellectual property; otherwise, stakeholders may never recoup their investments [17]. Even after product approval, the financial viability of bioreactor-based bone is currently unclear. Very conservative figures estimate that each bioengineered bone graft would likely cost between \$10,000 and 15,000 at a minimum which is much more expensive than the standard demineralized bone graft [18]. The steep prices of personalized bone are driven by the costs of materials, manufacturing, and properly trained personnel. The viability of tissue-engineered bone does not solely depend on its cost relative to that of stock bone substitutes. In healthcare, large expenditures are justifiable if savings are realized elsewhere. Tissue-engineered bone can gain traction if it is associated with shorter operative times, decreased lengths of stay, or if it can demonstrate reasonable healthcare value through measurable outcomes such as failure and reoperation rates.

There is a growing clinical need for bone tissue engineering. Bone grafts are currently used to reconstruct defects created by congenital conditions, pathologies, traumatic injuries, and degenerative diseases. In 2018, the global bone graft and substitute market was valued at \$2.58 billion, and it is projected to continue to grow at a compound annual rate of 4.1% [19]. In the USA, approximately 1.6 million bone grafts are performed annually [20]. As the overall population continues to age, the demand for orthopedic interventions is expected to increase. In 2017, there were roughly half a million spinal procedures performed, with the majority of spinal fusion cases occurring secondary to traumatic accidents [19]. From 2001 to 2011 there was a 40% rise in the number of hip replacements performed, and over the same period musculoskeletal operating room procedures saw the largest increase in utilization among all body systems [21]. By 2050, the Centers for Disease Control and Prevention expects the incidence of hip fractures to increase by roughly 200–300%. Bone loss secondary to failed hip and knee replacements is a growing problem as more and more joint replacements are being performed.

The challenges to bringing a concept demonstrated in the laboratory to fruition cannot be understated. Issuance of patents, negotiations with your University, maintaining compliance with conflict of interest laws, budgeting, procuring start-up funding and legal services, incorporating, recruiting, and hiring, renting appropriate space, purchasing equipment, building a good manufacturing practice facility to produce a safe product, instituting a quality assurance program, and interacting with the Food and Drug Administration are just some of the challenges faced when forming a start-up company. Finally, if phase 1 clinical trial demonstrating safety and efficacy is successful, then the company needs the financial resources to significantly ramp up the size of the company and its manufacturing facility. With this financial risk there is no guarantee phase 3 clinical trial will result in the successful launch of a new product.

There is optimism in the progress that has been achieved to date. Although tissue engineering cannot yet address composite hard and soft tissue defects, vascularized flaps can be used in tandem to obtain soft tissue bulk and coverage [22]. There appears to once again be a public appetite for regenerative solutions. Multiple off-label uses of rhBMP-2 have been developed (Fig. 4). PRP and PRF are routinely used in implant dentistry, orthopedic surgery, and facial cosmetics. Over the last 5 years, multiple promising cell-based bone tissue engineering studies have been conducted in both small and large animal models for alveolar bone defects [23]. In our experiments, we have found success not only in directing bone formation but also in differentiating a cartilaginous cap [14]. The ultimate goal is not to simply grow bone but to create functional, complex structures of different cell types that seamlessly take the place of lost organs. This book explores the current status of bone tissue engineering for maxillofacial and orthopedic applications with a focus on the implications of 3-dimensional printing. The translational feasibility and challenges will be discussed.

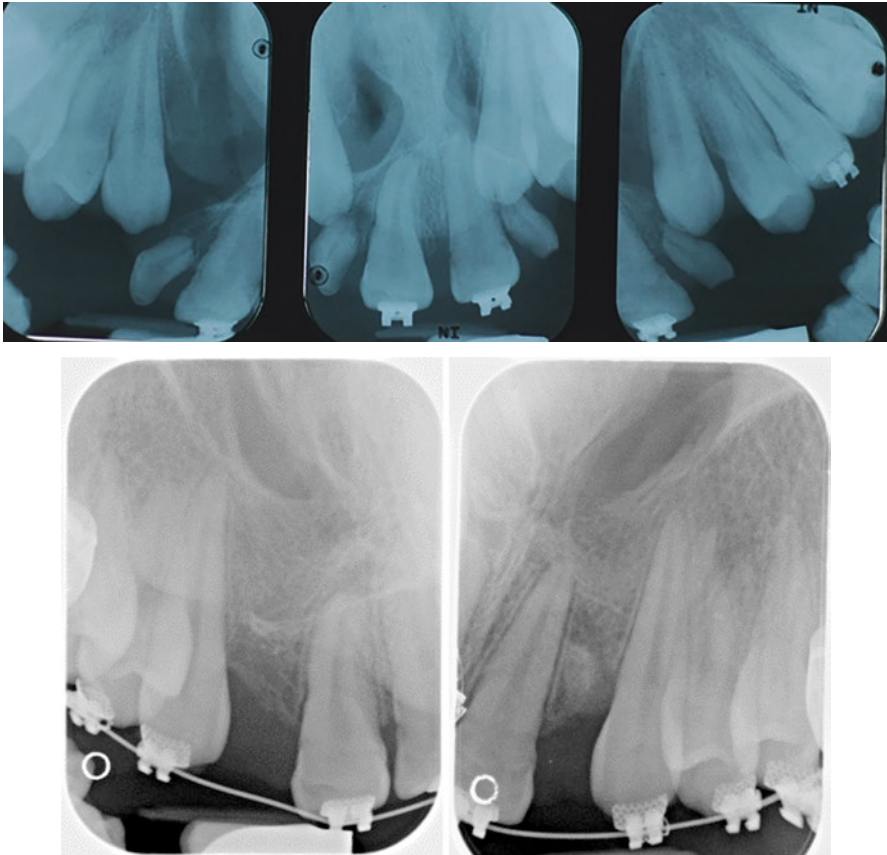


Fig. 4 Bilateral alveolar clefts in a cleft lip and palate patient (a) reconstructed with rhBMP-2/ACS (off-label use) (b)

References

1. Berthiaume F, Maguire TJ, Yarmush ML. Tissue engineering and regenerative medicine: history, progress, and challenges. *Annu Rev Chem Biomol Eng.* 2011;2:403.
2. O'Connor NE, Mulliken JB, Banks-Schlegel S, Kehinde O, Green H. Grafting of burns with cultured epithelium prepared from autologous epidermal cells. *Lancet.* 1981;317:75.
3. Brittberg M, Lindahl A, Nilsson A, Ohlsson C, Isaksson O, Peterson L. Treatment of deep cartilage defects in the knee with autologous chondrocyte transplantation. *N Engl J Med.* 1994;331:889.
4. Mason C. Regenerative medicine 2.0. *Regen Med.* 2007;2:11.
5. Lysaght MJ, Hazlehurst AL. Tissue engineering: the end of the beginning. *Tissue Eng.* 2004;10:309.
6. Gadjanski I, Vunjak-Novakovic G. Challenges in engineering osteochondral tissue grafts with hierarchical structures. *Expert Opin Biol Ther.* 2015;15:1583.
7. Urabe K, Itoman M, Toyama Y, Yanase Y, Iwamoto Y, Ohgushi H, Ochi M, Takakura Y, Hachiya Y, Matsuzaki H, Matsusue Y, Mori S. Current trends in bone grafting and the issue of banked bone allografts based on the fourth nationwide survey of bone grafting status from 2000 to 2004. *J Orthop Sci.* 2007;12:520.
8. Lad SP, Nathan JK, Boakye M. Trends in the use of bone morphogenetic protein as a substitute to autologous iliac crest bone grafting for spinal fusion procedures in the United States. *Spine (Phila Pa 1976).* 2011;36:E274.
9. Kim T-K, Cho W, Youn SM, Chang U-K. The effect of perioperative radiation therapy on spinal bone fusion following spine tumor surgery. *J Korean Neurosurg Soc.* 2016;59:597.
10. Delloye C, Cornu O, Druez V, Barbier O. Bone allografts: what they can offer and what they cannot. *J Bone Joint Surg (Br).* 2007;89:574.
11. Melville JC, Mañón VA, Blackburn C, Young S. Current methods of maxillofacial tissue engineering. *Oral Maxillofac Surg Clin North Am.* 2019;31:579.
12. Zhang K, Wang S, Zhou C, Cheng L, Gao X, Xie X, Sun J, Wang H, Weir MD, Reynolds MA, Zhang N, Bai Y, Xu HHK. Advanced smart biomaterials and constructs for hard tissue engineering and regeneration. *Bone Res.* 2018;6:31.
13. Parthasarathy J. 3D modeling, custom implants and its future perspectives in craniofacial surgery. *Ann Maxillofac Surg.* 2014;4:9.
14. Bhumiratana S, Bernhard JC, Alfi DM, Yeager K, Eton RE, Bova J, Shah F, Gimble JM, Lopez MJ, Eising SB, Vunjak-Novakovic G. Tissue-engineered autologous grafts for facial bone reconstruction. *Sci Transl Med.* 2016;8:343ra83.
15. Sathy BN, Mony U, Menon D, Baskaran VK, Mikos AG, Nair S. Bone tissue engineering with multilayered scaffolds-Part I: an approach for vascularizing engineered constructs in vivo. *Tissue Eng Part A.* 2015;21:2480.
16. Amini AR, Laurencin CT, Nukavarapu SP. Bone tissue engineering: recent advances and challenges. *Crit Rev Biomed Eng.* 2012;40:363.
17. Awad HA, O'Keefe RJ, Lee CH, Mao JJ. Chapter 83 - Bone tissue engineering: clinical challenges and emergent advances in orthopedic and craniofacial surgery. In: Lanza R, Langer R, Vacanti J, editors. *Principles of tissue engineering.* 4th ed. Boston, MA: Academic Press; 2014. p. 1733.
18. Salter E, Goh B, Hung B, Hutton D, Ghone N, Grayson WL. Bone tissue engineering bioreactors: a role in the clinic? *Tissue Eng Part B Rev.* 2012;18:62.
19. Research GV. Bone grafts and substitutes market size, share & trends analysis report by material type (allograft, synthetic), by application type (spinal fusion, craniomaxillofacial, long bone), by region, and segment forecasts, 2019–2026; 2020.
20. O'Keefe RJ, Mao J. Bone tissue engineering and regeneration: from discovery to the clinic--an overview. *Tissue Eng B Rev.* 2011;17:389.
21. Project HCaU. Trends in operating room procedures in U.S. hospitals, 2001–2011; 2014.

22. Melville JC, Tursun R, Green JM III, Marx RE. Reconstruction of a post-traumatic maxillary ridge using a radial forearm free flap and immediate tissue engineering (bone morphogenetic protein, bone marrow aspirate concentrate, and cortical-cancellous bone): case report. *J Oral Maxillofac Surg.* 2017;75:438.e1.
23. Shanbhag S, Pandis N, Mustafa K, Nyengaard JR, Stavropoulos A. Alveolar bone tissue engineering in critical-size defects of experimental animal models: a systematic review and meta-analysis. *J Tissue Eng Regen Med.* 2017;11:2935.

Basic Bone Biology



Matthew R. Allen, Corinne E. Metzger, Jaimo Ahn, and Kurt D. Hankenson

1 Introduction

Bone is a self-renewing, self-healing, composite material. It is organized as a hierarchical/multi-scale structure starting at the molecular level of mineral/collagen/water and scaling up to the structural organ level of a whole bone (Fig. 1). The composite nature of the organic matrix (~25%), inorganic mineral (~65%), and water (~10%) is organized in a way that makes bone both rigid (able to withstand load without bending too much) and tough (able to bend a bit without breaking) [2]. This combination of properties makes it ideally suited to carry out its functional roles of mechanical support and protection. Additionally, the structural characteristics of bone such as having a large surface area, having entombed cells within the mineralized matrix, and having a central marrow cavity allow it to function as a key site for mineral homeostasis, endocrine regulatory physiology, and hematopoiesis [1].

Throughout life, the skeleton is in a constant state of renewal through a cellular process called bone remodeling [3]. This intrinsic multicellular process identifies

M. R. Allen (✉)

Department of Anatomy, Cell Biology & Physiology, Indiana University School of Medicine, Indianapolis, IN, USA

Department of Biomedical Engineering, Indiana University Purdue University of Indianapolis, Indianapolis, IN, USA

Roudebush Veterans Administration Medical Center, Indianapolis, IN, USA
e-mail: matallen@iu.edu

C. E. Metzger

Department of Anatomy, Cell Biology & Physiology, Indiana University School of Medicine, Indianapolis, IN, USA

J. Ahn · K. D. Hankenson

Department of Orthopaedic Surgery, University of Michigan Medical School, Ann Arbor, MI, USA

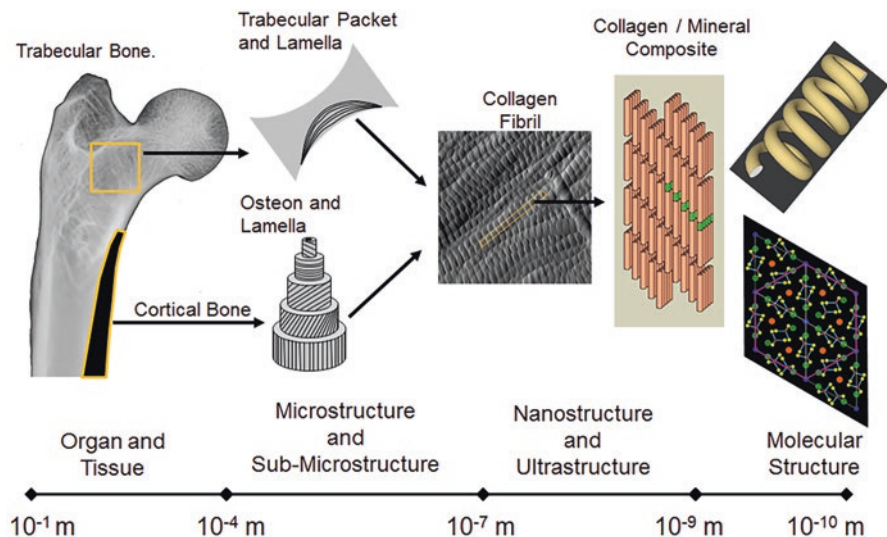


Fig. 1 The hierarchical organization of bone. At the macroscopic level, bone is seen as a composite, with dense cortical bone forming an outside shell and cancellous (spongy, trabecular) bone within the marrow cavity. The cancellous bone serves to attenuate loads and to direct forces to the stronger cortical bone. At the microscopic level, cortical bone is composed of many secondary Haversian systems, or osteons, that are the product of bone resorption and replacement with human new bone. These osteons are composed of a central canal carrying a blood vessel, nerves, and lymphatics surrounded by layers of concentric lamellae. Trabecular bone is also lamellar, but its structure comprises a combination of lamellae that run approximately parallel to the trabecular surface and the remnants of older remodeled bone that can appear osteonal in some cases. At the ultra- and nanostructural levels, bone is a composite of collagen fibers with plates of mineral interspersed within the collagen fibrils (intrafibrillar) and between the collagen fibers themselves (interfibrillar). Together, these can form a cross-fibrillar phase in which the crystals can expand beyond the dimensions of a single collagen fibril. The collagen fibrils are composed of molecules forming a triple helix composed of two $\alpha 1$ chains and a single $\alpha 2$ chain. (Reproduced with permission from [1])

regions of bone that are damaged, lack viable cells, or have other changes to the mineral or collagen that compromise mechanical properties and replaces them with new bone tissue [4]. Bone remodeling is also a central component to bone healing/regeneration. In bone healing, the early phases recapitulate aspects of bone development, involving unique stem cell populations, vascular interactions, and precursor tissues (cartilage) [5]. The later phases of healing utilize bone remodeling processes.

Normal homeostasis and physiological stressors such as healing and regeneration are all made possible by the unique macro/micro/ultrastructure of the skeleton and its interactions with associated cells/tissues. It is only through understanding these basic features and their intricate organization that one can begin to understand the foundation of skeletal tissue engineering.




	 Osteoblast	 Osteoclast	 Osteocyte
Main function	Form matrix	Resorb matrix	Orchestrate bone homeostasis
Morphology	Cuboidal, single nuclei, on bone surface	Large, multi-nucleated, on bone surface that is usually scalloped	Embedded in bone matrix, single nuclei, numerous projections
Cell lineage	Mesenchymal	Hematopoietic	Mesenchymal / Osteoblasts
Key products	Collagen (type I), osteocalcin, alkaline phosphatase	MMPs Acid Cathepsin-K	SOST FGF-23 RANK-L
Key factors driving differentiation	Ostrix Runx2 B-catenin	RANKL-L M-CSF	DMP-1

Fig. 2 Morphologic, functional, and physiological characteristics of the three bone cells

2 Bone Cells

The formation and removal of bone tissue is orchestrated by three cell types [6] (Fig. 2). Osteoblasts, which develop out of the mesenchymal stem cell population, are responsible for formation of the collagen scaffolding which forms the basis of mineralized tissue [7]. The differentiation from a mesenchymal stem cell to a mature osteoblast involves several key factors, including Runx2, osterix, and wnt/b-catenin. Once mature, osteoblasts actively secrete unmineralized matrix (osteoid) that is comprised of type I collagen and non-collagenous proteins. Osteoblasts undergo one of three fates. The majority of osteoblasts undergo apoptosis. Some osteoblasts become embedded in unmineralized osteoid and eventually further differentiate into osteocytes. A small number of osteoblasts become quiescent and line the bone surface (often termed bone lining cells). These quiescent osteoblasts can be reactivated to rapidly form new bone.

The osteoblast’s functional interactive partners the osteoclast, the cell that primarily resorbs bone but also has regulatory function with osteoblasts. Osteoclasts arise from the hematopoietic cell lineage, specifically in the line of the monocyte [8]. Key factors in osteoclast development and eventual fusion are monocyte colony stimulating factor (M-CSF) and receptor activator of the NF-kB ligand (RANKL). Mononucleated pre-osteoclasts undergo fusion in advance of polarization and

attachment to the bone surface where they seal tightly to the bone prior to resorption. Active bone resorption involves acidifying the region below the osteoclast to dissolve the mineral and secreting other factors to break up/remove the collagen. While actively resorbing osteoclasts are sealed tightly to the bone, the cells are dynamic in that they can retract the sealing zone, move along the bone surface, and then re-seal to the bone and continue resorption. The long-held paradigm of resorption was that osteoclasts undergo apoptosis at the end of their resorption phase, although emerging evidence suggests osteoclasts can undergo fission raising the potential that “recycling” of individual nuclei into new osteoclast may occur.

The osteocyte, entombed within the bone matrix, is involved in regulating both bone formation and resorption [6]. Although osteocytes originate from osteoblasts and retain several similarities, over time they express genes that clearly differentiate them from osteoblasts. These include genes such as *PEX*, *MEPE*, *DMP1*, and *FGF23*, which are all involved in phosphate metabolism, *E11* and *PDPN* which regulate filipodial process formation, *sclerostin* and *dkk1*, inhibitors of bone formation, and *M-CSF* and *RANKL* which are involved in osteoclast signaling. These expression profiles are consistent with the established role of osteocytes in regulating mineral metabolism, activating bone formation in response to stimuli such as mechanical loading, and signaling bone resorption in response to stimuli such as microdamage, disuse, or their own apoptosis.

2.1 Macrostructure

At an organ level, bone is classified as cortical or cancellous/trabecular (Fig. 3). Cortical bone forms the outer shell of all bones and comprises approximately 80% of total skeletal mass. The porosity of cortical bone is typically <5–10%, although in some pathologies, or with age, this can increase significantly. Cortical bone provides protection for bone marrow as well as imparting much of the mechanical strength to the skeleton. Increases in cortical porosity and decreases in cortical thickness are typically associated with reductions in mechanical properties of a bone [9, 10]. In most locations the outer surface of cortical bone is covered by periosteum. Periosteum has an inner cellular layer which contains osteoprogenitor cells and an outer fibrous layer containing collagen [11]. The periosteum plays an essential role in healing [12].

Trabecular bone, sometimes referred to as cancellous bone, is typically found at the ends of long bones and in various inner portions of other bones [1]. Trabecular bone has a lattice-like appearance, with more space than bone (porosity >70–80%). The architecture of the trabecular network and individual trabecular struts plays a role in mechanical properties. Individual trabeculae of humans are 100–200 μm thick with shapes that range from cylindrical rods to flattened plates. Most trabeculae in humans exist as plates with a transition of these plates to rods as individuals lose bone mass. The number of trabeculae is thought to be more important than the size of individual trabeculae because the number of trabecular has a greater effect

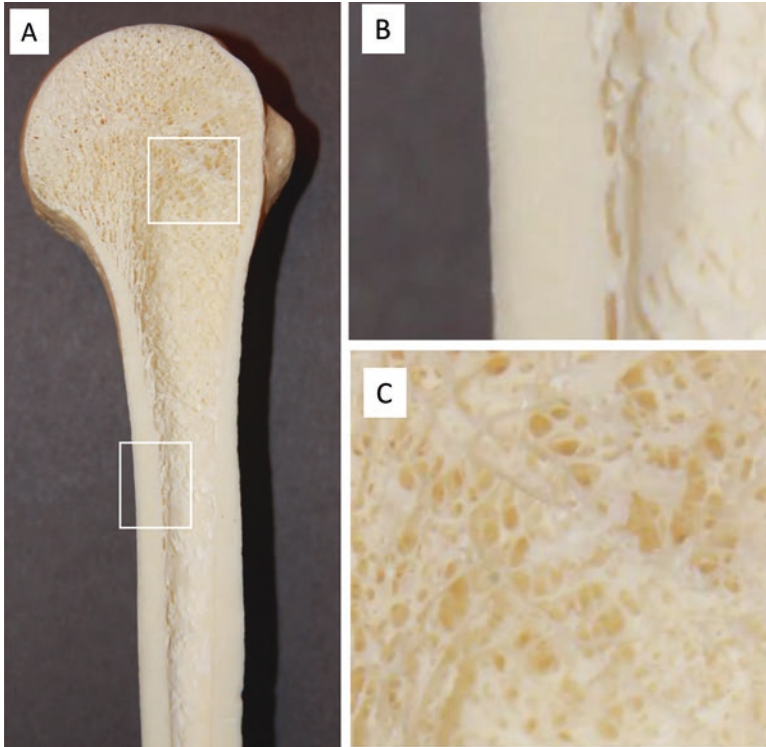


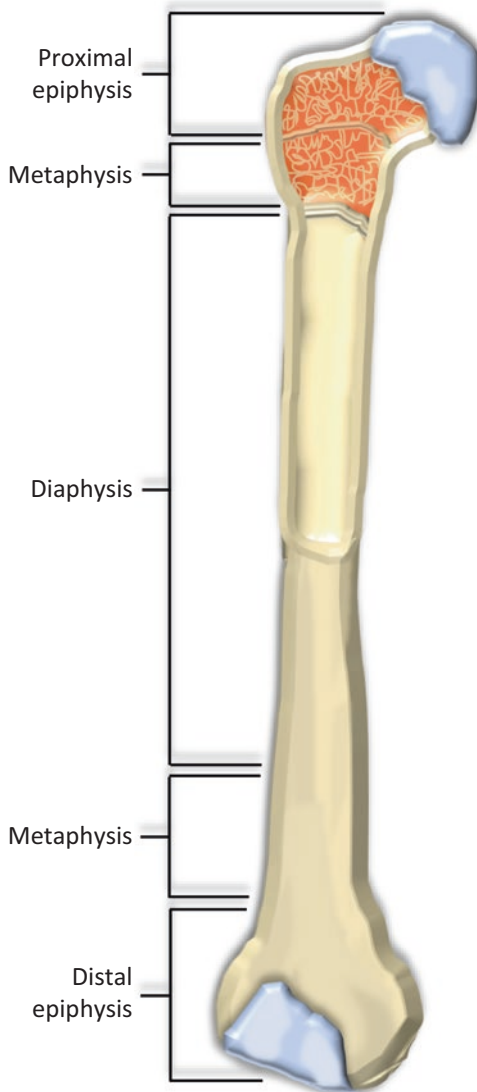
Fig. 3 (a) Whole bones are comprised of an outer dense shell of cortical bone (b) that covers the entire outer boundary and then a trabecular network (c) that is found internally among the bone marrow. Cortical and trabecular bone are both comprised of the same bone matrix (collagen, mineral, non-collagenous proteins), the main difference being the porosity of the tissue (with trabecular bone being more porous compared to cortical bone)

on connectivity; therefore, losing trabeculae (through resorption) has a 2–3 times greater effect on weakening the structure than does thinning of trabeculae.

Cortical and trabecular bone exist throughout the skeleton, which is divided into appendicular and axial portions. The appendicular skeleton includes the limbs and the pelvis; the axial portion includes the vertebra, the skull, and the thoracic cage. The bones of the appendicular skeleton (other than the pelvis, scapula, carpals, and tarsals) are referred to as long bones, each having three regions, epiphysis, metaphysis, and diaphysis (Fig. 4).

The epiphysis region only exists while the physes are present during skeletal immaturity. They are located at both ends of a long bone, in the region between the growth plate (physis) and the joint space. Each epiphysis is comprised of both a cortical shell and trabecular bone with the outer surface of the cortical bone that is found within the joint space covered with articular cartilage. The growth plate, as the name implies, permits long bones to grow in length while retaining the ability to bear load. In humans the growth plate fuses during puberty which means that

Fig. 4 Regions of long bones



longitudinal growth stops. Species such as rodents typically do not fuse their growth plates and thus long bones continually grow throughout life—although the rate of elongation slows notably with age [13].

The metaphysis is located adjacent to the epiphysis (opposite side toward the diaphysis) and is abundant in trabecular bone. The middle portion of a long bone is called the diaphysis and is comprised primarily of cortical bone. Bone marrow exists within the epiphysis, metaphysis, and diaphysis. Red marrow, which is comprised primarily of hematopoietic cells and connective tissue, is predominant around

trabecular bone. In growing bone, the shaft of long bones also has mostly red marrow. With age, the marrow transitions to yellow marrow which is largely comprised of adipocytes. In the long bones this transition begins in the central diaphysis and grows outward toward the metaphysis.

2.2 *Microstructure*

The microstructural components of bone have important anatomical, physiological, and mechanical roles [1]. Cortical bone is comprised of structures called osteons. These cylindrical structures are formed either during development (called primary osteons) or during remodeling (called secondary osteons). At the center of each osteon is a void, the central canal, containing vasculature and nerves. The outer boundary of secondary osteons is called the cement line. This structure, laid down first during formation of a new secondary osteon, differs in mineral content than the rest of the bone. This serves an important mechanical function by providing contrasting stiffness in material. This deflects (and sometimes traps) microdamage that may be propagating through the bone. Cement lines help enhance overall bone toughness. As secondary osteons form, growing from the cement line inward, the mineral and collagen are laid in different orientations, producing concentric lamellae that also serve to enhance the mechanical properties of the structure. A typical osteon in human bone is $\sim 200\ \mu\text{m}$ in diameter, although there is extreme heterogeneity in size both within and among humans. Many large animal species have both primary and secondary osteons. Rodents have primary osteons but unless they are provided physiological or pharmacological stressors do not typically form secondary osteons [13]. Trabecular bone typically does not have osteons although they can exist in nodes where trabeculae come together. Trabecular bone has structures, often referred to as “hemi-osteons,” which are formed during remodeling and have a cement line and lamellae.

Active remodeling that is unbalanced (more bone resorption than formation) causes two important structural features: cortical porosity and trabecular resorption cavities. Under normal physiological conditions, these structures are both formed temporarily, but are eventually filled in through formation. In numerous conditions, including post-menopausal osteoporosis and aging, osteoblasts do not fill in the excavated areas leaving void spaces. In cortical bone, porosity has a significant negative effect on bone mechanical properties with incomplete infilling in trabecular bone resulting in erosion cavities. Both voids produce stress risers in the tissue and can lead to formation of microcracks.

Embedded within the matrix, throughout the entire bone, are osteocytes. The cell bodies of osteocytes reside in a space called a lacunae while their filopodial processes extend through channels called canaliculi. Extracellular fluid exists within the free spaces within the lacunar/canalicular network. The lacunar/canalicular network is connected to the endosteal bone surface (to interface with the bone marrow), to the central canal (to interface with the vascular supply), and the periosteal

surface (to connect with the periosteal vasculature). Disrupting the lacunar/canalicular network, such as can occur with microdamage or micropetrosis (mineralization of the structures), can disrupt physiological regulation that is controlled by osteocytes. Dynamic activity occurs within the lacunae, orchestrated by the osteocyte. Osteolysis of the mineral/collagen matrix in the perilacunar space occurs in situations such as lactation, thought to be driven by the need for calcium liberation. Whether or not active formation exists at the perilacunar space is less clear although emerging evidence certainly points to mineral aggregation at this surface.

2.3 *Ultrastructure (Fig. 5)*

Mineral makes up the majority (by weight) of the bone matrix. Mineral crystals in the form of calcium phosphonate and calcium carbonate are initially deposited in spaces adjacent to the collagen fibrils—both between the ends and in spaces that run longitudinally between fibrils [14, 15]. This original deposition is often referred to as primary mineralization, which occurs quite rapidly (~3 weeks) and accounts for about 70% of total mineralization of the tissue. As the mineral matures, often called secondary mineralization, the carbonate content is reduced, and the crystals aggregate to form large plates that remain parallel to the fibrils. This occurs more slowly (months to years) until the local matrix achieves a physiological limit of mineral accumulation.

The organic fraction of bone consists mostly of type I collagen with associated non-collagenous proteins [16]. Type I collagen within bone is like that found elsewhere in the body, a triple helix comprised of repeating amino acids. The most abundant pattern of amino acids is glycine–proline–hydroxyproline, the latter serving an important role in hydrogen bonding with water within the matrix. Formation of the collagen propeptide occurs intracellularly; extrusion to the extracellular space results in cleavage of registration peptides which facilitate aggregation of fibrils to form fibers. This highly coordinated process results in fibers that are roughly 10 μm long and about 150 nm in diameter. The fibril aggregation occurs in a staggered pattern such that a gap between fibrils exists which is approximately 67 nm in size; this is eventually filled with mineral. Collagen fibers are abundant in crosslinks which impart mechanical rigidity [17]. Pyridinoline and deoxypyridinoline are two mature enzymatic collagen crosslinks that are common in bone. They are formed between adjacent collagen fibers through a lysyl oxidase-mediated reaction. Additionally, collagen in bone (as well as other tissues) accumulates nonenzymatically mediated crosslinks, such as pentosidine, vesperlysine, and carboxymethyllysine. These crosslinks also impart a mechanical effect on the fibers although high accumulation has been shown to produce a brittle mechanical phenotype as they do not allow normal sliding of adjacent fibers—an intrinsic toughening mechanism of the bone.

Although in relatively small amounts compared to mineral and collagen, non-collagenous proteins exist in the matrix and play key roles in the cellular processes that govern matrix formation [18, 19]. Non-collagenous proteins, often classified as

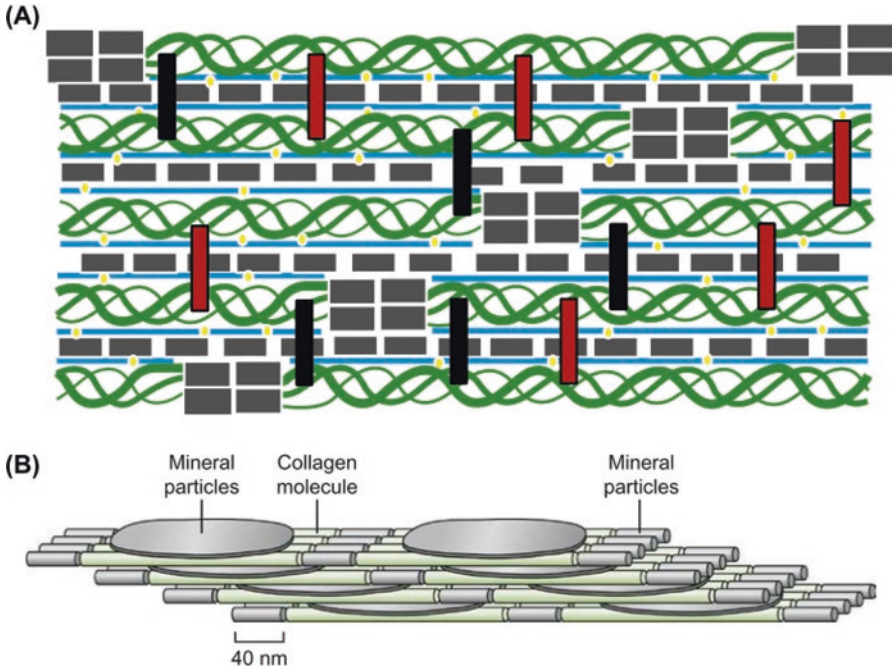


Fig. 5 (a) Collagen molecules (green helix) are cross-linked within the fibril by bonds that are formed through enzymatic processes and by those formed without the need for an enzymatic reaction. Enzymatically formed crosslinks (black bars), such as pyridinoline or deoxypyridinoline, form near the ends of the molecules, the C- and N-termini. Nonenzymatically formed bonds (red bars), such as pentosidine, are randomly located between the molecules. Mineral (gray blocks) is deposited in the hole and pore zones between the collagen fibrils. Water (blue lines) and hydrogen bonds contribute to the bonding of mineral and collagen within the fibril. (b) Hole and pore zones between the molecules contain plates of bone mineral (hydroxyapatite). Water is bound to collagen in these spaces, and this alters the distribution of load sharing between the collagen and bone mineral deposited in this location. (Reproduced with permission from [1])

proteoglycans, glycosaminoglycans, and glycoproteins, include such common factors as alkaline phosphatase, bone sialoprotein, dentin matrix acidic phosphoprotein 1 (DMP-1), osteopontin, osteocalcin, and osteonectin. These factors direct and influence osteoblast function and mineralization.

3 Bone Development

During fetal development, bone tissue develops in one of the two ways: intramembranous ossification or endochondral ossification [20]. Intramembranous ossification is the process that forms the flat bones of the face, the bones of the skull, and the clavicles. The process begins with mesenchymal cells coalescing to form a

highly vascularized connective tissue which then becomes ossified. Osteocytes are trapped within the ossified tissue and eventually, osteoblasts and osteoclasts form and resorb bone on the surface. The small islands of ossified tissue eventually coalesce together through the formation of bone on their surfaces.

Endochondral ossification is the process through which long bones develop (Fig. 6). The long bone begins as a cartilage template, in the shape of the bone, that was formed by chondrocytes. The multi-step process that transforms the cartilage template into bone begins with the formation of bone matrix on the outer surface at the mid-diaphysis. This bone matrix formation coincides with the death and calcification of the internal cartilage matrix at this location. Following vascular invasion at the mid-diaphysis (often called the primary center of ossification), the inner calcified cartilage is resorbed away, leaving a void which is then filled with cells and eventually becomes the marrow cavity. Secondary centers of ossification develop, through similar processes, at both ends of the long bone. Separating the primary and secondary centers of ossification is the physal (growth) plate.

The growth plate is what allows longitudinal growth of the mineralized bone (Fig. 7). The growth plate has five distinct zones that are classified according to the

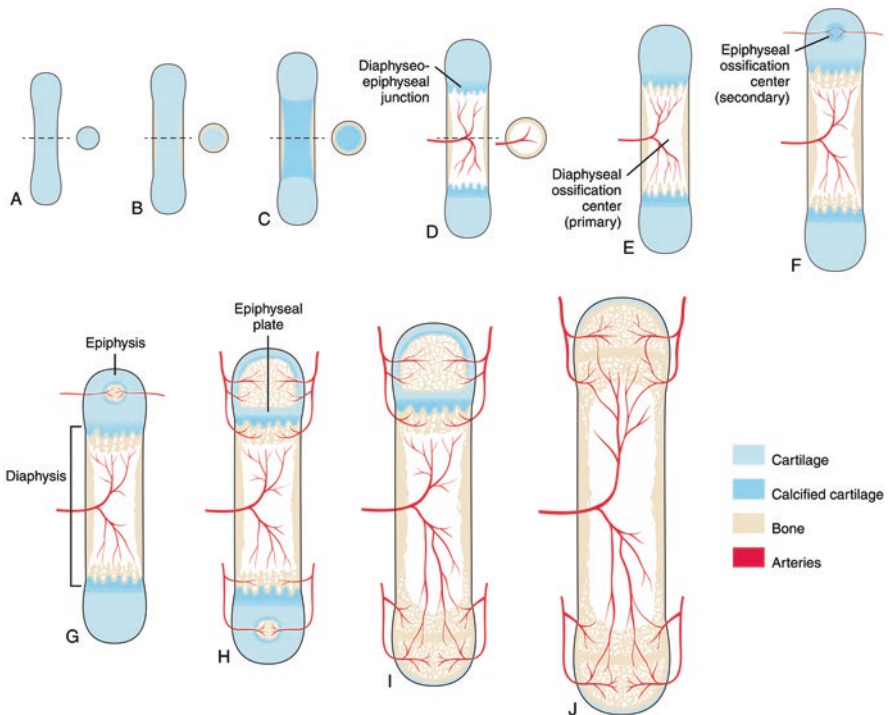


Fig. 6 (a–j) Endochondral ossification. The process of endochondral ossification begins with a cartilage template that transforms into bone through a series of stages involving the coordinated activity of chondrocytes, osteoblasts, and osteoclasts. (Reproduced with permission from [21])

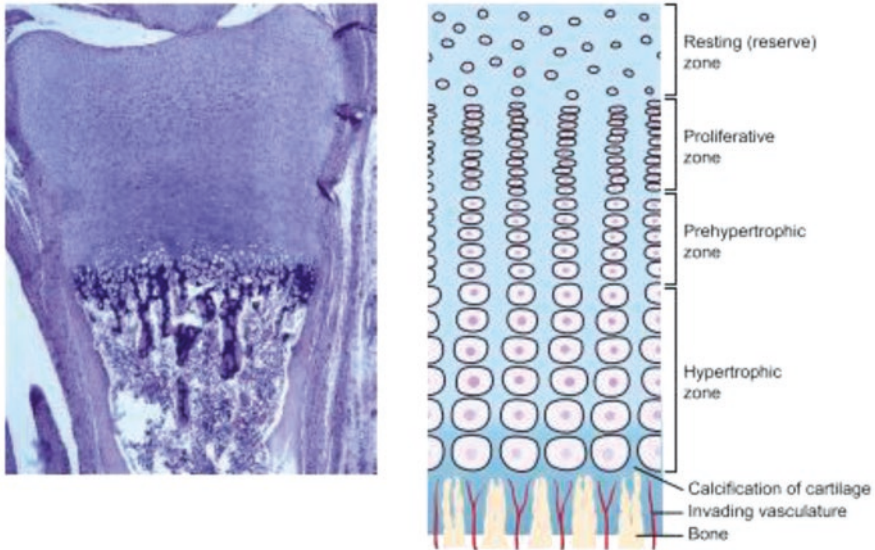


Fig. 7 The epiphyseal growth plate is classified into five zones (a, b) based on the different histologic appearance of the cells and matrix: resting (reserve) zone; proliferative zone; hypertrophic zone; zone of calcified cartilage; and zone of ossification. As long bone growth occurs, cells progress through the different zones. In the low power photomicrograph (a), the individual delineations between zones are not obvious, although the overall structure of the region can be appreciated. (b) The schematic more clearly shows the cell/tissue morphology of the zones within the growth plate. (Reproduced with permission from [21])

main cellular processes that occur at each location. Moving from the end of the bone inward, the zones are (1) resting, (2) proliferative, (3) hypertrophic, (4) zone of calcified cartilage, and (5) zone of ossification. The resting zone is primarily hyaline cartilage matrix with embedded chondrocytes. New resting zone matrix is continually produced by surface chondroblasts and embedded chondrocytes (thus not really resting as its name implies). The second region is called the proliferative zone and, fitting with its name, it is a site of active chondrocyte mitosis. The cell division is clearly notable histologically and often can be observed with the cells appearing as stacked coins/pancakes. Proliferative cells produce about twice their own volume of matrix. The third region is the hypertrophic zone, where the cells hypertrophy, increasing their volume by up to tenfold. The hypertrophic zone is complex in that the cells actively enlarge and secrete matrix while also undergoing the beginning stages of apoptosis. Signaling in this region is fundamental to not only bone elongation (cells actively produce both type II and type X collagen) but also secrete factors such as vascular endothelial growth factor, which is thought to regulate vascular permeability and mineralization. Type X collagen is exclusive to hypertrophic chondrocytes in the developing bone (although it can also be found in the fracture callus and damaged articular cartilage in adults) and is typically associated with cartilage degradation or aging. Although the fibers of type X collagen impart important

stiffening properties to the region, they create a matrix less able to diffuse nutrients to the cells. The matrix around the hypertrophied chondrocytes compresses between adjacent cells and eventually begins to mineralize (this is the fourth region—calcified cartilage). The chondrocytes in this region are either dead or in the process of dying, due to lack of nutrient diffusion or cellular waste removal. As the region becomes more calcified, local signaling leads to vascular invasion. The final zone of the growth plate is the zone of ossification, where bone is produced by osteoblasts on top of the calcified cartilage spicules that remain. Over time, the bone and calcified cartilage cores are remodeled, eventually leaving only bone in these regions (which are trabeculae).

Bone elongation eventually ceases, and the growth plate ossifies. Although there is a temporal connection between these two events, they are separate processes. Growth stops first, caused by an arresting of cell division in the resting and proliferative zones. Subsequent to cessation of growth, the epiphyseal plate ossifies, leaving behind a thin mineralized region of bone (the epiphyseal line) separating the epiphysis and metaphysis.

4 Bone Remodeling and Modeling

Beyond development and growth, bone remains a highly active and responsive tissue throughout life. The lifelong process of renewing or replacing of bone tissue is termed bone remodeling. Bone remodeling occurs through the action of osteoclasts and osteoblasts, temporally coordinated, on the same bone surface. It can occur on any of the bone surfaces/envelopes (trabecular, endocortical, intracortical, periosteal). An estimated 10% of the skeleton is renewed by bone remodeling per year [22].

The first step in bone remodeling is an activation signal to trigger bone resorption (Fig. 8). The signal can be systemic, such as disruptions in mineral homeostasis or hormonal signals. For example, decreased calcium leads to increased circulating

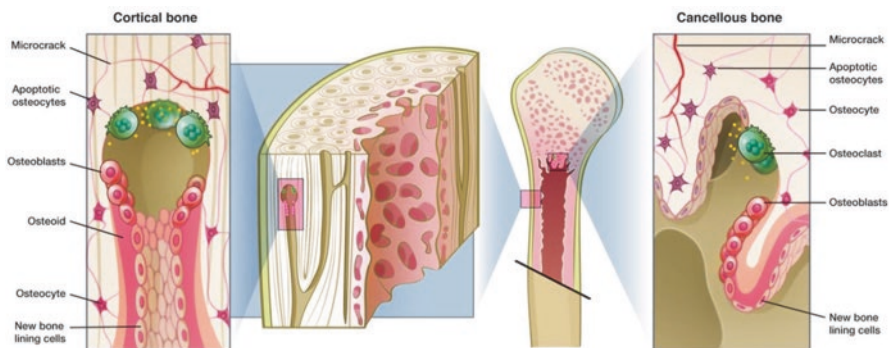


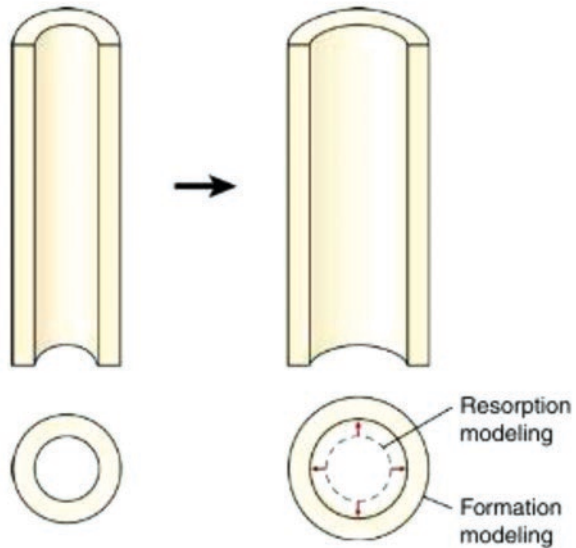
Fig. 8 Bone remodeling in cortical and cancellous bone tissue. (Reproduced with permission from [23])

parathyroid hormone which increases bone resorption in order to release calcium into the circulation. Local signals within bone tissue, like microdamage and osteocyte apoptosis, also serve as activation signals and trigger targeted bone resorption within a specific area. Following activation, osteoclasts are recruited to the site to initiate bone resorption. The process of remodeling, beginning with resorption, occurs under what is known as the canopy—a capillary-rich layer of cells above the remodeling site [24]. In the next stage, the reversal stage, the transition from resorption to formation occurs. It is not a stage per se, yet work has uncovered that important processes occur during this transition. While it is not completely known what factors are involved in the coupling of resorption to formation at the same remodeling site, factors released from the resorbed bone tissue, factors released by both osteoclasts and osteoblasts, and the integrity of the canopy cells over the remodeling site may all play roles in coupling resorption to formation [25, 26]. Following the reversal phase, osteoblasts begin laying down a protein matrix known as osteoid. Over time, this protein matrix becomes progressively embedded with mineral crystals which accumulate and grow around the collagenous matrix. Some of the osteoblasts working at the surface become buried within the matrix and differentiate into osteocytes which remain in the mineralized tissue. Once osteoblasts are finished laying down matrix at a site, the last remaining cells become quiescent and flatten out to cover the bone surface (termed bone lining cells).

Together, the osteoblasts and osteoclasts that work across time at the same bone site in the remodeling cycle are called the basic multicellular unit (BMU). The estimated lifespan of a BMU is 6–9 months with the resorption phase completed by the osteoclasts occurring more quickly (weeks) than the work of the osteoblasts (months). While initial mineralization (the first 70%) at a remodeling site may take only a few weeks, full mineralization can take up to 1 year. The net result of bone remodeling is the maintenance or slight decrease in bone mass. With aging, menopause, and various other diseases, the balance of remodeling favors resorption leading to net loss of bone over time. Anti-resorptive therapies for treatment of osteoporosis aim to prevent this net loss of bone and subsequent fracture by decreasing or inhibiting osteoclasts and suppressing remodeling.

In contrast to remodeling, bone modeling often leads to an increase in bone mass. Bone modeling occurs on trabecular, endocortical, and periosteal bone surfaces and involves the independent actions of either osteoblasts or osteoclasts on a given bone surface. Like remodeling, an activation signal can stimulate the recruitment of either osteoblasts or osteoclasts to a bone surface. However, in contrast to remodeling, there is no coordinated action of both osteoclasts and osteoblasts on the same bone surface. Modeling primarily occurs during childhood growth to maintain the shape of bones during longitudinal and radial growth. During radial growth of a long bone, for example, resorption-based modeling occurs on the endocortical surface, while formation-based modeling occurs on the periosteal surface (Fig. 9). Modeling can also be stimulated by mechanical loading. Bone is most responsive to these mechanical signals triggering modeling before puberty, but the stimulus for modeling remains post-puberty as demonstrated by differences in bone mass of the dominant and non-dominant arm of young tennis young athletes engaged in

Fig. 9 Radial bone growth involves formation modeling on periosteal surfaces and resorption modeling on the endocortical surface. Over time, these processes preserve cortical thickness while increasing the width of the bone. (Reproduced with permission from [21])



rigorous training [27]. There is some evidence for bone anabolic therapies stimulating formation-based modeling, thereby, increasing bone formation independent of the remodeling cycle [28].

5 Bone Healing and Regeneration

Bone is one of the few tissues that is capable of scarless healing and incorporates elements of bone development, modeling, and remodeling that have been previously covered in this chapter [29]. Bones of the appendicular skeleton heal through both endochondral ossification and intramembranous ossification processes. Conversely, bones that develop through intramembranous ossification, for instance, bones of the skull, heal primarily through intramembranous mechanisms although this is not absolute. In some cases, healing can be through both intramembranous and endochondral mechanisms.

Mechanical load is a major factor that influences the type of bone healing [30]. Thus, the mode of surgical fixation of injured bone becomes essential to understanding the mechanisms of healing. Bone that is highly stabilized (e.g., through compression)—either surgically or because of the extent of injury—heals exclusively by intramembranous ossification (Fig. 10a, b). Following injury progenitor cells are activated and differentiate to become bone forming osteoblasts directly. It is notable that rigidly opposed cortices of bone that have fractured will heal via intramembranous ossification and in this manner, the bone healing process is somewhat akin to the coupled activities of bone resorption and formation during

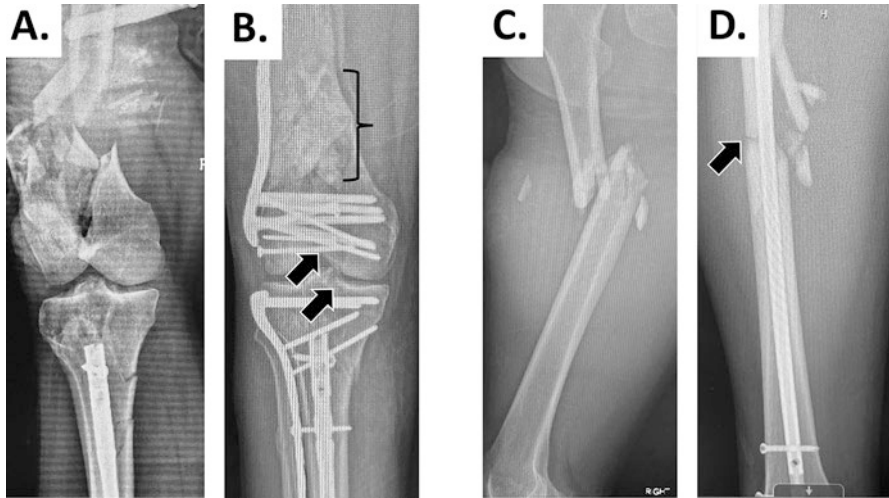


Fig. 10 Type of bone healing is dependent upon fixation and extent of injury. Radiographs of a patient injured in a motor vehicle collision with open, comminuted, and displaced intra-articular fracture of the distal femur with severe metaphyseal comminution and bone loss before (a) and after (b) surgical fixation. There was also a minimally displaced intra-articular fracture of the proximal tibia. The intra-articular fractures of the femur (and tibia) are fixed with high stability (plate and screws) after near anatomic reduction and are expected to heal via primary bone healing (black arrows), akin to intramembranous bone formation. The metaphyseal bone loss is fixed with “relative stability” using a spanning plate and because it is a critical sized defect will undergo a bone grafting procedure (induced membrane technique) for eventual healing via a process permissive of endochondral bone formation (bracket). (c, d) Radiographs of a second patient injured in a motor vehicle collision with open, comminuted, and displaced fracture of the femoral diaphysis. Fractures of the shaft are fixated with “relative stability” (intramedullary nail) after reduction of length-alignment-rotation and expected to heal via secondary bone healing akin to endochondral bone formation. A radiographically visible callus would be expected in this mode of healing

remodeling (primary bone healing). Interestingly, the contrasted mode of distraction osteogenesis also heals primarily through intramembranous ossification, although the injury site is under tensile force rather than compressive stabilizing force.

Conversely, a combination of intramembranous and endochondral ossification is responsible for the healing of most long bone injuries (secondary bone healing) (Fig. 10c, d). The presence of endochondral bone formation as a mechanism of healing is dependent upon the loading environment, and generally, is accompanied by increased inflammatory response. Loading directly increases the extent of endochondral bone formation [31]. It should also be noted that origin of progenitor cells can influence the phenotype of the healing callus and the extent of endochondral bone regeneration relative to intramembranous. Progenitor cells that are derived from the periosteum of long bones can become both osteoblasts and chondrocytes, whereas progenitors that are marrow-derived are more restricted to an osteoblast fate [32]. Increased hypoxia also contributes to bi-potential cells differentiating to

chondrocytes rather than osteoblasts [33]. Thus, fracture environments with significant vascular damage will likely result in healing through an endochondral process.

Secondary bone healing follows a well-coordinated temporal process, whereby following injury, a hematoma forms, which is followed by an inflammatory phase, a mesenchymal-angiogenic response phase, a bone forming phase, and eventually remodeling (Fig. 11). While these phases are often discussed as being temporally distinct, it is important to consider that they are occurring concurrently throughout healing. For example, callus tissue inflammatory cells remain elevated during the bone formation process. The hematoma (clot) that forms at the time of fracture repair prevents bleeding and serves to provide provisional stability (Fig. 11b). It was

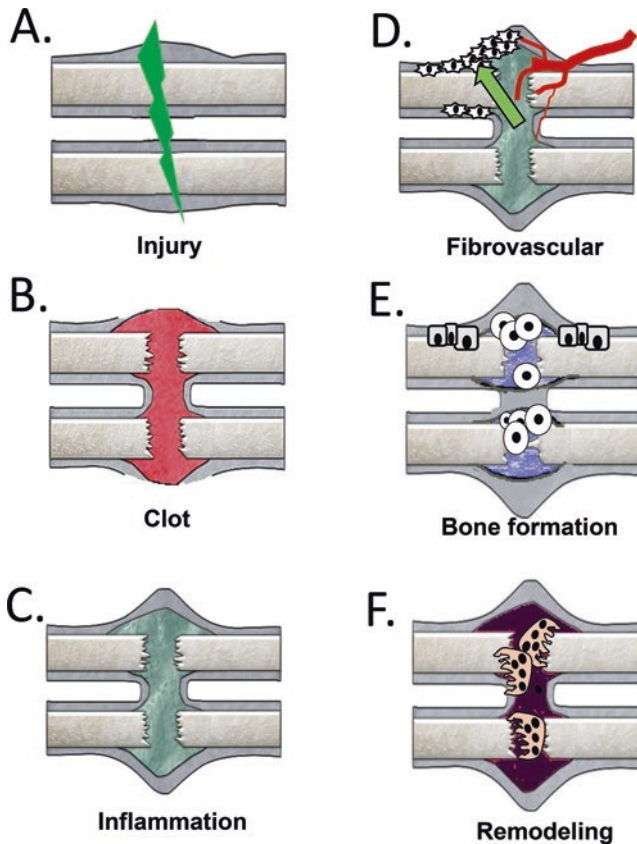


Fig. 11 Fracture healing is a temporally defined process. (a) At injury there is disruption of periosteum and bone (b) A clot forms immediately providing a provisional matrix. Platelet degranulation releases chemokines to recruit inflammation. (c) Inflammatory phase leads to a period of (d) mesenchymal expansion and migration from the periosteum and endosteum and angiogenesis, (e) bone is formed via both endochondral (round cells) and intramembranous ossification (cuboidal cells), (f) osteoclasts (multinucleated cells) resorb primary bone and the process of remodeling restores bone shape and structure. (Adapted from [29])

assumed that the clot was required for bone regeneration but studies have shown that fibrin during clot formation is dispensable, but clot dissolution (fibrinolysis) is an absolute requirement [34]. An influx of inflammatory cells follows the clot, and this inflammatory period is characterized by a mixed population of inflammatory cells, including T- and B-cell subtypes, monocyte/macrophages, eosinophils, and mast cells (Fig. 11c). Various models have been employed to interrogate the role and requirement of inflammatory cells, and perhaps the research is best summarized by indicating that while inflammatory cells are required for proper bone healing, particularly macrophages [35, 36], too much, or sustained inflammation, particularly T-cells [37–41], is deleterious to fracture healing. Systemic anti-inflammatory agents can improve healing and disruption of adaptive immune system accelerates healing [42–45]. While we have gained a deeper understanding of the cell-type requirements for bone healing, the mechanistic role of the various inflammatory cell types in bone healing is somewhat in its infancy. These cells produce a wide variety of cytokines and these undoubtedly play a key role in recruitment of mesenchymal progenitor cells and vasculature during the next phase of healing.

Cytokines secreted during the inflammatory phase recruit and promote proliferation of mesenchymal and endothelial progenitor cells [46]. New blood vessels begin to form and the mesenchymal progenitor cells proliferate during the fibrovascular phase (Fig. 11d). Failures during this phase of healing will result in atrophic healing or smaller calluses, as seen with radiation, ischemia, and aging [47–49]. VEGF signaling is known to be of prime importance during this early phase of bone healing to promote new blood vessel formation [50, 51], and delivery of VEGF has been shown to promote healing in a non-union model [52]. SDF1 signaling has been shown to be important for recruitment of both endothelial progenitors [53] and the recruitment of mesenchymal progenitors [54]. It should also be noted that BMP2 signaling, but not BMP4 or 7, is absolutely required for this phase of healing, as mice with BMP2 deficiency do not heal [55–57]. Similarly, an absence of Notch signaling results in the absence of mesenchymal expansion and a failure to heal [58].

Recruited mesenchyme at the periphery of fractures and proximal and distal ends differentiates to form bone via an intramembranous process, whereas the central portion of the mesenchyme becomes avascular and differentiates to form cartilage, which will then undergo endochondral ossification (Figs. 11e and 12). We previously mentioned that both hypoxia and mechanical loading can influence the extent of intramembranous and endochondral healing. Indeed, decreasing hypoxia will decrease the extent of endochondral bone formation [59], and similarly increasing mechanical stability will increase the proportion of endochondral bone in the callus [60]. Other factors, beyond mechanical loading and vascularization likely influence whether undifferentiated mesenchymal cells differentiate to become chondrocytes or osteoblasts, but these mechanisms are not well-described in the literature.

Endochondral bone formation occurs similarly to that described for development, whereas proliferative chondrocytes undergo hypertrophy, and then there is a phase of vascular invasion and cartilage template resorption. Signaling processes that are known to influence endochondral bone development likely play a significant role during this phase of healing. As an example, BMP increases and

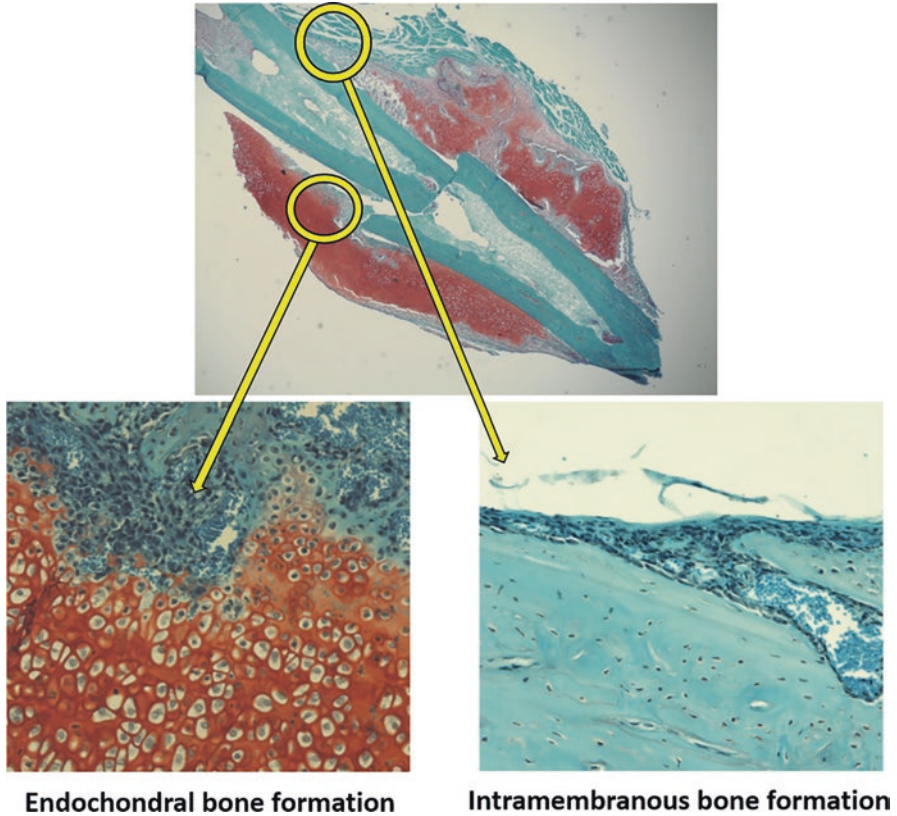


Fig. 12 Intramembranous and endochondral bone formation occurring concurrently during long bone fracture. Mouse tibiae were harvested 10 days post-fracture and fixated with an intramedullary pin. Longitudinal histological sections were stained with safranin-o and imaged at 2.5 \times . There is both endochondral ossification (red staining, safranin-o stains cartilage) and intramembranous bone formation occurring concurrently in this model

accelerates the extent of endochondral bone regeneration [61, 62], and inhibition of Wnt signaling decreases endochondral bone formation [63, 64]. Recent work shows that in fracture healing some chondrocytes do not undergo apoptosis and rather transdifferentiate to become chondrocytes through a process of dedifferentiation and redifferentiation [65] that may, in part, be guided by Wnt signaling. Of course, BMP and Wnt signaling are not the only relevant signaling pathways that influence endochondral bone formation, and other pathways should also be considered as potential therapeutic targets. Traditional endochondral development pathways such as FGF [66], PTHrP-Indian Hedgehog [67], and cytokines such as TNF [68] influence the extent of endochondral bone regeneration. Newer discovered protein families, such as CTRP3, also influence the extent of endochondral bone regeneration [67].

Signaling pathways that influence endochondral bone are also important for the intramembranous process. Osteoblast specific alterations of genes of interest in mice are useful to demonstrate that not only does Wnt signaling influence endochondral bone, but Wnt positively influences intramembranous bone formation [69]. Intramembranous bone healing is easily studied in models of mechanical stability, including with distraction osteogenesis, and in cranial healing models. Indeed, in a distraction osteogenesis model of induced intramembranous bone, VEGF production by osteolineage cells, in part driven by hypoxia, is responsible for secondary vessel recruitment. A loss of VEGF from osteocalcin expressing cells reduced bone formation in distraction osteogenesis model, which heals primarily through an intramembranous process [70, 71]. In cranial healing, BMP is a potent driver of intramembranous bone healing, and the extent of BMP-induced healing is regulated by Notch signaling [72].

Following the bone formation phase of healing, a callus composed of woven bone is established that has enhanced mechanical strength. Next follows a lengthy phase of bone remodeling during which the injured bone is remodeled to re-establish normal bone structure and function, including re-establishing material and mechanical properties. The coupled activities of osteoclasts and osteoblasts are required for this phase of healing similar to described earlier in the chapter. In the vast majority of experimental studies of healing in animal models, these long-term remodeling responses are not well studied, but osteoclasts clearly play an important role in the remodeling of callus to restore bone structure and function [73]. As would be expected, disruption of normal osteoclast function by inhibition of RANKL signaling results in retained cartilage [74]. Accelerating callus remodeling may be a useful strategy to promote enhanced bone formation, however, relatively few therapeutic strategies investigated in rodents are focused on targeting this phase of healing.

While most bone injuries heal with standard-of-care, which may include immobilization, surgical reduction, and combinations of external and internal fixation, some bone injuries fail to heal and thus require intervention. These poor healing bone injuries are the result of failures in the cellular and molecular processes previously outlined, but in many cases the systemic and/or local causative factors influencing healing are never identified. One injury type for which it is well understood that healing does not happen appropriately are “critical size defects” [75, 76]. In cases where bone has been lost to trauma, infection, or cancer, there can be large defects that are unable to heal (Fig. 10). Even with surgical intervention, including debridement and stabilization, injuries of this type fail to heal. It is interesting to note that the “rule of thumb” for long bone critical size healing is that defects that are larger than the width of the bone will not heal without surgical intervention. These critical size defects radiographically will form a small amount of bone at distal and proximal types, but the bone tips become fibrosed and healing will not progress without surgical intervention. Approaches to heal these critical size defects present numerous challenges and require innovative approaches as described in chapter “Bone Grafting in the Regenerative Reconstruction of Critical-Size Long Bone Segmental Defects” of this text.

References

1. Burr DB. Bone morphology and organization. In: Burr DB, Allen MR, editors. *Basic and applied bone biology*. London: Academic Press; 2019. p. 3–26.
2. Currey JD. How well are bones designed to resist fracture? *J Bone Miner Res*. 2003;18:591–8.
3. Seeman E. Bone modeling and remodeling. *Crit Rev Eukaryot Gene Expr*. 2009;19:219–33.
4. Burr DB. The complex relationship between bone remodeling and the physical and material properties of bone. *Osteoporos Int*. 2015;26:845–7.
5. Gerstenfeld LC, Cullinane DM, Barnes GL, Graves DT, Einhorn TA. Fracture healing as a post-natal developmental process: molecular, spatial, and temporal aspects of its regulation. *J Cell Biochem*. 2003;88:873–84.
6. Bellido T, Plotkin LI, Bruzzaniti A. Bone cells. In: Burr DB, Allen MR, editors. *Basic and applied bone biology*. London: Academic Press; 2019. p. 37–55.
7. Aubin JE. Mesenchymal stem cells and osteoblast differentiation. In: *Principles of bone biology, two-volume set*; 2008. p. 85–107.
8. Teitelbaum SL, Ross FP. Genetic regulation of osteoclast development and function. *Nat Rev Genet*. 2003;4:638–49.
9. Martin RB. Determinants of the mechanical properties of bones. *J Biomech*. 1991;24:79–88.
10. Seeman E. Growth and Age-related abnormalities in cortical structure and fracture risk. *Endocrinol Metab*. 2016;30:419.
11. Allen MR, Hock JM, Burr DB. Periosteum: biology, regulation, and response to osteoporosis therapies. *Bone*. 2004;35:1003–12.
12. Colnot C, Zhang X, Tate MLK. Current insights on the regenerative potential of the periosteum: molecular, cellular, and endogenous engineering approaches. *J Orthop Res*. 2012;30:1869–78.
13. Allen MR. Preclinical models for skeletal research: how commonly used species mimic (or don't) aspects of human bone. *Toxicol Pathol*. 2017;45:851–4.
14. Wagermaier W, Klaushofer K, Fratzl P. Fragility of bone material controlled by internal interfaces. *Calcif Tissue Int*. 2015;97:201–12.
15. Stock SR. The mineral–collagen interface in bone. *Calcif Tissue Int*. 2015;97:262–80.
16. Garnero P. The role of collagen organization on the properties of bone. *Calcif Tissue Int*. 2015;97:229–40.
17. Saito M, Marumo K. Effects of collagen crosslinking on bone material properties in health and disease. *Calcif Tissue Int*. 2015;97:242–61.
18. Gorski JP. Is all bone the same? Distinctive distributions and properties of non-collagenous matrix proteins in Lamellar vs. Woven bone imply the existence of different underlying osteogenic mechanisms. *Crit Rev Oral Biol Med*. 1998;9:201–23.
19. Gorski JP. Biomineralization of bone: a fresh view of the roles of non-collagenous proteins. *Front Biosci*. 2011;16:2598–621.
20. Berendsen A, Olsen B. Bone development Agnes. *Bone*. 2015;80:14–8.
21. Allen MR, Burr DB. Bone growth, modeling, and remodeling. In: Burr DB, Allen MR, editors. *Basic and applied bone biology*. London: Academic Press; 2019. p. 85–100.
22. Parfitt AM. Osteonal and hemi-osteonal remodeling: the spatial and temporal framework for signal traffic in adult human bone. *J Cell Biochem*. 1994;55:273–86.
23. Newman CL, Allen MR. Bone remodeling. In: Mooren FC, editor. *Encyclopedia of exercise medicine in health and disease*. Berlin: Springer; 2012. p. 140–3.
24. Andersen TL, Sondergaard TE, Skorzynska KE, Dagnaes-Hansen F, Plesner TL, Hauge EM, Plesner T, Delaïsse JM. A physical mechanism for coupling bone resorption and formation in adult human bone. *Am J Pathol*. 2009;174:239–47.
25. Jensen PR, Andersen TL, Hauge EM, Bollerslev J, Delaïsse JM. A joined role of canopy and reversal cells in bone remodeling - lessons from glucocorticoid-induced osteoporosis. *Bone*. 2015;73:16–23.
26. Matsuo K, Otaki N. Bone cell interactions through Eph/ephrin: bone modeling, remodeling and associated diseases. *Cell Adhes Migr*. 2012;6:148–56.

27. Kannus P, Haapasalo H, Sankelo M, Sievänen H, Pasanen M, Heinonen A, Oja P, Vuori I. Effect of starting age of physical activity on bone mass in the dominant arm of tennis and squash players. *Ann Intern Med.* 1995;123:27–31.
28. Dempster DW, Zhou H, Recker RR, et al. Remodeling- and modeling-based bone formation with teriparatide versus denosumab: a longitudinal analysis from baseline to 3 months in the AVA study. *J Bone Miner Res.* 2018;33:298–306.
29. Bahney CS, Zondervan RL, Allison P, Theologis A, Ashley JW, Ahn J, Miclau T, Marcucio RS, Hankenson KD. Cellular biology of fracture healing. *J Orthop Res.* 2019;37:35–50.
30. Augat P, Simon U, Liedert A, Claes L. Mechanics and mechano-biology of fracture healing in normal and osteoporotic bone. *Osteoporos Int.* 2005;16:S36–43.
31. Smith-Adaline EA, Volkman SK, Ignelzi MA Jr, Slade J, Platte S, Goldstein SA. Mechanical environment alters tissue formation patterns during fracture repair. *J Orthop Res.* 2004;22:1079–85.
32. Colnot C. Skeletal cell fate decisions within periosteum and bone marrow during bone regeneration. *J Bone Miner Res.* 2009;24:274–82.
33. O'Reilly A, Hankenson KD, Kelly DJ. A computational model to explore the role of angiogenic impairment on endochondral ossification during fracture healing. *Biomech Model Mechanobiol.* 2016;15:1279–94.
34. Yuasa M, Mignemi NA, Nyman JS, et al. Fibrinolysis is essential for fracture repair and prevention of heterotopic ossification. *J Clin Invest.* 2015;125:3117–31.
35. Rapp AE, Bindl R, Recknagel S, Erbacher A, Muller I, Schrezenmeier H, Ehrnthaller C, Gebhard F, Ignatius A. Fracture healing is delayed in immunodeficient NOD/scidIL2Rgammamacnull mice. *PLoS One.* 2016;11:e0147465.
36. Raggatt LJ, Wullschlegel ME, Alexander KA, Wu AC, Millard SM, Kaur S, Maughan ML, Gregory LS, Steck R, Pettit AR. Fracture healing via periosteal callus formation requires macrophages for both initiation and progression of early endochondral ossification. *Am J Pathol.* 2014;184:3192–204.
37. Claes L, Recknagel S, Ignatius A. Fracture healing under healthy and inflammatory conditions. *Nat Rev Rheumatol.* 2012;8:133–43.
38. Abou-Khalil R, Yang F, Mortreux M, et al. Delayed bone regeneration is linked to chronic inflammation in murine muscular dystrophy. *J Bone Miner Res.* 2014;29:304–15.
39. Dishowitz MI, Mutyaba PL, Takacs JD, Barr AM, Engiles JB, Ahn J, Hankenson KD. Systemic inhibition of canonical notch signaling results in sustained callus inflammation and alters multiple phases of fracture healing. *PLoS One.* 2013;8:e68726.
40. Könnecke I, Serra A, El Khassawna T, et al. T and B cells participate in bone repair by infiltrating the fracture callus in a two-wave fashion. *Bone.* 2014;64:155–65.
41. Jiao H, Xiao E, Graves DT. Diabetes and its effect on bone and fracture healing. *Curr Osteoporos Rep.* 2015;13:327–35.
42. Toben D, Schroeder I, El Khassawna T, et al. Fracture healing is accelerated in the absence of the adaptive immune system. *J Bone Miner Res.* 2011;26:113–24.
43. Lu C, Xing Z, Wang X, Mao J, Marcucio RS, Miclau T. Anti-inflammatory treatment increases angiogenesis during early fracture healing. *Arch Orthop Trauma Surg.* 2012;132:1205–13.
44. Timmen M, Hidding H, Wieskotter B, Baum W, Pap T, Raschke MJ, Schett G, Zwerina J, Stange R. Influence of antiTNF-alpha antibody treatment on fracture healing under chronic inflammation. *BMC Musculoskelet Disord.* 2014;15:184.
45. Josephson AM, Bradaschia-Correa V, Lee S, et al. Age-related inflammation triggers skeletal stem/progenitor cell dysfunction. *Proc Natl Acad Sci U S A.* 2019;116:6995–7004.
46. Einhorn TA, Majeska RJ, Rush EB, Levine PM, Horowitz MC. The expression of cytokine activity by fracture callus. *J Bone Miner Res.* 1995;10:1272–81.
47. Lu C, Miclau T, Hu D, Marcucio RS. Ischemia leads to delayed union during fracture healing: a mouse model. *J Orthop Res.* 2007;25:51–61.
48. Lopas LA, Belkin NS, Mutyaba PL, Gray CF, Hankenson KD, Ahn J. Fractures in geriatric mice show decreased callus expansion and bone volume. *Clin Orthop Relat Res.* 2014;472:3523–32.

49. Wang L, Tower RJ, Chandra A, et al. Periosteal mesenchymal progenitor dysfunction and extraskeletally-derived fibrosis contribute to atrophic fracture nonunion. *J Bone Miner Res.* 2019;34:520–32.
50. Street J, Bao M, deGuzman L, et al. Vascular endothelial growth factor stimulates bone repair by promoting angiogenesis and bone turnover. *Proc Natl Acad Sci U S A.* 2002;99:9656–61.
51. Hankenson KD, Dishowitz M, Gray C, Schenker M. Angiogenesis in bone regeneration. *Injury.* 2011;42:556–61.
52. Ogilvie CM, Lu C, Marcucio R, Lee M, Thompson Z, Hu D, Helms JA, Miclau T. Vascular endothelial growth factor improves bone repair in a murine nonunion model. *Iowa Orthop J.* 2012;32:90–4.
53. Kawakami Y, Ii M, Matsumoto T, et al. SDF-1/CXCR4 axis in Tie2-lineage cells including endothelial progenitor cells contributes to bone fracture healing. *J Bone Miner Res.* 2015;30:95–105.
54. Yellowley C. CXCL12/CXCR4 signaling and other recruitment and homing pathways in fracture repair. *Bonekey Rep.* 2013;2:300.
55. Tsuji K, Bandyopadhyay A, Harfe BD, Cox K, Kakar S, Gerstenfeld L, Einhorn T, Tabin CJ, Rosen V. BMP2 activity, although dispensable for bone formation, is required for the initiation of fracture healing. *Nat Genet.* 2006;38:1424–9.
56. Tsuji K, Cox K, Bandyopadhyay A, Harfe BD, Tabin CJ, Rosen V. BMP4 is dispensable for skeletogenesis and fracture-healing in the limb. *J Bone Jt Surg Am.* 2008;90(Suppl 1):14–8.
57. Tsuji K, Cox K, Gamer L, Graf D, Economides A, Rosen V. Conditional deletion of BMP7 from the limb skeleton does not affect bone formation or fracture repair. *J Orthop Res.* 2010;28:384–9.
58. Wang C, Inzana JA, Mirando AJ, Ren Y, Liu Z, Shen J, O’Keefe RJ, Awad HA, Hilton MJ. NOTCH signaling in skeletal progenitors is critical for fracture repair. *J Clin Invest.* 2016;126:1471–81.
59. Taylor DK, Meganck JA, Terkhorst S, Rajani R, Naik A, O’Keefe RJ, Goldstein SA, Hankenson KD. Thrombospondin-2 influences the proportion of cartilage and bone during fracture healing. *J Bone Miner Res.* 2009;24:1043–54.
60. Miclau T, Lu C, Thompson Z, Choi P, Puttlitz C, Marcucio R, Helms JA. Effects of delayed stabilization on fracture healing. *J Orthop Res.* 2007;25:1552–8.
61. Alden TD, Pittman DD, Hankins GR, Beres EJ, Engh JA, Das S, Hudson SB, Kerns KM, Kallmes DF, Helm GA. In vivo endochondral bone formation using a bone morphogenetic protein 2 adenoviral vector. *Hum Gene Ther.* 1999;10:2245–53.
62. Einhorn TA, Majeska RJ, Mohaideen A, Kagel EM, Bouxsein ML, Lurek TJ, Wozney JM. A single percutaneous injection of recombinant human bone morphogenetic protein-2 accelerates fracture repair. *J Bone Jt Surg Ser A.* 2003;85:1425–35.
63. Huang Y, Zhang X, Du K, Yang F, Shi Y, Huang J, Tang T, Chen D, Dai K. Inhibition of beta-catenin signaling in chondrocytes induces delayed fracture healing in mice. *J Orthop Res.* 2012;30:304–10.
64. Maupin KA, Droscha CJ, Williams BO. A comprehensive overview of skeletal phenotypes associated with alterations in wnt/beta-catenin signaling in humans and mice. *Bone Res.* 2013;1:27–71.
65. Hu DP, Ferro F, Yang F, Taylor AJ, Chang W, Miclau T, Marcucio RS, Bahney CS. Cartilage to bone transformation during fracture healing is coordinated by the invading vasculature and induction of the core pluripotency genes. *Development.* 2017;144:221–34.
66. Du X, Xie Y, Xian CJ, Chen L. Role of FGFs/FGFRs in skeletal development and bone regeneration. *J Cell Physiol.* 2012;227:3731–43.
67. Williams JN, Kambrath AV, Patel RB, et al. Inhibition of CaMKK2 enhances fracture healing by stimulating Indian hedgehog signaling and accelerating endochondral ossification. *J Bone Miner Res.* 2018;33:930–44.

68. Gerstenfeld LC, Cho TJ, Kon T, Aizawa T, Tsay A, Fitch J, Barnes GL, Graves DT, Einhorn TA. Impaired fracture healing in the absence of TNF- α signaling: the role of TNF- α in endochondral cartilage resorption. *J Bone Miner Res.* 2003;18:1584–92.
69. Chen Y, Whetstone HC, Lin AC, Nadesan P, Wei Q, Poon R, Alman BA. Beta-catenin signaling plays a disparate role in different phases of fracture repair: implications for therapy to improve bone healing. *PLoS Med.* 2007;4:1216–29.
70. Wang Y, Wan C, Deng L, et al. The hypoxia-inducible factor { α } pathway couples angiogenesis to osteogenesis during skeletal development. *J Clin Invest.* 2007;117:1616–26.
71. Jacobsen KA, Al-Aql ZS, Wan C, et al. Bone formation during distraction osteogenesis is dependent on both VEGFR1 and VEGFR2 signaling. *J Bone Miner Res.* 2008;23:596–609.
72. Wagley Y, Chesi A, Acevedo PK, Lu S, Wells AD, Johnson ME, Grant SFA, Hankenson KD. Canonical Notch signaling is required for bone morphogenetic protein-mediated human osteoblast differentiation. *Stem Cells.* 2020;38:1332. <https://doi.org/10.1002/stem.3245>.
73. McArdle A, Marecic O, Tevlin R, Walmsley GG, Chan CK, Longaker MT, Wan DC. The role and regulation of osteoclasts in normal bone homeostasis and in response to injury. *Plast Reconstr Surg.* 2015;135:808–16.
74. Gerstenfeld LC, Sacks DJ, Pelis M, Mason ZD, Graves DT, Barrero M, Ominsky MS, Kostenuik PJ, Morgan EF, Einhorn TA. Comparison of effects of the bisphosphonate alendronate versus the RANKL inhibitor denosumab on murine fracture healing. *J Bone Miner Res.* 2009;24:196–208.
75. Schmitz JP, Hollinger JO. The critical size defect as an experimental model for craniomandibulofacial nonunions. *Clin Orthop.* 1986:299–308.
76. Gomes PS, Fernandes MH. Rodent models in bone-related research: the relevance of calvarial defects in the assessment of bone regeneration strategies. *Lab Anim.* 2011;45:14–24.

Biomaterial Design Principles to Accelerate Bone Tissue Engineering



Marley J. Dewey and Brendan A. C. Harley

1 Bone Injury and Repair

1.1 *Types of Injuries*

In this chapter we will focus on the methods available to repair bone defects, focusing specifically on those that require surgical intervention to repair. These types of injuries include craniomaxillofacial defects, long bone segmental defects, and spinal fusion. Craniomaxillofacial injuries are classified as defects to the skull or jaw. These can arise from high energy impact trauma, cleft palate birth defects, and oral cancer [1–4]. Similar to craniofacial defects, long bone defects can arise from trauma, tumor resection, and nonunion [5]. Spinal fusions involve surgery to place an implant within the space of vertebrae to eliminate motion. Spinal fusion is used to treat spinal fractures, deformities, and instability [6]. Craniomaxillofacial and other segmental bone defects are particularly challenging due to their irregular size and shape and the amount of missing bone tissue. These types of defects are usually critical in size, in which the section of bone missing is too large for the body to regenerate. Biomaterial implants need to be optimized to repair these defects in

M. J. Dewey

Department of Materials Science and Engineering, University of Illinois at Urbana-Champaign, Urbana, IL, USA

B. A. C. Harley (✉)

Department of Materials Science and Engineering, University of Illinois at Urbana-Champaign, Urbana, IL, USA

Department Chemical and Biomolecular Engineering, University of Illinois at Urbana-Champaign, Urbana, IL, USA

Carl R. Woese Institute for Genomic Biology, University of Illinois at Urbana-Champaign, Urbana, IL, USA

e-mail: bharley@illinois.edu

© Springer Nature Switzerland AG 2022

F. P. S. Guastaldi, B. Mahadik (eds.), *Bone Tissue Engineering*,
https://doi.org/10.1007/978-3-030-92014-2_3

order to promote new bone formation as well as avoid implant inflammation and infection, which is common in large missing portions of bone [7].

1.2 *The Healing Cascade*

In normal homeostasis, uninjured bone is constantly being remodeled. Bone is resorbed by a resident population of osteoclasts and new bone synthesized by resident osteoblasts in a precise balance [8]. This process is facilitated by mechanosensitive processes that respond to bone deformation and provide the stimuli to alternately produce or resorb more bone and maintain the mechanical support of soft tissues. In order to design materials for bone regeneration, the coupling of osteoclasts and osteoblasts needs to be recognized and kept in balance in order to avoid complete resorption of implants or unnecessary and often painful excess bone formation.

Bones of the body heal via either endochondral ossification or intramembranous ossification. The two methods have similar healing endpoints; however, endochondral ossification involves a cartilage intermediate and is typically the process involved in long bone healing, while intramembranous ossification does not involve cartilage formation and is the process by which the flat bones of the skull and jaw heal [9–11]. Bone healing occurs in stages; for segmental defects this can take several months to complete. Firstly, a hematoma is formed and inflammation occurs, bringing in various immune cells and bone progenitor cells. During a typical immune response, undifferentiated macrophages would migrate to the wound site and polarize to the M1 phenotype in the early stages (1–3 days) [12, 13]. This phenotype is considered “pro-inflammatory” and is responsible for the initial removal of any cellular debris and host defense mechanisms. After 3 days and continuing for weeks, M1 macrophages should shift in phenotype to the “anti-inflammatory” M2 macrophages, which remodel the tissue and deposit matrix [12, 13]. In the case of a biomaterial implant, M1 macrophages are responsible for graft resorption and rejection, while M2 macrophages are accountable for graft acceptance by the body. The M1 to M2 transition over the course of a week is important in avoiding persistent or chronic inflammation, which can lead to a foreign body reaction and ultimate need for a secondary surgery [14, 15]. The way in which mesenchymal stem cells and immune cells differentiate can be partly attributed to the pore size of implant materials. Pore size can determine how vessels form, how cells infiltrate and differentiate, whether inflammation or infection will occur, and how macrophages polarize [16], and suggest exciting opportunities to engineer biomaterial design to not only promote osteogenic activity but also modulate the immune and inflammatory cascade after injury. Ultimately, these macrophages and the topography of an implant can determine the success early-on in the wound healing process. After inflammation, cartilage formation occurs in long bones and vascular growth occurs within the cartilage [17]. Next, chondrocytes die off and cartilage is resorbed in order for mesenchymal stem cells to differentiate into osteoblasts. In intramembranous

ossification this cartilage step is skipped and mesenchymal stem cells differentiate and mature, while blood vessels are formed during the primary bone formation step [17]. Finally, secondary bone formation occurs and bone is remodeled by osteoclasts in order to create the anisotropic nature of bone [17].

2 Current State of the Art in Repair: Bone Grafting

The gold standard to repair many bone defects is through the use of bone grafting. Autografts, allografts, and xenografts fall under this category. Grafting typically uses human or mammalian bone in order to repair a patient's defect. Here, we will discuss the various types of bone grafting used to repair critical-sized bone defects.

2.1 Autografts

Autografts involve using bone from a secondary site in the patient's own body in order to regenerate bone missing in the wound site. Multiple types of bone can be used, such as cancellous, cortical, vascularized bone, and bone marrow [18]. One of the most commonly used grafting sites is the iliac crest, a part of the pelvis. From this, one can take segments of cortical or cancellous bone for a variety of sized defects [18]. For craniofacial and long bone defects, bone can be repaired using iliac crest autografts with 70–95% success rates [19]. For repairing small bone defects, a chin graft or a retromolar graft from the area behind the third molar can be used [18, 20]. Other less commonly used grafts include tibial, rib, scapula, fascia, sternum, pedicled clavicle, and pedicled temporal bone [18, 20]. Unfortunately, defects longer than 6 cm have much lower success rates, and 50% failure rates have been reported for long bone defects [5, 19]. Drawbacks to removing the iliac crest include iliac fractures, pain, vascular and nerve injury, and persistent hematomas [18]. A popular cortical bone graft in craniofacial reconstruction is the calvarial graft, due to its slow resorption rate [18]. However, the thickness of this graft is highly variable and important vessels exist near this area of bone which should avoid being damaged. Removing this bone from a patient can cause deformity at the removal site and fracture of the bone. Although drawbacks limit the use of this graft, typically success rates are high. A study on 211 patients with calvarial grafts found that after 10–11 months there was a 95% chance of implant integration which matched with other findings of high success rates [21]. However, there was a high number of secondary procedures due to bone resorption, which was attributed to the need for a large amount of bone to be used as an autograft, and patient health differences [21].

General advantages of autografts include retention of some osteogenic cells and an immune response that does not persist [18]. Drawbacks to these methods include limited availability of bone and high chance of morbidity of bone at the site where the graft was taken from [18].

2.2 *Allografts*

Allografts use bone typically from a deceased donor, with cellular materials removed before implantation [18]. Repair using allografts involves demineralized bone matrix as particles, blocks, or sheets. This removal involves thorough treatment to eliminate any pathogenic agents and genetic material in order to minimize disease transmission. Removal of these pathogenic agents is necessary; however, in order to promote bone repair the extracellular matrix and collagen should not be removed [22]. A main drawback to using allografts is that the osteogenic properties of these vary from one commercial supplier to another due to the treatment and cleaning process [22, 23]. In general there can be high infection rates even after sterilization due to foreign substances remaining in the graft, but more vigorous removal of graft material ultimately leads to the bone being less likely to promote regeneration [20]. A study investigated four different allogenic bone matrices found that in all of the samples there were cells and cell residues before implantation, which in canine studies has shown to illicit an immune response [24]. Although cleaning of the bone matrix can be difficult, the implant survival rate is more than 95%, and new bone formation at 30% after 6 months [24].

2.3 *Xenografts*

Xenografts use bone from a mammalian source, typically bovine or porcine derived. Similar to allografts, infectious materials and cells must be removed from the bone prior to implantation. One study examined the structure of five different suppliers' allograft and xenograft materials and discovered that three of the five bone substitutes failed to meet criteria the manufacturers had promised [22]. This was due to the grafts either containing cellular content, loss of lamellar bone structure, or no collagen present [22]. Xenografts do not repair as well as autografts, they have a slower integration with host bone than autografts, and disease transmission such as bovine spongiform encephalopathy is a concern [25, 26].

Given some of the disadvantages associated with existing autograft, allograft, or xenograft procedures, biomaterials for regenerative repair of bone have become increasingly popular conceptually. One advantage of biomaterial approaches is the ability to potentially generate shelf-stable implants in order to remove considerations regarding time between graft harvest and use.

3 **Implant Design to Optimize Bone Regeneration**

In the next sections we will discuss design strategies for biomaterial implants as alternatives to graft materials. We will discuss the properties of an such an implant, specifically what criteria need to be met in order to successfully regenerate bone.

These criteria include selecting biocompatible materials that can promote bone and vessel formation, creating designs that can mimic the mechanical properties of bone and provide mechanical stability, altering the pore size and orientation through fabrication methods, and controlling degradation of the material. We will also discuss the variety of material classes available for implantation and the ways in which these can be modified to fit bone repair applications. These include polymers, both synthetic and natural, metals, and ceramics, focusing on their outcomes *in vitro* and *in vivo* and their specific advantages and disadvantages. We also highlight the method of 3D printing, which can be used to add functionality in shape, porosity, and release of biomolecules and cells. Finally, we will discuss cellular and growth factor additions to scaffold materials in order to improve bone formation.

4 Biomaterial Implants for Bone Regeneration

Biomaterial design criteria have to meet a wide range of benchmarks along with considerations of ease of surgical use and economic feasibility [20]. These criteria include biocompatibility, mechanical properties, pore size and orientation, and degradation and bioresorption. Presently, no biomaterial exists that meets all the following criteria. However, in Fig. 1 we outline a series of design criteria for biomaterial implants to address challenges in bone repair.

4.1 Biocompatibility

A biomaterial used for bone regeneration must be able to recruit cells from the surrounding tissues and provide nutrition and signals to support the vitality of these cells. There are many facets of biocompatibility related to bone repair; an implant

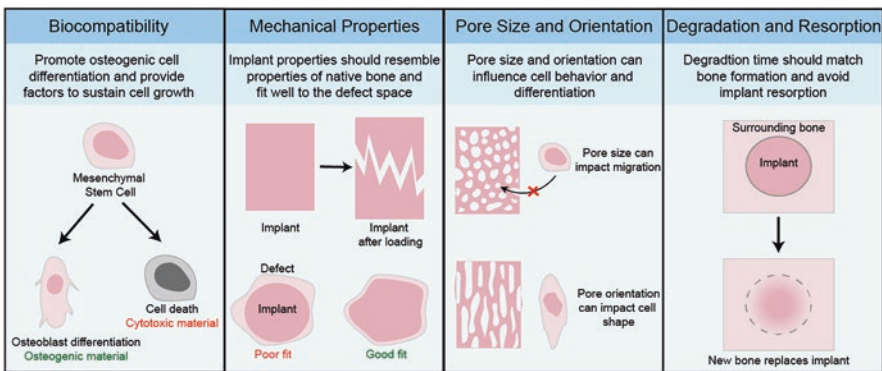


Fig. 1 Biomaterial properties for enhancing bone repair

should promote osteoconduction, osteoinduction, and osteogenesis. Cells should adhere to the biomaterial implant, enhance mineral formation and deposition of new bone, also known as osteoconduction. A variety of signals need to be provided to cells; ones that include osteoinduction, the promotion of differentiation of stem cells to mature bone cells. In addition to this, avoiding signals that may cause persistent inflammation, macrophage fusion, and foreign body response will lead to a more successful outcome. An implant also needs to promote osteogenesis, such that it attracts new cells from the surrounding tissue to the implant site to remodel and form bone [18]. A final important aspect of biocompatibility is the need for the implant to promote the formation of blood vessels. This should occur within a few weeks of biomaterial implantation to support nutrient transport and cell viability and induce osteoconduction, osteoinduction, and osteogenesis [27].

4.2 *Mechanical Properties*

Ideally, the mechanical properties of an implant would match the properties of the host bone at implant. However, this is extraordinarily difficult to meet, for a number of reasons. Firstly, bone is a multi-scale composite, with cortical and cancellous bone having vastly different mechanical properties. The Young's modulus and compressive strength of cortical and cancellous bone can vary from a Young's Modulus of 0.1–20 GPa (Table 1) [27]. Further, these properties reflect the mechanical properties of fully mature bone tissue with integrated vasculature; conceptually, biomaterials for bone repair may be much better suited having an environment designed for diffusive transport of nutrients and oxygen to facilitate cell penetration, proliferation, and extensive remodeling required to form new bone. An additional challenge with designing modulus-matched biomaterials is that many bone defects, notably craniomaxillofacial defects, are typically irregular in size and shape. This makes for difficulties shaping the implant to fit the defect site, which can affect mechanical stability. In general, the mechanical stability of the implant can also affect the healing outcome, as micromotion can directly inhibit osseointegration, so a mechanically stable implant is desired [28, 29].

4.3 *Pore Size and Orientation*

Typically, porous implants are used for bone regeneration as they provide a template for rapid cell infiltration and metabolic support via diffusion. The pore size of an implant greatly influences the cell behavior and ultimate success or failure of the surgery. There exists debate about optimal pore size to promote bone regeneration, as multiple cell types are involved in the healing process. *Bose et al.* suggest that pore sizes should be at least 100 μm in diameter for diffusion of nutrients and

oxygen, and pore sizes ranging from 200 to 350 μm are optimal for the in-growth of bone tissue [27, 30]. As for macrophages, a pore size of 34 μm promotes a more pro-inflammatory phenotype [31], yet other sources have suggested that 30–40 μm pores promote a pro-healing phenotype and avoid a foreign body response [32, 33]. Bone is an anisotropic tissue, and thus the pore orientation is increasingly considered as an important design parameter to consider in implant design. Recent work have begun to describe the use of aligned pores to promote bone formation by structural guidance cues to increase blood vessel ingrowth, accelerate cellular migration, and guide osteogenic cell differentiation [34–36].

4.4 Degradation and Bioresorption

In order to fully repair bone, the implant must be able to degrade while still providing signals for the patient’s own cells to form new bone. This degradation time should match the time it takes for new bone to be formed in order to replace the implant. Different bones regenerate over different times, which are summarized in Table 1 [27, 37]. If a material degrades too quickly, then there will not be enough material to continue to promote host bone regeneration and mechanically support the implant site [38]. Conversely, if a material degrades too slowly, remaining material will block new bone formation, as seen in Fig. 2. Any degradation to a material leads to a loss of mechanical properties, and if this is controlled correctly, then load transfer from the implant to the host bone will occur [40–42]. Therefore, to create a biomaterial that can successfully regenerate bone, the design must have a controlled material degradation rate.

Table 1 Properties of a biomaterial implant for bone regeneration

Property	Optimal range
Mechanics	
Young’s modulus	Cortical: 15–20 GPa; Cancellous: 0.1–2 GPa
Compressive strength	Cortical: 100–200 MPa; Cancellous: 2–20 MPa
Pore size and orientation	
Nutrient diffusion	At least 100 μm in diameter
Bone in-growth	200–350 μm in diameter
Immune cells	30–40 μm in diameter to avoid foreign body reaction
Cell migration	Anisotropic pores promote faster migration
Direction vessel growth	Anisotropic pores promote aligned vessels
Degradation and bioresorption	
Spinal fusion	9 months or more
Craniomaxillofacial	3–6 months
Long bone	5–7 months

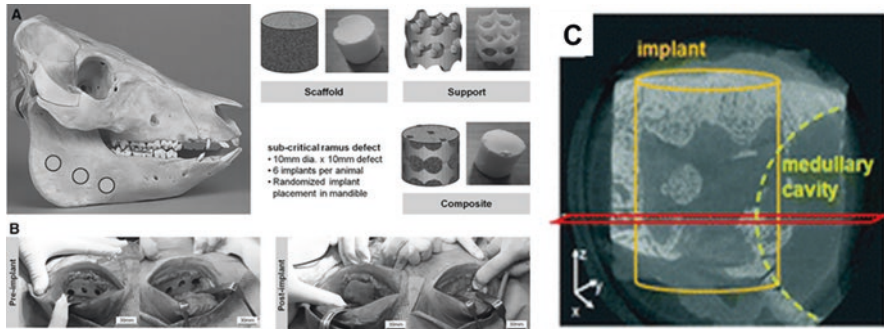


Fig. 2 PCL and mineralized collagen implant in porcine ramus defect model. (a) Schematic of subcritical ramus defect locations along with 10 mm diameter, 10 mm thick mineralized collagen (CGCaP) scaffold, PCL support, and mineralized collagen-PCL composite implants. (b) Specimen locations were randomized on each side of the mandible and within each porcine animal model. Representative images of the subcritical ramus defect preimplant and postimplant. *CGCaP* collagen-glycosaminoglycan calcium phosphate, *PCL* polycaprolactone. (c) Representative μ CT data showing partial penetration of the implant into the medullary cavity. Light regions represent bone mineral and dark regions represent no mineral or PCL still present within the implant. (Image adapted from [39])

5 Scaffolds: Mechanical, Chemical, and Biological Properties

Scaffolds are commonly thought of as an initial template that provides a constellation of structural, compositional, and mechanical signals to potentially accelerate the process of bone regeneration. Common scaffold materials include polymers, ceramics and hydroxyapatite materials, metals, and collagen-based implants. Some advantages of scaffolds are their ability to be tailored to specific patients and avoid the cellular material cleaning process that bone-derived graft materials require. When deciding between allograft or xenograft materials versus synthetic or other scaffold materials, sources have found a variety of results, ranging from better to worse healing outcomes [43, 44]. Alternatively, autograft materials have shown favorable healing and mechanics over scaffold materials, but autografts drawbacks outweigh their benefits [45–47]. Scaffolds do not require a secondary surgery as autografts do and do not suffer from a limited supply of material. If materials have the same or very similar healing outcomes, it is then favorable to use scaffolds over grafts due to their advantages over bone-derived materials. Scaffolds can also be patient-tailored, such as 3D printed or cast in the particular size and shape of the defect. In addition to this, patient-derived cells can be added to affect the outcome, and growth factors can be added to target specific cell functions to improve osteogenesis and angiogenesis [48]. A summary of clinically available implant materials and their outcomes *in vitro* and *in vivo* can be found in Table 2.

Table 2 Commercially available bone implant materials and their healing outcomes *in vivo* and *in vitro*

Implant type	Outcome	References
Demineralized bone matrix		
Grafton Putty (Synthes, USA)	Good handling, complete spinal fusion in all animals, promotes new and mature bone formation in critical-sized defects	[49, 50]
DBX® Putty (Synthes, USA)	Good handling, half of animals tested had spinal fusion, promotes mature bone formation in critical-sized defects	[49, 50]
AlloMatrix Injectable Putty (Wright Medical Technology Inc, USA)	Fair handling, no spinal fusion occurred, limited bone formation in critical-sized defects	[49, 50]
Regenafil (Regeneration Technologies Inc, USA)	Fair handling, limited bone formation in critical-sized defects	[50]
Dynagraft (Gensci Regeneration Sciences Inc, Canada)	Good handling, limited bone formation in critical-sized defects	[50]
Lubloc® bovine xenograft	Better bone healing than Grafton, Ceraform, and Osteoset, induced activation of host bone cells	[25, 51]
Biocoral® coral xenograft (Biocoral Inc, USA)	Superior healing compared to ceramic and hydroxyapatite materials in alveolar bone defects, bone formation within 2 weeks post-operation	[51, 52]
Metals		
Plasma sprayed titanium	Good osteoblast adhesion, proliferation, and differentiation, better early-stage healing conditions	[53]
Sand-blasted, acid-etched titanium	Similar results to plasma sprayed, but worse early-stage healing, osseointegration in dental implants	[53, 54]
Actipore™ porous NiTi (Biorthex, Canada)	High bone ingrowth stimulation, performs similarly to traditional titanium implants, complete bone bridging after 12 months	[55, 56]
Ceramics and hydroxyapatites		
ZrO ₂ ceramic (Ziterion GmbH, Germany)	Osseointegration with surface-modification comparable to titanium for dental implants	[54]
Ceraform® hydroxyapatite substitute (Teknimed, France)	Newly formed bone was restricted to graft area, osteoconductive properties, poor healing compared to Osteoset and Lubloc	[25, 51]
SRS® carbonated apatite bone cement (Norian Coporation, USA)	Extraosseous extrusion of bone cement, remodels into natural bone but occurs slowly in the distal radius repair	[51, 57]
Osteoset® calcium sulfate substitute (Synthes, USA)	Osteoconductive properties, no evidence of osteoinductive activity, superior to Ceraform and similar to demineralized bone substitute	[25, 51]
BonAlive® bioactive glass (Vivoxid, Finland)	Longer time for material to biodegrade, form and remodel bone compared to autografts, cortical bone grew in thickness over time	[51, 58]

(continued)

Table 2 (continued)

Implant type	Outcome	References
Biosilicate®/Bioglass® 45S5	Biosilicate has higher osteogenic activity and higher amounts of fully formed bone compared to bioglass, biosilicate does not have the potential to be cytotoxic/genotoxic that bioglass does	[51, 59]
ProOsteon 500R (Interpore International, USA)	Better option than collagraft for spine and lower extremity applications with need for more mechanical support, slow resorption of material	[60]
Polymers		
Poly(DL-lactide) mesh plate (Synthes, USA)	Fair handling, poor healing response, and scant new bone formation in critical-sized defects, mesh was replaced by fibrous tissue	[50]
Cortoss® Bisphenol-a-glycidyl dimethacrylate resin (Orthovita, USA)	Minimal formation of apatite layer <i>in vitro</i> , less leachable toxic monomer than compared to PMMA cements, possibly cytotoxicity	[51, 61]
Collagen scaffolds		
Healos® type I collagen/hydroxyapatite matrix (DuPuy Spine Inc, USA)	Osteoconductive and osteoinductive, not recommended for interbody cages for spinal fusion, similar healing to autografts in posterolateral fusions	[51, 62]
Collagraft® collagen/hydroxyapatite/tricalcium phosphate composite (Zimmer and Collagen Corporation, USA)	Greatest ingrowth of bone compared to ProOsteon and demineralized bone xenograft, rapid resorption	[51, 60]

5.1 Synthetic Polymeric Scaffolds

Synthetic polymers are man-made polymers, commonly seen in household items such as plastics, rubbers, and glue. Synthetic polymers for tissue engineering must be biodegradable and biocompatible while avoiding a negative immune reaction and matching biomaterial properties as closely as possible. Much of this can be accomplished through modifying the polymer itself, and careful consideration must be made when examining the degradation byproducts. An advantage to using synthetic polymers are their large scale reproducibility with controlled mechanical properties, degradation, and structure [63].

A wide variety of techniques can be used to create porous scaffold architectures. These include casting and forming based methods such as solvent-casting, particulate leaching, and gas-foaming. Solvent-casting and particulate leaching techniques are simple, involving a water-soluble salt homogeneously distributed through the polymer solution. The polymer is cast into shape and the solvent is removed by evaporation or lyophilization, while the salt is leached out by soaking in water to create an open-porous polymer [63]. Gas-foaming removes the need for organic solvents and instead carbon dioxide is used to create a polymer foam. In brief, the solid polymer is exposed to high pressure carbon dioxide, which is then saturated into the polymer, and then gas bubbles expand to create a closed-pore structure [63].

Increasingly, more exotic methods are also being used such as electrospinning, 3D printing, and thermally induced phase separation. Electrospinning can create polymeric fibers on the nanoscale by applying a high voltage and an electric field to a polymer solution on a collector which can be rotated in order to create various alignments of fibers. This method can easily create fine fibers; however, it can be difficult to create small diameter fibers with biocompatible materials, and creating 3D scaffolds and complex pore geometry still remain a challenge [64]. Scaffolds with nanofibers have shown to improve stem cell differentiation toward the osteogenic lineage and can be beneficial to bone repair due to their ability to mimic the type I collagen alignment in bone [64]. In addition, sacrificial nanofibers can be added to poly(caprolactone) fibers in order to align cells, direct the formation of extracellular matrix, increase tensile properties, and control the release of collagenase and growth factors to increase cellularity [65, 66]. 3D printing can be used to fabricate scaffolds with complex architectures; however, small pore sizes are difficult to achieve. Various methods of 3D printing exist, such as laser sintering, photopolymerization printing, and extrusion printing, which will be expanded on in Sect. 6. Thermally induced phase separation can be used to fabricate biodegradable 3D polymers by first dissolving the polymer in a solvent at high temperature and then phase separation occurs by lowering the temperature and final sublimation to create a porous polymer [63]. Ultimately, another advantage to this is the ability to modify the surface of polymers in order to alter cell interactions with the polymer surface.

The most extensively used polymeric material in cranioplasty is poly(methylmethacrylate) (PMMA). This is an easy to shape and lightweight material and does not radiate heat [20]. Polyethylene has also been used due to its porous nature, and if infections occur antibiotics can be used instead of complete removal of the implant [67–69]. Polyethylene glycol (PEG) hydrogels have been investigated for new bone formation due to their ability to slowly release growth factors. However, unlike other polymers, PEG hydrogels added to a mandibular defect saw no difference in new bone formation and did not have an osteogenic effect [70].

Other commonly used polymers in bone tissue engineering are poly(lactic acid) (PLA), poly(lactide-co-glycolide) (PLGA), 3-hydroxybutyric acid (PHB), and poly(caprolactone) (PCL) [39, 71–74]. PLA degradation byproducts are expected to be nontoxic; however, degradation by hydrolysis releases lactic acid and in a zygomatic fracture fixation, PLA caused swelling at the implant site in 60% of patients [75–77]. Some polymers used for bone regeneration, such as lactic acid based polymers, have caused fibrous tissue formation and foreign body responses [78]. Alternatively, PHB scaffolds have been shown to be highly compatible with osteoblasts and can induce ectopic, or abnormal, bone formation [79]. Benefits to using PLA, PCL, and PLGA are their FDA approval for certain use in humans and degradation rates can be tailored by altering the molecular weight and composition. However, drawbacks include poor mechanical properties compared to bone and the possibility of rejection by the body and foreign body responses. Mechanical properties can be tailored based on polymer crystallinity, and growth factor release can be added to these polymer systems, in the future these two factors can possibly eliminate the drawbacks of polymer systems.

5.2 *Natural Polymeric Scaffolds*

Natural polymers, such as collagen scaffolds, have been used extensively as an alternative material to heal bone defects. A common variant of the collagen scaffolds contains type I collagen, glycosaminoglycans such as chondroitin-6-sulfate, and acid [80–84]. These materials are homogenized together to create a liquid suspension and then freeze dried in order to create an open-porous structure that enables cell migration and penetration through the material. Other natural polymers, such as chitosan have also been investigated [51]. Chitosan is also highly biodegradable and biocompatible and can differentiate osteoblasts *in vitro*. However, this material is not osteoconductive and has caused allergic reactions [51]. Typically, collagen scaffolds without any mineral supplements are used to regenerate tendon or skin due to their poor ability to heal bone [51, 85–88]. A benefit to using collagen scaffolds is their tunable pore size and orientation, which can be achieved by using molds with different thermal properties in which scaffolds are lyophilized and altering the freezing rate and temperature [30, 81, 86, 89, 90]. Issues with using naturally derived polymers are that they may contain pathogenic impurities and produce a negative immune response, and it is harder to control the mechanical properties, however, they typically support cell adhesion and proliferation [63].

Variants of collagen materials can be made in order to heal different tissues in the body, such as scaffolds containing calcium phosphate mineral in order to repair bone defects [83, 84, 91–95]. These scaffolds have been shown to be more appropriate for bone repair, due to their biocompatible, biodegradable, and bone formation-inducing behaviors. This has been demonstrated by mineral formation *in vitro* and bone formation *in vivo* without additional osteogenic supplements and inhibiting bone resorption [96–98]. Disadvantages to these scaffolds are their weak mechanical properties, due to their extremely porous nature. However, mechanical properties can be altered by adding additional materials during freeze drying, such as polymer reinforcements like PLA and PCL [99, 100]. These reinforcements can be 3D printed in various architectures, and one design in particular has been used to achieve shape-fitting in order to avoid micromotion upon implantation [99]. Mineralized collagen scaffolds combined with laser-sintered PCL have demonstrated a 6000-fold increase in Young's Modulus compared to scaffolds alone [100], and in a porcine ramus defect model this composite material had greater bone repair than the scaffold or PCL construct alone [74]. Other elements such as allogenic tissues, growth factors, and other minerals can easily be added to these scaffolds by mixing into the suspension step before lyophilization [101–103]. Specifically, the amniotic membrane derived from placentas has been added to collagen and mineralized collagen scaffolds in order to control the wound healing process and avoid inflammation while increasing bone formation [101, 102, 104].

Increasingly, the delivery or endogenous production of growth factors has been investigated in collagen scaffolds. For example, PDGF-BB and IGF-I delivery was shown to influence migration into these scaffolds [87]. Additionally, current research is focused on sequestering and tethering these growth factors to collagen scaffolds

or using micelles as controlled release mechanisms. Other minerals, most notably zinc, have been investigated to improve osteogenesis, and various glycosaminoglycans can be used in order to alter the mineral formation [103, 105]. Additionally, pore sizes and orientations have been investigated in collagen and mineralized collagen scaffolds in order to drive a response to increase viability of tenocytes or increase bone mineral formation [30, 34, 80, 81, 89, 105–107]. Finally, the important interaction of mesenchymal stem cells and osteoclasts has been investigated in these scaffolds, and research has shown that mineralized collagen scaffolds inhibit osteoclastogenesis by releasing osteoprotegerin [97, 98]. These scaffolds have the vast potential to be expanded on in order to achieve the criteria for bone regeneration. Whether it be altering the pore size and orientation, adding other minerals, glycoproteins, or tissue matrices, or adding growth factors and specific cell types, there is much work to be done to advance these mineralized scaffolds.

Commercially available natural polymers, such as the mineralized collagen material Healos[®], have found comparable results in some cases to autografts. Healos[®] soaked in bone marrow aspirate without any exogenous factors demonstrated similar healing to autografts in posterolateral fusions. However, this same material performed poorly for interbody cages in spinal surgeries, due to volume of material and mechanical properties [62]. Thus, improvements still need to be made in order to increase mechanical strength and stability to repair other bone defects.

5.3 *Metallic Scaffolds*

Metal scaffold use is limited due to their ability to conduct heat, difficulty to shape during implantation, and radio-opacity [20]. Metal screws or plates can interfere with imaging of the defect site and monitoring the patient's health. In addition to this, metals risk corrosion and fatigue over time, the stress shielding effect can cause bone atrophy, and it is difficult to have a metal implant fit well to the implant site without micromotion [75, 108, 109].

Titanium has been the metal of choice for use in large bone defects and like most metals is hard to shape, but resists infection and will be accepted by the body [20]. In order for titanium and its alloys to be successful in bone repair, typically surface modifications are necessary to promote cell attachment and integration. Various methods to do this include mechanical grinding or polishing the surface, physical vapor deposition, acid etching, or chemical vapor deposition [110].

Other metallic materials used include stainless steel 316 L, cobalt based alloys, porous tantalum, and magnesium. Disadvantages include their lack of biocompatibility, wear, and corrosion can release ions and particles that can lead to inflammation. Stainless steel specifically has a very high stiffness, so high in fact that it can lead to bone resorption due to the mismatch in mechanical properties of bone and the implant [111]. Unfortunately, in order to make porous metallic materials to mimic the natural structure of bone, these usually end up too weak to be a viable option [110]. Porous tantalum, however, has a high porosity, a Young's modulus

comparable to bone, and has been shown to be biocompatible in animal models [110]. Magnesium and its alloys are fully bioresorbable, have mechanical properties similar to native bone, do not induce a negative immune response, and promote bone growth [110]. Concerns of using magnesium are the hazards associated with rapid dissolution of the magnesium in the body. An alloy of titanium, nickel-titanium (Nitinol) can be used as a shape-memory material and has demonstrated biocompatibility and mechanical properties similar to bone. Studies have shown that nitinol is more biocompatible than stainless steel [110]; however, release of nickel ions poses a toxicity and allergy concern.

In vivo studies comparing metal implants have shown that porous nitinol had increased osseointegration compared to titanium alloys [112]. Of the metals available, nitinol and resorbable magnesium are the most promising due to low stiffness [111]. In general metals suffer from stress shielding, corrosion, and biofilm formation, all of which contribute to their concerns with clinical use. Overall, the use of metals is mostly desired for permanent implants at sites that need high mechanical loading or as fixation devices.

5.4 *Ceramic and Hydroxyapatite Scaffolds*

Hydroxyapatite and bioactive ceramics are the most widely used alternative to autografts and allografts in the preclinical and clinical settings [113]. One very common ceramic used in healing of bone defects are bioactive glasses. Bioglass is comprised of sodium, silicone, magnesium, potassium, oxygen, phosphorous, and calcium [114]. As far as healing results, a study examined two different versions of compressed hydroxyapatite scaffolds versus a xenogenic graft in mandibular defects and found no healing differences between the groups at the end of the study [43]. Another study used bioreactors to create bone over time in an autograft and a commercially available bioceramic and found that both were able to create mineral tissue, but autograft materials had more mature bone and mechanical properties more similar to bone [45]. In general, calcium phosphate or hydroxyapatite bone substitutes have less osteogenic potential than autografts [25, 45, 46]. However, hydroxyapatite coatings have different effects than used as a bulk material, and coatings promote cellular contact of osteoblasts [115]. Bioceramics can have various degradation times in the body, an example being hydroxyapatite and tricalcium phosphate (TCP), with hydroxyapatite scaffolds degrading after 2–5 years and TCP degrading within 1 year [113]. This degradation time impacts healing outcomes, as a clinical trial involving hydroxyapatite scaffolds demonstrated that after 15 months the scaffold was still present, and another study claimed the scaffolds were still present even after 7 years [37, 116]. In contrast to this, a β -TCP scaffold deposited new bone after 9 months but complete regeneration of the fibula was only found in 1 out of 14 patients [117].

An alternative to bioactive ceramics is bioinert nanoceramics. These include implants made of titanium, alumina, and zirconia [118]. These ceramics are not

designed to regenerate the host bone due to their inert nature; however, they have high fracture toughness and mechanical strength at the implant site [118]. Titanium implants can be modified with Ca^{2+} ions in order to create titanium oxide, which helps prevent corrosion and absorb proteins to the surface of the material [118]. In addition, other treatments to titanium can be made to modify the surface to promote integration with the host bone, such as etching or sand blasting [118]. Similar to other bioinert ceramics, alumina does not promote osseointegration due to its inert nature, and thus coatings must be added, or the surface topography must be altered to enhance protein adhesion. Zirconia-yttria ceramics are often used as bone fillers due to the ability to prevent biofilms [119]. However, the drawback to these is their inert nature, and these ceramics will still remain in the body instead of host bone.

Bioceramics are thought of to be one of the preferred scaffolds for bone repair due to biocompatibility and high mechanical properties. However, due to the nature of ceramics, these materials can be brittle and only so much of the material can be resorbed by the body [115]. In order to achieve a biomaterial implant it is likely that a composite material will be needed that balances mechanical, chemical, and biological properties. Composite materials have already been discussed as better choices for tissue engineering applications, as no implant material exists today that includes all of the implant criteria [63].

6 3D Printing as a Tool to Improve Bone Formation

3D printing, also known as additive manufacturing, has been used to create materials in our daily lives as well as materials for the medical field. Various methods for creating designs and architectures that would be difficult or impossible using other methods can be accomplished by 3D printing. 3D printing involves a user-created design, which the printer then creates layer-by-layer. This approach overcomes the issue of irregular size and shape defects for bone repair, as the design can be tailored to fit a patient-specific shape. A patient's defect can be scanned using MRI or CT technology to map the defect space, and subsequently this scan can be converted and used on a 3D printer to fill the defect space [120–122]. 3D printing methods can fall into four categories: extrusion, polymerization, laser sintering, and direct writing [123]. The extrusion method takes a solid polymer, extrudes the material through a nozzle by the application of heat and pressure, and allows the print to cool to room temperature to solidify. Fused deposition printing is an example of extrusion-based printing. Polymerization printing uses a bed of resin that is polymerized by lasers, for example, stereolithography [124]. Selective laser sintering involves a bed of polymer powder in which lasers are used to fuse the powder together to create a 3D print. Finally, direct writing uses powder and a regular inkjet printing head with binder, in which the binder is printed onto the loose powder. This method can be used to create interconnected pores; however, intensive optimization of the printing process for a new material is required [122, 123].

An expanding range of materials can be 3D printed, such as the polymers polyethylene, polylactic acid, and polycaprolactone, as well as ceramic materials such as TCP and HA. In addition to these, metals can also be 3D printed; however, this is less common, with an example being bioactive titanium scaffolds fabricated by ink-jet 3D printing [125]. In this case, titanium was printed and then fired in order to strengthen the material, and the bioactivity was modified by the deposition of hydroxyapatite on the surface [125]. 3D printing can be used to make these materials very porous; however, a drawback to this is that the mechanical strength is lowered, which limits their use in load-bearing applications. Not only can 3D printing offer a better implant fit, it also can be modified with growth factors and cells. Growth factors and cells for use in 3D printing, also known as bioprinting, will be elaborated on in the following sections, but can be incorporated into polymers such as hydrogels for encapsulating cells and the slow release of biomolecules.

A further opportunity for 3D printing is the addition of these 3D prints to existing materials for bone regeneration. As it can be difficult to create load-bearing 3D prints with very porous structures, an alternative is to use 3D prints as mechanical supports and other biomaterials as the bioactive matrix. This has been demonstrated with mineralized collagen scaffolds and 3D printed polymers. The mineralized collagen acts as the bioactive and osteogenic matrix, and the polymer 3D print acts to give mechanical strength to the whole material in order to better match the mechanical properties of bone [29, 39, 74, 100]. This method provides another way to consider 3D printing; besides using the method to create a scaffold, 3D printing can be used to fabricate pieces of the overall structure. Overall, 3D printing is an extremely useful tool for creating patient-specific implants as it can create complex and porous shapes using a wide variety of materials and methods while also including the option of printing cells and growth factors. More research needs to be performed on optimizing 3D printed materials, as well as investigating combinations of 3D printing with other factors to create composites which can leverage multiple benefits.

7 Stem Cells: Biology and the Application for Tissue Regeneration

7.1 Stem Cells for Bone Repair

Multiple cell types are involved in the bone formation and remodeling process, such as osteocytes, osteoblasts, osteoclasts, and immune cells. Osteocytes maintain the existing bone and are considered mature bone cells. Osteoblasts are responsible for bone growth and can differentiate into osteocytes, while osteoclasts are responsible for bone resorption. Finally, immune cells are important for the healing outcome of the wound, as they clean the area and can lead to fibrous tissue formation or a foreign body reaction if a negative immune response persists [14, 15].

Based on literature, the addition of stem cells to implant materials before implantation has shown more success than implants without stem cells [126, 127]. Overall, the use of autologous or allogenic cells in combination with scaffolds for long bone repair has resulted in positive healing outcomes [5]. The most commonly used stem cells used are embryonic stem cells (ESCs), induced pluripotent stem cells (iPSCs), and adult mesenchymal stem cells (MSCs). ESCs are derived from embryos through *in vitro* fertilization, can proliferate infinitely, and can differentiate into any cell type. iPSCs are somatic cells that have been genetically reprogrammed to express the pluripotent properties similar to ESCs. Finally, MSCs, which are the most commonly used cell type for bone repair, are isolated from the liver, fetal blood, bone marrow, and umbilical cord. All of these cell types are able to differentiate into various bone cells, making them important in the bone repair process.

Typically, cells are cultured to a pre-confluent state and then added to graft materials and cultured for a short period of time before implantation into the defect space. Alternatively, cells can be injected directly into defects, which has shown some promise *in vivo* [128]. Cell death upon transplantation is a drawback; however, MSCs can be contained in spheroids to improve survival, and these have been injected into damaged tissues to promote repair [129, 130]. Interestingly, these have also shown that restricting MSC migration out of these spheroids can enhance the osteogenic potential of these spheroids [130]. In general, adult stem cells have a wide variety of results which can be due to the differences in donors, such as where the cells were sampled, the age of the donor, and life habits [115].

Of the mesenchymal stem cells used, bone marrow stromal cells are favored and can differentiate into almost all mesoderm-derived cell types, including cartilage, bone, hematopoietic stroma, tenocytes, and skeletal muscle cells [115]. However, loss of differentiation properties toward the adipocyte or chondrocyte lineage has been observed after multiple cell passages [131]. Pericytes have also been investigated and are derived from the peripheral blood. These cells are positive for some osteogenic markers and can differentiate along the osteogenic, chondrogenic, and adipogenic lineage [115]. Another commonly used cell line are adipose-derived stem cells, due to their being easy to acquire, abundant, and can differentiate into adipocytes, chondrocytes, osteoblasts, and myocytes. However, this cell line is more biased toward the osteogenic lineage, which can make for biased *in vitro* studies and have demonstrated less favorable outcomes compared to bone marrow stromal cells [132, 133]. In a study by *Follmar et al.*, combining adipose-derived stem cells with allografts in a rabbit model demonstrated a foreign body response; however, these same cells in a porcine model accelerated bone healing [128, 134]. Another alternative is to use cells derived from pregnancies, such as umbilical cord and placental stem cells. Umbilical cord blood multilineage cells take longer to culture and express lower bone antigens, but exposure to osteoblast-conditioned media enhanced their rate of osteogenic differentiation [135, 136]. Placental stem cells have also been shown to have a bone marrow stromal cell-like behavior and possess multilineage differentiation potentials [115].

3D printing offers the unique opportunity to encapsulate cells into printed constructs and even encapsulate various cell types into the same print. These cells can

be cultured and encapsulated into hydrogels, which can then be used in syringe pumps in bioprinters to print layer-by-layer. Mesenchymal stem cells and chondrocytes have been embedded into alginate hydrogels, and this hydrogel exhibited extracellular matrix formation both *in vitro* and *in vivo* [123]. Organ bioprinting, an approach to print fully capable organs, can be accomplished through printing a variety of cells and culturing the resultant scaffold post-printing. Firstly, the organ blueprint must be designed, next, stem cells required for the organ are isolated and differentiated, and then these are encapsulated into hydrogels or other medium to support the life of the cells, and finally, these are printed and placed into a bioreactor or incubator to continue cell growth [137]. Bioprinting enables cells to be printed in distinct areas using various nozzles containing hydrogels with different encapsulated cells. This can make for interesting studies comparing co-cultures in different compartments. Bioprinting with cells offers new complex architectures with a wide variety of cells; however, the material in which the cells are encapsulated within still needs to meet bioactivity requirements while being able to be printed. Cells must remain viable within these materials and further research needs to investigate improving these printers and materials to sustain cell viability.

7.2 *Cells Involved in the Wound Healing Cascade*

There are a wide variety of cells to consider using in biomaterial implants, and more research needs to be performed on using patient-derived cells in order to accelerate healing as well as the interactions of each cell type on the biomaterial implant. Maintaining the balance between osteoclasts and osteoblasts, creating a controlled environment for M1 to M2 macrophage phenotype transition, and allowing blood vessels to grow and deliver nutrients are all factors that need consideration in biomaterial implant design. The promise of better healing using biomaterial scaffold implants lies in the ability for these to be tailored to meet these requirements. In order to balance osteoclasts and osteoblasts, these cell types could be examined in a co-culture on the implant in order to determine the possible mechanisms and healing that may proceed *in vivo*. This has been performed on collagen-based scaffolds in order to determine that these scaffolds inhibit osteoclastogenesis [97, 98]. Similar studies should be carried out investigating this balance in other biomaterial implants as well. Uncovering the type of M1 to M2 macrophage transition in implants can be investigated by seeding M0 macrophages or monocytes on scaffolds *in vitro*. These transitions have been investigated by Spiller *et al.* [13, 138–141], and this can provide useful information over time about how these cells polarize in response to implant released factors and implant topography and composition. This phenotype transition could be helpful to elucidate whether inflammation may persist or if a foreign body response may occur before an *in vivo* experiment is undertaken. In addition to investigating these specific cells, placental-derived tissues have shown promise in modulating this transition and ultimately the immune response. The amnion and chorion membrane of the placenta have been investigated as an addition

to scaffolds and have shown to dampen the pro-inflammatory immune response while promoting osteogenesis [101, 102, 104, 139, 142, 143]. Finally, angiogenesis is important for delivery of nutrients to the growing bone and inadequate vascularization of bone has been associated with a decrease in bone mass [144]. An interesting opportunity exists to test vessel formation in biomaterial implants for bone regeneration, an example being endothelial vessel formation created in hydrogels by co-culture of umbilical vein endothelial cells and normal lung fibroblasts [145]. This type of study could be expanded using released factors from implant or solely focusing on blood vessel formation in implants for bone regeneration. This may give a better understanding of how blood vessel formation would occur *in vivo*.

Overall there are many variables to consider when using stem cells and more research needs to be examined on the effect of adding these to implants. There exists potential for these cells to accelerate healing, and in combination with 3D printing even greater potential exists to improve bone repair with complex tissue architectures.

8 Growth Factors, Chemical Cues, Differentiating Agents for Bone

8.1 Growth Factors to Enhance Bone Repair

Growth factors are polypeptides and are used in bone regeneration to differentiate bone cells, promote angiogenesis, or promote migration and retention of cells to the implant site. These can act on the autocrine (influences the cell of origin), paracrine (influences nearby cells), or endocrine (influences the nearby microenvironment) systems. Growth factors bind to cell receptors and induce intracellular signal transduction which determines the biological response upon reaching the cell nucleus [146]. Additionally, a single growth factor may bind to different receptors. Growth factors are typically introduced to the body in one of the two methods, as a protein therapy or gene therapy. Protein therapy involves direct recombinant growth factor delivery to the site of interest, whereas gene therapy delivers growth factors to cells by gene encoding [146].

Most common growth factors interacting with the skeletal system are bone morphogenic proteins (BMPs), fibroblast growth factors (FGF), platelet-derived growth factor (PDGF), insulin-like growth factors (IGFs), transforming growth factor- β (TGF- β), and vascular endothelial growth factor (VEGF) to name a few. A summary of growth factors and their impact on bone and cartilage formation can be found in Table 3. Using growth factors to heal critically sized defects has shown to mostly improve the healing process; however, there have been reports that BMPs and TGF β -3 did not improve healing [5].

Bone morphogenic proteins are typically considered the most promising approach to repair bone due to their osteoinductive nature. BMP-2, -4, -6, -7, and -9

Table 3 Growth factors used in bone repair and their functions

Growth factor	Function	References
BMPs	Promotes osteoprogenitor migration	[146]
	Promotes proliferation and differentiation of chondrocytes and osteoblasts	
	Promotes bone formation	
EGF	Promotes osteoblast proliferation	[147]
	Combined with BMP-2 and -7 can further upregulate proliferation	
FGFs	Promotes chondrocyte maturation (FGF-1)	[146, 148]
	Differentiates osteoblasts	
	Involvement in bone resorption and formation (FGF-2)	
HGF	Promotes osteoblast proliferation	[149, 150]
	Promotes osteoblast migration	
	In some instances it has been found to inhibit BMP-2-induced bone formation	
IGFs	Promotes osteoblast proliferation	[146, 148]
	Promotes bone formation and controls resorption	
	Induces the deposition of type I collagen	
MGF	Repairs tissues	[151, 152]
	Improves osteoblast proliferation	
PDGF	Promotes osteoprogenitor migration and differentiation	[146, 153, 154]
	Promotes wound healing and bone repair	
TGF- β	Stimulates differentiation of mesenchymal stem cells to osteoblasts and chondrocytes	[146, 155, 156]
	Promotes bone formation	
	Recruits osteoblast and osteoclast precursors	
VEGF	Mineralized cartilage	[146]
	Promotes osteoblast proliferation	
	Control angiogenesis	

have shown to have the greatest osteogenic success *in vitro* [157]. However, there have been mixed results with using BMPs. A review found that 11 results supported the use of BMPs, three results found no effect on bone repair, and two demonstrated negative outcomes [158]. This variability can be attributed to the variety of BMPs used and the treatment conditions. To repair fractures, recombinant human BMP-2 (rhBMP-2) is used most frequently, and rhBMP-7 is most commonly used for non-union repairs [158]. Overall, rhBMPs have been shown to accelerate healing of tibial fractures and reduce infection rates [158]. There exist drawbacks to using BMPs, especially rhBMP-2 which has resulted in surgery complications, especially spinal surgeries. The majority of these complications stem from heterotopic ossification, or bone growth in areas of other tissues. Literature finds it difficult to compare the two BMPs, BMP-2 and -7, as most studies lack comparisons between the two which can elucidate differences. Another issue with BMPs and many growth factors is the delivery method. Due to their soluble nature, if these growth factors

are not appropriately carried to the site of interest they can diffuse into nearby tissues and form bone in undesirable locations. In general, large doses of BMPs are required to achieve osteogenic effects, which can be both expensive and increase the risk of heterotopic ossification [158]. Thus, further research into BMP delivery needs to be performed in order to control the release of these factors better.

Fibroblast growth factors have been found to be suitable for regeneration of a wide range of tissues and are key regulators of bone development [148]. In particular, FGF-2, -9, and -18 are involved in bone development and FGF signaling can stimulate proliferation of osteogenic cells and angiogenesis [148]. Recombinant FGF-2 has shown to accelerate bone repair in rabbits, but its anabolic effect is limited to the first 24 h after fracture occurs [159]. In a rabbit model, FGF-2-coated hydroxyapatite scaffolds were shown to greatly enhance the osteoinductive effect compared to uncoated implants [160].

Platelet-derived growth factor is involved in the development of embryos but also plays important roles in bone repair in adults. Systemic application of PDGF has shown to result in increased bone mineral density and compressive properties in rat vertebrae [161], conversely, PDGF inhibited bone regeneration in rat calvarial defects [162]. However, with the appropriate carrier, the opposite was true and bone formation was increased in rat calvarial defects [163].

Insulin-like growth factors can influence both metabolic and growth activity in many cell and tissue types, and of the isoforms IGF-I and IGF-II, IGF-I has been typically only used in skeletal reconstruction [164]. IGF-I is the most abundant growth factor found in the skeletal system and regulates bone development and osteoblasts [165]. IGF-I has also been used to increase bone formation, but this did not have the desired effect in young animals [166]. IGF-I delivered via PLGA microparticles was shown to enhance new bone formation, but there was little therapeutic effect of using IGF-I alone for cartilage and bone repair in osteoarthritic joints [167, 168]. IGF-II is the most abundant growth factor in bone and both IGFs play important roles in stimulating osteoblast differentiation, deposition of bone, and collagen protein expression [169]. Insulin-like growth factors can be differentiated from one other by their functions, as IGF-II can induce proliferation and differentiation of MSCs to osteoblasts, while IGF-I cannot, and functions to maintain and grow bone [169].

Transforming growth factor beta is one of the most common cytokines and influences the development of various tissues [164]. The carrier of TGF- β plays an important role in its activity, as single doses of TGF- β_1 had no effect in rabbit calvarial defects but gelatin capsules enhanced bone formation [170]. Similar to this, TGF- β hydrogels with very rapid or very slow degradation times had no effect on bone formation [171].

Finally, vascular endothelial growth factor not only controls vasculogenesis and angiogenesis, but is involved in recruitment and activity of bone forming cells [148]. VEGF had been shown to enhance blood vessel formation and ossification in murine femur fractures [172]. In addition, VEGFs have been shown to enhance bone formation when combined with other growth factors [148].

An alternative to growth factors is platelet rich plasma (PRP), which is centrifuged autogenous blood that contains high concentrations of cells containing various growth factors such as PDGF, TGF- β , IGF, and VEGF [164]. PRP has been considered a better alternative to the single use of growth factors due to its composition of many growth factors and its cost-effective sourcing [173]. However, there are variabilities in success due to the preparation methods, concentration, and methods of application of PRP. *In vitro*, PRP has shown to induce proliferation of bone marrow stem cells and promote osteogenic differentiation [174]. *In vivo* studies have demonstrated various outcomes, with most improving the histological appearance of bone but some reporting harmful or non-significant effects [173].

Drawbacks to using recombinant growth factors in general are their roles in tumor formation or negative immune reactions, which has been demonstrated for BMP2 and VEGF [146, 175]. As with all growth factors, the design of the delivery system can greatly affect the outcome of the surgery. This adds another element to designing a biomaterial implant. If the biomaterial includes the release of a growth factor, then further consideration on the kinetics of release needs to be tailored to the wound of interest, whether it be a short or sustained release. Interestingly, combinations of scaffolds, cells, and growth factors have been shown both positive and negative results when compared to combinations of scaffolds and cells or growth factors [5].

8.2 *Application of Growth Factors to Tissue Engineering*

In addition to printing unique structures and multiple cell types, growth factors can be combined with bioprinting. Growth factors, like cells, can be added to the printing medium in order to drive cellular responses. Hydrogels have been effectively loaded with BMP-2 and VEGF in order to induce bone regeneration. In one study, BMP-2 was loaded into collagen hydrogels for a sustained release and VEGF was loaded into alginate and gelatin hydrogels for a burst release [176]. In this example, multiple print heads were used to create a scaffold with two different growth factors located in different regions of the scaffold that released at different rates based on material properties [176]. Bioprinting offers a simple way to incorporate various growth factors in order to study their interactions with cells; however, the material that these growth factors are encapsulated in determines their release. Further research needs to be performed in order to optimize these materials, especially materials other than hydrogels, as bioprinting is an incredibly useful tool if optimized.

There exist a wide variety of growth factors available to promote bone regeneration, and more research needs to be investigated on how to adequately deliver these and control cell fate. Again, factors that can control the balance of osteoclasts and osteoblasts, the M1 to M2 macrophage transition, and angiogenesis need to be examined. Research has demonstrated that osteoprotegerin plays a critical role in inhibiting osteoclastogenesis, which could be potentially used as a growth factor in

order to maintain this balance between osteoclasts and osteoblasts [97, 98]. In addition to this, macrophage phenotype impacts the wound outcome and growth factors could be delivered in order to promote a more M1 or M2-like phenotype. Cytokines that can induce an M1 response include LPS and IFN- γ , while cytokines that can induce an M2 response include IL-4, IL-13, and IL-10 [13, 141, 177]. An interesting opportunity exists to combine these cytokines in 3D-printed scaffolds in order to drive a particular immune response depended on release rates and specific cytokines released. Finally, angiogenesis can be accomplished by introducing VEGF to scaffolds, and more research should involve examining blood vessel formation with and without this growth factor and its potential to induce vessel formation quicker in scaffolds. Overall, growth factor addition to implant materials holds promise, but more investigation must be performed on the negative outcomes of these factors, controlling delivery, and leveraging multiple growth factors in order to drive osteogenesis, wound healing, and angiogenesis.

9 Conclusions

There are many strategies to repair bones; however, no such strategy exists without its drawbacks. Autografts have the greatest potential to heal but require another surgery within the patient's body. Allografts and xenografts have shown promising results, but processing methods can destroy important components in these materials. Other scaffold types are easy to manipulate and can be patient-specific; however, their results cannot yet compare to autografts. The future of bone regeneration involves combining these various methods to heal bone in order to achieve the properties of a biomaterial implant (Fig. 3): biocompatible materials, mechanics that match the properties of bone and prevent micromotion, a pore size and orientation that guides vessel formation and cell migration, and a material that degrades and allows new bone formation to occur. 3D printing can be used to print multiple material types, unique and challenging structures, and patient-specific implants. This can be useful in combination with the various materials, cells, and growth factors discussed here, to one day create a biomaterial implant that addresses all necessary criteria. Research efforts should also focus on targeting the balance between osteoclasts and osteoblasts, macrophage phenotype transition, and angiogenesis. These can be addressed by material design, studies investigating multiple cell-type interactions, and growth factor addition. Overall, there exists a vast amount of research and development left in the area of bone repair, and many factors need to be addressed. Optimizing materials, fabrication, cell types, and growth factors included in biomaterial implants must be accomplished in order to create the optimal biomaterial for bone repair.

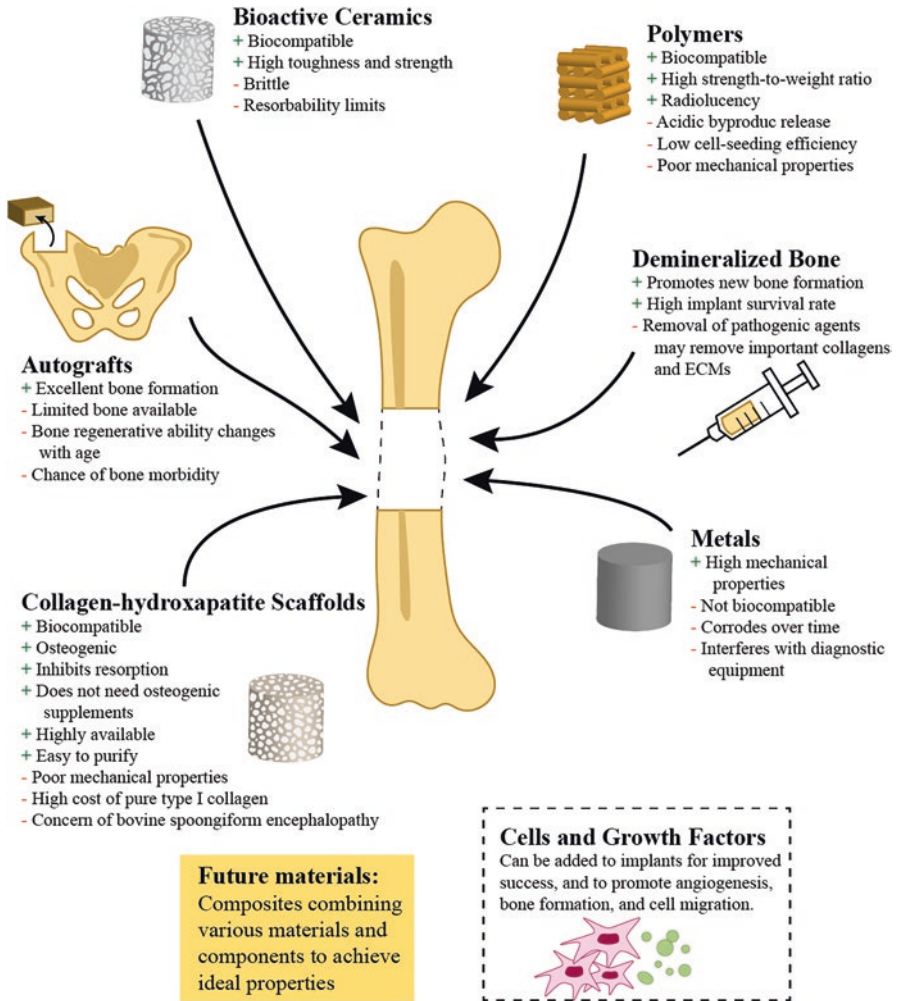


Fig. 3 Advantages and disadvantages of implant materials for bone regeneration. Future materials need to combine these advantages and supplemental materials, such as cells and growth factors, to reach optimal properties

Acknowledgements This work was supported by the Office of the Assistant Secretary of Defense for Health Affairs Broad Agency Announcement for Extramural Medical Research through the Award No. W81XWH-16-1-0566 (BACH). Opinions, interpretations, conclusions, and recommendations are those of the authors and are not necessarily endorsed by the Department of Defense. This work was also supported by the National Institute of Dental and Craniofacial Research of the National Institutes of Health under Award Number R21 DE026582 (BACH). The content is solely the responsibility of the authors and does not necessarily represent the official views of the NIH. We are grateful for the funding for this study provided by the NSF Graduate Research Fellowship DGE-1144245 (MJD). The authors would like to acknowledge Vasiliki Kolliopoulos and Andrey Nosatov for assistance with manuscript editing.

References

1. Lew T, Walker J, Wenke J, Blackburne L, Hale R. Characterization of craniomaxillofacial battle injuries sustained by United States service members in the current conflicts of Iraq and Afghanistan. *J Oral Maxillofac Surg*. 2010;68(1):3–7.
2. Fong A, Lemelman B, Lam S, Kleiber G, Reid R, Gottlieb L. Reconstructive approach to hostile cranioplasty: a review of the University of Chicago experience. *J Plast Reconstr Aesthet Surg*. 2015;68(8):1036–43.
3. Lee J, Kleiber G, Pelletier A, Reid R, Gottlieb L. Autologous immediate cranioplasty with vascularized bone in high-risk composite cranial defects. *Plast Reconstr Surg*. 2013;132(4):967–75.
4. Lee E, Chao A, Skoracki R, Yu P, DeMonte F, Hanasono M. Outcomes of calvarial reconstruction in cancer patients. *Plast Reconstr Surg*. 2014;133(3):675–82.
5. Roffi A, Krishnakumar GS, Gostynska N, Kon E, Candrian C, Filardo G. The role of three-dimensional scaffolds in treating long bone defects: evidence from preclinical and clinical literature — a systematic review. *Biomed Res Int*. 2017;2017:13.
6. Staff MC. Spinal fusion. Mayo Clinic. <https://www.mayoclinic.org/tests-procedures/spinal-fusion/about/pac-20384523>. Accessed on 23 Jan 2020
7. Trampuz A, Zimmerli W. Diagnosis and treatment of implant-associated septic arthritis and osteomyelitis. *Curr Infect Dis Rep*. 2008;10(5):394–403.
8. Rodan GA. Bone homeostasis. *PNAS*. 1998;95(23):13361–2.
9. Thompson E, Matsiko A, Farrell E, Daniel JK, O'Brien F. Recapitulating endochondral ossification: a promising route to in vivo bone regeneration. *J Tissue Eng Regen Med*. 2015;9:889–902.
10. Kruijt Spanjer EC, Bittermann GKP, van Hooijdonk IEM, Rosenberg AJWP, Gawlitza D. Taking the endochondral route to craniomaxillofacial bone regeneration: a logical approach? *J Craniomaxillofac Surg*. 2017;45(7):1099–106. <https://doi.org/10.1016/j.jcms.2017.03.025>.
11. Scott CK, Hightower JA. The matrix of endochondral bone differs from the matrix of intramembranous bone. *Calcif Tissue Int*. 1991;49(5):349–54.
12. Ribeiro M, Monteiro FJ, Ferraz MP. Infection of orthopedic implants with emphasis on bacterial adhesion process and techniques used in studying bacterial-material interactions. *Biomater*. 2012;2(4):176–94.
13. Spiller KL, Freytes DO, Vunjak-Novakovic G. Macrophages modulate engineered human tissues for enhanced vascularization and healing. *Ann Biomed Eng*. 2015;43(3):616–27.
14. Kim YK, Chen EY, Liu WF. Biomolecular strategies to modulate the macrophage response to implanted materials. *J Mater Chem B*. 2016;4(9):1600–9.
15. Gibon E, Lu LY, Nathan K, Goodman SB. Inflammation, ageing, and bone regeneration. *J Orthop Transl*. 2017;10:28–35. <https://doi.org/10.1016/j.jot.2017.04.002>.
16. Lee J, Byun H, Madhurakkat Perikamana SK, Lee S, Shin H. Current advances in immunomodulatory biomaterials for bone regeneration. *Adv Healthc Mater*. 2019;8:1–20.
17. Runyan CM, Gabrick KS. Biology of bone formation, fracture healing, and distraction osteogenesis. *J Craniofac Surg*. 2017;28(5):1380–9.
18. Elsalanty M, Genecov D. Bone grafts in craniofacial surgery. *Craniofacial Trauma Reconstr*. 2009;2(03):125–34.
19. Pogrel M, Podlesh S, Anthony J, Alexander J. A comparison of vascularized and nonvascularized bone grafts for reconstruction of mandibular continuity defects. *J Oral Maxillofac Surg*. 1997;55(11):1200–6.
20. Abuzayed B, Aydin S, Aydin S, Kucukyuruk B, Sanus G. Cranioplasty: review of materials and techniques. *J Neurosci Rural Pract*. 2011;2(2):162.
21. Depeyre A, Touzet-Roumazielle S, Lauwers L, Raoul G, Ferri J. Retrospective evaluation of 211 patients with maxillofacial reconstruction using parietal bone graft for implants insertion. *J Craniomaxillofac Surg*. 2016;44(9):1162–9. <https://doi.org/10.1016/j.jcms.2016.06.034>.

22. Ghanaati S, Barbeck M, Booms P, Lorenz J, Kirkpatrick CJ, Sader RA. Potential lack of “standardized” processing techniques for production of allogeneic and xenogeneic bone blocks for application in humans. *Acta Biomater.* 2014;10(8):3557–62. <https://doi.org/10.1016/j.actbio.2014.04.017>.
23. Bae H, Zhao L, Kanim L, Wong P, Delamarter R, Dawson E. Intervariability and intravariability of bone morphogenetic proteins in commercially available demineralized bone matrix products. *Spine (Phila Pa 1976).* 2006;31(12):1299–306.
24. Nelson K, Fretwurst T, Stricker A, Steinberg T, Wein M, Spanou A. Comparison of four different allogeneic bone grafts for alveolar ridge reconstruction: a preliminary histologic and biochemical analysis. *Oral Surg Oral Med Oral Pathol Oral Radiol.* 2014;118(4):424–31. <https://doi.org/10.1016/j.oooo.2014.05.020>.
25. Athanasiou V, Papachristou D, Panagopoulos A, Saridis A, Scopa C, Megas P. Histological comparison of autograft, allograft-DBM, xenograft, and synthetic grafts in a trabecular bone defect: an experimental study in rabbits. *Med Sci Monit.* 2010;16(1):BR24–31.
26. Hartl A, Bitzan P, Wanivenhaus A, Kotz R. Faster integration of human allograft bone than of the bovine substitute Lubbock: non-randomized evaluation of 20 cases with benign tumors or tumor-like conditions. *Acta Orthop Scand.* 2004;75(2):217–20.
27. Bose S, Roy M, Bandyopadhyay A. Recent advances in bone tissue engineering scaffolds. *Trends Biotechnol.* 2012;30(10):546–54.
28. Dimitriou R, Babis GC. Biomaterial osseointegration enhancement with biophysical stimulation. *J Musculoskelet Neuronal Interact.* 2007;7(3):253–65.
29. Dewey MJ, Johnson EM, Weisgerber DW, Wheeler MB, Harley BAC. Shape-fitting collagen-PLA composite promotes osteogenic differentiation of porcine adipose stem cells. *J Mech Behav Biomed Mater.* 2019;95:21.
30. Murphy CM, Haugh MG, O’Brien FJ. The effect of mean pore size on cell attachment, proliferation and migration in collagen-glycosaminoglycan scaffolds for bone tissue engineering. *Biomaterials.* 2010;31(3):461–6. <https://doi.org/10.1016/j.biomaterials.2009.09.063>.
31. Sussman EM, Halpin MC, Muster J, Moon RT, Ratner BD. Porous implants modulate healing and induce shifts in local macrophage polarization in the foreign body reaction. *Ann Biomed Eng.* 2014;42(7):1508–16.
32. Ratner BD. A pore way to heal and regenerate : 21st century thinking on biocompatibility. *Regen Biomater.* 2016;3:107–10.
33. Madden LR, Mortisen DJ, Sussman EM, Dupras SK, Fugate JA, Cuy JL. Proangiogenic scaffolds as functional templates for cardiac tissue engineering. *PNAS.* 2010;107(34):15211–6.
34. Seong Y, Kang I, Song E, Kim H, Jeong S. Calcium phosphate – collagen scaffold with aligned pore channels for enhanced osteochondral regeneration. *Adv Healthc Mater.* 2017;6:1–11.
35. Bobbert FSL, Zadpoor AA. Effects of bone substitute architecture and surface properties on cell response, angiogenesis, and structure of new bone. *J Mater Chem B.* 2017;5(31):6175–92.
36. Lin W, Lan W, Wu Y, Zhao D, Wang Y, He X, et al. Aligned 3D porous polyurethane scaffolds for biological anisotropic tissue regeneration. *Regen Biomater.* 2019;7:19–27.
37. Marcacci M, Kon E, Moukhachev V, Lavroukov A, Kutepov S, Quarto R, et al. Stem cells associated with macroporous bioceramics for long bone repair: 6- to 7-year outcome of a pilot clinical study. *Tissue Eng.* 2007;13(5):947.
38. Sheikh Z, Sima C, Glogauer M. Bone replacement materials and techniques used for achieving vertical alveolar bone augmentation. *Materials (Basel).* 2015;8:2953–93.
39. Weisgerber DW, Milner DJ, Lopez-Lake H, Rubessa M, Lotti S, Polkoff K, et al. A mineralized collagen-polycaprolactone composite promotes healing of a porcine mandibular defect. *Tissue Eng Part A.* 2017;24(11–12):943–54.
40. Sheikh Z, Najeeb S, Glogauer M. Biodegradable materials for bone repair and tissue engineering applications. *Materials (Basel).* 2015;8(9):5744–94.
41. Huttmacher D, Hurzeler MB, Schliephake H. A review of material properties of biodegradable and bioresorbable polymers and devices for GTR and GBR applications. *Int J Oral Maxillofac Implants.* 1996;11:667–78.

42. Chanlalit C, Shukla DR, Fitzsimmons JS, An KN, O'Driscoll SW. Stress shielding around radial head prostheses. *J Hand Surg [Am]*. 2012;37:2118–25.
43. Dau M, Kämmerer PW, Henkel KO, Gerber T, Frerich B, Gundlach KKH. Bone formation in mono cortical mandibular critical size defects after augmentation with two synthetic nano-structured and one xenogenous hydroxyapatite bone substitute - in vivo animal study. *Clin Oral Implants Res*. 2016;27(5):597–603.
44. Buser Z, Brodke D, Youssef J, Meisel H, Myhre S, Hashimoto R, et al. Synthetic bone graft versus autograft or allograft for spinal fusion: a systematic review. *J Neurosurg Spine*. 2016;25(4):509–16.
45. Tatara AM, Koons GL, Watson E, Piepergerdes TC, Shah SR. Biomaterials-aided mandibular reconstruction using in vivo bioreactors. *PNAS*. 2019;116(14):6954–63.
46. Brogginini N, Bosshardt DD, Jensen SS, Bornstein MM, Wang C, Buser D. Bone healing around nanocrystalline hydroxyapatite, deproteinized bovine bone mineral, biphasic calcium phosphate, and autogenous bone in mandibular bone defects. *J Biomed Mater Res B Appl Biomater*. 2015;103:1478–87.
47. Wang W, Yeung KWK. Bone grafts and biomaterials substitutes for bone defect repair: a review. *Bioact Mater*. 2017;2(4):224–47.
48. Ghassemi T, Shahroodi A, Moradi A. Current concepts in scaffolding for bone tissue engineering. *Arch Bone Jt Surg*. 2018;6(2):90–9.
49. Peterson B, Whang P, Iglesias R, Wang J, Lieberman J. Osteoinductivity of commercially available demineralized bone matrix. *J Bone Jt Surg*. 2004;86(10):2243–50.
50. Acarturk T, Hollinger J. Commercially available demineralized bone matrix compositions to regenerate calvarial critical-sized bone defects. *Plast Reconstr Surg*. 2006;118(4):862–73.
51. Oryan A, Alidadi S, Moshiri A, Maffulli N. Bone regenerative medicine: classic options, novel strategies, and future directions. *J Orthop Surg Res*. 2014;9:18.
52. Goa T-J, Tuominen TK, Lindholm TS, Kommonen B, Lindholm TC. Morphological and biomechanical difference in healing in segmental tibial defects implanted with Biocoral(R) or tricalcium phosphate cylinders. *Biomaterials*. 1997;18:219–23.
53. Galli C, Guizzardi S, Passeri G, Martini D, Tinti A, Mauro G, et al. Comparison of human mandibular osteoblasts grown on two commercially available titanium implant surfaces. *J Periodontol*. 2005;76(3):364–72.
54. Gredes T, Kubasiewicz-Ross P, Gedrange T, Dominiak M, Kunert-Keil C. Comparison of surface modified zirconia implants with commercially available zirconium and titanium implants: a histological study in pigs. *Implant Dent*. 2014;23(4):502–7.
55. Bansiddhi A, Sargeant T, Stupp S, Dunand D. Porous NiTi for bone implants: a review. *Acta Biomater*. 2008;4(4):773–82.
56. Bai X, Gao M, Syed S, Zhuang J, Xu X, Zhang X-Q. Bioactive hydrogels for bone regeneration. *Bioact Mater*. 2018;3(4):401–17.
57. Sanchez-Sotelo J, Munuera L, Madero R. Treatment of fractures of the distal radius with a remodelable bone cement. *J Bone Jt Surg*. 2000;82:856–63.
58. Lidfors N, Heikkila J, Koski I, Mattila K, Aho A. Bioactive glass and autogenous bone as bone graft substitutes in benign bone tumors. *J Biomed Mater Res B*. 2008;90B(1):131–6.
59. Crovace M, Souza M, Chinaglia C, Peitl O, Zanutto E. Biosilicate® — a multipurpose, highly bioactive glass-ceramic. In vitro, in vivo and clinical trials. *J Non-Cryst Solids*. 2016;432:90–110.
60. Leupold J, Barfield W, Han Y, Hartsock L. A comparison of ProOsteon, DBX, and collagraft in a rabbit model. *J Biomed Mater Res B*. 2006;79B(2):292–7.
61. Boyd D, Towler M, Wren A, Clarkin O. Comparison of an experimental bone cement with surgical Simplex® P, Spineplex® and Cortoss®. *J Mater Sci Mater Med*. 2008;19:1745–52.
62. Nee D, Noyes D, Shaw M, Gwilym S, Fairlie N, Birch N. Healos and bone marrow aspirate used for lumbar spine fusion: a case controlled study comparing healos with autograft. *Spine (Phila Pa 1976)*. 2006;31(18):E636–40.

63. Liu X, Ma P. Polymeric scaffolds for bone tissue engineering. *Ann Biomed Eng.* 2004;32(3):477–86.
64. Gupte MJ, Ma PX. Nanofibrous scaffolds for dental and craniofacial applications. *J Dent Res.* 2012;91(3):227–34.
65. Qu F, Holloway J, Esterhai J, Burdick J, Mauck R. Programmed biomolecule delivery to enable and direct cell migration for connective tissue repair. *Nat Commun.* 2017;8:1780.
66. Baker B, Shah R, Silverstein A, Esterhai J, Burdick J, Mauck R. Sacrificial nanofibrous composites provide instruction without impediment and enable functional tissue formation. *PNAS.* 2012;109(35):14176–81.
67. Abuzayed B, Tuzgen S, Canbaz B, Yuksel O, Tutunculer B, Sanus G. Reconstruction of growing skull fracture with in situ galeal graft duraplasty and porous polyethylene sheet. *J Craniofac Surg.* 2009;20(4):1245–9.
68. Abuzayed B, Dashti R, Turk O, Kaynar M. Aneurysmal frontal bone cyst in a child with history of acute lymphoblastic leukemia: a case of rare location and history. *J Pediatr Hematol Oncol.* 2010;32(1):e1–3.
69. Kucukyuruk B, Biceroglu H, Abuzayed B, Ulu M, Sanus G. Intraosseous meningioma: a rare tumor reconstructed with porous polyethylene. *J Craniofac Surg.* 2010;21(3):936–9.
70. Brockmeyer P, Kramer K, Krohn S, Kauffmann P, Mauth C, Dard M, et al. Influence of synthetic polyethylene glycol hydrogels on new bone formation during mandibular augmentation procedures in Goettingen minipigs. *J Mater Sci Mater Med.* 2015;26(6):1–7.
71. Gregor A, Filová E, Novák M, Kronek J, Chlup H, Buzgo M, et al. Designing of PLA scaffolds for bone tissue replacement fabricated by ordinary commercial 3D printer. *J Biol Eng.* 2017;11(1):1–21.
72. Zhang H, Mao X, Zhao D, Jiang W, Du Z, Li Q, et al. Three dimensional printed polylactic acid-hydroxyapatite composite scaffolds for prefabricating vascularized tissue engineered bone: an in vivo bioreactor model. *Sci Rep.* 2017;7:15255.
73. Park SA, Lee H-J, Park S-Y. In vivo evaluation of 3D-printed polycaprolactone scaffold implantation combined with β -TCP powder for alveolar bone augmentation in a beagle defect model. *Materials (Basel).* 2018;11(2):238.
74. Weisgerber DW, Milner DJ, Lopez-Lake H, Rubessa M, Lotti S, Polkoff K, et al. A mineralized collagen-polycaprolactone composite promotes healing of a porcine mandibular ramus defect. *Tissue Eng Part A.* 2017;24(11–12):943–54.
75. Gredes T, Kunath F, Gedrange T, Kunert-Keil C. Bone regeneration after treatment with covering materials composed of flax fibers and biodegradable plastics: a histological study in rats. *Biomed Res Int.* 2016;2016:1–8.
76. Athanasiou K, Niederauer G, Agrawal CM. Sterilization, toxicity, biocompatibility and clinical applications of polylactic acid/polyglycolic acid copolymers. *Biomaterials.* 1996;17(2):93–102.
77. Athanasiou K, Agrawal C, Barber F, Burkhart S. Orthopaedic applications for PLA-PGA biodegradable polymers. *Arthrosc J Arthrosc Relat Surg.* 1998;14(7):726–37.
78. Kroeze RJ, Helder MN, Smit TH. Biodegradable polymers in bone tissue engineering. *Materials (Basel).* 2009;2(3):833–56.
79. Mai R, Hagedorn MG, Gelinsky M, Werner C, Turhani D, Spath H, et al. Ectopic bone formation in nude rats using human osteoblasts seeded poly(3)hydroxybutyrate embroidery and hydroxyapatite-collagen tapes constructs. *J Craniomaxillofac Surg.* 2006;34(2):101–9.
80. Harley BA, Leung JH, Silva ECCM, Gibson LJ. Mechanical characterization of collagen-glycosaminoglycan scaffolds. *Acta Biomater.* 2007;3(4):463–74.
81. O'Brien FJ, Harley BA, Yannas IV, Gibson LJ. The effect of pore size on cell adhesion in collagen-GAG scaffolds. *Biomaterials.* 2005;26(4):433–41.
82. Florent D, Levingstone T, Schneeweiss W, de Swartw M, Jahns H, Gleeson J, et al. Enhanced bone healing using collagen-hydroxyapatite scaffold implantation in the treatment of a large multiloculated mandibular aneurysmal bone cyst in a thoroughbred filly. *J Tissue Eng Regen Med.* 2015;9:1193–9.

83. Cunniffe G, Dickson G, Partap S, Stanton K, O'Brien FJ. Development and characterisation of a collagen nano-hydroxyapatite composite scaffold for bone tissue engineering. *J Mater Sci Mater Med.* 2010;21:2293–8.
84. Al-Munajjed A, Gleeson J, O'Brien F. Development of a collagen calcium-phosphate scaffold as a novel bone graft substitute. *Stud Heal Technol Inf.* 2008;133:11–20.
85. Ren X, Bischoff D, Weisgerber DW, Lewis MS, Tu V, Yamaguchi DT, et al. Osteogenesis on nanoparticulate mineralized collagen scaffolds via autogenous activation of the canonical BMP receptor signaling pathway. *Biomaterials.* 2015;50:107–14.
86. Caliarì SR, Harley BAC. Structural and biochemical modification of a collagen scaffold to selectively enhance MSC tenogenic, chondrogenic, and osteogenic differentiation. *Adv Healthc Mater.* 2014;3:1086–96.
87. Caliarì SR, Harley BAC. Composite growth factor supplementation strategies to enhance tenocyte bioactivity in aligned collagen-GAG scaffolds. *Tissue Eng Part A.* 2012;19(9–10):1100–12.
88. Kanungo BP, Gibson LJ. Density-property relationships in collagen-glycosaminoglycan scaffolds. *Acta Biomater.* 2010;6(2):344–53. <https://doi.org/10.1016/j.actbio.2009.09.012>.
89. O'Brien FJ, Harley BA, Yannas IV, Gibson L. Influence of freezing rate on pore structure in freeze-dried collagen-GAG scaffolds. *Biomaterials.* 2004;25(6):1077–86.
90. Murphy CM, O'Brien FJ. Understanding the effect of mean pore size on cell activity in collagen-glycosaminoglycan scaffolds. *Cell Adhes Migr.* 2010;4(3):377–81.
91. Weisgerber DW, Caliarì SR, Harley BAC. Mineralized collagen scaffolds induce hMSC osteogenesis and matrix remodeling. *Biomater Sci.* 2015;3(3):533–42.
92. Yamaguchi DT, Lee JC, Tu V, Ren X, Harley BAC, Weisgerber DW, et al. Osteogenesis on nanoparticulate mineralized collagen scaffolds via autogenous activation of the canonical BMP receptor signaling pathway. *Biomaterials.* 2015;50:107–14. <https://doi.org/10.1016/j.biomaterials.2015.01.059>.
93. Kanungo BP, Silva E, Van Vliet K, Gibson LJ. Characterization of mineralized collagen-glycosaminoglycan scaffolds for bone regeneration. *Acta Biomater.* 2008;4(3):490–503.
94. Harley BA, Lynn AK, Wissner-Gross Z, Bonfield W, Yannas IV, Gibson LJ. Design of a multiphase osteochondral scaffold. II. Fabrication of a mineralized collagen-glycosaminoglycan scaffold. *J Biomed Mater Res A.* 2010;92(3):1066–77.
95. Lyons FG, Gleeson JP, Partap S, Coghlan K, O'Brien FJ. Novel microhydroxyapatite particles in a collagen scaffold: a bioactive bone void filler? *Clin Orthop Relat Res.* 2014;472(4):1318–28.
96. Ren X, Tu V, Bischoff D, Weisgerber DW, Lewis MS, Yamaguchi DT, et al. Nanoparticulate mineralized collagen scaffolds induce in vivo bone regeneration independent of progenitor cell loading or exogenous growth factor stimulation. *Biomaterials.* 2016;89:67–78.
97. Ren X, Dewey MJ, Bischoff D, Miller TA, Yamaguchi DT, Harley BAC, et al. Nanoparticulate mineralized collagen glycosaminoglycan materials directly and indirectly inhibit osteoclastogenesis and osteoclast activation. *J Tissue Eng Regen Med.* 2019;13:823–34.
98. Ren X, Zhou Q, Foulad D, Tiffany AS, Dewey MJ, Bischoff D, et al. Osteoprotegerin reduces osteoclast resorption activity without affecting osteogenesis on nanoparticulate mineralized collagen scaffolds. *Sci Adv.* 2019;5:1–12.
99. Dewey MJ, Weisgerber DW, Johnson E, Wheeler MB, Harley BAC. Shape-fitting collagen-PLA composite promotes osteogenic differentiation of porcine adipose stem cells. *J Mech Behav Biomed Mater.* 2019;95:21.
100. Weisgerber DW, Erning K, Flanagan CL, Hollister SJ, Harley BAC. Evaluation of multi-scale mineralized collagen-polycaprolactone composites for bone tissue engineering. *J Mech Behav Biomed Mater.* 2016;61:318–27. <https://doi.org/10.1016/j.jmbbm.2016.03.032>.
101. Hortensius RA, Ebens JH, Dewey MJ, Harley BAC. Incorporation of the amniotic membrane as an immunomodulatory design element in collagen scaffolds for tendon repair. *ACS Biomater Sci Eng.* 2018;4(12):4367–77.

102. Hortensius RA, Ebens JH, Harley BAC. Immunomodulatory effects of amniotic membrane matrix incorporated into collagen scaffolds. *J Biomed Mater Res A*. 2016;104(6):1332–42.
103. Tiffany AS, Gray DL, Woods TJ, Subedi K, Harley BAC. The inclusion of zinc into mineralized collagen scaffolds for craniofacial bone repair applications. *Acta Biomater*. 2019;93:86–96. <https://doi.org/10.1016/j.actbio.2019.05.031>.
104. Dewey M, Johnson E, Slater S, Milner D, Wheeler M, Harley B. Mineralized collagen scaffolds fabricated with amniotic membrane matrix increase osteogenesis under inflammatory conditions. *Regen Biomater*. 2020;7:247.
105. Dewey M, Nosatov A, Subedi K, Harley B. Anisotropic mineralized collagen scaffolds accelerate osteogenic response in a glycosaminoglycan-dependent fashion. *RSC Adv*. 2020;10:15629.
106. Offeddu GS, Ashworth JC, Cameron RE, Oyen ML. Multi-scale mechanical response of freeze-dried collagen scaffolds for tissue engineering applications. *J Mech Behav Biomed Mater*. 2015;42:19–25.
107. Klaumünzer A, Leemhuis H, Schmidt-Bleek K, Schreivogel S, Woloszyk A, Korus G, et al. A biomaterial with a channel-like pore architecture induces endochondral healing of bone defects. *Nat Commun*. 2018;9(1):4430. <https://doi.org/10.1038/s41467-018-06504-7>.
108. Radzi S, Cowin G, Schmutz B. Metal artifacts from titanium and steel screws in CT, 1.5T and 3T MR images of the tibial Pilon: a quantitative assessment in 3D. *Quant Imag Med Surg*. 2014;4(3):163–72.
109. Terjesen T, Nordby A, Arnulf V. Bone atrophy after plate fixation: compute tomography of femoral shaft fractures. *Acta Orthop Scand*. 1985;56(5):416–8.
110. Alvarez K, Nakajima H. Metallic scaffolds for bone regeneration. *Materials (Basel)*. 2009;2(3):790–832.
111. Moghaddam NS, Andani MT, Amerinatanzi A, Haberland C, Huff S, Miller M, et al. Metals for bone implants: safety, design, and efficacy. *Biomanufact Rev*. 2016;1:1.
112. Assad M, Jarzem P, Leroux M, Coillard C, Chernyshov AV, Charette S, et al. Porous titanium-nickel for intervertebral fusion in a sheep model: Part 1. Histomorphometric and radiological analysis. *J Biomed Mater Res Part B Appl Biomater*. 2003;64B(2):107.
113. Bohner M. Physical and chemical aspects of calcium phosphates used in spinal surgery. *Eur Spine J*. 2001;10:S114–21.
114. Durgalakshmi D, Subhathirai S, Balakumar S. Nano-bioglass: a versatile antidote for bone tissue engineering problems. *Proc Eng*. 2014;92:2–8.
115. Scaglione S, Quarto R, Giannoni P. Stem cells and tissue scaffolds for bone repair. In: *Cellular response to biomaterials*. Cambridge: Woodhead Publishing Limited; 2008. p. 291–312. <https://doi.org/10.1016/B978-1-84569-358-9.50012-0>.
116. Werber K, Brauer R, Weiss W, Becker K. Osseous integration of bovine hydroxyapatite ceramic in metaphyseal bone defects of the distal radius. *J Hand Surg [Am]*. 2000;25(5):833–41.
117. Arai E, Nakashima H, Tsukushi S, Shido Y, Nishida Y, Yamada Y, et al. Regenerating the fibula with beta-tricalcium phosphate minimizes morbidity after fibula resection. *Clin Orthop Relat Res*. 2005;431:233–7.
118. Devendran S, Namashivayam S, Ambigapathi M, Nagarajan S, Tsai W-B, Sethu SN, et al. Nanoceramics on osteoblast proliferation and differentiation in bone tissue engineering. *Int J Biol Macromol*. 2017;98:67–74. <https://doi.org/10.1016/j.ijbiomac.2017.01.089>.
119. Roualdes O, Duclos M-E, Gutknecht D, Frappart L, Chevalier J, Hartmann D. In vitro and in vivo evaluation of an alumina–zirconia composite for arthroplasty applications. *Biomaterials*. 2010;31(8):2043–54.
120. Canzi P, Marconi S, Benazzo M. From CT scanning to 3D printing technology: a new method for the preoperative planning of a transcutaneous bone-conduction hearing device. *Acta Otorhinolaryngol Ital*. 2018;38(3):251–6.
121. Haleem A, Javaid M. Role of CT and MRI in the design and development of orthopaedic model using additive manufacturing. *J Clin Orthop Trauma*. 2018;9(3):213–7.

122. Brunello G, Sivoletta S, Meneghello R, Ferroni L, Gardin C, Piattelli A, et al. Powder-based 3D printing for bone tissue engineering. *Biotechnol Adv.* 2016;34(5):740–53.
123. Bose S, Vahabzadeh S, Bandyopadhyay A. Bone tissue engineering using 3D printing. *Mater Today.* 2013;16(12):496–504.
124. Trombetta R, Inzana J, Schwarz E, Kates S, Awad H. 3D printing of calcium phosphate ceramics for bone tissue engineering and drug delivery. *Ann Biomed Eng.* 2017;45(1):23–44.
125. Maleksaeedi S, Wang JK, El-Hajje A, Harb L, Guneta V, He Z, et al. Toward 3D printed bioactive titanium scaffolds with bimodal pore size distribution for bone ingrowth. *Proc CIRP.* 2013;5:1558–163.
126. Scarano A, Crincoli V, Di Benedetto A, Cozzolino V, Lorusso F, Podaliri Vulpiani M, et al. Bone regeneration induced by bone porcine block with bone marrow stromal stem cells in a minipig model of mandibular “critical size” defect. *Stem Cells Int.* 2017;2017:9082869.
127. Walmsley GG, Ransom RC, Wan DC. Stem cells in bone regeneration. *Stem Cell Rev.* 2016;12(5):524–9.
128. Wilson SM, Goldwasser MS, Clark SG, Monaco E, Bionaz M, Hurley WL, et al. Adipose-derived mesenchymal stem cells enhance healing of mandibular defects in the ramus of swine. *J Oral Maxillofac Surg.* 2012;70(3):e193–203. <https://doi.org/10.1016/j.joms.2011.10.029>.
129. Ho S, Murphy K, Leach K. Increased survival and function of mesenchymal stem cell spheroids entrapped in instructive alginate hydrogels. *Stem Cells Transl Med.* 2016;5(6):773–81.
130. Ho S, Keown A, Leach K. Cell migration and bone formation from mesenchymal stem cell spheroids in alginate hydrogels are regulated by adhesive ligand density. *Biomacromolecules.* 2017;18(12):4331–40.
131. DiGirolamo C, Stokes D, Colter D, Phinney D, Class R, Prockop D. Propagation and senescence of human marrow stromal cells in culture: a simple colony-forming assay identifies samples with the greatest potential to propagate and differentiate. *Br J Haematol.* 2001;107(2):275–81.
132. Im GI, Shin YW, Lee KB. Do adipose tissue-derived mesenchymal stem cells have the same osteogenic and chondrogenic potential as bone marrow-derived cells? *Osteoarthr Cartil.* 2005;13:845–53.
133. Luby A, Ranganathan K, Lynn J, Nelson N, Donneys A, Buchman S. Stem cells for bone regeneration: current state and future directions. *J Craniofac Surg.* 2019;30(3):730–5.
134. Follmar K, Prichard H, DeCroos F, Wang H, Levin L, Klitzman B, et al. Combined bone allograft and adipose-derived stem cell autograft in a rabbit model. *Ann Plast Surg.* 2007;58(5):561–5.
135. Kubo M, Sonoda Y, Muramatsu R, Usui M. Immunogenicity of human amniotic membrane in experimental xenotransplantation. *Invest Ophthalmol Vis Sci.* 2001;42:1539–46.
136. Hutson E, Boyer S, Genever P. Rapid isolation, expansion, and differentiation of osteoprogenitors from full-term umbilical cord blood. *Tissue Eng.* 2005;11(9–10):1407.
137. Ventola CL. Medical applications for 3D printing: current and projected uses. *Pharm Ther.* 2014;39(10):704–11.
138. Graney PL, Zreiqat H, Spiller KL, Spiller KL. In vitro response of macrophages to ceramic scaffolds used for bone regeneration. *J R Soc Interface.* 2016;13:20160346.
139. Witherel CE, Yu T, Concannon M, Dampier W, Spiller K. Immunomodulatory effects of human cryopreserved viable amniotic membrane in a pro-inflammatory environment in vitro. *Cell Mol Bioeng.* 2017;10:451.
140. Weingarten MS, Witherel CE, Spiller KL, Graney PL, Freytes DO. Response of human macrophages to wound matrices in vitro. *Wound Repair Regen.* 2016;24(3):514–24.
141. Spiller KL, Anfang RR, Spiller KJ, Ng J, Nakazawa KR, Daulton JW, et al. The role of macrophage phenotype in vascularization of tissue engineering scaffolds. *Biomaterials.* 2014;35(15):4477–88. <https://doi.org/10.1016/j.biomaterials.2014.02.012>.
142. Go YY, Kim SE, Cho GJ, Chae S, Song J. Differential effects of amnion and chorion membrane extracts on osteoblast-like cells due to the different growth factor composition of the extracts. *PLoS One.* 2017;12(8):1–20.

143. Go YY, Kim SE, Cho GJ, Chae S-W, Song J-J. Promotion of osteogenic differentiation by amnion/chorion membrane extracts. *J Appl Biomater Funct Mater*. 2016;14(2):e171–80.
144. Carano R, Filvaroff E. Angiogenesis and bone repair. *Drug Discov Today*. 2003;8(21):980–9.
145. Ngo M, Harley B. The influence of hyaluronic acid and glioblastoma cell coculture on the formation of endothelial cell networks in gelatin hydrogels. *Adv Healthc Mater*. 2017;6(22)
146. Devescovi V, Leonardi E, Ciapetti G, Cenni E. Growth factors in bone repair. *Chir Organi Mov*. 2008;92:161–8.
147. Laflamme C, Curt S, Rouabhia M. Epidermal growth factor and bone morphogenetic proteins upregulate osteoblast proliferation and osteoblastic markers and inhibit bone nodule formation. *Arch Oral Biol*. 2010;55(9):689–701.
148. Yun Y-R, Jang JH, Jeon E, Kang W, Lee S, Won J-E, et al. Administration of growth factors for bone regeneration. *Regen Med*. 2012;7(3):369.
149. Hossain M, Irwin R, Baumann M, McCabe L. Hepatocyte growth factor (HGF) adsorption kinetics and enhancement of osteoblast differentiation on hydroxyapatite surfaces. *Biomaterials*. 2005;26(15):2595–602.
150. Kawasaki T, Niki Y, Miyamoto T, Horiuchi K, Matsumoto M, Aizawa M, et al. The effect of timing in the administration of hepatocyte growth factor to modulate BMP-2-induced osteoblast differentiation. *Biomaterials*. 2010;31(6):1191–8.
151. Deng M, Zhang B, Wang K, Liu F, Xiao H, Zhao J, et al. Mechano growth factor E peptide promotes osteoblasts proliferation and bone-defect healing in rabbits. *Int Orthop*. 2011;35(7):1099–106.
152. Dai Z, Wu F, Yeung E, Li Y. IGF-IEc expression, regulation and biological function in different tissues. *Growth Hormon IGF Res*. 2010;20(4):275–81.
153. Young CS, Bradica G, Hollinger JO. Preclinical toxicology studies of recombinant human platelet-derived growth factor-bb either alone or in combination with beta-tricalcium phosphate and type I collagen. *J Tissue Eng*. 2011;2010:246215.
154. Chang P-C, Seol Y-J, Cirelli J, Pellegrini G, Jin Q, Franco L, et al. PDGF-B gene therapy accelerates bone engineering and oral implant osseointegration. *Gene Ther*. 2010;17:95–104.
155. Andrew J, Hoyland J, Andrew S, Freemont A, Marsh D. Demonstration of TGF- β 1 mRNA by in situ hybridization in normal human fracture healing. *Calcif Tissue Int*. 1993;52(2):74–8.
156. Bourque W, Gross M, Hall B. Expression of four growth factors during fracture repair. *Int J Dev Biol*. 1993;37(4):573–9.
157. Cheng H, Jiang W, Phillips F, Haydon R, Peng Y, Zhou L, et al. Osteogenic activity of the fourteen types of human bone morphogenetic proteins (BMPs). *J Bone Jt Surg Am*. 2003;85(8):1544–52.
158. Krishnakumar GS, Roffi A, Reale D, Kon E, Filardo G. Clinical application of bone morphogenetic proteins for bone healing: a systematic review. *Int Orthop*. 2017;41(6):1073–83.
159. Chen W-J, Jingushi S, Aoyama I, Anzai J, Hirata G, Tamura M, et al. Effects of FGF-2 on metaphyseal fracture repair in rabbit tibiae. *J Bone Miner Metab*. 2004;22(4):303–9.
160. Draenert G, Draenert K, Tischer T. Dose-dependent osteoinductive effects of bFGF in rabbits. *Growth Factors*. 2009;27(6):419–24.
161. Mitlak B, Finkelman R, Hill E, Li J, Martin B, Smith T, et al. The effect of systemically administered PDGF-BB on the rodent skeleton. *J Bone Miner Res*. 1996;11(2):238.
162. Marden L, Ran R, Pierce G, Reddi A, Hollinger J. Platelet-derived growth factor inhibits bone regeneration induced by osteogenin, a bone morphogenetic protein, in rat craniotomy defects. *J Clin Inven*. 1993;92(6):2897–905.
163. Chung C, Kim D, Park Y, Nam K, Lee S. Biological effects of drug-loaded biodegradable membranes for guided bone regeneration. *J Periodont Res*. 1997;32:172–5.
164. Schliephake H. Bone growth factors in maxillofacial skeletal reconstruction. *Int J Oral Maxillofac Surg*. 2002;31:469–84.
165. Canalis E. Growth factor control of bone mass. *J Cell Biochem*. 2009;108:769–77.
166. Specer E, Liu C, Si E, Howard G. In vivo actions of insulin-like growth factor-I (IGF-I) on bone formation and resorption in rats. *Bone*. 1991;12:21–6.

167. Akeno N, Robins J, Zhang M, Czyzyk-Krzeska M, Clemens T. Induction of vascular endothelial growth factor by IGF-I in osteoblast-like cells is mediated by the PI3K signaling pathway through the hypoxia-inducible factor-2alpha. *Endocrinology*. 2002;143(2):420–5.
168. Meinel L, Zoidis E, Zapf J, Hassa P, Hottiger M, Auer J, et al. Localized insulin-like growth factor I delivery to enhance new bone formation. *Bone*. 2003;33(4):660–72.
169. Hayrapetyan A, Jansen JA, van den Beucken JJJP. Signaling pathways involved in osteogenesis and their application for bone regenerative medicine. *Tissue Eng Part B Rev*. 2014;21(1):75–87.
170. Hong L, Tabata Y, Miyamoto S, Yamada K, Aoyama I, Tamura M, et al. Promoted bone healing at a rabbit skull gap between autologous bone fragment and the surrounding intact bone with biodegradable microspheres containing transforming growth factor- β 1. *Tissue Eng*. 2004;6(4):331.
171. Yamamoto M, Tabata Y, Hong L, Miyamoto S, Hashimoto N, Ikada Y. Bone regeneration by transforming growth factor β 1 released from a biodegradable hydrogel. *J Control Release*. 2000;64(1–3):133–42.
172. Street J, Bao M, DeGuzman L, Bunting S, Peale FJ, Ferrara N, et al. Vascular endothelial growth factor stimulates bone repair by promoting angiogenesis and bone turnover. *Proc Natl Acad Sci U S A*. 2002;99(15):9656–61.
173. Oryan A, Alidadi S, Moshiri A. Platelet-rich plasma for bone healing and regeneration. *Expert Opin Biol Ther*. 2016;16:213.
174. Zou J, Yuan C, Chunshen W, Cao C, Yang H. The effects of platelet-rich plasma on the osteogenic induction of bone marrow mesenchymal stem cells. *Connect Tissue Res*. 2014;55(4):304.
175. Raida M, Heymann A, Gunther C, Niederwieser D. Role of bone morphogenetic protein 2 in the crosstalk between endothelial progenitor cells and mesenchymal stem cells. *Int J Mol Med*. 2006;18:735–9.
176. Park JY, Shim JH, Choi S-A, Jang J, Kim M, Lee SH, et al. 3D printing technology to control BMP-2 and VEGF delivery spatially and temporally to promote large-volume bone regeneration. *J Mater Chem B*. 2015;2:5415–25.
177. Spiller KL, Nassiri S, Witherel CE, Anfang RR, Ng J, Nakazawa KR, et al. Sequential delivery of immunomodulatory cytokines to facilitate the M1-to-M2 transition of macrophages and enhance vascularization of bone scaffolds. *Biomaterials*. 2015;37:194–207.

Additive Manufacturing Technologies for Bone Tissue Engineering



Joshua Copus, Sang Jin Lee, James J. Yoo, and Anthony Atala

1 Introduction

Additive manufacturing (AM) is the process of joining materials together in order to form a three-dimensional (3D) object typically in a layer-by-layer fashion. There are a variety of different approaches, from vat photopolymerization to material extrusion, but all involve the use of 3D modeling software to create a computer-aided design (CAD). AM technologies have been improved upon since their invention in the early 1980s to become compatible with all types of materials from plastics, metals, ceramics, and even cell-laden hydrogels for the formation of human tissues and organs [1]. In the early 1980s, Charles Hull was able to successfully produce the first 3D printed part by utilizing a process which he coined “stereolithography.” Using his stereolithography apparatus (SLA), he was able to cure a vat of photo-crosslinkable polymer resin with an ultraviolet (UV) light beam. By using a computer-generated code, he could direct the light beam to create the computer-designed structure. The code generated to do this was called an STL file, which is short for stereolithography, which specified the geometry, dimensions, and thickness of the desired object [1]. The first 3D printed objects were typically used to create rapid prototypes for various commercial purposes, and it was not until the early 2000s that the technology was applied to the medical field in order to create dental implants and prosthetic devices [1].

Researchers have utilized these AM technologies to develop orthopedics implants that closely mimic the native structures of a patient. Severely damaged bone would typically require a bone grafting procedure which can result in donor site morbidity as well as other complications associated with the surgical procedure. However, now with advances in AM, surgeons can improve outcomes without the need for a

J. Copus · S. J. Lee (✉) · J. J. Yoo · A. Atala
Wake Forest Institute for Regenerative Medicine, Wake Forest School of Medicine,
Winston-Salem, NC, USA
e-mail: sjlee@wakehealth.edu

bone grafting procedure by using 3D printed titanium implants that allow for native bone integration [2, 3]. Currently AM has allowed for the creation of patient-specific hips, jaws, and even entire skull implants [3]. Since the shape of bones varies from patient to patient, a patient-specific implant will have better fit, be easier to insert and secure, and can also produce a better cosmetic result [4, 5].

The fabrication of bone tissue requires complex manufacturing techniques due to its heterogeneity in biology, structure, and architecture. AM technologies allow for greater control over many parameters in addition to size and shape. Porosity and pore size are easily controlled by these techniques, and they are both important parameters for bone as the native mineral components are structured in a porous manner. The surface and mechanical properties of the constructs are dependent on the manufacturing technique and material used and play a vital role in bone regeneration by affecting cell adhesion and preventing stress shielding in vivo. Lastly, osteoconductivity can be controlled in these techniques by the inclusion of calcium phosphates or hydroxyapatite [6]. There have been a wide range of AM techniques developed, and each technique has its own benefits and limitations. Herein, we explore the principles, components, and capabilities for bone tissue engineering that each AM technique possesses.

2 3D Printing via Medical Imaging

One of the most important developments for the field of AM came in 1986 with the development of the STL file. The STL file is used to “complete the electronic ‘handshake’ from the CAD software and transmit files for the printing of 3D objects [7].” The file stores surface information based on the CAD design and can create a text file with information on the coordinates of each of the surface vertices. Slicer software is then used to convert the 3D surface information into 2D cross-sections with predetermined thickness in the form of a G-file. This then allows the 3D structure to be printed by depositing material following the shape and path of the 2D cross-sections. These cross-sections are stacked upon the previous layer consecutively to create the final structure. Figure 1 shows 3D printing workflow from a medical image from a patient to 3D printed bone construct for reconstruction.

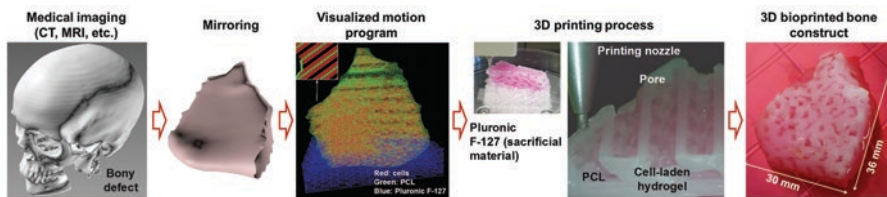


Fig. 1 The process of converting medical images into .STL format for 3D printing. (Reprinted with permission from ref [8] Copyright © 2016 Springer Nature)

In the medical field, technology has advanced rapidly to create CAD files based on medical imaging techniques. Currently, 3D printed structures can be created from computed tomography (CT), laser scanning, and even magnetic resonance imaging (MRI) [7]. While acquiring images of the region of interest, each medical imaging technique offers varying resolution, which can result in a discrepancy between the desired model and the generated model. Model resolution is also impacted by the slice thickness chosen during the image acquisition process [9]. The next step required is segmentation and mesh generation. During segmentation, the region of interest is identified from the medical images and extracted in order to create the mesh required for surface generation. There is a variety of open-source software that assists with mesh generation and automates the surface rendering process, and the preference of individual programs is ultimately up to the user, but most programs allow for manual rendering should the generated model not match the desired model [9]. Once segmentation and mesh generation are complete the data is in the STL format in order to be compatible with the AM technology. Ultimately, the goal of utilizing medical imaging techniques to generate models for AM is to improve clinical success rates by creating a patient-specific and personalized model.

The computational models built from medical imaging technologies allow doctors to make rapid prototypes of patient-specific bone defect areas. This allows the doctors to have a physical model which they can use to develop a plan of action and ultimately to improve the surgical outcome [10]. In other cases, medical imaging technologies are being used to scan the defect site and create a computational model that has the same geometry and dimensions as the bone defect. This model is then coupled with one of the various AM technologies to create a bone transplant identical to the bone defect area [10]. From these models, many parameters can be altered to improve tissue ingrowth and mechanical properties such as composition, density, pore shape and size, and pore interconnectivity [10].

3 Vat Photopolymerization

Stereolithography, or vat photopolymerization, is an AM technique that is used to fabricate 3D structures from STL files by selectively solidifying a liquid resin. The photo-crosslinkable resin is typically contained within a vat or tank and then is exposed to a light source in the form of a computer-controlled laser beam or a digital light projector with a computer-controlled mask [11]. When using a laser beam to crosslink the resin, the process is typically referred to as stereolithography (SLA) (Fig. 2a: a) but when using a projector, the process is referred to as digital light processing (DLP), but both methods rely on the same principle of crosslinking a liquid resin that is contained within a vat. SLA setups have remained relatively constant since their invention in the 1980s. In this method, a laser is used to crosslink resin in the desired pattern based on the STL file. This creates structures in a bottom-up method. After the first layer solidifies and adheres to the build platform, the platform is then submerged again in liquid resin and the laser then crosslinks the

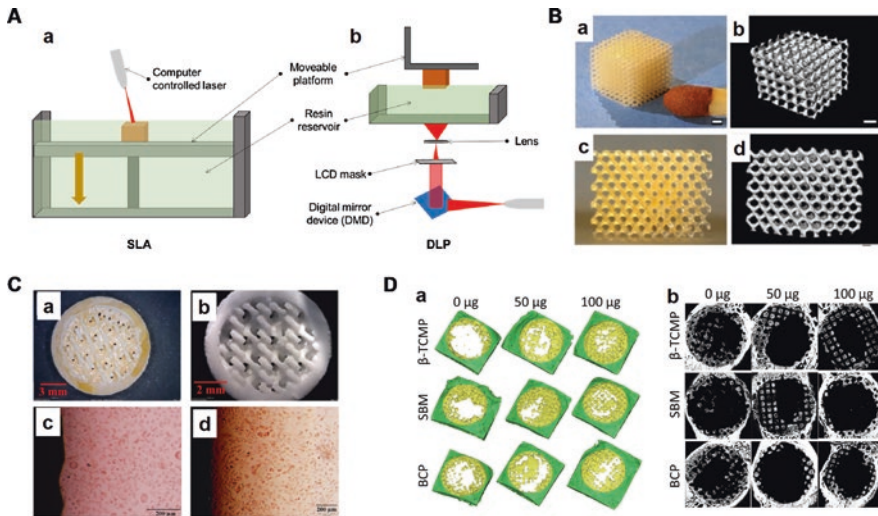


Fig. 2 (a) Schematic diagram of SLA and DLP methods of vat photopolymerization. (b) Scaffolds created by SLA that demonstrate the complex geometries that can be achieved with vat photopolymerization (reprinted with permission from ref. [12] Copyright © 2019 Elsevier). (c) Hydroxyapatite scaffolds created by vat photopolymerization showing improved cell differentiation in vitro (reprinted with permission from ref. [13] Copyright © 2015 IOS Press). (d) Poly(propylene fumarate) resins coated with BMP-2 that demonstrated improved bone regeneration when implanted in calvarial defect in vivo. (Reprinted with permission from ref. [14] Copyright © 2015 Elsevier)

second layer onto the first. This process is then repeated layer-by-layer until the final design is completed. Some SLA techniques have the ability to build structures from a top-down approach as well, but this is more commonly accomplished utilizing DLP techniques [11].

DLP is typically based on a top-down approach, where the first layer that forms is considered the top of the scaffold. With this technique, the light source arrives underneath the vat which requires the bottom of the vat to be composed of a transparent, non-adhesive material. The build stage is lowered to the bottom of the vat where the first layer is crosslinked and adheres onto the plate. The stage is then raised incrementally, depending on the layer thickness, where each successive layer is crosslinked. Once the final layer has been crosslinked, the build platform raises completely out of the liquid resin with the final solidified structure. In this method of photo-crosslinking, a digital mirror device (DMD) is used to create the desired pattern (Fig. 2a: b), which limits the resolution to the size of the micromirrors contained on the device. The device contains an array of millions of mirrors that are computer-controlled on a microscale level to only reflect light onto the stage in the shape defined by the STL file. This light is then directed to the uncured resin where the structure is crosslinked layer-by-layer [11].

Both DLP and SLA methods of photopolymerization are compatible with polymers, composite materials, hydrogels, and cells. This method also offers accuracy

down to 20 μm , while other AM techniques typically have a resolution around 50–200 μm . Layer thickness control is one of the more difficult aspects of stereolithography as it depends on many variables such as the resin, photoinitiator used, power of the light source, and exposure time. Overexposure is a significant challenge in stereolithography techniques, and especially when attempting to create porous structures so it is very important to optimize these parameters [11]. This technique can be used to create complex geometries and overhangs not typically capable by other AM techniques as demonstrated by Madrid et al. (Fig. 2b) [12].

One of the early limitations for both SLA and DLP techniques was with the photocurable resins available for use. Many of these resins caused skin irritation and were cytotoxic which prevented them from being implanted, but now a variety of polymers and associated resins, such as those based on vinyl esters, are available for use with these systems [15]. Tesavibul et al. have developed a method to use lithography based techniques to produce biocompatible hydroxyapatite scaffolds (Fig. 2c) [13]. Various hydrogels also have been developed for this technique which allows for the inclusion of cells within the tissue-engineered constructs [16]. Scaffolds produced by this technique have also been implanted *in vivo* previously. Dadsetan et al. used a photo-crosslinkable poly(propylene fumarate) resin to create porous scaffolds that allowed for bone ingrowth when implanted [14]. They coated these SLA fabricated resin with recombinant human bone morphogenic protein-2 (rhBMP-2) and observed bone regeneration *in vivo* via micro-CT scans (Fig. 2d).

These vat photopolymerization techniques offer a wide variety of approaches to design tissue-engineered bone constructs. Although not compatible with metals or ceramics, the range of polymers available for use and the ability to manufacture cellularized hydrogels make this one of the most used AM techniques for bone tissue engineering applications.

4 Powder Bed Fusion

Powder bed fusion, also known as selective laser sintering (SLS), is an AM technique that uses a high-power laser system to sinter or fuse regions of a powder bed together to form a scaffold [17]. It was first developed by Carl Deckard and patented in 1989 and rapidly changed the manufacturing process of prosthetics and osseointegration [18]. This method is compatible with metals, ceramics, polymers, and many composite materials, as long as they are available in powder form, and the material is able to melt or sinter together [19]. Unlike stereolithography, this method is not compatible with cells unless they are added to the scaffolds after manufacturing. This technique consists of a high-power laser, a beam deflection system, a powder bed container, and a deposition system (Fig. 3a), and like other systems utilizes an STL file to determine the laser pathway to fuse materials in the desired pattern.

The laser utilized in this system is highly dependent on the material of powder that is being fused. Most commercial devices utilize CO_2 lasers that have power

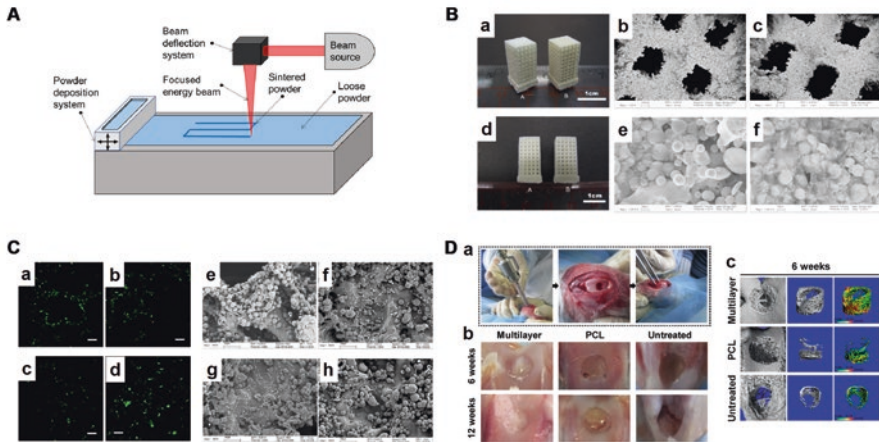


Fig. 3 (a) Schematic diagram of powder bed fusion. (b) A porous scaffold created by sintering of PLLA and calcium phosphate microspheres (reprinted with permission from ref. [20] Copyright © 2010 Elsevier). (c) In vitro study assessing the cell viability of osteoblasts when cultured on PLLA-calcium phosphate sintered scaffolds (reprinted with permission from ref. [20] Copyright © 2010 Elsevier). (d) In vivo bone regeneration within an osteochondral defect due to powder bed fusion created scaffolds. (Reprinted with permission from ref [21] Copyright © 2017 Elsevier)

ratings between 50 and 200 W [19]. The properties of the constructs can be easily modified by varying laser parameters such as wavelength, power, scan speed, and spacing. The powder characteristics and deposition system also can easily control scaffold parameters. By varying powder mixing, particle size, and composition, the surface quality and part density will vary [19]. Once the initial layer has been sintered or fused within the powder bed container, the container lowers in the Z-direction in a predefined distance, and then the powder deposition system deposits a new powder layer on top of the previous layer. This process is repeated and allows the following layers to be successively fused to the previous layer in a similar method to other AM techniques such as stereolithography. Typically powder layers are 0.1–0.3 mm thick, but this is also dependent upon the laser strength and particle size of the powder [19]. The resolution of the final product is also dependent on the laser and particle parameters. For instance, finer particle size will result in better resolution due to thinner layers being formed, particles flowing easier out of the powder deposition device, and less shrinkage during sintering or fusing [19].

In the biomedical field, powder bed fusion offers superior resolution and mechanical properties when compared to other AM techniques for metals such as directed energy deposition [22]. The most common use for these in the medical field is the fabrication of porous metal orthopedic implants [22]. The porous nature of these implants, typically composed of a biocompatible material such as titanium, improves bone ingrowth into the prosthetic and also promotes bone regeneration as well [23]. The importance of using calcium phosphate-based ceramics due to their osteoconductive properties has been instrumental in bone tissue engineering, and powder bed

fusion techniques expanded the complexity of scaffolds that are able to be fabricated with these ceramics. Previously, their use was limited to being fabricated in simple geometries unless incorporated into a polymeric material [24, 25]. To create complex scaffolds composed of bioceramic materials such as calcium phosphates, powder bed fusion was used to sinter the materials together with the aid of an intermediate polymer binder that was later removed from the scaffold by placing it in a heat furnace [26].

The inclusion of these calcium phosphate particles into polymeric constructs has shown promising results and has been manufactured via powder bed fusion previously [20]. In this study, Duan et al. combined nanosized calcium phosphate particles into poly(L-lactic acid) (PLLA) microspheres which were then sintered together into a 3D structure (Fig. 3b). After manufacturing these scaffolds, osteoblasts were seeded onto the osteoconductive material, and they found that there was increased osteoblast activity, as well as alkaline phosphatase (ALP) activity (Fig. 3c) [20]. Pure poly(ϵ -caprolactone) (PCL) scaffolds for bone tissue engineering have also been manufactured with this technique [27], but are still limited without the inclusion of cells. Most polymeric scaffolds manufactured with a powder bed fusion approach require post-processing techniques, like coating cells or growth factors onto the scaffold, in order to be effective for bone tissue engineering. This technique has also been used to create scaffolds composed of (HA)/PCL, which were then implanted into an osteochondral defect where the scaffolds accelerated early subchondral bone regeneration (Fig. 3d) [21].

Powder bed fusion is a versatile manufacturing method for metals, ceramics, and polymers for bone tissue engineering. Most of the advantages of this technique lie in the ability to create porous 3D structures from ceramic and metals. For bone tissue engineering applications, this technique has seen the most success in the production of patient-specific implants composed of porous metals or ceramics. Other approaches may be better suited if the desired outcome is to produce a cellularized bone tissue construct.

5 Directed Energy Deposition

Directed energy deposition is similar to powder bed fusion but is much more limited in its applications to bone tissue engineering. In this process, the material is melted as it is being deposited [28]. This process is in theory compatible with ceramics and polymers but is mainly used for metals and often even referred to as metal deposition. This technique differs from powder bed fusion as the high energy beam is not used to melt pre-deposited materials, but rather a high energy beam is created and melts materials at the same time as they are being deposited [28].

In directed energy deposition, a high-powered laser or electron beam is focused into a narrow region (Fig. 4a). Typically, this laser beam is stationary, and the stage below is controlled by an X-Y-Z motor controller; however, additional systems that utilize a robotic arm or rotary table are also available. Material is stored in powder

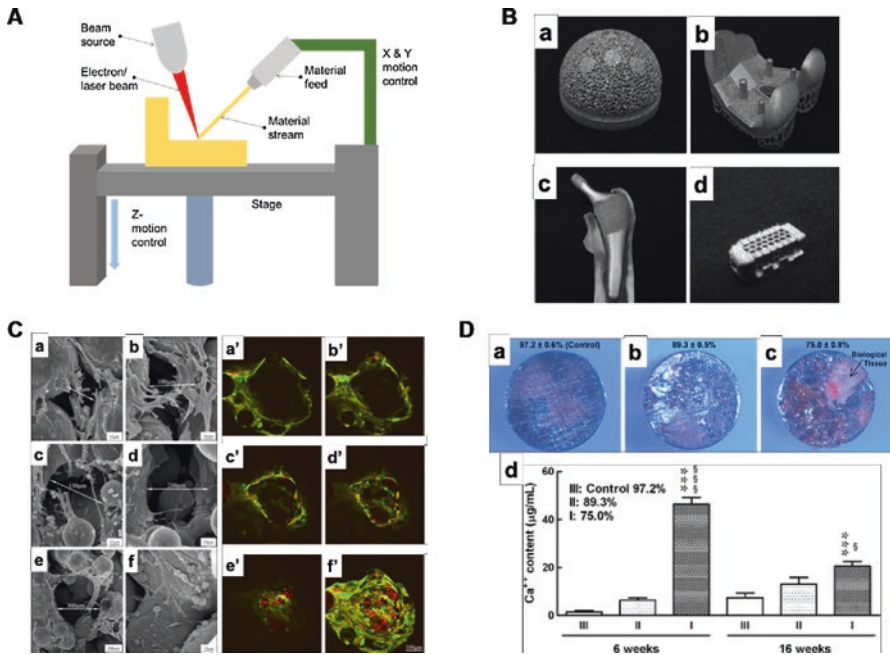


Fig. 4 (a) Schematic diagram of directed energy deposition technique. (b) Metallic orthopedic implants created by directed energy deposition (reprinted with permission from [Basicmedicalkey.com](https://www.basimedicalkey.com) Copyright © 2020). (c) Cell viability of osteoblasts cultured on titanium scaffolds created via directed energy deposition (reprinted with permission from ref. [29] Copyright © 2007 Elsevier). (d) In vivo tissue ingrowth into porous titanium constructs and the increased calcium content associated with improved bone regeneration within the constructs. (Reprinted with permission from ref. [29] Copyright © 2007 Elsevier)

feed nozzles, which deposit the material into the region of focus of the laser or electron beam [28]. Most deposition heads are composed of both the powder feed nozzle and an adjacent laser beam, as well as inert gases to help control the parameters with the beam. As the stage moves and material is melted and deposited, layers can be formed and eventually stacked to create the 3D structure. One interesting aspect of the direct energy deposition method is that the fabrication of vertical components does not always require differential Z-slices meaning that material can be deposited directly in a vertical beam. This technique can also be used for surface modification of pre-existing parts, as well as fabricating new structures onto parts [28].

Due to the high energy of the focused beam, materials are fairly limited to powdered metals, which therefore restricts applications in bone tissue engineering to those of metallic implants (Fig. 4b). This process also struggles to make smooth surface features. Lastly, the cost to operate direct energy deposit devices is significant so for many medical devices other fabrication techniques are used [28]. Nevertheless, direct energy deposition is still used for some applications in the medical field and specifically for bone tissue engineering applications. One application

is to deposit thin layers of titanium onto the surface of biomedical implants in order to make them more corrosion resistant and improve wear resistance [28]. Specifically, some orthopedic implants have been fabricated with novel titanium alloys which would be difficult to manufacture elsewhere, especially when attempting to fabricate them in a patient-specific geometry [30]. Xue et al. evaluated the biocompatibility of porous titanium constructs fabricated by this technique and found that osteoblasts had strong local adhesion and the cells expressed higher levels of alkaline phosphatase compared to cells on smooth non-fabricated titanium scaffolds (Fig. 4c) [29]. Metallic biomaterials fabricated by this method have been implanted in vivo previously, where Bandyopadhyay et al. demonstrated a significant increase of calcium within the implants as well as tissue ingrowth throughout the interconnected pores of the scaffold (Fig. 4d).

6 Binder Jetting

Binder jetting is a technique that builds upon the powder bed fusion, but instead of utilizing a high-powered laser to sinter the binder a drop of liquid bonding agent is deposited onto the bed of powder [15]. Binder jetting is one of the few AM technologies that does not rely on either a light or heat source in order to fabricate scaffolds [31]. This technique was first invented in 1993 and very quickly became commercialized to fabricate rapid prototypes [31]. This approach is compatible with all materials as long as they are available in powder form. It also has one of the fastest build rates of all AM techniques.

In this approach, the build plate is contained within an enclosed system (Fig. 5a). A layer of powder is spread onto the build plate before an inkjet print head deposits the liquid bonding agent onto the desired positions. Next, the build plate lowers, and a powder depositor typically in the form of a counter roller spreads more powder over the first layer. The bonding agent is again deposited in the desired positions and this process repeats until the final construct is assembled. One advantage of this system is that when building structures with overhangs or vertical columns, powder from previous layers can be used to stack upon and is removed at the end of the print [31]. This allows for the manufacture of scaffolds with complex geometries and overhangs that other AM processes would fail to create. One of the limitations of this process is that since the final construct consists of powdered particles that are bound together the constructs are typically fragile. In order to be utilized for bone tissue engineering applications, these constructs require post-processing techniques in order to improve their mechanical properties [34].

The use of metals in binder jetting techniques is the most common, although they are still limited due to the low geometric accuracy that results from the process. Another limitation of using metal powders with this technique is a large amount of post-processing that occurs. Typically, sintering or isostatic pressing is required to create scaffolds with significant mechanical properties [35]. The creation of prosthetics or implants with this technique is somewhat rare, as the amount of

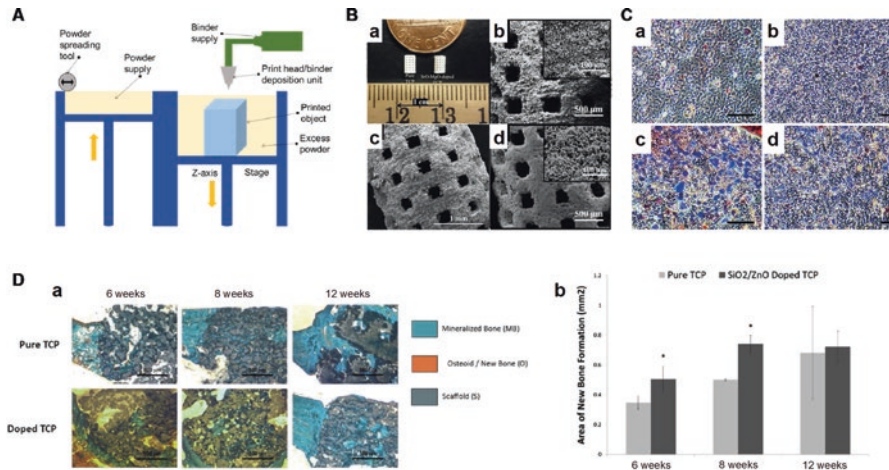


Fig. 5 (a) Schematic diagram of binder jetting technique. (b) Porous calcium phosphate scaffolds with complex geometries created by powder bed fusion (reprinted with permission from ref. [12] Copyright © 2019 Elsevier). (c) Histological images of binder jetting scaffolds showing improved collagen deposition from osteogenic differentiation (reprinted with permission from ref. [32] Copyright © 2014 Wiley Online Library). (d) TCP based scaffolds created by binder jetting which exhibit improved mineralization when implanted in vivo. (Reprinted with permission from ref. [33] Copyright © 2013 Elsevier)

post-processing required makes other AM processes much more appealing for this purpose. Regardless, binder jetting has been used to develop biodegradable alloys that can be utilized as a substitute for bone grafts [36]. Binder jetting's applications for bone tissue engineering are more commonly associated with manufacturing ceramics such as hydroxyapatite and calcium phosphates [37]. These are commonly available in powder form and have excellent biocompatibility alone but are still somewhat limited for clinical translation when manufactured with this process due to residues left behind from the bonding agent. The binders for ceramics can include toxic materials such as chloroform or various acid-based binders [38]. This technique has been used previously to fabricate complex porous scaffolds composed of calcium phosphates, which exhibit surface roughness that is well-suited for bone regeneration purposes (Fig. 5b).

The use of polymers as the sole material in binder jetting is fairly limited owing to the fact that polymer formulations are rarely powdered. However, some polymers have been utilized in binder jetting, such as PCL, when bound with appropriate solvents. These can be utilized for bone tissue engineering applications, but typically other AM methods are used to create these scaffolds [31]. Gao et al. have developed a method that utilizes bioactive glass nanoparticles and a PEG-HA hydrogel as the binder which allows for the creation of cell-seeded scaffolds. In vitro studies with this method showed increased collagen deposition in the presence of osteogenic differentiation media (Fig. 5c) [32]. Fielding et al. have utilized binder jetting techniques to create TCP scaffolds that enhance both osteogenesis and angiogenesis in vivo (Fig. 5d) [33].

7 Material Jetting

Material jetting, also known as inkjet 3D printing, is a technique where liquid photopolymer droplets are selectively deposited and then crosslinked, usually with UV light [39]. In this technique, multiple print heads can be utilized to deposit many different material compositions, or even cell-laden hydrogels, within the same scaffold. Material jetting devices are very similar to the original inkjet printers designed in the 1950s. It took until the year 2000 for an inkjet-based 3D printer to be developed by Objet Geometries [40].

The material jetting technique physically manipulates a resin or cell-laden hydrogel in order to create droplets that can be deposited in specific locations based on code generated from the STL file. The droplet formation can be accomplished by several different mechanisms. One of such mechanisms relies on the Rayleigh–Plateau instability in order to break up a continuous stream into droplets [41]. In this method, referred to as continuous ink jetting, the resin or bioink is contained within a syringe and air pressure is used to force it from a nozzle. Another approach, drop-on-demand, can utilize either a thermal actuator, piezoelectric actuator, or electrode to generate pressure pulses which can deposit a controlled amount of ink from the nozzle (Fig. 6a) [40, 45, 46].

Like other AM techniques, the scaffold design is based on 2D patterns generated from an STL file. In order to generate these patterns an *X-Y-Z* axis motor controller is used to move either the print head or stage being printed onto. *Z*-slice thickness can be controlled in material jetting applications by altering the amount of material deposited with each droplet. One of the main limitations of this modality is that it is limited to photo-crosslinkable polymers with a low enough viscosity that they can be deposited in small droplets [40]. The main advantage of this technique is that multiple different bioinks or resins can be used, which allows for the manufacturing of tissues with multiple cells types in the same scaffold.

Specific to bone tissue engineering, material jetting can be used to create biocompatible polymeric scaffolds with the optimal pore design for bone tissue ingrowth such as the octacalcium phosphate scaffolds produced by Komlev et al. (Fig. 6b: a) [42]. With this technique, researchers have also been able to print complex multi-cell constructs (Fig. 6b: d). Xu et al. manufactured constructs that incorporate both mesenchymal stem cells that are capable of osteogenic differentiation as well as smooth muscle cells that aid in vascular network formation [43]. In this study, the inkjet printer was loaded with a sodium alginate-based bioink that encapsulated their cells. Calcium chloride was then used as a crosslinker to ensure mechanical stability when printing multiple layers [43]. In some cases, this technique can even be used to biopattern bone morphogenic protein into a scaffold to spatially control bone formation (Fig. 6c) [44]. In this study, BMP-2 was patterned in scaffolds via material jetting techniques which then saw osteogenic differentiation *in vitro*, as well as improved bone formation in a rat calvarial defect *in vivo* (Fig. 6d).

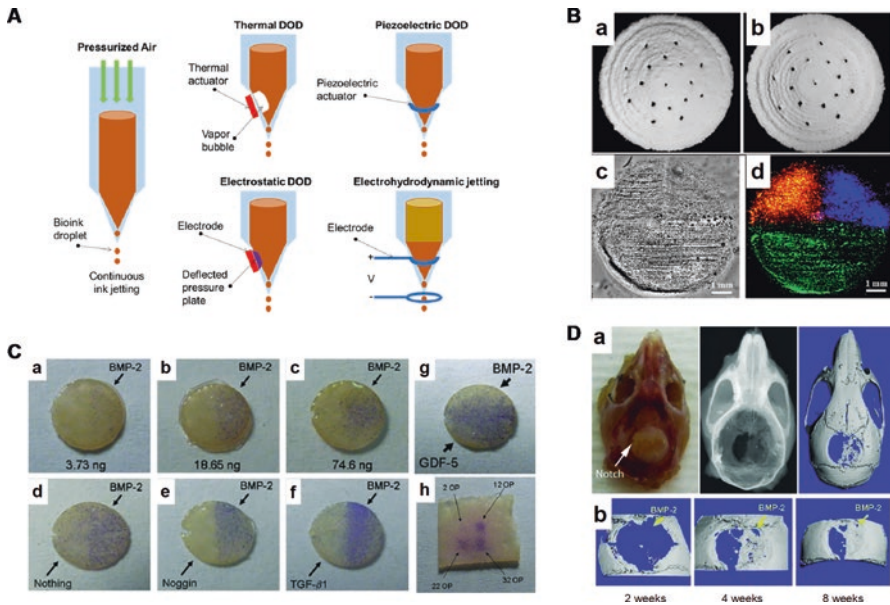


Fig. 6 (a) Schematic diagram of the various material jetting techniques. DOD: drop-on-demand. (b) (a, b) Octacalcium phosphate scaffolds created by material jetting (reprinted with permission from ref. [42] Copyright © 2015 Frontiers). (c, d) Constructs with multiple cell types capable of vascular network formation and osteogenic differentiation fabricated via material jetting (reprinted with permission from ref. [43] Copyright © 2013 Elsevier). (c) Material jetting fabricated scaffolds with patterned BMP-2 to control osteogenic differentiation in vitro (reprinted with permission from ref. [44] Copyright © 2010 Mary Ann Liebert, Inc.) (d) In vivo bone regeneration of BMP-2 patterned scaffolds implanted in calvarial defect. (Reprinted with permission from ref. [44] Copyright © 2010 Mary Ann Liebert, Inc.)

Since material jetting is capable of printing both polymeric material and cell-seeded hydrogels within the same print it offers a distinct advantage over other single material AM techniques. The delivery of cells, growth factors, and the high precision droplet placement associated with this technique makes it a promising candidate for the manufacture of transplantable bone tissues.

8 Sheet Lamination

Sheet lamination is another AM technique based on the application of heat to materials. In this process, sheets of material, whether polymer, metal, or ceramic, are cut into shapes with laser and then are fused using heat and pressure [17, 47]. This technique is fairly limited for tissue engineering applications as it can only create very dense structures. Sheet lamination involves the use of a laser that typically rests on an X-Y plotter, a heated roller that can apply pressure, a build platform, and

material rolls for housing. Typically, the material is stored on the roller in the form of a sheet and stretched to another roller that houses the excess material. As it passes by the build platform, the full sheet is cut into the desired geometry before being pressed by a heated roller which is optimized with the temperature and pressure at which to fuse the materials. The excess material is then rolled past the build stage where the next layer is then pressed [48]. This process is compatible with metals, ceramics, and polymers [47].

Due to the high pressure and temperature required to fuse materials, cells cannot be used in this process. This limits the applications for bone tissue engineering, especially considering that the final manufactured products are very dense and have a low void volume. This makes it very difficult to create highly cellularized constructs, as the cells are not able to penetrate deep due to the low pore sizes [47]. 3D constructs are capable of this process, but it is much more applicable to use them for rapid prototyping purposes. Regardless, this process has been used, albeit rarely, in bone tissue engineering applications in order to create ceramic-based constructs. Tanimoto et al. utilized this sheet lamination technique to stack individual tricalcium phosphate sheets to create a 3D scaffold. This sheet lamination process required temperatures up to 1200 °C and converted the β -tricalcium phosphate sheets into α -tricalcium phosphate which increased both strength and modulus of the scaffold [49]. Of all the AM techniques, sheet lamination is the most limited in terms of bone tissue engineering applications.

9 Material Extrusion

Material extrusion, also known as fused deposition modeling, is arguably the most commonly used technique for AM. In this method, the constructs are manufactured by a controlled extrusion of material which is deposited onto a substrate by an extrusion head [50]. These printers usually consist of a temperature controlled unit that is capable of dispensing the material, an X-Y-Z motor controller, the stage, and sometimes a light source that is capable of photo-crosslinking materials [50]. Many of these material extruders contain multiple print heads, which allows them to use multiple materials, including those that contain cells.

Within this system, either pneumatic or mechanical dispensing systems are used to force the material through the nozzle (Fig. 7a) [54, 55]. Pneumatic systems rely on pressurized air to force the material through the nozzle, while the mechanical dispensing systems can use either a piston or screw-based system to achieve this. Mechanical systems can have more precise flow than pneumatic as there is a residual pressure within the syringe head that often occurs with pneumatic-based systems [50]. A large variety of materials can be printed by this method, but for bone tissue engineering applications the use of polymers, ceramic composites, and cell-seeded hydrogels offers the most advantage over other AM techniques.

In material extrusion techniques, materials with a viscosity between 30 mPa/s and some greater than 6×10^7 mPa/s are capable of being extruded [50]. When using

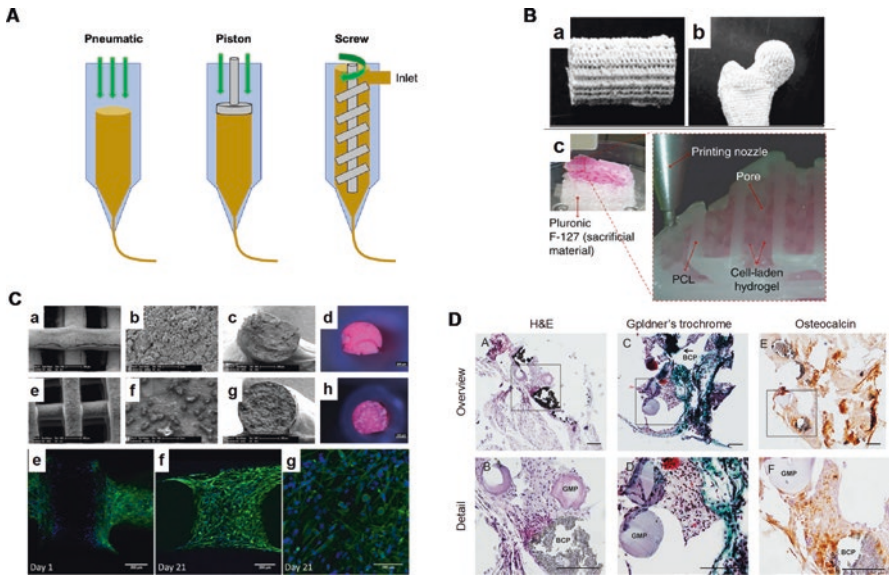


Fig. 7 (a) Schematic diagram of material extrusion techniques. (b) Patient-specific bone geometries fabricated by material extrusion that include both polymer-ceramic composites and cell-seeded hydrogels (reprinted with permission from refs [51] (b: a, b) and [8] (b: c), copyright © 2018 Whioce Publishing Pte. Ltd. and copyright © 2016 Springer, respectively). (c) In vitro viability of MSCs seeded within a bone tissue construct (reprinted with permission from ref. [52] Copyright © 2015 Elsevier). (d) Histological analysis of implanted material extrusion scaffolds that allow for the controlled release of BMP-2 in vivo. (Reprinted with permission from ref. [53] Copyright © 2013 PLOS)

polymers, an initial molten layer is deposited onto the stage where it rapidly cools before the next molten layer is deposited on top of it. This fuses the materials and allows for stacking in a layer-by-layer fashion. When using hydrogels or other soft materials, due to the lack of structural integrity, crosslinking may be required before depositing the following layer; otherwise, the structure can collapse upon itself due to the forces being imposed on it [50]. The development of novel bioinks that maintain cell viability during the printing process has been one of the most important developments for extrusion-based bioprinting. Previously, cell viability was limited due to the shear stress during the printing process that they were subjected to, but with the advancement of shear-thinning materials available for use, high cell densities can now be achieved [50].

Specifically for polymeric materials, melt electrospinning writing has been utilized to fabricate highly ordered fibers that are deposited in a layer-by-layer fashion. This process is similar to material extrusion except that a large voltage is applied to the molten polymer which allows nanometer-scale fibers to be precisely deposited [56], whereas material extrusion is limited to the diameter of the nozzle used. Although this technique can offer higher fiber resolution, it is a complex process that requires balancing many parameters. In order to successfully fabricate a

scaffold, it requires a high voltage which can result in charge accumulation in the fibers which ultimately results in structural distortion. The electric field, in addition to the numerous other material extrusion parameters, must be carefully controlled which makes it difficult to fabricate large-scale structures. Researchers have successfully fabricated 7-mm structures [57] and structures with 100 layers of filament [58] with this approach, but large-scale structure fabrication has been limited. As improvements in parameter optimization occur, this technique may become more widely used for applications in bone tissue engineering.

The use of biocompatible polymers is commonplace in material extrusion, especially when attempting to create engineered bone scaffolds. With this method, scaffolds with patient-specific geometry can be created with predefined pore sizes, and cell-seeded hydrogels can be incorporated within the scaffolds in the same print (Fig. 7b). Polymeric materials are usually utilized for their mechanical properties, although they are frequently mixed with a ceramic such as calcium phosphate in order to improve the osteoconductive properties of the scaffold [59]. Cell-seeded bioinks are included to improve osteogenesis within the scaffold, aided by the inclusion of mesenchymal stem cells [60]. Commonly, bioinks that contain cells are either modified synthetic materials, such as poly(ethylene glycol) (PEG), or naturally derived materials including those based on alginate, cellulose, or gelatin [61–63]. Many *in vitro* studies have utilized this method to incorporate MSCs into their constructs such as the study by Akkineni et al. (Fig. 7c) [52]. This technique also allows for the controlled release of BMP-2 and other growth factors as shown by the *in vivo* study (Fig. 7d) [53].

Overall, extrusion-based bioprinting offers the creation of complex, multi-material cell-seeded scaffolds with high resolution and low print times. Since it is one of the most common AM techniques, commercial extrusion printers are becoming cheaper and more readily available, and as advances in materials continue, the likelihood of this technique producing clinical-grade implants has improved greatly. Table 1 summarizes AM techniques for bone tissue engineering applications.

10 Conclusions and Future Perspectives

AM techniques allow for the creation of patient-specific bone implants with superior biocompatibility, porosity, surface and mechanical properties, osteoconductivity, and osteoinductivity. Currently, AM techniques are limited mainly by material availability and achievable resolution. The resolution will improve as manufacturing techniques are optimized and new technologies developed, while novel biomaterials are continually being developed and improved upon. Additionally, the inclusion of cells and bioactive molecules is being investigated more frequently and researchers are learning which cell type or bioactive molecule may be optimal to treat the various bone tissue diseases or disorders. While each AM technique has its own advantages and limitations, AM as a whole remains a promising approach for the development of tissue-engineered bone constructs with clinical significance.

Table 1 Additive manufacturing techniques for bone tissue engineering applications

AM technique	Description	Compatible materials	Resolution	Advantages	Disadvantages	Refs.
Vat photopolymerization	A liquid vat of resin is photo-crosslinked in a layer-by-layer fashion	Photopolymers/resins, hydrogels	10 μm	<ul style="list-style-type: none"> No support materials needed Can encapsulate cells High resolution 	<ul style="list-style-type: none"> Typically limited to one material Long UV exposure time 	[16, 64–67]
Powder bed fusion	A laser/electron beam is used to melt layers of powdered material together	Polymers, metals, ceramics	80–250 μm	<ul style="list-style-type: none"> No support materials needed Scaffolds with high mechanical properties can be made 	<ul style="list-style-type: none"> High-powered laser can destroy some materials Limited to powdered materials Non-fused materials remain in the scaffold 	[20, 22, 64, 68, 69]
Directed energy deposition	A feed of material is directed into an energy source which melts it onto a substrate	Polymers, metals, ceramics	250 μm	<ul style="list-style-type: none"> Can create scaffolds or add coatings on pre-existing scaffolds Can create large scaffolds Fast print speed and relatively low material cost 	<ul style="list-style-type: none"> Limited to wire or powdered materials High energy input required 	[17, 30, 70]
Binder jetting	A liquid binder is deposited into a bed of powdered material	Polymers, metals, ceramics	20–200 μm	<ul style="list-style-type: none"> Heat not required Large size scaffolds can be fabricated Scaffolds can be made quickly Low part cost 	<ul style="list-style-type: none"> Scaffolds have poor mechanical properties Limited to powdered materials 	[31, 37, 71–73]

Material jetting	Droplets of material are selectively deposited onto a substrate	Photopolymers, hydrogels	5–200 µm	<ul style="list-style-type: none"> • High dimensional accuracy • Can encapsulate cells • Multi-material compatible 	<ul style="list-style-type: none"> • Excessive cost • Limited materials available 	[43, 44, 74–76]
Sheet lamination	Thin sheets of material are shaped and bonded together to create a single object	Polymers, metals, ceramics	Dependent on sheet thickness	<ul style="list-style-type: none"> • Large size scaffolds can be made • Low cost • Good surface finish 	<ul style="list-style-type: none"> • Susceptible to shear and tensile loading • Limited to materials available in sheets 	[49, 77]
Material extrusion	Material is forced through a nozzle and patterned in a layer-by-layer fashion	Polymers, ceramic composites, hydrogels	50–200 µm	<ul style="list-style-type: none"> • Multi-material compatible • Can encapsulate cells 	<ul style="list-style-type: none"> • Support structures needed • Resolution limited to nozzle size • Large print times 	[59, 61, 64, 78, 79]
				<ul style="list-style-type: none"> • Good mechanical properties 		

Acknowledgments This study was supported by the National Institutes of Health (1P41EB023833-346 01).

References

1. Ventola CL. Medical applications for 3D printing: current and projected uses. *Pharm Ther.* 2014;39(10):704.
2. Greenwald AS, Boden SD, Goldberg VM, Khan Y, Laurencin CT, Rosier RN. Bone-graft substitutes: facts, fictions, and applications. *JBJS.* 2001;83(2 Suppl 2):S98–103.
3. Whitaker M. The history of 3D printing in healthcare. *Bull Roy Coll Surg Engl.* 2014;96(7):228–9.
4. Hollister SJ. Porous scaffold design for tissue engineering. *Nat Mater.* 2005;4(7):518–24.
5. Stoodley MA, Abbott JR, Simpson DA. Titanium cranioplasty using 3-D computer modelling of skull defects. *J Clin Neurosci.* 1996;3(2):149–55.
6. Salgado AJ, Coutinho OP, Reis RL. Bone tissue engineering: state of the art and future trends. *Macromol Biosci.* 2004;4(8):743–65.
7. Gross BC, Erkal JL, Lockwood SY, Chen C, Spence DM. Evaluation of 3D printing and its potential impact on biotechnology and the chemical sciences. *ACS Publ.* 2014;86:3240.
8. Kang H-W, Lee SJ, Ko IK, Kengla C, Yoo JJ, Atala A. A 3D bioprinting technology to produce human-scale tissue constructs with structural integrity. *Nat Biotechnol.* 2016;34(3):312–9.
9. Marro A, Bandukwala T, Mak W. Three-dimensional printing and medical imaging: a review of the methods and applications. *Curr Probl Diagn Radiol.* 2016;45(1):2–9.
10. Wong KV, Hernandez A. A review of additive manufacturing. *Int Scholar Res Notice.* 2012;2012:208760.
11. Melchels FPW, Feijen J, Grijpma DW. A review on stereolithography and its applications in biomedical engineering. *Biomaterials.* 2010;31(24):6121–30.
12. Madrid APM, Vrech SM, Sanchez MA, Rodriguez AP. Advances in additive manufacturing for bone tissue engineering scaffolds. *Mater Sci Eng C.* 2019;100:631–44.
13. Tesavibul P, Chantawerod S, Laohaprapanon A, Channasanon S, Uppanan P, Tanodekaew S, Chalermkamnon P, Sitthiseripratip K. Biocompatibility of hydroxyapatite scaffolds processed by lithography-based additive manufacturing. *Biomed Mater Eng.* 2015;26(1–2):31–8.
14. Dadsetan M, Guda T, Runge MB, Mijares D, LeGeros RZ, LeGeros JP, Silliman DT, Lu L, Wenke JC, Baer PRB. Effect of calcium phosphate coating and rhBMP-2 on bone regeneration in rabbit calvaria using poly (propylene fumarate) scaffolds. *Acta Biomater.* 2015;18:9–20.
15. Roseti L, Parisi V, Petretta M, Cavallo C, Desando G, Bartolotti I, Grigolo B. Scaffolds for bone tissue engineering: state of the art and new perspectives. *Mater Sci Eng C.* 2017;78:1246–62.
16. Dhariwala B, Hunt E, Bolan T. Rapid prototyping of tissue-engineering constructs, using photopolymerizable hydrogels and stereolithography. *Tissue Eng.* 2004;10(9–10):1316–22.
17. Gu BK, Choi DJ, Park SJ, Kim MS, Kang CM, Kim C-H. 3-dimensional bioprinting for tissue engineering applications. *Biomater Res.* 2016;20(1):12.
18. Mazzoli A. Selective laser sintering in biomedical engineering. *Med Biol Eng Comput.* 2013;51(3):245–56.
19. Kruth J-P, Wang X, Laoui T, Froyen L. Lasers and materials in selective laser sintering. *Assem Autom.* 2003;23:357.
20. Duan B, Wang M, Zhou WY, Cheung WL, Li ZY, Lu WW. Three-dimensional nanocomposite scaffolds fabricated via selective laser sintering for bone tissue engineering. *Acta Biomater.* 2010;6(12):4495–505.
21. Du Y, Liu H, Yang Q, Wang S, Wang J, Ma J, Noh I, Mikos AG, Zhang S. Selective laser sintering scaffold with hierarchical architecture and gradient composition for osteochondral repair in rabbits. *Biomaterials.* 2017;137:37–48.

22. Yuan L, Ding S, Wen C. Additive manufacturing technology for porous metal implant applications and triple minimal surface structures: a review. *Bioact Mater.* 2019;4:56–70.
23. Chia HN, Wu BM. Recent advances in 3D printing of biomaterials. *J Biol Eng.* 2015;9(1):4.
24. Burg KJL, Porter S, Kellam JF. Biomaterial developments for bone tissue engineering. *Biomaterials.* 2000;21(23):2347–59.
25. Bertrand P, Bayle F, Combe C, Gœuriot P, Smurov I. Ceramic components manufacturing by selective laser sintering. *Appl Surf Sci.* 2007;254(4):989–92.
26. Lee G, Barlow JW. Selective laser sintering of bioceramic materials for implants. In: 1993 International Solid Freeform Fabrication Symposium; 1993. p. 376–80.
27. Williams JM, Adewunmi A, Schek RM, Flanagan CL, Krebsbach PH, Feinberg SE, Hollister SJ, Das S. Bone tissue engineering using polycaprolactone scaffolds fabricated via selective laser sintering. *Biomaterials.* 2005;26(23):4817–27.
28. Gibson I, Rosen D, Stucker B. Directed energy deposition processes. In: *Additive manufacturing technologies.* New York, NY: Springer; 2015. p. 245–68.
29. Xue W, Krishna BV, Bandyopadhyay A, Bose S. Processing and biocompatibility evaluation of laser processed porous titanium. *Acta Biomater.* 2007;3(6):1007–18.
30. Banerjee R, Nag S, Fraser HL. A novel combinatorial approach to the development of beta titanium alloys for orthopaedic implants. *Mater Sci Eng C.* 2005;25(3):282–9.
31. Ziaee M, Crane NB. Binder jetting: a review of process, materials, and methods. *Addit Manufact.* 2019;28:781.
32. Gao G, Schilling AF, Yonezawa T, Wang J, Dai G, Cui X. Bioactive nanoparticles stimulate bone tissue formation in bioprinted three-dimensional scaffold and human mesenchymal stem cells. *Biotechnol J.* 2014;9(10):1304–11.
33. Fielding G, Bose S. SiO₂ and ZnO dopants in three-dimensionally printed tricalcium phosphate bone tissue engineering scaffolds enhance osteogenesis and angiogenesis in vivo. *Acta Biomater.* 2013;9(11):9137–48.
34. Gaytan SM, Cadena MA, Karim H, Delfin D, Lin Y, Espalin D, Macdonald E, Wicker RB. Fabrication of barium titanate by binder jetting additive manufacturing technology. *Ceram Int.* 2015;41(5):6610–9.
35. Kumar A, Bai Y, Eklund A, Williams CB. Effects of hot isostatic pressing on copper parts fabricated via binder jetting. *Proc Manufact.* 2017;10:935–44.
36. Hong D, Chou D-T, Velikokhatnyi OI, Roy A, Lee B, Swink I, Issaev I, Kuhn HA, Kumta PN. Binder-jetting 3D printing and alloy development of new biodegradable Fe-Mn-Ca/Mg alloys. *Acta Biomater.* 2016;45:375–86.
37. Sheydaeian E, Vlasea M, Woo A, Pilliar R, Hu E, Toyserkani E. Effect of glycerol concentrations on the mechanical properties of additive manufactured porous calcium polyphosphate structures for bone substitute applications. *J Biomed Mater Res B Appl Biomater.* 2017;105(4):828–35.
38. Zhou Z, Buchanan F, Mitchell C, Dunne N. Printability of calcium phosphate: calcium sulfate powders for the application of tissue engineered bone scaffolds using the 3D printing technique. *Mater Sci Eng C.* 2014;38:1–10.
39. Yap YL, Wang C, Sing SL, Dikshit V, Yeong WY, Wei J. Material jetting additive manufacturing: an experimental study using designed metrological benchmarks. *Precis Eng.* 2017;50:275–85.
40. Gudapati H, Dey M, Ozbolat I. A comprehensive review on droplet-based bioprinting: past, present and future. *Biomaterials.* 2016;102:20–42.
41. Derby B. Bioprinting: inkjet printing proteins and hybrid cell-containing materials and structures. *J Mater Chem.* 2008;18(47):5717–21.
42. Komlev VS, Popov VK, Mironov AV, Fedotov AY, Teterina AY, Smirnov IV, Bozo IY, Rybko VA, Deev RV. 3D printing of octacalcium phosphate bone substitutes. *Front Bioeng Biotechnol.* 2015;3:81.

43. Xu T, Zhao W, Zhu J-M, Albanna MZ, Yoo JJ, Atala A. Complex heterogeneous tissue constructs containing multiple cell types prepared by inkjet printing technology. *Biomaterials*. 2013;34(1):130–9.
44. Cooper GM, Miller ED, DeCesare GE, Usas A, Lensie EL, Bykowski MR, Huard J, Weiss LE, Losee JE, Campbell PG. Inkjet-based biopatterning of bone morphogenetic protein-2 to spatially control calvarial bone formation. *Tissue Eng A*. 2010;16(5):1749–59.
45. Wijshoff H. The dynamics of the piezo inkjet printhead operation. *Phys Rep*. 2010;491(4–5):77–177.
46. Kamisuki S, Hagata T, Tezuka C, Nose Y, Fujii M, Atobe M. A low power, small, electrostatically-driven commercial inkjet head. Washington, DC: IEEE; 1998. p. 63–8.
47. Tsang VL, Bhatia SN. Three-dimensional tissue fabrication. *Adv Drug Deliv Rev*. 2004;56(11):1635–47.
48. Gibson I, Rosen DW, Stucker B. Sheet lamination processes. In: *Additive manufacturing technologies*. New York, NY: Springer; 2010. p. 223–52.
49. Tanimoto Y, Nishiyama N. Preparation and physical properties of tricalcium phosphate laminates for bone-tissue engineering. *J Biomed Mater Res A*. 2008;85(2):427–33.
50. Murphy SV, Atala A. 3D bioprinting of tissues and organs. *Nat Biotechnol*. 2014;32(8):773.
51. Liu F, Liu C, Chen Q, Ao Q, Tian X, Fan J, Tong H, Wang X. Progress in organ 3D bioprinting. *Int J Bioprint*. 2018;4(1):128.
52. Akkineni AR, Luo Y, Schumacher M, Nies B, Lode A, Gelinsky M. 3D plotting of growth factor loaded calcium phosphate cement scaffolds. *Acta Biomater*. 2015;27:264–74.
53. Poldervaart MT, Wang H, van der Stok J, Weinans H, Leeuwenburgh SCG, Öner FC, Dhert WJA, Alblas J. Sustained release of BMP-2 in bioprinted alginate for osteogenicity in mice and rats. *PLoS One*. 2013;8(8):e72610.
54. Censi R, Van Putten S, Vermonden T, Di Martino P, Van Nostrum CF, Harmsen MC, Bank RA, Hennink WE. The tissue response to photopolymerized PEG-p (HPMAm-lactate)-based hydrogels. *J Biomed Mater Res A*. 2011;97(3):219–29.
55. Visser J, Peters B, Burger TJ, Boomstra J, Dhert WJA, Melchels FPW, Malda J. Biofabrication of multi-material anatomically shaped tissue constructs. *Biofabrication*. 2013;5(3):035007.
56. Afghah F, Dikyol C, Altunbek M, Koc B. Biomimicry in bio-manufacturing: developments in melt electrospinning writing technology towards hybrid biomanufacturing. *Appl Sci*. 2019;9(17):3540.
57. Wunner FM, Wille ML, Noonan TG, Bas O, Dalton PD, De-Juan-Pardo EM, Hutmacher DW. Melt electrospinning writing of highly ordered large volume scaffold architectures. *Adv Mater*. 2018;30(20):1706570.
58. Hochleitner G, Jüngst T, Brown TD, Hahn K, Moseke C, Jakob F, Dalton PD, Groll J. Additive manufacturing of scaffolds with sub-micron filaments via melt electrospinning writing. *Biofabrication*. 2015;7(3):035002.
59. Shim J-H, Moon T-S, Yun M-J, Jeon Y-C, Jeong C-M, Cho D-W, Huh J-B. Stimulation of healing within a rabbit calvarial defect by a PCL/PLGA scaffold blended with TCP using solid freeform fabrication technology. *J Mater Sci Mater Med*. 2012;23(12):2993–3002.
60. Weinand C, Pomerantseva I, Neville CM, Gupta R, Weinberg E, Madisch I, Shapiro F, Abukawa H, Troulis MJ, Vacanti JP. Hydrogel- β -TCP scaffolds and stem cells for tissue engineering bone. *Bone*. 2006;38(4):555–63.
61. Fedorovich NE, De Wijn JR, Verbout AJ, Alblas J, Dhert WJA. Three-dimensional fiber deposition of cell-laden, viable, patterned constructs for bone tissue printing. *Tissue Eng A*. 2008;14(1):127–33.
62. Sangeetha K, Thamizhavel A, Girija EK. Effect of gelatin on the in situ formation of Alginate/Hydroxyapatite nanocomposite. *Mater Lett*. 2013;91:27–30.
63. Gopinathan J, Noh I. Recent trends in bioinks for 3D printing. *Biomater Res*. 2018;22(1):11.
64. Hao ZC, Lu J, Wang SZ, Wu H, Zhang YT, Xu SG. Stem cell-derived exosomes: a promising strategy for fracture healing. *Cell Prolif*. 2017;50(5):e12359.

65. Schmidleithner C, Malferarri S, Palgrave R, Bomze D, Schwentenwein M, Kalaskar DM. Application of high resolution DLP stereolithography for fabrication of tricalcium phosphate scaffolds for bone regeneration. *Biomed Mater.* 2019;14(4):045018.
66. Zeng Y, Yan Y, Yan H, Liu C, Li P, Dong P, Zhao Y, Chen J. 3D printing of hydroxyapatite scaffolds with good mechanical and biocompatible properties by digital light processing. *J Mater Sci.* 2018;53(9):6291–301.
67. Scalera F, Corcione CE, Montagna F, Sannino A, Maffezzoli A. Development and characterization of UV curable epoxy/hydroxyapatite suspensions for stereolithography applied to bone tissue engineering. *Ceram Int.* 2014;40(10):15455–62.
68. Cahill S, Lohfeld S, McHugh PE. Finite element predictions compared to experimental results for the effective modulus of bone tissue engineering scaffolds fabricated by selective laser sintering. *J Mater Sci Mater Med.* 2009;20(6):1255–62.
69. Tan KH, Chua CK, Leong KF, Cheah CM, Cheang P, Bakar MSA, Cha SW. Scaffold development using selective laser sintering of polyetheretherketone–hydroxyapatite biocomposite blends. *Biomaterials.* 2003;24(18):3115–23.
70. Gibson I, Rosen D, Stucker B. Direct digital manufacturing. In: Additive manufacturing technologies. New York, NY: Springer; 2015. p. 375–97.
71. Mirzababaei S, Pasebani S. A review on binder jet additive manufacturing of 316L stainless steel. *J Manufact Mater Process.* 2019;3(3):82.
72. Tarafder S, Balla VK, Davies NM, Bandyopadhyay A, Bose S. Microwave-sintered 3D printed tricalcium phosphate scaffolds for bone tissue engineering. *J Tissue Eng Regen Med.* 2013;7(8):631–41.
73. Trombetta R, Inzana JA, Schwarz EM, Kates SL, Awad HA. 3D printing of calcium phosphate ceramics for bone tissue engineering and drug delivery. *Ann Biomed Eng.* 2017;45(1):23–44.
74. Kazemian A, Yuan X, Cochran E, Khoshnevis B. Cementitious materials for construction-scale 3D printing: laboratory testing of fresh printing mixture. *Constr Build Mater.* 2017;145:639–47.
75. Saijo H, Igawa K, Kanno Y, Mori Y, Kondo K, Shimizu K, Suzuki S, Chikazu D, Iino M, Anzai M. Maxillofacial reconstruction using custom-made artificial bones fabricated by inkjet printing technology. *J Artif Organs.* 2009;12(3):200–5.
76. Zhang Y, Tse C, Rouholamin D, Smith P. Scaffolds for tissue engineering produced by inkjet printing. *Open Eng.* 2012;2(3):325–35.
77. Hollinger JO. Unique bone regeneration tricalcium phosphate. Google Patents; 1991.
78. Shao H, He J, Lin T, Zhang Z, Zhang Y, Liu S. 3D gel-printing of hydroxyapatite scaffold for bone tissue engineering. *Ceram Int.* 2019;45(1):1163–70.
79. Cox SC, Thornby JA, Gibbons GJ, Williams MA, Mallick KK. 3D printing of porous hydroxyapatite scaffolds intended for use in bone tissue engineering applications. *Mater Sci Eng C.* 2015;47:237–47.

3D Printing for Oral and Maxillofacial Regeneration



Fernando Pozzi Semeghini Guastaldi, Toru Takusagawa,
Joao L. G. C. Monteiro, Yan (Helen) He, Qingsong (Adam) Ye,
and Maria J. Troulis

1 Introduction

The management and regeneration of large maxillofacial bone defects present significant challenges for surgeons and scientists. In order to restore adequate form and function of traumatic, congenital, and ablative missing bone, autologous bone transplantation is still considered the gold standard, especially for large mandibular and maxillary continuity defects [1, 2]. Anterior or posterior iliac non-vascularized grafts were initially used for reconstruction; however, resorption and infection of grafts are common due to a lack of immediate blood supply [3].

Advancements in microvascular surgery made possible the use of vascularized grafts, such as the fibula flap, which provides a soft tissue paddle for external cover and intra-oral lining. Conversely, many centers do not have the expertise and infrastructure to perform the anastomosis of these grafts [3]. Additionally, donor site morbidity is still a concern and is associated with both types of grafts [1]. These factors compromise stability in the long-term and have detrimental effects on patient's quality of life [2, 3].

Emerging technologies and innovative techniques such as tissue engineering (TE) may represent an interesting minimally invasive alternative to autogenous bone graft procedures [4–6]. Bioengineering strategies used in developing scaffolds for applications in bone tissue damage regeneration come in multiple ways. Each of the strategies employed is directly guided by the defect and can be influenced by several general factors [7, 8].

In addition, an increasing number of patients with maxillofacial bone defects have triggered the development of new bioactive synthetic biomaterials. The

F. P. S. Guastaldi (✉) · T. Takusagawa · J. L. G. C. Monteiro · Y. (H). He
Q. (A). Ye · M. J. Troulis
Skeletal Biology Research Center, Department of Oral and Maxillofacial Surgery,
Massachusetts General Hospital, Harvard School of Dental Medicine, Boston, MA, USA
e-mail: fguastaldi@mgh.harvard.edu

combination of these new biomaterials with the establishment of rigorous protocols using mesenchymal stem cell therapies and growth factors can guide cellular and molecular pathways to improve maxillofacial regeneration. Mimicking the complex 3D architecture and functional dynamics of the maxillofacial bones is a challenging proposal that generates the need for a customized and on-demand tissue replacement strategy to obtain patient specificity that could not be achieved to date.

In the last decade, computer-assisted planning and 3D printing technology are allowing more personalized reconstructive strategies with scaffolds designed with precise dimensions, tailored structure, and complex morphologies for maxillofacial regeneration [8–10].

Maxillofacial bone forms via intramembranous ossification, in which mesenchymal stem cells differentiate into osteoblasts. They accumulate locally to form ossification centers, secrete extracellular matrix, and form calcified bone tissue [11]. This type of bone formation is also seen in bone formation of the cranium [12]. The mandible is composed of an arched body, which runs posteriorly on each side to attach to the flat ramus, which articulates the mandible to the skull through the condylar process. The maxilla houses the maxillary sinus and articulates with many other bones of the facial skeleton. This makes the maxillofacial skeletal bone complex in geometry. Moreover, it needs to be adapted to a high mechanical requirement, since these bones participate in mastication [13].

Therefore, scaffolds designed for maxillofacial bone regeneration need to meet specific strength requirements compatible with areas that are subjected to constant load [10]. Additionally, these scaffolds should be biodegradable and porous, so an ideal 3D microstructure is provided for bone ingrowth [10]. Three-dimensional printed scaffolds have been studied in large animal models either in conjunction with stem cells to engineer bone *in vitro* [14, 15] or in combination with osteoinductive materials for ectopic implantation *in vivo* before transfer to the defect site [8].

The aim of this chapter is to provide an overview of BTE strategies in conjunction with 3D printing technology to regenerate large maxillofacial bone defects. The recent evidence from both small and large animal studies is revised. The clinical application of 3D printing combined with BTE, the current limitations, and future directions are also discussed.

2 BTE for Maxillofacial Regeneration

Bone regeneration facilitated by biomaterial scaffolds, stem cells, and growth factors has been currently regarded as the most effective approach in the field of TE. For the convenience of content delivery, this part will be separately introduced. Chapter “Biomaterial Design Principles to Accelerate Bone Tissue Engineering” discussed in detail the principles of BTE that build upon the effective application of these three elements—scaffolds, cells, growth factors—for bone regeneration. This section will focus only on BTE for maxillofacial regeneration.

As previously mentioned, large jawbone defects (i.e. mandible and/or maxilla) can result from, but not limited to, congenital abnormalities, after traumatic injuries to the maxillofacial area and tumor resection. The current therapies available for surgeons for the treatment of these challenging large bone defects are mainly limited to non-vascularized autogenous bone grafts, vascularized autogenous bone grafts, and titanium-based reconstruction plates. To overcome some of the limitations of these methods, 3D printing technologies combined with TE approach may enable the production of customized bioengineered bone scaffolds. A general overview of maxillofacial regeneration using BTE approach combined with 3D printing technology is shown in Fig. 1.

In the last two decades, there have been two major leaps in understanding the osteogenesis process, which have impacted and are redirecting the BTE and regeneration efforts—immunomodulation and angiogenesis.

Immunomodulation in Bone Remodeling

First, the concept of immunomodulation is based on the idea that macrophage is related to osteogenic process in addition to its original relation with osteoclastic activity [16]. This concept in conjunction with the understanding of foreign body reaction (cell–cell and cell–materials) has fostered research aimed at establishing a passive relation between foreign bodies and the host. Immune inhibition in organ transplant serves as a good example of a passive relation. And it is still the case in today's practice. Since it is accepted that macrophages can present different modes of action (polarization) and that activated macrophages are highly related to osteogenesis enhancement, immunomodulating bone formation has become a hot topic. This osseo-immunomodulation has become a game changing concept in biomaterials fabrication for bone regeneration [17] and provided people to view the use of stem cells [18] and growth factors [19] from different perspectives.

The application of gel-based biomaterials in bone formation has been possible as it has been proved feasible using immunomodulation approaches. For instance, a stiff hydrogel has desirable mechanical property to repair bone defect. Yet it promotes osteoclastic activities when implanted. A recent study modified this stiff hydrogel to polarize macrophages and attenuated inflammatory response, which resulted in high level of bone formation [20]. Gelatin is often used in BTE due to its biodegradability. With calibrated macrophage polarization, scaffold can be controlled to release bone forming growth factor during degradation [19].

Angiogenesis in BTE

The relation between angiogenesis and bone formation has been always discussed. This discussion has evolved, and the research has shown a promising advancement in the treatment of critical size bone defects. In critical size defect repair, vasculature is a key factor to ensure the success of bone regeneration.

Because of the lack of blood vessels inside a large defect, the current best bone regeneration strategy is a combination of a biomaterial scaffold, stem cells, and growth factors, which are the key components to regenerate bone [11, 18, 21]. Angiogenesis in BTE techniques is achieved through growth factors [22] and/or stem cells [23] application to stimulate vessel formation and vessel by-pass surgical

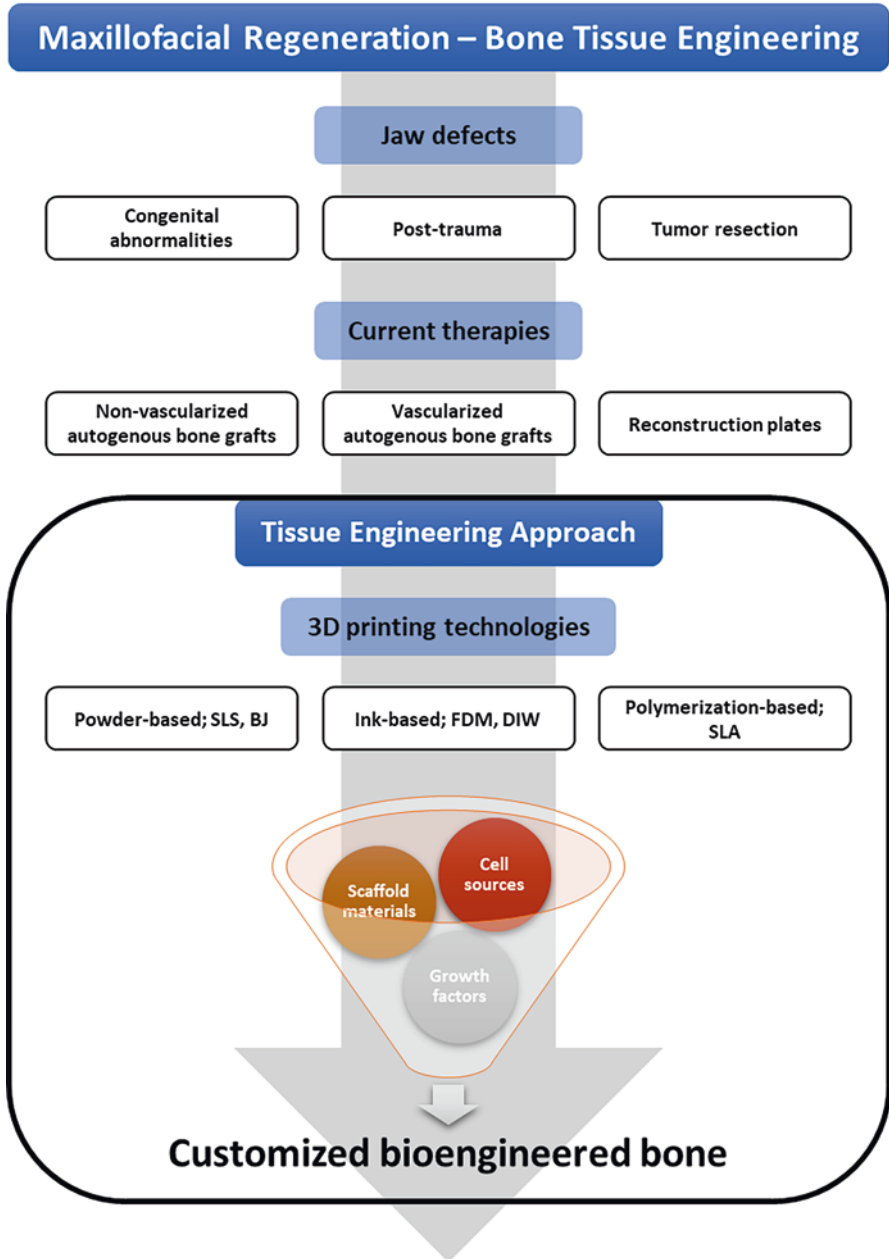


Fig. 1 General overview of maxillofacial regeneration using BTE approach. Main etiologies of large jaw defects, most used therapies in the clinical setting, 3D printing technologies combined with TE approach to produce customized bioengineered bone scaffolds. *SLS* selective laser sintering, *BJ* binder jetting, *FDM* fused deposition modeling, *DIW* direct ink writing, *SLA* stereolithography

procedures to provide direct access to blood supply [24]. In 2005 research reported capillary penetration in pure scaffold materials with certain microstructure prior to bone formation [25–27]. Chapter “Strategies for 3D Printing of Vascularized Bone” will discuss in more detail the current vascularization strategies in 3D printing for BTE.

In the last decade, a growing body of research has proved that angiogenesis could also be achieved via biomaterials. Due to various kinds and forms of scaffold materials, there has not been developed a universal fabrication parameter of biomaterials promoting angiogenesis and osteogenesis. Keeping in mind that angiogenesis as one of many expectations in an ideal BTE process, a balanced strategy incorporating all essential properties will be optimal.

2.1 Scaffolding Biomaterials

For a feasible clinical application, besides common properties such as biocompatibility, biodegradability (optional), and immunomodulation, scaffold properties like porosity, interconnectivity, and mechanical integrity are required for optimal bone regeneration [28] (Figs. 2 and 3). To satisfy these properties, various types of materials (metal, polymers, ceramics, etc.) in diverse forms (block vs. mesh in metal; solid vs. gel in polymer; granule powder vs. porous bulk in ceramic; etc.) have been synthesized and further modified [29, 30].

In Vivo Evaluation of Biomaterials for BTE in the Field of OMFS

Biomaterials have been used as scaffolds for bone engineering and studied extensively. The commonly used ones are β -TCP, titanium (Ti), and chitosan. Previous studies showed that the bone regeneration could be enhanced significantly if these biomaterials were used with other bioactive factors, i.e. stem cells and/or growth factors.

In the field of oral and maxillofacial surgery, β -TCP showed an increase in bone tissue regeneration when BMSC in combination with growth factors were used in comparison to a pure β -TCP scaffold [31]. Clinical studies showed that Ti scaffolds incorporated with BMSCs and PRP have repaired alveolar cleft defects [32]. A study using rat mandible showed that Ti membranes coated with TGF- β 1/IGF-I could significantly accelerate the healing process and lead to nearly full bony bridging of critical-sized defects [33]. Another study used different amounts of resin (RS) incorporated with chitosan-hydroxyapatite (CHA) to develop a triconstituent nanoensemble CHA-RS. The results suggested that, within 2 weeks, the optimal group (CHA-1RS) enhanced the bone regeneration significantly, indicating CHA-1RS as a potential alternative scaffold for BTE in critical calvaria defects [34]. Table 1 shows the application of scaffold biomaterials for maxillofacial regeneration in animal models.

With the development of additive manufacturing technology, 3D-printed scaffolds have drawn more and more attention for BTE. A previous study showed that

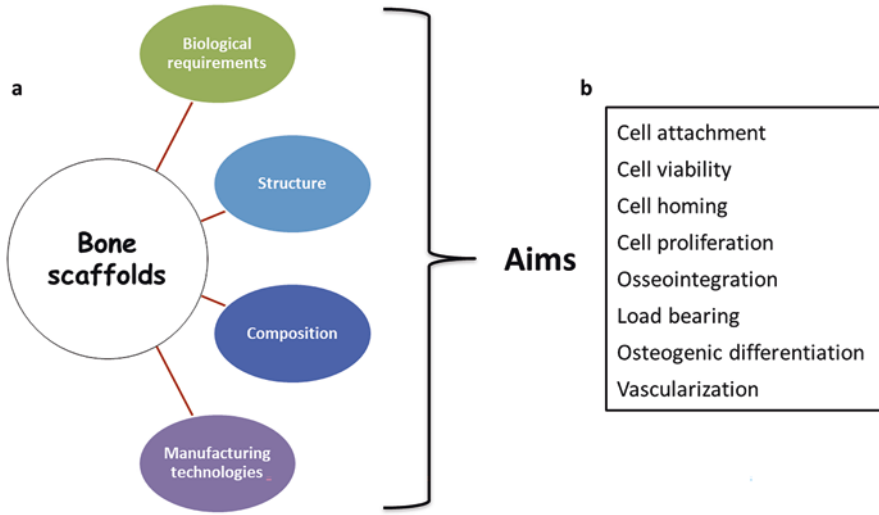


Fig. 2 (a) Characteristics of bone scaffolds for BTE applications and maxillofacial regeneration; (b) desired biological behavior of bone scaffolds after in vivo implantation

Biological requirements	Structure	Composition	Manufacturing technologies
Non-toxic	Biomimetic	Ceramics	Conventional
Biocompatible	Tailored architecture	Polymers	Gas foaming
Biodegradable	Customized shape	Metals	Solvent casting
Non-immunogenic	High porosity	Composites	Freeze drying
Bioactive	Pore size		Advanced
Osteoconductive	Pore interconnection		Electrospinning
	Mechanical properties		Rapid prototyping
	Surface topography		

Fig. 3 The biological requirements, structure properties, composition, and manufacturing technologies of bone scaffolds for maxillofacial regeneration

3D-printed β -TCP scaffolds coated with sphingosine 1-phosphate could play dual roles, either promoting osteogenesis or inhibiting inflammatory responses [36]. Gelatin and modified gelatin have been used as scaffolds to repair cleft defects. Results showed that modified scaffolds with bioactive factors led to more bone formation in comparison to unmodified ones [37]. Furthermore, gelatin-methacryloyl (GelMA) based photosensitive hydrogels can be used as bio-ink for 3D printing

Table 1 In vivo application of scaffold biomaterials for maxillofacial regeneration (animal models)

Biomaterials	Applied with	Animal model	Defect site	Follow-up	Evaluation method	Bone formation fold to control
PCL	BMSCs	Rodent	Femur	12 weeks	Micro-CT	Bone volume (mm ³): 25/10 = 2.5
Hyaluronic acid	BMSCs	Rodent	Calvaria	4 weeks	Histology	Bone percentage (%): 61/16 = 3.8
PLGA	ADSCs	Rodent	Calvaria	12 weeks	Histology	Bone percentage (%): 72/38 = 1.9
Ti	ADSCs	Rodent	Calvaria	8 weeks	Histology	Bone percentage (%): 151/57 = 2.6
Chitosan	BMSCs	Rodent	Calvaria	8 weeks	Micro-CT	More bone formation in cell-seeded constructs: (no quantitative analysis)
PCL/ Beta-TCP	BMSCs	Rodent	Femur	3 weeks	Micro-CT	Bone volume (mm ³): 1/0.3 = 3.3
PLGA	BMSCs	Rodent	Calvaria	20 weeks	Histology	Bone percentage (%): 54/20 = 2.7
Collagen	BMSCs/ ADSCs	Rodent	Calvaria	8 weeks	X-ray	BMD percentage (%): 100/60 = 1.7 (both BMSCs and ADSCs)
Collagen; PLGA; HA	ADSCs	Rodent	Calvaria	18 weeks	Histology	BMD (g/cm ²): 4 collagen; 1.6 PLGA; 2 HA
PLGA	ADSCs	Rodent	Calvaria	8 weeks	Histology	Bone percentage (%): 100/42 = 2.4
BCP	ADSCs	Rodent	Femur	16 weeks	Histology	Bone percentage (%): 89/40 = 2.2
Collagen	DPSCs	Rodent	Parietal bone	6 weeks	Histology	Bone percentage (%): 69/38 = 1.8

PCL polycaprolactone, *BMSCs* bone marrow stem cells, *PLGA* poly(lactic-co-glycolic acid), *ADSCs* adipose-derived stem cells, *Ti* titanium, *β-TCP* beta-tricalcium phosphate, *BMD* bone mineral density, *HA* hydroxyapatite, *BCP* biphasic calcium phosphate

Note: Table adapted from Ma et al. [35]

when exposed to UV lights or visible light (depending on the photo-initiators). This is a promising technique for 3D biofabrication.

2.2 Stem Cells as Seeding Cells

In bone regeneration, three types of stem cells have been extensively explored: bone marrow mesenchymal stem cells (BMSCs), adipose stem cells (ADSCs), and stem cells from dental tissue. The combination of biomaterials, stem cells, and growth factors is regarded as the best bone formation strategy currently. Research has been developing to maximize the potency of stem cells. In critical size bone defect, the

cell quantity in need is large. To address this issue, several approaches have been made, such as optimizing cell seeding density, promoting cell proliferation, and preventing cell apoptosis [38].

Due to higher proliferation capacity of these stem cells, the seeding density should be set at a relative low level because of contact inhibition and nutrition perfusion. As discussed in the previous section, there are so many types of scaffold materials being studied in osteogenesis. Scaffold properties vary and could not yield a systematic conclusion on optimal cell seeding density. Yet, it has been suggested that mineralization activity is proportional to cell density. When the cell density exceeds a certain limit, mineralization activity decreases [35]. The affinity of scaffold to stem cells affects the seeding efficiency, which influences the seeding density and bone forming capacity. Generally, a high affinity of scaffold is appreciated and is achieved by screening proper scaffold material and modifying the scaffold. Another approach to increase the seeding efficiency is to optimize the seeding methodology [39], i.e. bioreactor [15] and vacuum pressure [35].

Cellular proliferation varies in different cell types. For example, stem cells from dental tissue have shown a better proliferation than BMSCs. Maintaining the tissue regenerative potency of stem cells stored in liquid nitrogen is a shared challenge both in research studies and clinical application where cryopreservation and defrosting are part of routine procedures. It has been found that basic fibroblast growth factor (bFGF) can improve cellular proliferation and prevent apoptosis of dental pulp stem cells (DPSCs) after cryopreservation [40].

Bone Marrow Derived Stem Cells

The bone forming capacity of BMSCs was first studied among all stem cells. As discussed, despite BMSCs not being as efficient in bone formation as lipid-free dedifferentiated fat cells (DFAT) or stem cells from dental tissue, they usually serve as a positive control when studying tissue regeneration potency of other types of stem cells. Many approaches have been employed to enhance its capacity in bone formation especially in critical size defects. miRNA21 has been suggested to maintain the homeostasis in bone tissue [41]. When the expression of miRNA21 is inhibited, the bone formation ability of osteoblast is lost, and the apoptosis of osteoclasts is increased. Recently miRNA21 was applied in conjunction with BMSCs to improve osteogenesis in critical size defects located at load bearing areas of dog's mandibles [42] via the PTEN/PI3K/Akt/HIF-1 α pathway, an important regulatory pathway in osteoblast differentiation [43].

Vasculature is important to the successful repair of critical size bone defects. HIF-1 α is generally accepted to influence all critical angiogenic growth factors in hypoxia condition [44]. HIF-1 α is recently related to enhance osteogenesis of human mesenchymal stromal cells in hypoxia condition [45]. As a protein, the stability and activity of HIF-1 α at nonhypoxic condition are poor [46]. With genetic modification via lentivirus transfection, BMSCs could express a constitutively active hypoxia-inducible factor-1 α (HIF-1 α) protein. When these genetically modified BMSCs were applied on a critical size calvaria defect, an improved bone formation was observed in 8-week post-surgery [47].

Adipose-Derived Stem Cells

Generally, BMSCs work better in bone formation than adipose tissue-derived stem cells (ADSCs) [48]. However, it has been shown that DFAT have a higher differentiation capability of becoming osteoblasts than BMSCs and ADSCs do [49]. In critical size bone defect repair, DFAT could effectively regrow bone in rat mandibles [50], alveolar bone defects (three wall periodontal bone defect) [51], a severe alveolar defect in the maxillofacial region and periodontal fenestration defect [52], and cleft defects [37].

Dental Tissue Derived Stem Cells

Compared with BMSCs and ADSCs, stem cells from dental tissue showed promising bone formation application due to their immunomodulatory capacity, where osteoclastogenesis has been regarded important during bone formation [53]. Dental stem cells were found to regulate inflammatory cytokine levels and bone resorption in response to the inflammation status.

So far several sub-types of stem cells from dental tissue have been identified: stem cells from human exfoliated deciduous teeth (SHED), dental follicle stem cells (DFSC), stem cells from apical papilla (SCAP), dental pulp stem cells (DPSCs), gingival mesenchymal stem cells, periodontal ligament stem cells, bone marrow mesenchymal stem cells from alveolar bone, periapical cyst-mesenchymal stem cells. Most of them are collected involving less invasive procedures. The collection of SHED and DPSCs requires no additional harm to individual and they have long period for collection. Table 2 summarizes the bone regenerative application of all stem cells from dental tissue.

The safety of the use of stem cell conditioned medium in human alveolar bone repair has been verified in clinic [55]. Human mesenchymal stem cell could provide similar bone healing outcome compared to β -TCP. Potential underlying mechanisms may lie on that the growth factors secreted by the stem cells enhance bone formation as well regulate inflammation.

2.3 Growth Factors

Growth factors are used in bone regeneration for various purposes including angiogenesis, proliferation, and osteogenesis. For angiogenesis and cell proliferation purpose, the application of growth factors has been discussed in previous sections. Growth factors that directly enhance bone formation will be discussed in this section.

Platelet-Rich Plasma (PRP)

Platelet-rich plasma (PRP), first introduced by Marx et al. [56] to perform tissue regeneration in maxillofacial reconstruction, has been extensively proved in bone regeneration. It contains a cocktail of growth factors including platelet-derived growth factor (PDGF), transforming growth factor- β (TGF- β), and insulin-like growth factor-1 (IGF-1) [57]. PRP may accelerate bone formation at early stage,

Table 2 Stem cells from dental tissue and its application in bone formation

Cells	Bone regeneration capacity	In vivo/in vitro	Easy access	References
Stem cells from human exfoliated deciduous teeth (SHED)	+++	In vivo	+++	Nakajima et al. [53]
Dental pulp stem cells (DPSCs)	++	In vivo	+++	Nakajima et al. [53]
Dental follicle stem cells (DFSCs)	++	In vivo	+	Nakajima et al. [53]
Periodontal ligament stem cells	–	In vitro and in vivo	+	Li et al. [54]

2 weeks after implantation. There is no obvious additional impact on bone formation when PRP is used alone with scaffold in animal studies (Table 3). Yet when PRP is teamed up with stem cells or other growth factors, the combination could provide a significant osteogenic effect [64].

Bone Morphogenetic Proteins (BMPs)

Most studied growth factors for bone formation are bone morphogenetic proteins (BMPs). Despite there might be variation, BMPs influence the bone formation in different manners. For example, out of more than 15 types of known BMPs, only BMP-2, 6, and 9 could direct the osteoblast differentiation of mesenchymal stem cells. Most BMPs could enhance the osteogenesis of mature osteoblasts [65]. Among all families, only recombinant human BMP-2 and 7 (rhBMP-2, rhBMP-7) have been approved by the US Food and Drug Administration (FDA) for clinical application [66, 67].

Besides a strong bone forming ability, BMPs also showed immunomodulation in pathological conditions. For instance, BMP-2 and BMP-4 mediate inflammatory phenotype of endothelium in response to tissue injury [68]. A recent study on BMP-2 summarized a good angiogenic and osteogenic ability when applied with scaffold material in murine bone defect models [69].

Direct application of growth factor has several drawbacks including short half-life, high costs, potential systemic side-effects, and an incompletely understood dose dependency. Hence solutions have been tried to resolve these shortcomings including dual delivery of growth factors, BMP-2 gene transfection by a virus, and application of BMP-2 antibody. The use of monoclonal antibodies against BMP-2 captures the endogenous BMP-2 ligands and presents them to progenitor cells [70].

To reduce undesired side effect of BMP-2, cell homing factor (SDF-1) and BMP-2 were loaded in hydrogel to repair a critical size calvaria model. The study showed osteogenesis outcome was maintained and even enhanced compared with the control when BMP-2 level in dual growth factor delivery was reduced to 1/10 of the concentration used in control (BMP-2 only) [71].

Table 3 Comparison of PRP application for bone formation

	Additional materials	Defect model	Outcome
PRP	Scaffold material: autogenous bone and inorganic bovine bone (Bio-Oss) particles	Goat, forehead, round	Compared with scaffold material: addition of PRP failed to enhance early and late bone healing was not enhanced when PRP was used [58]
PRP	Scaffold material: inorganic bovine bone (Bio-Oss) or autologous rib bone	Rat, mandible	Compared with BMP-7: addition of PRP failed to enhance bone formation in either scaffold [59]
PRP	Scaffold material: autogenous bone, tricalcium-phosphate granules (Cerasorb), bovine spongius blocks (Bio-Oss) and a bovine bone inducing collagenous sponge (Colloss, with BMP-2)	Mini-pig, forehead	Compared with BMP-2: addition of PRP failed to enhance bone formation in xenogeneic bone substitutes PRP significantly promoted bone formation of autogenous bone in early stage, 2 w post implantation [60]
PRP autologous	HA/ β -TCP	Rabbit, cranium, bi-cortical	Compared with scaffold: addition of PRP failed to enhance bone formation in 2, 4, and 6-week post-implantation [61]
PRP	β -TCP and angiogenic components (combination of VEGF and platelet microparticle)	Rat, cranium	Compared with scaffold: addition of PRP failed to enhance bone formation; addition of PRP + angiogenic components significantly enhanced bone formation [62]
PRP	Autogenous bone/bovine collagen-based scaffold	Pig, forehead	Compared with scaffold: addition of PRP failed to enhance bone formation Autogenous bone + PRP showed a significant accelerating effect on early bone regeneration (2 weeks) [63]

3 Preclinical Studies: BTE of the Mandible

In the past, different techniques have been described and used to fabricate scaffolds, such as gas foaming, solvent casting, and freeze drying. However, there are important limitations associated with these techniques: the use of organic solvents, long fabrication periods, labor-intensive process, effects of residual particulates in the scaffold matrix, poor repeatability, irregularly shaped pores, insufficient interconnectivity of pores and thin structures [72]. These drawbacks have been addressed with rapid prototyping technologies such as 3D printing [7, 8, 10, 14, 15, 73]. Table 4 presents a summary of BTE strategies for mandible reconstruction in pre-clinical large animals.

Table 4 BTE of the mandible in preclinical large animals

Author/year	Animal model	Anatomical area	Biomaterials	Stem cells	Growth factors	Bioreactor	Follow-up	Evaluation methods
[74]	Swine	Mandible; body and ramus	PLGA	Autologous pBMPCs differentiated into osteoblast	–	ROBS; 10 days	6 weeks	<ul style="list-style-type: none"> • X-ray • Histology
[75]	Swine	Mandible; body	PLGA and tooth-constructs	Autologous pBMPCs differentiated into osteoblast	–	ROBS; 10 and 14 days	12 and 20 weeks	<ul style="list-style-type: none"> • X-ray • VCT • Histology
[15]	Swine	Mandible; body	β -TCP/PCL	Autologous pBMSCs differentiated into osteoblast	–	ROBS; 10 and 14 days	8 weeks	<ul style="list-style-type: none"> • Histology • Immunohistochemistry • Histomorphometry
[14]	Swine	Mandible; ramus-condyle unit	Decellularized bovine cancellous bone	Autologous ADSCs	–	Advanced bioreactor system that provided environmental control and the exchange of nutrients, oxygen, and metabolites (3 weeks)	24 weeks	<ul style="list-style-type: none"> • CT, micro-CT • Mechanical testing • Histology • Immunohistochemistry
[8]	Sheep	Mandible; angle	Morcellized autologous bone, synthetic ceramic particles, or a combination of both	–	–	Implanted against the rib periosteum of 3–4-year-old sheep (9 weeks)	12 weeks	<ul style="list-style-type: none"> • X-ray • Histology • Mechanical • Biomolecular
[76]	Swine	Mandible; body and angle	TCP-PLGA	Heterologous p-ADSCs differentiated into osteoblast	–	–	12 weeks	<ul style="list-style-type: none"> • Live/dead staining of seeded scaffolds • Micro-CT • Histology • Immunohistochemistry • Histomorphometry

PLGA poly(D,L-lactide-co-glycolide), pBMSCs porcine bone marrow stem cells, ROBS rotational oxygen-permeable bioreactor, H&E hematoxylin and eosin staining, VCT ultra high-resolution volume computed tomography (VCT), volume computed tomography, ADSCs adipose-derived stem cells, p-ADSCs porcine adipose-derived mesenchymal stem cells

3.1 Swine Mandible Reconstruction: 3D-Printed Bone Scaffolds, Autologous BMSCs, Engineered Bone In Vitro

At our Laboratory, the Skeletal Biology Research Center, Department of Oral and Maxillofacial Surgery in collaboration with the Laboratory for Tissue Engineering and Organ Fabrication, at Massachusetts General Hospital, Boston, MA, bone has been successfully bioengineered in an autologous minipig model [77]. To be clinically relevant, uniform bone and blood supply must be achieved. To address these fundamental aspects, scaffolds and seeding protocols using a rotational bioreactor system (ROBS) were modified and combined with earlier implantation protocols in Yucatan minipigs [15, 74, 75, 78].

In 2004, the SBRC at MGH first reported the reconstruction of a mandibular defect using autologous porcine mesenchymal stem cells (pBMSCs) in which bone formation was observed on the surface; however, a clinical application would require bone formation and vascularization throughout the whole construct [74]. The technique was further consolidated by attempts to generate a jaw with tooth buds by using PGA/PLLA (polyglycolide/poly L-lactic acid) scaffolds in conjunction with dental endothelial cells; however, a robust bioengineered bone was not observed in this study [75].

In 2012, Sharaf et al. reported an in vitro study of the successful use of 3D-printed β -TCP/PCL (50:50) and PCL scaffolds. The effect of small and large channel sizes (1 mm vs. 2 mm, respectively) on cellular penetration was evaluated. After 2 weeks of culturing, the β -TCP/PCL scaffolds with a small channel size showed increased cellular proliferation and depth of cell penetration.

To regenerate the bone in porcine mandibular defects, a study performed in 2015 by Konopnicki et al. used the 3D-printed β -TCP/PCL (50:50%) scaffolds with the small channel size seeded with pBMPCs and an early implantation protocol (14 days). After 8 weeks of healing the 3D-printed scaffolds seeded with pBMSCs showed good penetration of bone forming cells and neovascularization in the center of the construct.

In a recent study, we successfully fabricated a 4 × 2 cm β -TCP/PCL (50:50%) scaffold implanted in a 4 × 2 cm critical-sized defect in a minipig mandible. The scaffolds were seeded with autologous pBMSCs. The cells were treated with osteogenic medium in a rotational bioreactor (10 days) prior to implantation. After 4 and 8 weeks of healing, the results have indicated good osseointegration at the interface, and early bone formation at the center of the scaffold, as well as angiogenesis (unpublished data). However, for clinical applicability, large animal sample and long-time points are required to evaluate angiogenesis and bone formation throughout the whole construct as well as degradation of the scaffold materials (Fig. 4).

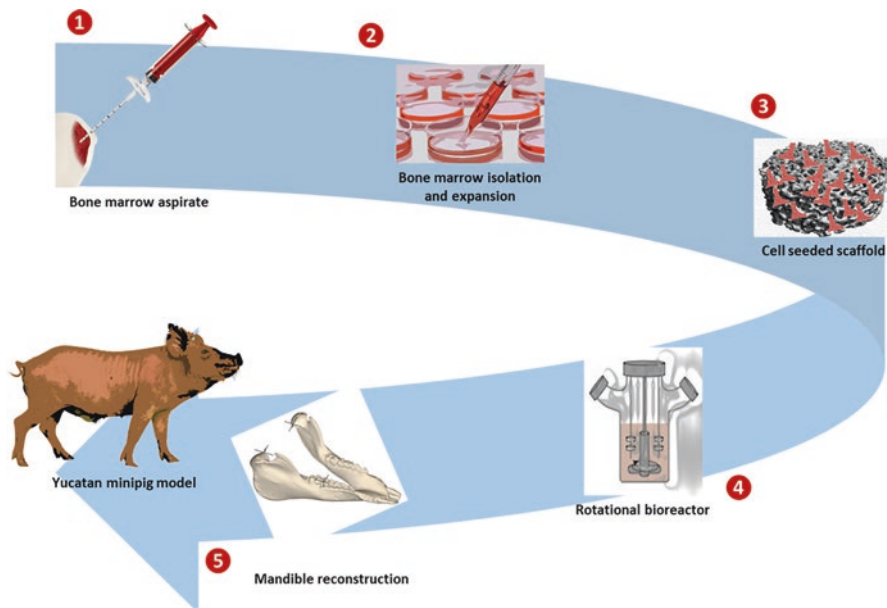


Fig. 4 Schematic sequence for the reconstruction of a Yucatan minipig model. (1) Autogenous bone marrow aspiration; (2) Isolation and expansion of porcine bone marrow stem cells (pBMSCs); (3) Scaffolds seeded with pBMSCs (constructs); (4) Incubation in a rotational oxygen-permeable bioreactor system (ROBS); (5) Construct implantation to reconstruct a critical-sized minipig mandibular defect

3.2 *Swine Mandible Reconstruction: Anatomical Shaped Bioreactor, Autologous ADSCs, Engineered Bone In Vitro*

In recent years, decellularized tissues have been widely applied as a transplant material, serving as three-dimensional extracellular matrixes (ECM) for tissue regeneration purposes. The cellular components can be removed by various decellularization techniques, which have a strong influence on the morphology, structure, mechanical properties, and biological activity of the obtained tissue. The ECMs are conserved between species in terms of structure and composition, hindering the chance of immune rejections. Moreover, it has been reported that cells cultured on ECM of a specific tissue differentiate into cells of that tissue [79].

The study by Bhumiratana et al. [14] investigated the use of a clinically approved decellularized bovine cancellous bone as a scaffold material to reconstruct the ramus-condyle unit in a swine model. The decellularized bone was crafted into an anatomical shape of a condyle by image-guided micromilling. Before implantation and fixation to repair the defect, these scaffolds were seeded with autologous adipose-derived stem cells (ADSCs) and were cultured in a perfusion culture for 3 weeks to allow osteogenic differentiation. The engineered constructs were either compared to non-seeded scaffolds or untreated defects (condylectomy only). Six

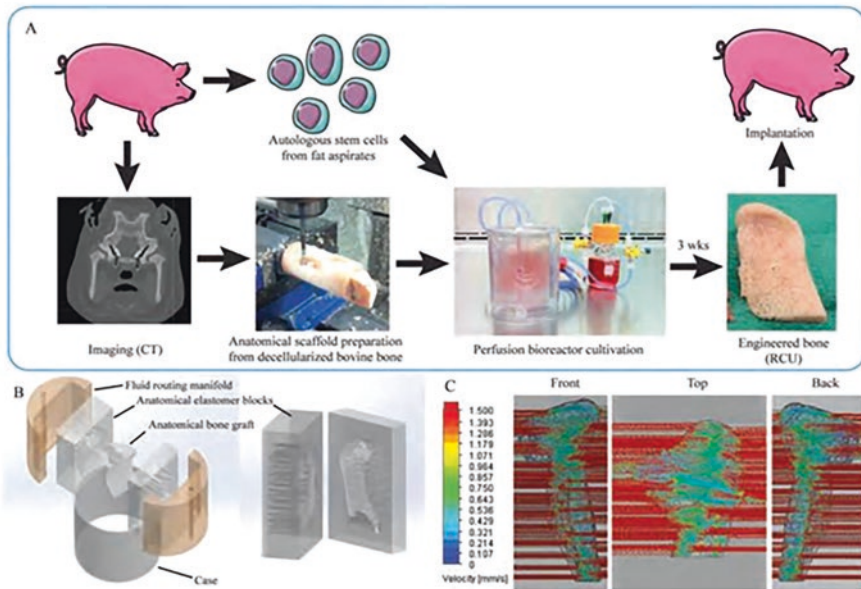


Fig. 5 (a) Personalized bone tissue engineering process. Autologous mesenchymal stem cells (from fat aspirates) and CT images were obtained for each animal subject. The anatomical scaffold was fabricated from the bovine stifle bone that had been processed to remove any cellular material while preserving the tissue matrix. The cells were seeded into the scaffold and cultured in the specially designed perfusion bioreactor. After 3 weeks, the engineered RCU was implanted back into the pig for 6 months. (b) The bioreactor culture chamber consisted of five components designed to provide tightly controlled perfusion through the anatomical scaffold: anatomical inner chamber with bone scaffold; two halves of the polydimethylsiloxane (PDMS) (elastomer) block with incorporated channels; two manifolds; and an outer casing. The PDMS block was designed as an impression of the anatomical RCU structure and contained flow channels at both sides for the flow of culture medium in and out of the scaffold. The flow rate necessary for providing nutrient supply and hydrodynamic shear was defined by the design of parallel channels in the elastomer block (with the channel diameters and distribution dictated by the geometry of the graft) and the fluid routing manifold. The channel diameters and spacing were specifically designed by flow simulation software for each pig, to provide a desired interstitial flow velocity for a given shape and size of the anatomical RCU. (c) Flow simulation of the medium flow through the anatomically shaped scaffold reveals uniform flow velocity throughout the volume of the graft. (From “Tissue-engineered autologous grafts for facial bone reconstruction” by Bhumiratana S, Bernhard JC, Alfi DM, Yeager K, Eton RE, Bova J, Shah F, Gimble JM, Lopez MJ, Eisig SB, Vunjak-Novakovic G, 2016, *Sci Transl Med.*, 8(343), 343ra83. Reprinted with permission)

months after transplantation, the engineered construct retained its anatomical structure, integrated with native tissue, and generated bone of superior quality in comparison to the other groups. Despite the relevance of obtaining new bone without harvesting it from other sites, future studies need to address some points. First, the real effect of using ADSC needs to be evaluated; for instance, using cell-lineage tracing. Secondly, since a complete decellularization might be difficult to achieve, careful discussion is required before clinical application (Fig. 5).

3.3 Sheep Mandible Reconstruction: 3D-Printed Bioreactor, Biomaterials, Ectopic Implantation In Vivo

In contrast to previous studies in which angle defects were analyzed, the study by Tataru et al. [8] used a more superior and marginal defect in a region subjected to mechanical forces and that is adjacent to the oral mucosa. A two-stage mandibular reconstruction was used. First, the mandibular defect was created, and a customized porous space maintainer made of poly(methylmethacrylate) (PMMA) was implanted. Meanwhile, 3D-printed bioreactors with the dimensions of the defect were obtained and filled with either a synthetic (SG) or autogenous graft (AG) and further implanted against the periosteum of the rib cage. This allowed the migration of native cell populations for osteogenic differentiation. After a period of 9 weeks, the bone generated inside the bioreactors was transferred and plated into the mandibular defect gap. Sheep were euthanized after 12 weeks and the reconstructed samples were analyzed. The results suggested the both materials (SG and AG) could produce mineralized tissue suitable for transfer; however, AG generated a more mature bone with mechanical properties similar to the native bony tissue (Fig. 6).

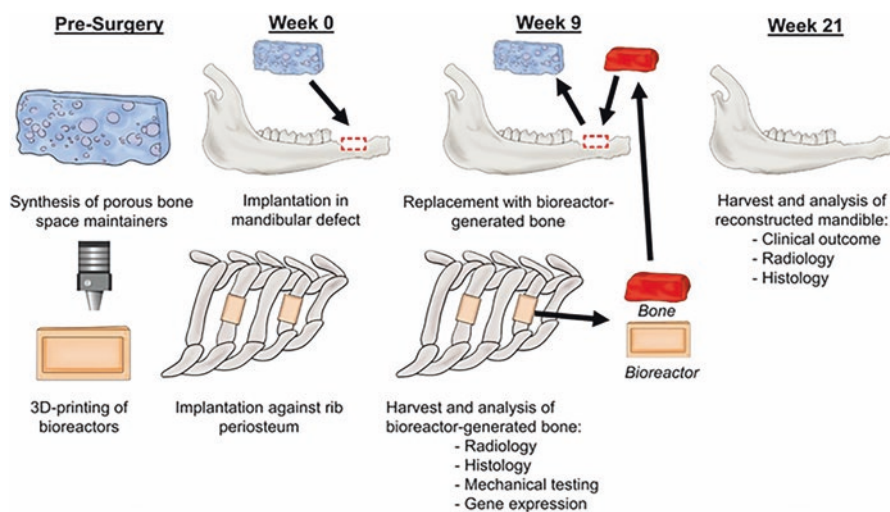


Fig. 6 Schematic of the use of the in vivo bioreactor strategy for reconstruction in a sheep model. PBSMs were fabricated, and bioreactors were 3D printed to the shape of the mandibular defect. At Week 0, a defect was made in the mandible and four bioreactors were implanted against the periosteum of the rib. The mandibular defect space was preserved by insertion of the PBSM. At Week 9, bioreactors were harvested for analysis or for use as vascularized free flaps in the reconstruction of the mandible. At Week 21, the mandibles were harvested to analyze the success of the strategy for mandibular reconstruction. (From “Biomaterials-aided mandibular reconstruction using in vivo bioreactors” by Tataru AM, Koons GL, Watson E, Piepergerdes TC, Shah SR, Smith BT, Shum J, Melville JC, Hanna IA, Demian N, Ho T, Ratcliffe A, van den Beucken JJJP, Jansen JA, Wong ME, Mikos AG, 2019, PNAS, 166(14), 6954–6963. Reprinted with permission)

4 Clinical Application of BTE and 3D Printing in OMFS

Three-dimensional (3D) printing technology, also named additive manufacturing or rapid prototyping technology, was first described in 1986 and has wide applications in medicine and dentistry and is rapidly expanding. It has revolutionized the health-care system by building biomedical models, customized implants, and prostheses.

In the field of oral and maxillofacial surgery, 3D printing is being used in the creation of anatomical models to assist surgeons in surgical planning, in obtaining surgical guides, in medical training and education, and in the production of customized medical devices (implants and prostheses) [73, 80]. Table 5 describes the current applications along with the main advantages of 3D printing technology in OMFS.

Also, it is a very interesting process because of its great potential use in fabricating scaffolds for BTE applications [73]. This approach can design scaffolds with customized shapes and fully interconnected porous structures. Thus, 3D-printed scaffolds can mimic native bone tissue and provide an appropriate environment for cell migration, proliferation, and differentiation. This emerging technology based on a computer-aided design (CAD)/computer-aided manufacturing (CAM) process became of high interest for the regeneration of maxillofacial bone defects and in the field of TE, due to its capacity of creating complex scaffolds with a custom, patient-specific design and high precision [10, 73, 81].

In a recent integrative review ([82]; unpublished data) of articles published up to date, only 20 reports were found describing patients that were treated with 3D printing technology and/or TE for reconstruction of segmental bone defects of the mandible or the maxilla. Fifteen defects were due to tumor ablation, four were cleft cases, and one was related to trauma. The defects had a mean size of 8.1 cm. In all cases, patient-specific devices and scaffolds were manufactured with the aid of CT-imaging, and the printing techniques reported were stereolithography (SLA), selective laser sintering (SLS), and selective laser melting (SLM). The devices were

Table 5 Applications and advantages of 3D printing technology in oral and maxillofacial surgery (OMFS)

3D printing in OMFS	
Applications	Advantages
Surgery plan	Visualize the lesion realistically
Pre-bending of reconstruction plates for trauma and defects	Preoperative plate pre-bending
Orthognathic surgery	Preoperative simulation
Facial prosthesis	Esthetic improvement
TMJ reconstruction	Accurate functional recovery
Dental implant	Improve its accuracy and treatment time
Surgeon training	Perform the treatment method on the model
Information sharing with patients	Help visual understanding and help avoid medical disputes

mainly made of titanium (Ti); however, one case mentioned a biodegradable material (PCL).

Cases were treated with 3D-printed Ti devices only or using 3D-printing technology in conjunction with a variety of TE approaches such as: seeding of scaffolds with bone marrow stem cells (BMSCs), filling Ti meshes with autogenous bone alone or together with deproteinized bovine bone (Bio-Oss[®], Geistlich Pharma AG, Switzerland) or BMP-2, or with beta-tricalcium phosphate (β -TCP) granules after an incubation period in media containing BMP-2. Three cases reported the patient's body as a bioreactor. Taking a closer look at the timepoint of publication, it turns out that in early stage clinical trials only TE approaches were reported. In the recent years, the combination of TE approach and 3D printing technology represents most cases.

5 3D Printing of Customized Bone Scaffolds: Workflow

The production of custom 3D-printed scaffolds using medical imaging combined with computer modeling and designing should be considered as a promising alternative for the regeneration of large maxillofacial bone defects. Over the last decade 3D printing technology is becoming affordable for surgeons and patients, and devices and scaffolds can be manufactured in a cost and time-efficient manner, leading to personalized implants that fit one unique individual matching the concept of individualized medicine.

The process starts with the proper selection of the patient and a thorough evaluation of the bone defect that requires maxillofacial regeneration (i.e. mandible and/or maxilla). A 3D-printed scaffold can be produced using the rapid prototyping (RP) technique, using data from medical images such as: computed tomography (CT) and magnetic resonance imaging (MRI) [83–85]. Details of this method are discussed in chapter “Additive Manufacturing Technologies for Bone Tissue Engineering”.

The process from image acquisition to the final 3D-printed customized bone scaffold is as follows (Fig. 7): the patient with a jaw defect will undergo a CT scan. This will enable the acquisition and storage of DICOM (Digital Imaging and Communication in Medicine) files; next, the DICOM files will be imported into a medical image computer-aided design (CAD) software; then, CT images will be segmented, 3D virtual models will be generated, and the file will be converted in STL (Standard Tessellation Language) files.

Once this part is successfully completed, the next step requires the proper selection of the biomaterial(s) and the selection of the 3D printing technique; this will lead to the production, layer-by-layer, of the 3D-printed customized bone scaffold; once the 3D printing process is completed the last, but not least step is the

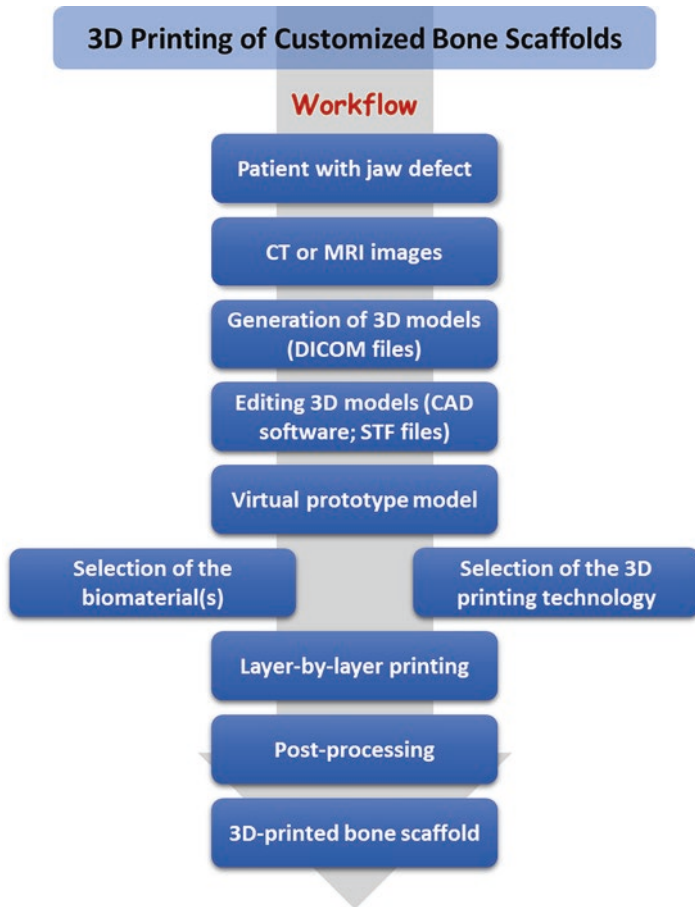


Fig. 7 Workflow to produce 3D-printed customized bone scaffolds for maxillofacial regeneration

post-processing of the 3D-printed bone scaffold (cleaning, heat treatment, sterilization, and packaging) [83–86]. The heat treatment and the sterilization of 3D-printed bone scaffolds will be determined and guided by the printed biomaterial(s); inappropriate post-processing care can damage the 3D-printed bone scaffold compromising its final use.

The overall goal after the reconstructive procedure is the rehabilitation of the patient with dental implants and prosthesis. Even though it seems obvious that the regenerated bone is capable of anchoring dental implants, there is a lack of studies showing dental implants placed in reconstructed jaws using 3D-printed bone scaffolds and the long-term stability of these implants.

6 Current Limitations of 3D-Printed Bone Scaffolds for Maxillofacial Regeneration

In this section we will discuss two of the main limitations for the clinical use of 3D-printed bone scaffolds for maxillofacial regeneration: (a) the scarcity of clinical trials and (b) the vascularization of bone scaffolds. In chapter “Strategies for 3D Printing of Vascularized Bone” we will discuss in detail vascularization strategies to overcome the current hurdles in BTE, and in chapter “Development of Additive Manufacturing-Based Medical Products for Clinical Translation and Marketing” we will cover the current barriers to translate 3D-printed products to the marketplace and the clinic.

The overall goal in BTE is to create customized bone scaffolds or co-constructs (bone, teeth, nerve, etc.) with precise form and shape to reconstruct missing structures of the mandible and the maxilla [5]. The greatest limitation of this approach to date is the scarcity of clinical trials. Nevertheless, data from several preclinical studies [8, 14, 15, 75, 87], as well as the positive outcomes reported in a few clinical trials [88–90]. Positive outcomes are generally defined as absence of complications, postoperative corrections, or total revision after the maxillofacial regeneration. Just a few studies state a positive outcome with objective criteria such as bone mineral density, measured in Hounsfield Units (HU), millimeters of mouth opening, and stable occlusion [88–90]. In contrast, in cases which postoperative second surgical interventions were performed, or complications occurred, are considered as partially successful. Postoperative complications are described as suture dehiscence, fistula occurrence, and necrosis of the reconstructed bone. In most clinical trials there is a lack in reporting the outcome with objective and standardized data and long-term follow-up.

Results from both preclinical and clinical studies are encouraging and suggest that BTE approach using 3D printing technology has great potential to be translated to the clinical setting of maxillofacial regeneration. Future developments in the field of TE will have a significant impact on managing anatomic and physiological changes and will definitively drive the way surgeons restore damaged tissues of the skeleton.

Although BTE strategies and 3D printing technology represent a promising alternative to current approaches and techniques for maxillofacial bone regeneration, there are some important questions that need to be addressed before the translation of 3D-printed bone scaffolds to the marketplace and the clinic (i.e. regulatory considerations, large scale production, safety, costs). In addition, the current available techniques for the surgeon have extensive scientific evidence and long-term follow-up studies showing the advantages and disadvantages that should be taken into consideration when deciding the best approach for each patient.

Vascularization

Deep cell penetration and angiogenesis are crucial conditions for the survivor and for the clinical success of a bone scaffold. Vascularization is considered one of the

biggest challenges in the field of BTE [91]. Clinical success of autologous bone grafting depends on the angiogenesis induced at the recipient site within the first 48 h after implantation.

In order to maintain the viability of the grafted cells, the process of forming new vessels is essential. For this, the implanted construct should contain implementing pro-angiogenic factors (such as vascular endothelial growth factor secreted by osteoblastic cells) to induce formation of new vessels from adjacent connective tissue. Furthermore, prior to deposition of the extracellular matrix, the construct should physically allow the vessels to reach the center of the scaffold [15, 78].

Several strategies have been suggested to overcome this challenge. Two ways currently described for maxillofacial regeneration are: (a) *in vitro* pre-vascularization and (b) *in vivo* pre-vascularization [91]. Chapter “Strategies for 3D Printing of Vascularized Bone” describes these strategies in detail.

7 Conclusion

The regeneration of large maxillofacial bone defects presents significant challenges for surgeons and scientists. With the constant advancement of technology, with the development of new materials and approaches, the ability to develop customized bioactive scaffolds will become more sophisticated.

Successful BTE is mainly determined by the following three components: a suitable scaffolding biomaterial, osteogenic stem cells, and bioactive growth factors. Among the various BTE technologies tested *in vitro* and *in vivo*, few have moved forward to clinical trial. The translational (from bench to bed) efficacy of these techniques has not yet reached its full potential.

Three-dimensional printing technology has drawn significant attention in the field of BTE, as an attractive process due to its great potential for use in the manufacture of artificial substitutes. It is considered a relatively fast manufacturing technique, has become economically viable, and allows the customization of bone scaffolds. This technology has provided a new platform for basic and translational research and has shown promising results for maxillofacial regeneration.

Looking to the future, 3D biofabrication technique will emerge. Therefore, more requirements will be added to the three key components of bone engineering: (a) the scaffolding biomaterial should be printable; (b) the stem cells will be cultured in a 3D system; (c) more stable growth factors are needed so the bioactivity will not be lost during the 3D printing process. Furthermore, well-designed clinical trials are needed to speed up the translation from lab bench to the clinical bedside.

A future in which medical treatment has become highly personalized, with specific and individualized treatments, contrary to the “one size fits all” concept, is being practiced. Precision medicine is in focus and has become more relevant to clinical practice based on scientific evidence.

References

1. Nkenke E, Neukam FW. Autogenous bone harvesting and grafting in advanced jaw resorption: morbidity, resorption and implant survival. *Eur J Oral Implantol*. 2014;7(Suppl 2):S203–17.
2. Sethi A, Kaus T, Cawood JI, Plaha H, Boscoe M, Sochor P. Onlay bone grafts from iliac crest: a retrospective analysis. *Int J Oral Maxillofac Surg*. 2020;49(2):264–71.
3. Akinbami BO. Reconstruction of continuity defects of the mandible with non vascularized bone grafts. Systematic literature review. *Craniomaxillofac Trauma Reconstr*. 2016;9(3):195–205.
4. Aghaloo TL, Hadaya D. Basic principles of bioengineering and regeneration. *Oral Maxillofac Surg Clin North Am*. 2017;29(1):1–7.
5. Konopnicki S, Troulis MJ. Mandibular tissue engineering: past, present, future. *J Oral Maxillofac Surg*. 2015;73(12 Suppl):S136–46.
6. Melville JC, Mañón VA, Blackburn C, Young S. Current methods of maxillofacial tissue engineering. *Oral Maxillofac Surg Clin North Am*. 2019;31(4):579–91.
7. Roseti L, Parisi V, Petretta M, Cavallo C, Desando G, Bartolotti I, Grigolo B. Scaffolds for bone tissue engineering: state of the art and new perspectives. *Mater Sci Eng C Mater Biol Appl*. 2017;78:1246–62.
8. Tataru AM, Koons GL, Watson E, Piepergerdes TC, Shah SR, Smith BT, Shum J, Melville JC, Hanna IA, Demian N, Ho T, Ratcliffe A, van den Beucken JJJP, Jansen JA, Wong ME, Mikos AG. Biomaterials-aided mandibular reconstruction using in vivo bioreactors. *PNAS*. 2019;116(14):6954–63.
9. Largo RD, Garvey PB. Updates in head and neck reconstruction. *Plast Reconstr Surg*. 2018;141(2):271e–85e.
10. Shao H, Sun M, Zhang F, Liu A, He Y, Fu J, Yang X, Wang H, Gou Z. Custom repair of mandibular bone defects with 3D printed bioceramic scaffolds. *J Dent Res*. 2018;97(1):68–76.
11. Sivaraj KK, Adams RH. Blood vessel formation and function in bone. *Development*. 2016;143(15):2706–15.
12. Schmitz JP, Hollinger JO. The critical size defect as an experimental model for craniomandibulofacial nonunions. *Clin Orthop Relat Res*. 1986;205:299–308.
13. Alvarez C, Monasterio G, Cavalla F, Córdova LA, Hernández M, Heymann D, Garlet GP, Sorsa T, Pärnänen P, Lee H, Golub L, Vernal R, Kantarci A. Osteoimmunology of oral and maxillofacial diseases: translational applications based on biological mechanisms. *Front Immunol*. 2019;10:1664.
14. Bhumiratana S, Bernhard JC, Alfi DM, Yeager K, Eton RE, Bova J, Shah F, Gimble JM, Lopez MJ, Eising SB, Vunjak-Novakovic G. Tissue-engineered autologous grafts for facial bone reconstruction. *Sci Transl Med*. 2016;8(343):343ra83.
15. Konopnicki S, Sharaf B, Resnick C, Patenaude A, Pogal-Sussman T, Hwang KG, Abukawa H, Troulis MJ. Tissue-engineered bone with 3-dimensionally printed beta-tricalcium phosphate and polycaprolactone scaffolds and early implantation: an in vivo pilot study in a porcine mandible model. *J Oral Maxillofac Surg*. 2015;73(5):1016.e1011.
16. Horwood NJ. Macrophage polarization and bone formation: a review. *Clin Rev Allergy Immunol*. 2016;51(1):79–86.
17. Chen Z, Yuen J, Crawford R, Chang J, Wu C, Xiao Y. The effect of osteoimmunomodulation on the osteogenic effects of cobalt incorporated β -tricalcium phosphate. *Biomaterials*. 2015;61:126–38.
18. Zhu S, Bennett S, Kuek V, Xiang C, Xu H, Rosen V, Xu J. Endothelial cells produce angiocrine factors to regulate bone and cartilage via versatile mechanisms. *Theranostics*. 2020;10(13):5957–65.
19. Annamalai RT, Turner PA, Carson WF 4th, Levi B, Kunkel S, Stegemann JP. Harnessing macrophage-mediated degradation of gelatin microspheres for spatiotemporal control of BMP2 release. *Biomaterials*. 2018;161:216–27.

20. He XT, Li X, Xia Y, Yin Y, Wu RX, Sun HH, Chen FM. Building capacity for macrophage modulation and stem cell recruitment in high-stiffness hydrogels for complex periodontal regeneration: experimental studies in vitro and in rats. *Acta Biomater.* 2019;88:162–80.
21. Watson EC, Adams RH. Biology of bone: the vasculature of the skeletal system. *Cold Spring Harb Perspect Med.* 2018;8(7):a031559.
22. Schnettler R, Alt V, Dingeldein E, Pfefferle H, Kilian O, Meyer C, Heiss C, Wenisch S. Bone ingrowth in bFGF-coated hydroxyapatite ceramic implants. *Biomaterials.* 2003;24(25):4603–8.
23. Annabi B, Lee YT, Turcotte S, Naud E, Desrosiers RR, Champagne M, Eliopoulos N, Galipeau J, Béliveau R. Hypoxia promotes murine bone-marrow-derived stromal cell migration and tube formation. *Stem Cells.* 2003;21(3):337–47.
24. Pelissier P, Villars F, Mathoulin-Pelissier S, Bareille R, Lafage-Proust MH, Vilamitjana-Amedee J. Influences of vascularization and osteogenic cells on heterotopic bone formation within a madreporic ceramic in rats. *Plast Reconstr Surg.* 2003;111(6):1932–41.
25. Du B, Liu W, Deng Y, Li S, Liu X, Gao Y, Zhou L. Angiogenesis and bone regeneration of porous nano-hydroxyapatite/coralline blocks coated with rhVEGF165 in critical-size alveolar bone defects in vivo. *Int J Nanomedicine.* 2015;10:2555–65.
26. Hing KA, Annaz B, Saeed S, Revell PA, Buckland T. Microporosity enhances bioactivity of synthetic bone graft substitutes. *J Mater Sci Mater Med.* 2005;16(5):467–75.
27. Rustom LE, Boudou T, Lou S, Pignot-Paintrand I, Nemke B, Lu Y, Markel M, Picart C, Wagoner Johnson A. Micropore-induced capillarity enhances bone distribution in vivo in biphasic calcium phosphate scaffolds. *Acta Biomater.* 2016;44:144–54.
28. Liu C, Fu X, Pan H, Wan P, Wang L, Tan L, Wang K, Zhao Y, Yang K, Chu P. Biodegradable Mg-Cu alloys with enhanced osteogenesis, angiogenesis, and long-lasting antibacterial effects. *Sci Rep.* 2016;6:27374.
29. Carluccio D, Xu C, Venezuela J, Cao Y, Kent D, Bermingham M, Demir AG, Previtali B, Ye Q, Dargusch M. Additively manufactured iron-manganese for biodegradable porous load-bearing bone scaffold applications. *Acta Biomater.* 2020;103:346–60.
30. Xie H, Gu Z, Li C, Franco C, Wang J, Li L, Meredith N, Ye Q, Wan C. A novel bioceramic scaffold integrating silk fibroin in calcium polyphosphate for bone tissue-engineering. *Ceram Int.* 2016;42(2):2386–92.
31. Tee BC, Desai KG, Kennedy KS, Sonnichsen B, Kim DG, Fields HW, Mallery SR, Schwendeman SP, Sun Z. Reconstructing jaw defects with MSCs and PLGA-encapsulated growth factors. *Am J Transl Res.* 2016;8(6):2693–704.
32. Hibi H, Yamada Y, Ueda M, Endo Y. Alveolar cleft osteoplasty using tissue-engineered osteogenic material. *Int J Oral Maxillofac Surg.* 2006;35(6):551–5.
33. Deppe H, Stemberger A, Hillemanns M. Effects of osteopromotive and anti-infective membranes on bone regeneration: an experimental study in rat mandibular defects. *Int J Oral Maxillofac Implants.* 2003;18(3):369.
34. Shakir M, Jolly R, Khan A, Ahmed S, Alam S, Rauf M, Owais M, Farooqi M. Resol based chitosan/nano-hydroxyapatite nanoensemble for effective bone tissue engineering. *Carbohydr Polym.* 2018;179:317–27.
35. Ma J, Both SK, Yang F, Cui F, Pan J, Meijer G, Jansen J, van den Beucken J. Concise review: cell-based strategies in bone tissue engineering and regenerative medicine. *Stem Cells Transl Med.* 2014;3(1):98–107.
36. Cao Y, Xiao L, Cao Y, Nanda A, Xu C, Ye Q. 3D printed β -TCP scaffold with sphingosine 1-phosphate coating promotes osteogenesis and inhibits inflammation. *Biochem Biophys Res Commun.* 2019;512(4):889–95.
37. Sasayama S, Hara T, Tanaka T, Honda Y, Baba S. Osteogenesis of multipotent progenitor cells using the epigallocatechin gallate-modified gelatin sponge scaffold in the rat congenital cleft-jaw model. *Int J Mol Sci.* 2018;19(12):3803.

38. Chen X, Zhang T, Shi J, Xu P, Gu Z, Sandham A, Yang L, Ye Q. Notch1 signaling regulates the proliferation and self-renewal of human dental follicle cells by modulating the G1/S phase transition and telomerase activity. *PLoS One*. 2013;8(7):e69967.
39. Polak SJ, Rustom LE, Genin GM, Talcott M, Wagoner Johnson AJ. A mechanism for effective cell-seeding in rigid, microporous substrates. *Acta Biomater*. 2013;9(8):7977–86.
40. Albashari A, He Y, Zhang Y, Ali J, Lin F, Zheng Z, Zhan K, Cao Y, Xu C, Luo L, Wang J, Ye Q. Thermosensitive bFGF-modified hydrogel with dental pulp stem cells on neuroinflammation of spinal cord injury. *ACS Omega*. 2020;5:16064.
41. Smieszek A, Marcinkowska K, Pielok A, Sikora M, Valihrach L, Marycz K. The role of miR-21 in osteoblasts-osteoclasts coupling in vitro. *Cells*. 2020;9(2):479.
42. Hu B, Li Y, Wang M, Zhu Y, Zhou Y, Sui B, Tan Y, Ning Y, Wang J, He J, Yang C, Zou D. Functional reconstruction of critical-sized load-bearing bone defects using a Sclerostin-targeting miR-210-3p-based construct to enhance osteogenic activity. *Acta Biomater*. 2018;76:275–82.
43. Yang J, Park OJ, Kim J, Kwon Y, Yun CH, Han SH. Modulation of macrophage subtypes by IRF5 determines osteoclastogenic potential. *J Cell Physiol*. 2019;234(12):23033–42.
44. Manalo DJ, Rowan A, Lavoie T, Natarajan L, Kelly BD, Ye SQ, Garcia JG, Semenza GL. Transcriptional regulation of vascular endothelial cell responses to hypoxia by HIF-1. *Blood*. 2005;105(2):659–69.
45. Costa V, Raimondi L, Conigliaro A, Salamanna F, Carina V, De Luca A, Bellavia D, Alessandro R, Fini M, Giavaresi G. Hypoxia-inducible factor 1A may regulate the commitment of mesenchymal stromal cells toward angio-osteogenesis by mirna-675-5P. *Cytherapy*. 2017;19(12):1412–25.
46. Majmundar AJ, Wong WJ, Simon MC. Hypoxia-inducible factors and the response to hypoxic stress. *Mol Cell*. 2010;40(2):294–309.
47. Zou D, Zhang Z, Ye D, Tang A, Deng L, Han W, Zhao J, Wang S, Zhang W, Zhu C, Zhou J, He J, Wang Y, Xu F, Huang Y, Jiang X. Repair of critical-sized rat calvarial defects using genetically engineered bone marrow-derived mesenchymal stem cells overexpressing hypoxia-inducible factor-1 α . *Stem Cells*. 2011;29(9):1380–90.
48. Zhang W, Zhang X, Wang S, Xu L, Zhang M, Wang G, Jin Y, Zhang X, Jiang X. Comparison of the use of adipose tissue-derived and bone marrow-derived stem cells for rapid bone regeneration. *J Dent Res*. 2013;92(12):1136–41.
49. Kishimoto N, Honda Y, Momota Y, Tran SD. Dedifferentiated Fat (DFAT) cells: a cell source for oral and maxillofacial tissue engineering. *Oral Dis*. 2018;24(7):1161–7.
50. Tateno A, Asano M, Akita D, Toriumi T, Tsurumachi N, Kazama T, Arai Y, Matsumoto T, Kano K, Honda M. Transplantation of dedifferentiated fat cells combined with a biodegradable type I collagen-recombinant peptide scaffold for critical-size bone defects in rats. *J Oral Sci*. 2019;61(4):534–8.
51. Suzuki D, Akita D, Tsurumachi N, Kano K, Yamanaka K, Kaneko T, Kawano E, Iguchi S, Toriumi T, Arai Y, Matsumoto T, Sato S, Honda M. Transplantation of mature adipocyte-derived dedifferentiated fat cells into three-wall defects in the rat periodontium induces tissue regeneration. *J Oral Sci*. 2017;59(4):611–20.
52. Akita D, Kano K, Saito-Tamura Y, Mashimo T, Sato-Shionome M, Tsurumachi N, Yamanaka K, Kaneko T, Toriumi T, Arai Y, Tsukimura N, Matsumoto T, Ishigami T, Isokawa K, Honda M. Use of rat mature adipocyte-derived dedifferentiated fat cells as a cell source for periodontal tissue regeneration. *Front Physiol*. 2016;7:50.
53. Nakajima K, Kunitatsu R, Ando K, Hayashi Y, Kihara T, Hiraki T, Tsuka Y, Abe T, Kaku M, Nikawa H, Takata T, Tanne K, Tanimoto K. Comparison of the bone regeneration ability between stem cells from human exfoliated deciduous teeth, human dental pulp stem cells and human bone marrow mesenchymal stem cells. *Biochem Biophys Res Commun*. 2018;497(3):876–82.

54. Li J, Zhang F, Zhang N, Geng X, Meng C, Wang X, Yang Y. Osteogenic capacity and cytotherapeutic potential of periodontal ligament cells for periodontal regeneration in vitro and in vivo. *PeerJ*. 2019;7:e6589.
55. Katagiri W, Osugi M, Kawai T, Hibi H. First-in-human study and clinical case reports of the alveolar bone regeneration with the secretome from human mesenchymal stem cells. *Head Face Med*. 2016;12:5.
56. Marx RE, Carlson ER, Eichstaedt RM, Schimmele SR, Strauss JE, Georgeff KR. Platelet-rich plasma: growth factor enhancement for bone grafts. *Oral Surg Oral Med Oral Pathol Oral Radiol Endod*. 1998;85(6):638–46.
57. Schilephake H. Bone growth factors in maxillofacial skeletal reconstruction. *Int J Oral Maxillofac Surg*. 2002;31(5):469–84.
58. Mooren RE, Dankers AC, Merckx MA, Bronkhorst EM, Jansen JA, Stoelinga PJ. The effect of platelet-rich plasma on early and late bone healing using a mixture of particulate autogenous cancellous bone and Bio-Oss®: an experimental study in goats. *Int J Oral Maxillofac Surg*. 2010;39(4):371–8.
59. Roldán JC, Jepsen S, Miller J, Freitag S, Rueger DC, Açil Y, Terheyden H. Bone formation in the presence of platelet-rich plasma vs. bone morphogenetic protein-7. *Bone*. 2004;34(1):80–90.
60. Wiltfang J, Kloss FR, Kessler P, Nkenke E, Schultze-mosgau S, Zimmermann R, Schlegel KA. Effects of platelet-rich plasma on bone healing in combination with autogenous bone and bone substitutes in critical-size defects: an animal experiment. *Clin Oral Implants Res*. 2004;15(2):187–93.
61. Faratzis G, Leventis M, Chrysomali E, Khaldi L, Eleftheriadis A, Eleftheriadis I, Dontas I. Effect of autologous platelet-rich plasma in combination with a biphasic synthetic graft material on bone healing in critical-size cranial defects. *J Craniofac Surg*. 2012;23(5):1318–23.
62. Kim ES, Kim JJ, Park EJ. Angiogenic factor-enriched platelet-rich plasma enhances in vivo bone formation around alloplastic graft material. *J Adv Prosthodont*. 2010;2(1):7–13.
63. Schlegel KA, Donath K, Rupprecht S, Falk S, Zimmermann R, Felszeghy E, Wiltfang J. De novo bone formation using bovine collagen and platelet-rich plasma. *Biomaterials*. 2004;25(23):5387–93.
64. Engler-Pinto A, Siéssere S, Calefi A, Oliveira L, Ervolino E, de Souza S, Furlaneto F, Messori MR. Effects of leukocyte- and platelet-rich fibrin associated or not with bovine bone graft on the healing of bone defects in rats with osteoporosis induced by ovariectomy. *Clin Oral Implants Res*. 2019;30(10):962–76.
65. Chen X, Yang L, Tian W. Heterotopic osteogenesis of autogenous marrow stromal cells with recombinant human bone morphogenetic protein 2 gene transfection and porous calcium phosphate ceramic as scaffold. *Hua Xi Kou Qiang Yie Xue Za Zhi*. 2003;21(6):419–21.
66. Hsu WK, Wang JC. The use of bone morphogenetic protein in spine fusion. *Spine J*. 2008;8(3):419–25.
67. Jones AL, Bucholz RW, Bosse MJ, Mirza SK, Lyon TR, Webb LX, Pollak AN, Golden JD, Valentin OA. Recombinant human BMP-2 and allograft compared with autogenous bone graft for reconstruction of diaphyseal tibial fractures with cortical defects. A randomized, controlled trial. *J Bone Joint Surg Am*. 2006;88(7):1431–41.
68. Wu DH, Hatzopoulos AK. Bone morphogenetic protein signaling in inflammation. *Exp Biol Med (Maywood)*. 2019;244(2):147–56.
69. Zeng JH, Qiu P, Xiong L, Liu SW, Ding LH, Xiong SL, Li JT, Xiao ZB, Zhang T. Bone repair scaffold coated with bone morphogenetic protein-2 for bone regeneration in murine calvarial defect model: systematic review and quality evaluation. *Int J Artif Organs*. 2019;42(7):325–37.
70. Ansari S, Freire MO, Pang EK, Abdelhamid AI, Almohaimeed M, Zadeh HH. Immobilization of murine anti-BMP-2 monoclonal antibody on various biomaterials for bone tissue engineering. *Biomed Res Int*. 2014;2014:940860.

71. Holloway JL, Ma H, Rai R, Hankenson KD, Burdick JA. Synergistic effects of SDF-1 α and BMP-2 delivery from proteolytically degradable hyaluronic acid hydrogels for bone repair. *Macromol Biosci*. 2015;15(9):1218–23.
72. Wubneh A, Tsekoura EK, Ayranci C, Uludag H. Current state of fabrication technologies and materials for bone tissue engineering. *Acta Biomater*. 2018;80:1–30.
73. Maroulakos M, Kamperos G, Tayebi L, Halazonetis D, Ren Y. Applications of 3d printing on craniofacial bone repair: a systematic review. *J Dent*. 2019;80:1–14.
74. Abukawa H, Shin M, Williams WB, Vacanti JP, Kaban LB, Troulis MJ. Reconstruction of mandibular defects with autologous tissue-engineered bone. *J Oral Maxillofac Surg*. 2004;62(5):601–6.
75. Abukawa H, Zhang W, Young CS, Asrican R, Vacanti JP, Kaban LB, Troulis MJ, Yelick PC. Reconstructing mandibular defects using autologous tissue-engineered tooth and bone constructs. *J Oral Maxillofac Surg*. 2009;67(2):335–47.
76. Probst FA, Fliefel R, Burian E, Probst M, Eddicks M, Cornelsen M, Riedl C, Seitz H, Aszodi A, Schieker M, Otto S. Bone regeneration of minipig mandibular defect by adipose derived mesenchymal stem cells seeded tri-calcium phosphate- poly(D,L-lactide-co-glycolide) scaffolds. *Sci Rep*. 2020;10(1):2062.
77. Abukawa H, Terai H, Hannouche D, Vacanti JP, Kaban LB, Troulis MJ. Formation of a mandibular condyle in vitro by tissue engineering. *J Oral Maxillofac Surg*. 2003;61(1):94–100.
78. Sharaf B, Faris CB, Abukawa H, Susarla SM, Vacanti JP, Kaban LB, Troulis MJ. Three-dimensionally printed polycaprolactone and β -tricalcium phosphate scaffolds for bone tissue engineering: an in vitro study. *J Oral Maxillofac Surg*. 2012;70(3):647–56.
79. Mao Y, Hoffman T, Wu A, Goyal R, Kohn J. Cell type-specific extracellular matrix guided the differentiation of human mesenchymal stem cells in 3D polymeric scaffolds. *J Mater Sci Mater Med*. 2017;28(7):100.
80. Aldaadaa A, Owji N, Knowles J. Three-dimensional printing in maxillofacial surgery: hype versus reality. *J Tissue Eng*. 2018;9:2041731418770909.
81. Sakkas A, Schramm A, Winter K, Wilde F. Risk factors for post-operative complications after procedures for autologous bone augmentation from different donor sites. *J Craniomaxillofac Surg*. 2018;46(2):312–22.
82. Mueller ML, Thamm JR, Troulis MJ, Guastaldi FPS. Clinical application of three-dimensional printing and tissue engineering for maxillofacial reconstruction. A review of reported cases. *JSM Oro Facial Surg*. 2020;4(1):1013.
83. Hollister SJ, Flanagan CL, Morrison RJ, Patel JJ, Wheeler MB, Edwards SP, Green GE. Integrating image-based design and 3D biomaterial printing to create patient specific devices within a design control framework for clinical translation. *ACS Biomater Sci Eng*. 2016;2(10):1827–36.
84. VanKoeveering KK, Zopf DA, Hollister SJ. Tissue engineering and 3-dimensional modeling for facial reconstruction. *Facial Plast Surg Clin North Am*. 2019;27(1):151–61.
85. Wong ME, Kau CH, Melville JC, Patel T, Spagnoli DB. Bone reconstruction planning using computer technology for surgical management of severe maxillomandibular atrophy. *Oral Maxillofac Surg Clin North Am*. 2019;31(3):457–72.
86. Bruyas A, Moeinzadeh S, Kim S, Lowenberg DW, Yang YP. Effect of electron beam sterilization on three-dimensional-printed polycaprolactone/beta-tricalcium phosphate scaffolds for bone tissue engineering. *Tissue Eng Part A*. 2019;25(3–4):248–56.
87. Khojasteh A, Behnia H, Hosseini FS, Dehghan MM, Abbasnia P, Abbas FM. The effect of PCL-TCP scaffold loaded with mesenchymal stem cells on vertical bone augmentation in dog mandible: a preliminary report. *J Biomed Mater Res B Appl Biomater*. 2013;101(5):848–54.
88. Ahn G, Lee JS, Yun WS, Shim JH, Lee UL. Cleft alveolus reconstruction using a three-dimensional printed bioresorbable scaffold with human bone marrow cells. *J Craniofac Surg*. 2018;29(7):1880–3.

89. Sandor GK, Numminen J, Wolff J, Thesleff T, Miettinen A, Tuovinen VJ, Mannerstrom B, Patrikoski M, Seppanen R, Miettinen S, Rautiainen M, Ohman J. Adipose stem cells used to reconstruct 13 cases with cranio-maxillofacial hard-tissue defects. *Stem Cells Transl Med.* 2014;3(4):530–40.
90. Wiltfang J, Rohnen M, Egberts JH, Lutzen U, Wieker H, Acil Y, Naujokat H. Man as a living bioreactor: prefabrication of a custom vascularized bone graft in the gastrocolic omentum. *Tissue Eng Part C Methods.* 2016;22(8):740–6.
91. Tian T, Zhang T, Lin Y, Cai X. Vascularization in craniofacial bone tissue engineering. *J Dent Res.* 2018;97(9):969–76.

3D Printing for Orthopedic Joint Tissue Engineering



Michael S. Rocca, Matthew Kolevar, Jocelyn Wu, and Jonathan D. Packer

1 Overview

The treatment of articular cartilage defects is one of the most challenging clinical problems in orthopedic surgery. Cartilage defects can cause debilitating pain, functional limitations, and lead to further intraarticular injury and eventually osteoarthritis. Over the past few decades, extensive research has been dedicated to articular cartilage and osteochondral defects; however, these efforts have not yet led to significant improvements on patient outcomes and the development of new treatment options. While the currently available cartilage repair and restoration treatment options have limitations, the field of 3D printing and bioengineering may offer promising and exciting future treatments for patients with articular cartilage and osteochondral defects.

In this chapter we will review articular cartilage defects and discuss the current treatment strategies from the standpoint of an orthopedic surgeon. Our goal is to provide an overview for the indications, technique, and outcomes for each common treatment strategy and conclude by highlighting the rapidly evolving field of cartilage tissue engineering.

2 Articular (Hyaline) Cartilage

Articular or hyaline cartilage is complex and specialized tissue [1]. Articular cartilage is composed of extracellular matrix, the majority of which is water, as well as collagen, primarily type II collagen, proteoglycans, and chondrocyte cells [2].

M. S. Rocca, MD · M. Kolevar, MD · J. Wu · J. D. Packer (✉)
Department of Orthopaedics, University of Maryland School of Medicine,
Baltimore, MD, USA
e-mail: jpacker@som.umaryland.edu

Cartilage is avascular and does not contain any nerves or lymphatics, while the chondrocytes, as the only cell, comprise only a small percentage of the total cartilage volume. Chondrocytes help maintain the extracellular matrix of the cartilage as well as metabolically respond to the substances within the extracellular matrix, including growth factors, acute phase reactants, and systemic or intraarticular pharmaceuticals [2]. Chondrocytes are derived from mesenchymal stems cells (MSCs) and thus is the rationale for focusing many research efforts on utilizing MSCs as a treatment strategy.

Hyaline cartilage is integral for joint function because its biomechanical properties allow for low-friction joint motion, resistance to high forces and strain, and the ability to distribute load and absorb shock [2]. Despite its importance to healthy joint function, hyaline cartilage has poor capacity to heal [3] and does not “regenerate.” Unfortunately, these qualities frequently result in areas of cartilage injury in joints (cartilage defects), which are often a source of morbidity and disability for patients. Patients with cartilage defects can have symptoms such as pain, swelling, catching, locking, and instability [2, 4]. The pain can be debilitating and worsen with walking, activities of daily living, and especially high impact activities including running or participation in sports. Mechanical symptoms such as locking, catching, or instability can be due to a piece of cartilage that has broken free (“loose body”) and floating in the synovial fluid. Other causes of pain from articular cartilage lesions are the uneven or “aberrant” loading [2, 5] and also by increased load in the subchondral bone resulting in the subchondral edema [5–7].

Patients experience a wide range of symptom quality and intensity from partial and full thickness chondral defects. Frequently, full thickness cartilage defects are asymptomatic and incidental findings on MRI or arthroscopy. In other patients, however, even small defects can be extremely painful and debilitating. In theory, cartilage repair and restoration would slow or prevent further articular cartilage damage and the development of osteoarthritis. However, support for this theory is lacking in the literature. Therefore, current treatment goals are focused on pain relief rather than prevention of subsequent cartilage damage and osteoarthritis. Initial treatment involves activity modification, anti-inflammatory medications, weight loss, physical therapy/strengthening exercises, intraarticular injections, and bracing. If the symptoms are controlled and tolerable, surgery is not recommended. If the patient is still symptomatic after a course of non-operative treatments, then surgery is considered. Frequently, there are other concomitant intraarticular pathologies, such as meniscus tears, synovitis, loose bodies, instability, and joint malalignment that could also be a source of pain and functional impairment and must be considered in the preoperative evaluation.

Articular cartilage defects are common and were found in 50% of 30,000 knee arthroscopies in one published case series [8]. Arthroscopic knee surgery is one of the most common procedures performed by orthopedic surgeons and involves using a small camera, an arthroscope, and instruments to perform minimally invasive surgery. The arthroscopic technique allows for complex surgery to occur by using only a few small skin incisions, typically less than 1 cm in length.

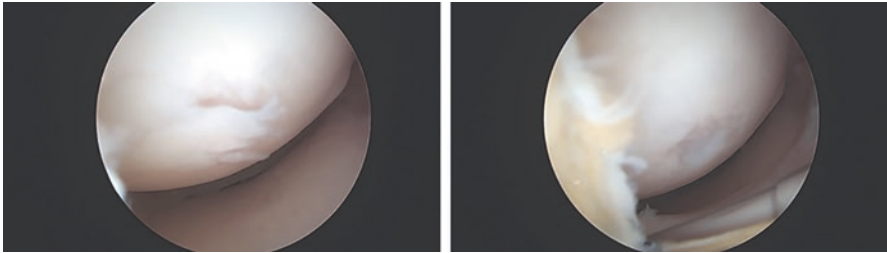


Fig. 1 The arthroscopic images above show the femoral condyle with a small cartilage flap tear and underlying chondral defect. There is intact cartilage on the periphery and around the lesion. The images are before (left) and after (right) the cartilage flap has been debrided with the chondroplasty technique

Although many different cartilage repair and restoration techniques exist, a simple and effective treatment of cartilage flap tears is a “chondroplasty,” which involves removal of any torn and damaged cartilage flaps and contouring the edge so that all remaining cartilage is healthy and stable (Fig. 1). A chondroplasty can be performed arthroscopically and the rehabilitation involves immediate weight-bearing and a 4 to 6-week recovery period. For comparison, cartilage restoration surgery can require 6 weeks of no weight-bearing on crutches and a 6 to 9-month recovery. Therefore, chondroplasty can be an attractive option for patients with smaller cartilage defects, cartilage flap tears, and patients seeking a quick recovery. However, for patients who have failed a chondroplasty and/or have larger cartilage defects, cartilage restoration surgeries are considered.

An important clinical decision for orthopedic surgeons is to determine who will benefit from these cartilage restoration surgeries. Patient selection is critical since other factors can contribute to preoperative and persistent postoperative symptoms regardless of which technique is used. Cartilage lesion related factors that are considered include lesion size on MRI, involvement of underlying bone (osteochondral lesion), and location of lesion.

Other patient factors also influence long-term clinical outcomes from cartilage restoration procedures [2]. These factors include the patient’s age, activity status, duration of symptoms, medical comorbidities (diabetes, smoking, etc.), and body mass index (BMI). Knee instability, lower extremity malalignment, and meniscus deficiency also should be addressed to decrease the stress on the cartilage repair site and improve success rates. It is also important to recognize that cartilage repair and restoration efforts are most successful when treating isolated cartilage defects rather than multiple defects or osteoarthritis, which involves diffuse and global cartilage thinning and degeneration. Therefore, addressing one area of damaged cartilage in a patient with many cartilage defects or diffuse osteoarthritis is unlikely to be beneficial.

In the following section, we will review the different cartilage restoration procedures that are currently performed by orthopedic surgeons.

3 Marrow Stimulating Techniques of Cartilage Defect Repair: Microfracture, Osteochondral Drilling, Abrasion Arthroplasty

3.1 *Microfracture*

Microfracture surgery is one of the first procedures described for the treatment of osteochondral lesions. The technique was initially described by J. Richard Steadman and has been in the repertoire of orthopedic surgeons for decades. Microfracture surgery had gained so much traction through the early 2000s with famous professional athletes that the procedure was a common topic in the mainstream media, including in the New York Times [9].

The main premise behind microfracture surgery is to create small bone channels to the bone marrow within the lesion as a means of providing a suitable environment for tissue regeneration [10–12]. The original technique is an arthroscopic procedure in which the cartilage lesion is debrided down to the subchondral bone with circumferentially stable healthy cartilage edges [10]. The microfracture is then performed using an awl to “fracture” the subchondral bone plate by creating small holes with the awl. There should be approximately 3–4 holes per square centimeter of subchondral bone in order to give enough space for bone marrow stimulation without having the holes fracture into each other [10–12]. After the microfracture is complete, the release of fat droplets from the subchondral bone can be visualized, representing release of bone marrow into the defects [2, 10–12]. On a cellular level, the goal of the procedure is to have the MSCs released from bone marrow and a fibrin clot fill in the defect and eventually differentiate into cartilage-like tissue.

A microfracture can be performed relatively quickly, is not technically difficult, has a low patient morbidity, and also can be performed in combination with other arthroscopic procedures, such as anterior cruciate ligament (ACL) reconstruction or meniscus surgery [2, 12]. Another advantage of the microfracture technique is that there is very little to no thermal necrosis of the subchondral bone, as opposed to drilling through the bone. Furthermore, this procedure is cost effective, especially compared to many of the cell-based techniques.

The primary concern with microfracture is that the osteochondral defect is ultimately filled with fibrocartilage, which is biomechanically and biochemically inferior to the native specialized articular hyaline cartilage [2, 13]. Although early clinical studies were promising [12], long term follow-up studies have demonstrated deteriorating outcomes with microfracture over time [3, 14]. Another limitation of microfracture is that the technique is ideally used for smaller cartilage defects. Many published studies have included lesions up to 4 cm²; however, most surgeons would agree that microfracture is best indicated for lesions <2 cm². Patient compliance with postoperative rehabilitation is critical to achieve the best outcomes, which typically involves 6 weeks of protected weight-bearing and use of a continuous passive motion device. Patients may resume running and jumping after 6 months post op.

3.2 Osteochondral Drilling

Osteochondral drilling has recently become a common modification of the microfracture technique (Fig. 2). Osteochondral drilling is similar to microfracture, but utilizes a small diameter drill instead of awls to create small drill holes into subchondral bone [15]. This process parallels that of microfracture in that it stimulates bone marrow to create a fibrin clot of MSCs, platelets and ECM proteins to fill in the osteochondral defect [2]. However, some authors argue against the use of osteochondral drilling due to concern that the heat generated by the drilling process may cause thermal necrosis of subchondral bone and possibly affect the viability of MSCs released by the subchondral drilling [2, 16].

Chen et al. investigated drilling versus microfracture in rabbit models of cartilage defects. They found that compared to microfracture, drilling could create cleaner and deeper channels to access more bone marrow, potentially increasing the yield of regenerative cells given that the drill holes provide direct, uninhibited access to bone marrow stroma [16]. The researchers found that with microfracture, the subchondral bone around the holes can be fractured, thus decreasing the amount

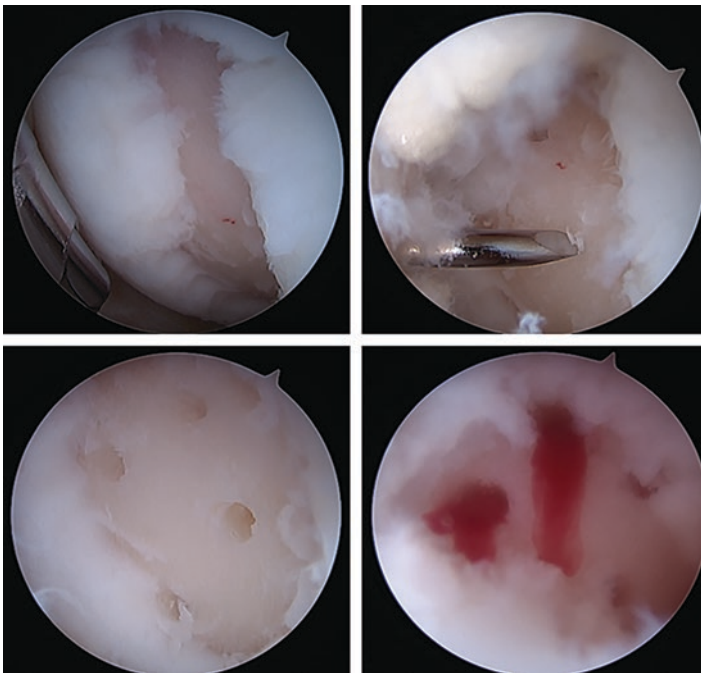


Fig. 2 Below are four intraoperative arthroscopic images demonstrating drilling of an osteochondral lesion. Top left: a femoral condyle cartilage lesion that has been debrided down to subchondral bone with surrounding healthy cartilage. Top right: a drill is used to penetrate the subchondral bone. Bottom left: after drilling of multiple, evenly spaced subchondral drill holes. Bottom right: release of bone marrow and its associated MSCs, platelets, and ECM proteins from the drill holes/channels that will form the clot which will fill the defect with cartilage-like tissue

of bone marrow progenitor cells that can access the defect. Whereas with osteochondral drilling, the holes to the subchondral bone are cleaner, containing more open channels since the drill had removed any inhibiting bone fragments within the holes. However, this study only evaluated the first 24 h after procedure, thus making it difficult to draw distinct conclusions for long term outcomes.

3.3 Abrasion Chondroplasty

Arthroscopic abrasion chondroplasty or abrasion arthroplasty is a technique that was developed in the 1980s to treat osteoarthritis in areas of exposed subchondral bone. It is thought that gaining access to the vasculature located deep in the subchondral bone would allow for infiltration of bone marrow elements such as MSCs. This method utilizes a curette or motorized burr to remove the superficial subchondral bone plate, resulting in a bleeding response and clot formation. In humans, histology of the abraded regions showed healed fibrocartilage containing type I collagen and fibroblasts due to stimulation of bone marrow elements [17]. Beckmann et al. 2015 observed higher contents of MSCs in postoperative joint effusion following abrasion compared to arthroscopic chondroplasty [18]. Despite the infiltration of MSCs, chondrocyte differentiation still failed to create desired hyaline cartilage.

In all of these bone marrow stimulation techniques, fibrocartilage fills in the defect over exposed subchondral bone, but has relatively low functional capacity and poorly redistributes pressure across the articular surface. This can lead to wear and breakdown of the repaired tissue [19]. Clinically, the fibrocartilage seen on second arthroscopy or imaging did not lead to better clinical outcomes and there is high variability in defect filling between patients [18]. When comparing arthroscopic abrasion to standard arthroscopic debridement, there is little indication that abrasion is superior to debridement, despite cartilage formation seen after abrasion [20]. Risks of abrasion chondroplasty include destruction of subchondral bone and necrosis of adjacent tissue which can lead to postoperative complications [21]. Compared to other bone marrow stimulating techniques, abrasion chondroplasty may accelerate cartilage repair at 1 year post-op but there is no difference in clinical outcomes, patient-reported outcome scores, or revision rates within 5 years post-op [22, 23].

4 Adipose Derived and Bone Marrow Derived Stem Cells

The use of adipose derived stem cells (ADSCs) and bone marrow derived stem cells (BMSCs) in the treatment of osteochondral defects and osteoarthritis has increased over the last decade, especially in Asia. BMSCs were the first discovered multipotent cell which could differentiate into chondrocytes and osteocytes. The use of ADSCs and BMSCs in the USA has been limited due to FDA regulations since most isolation techniques are not considered “minimally manipulative.”

The technique of BMSC harvest typically involves bone marrow extraction from the iliac crest which is then centrifuged to isolate the BMSCs. Following collection, the solution can be immediately injected, stored at -80°C until ready for use, or cultured and expanded for later use. However, the MSCs make up a small proportion of cells in this solution, meaning larger quantities may be required to have a clinical effect [24].

The basic technique of harvesting ADSCs relies on using liposuction to isolate “lipoaspirate” which contains stem cells. This fluid is then combined with specific enzymes and centrifuge gradient separation to isolate the specific ADSCs. Alternative non-enzymatic methods of isolating ADSCs that would be FDA-approved have been studied, but have not yet been successful [25]. The isolated ADSCs are then either injected into the joint, placed into an osteochondral defect, or used to augment other cartilage restoration procedures. It is thought that the ADSCs improve function by interacting with resident chondrocytes through paracrine signaling involving growth factors, but the exact mechanism has not been elucidated [26, 27]. Compared to BMSCs, ADSCs are attractive because it is relatively easy to harvest fat and once isolated, ADSCs, like MSCs, can differentiate into mesodermal tissues, including cartilage, without provoking immunogenicity [28].

There has been increasing evidence in the literature for the use of ADSCs and BMSCs for treating cartilage pathology [24, 29, 30]. Freitag et al. conducted the first randomized controlled trial on autologous ADSCs injection for the treatment of osteoarthritis and found improvements in pain scores and functional outcomes in 1 year [31]. Similar to bone marrow stimulation techniques, the propensity of BMSCs and ADSCs to differentiate into fibrous tissue rather than hyaline cartilage is a major limitation [32, 33]. However, there are encouraging results from in vitro studies showing that these cells could be guided towards becoming chondrocytes when the optimal environment is created. Li et al. utilized a 3D nanofibrous scaffold treated with TGF- β to culture BMSCs, which was able to differentiate into phenotypic chondrocytes in vitro [34]. Similarly, Rosadi et al. demonstrated chondrocyte differentiation in vitro from ADSCs utilizing a silk fibroin scaffold and platelet rich plasma [35]. Such strategies can be combined with 3D printing to create a scaffold for optimal chondrocyte differentiation utilizing ADSCs.

5 Cell-Based Techniques for Treatment of Cartilage Defects: Osteochondral Grafting

5.1 Autologous Chondrocyte Implantation

The appeal of cell-based methods for the treatment of cartilage defects is the induction and/or implantation of hyaline and hyaline-like cartilage as compared to the fibrocartilage generated by bone marrow stimulation techniques. Autologous chondrocyte implantation (ACI) is a cell-based technique for the treatment of chondral

lesions. ACI involves the harvesting and culturing of chondrocytes and then using these harvested chondrocytes in an implanted patch to “fill-in” the cartilage defect. This method utilizes the harvesting of chondrocytes from a non or lesser weight-bearing area of the joint [2, 36, 37]. Once harvested, the chondrocytes are enzymatically optimized into a suspension for reimplantation into the cartilage defect via a periosteal or collagen patch covering [2, 36, 37]. The patch is sutured in place which can be a technically demanding aspect of the operation.

Recently, ACI has progressed to a newer technique known as MACI or matrix-induced autologous chondrocyte implantation. This procedure utilizes a matrix scaffold as the vehicle to implant harvested chondrocytes into the cartilage lesion. The chondrocyte suspension is directly adhered to the MACI degradable collagen membrane matrix [38]. With the use of the MACI technique, the chondral graft for implant is more durable and easier to handle surgically than the earlier generation ACI technique grafts, thus likely to lead to improved outcomes [39]. Although long-term outcomes are lacking, some trials have reported improved outcomes with MACI compared to microfracture at 2 year follow-up for symptomatic cartilage defects of the knee [39]. Currently, MACI has largely replaced the earlier generations of autologous chondrocyte implantation given its ease of use profile, decreased operative times, decreased surgical complications, and its ability to be used in more chondral defect areas within the knee [39]. ACI/MACI has typically been reserved for cartilage lesions that are greater than 2 cm² but still has an intact subchondral plate, i.e. the lesion only affects the cartilage surface. Disadvantages are that ACI/MACI involves two separate operations and is expensive compared to other techniques [38].

5.2 *Osteochondral Autograft Transfer*

Osteochondral autograft transfer (OATS) is a technique that involves the transfer of osteochondral plugs from low weight-bearing areas of the knee to cartilage defects in high weight-bearing areas of the knee. The transferred tissue is a cylindrical “plug” of healthy cartilage and subchondral bone which is used to replace chondral defects (Fig. 3) [40, 41]. The goal is to utilize the osteochondral plugs to match articular surface and allow for a healing graft that restores the articular surface with native hyaline cartilage [41]. A major advantage of this technique is that the transferred native bone reliably and quickly heals to the surrounding bone allowing for a relatively quick recovery. Additionally, the OATS procedure allows for any chondral defect to be replaced with native hyaline cartilage and subchondral bone, thus giving this technique a biomechanical and biochemical advantage over marrow stimulating techniques like microfracture or drilling [40, 41].

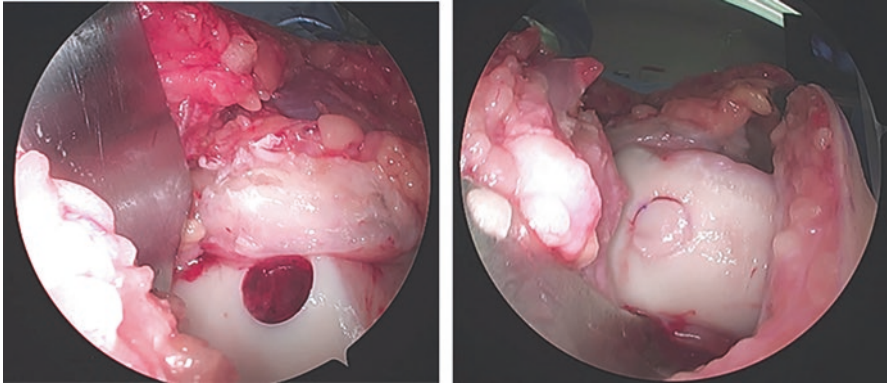


Fig. 3 The below images are intraoperative images from an OATS procedure performed on a young patient with a symptomatic cartilage lesion. The lesion on the weight-bearing aspect of the femoral condyle was replaced by a transferred osteochondral plug from a less weight-bearing area on the femoral condyle

OATS can be completed during one operation, which decreases the patient morbidity compared to other procedures, such as ACI and MACI, that require multiple operations. Additionally, there are surgical instrument systems available that are inexpensive and intuitive. Overall, the OATS procedure has had excellent clinical outcomes and has demonstrated a quicker return to sport for athletes than the other cartilage procedures mentioned in this chapter, including ACI/MACI and microfracture [40, 42, 43]. OATS is reserved for smaller lesions since the largest harvest plug size is 10 mm in diameter. For the treatment of larger osteochondral lesions, multiple plugs can be used to fill the larger lesion in a procedure called “mosaicplasty” [40]. A drawback to mosaicplasty is the potential donor site morbidity since more donor cartilage and bone plugs are harvested encompassing a larger donor area [40]. Mosaicplasty has been shown to be more successful in long term studies compared to microfracture in certain patient populations representing its importance in the repertoire for treatment of cartilage lesions [44].

5.3 Osteochondral Allograft Transplant and Allograft Implants

Many allograft options are available for the treatment of symptomatic osteochondral lesions, such as an osteochondral allograft (OCA) transplantation. An OCA is a fresh cadaver joint with live chondrocytes that is sized to the recipient patient through either an MRI or radiograph. The transfer process is similar to the OATS procedure, but without graft size limitations since the donor is the cadaver knee (no

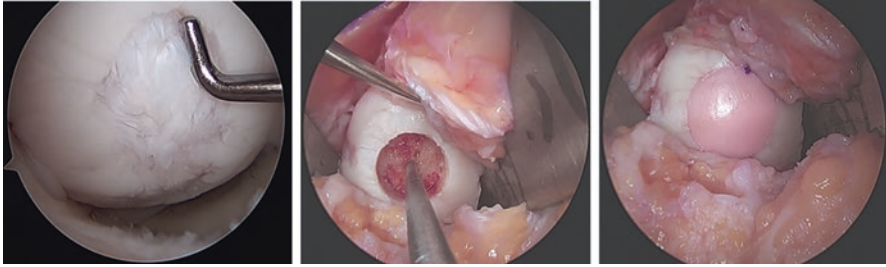


Fig. 4 Intraoperative images from an OCA procedure performed on a young patient with a large symptomatic cartilage lesion. Left image: a near full thickness large osteochondral lesion in the weight-bearing surface of the lateral femoral condyle. Middle image: the bone and cartilage have been removed from the osteochondral lesion in preparation of OCA implantation. Right image: after OCA transplant. The osteochondral allograft is well fixed in the femoral weight-bearing surface replacing the osteochondral defect (left image)

donor site morbidity). The use of fresh OCA transplant allows for defects to be filled by fresh, transplanted mature hyaline cartilage from the cadaver, typically femoral condyles (Fig. 4). Depending on the defect size and location, fixation with screws, dowels, or pins may be required for stability and to stimulate healing of the allograft into the patient's cartilage defect [2]. Similar to OATS, one of the keys to osteochondral allograft transplantation is the bony healing between the transplanted osteochondral graft and the surrounding subchondral bone. One of the disadvantages of osteochondral allograft is the high expense, as well as the specific storage requirements so that the chondrocytes and associated ECM does not denature [2]. The grafts have to be stored under specific conditions and must be implanted within 4 weeks, which creates logistical challenges as well [45, 46]. Given the nature of allograft tissue, there is risk of immunologic response and poor healing between the donor graft and surrounding native bone at the bone–bone healing interface [40]. Classically, many of the methods and industry formulations for osteochondral allografts were used for large defects or as salvage options when other treatment methods for osteochondral lesions had failed [2, 40, 46, 47]. Recently, multiple allograft implantable products have been introduced by industry as an alternative to a fresh cadaver knee. These include Cartiform (Arthrex, USA), Biocartilage (Arthrex, USA), DeNovo (Zimmer Biomet, USA), and Chondrofix (Zimmer Biomet, USA). These allograft options represent a target of 3D printing and scaffolds for defects that we will expand on in the next section.

Summary table

Treatments for symptomatic cartilage lesions			
Type	Goal	Example	Pros/Cons
Debridement	Remove loose cartilage flaps	Chondroplasty	<ul style="list-style-type: none"> • Can often provide significant symptomatic relief for isolated lesions • Cost effective • Single arthroscopic operation • Quick recovery • Does not address cartilage loss
Bone marrow stimulating procedures	Stimulate bone marrow to form a fibrin clot to replace/“repair” damaged articular cartilage	Microfracture, osteochondral drilling, abrasion arthroplasty	<ul style="list-style-type: none"> • Use of specialized awls • Typically, lesions <2 cm² • Healthy surrounding cartilage rim required • One operation • Cost effective • Produces/repairs with fibrocartilage • Lengthy and involved post-op rehabilitation and restrictions
Stem cell treatments	Use of multipotent stems cells to differentiate into chondrocyte lineage to repair/regenerate cartilage defects	Adipose derived stem cells (ADSC)	<ul style="list-style-type: none"> • Limited use in USA • Relatively simple and easy harvesting procedure • Require specific enzymes to isolate
		Bone marrow derived stem cells (BMSC)	<ul style="list-style-type: none"> • Limited use in USA • Invasive and painful harvest
<i>Cartilage restoration</i>			
Cell based	Use of autologous chondrocytes that are expanded and reimplanted to fill a cartilage lesion	Autologous chondrocyte implantation (ACI)	<ul style="list-style-type: none"> • Larger lesions • Requires intact subchondral bone • Requires two operations • Requires periosteal or collagen patch to seal chondrocyte solution in place
		Matrix-induced autologous chondrocyte implantation (MACI)	<ul style="list-style-type: none"> • Recently favored over ACI due to improved durability, handling, and less difficult surgical technique • Matrix seeded with chondrocyte solution and directly placed into defect • Requires two operations

Treatments for symptomatic cartilage lesions			
Type	Goal	Example	Pros/Cons
Autograft transfer	Transfer of healthy cartilage via an osteochondral bone plug from a low weight-bearing area of the joint to the cartilage defect	OATS	<ul style="list-style-type: none"> • Technically demanding • Donor site morbidity
		Mosaicplasty	<ul style="list-style-type: none"> • Same as OATS but with more bone plugs for larger lesions than OATS • Significant donor site morbidity
Allograft transplant	Replacement of damaged cartilage lesion with cadaveric donor cartilage or with synthetically made cartilage-type materials	Osteochondral allograft transplant	<ul style="list-style-type: none"> • Large lesions (>2 cm²) • Salvage following other restoration techniques • No donor site morbidity • Expensive (due to specificity and storage of allografts) • Need for fresh allograft cadaveric cartilage and bone • Possible immune response
		Allograft implants	<ul style="list-style-type: none"> • Expensive • Longer shelf life than fresh cadavers • Can replace need for fresh cadaveric distal femur • Treated allograft and/or synthetically created, and can be combined with other modalities

6 Cartilage Tissue Engineering: Moving into the Future and the Prospects of Using of 3D Printing for Cartilage Defects

Cartilage tissue engineering is a rapidly evolving field and research in this area has the potential to benefit millions of people suffering from chondral defects and osteoarthritis. Articular cartilage is a complex tissue with zonal architecture which is critical to its function. The architecture and interactions between chondrocytes, extracellular matrix, and subchondral bone are what give articular cartilage its mechanical properties [48, 49]. Because of the spatial arrangement of chondrocytes and molecular variability of the extracellular matrix contents of articular cartilage, 3D printing is an attractive technology for its engineering and design. 3D printing allows for customization and mixing of materials and microstructures with the goal of mimicking native cartilage or creating a new microenvironment to enable or facilitate the synthesis of new articular cartilage. To date, no 3D bioprinted product

has been successfully translated clinically from bench to bedside [50, 51]. This section will discuss principles that are important for articular cartilage engineering and 3D printing, current successes and shortcomings, artificial cartilage products currently in clinical use, and goals for future research and development. We will also briefly discuss the current use of 3D printing in joint replacement surgery.

Current research in cartilage engineering and 3D printing has involved cartilage and osteochondral replacement, hydrogel materials, composite materials, cell-based designs, cell-free designs, and many combinations of the aforementioned components [50]. When designs utilize chondrocytes or stem cells, important cell properties must be considered including sufficient number of cells, ability of these cells to proliferate either *in vitro* or *in vivo*, cell survival during the 3D printing process and shelf life, interaction with the environment, and ability to maintain function *in vivo*. Hydrogels made of materials such as alginate, hyaluronic acid (HA), and collagen have been a popular area of research because cells retain their viability and metabolic activity [49, 52, 53]. Researchers are also developing photopolymerizable hydrogels for ease of application [54]. Extrusion and droplet-based printing are forms of 3D printing that can easily use bioinks made of these materials to create chondral grafts [48]. Hydrogels are attractive because they can easily be seeded with patterns of cells, are low cost, and are highly compatible with different methods of 3D printing such as droplet based, extrusion based, laser based, and printing of tissue spheroids. Disadvantages of hydrogels include the weak mechanical properties, inability to retain a uniform 3D structure well, and limitations in the complexity of shapes that can be printed [49, 53]. These limitations have led to the development of composite materials, or hydrogels mixed with synthetic, high molecular weight biomaterials such as polylactic acid (PLA), poly-lactic-co-glycolic acid (PLGA), and polycaprolactone (PCL) [53].

Osteochondral designs are a popular new type of graft that commonly use scaffold-based designs composed of composite bioinks, such as PCL or PLGA combined with osteoconductive materials such as tri-calcium phosphates and HA. These polymers enhance the biomechanical properties of the construct compared to hydrogel alone and can achieve a compressive modulus more closely resembling that of articular cartilage [48]. Constructs can even be co-printed in a layer by layer fashion, mixing cell-containing bioinks and polymers to create varying mechanical properties and macroscopic anatomy similar to the anisotropic structure seen in articular cartilage [49]. Lee et al. have demonstrated success in this approach using a composite, osteochondral graft in a rabbit model [55]. In this study, an anatomically accurate 3D printed bioscaffold composed of PCL and HA was infused with a transforming growth factor- β 3-adsorbed collagen hydrogel. This cell-free scaffold was surgically implanted into a proximal humerus osteochondral defect. At four months, this scaffold demonstrated increased hyaline cartilage formation, better compressive and shear properties, and higher cell content compared to control groups as demonstrated in Fig. 5. Additionally, rabbits with this growth factor laden scaffold resumed full weight-bearing and locomotion more consistently than control groups. This demonstrated that a scaffold-based design could be printed with an anatomic geometry and its materials could be enhanced with growth factors to improve cartilage formation and function. Additionally, use of 3D printing could

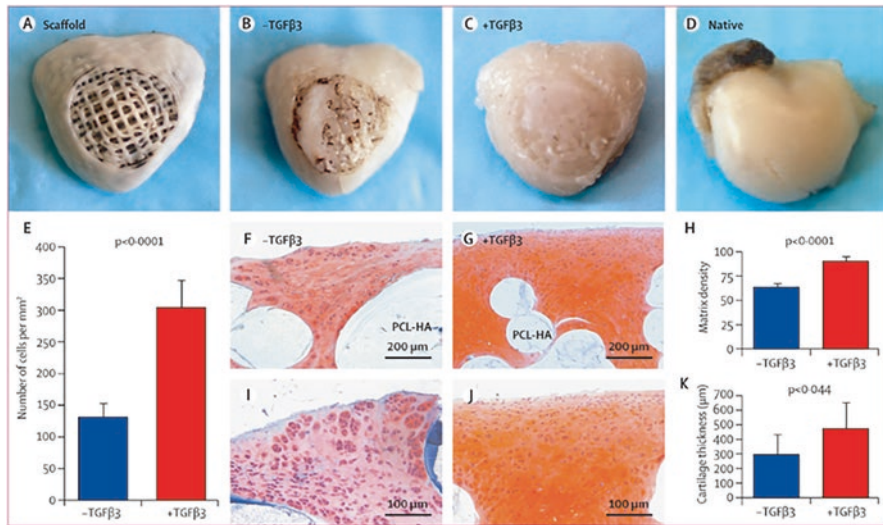


Fig. 5 Articular cartilage regeneration. India ink staining of (a) unimplanted bioscaffold, (b) TGFβ3-free and (c) TGFβ3-infused bioscaffolds after 4 months' implantation, and (d) native cartilage. (e) Number of chondrocytes present in TGFβ3-infused and TGFβ3-free regenerated articular cartilage samples (n = 8 per group). Safranin O staining of TGFβ3-free (f, i) and TGFβ3-infused (g, j) articular cartilage. Matrix density (h) and cartilage thickness (k) of TGFβ3-infused and TGFβ3-free samples (n = 8 per group for both comparisons). TGFβ3 transforming growth factor β3, PCL-HA poly-ε-caprolactone hydroxyapatite. (From "Regeneration of the articular surface of the rabbit synovial joint by cell homing: A proof of concept study" by Lee CH, Cook JL, Mendelson A, Moiola EK, Yao H, Mao JJ, 2010, *The Lancet*, 376(9739), 440–448. [Reprinted with permission])

allow for more personalized design of the scaffold to allow for better fit into the defect and tissue incorporation.

In a recent study by Guo et al., researchers developed a 3D printed PLCL-amine scaffold which was functionalized by covalent bond addition of aggrecan [13]. PLCL has mechanical properties of toughness that is more similar to cartilage than PLA and PLGA scaffolds. Also, aggrecan is the most abundant proteoglycan within the ECM of articular cartilage, making this an attractive combination. Cartilage defects were created in the femoral trochlear groove of rabbits and repaired by microfracture technique combined with implantation of the biofunctionalized acellular scaffold. Acellular scaffolds have the advantages of improved availability and shelf life compared to live, cellular scaffolds, and also obviates the need for a second procedure or cell harvest or culture. Results showed that this scaffold doubled the thickness of regenerated cartilage tissue, tripled the number of chondrocytes present (Fig. 6), and increased the expression of type II collagen nearly tenfold

Fig 6 (continued) Noshin M, Baker HB, Taskoy E, Meredith SJ, Tang Q, Ringel JP, Lerman MJ, Chen Y, Packer JD, Fisher JP, 2018, *Biomaterials*, 185, 219–231. [Reprinted with permission])

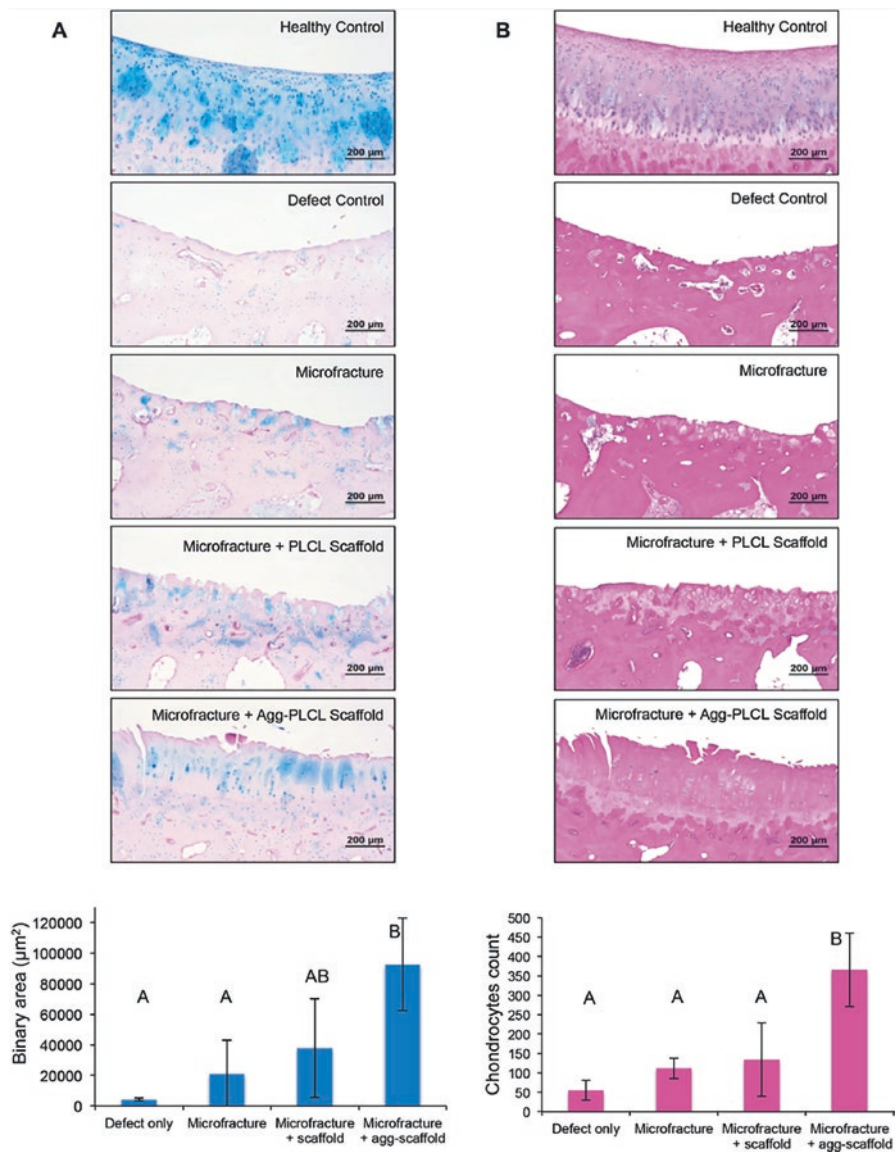


Fig. 6 Histological examination of regenerated cartilage tissue using H&E and Alcian blue staining. (a) Alcian Blue staining showing the GAGs production in different groups. Cell nuclei were stained purple and surrounding GAGs were stained blue. The GAGs expression level was quantified by binary area. Compared to defect control, microfracture and PLCL showed increased production of GAGs from the histology staining. The addition of aggrecan further improved the quality of regenerated tissue, with visible lined chondrocytes surrounded by GAGs. (b) H&E staining showing newly regenerated cartilage tissue. Cell nuclei were stained purple, and the background tissue was stained pink. The cartilage layer presents a lighter pink than the bone tissue. The number of chondrocytes was calculated and compared among groups. The chondrocytes number in the aggrecan functionalized group was significantly higher than other experimental groups. $N = 3$. Data is shown as mean \pm standard deviation. ANOVA was performed to compare the significance among groups. Means that do not share the same letter are significantly different. (From “3D printed biofunctionalized scaffolds for microfracture repair of cartilage defects” by Guo Y,

compared to microfracture alone. This study demonstrated that the biofunctionalized scaffold augmentation of microfracture could be an effective future strategy for the treatment of symptomatic cartilage defects by filling the defect with tissue more akin to hyaline cartilage than fibrocartilage. Both studies demonstrate the potential of 3D printing for treating cartilage defects.

One very important characteristic of articular cartilage which to date has been the most challenging to recreate is the layered architecture. Hyaline cartilage contains three zones, the superficial, middle, and deep zone, with each differing in chondrocyte number and morphology and extracellular composition. This architecture, which fibrocartilage lacks, helps provide hyaline cartilage resistance to compression and shear stress [49]. Different strategies for creating articular cartilage with zone-specific properties include using zonal chondrocyte subpopulations, scaffolds that differ in material composition and characteristics by level, and zone-specific growth factors and cell signaling [56]. Although it is possible to harvest and isolate chondrocytes from different zones of cartilage, it is challenging to isolate pure zonal populations. It has also proven difficult to expand these populations due to de-differentiation and loss of zone-specific characteristics. The cells do not self-organize in layers, but mechanical loading influences their phenotypic development. Current research efforts are focused on the engineering of zonal scaffolds. Zhu et al. synthesized a gradient hydrogel from 8-arm-PEG-norbornene, PEG-dithiol, and 25% methacrylated chondroitin sulfate by varying the amount of PEG in the hydrogel as it was printed, thus creating a hydrogel with a three-dimensional gradient [57]. The continuous gradient of PEG created zonal variabilities in stiffness of the hydrogel, which was shown to influence chondrocyte proliferation and glycosaminoglycans and collagen production in each zone, as well as cartilage specific gene expression by stem cells. Although much research is needed prior to clinical applications, this study demonstrates that advanced printing and tissue engineering techniques can be used to recapitulate zonal properties to optimize and customize cartilage regeneration.

Although there are no current clinical applications of cartilage zone-specific grafts, many implants, which take advantage of the bone-cartilage interface are gaining popularity. An example of a biphasic implant which was used in humans but has since been removed from the market due to regulatory issues is the TruFit (Smith and Nephew, USA) bone graft substitute. The TruFit plug was a synthetic, biphasic, acellular scaffold made of a 3D polymer blend of polylactide-*co*-glycolide (PLG) copolymer, calcium sulfate, polyglycolide (PGA) fibers, and surfactant. The chondral component was the 4 mm-thick articular portion of graft which was devoid of calcium sulfate [58]. According to the manufacturer, the plug was indicated only to fill bony defects and donor graft sites, but it was also frequently used off label for primary cartilage defects. This product was attractive because it could be used in a single stage procedure and donor site morbidity, such as in an OATS procedure, could be avoided. The theoretical benefit of using a synthetic plug to backfill a donor defect is that this achieves hemostasis. The plug prevents the release of

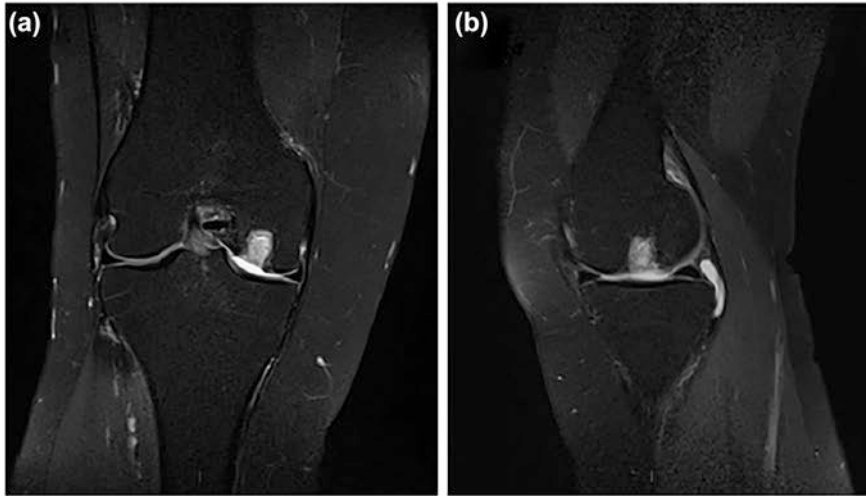


Fig. 3 Pre-operative coronal (a) and sagittal images (b). The same patient at two years following implantation (c, d)



Fig. 4 Two-year post-operative images demonstrating an incorporated TruFit plug on coronal (d) and sagittal (c)

Fig. 7 From “Autologous osteochondral mosaicplasty or TruFit™ plugs for cartilage repair” by Hindle P, Hendry JL, Keating JF, Biant LC, 2014, *Knee Surg. Sports Traumatol. Arthrosc.*, 22(6), 1235–1240. (Reprinted with permission)

proinflammatory cytokines which may inhibit osteochondral healing, and the plug promotes native tissue integration and healing with an osteoconductive material. Donor site morbidity for osteochondral autograft has been reported from 0 to 50% in the literature [59]. Fraser et al. published a retrospective case series looking at use of the TruFit to backfill autologous osteochondral transplantation donor sites in the knee. They demonstrated a low donor site morbidity of 12.5% at 2 years, but magnetic resonance observation of cartilage repair tissue (MOCART) scores did not correlate with patient-reported clinical outcome scores [26]. Hindle et al. performed a retrospective review comparing pain and functional outcomes in patients after either TruFit implantation or autologous osteochondral mosaicplasty. Although some MRI scans demonstrated mild incorporation of the graft at 2 years, others did not (Fig. 7).

More importantly, patients in the TruFit group had significantly lower clinical outcome scores as well as a lower rate of return to sport [58]. A systematic review performed by Verhaegen et al. did not demonstrate superiority or equality of TruFit compared to conservative management or mosaicplasty for osteochondral articular defects or gap filling of donor sites [60]. Although this product was safe for clinical use, its superiority over other techniques has not been demonstrated.

Other attempts to maintain the native 3D microenvironment of cartilage include osteochondral allografts and grafts designed to augment bone marrow stimulation techniques. Cartiform (Arthrex, USA) is an off the shelf cryopreserved osteochondral allograft which contains a layer of full thickness articular cartilage over a thin layer of subchondral bone (Fig. 8). This graft contains viable endogenous chondrocytes surrounded by their native extracellular matrix proteins and chondrogenic growth factors [61]. Cartiform is intended to supplement bone marrow stimulation and has a porous design which allow for suture fixation to secure the graft and also for bone marrow stem cells to easily penetrate into the graft. This enhanced microenvironment is thought to regenerate hyaline cartilage rather than only fibrocartilage. Although the graft is available in different sizes, it may not fit the curvature of the joint surface or match the native cartilage thickness. The long shelf life of Cartiform is a distinct logistical and practical advantage compared to fresh osteochondral allografts that must be used within 2 weeks of availability. However, Cartiform is currently expensive and not covered by all insurance companies. Melugin et al. published a prospective case series following 19 patients with full



Fig. 8 Left: large full thickness chondral defect in the central patella. Middle: implantation of Cartiform using an absorbable suture. Right: final fixation of the Cartiform implant after application of a fibrin sealant TISSEEL (Baxter, USA)



Fig. 9 A full thickness patellar cartilage defect before (left) and after (right) BioCartilage implant

thickness cartilage defects of the patellofemoral compartment [62]. Nineteen (19) patients received the Cartiform graft in addition to microfracture and 17 underwent concomitant surgery such as lateral retinacular release or tibial tubercle osteotomy to improve patellar tracking. They demonstrated that at a minimum of 2 years and average of 42 months, patients had significant clinical improvements from baseline in validated outcome scores. Second look arthroscopy at 8 weeks to 1 year showed good incorporation of the graft, yet 2 out of 19 patients went on to develop patellofemoral arthritis which required a joint replacement. This study demonstrates promising results, but further studies and randomized controlled trials are necessary to determine functional and economic superiority over other techniques.

Another similar strategy for cartilage reconstruction is the use of a minced juvenile articular cartilage allograft, DeNovo (Zimmer Biomet, USA), which is harvested from the femoral condyle of donors age <13 years old. The minced allograft contains viable chondrocytes that are implanted and secured into the defect with fibrin glue. The theory is that these viable chondrocytes migrate from the allograft cartilage and proliferate to form new cartilage which then integrates with the surrounding cartilage and subchondral bone. This single stage procedure is indicated for cartilage defects less than 5 cm² in young patients with intact subchondral bone. The disadvantages are that the graft is expensive and has a shelf life of only 40–45 days [63]. DeNovo is a relatively new product and only limited data are currently available. One case series followed 25 patients who received DeNovo for symptomatic articular cartilage lesions and received intermittent MRIs and pain, function, and recreations scores [61]. At 2 years post-operation, functional outcomes had significantly improved compared to baseline, histology demonstrated a mixture of hyaline and fibrocartilage formed along with type two collagen, and MRI demonstrated mean lesion filling of 109%. Although this study suggested that DeNovo is safe and effective in the short term, long term results and superiority to other treatments are not known.

Other strategies involve harvesting allograft for only the extracellular matrix instead of whole cartilage. An example is BioCartilage (Arthrex, USA), which is a dehydrated allograft extracellular matrix scaffold made up of type 2 collagen, proteoglycans, and cartilaginous growth factors from native cartilage. This product is

designed to augment bone marrow stimulation techniques as it is thought to lead to more hyaline cartilage and less fibrocartilage formation. A study by Fortier et al. compared BioCartilage with platelet rich plasma and microfracture to microfracture alone in an equine model [59]. They demonstrated that the BioCartilage group had higher International Cartilage Repair Society (ICRS) scores, better histologic scores, and more formation of type 2 collagen than the control group. In humans, BioCartilage is indicated for most of the same indications as microfracture. It is an attractive option because it is a single stage procedure, can be used in either arthroscopic or open technique, does not contain living cells and therefore has a shelf life of multiple years, and is less expensive than many of the other available products. The allograft is mixed with either PRP or whole blood, placed in the defect, and sealed in place with fibrin glue (Fig. 9) [64]. BioCartilage has been shown to be safe in humans, and case studies have demonstrated improvement in clinical outcomes and MRI parameters of articular cartilage repair quality, but longer term and high quality outcomes data are currently unavailable [65].

Summary of the commercial grafts that are currently available in the USA

Graft type	Advantages	Disadvantages	Trade name	Manufacturer/Tissue Bank
Juvenile particulate cartilage allograft	– Single stage procedure	– 40–45-day shelf life – More expensive	DeNovo	Zimmer Biomet
Dehydrated allograft extracellular matrix	– Single stage procedure – Multiple year shelf life – Less expensive		Biocartilage	Arthrex
Cryopreserved viable osteochondral allograft	– Single stage procedure – Long shelf life – Easily contoured to desired shape	– More expensive	Cartiform	Arthrex
Fresh osteochondral allograft	– Single stage procedure – Can replace largest defects – Can address bone loss – Bone to bone healing	– Strict storage conditions – Surgical timing constraints – Possible immune response – More expensive	N/A	– Joint Research Foundation – Musculoskeletal Transplant Foundation – LifeNet Health – Regeneration Technology Incorporated

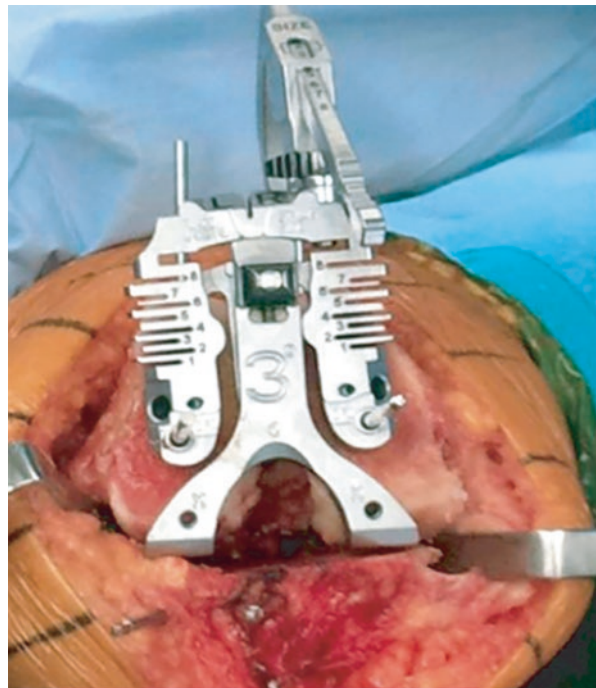
To date, the ideal graft for articular cartilage repair remains unknown in clinical practice. There is limited data comparing all the different cartilage restoration techniques and products. It is extremely complex and challenging to design cartilage restoration clinical research studies for many reasons including different cartilage

defect sizes, different locations (femoral condyle versus patella), presence of mal-tracking and malalignment, instability, or increased cartilage strains from meniscus insufficiency. There are also patient related factors that are confounding variables such as age, weight, nutritional status, smoking history. Further, a second surgery and biopsy would be required for histological evaluation of the cartilage in human patient. Additionally, FDA regulations require a high expense and time investment prior to translating the research from bench to bedside. In order to avoid the need for premarket approval and animal and clinical studies, products cannot be combined with another product and must follow principles of minimal manipulation and homologous use [66].

In our opinion, the ideal graft will either contain or be able to generate true hyaline articular cartilage, integrate well with the patient's existing cartilage and bone, be as durable as native cartilage, and fit the patient's specific anatomy. This could be achieved with cell-based or cell-free therapies and will be highly dependent on the available mechanical, chemical, and tissue engineering technology. The graft would ideally be low cost, have a long shelf life, be easily available, and could be implanted during a single procedure. Such a graft has the potential to impact millions of people who suffer from chondral defects and osteoarthritis. 3D printing will likely have an important role in the development of this ideal graft for the ability to customize materials, mechanical properties, and patient-specific shapes.

Despite our best efforts to repair and regenerate articular cartilage, many patients will eventually require a joint replacement (arthroplasty) procedure. A joint

Fig. 10 Distal femur cutting jig with adjustable guides for intra-op measurement and resection during total knee arthroplasty. (Image from "Daines & Dennis. Gap Balancing vs. Measured Resection Technique in Total Knee Arthroplasty. Clin Orthop Surg. 2014; 6: 1–8. <https://ecios.org/DOIX.php?id=10.4055/cios.2014.6.1.1>")



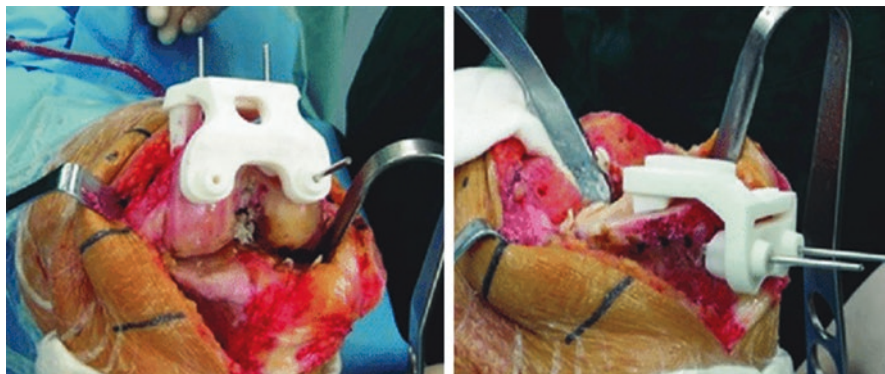


Fig. 11 Example of 3D printed patient-specific distal femur and proximal tibia cutting guides. (Image taken from: Patient-Specific Instruments Based on Knee Joint Computed Tomography and Full-Length Lower Extremity Radiography in Total Knee Replacement - Scientific Figure on ResearchGate. Available from: https://www.researchgate.net/figure/Representative-images-of-primary-total-knee-replacement-guided-by-patient-specific_fig1_323558012 [accessed 22 Sep 2020])

replacement is the final step in management of cartilage damage resulting from post-traumatic arthritis, osteoarthritis, rheumatoid arthritis, or other causes of joint destruction. An estimated 5.2 million total knee replacements were performed in the USA between 2000 and 2010, and this number is only increasing with an aging population [67]. While joint replacement is historically one of the most successful procedures in all of surgery, implant position and alignment affects implant performance and patient outcomes and is especially critical in total knee arthroplasty. 3D printing has been used in clinical practice in the field of total knee arthroplasty for years with the goal of improving alignment. Knee replacement involves bony cuts and resection of the arthritic cartilage surface of the distal femur and proximal tibia. Measurements for these cuts are traditionally taken intraoperatively by the surgeon and based on anatomic landmarks and preoperative radiographs. Adjustable cutting jigs are placed on the bone to guide resection as shown in Fig. 10 [68], and different sized implants are available and trialed for proper fit. Patient-specific implants (PSI) differ in the way measurements are taken, the steps performed during surgery, and how 3D printing technology is utilized. There are many PSI currently on the market from different companies, but all use a preoperative MRI or CT scan of the patient to create a 3D image of the joint. This 3D image is used instead of intraoperative measurements and anatomic landmarks. The 3D data may be used to create a patient-specific cutting block or “jig” which can be 3D printed by the device manufacturer before the surgery is performed. This custom jig is then used intraoperatively as shown in Fig. 11 [69]. The printed block is designed to conform to the patient’s specific anatomy and may guide the placement of pins to then further secure a traditional cutting block, or may actually be the cutting block itself. The iTotal Identity (Conformis, USA) is a total knee arthroplasty system in which jigs are 3D printed out of nylon for use intraoperatively, and wax molds are 3D printed

for casting of the patient-specific cobalt-chromium and titanium implant. Theoretically, this improves the precision and accuracy of implant positioning and thus patient outcomes [70]. Studies have shown that surgeries involving PSI use significantly less instruments trays and have less steps to the surgical procedure, but the clinical significance of this is unknown. A systematic review concluded that PSI has not reliably demonstrated improvement in postoperative limb or component alignment, implant longevity, cost, or patient outcomes when compared with standard instrumentation [71].

For further readings about 3D printing in other fields of orthopedics which are outside of the scope of this book, the reader is directed to articles by Galvez, McMemamin, Skelley, and Zuniga covering the topics of surgical planning, education, surgical simulation, and prosthesis development, respectively [72–75].

7 Conclusion

Osteochondral defects and cartilage injury are common causes of joint pain and disability in patients of all ages. Many surgical treatment options exist with some clinical success, but all have limitations and there is a need for innovative and cost-efficient solutions that will result in improved patient outcomes. The ideal cartilage implants of the future will likely involve both tissue engineering and 3D printing to create individualized scaffolds or tissue that can mimic hyaline cartilage. The development of this type of implant could result in symptomatic improvements and prevention of osteoarthritis in millions of patients throughout the USA.

References

1. Hunziker EB, Lippuner K, Keel MJB, Shintani N. An educational review of cartilage repair: precepts & practice—myths & misconceptions—progress & prospects. *Osteoarthr Cartil.* 2015;23(3):334–50. <https://doi.org/10.1016/j.joca.2014.12.011>.
2. Williams RJ. *Cartilage repair strategies*. Humana Press. 2007.
3. Bedi A, Feeley BT, Williams RJ. Management of articular cartilage defects of the knee. *J Bone Joint Surg Am.* 2010;92(4):994–1009. <https://doi.org/10.2106/JBJS.I.00895>.
4. Shelbourne KD, Jari S, Gray T. Outcome of untreated traumatic articular cartilage defects of the knee: a natural history study. *J Bone Joint Surg Am.* 2003;85-A(Suppl):8–16. <https://doi.org/10.2106/00004623-200300002-00002>.
5. Neogi T, Nevitt M, Niu J, et al. Subchondral bone attrition may be a reflection of compartment-specific mechanical load: the MOST study. *Ann Rheum Dis.* 2010;69(5):841–4. <https://doi.org/10.1136/ard.2009.110114>.
6. Kornaat PR, Kloppenburg M, Sharma R, et al. Bone marrow edema-like lesions change in volume in the majority of patients with osteoarthritis; associations with clinical features. *Eur Radiol.* 2007;17(12):3073–8. <https://doi.org/10.1007/s00330-007-0711-1>.
7. Felson DT, Chaisson CE, Hill CL, et al. The association of bone marrow lesions with pain in knee osteoarthritis. *Ann Intern Med.* 2001;134(7):541–9. <https://doi.org/10.7326/0003-4819-134-7-200104030-00007>.

8. Curl WW, Krome J, Gordon ES, Rushing J, Smith BP, Poehling GG. Cartilage injuries: a review of 31,516 knee arthroscopies. *Arthroscopy*. 1997;13(4):456–60. [https://doi.org/10.1016/S0749-8063\(97\)90124-9](https://doi.org/10.1016/S0749-8063(97)90124-9).
9. Lowry V. Older knees now have new option. *The New York Times*. 2005, April 5. <https://www.nytimes.com/2005/04/05/health/nutrition/older-knees-now-have-new-option.html>.
10. Steadman JR, Rodkey WG, Singleton SB, Briggs KK. Microfracture technique for full-thickness chondral defects: technique and clinical results. *Oper Tech Orthop*. 1997;7(4):300–4. [https://doi.org/10.1016/S1048-6666\(97\)80033-X](https://doi.org/10.1016/S1048-6666(97)80033-X).
11. Steadman JR, Briggs KK, Rodrigo JJ, Kocher MS, Gill TJ, Rodkey WG. Outcomes of microfracture for traumatic chondral defects of the knee: average 11-year follow-up. *Arthroscopy*. 2003;19(5):477–84. <https://doi.org/10.1053/jars.2003.50112>.
12. Steadman JR, Rodkey WG, Briggs KK. Microfracture: its history and experience of the developing surgeon. *Cartilage*. 2010;1(2):78–86. <https://doi.org/10.1177/1947603510365533>.
13. Guo T, Noshin M, Baker HB, et al. 3D printed biofunctionalized scaffolds for microfracture repair of cartilage defects. *Biomaterials*. 2018;185:219–31. <https://doi.org/10.1016/j.biomaterials.2018.09.022>.
14. Gobbi A, Karnatzikos G, Kumar A. Long-term results after microfracture treatment for full-thickness knee chondral lesions in athletes. *Knee Surg Sports Traumatol Arthrosc*. 2014;22(9):1986–96. <https://doi.org/10.1007/s00167-013-2676-8>.
15. Müller B, Kohn D. [Indication for and performance of articular cartilage drilling using the Pridie method]. *Der Orthopäde*. 1999;28(1):4–10. <https://doi.org/10.1007/s001320050315>.
16. Chen H, Sun J, Hoemann CD, et al. Drilling and microfracture lead to different bone structure and necrosis during bone-marrow stimulation for cartilage repair. *J Orthop Res*. 2009;27(11):1432–8. <https://doi.org/10.1002/jor.20905>.
17. Dandy DJ. Abrasion chondroplasty. *Arthroscopy*. 1986;2(1):51–3. [https://doi.org/10.1016/S0749-8063\(86\)80011-1](https://doi.org/10.1016/S0749-8063(86)80011-1).
18. Beckmann R, Lippross S, Hartz C, et al. Abrasion arthroplasty increases mesenchymal stem cell content of postoperative joint effusions. *BMC Musculoskelet Disord*. 2015;16(1):1–7. <https://doi.org/10.1186/s12891-015-0705-0>.
19. Hunt SA, Jazrawi LM, Sherman OH. Arthroscopic Management of Osteoarthritis of the knee. *J Am Acad Orthop Surg*. 2002;10(5):356–63. <https://doi.org/10.1136/bmj.e4934>.
20. Rand JA. Role of arthroscopy in osteoarthritis of the knee. *Arthroscopy*. 1991;7(4):358–63. [https://doi.org/10.1016/0749-8063\(91\)90004-h](https://doi.org/10.1016/0749-8063(91)90004-h).
21. Redman SN, Oldfield SF, Archer CW, Roughley PJ, Lee C. Current strategies for articular cartilage repair. *Eur Cells Mater*. 2005;9:23–32. <https://doi.org/10.22203/eCM.v009a04>.
22. Matsunaga D, Akizuki S, Takizawa T, Yamazaki I, Kuraishi J. Repair of articular cartilage and clinical outcome after osteotomy with microfracture or abrasion arthroplasty for medial gonarthrosis. *Knee*. 2007;14(6):465–71. <https://doi.org/10.1016/j.knee.2007.06.008>.
23. Hevesi M, Bernard C, Hartigan DE, Levy BA, Domb BG, Krych AJ. Is microfracture necessary? Acetabular chondrolabral debridement/abrasion demonstrates similar outcomes and survival to microfracture in hip arthroscopy: a multicenter analysis. *Am J Sports Med*. 2019;47(7):1670–8. <https://doi.org/10.1177/0363546519845346>.
24. Cotter EJ, Wang KC, Yanke AB, Chubinskaya S. Bone marrow aspirate concentrate for cartilage defects of the knee: from bench to bedside evidence. *Cartilage*. 2018;9(2):161–70. <https://doi.org/10.1177/1947603517741169>.
25. Packer JD, Chang W-T, Dragoo JL. The use of vibrational energy to isolate adipose-derived stem cells. *Plast Reconstr Surg Global Open*. 2018;6(1):e1620. <https://doi.org/10.1097/GOX.0000000000001620>.
26. Fraser EJ, Savage-Elliott I, Yasui Y, et al. Clinical and MRI donor site outcomes following autologous osteochondral transplantation for Talar osteochondral lesions. *Foot Ankle Int*. 2016;37(9):968–76. <https://doi.org/10.1177/1071100716649461>.

27. Zhong J, Guo B, Xie J, et al. Crosstalk between adipose-derived stem cells and chondrocytes: when growth factors matter. *Bone Res.* 2016;4:15036. <https://doi.org/10.1038/boneres.2015.36>.
28. Frese L, Dijkman PE, Hoerstrup SP. Adipose tissue-derived stem cells in regenerative medicine. *Transfusion medicine and hemotherapy* : offizielles Organ der Deutschen Gesellschaft für Transfusionsmedizin und Immunhamatologie. 2016;43(4):268–74. <https://doi.org/10.1159/000448180>.
29. Mehrabani D, Mojtahed Jaber F, Zakerinia M, et al. The healing effect of bone marrow-derived stem cells in knee osteoarthritis: a case report. *World J Plast Surg.* 2016;5(2):168–74.
30. Freitag J, Li D, Wickham J, Shah K, Tenen A. Effect of autologous adipose-derived mesenchymal stem cell therapy in the treatment of a post-traumatic chondral defect of the knee. *BMJ Case Rep.* 2017;2017:bcr-2017-220852. <https://doi.org/10.1136/bcr-2017-220852>.
31. Freitag J, Bates D, Wickham J, et al. Adipose-derived mesenchymal stem cell therapy in the treatment of knee osteoarthritis: a randomized controlled trial. *Regen Med.* 2019;14(3):213–30. <https://doi.org/10.2217/rme-2018-0161>.
32. Lee WY-W, Wang B. Cartilage repair by mesenchymal stem cells: clinical trial update and perspectives. *J Orthop Transl.* 2017;9:76–88. <https://doi.org/10.1016/j.jot.2017.03.005>.
33. Kuah D, Sivell S, Longworth T, et al. Safety, tolerability and efficacy of intra-articular Progenza in knee osteoarthritis: a randomized double-blind placebo-controlled single ascending dose study. *J Transl Med.* 2018;16(1):49. <https://doi.org/10.1186/s12967-018-1420-z>.
34. Li W-J, Tuli R, Okafor C, et al. A three-dimensional nanofibrous scaffold for cartilage tissue engineering using human mesenchymal stem cells. *Biomaterials.* 2005;26(6):599–609. <https://doi.org/10.1016/j.biomaterials.2004.03.005>.
35. Rosadi I, Karina K, Rosliana I, et al. In vitro study of cartilage tissue engineering using human adipose-derived stem cells induced by platelet-rich plasma and cultured on silk fibroin scaffold. *Stem Cell Res Ther.* 2019;10(1):369. <https://doi.org/10.1186/s13287-019-1443-2>.
36. Batty L, Dance S, Bajaj S, Cole BJ. Autologous chondrocyte implantation: an overview of technique and outcomes. *ANZ J Surg.* 2011;81(1–2):18–25. <https://doi.org/10.1111/j.1445-2197.2010.05495.x>.
37. Knutsen G, Drogset JO, Engebretsen L, et al. A randomized multicenter trial comparing autologous chondrocyte implantation with microfracture. *J Bone Joint Surg.* 2016;98(16):1332–9. <https://doi.org/10.2106/JBJS.15.01208>.
38. Brittberg M. Cell carriers as the next generation of cell therapy for cartilage repair. *Am J Sports Med.* 2010;38(6):1259–71. <https://doi.org/10.1177/0363546509346395>.
39. Saris D, Price A, Widuchowski W, et al. Matrix-applied characterized autologous cultured chondrocytes versus microfracture. *Am J Sports Med.* 2014;42(6):1384–94. <https://doi.org/10.1177/0363546514528093>.
40. Camp CL, Stuart MJ, Krych AJ. Current concepts of articular cartilage restoration techniques in the knee. *Sports Health.* 2014;6(3):265–73. <https://doi.org/10.1177/1941738113508917>.
41. Richter DL, Tanksley JA, Miller MD. Osteochondral autograft transplantation. *Sports Med Arthrosc Rev.* 2016;24(2):74–8. <https://doi.org/10.1097/JSA.0000000000000099>.
42. Krych AJ, Robertson CM, Williams RJ. Return to athletic activity after osteochondral allograft transplantation in the knee. *Am J Sports Med.* 2012;40(5):1053–9. <https://doi.org/10.1177/0363546511435780>.
43. Rowland R, Colello M, Wyland DJ. Osteochondral autograft transfer procedure: arthroscopic technique and technical pearls. *Arthrosc Tech.* 2019;8(7):e713–9. <https://doi.org/10.1016/j.eats.2019.03.006>.
44. Solheim E, Hegna J, Inderhaug E. Early determinants of long-term clinical outcome after cartilage repair surgery in the knee. *J Orthop.* 2018;15(1):222–5. <https://doi.org/10.1016/j.jor.2018.01.021>.
45. LaPrade RF, Botker J, Herzog M, Agel J. Refrigerated osteoarticular allografts to treat articular cartilage defects of the femoral condyles. *J Bone Joint Surg Am Vol.* 2009;91(4):805–11. <https://doi.org/10.2106/JBJS.H.00703>.

46. Torrie AM, Kesler WW, Elkin J, Gallo RA. Osteochondral allograft. *Curr Rev Musculoskelet Med.* 2015;8(4):413–22. <https://doi.org/10.1007/s12178-015-9298-3>.
47. Gracitelli GC, Ymoraes V, Franciozi CES, Luzo MV, Belloti JC. Surgical interventions (microfracture, drilling, mosaicplasty, and allograft transplantation) for treating isolated cartilage defects of the knee in adults. *Cochrane Database Syst Rev.* 2016;(9). <https://doi.org/10.1002/14651858.CD010675.pub2>. www.cochranelibrary.com
48. Daly AC, Freeman FE, Gonzalez-Fernandez T, Critchley SE, Nulty J, Kelly DJ. 3D bioprinting for cartilage and osteochondral tissue engineering. *Adv Healthc Mater.* 2017;6(22):1–20. <https://doi.org/10.1002/adhm.201700298>.
49. Di Bella C, Fosang A, Donati DM, Wallace GG, Choong PFM. 3D bioprinting of cartilage for orthopedic surgeons: reading between the lines. *Front Surg.* 2015;2:1–7. <https://doi.org/10.3389/fsurg.2015.00039>.
50. Dhawan A, Kennedy PM, Rizk EB, Ozbolat IT. Three-dimensional bioprinting for bone and cartilage restoration in orthopaedic surgery. *J Am Acad Orthop Surg.* 2019;27(5):E215–26. <https://doi.org/10.5435/JAAOS-D-17-00632>.
51. Mouser VHM, Levato R, Bonassar LJ, et al. Three-dimensional bioprinting and its potential in the field of articular cartilage regeneration. *Cartilage.* 2017;8(4):327–40. <https://doi.org/10.1177/1947603516665445>.
52. Izadifar Z, Chen X, Kulyk W. Strategic design and fabrication of engineered scaffolds for articular cartilage repair. *J Funct Biomater.* 2012;3(4):799–838. <https://doi.org/10.3390/jfb3040799>.
53. Lim W, Kim B, Moon YL. Three-dimensional bioprinting for bone and cartilage transplantation. *Ann Joint.* 2019;4(5):7. <https://doi.org/10.21037/aoj.2018.12.06>.
54. Meng W, Gao L, Venkatesan JK, Wang G, Madry H, Cucchiari M. Translational applications of photopolymerizable hydrogels for cartilage repair. *J Exp Orthop.* 2019;6(1):47. <https://doi.org/10.1186/s40634-019-0215-3>.
55. Lee CH, Cook JL, Mendelson A, Moioli EK, Yao H, Mao JJ. Regeneration of the articular surface of the rabbit synovial joint by cell homing: a proof of concept study. *Lancet.* 2010;376(9739):440–8. [https://doi.org/10.1016/S0140-6736\(10\)60668-X](https://doi.org/10.1016/S0140-6736(10)60668-X).
56. Schuurman W, Klein TJ, Dhert WJA, van Weeren PR, Hutmacher DW, Malda J. Cartilage regeneration using zonal chondrocyte subpopulations: a promising approach or an over-complicated strategy? *J Tissue Eng Regen Med.* 2015;9(6):669–78. <https://doi.org/10.1002/term.1638>.
57. Zhu D, Tong X, Trinh P, Yang F. Mimicking cartilage tissue zonal organization by engineering tissue-scale gradient hydrogels as 3D cell niche. *Tissue Eng Part A.* 2018;24(1–2):1–10. <https://doi.org/10.1089/ten.TEA.2016.0453>.
58. Hindle P, Hendry JL, Keating JF, Biant LC. Autologous osteochondral mosaicplasty or TruFit™ plugs for cartilage repair. *Knee Surg Sports Traumatol Arthrosc.* 2014;22(6):1235–40. <https://doi.org/10.1007/s00167-013-2493-0>.
59. Fortier LA, Chapman HS, Pownder SL, et al. BioCartilage improves cartilage repair compared with microfracture alone in an equine model of full-thickness cartilage loss. *Am J Sports Med.* 2016;44(9):2366–74. <https://doi.org/10.1177/0363546516648644>.
60. Verhaegen J, Clockaerts S, Van Osch GJVM, Somville J, Verdonk P, Mertens P. TruFit plug for repair of osteochondral defects—where is the evidence? Systematic review of literature. *Cartilage.* 2015;6(1):12–9. <https://doi.org/10.1177/1947603514548890>.
61. Vangsness CT, Higgs G, Hoffman JK, et al. Implantation of a novel cryopreserved viable osteochondral allograft for articular cartilage repair in the knee. *J Knee Surg.* 2018;31(6):528–35. <https://doi.org/10.1055/s-0037-1604138>.
62. Melugin HP, Ridley TJ, Bernard CD, et al. Prospective outcomes of cryopreserved osteochondral allograft for patellofemoral cartilage defects at minimum 2-year follow-up. *Cartilage.* 2020. <https://doi.org/10.1177/1947603520903420>.

63. Yanke AB, Tilton AK, Wetters NG, Merkow DB, Cole BJ, DeNovo NT. Particulated juvenile cartilage implant. *Sports Med Arthrosc Rev.* 2015;23(3):125–9. <https://doi.org/10.1097/JSA.0000000000000077>.
64. Hirahara AM, Mueller KW. BioCartilage: a new biomaterial to treat chondral lesions. *Sports Med Arthrosc Rev.* 2015;23(3):143–8. <https://doi.org/10.1097/JSA.0000000000000071>.
65. Carter AH, Guttierrez N, Subhawong TK, et al. MR imaging of BioCartilage augmented microfracture surgery utilizing 2D MOCART and KOOS scores. *J Clin Orthop Trauma.* 2018;9(2):146–52. <https://doi.org/10.1016/j.jcot.2017.08.017>.
66. Anz AW, Hackel JG, Nilssen EC, Andrews JR. Application of biologics in the treatment of the rotator cuff, meniscus, cartilage, and osteoarthritis. *J Am Acad Orthop Surg.* 2014;22(2):68–79. <https://doi.org/10.5435/JAAOS-22-02-68>.
67. Williams SN, Wolford ML, Bercovitz A. Hospitalization for total knee replacement among inpatients aged 45 and over: United States, 2000–2010. *NCHS Data Brief.* 2015;210:1–8.
68. Daines BK, Dennis DA. Gap balancing vs. measured resection technique in total knee arthroplasty. *Clin Orthop Surg.* 2014;6(1):1–8. <https://doi.org/10.4055/cios.2014.6.1.1>.
69. Haglin JM, Eltorai AEM, Gil JA, Marcaccio SE, Botero-Hincapie J, Daniels AH. Patient-specific orthopaedic implants. *Orthop Surg.* 2016;8(4):417–24. <https://doi.org/10.1111/os.12282>.
70. Krishnan SP, Dawood A, Richards R, Henckel J, Hart AJ. A review of rapid prototyped surgical guides for patient-specific total knee replacement. *J Bone Joint Surg.* 2012;94-B(11):1457–61. <https://doi.org/10.1302/0301-620x.94b11.29350>.
71. Sassoon A, Nam D, Nunley R, Barrack R. Systematic review of patient-specific instrumentation in total knee arthroplasty: new but not improved. *Clin Orthop Relat Res.* 2015;473(1):151–8. <https://doi.org/10.1007/s11999-014-3804-6>.
72. Zuniga JM, Peck J, Srivastava R, Katsavelis D, Carson A. An open source 3D-printed transitional hand prosthesis for children. *J Prosthet Orthot.* 2016;28(3):103–8. <https://doi.org/10.1097/JPO.0000000000000097>.
73. Skelley NW, Smith MJ, Ma R, Cook JL. Three-dimensional printing technology in orthopaedics. *J Am Acad Orthop Surg.* 2019;27(24):918–25. <https://doi.org/10.5435/JAAOS-D-18-00746>.
74. McMenamin PG, Quayle MR, McHenry CR, Adams JW. The production of anatomical teaching resources using three-dimensional (3D) printing technology. *Anat Sci Educ.* 2014;7(6):479–86. <https://doi.org/10.1002/ase.1475>.
75. Galvez M, Asahi T, Baar A, et al. Use of three-dimensional printing in orthopaedic surgical planning. *JAAOS Global Res Rev.* 2018;2(5):e071. <https://doi.org/10.5435/jaaosglobal-d-17-00071>.

3D Printing in Pediatric Orthopedics



Anirejuoritse Bafor, Jayanthi Parthasarathy, and Christopher A. Iobst

1 Introduction and Historical Perspective

Pediatric orthopedics is the surgical specialty that deals with the management of musculoskeletal conditions in growing children. The origin of the field is credited to a French physician, Nicholas Andry. In 1741, he coined the term “Orthopedia” which has its origins from two Greek words: *orthos* meaning straight and *paidios* meaning child [1].

Prior to the advent of 3D printing technology, orthopedic operative planning and templating were primarily limited to information derived from two-dimensional X-ray images obtained as part of the patient evaluation. This made precise assessment of complex fracture patterns and deformities difficult. Consequently, potentially less accurate treatment plans with subsequently higher unsatisfactory outcomes were the result. To overcome this, magnetic resonance imaging (MRI) and computerized tomography (CT) scans with 3D reconstruction were introduced to provide three-dimensional visualization of the anatomy. While these advanced imaging modalities have helped to improve diagnostic accuracy and treatment planning, 3D printing delivers the next level in the evolution of imaging technology. The ability to create a handheld model (or models) that can allow surgical plans to be trialed prior to the actual surgery is immensely valuable for complex cases.

3D printing has been around since the early 1980s. In 1984, Charles W. Hull, who was one of the founders of 3D systems, successfully filed a US patent for the world’s first 3D printer marking the beginning of the 3D printing technology era [2]. 3D printing can occur by either an additive or subtractive process. The concept of additive manufacturing adds successive layers of material to produce a solid object. In contrast, subtractive printing entails the removal of unwanted material from the

A. Bafor · J. Parthasarathy · C. A. Iobst (✉)

Orthopaedic Surgery, The Ohio State University, College of Medicine, Nationwide Children’s Hospital, Columbus, OH, USA

e-mail: Christopher.Iobst@nationwidechildrens.org

base source, leaving the desired 3D structure as the result of the process. The process of 3D printing is facilitated by a complex computer-aided design (CAD) software. Some of its earliest uses were in rapid prototyping in the engineering sector but it has since found applicability in almost all spheres of life. As improvements in technology and design have evolved, 3D printing has been utilized to produce everything from simple homogenous solid structures to complex structures like cars, aircraft, and ironically even 3D printers! Because of the vast potential inherent in this process, it is no surprise that it has gained rapid acceptance and applicability in healthcare, especially in orthopedics.

2 The 3D Printing Process

The pathway to 3D printing patient-specific models, implants, and instruments (Fig. 1) consists of two phases: a design phase and a manufacturing phase. The design input commences with the accurate capture and acquisition of an image of the structure to be 3D printed. This is achieved using computerized tomography (CT) scanning and/or magnetic resonance imaging (MRI). High quality images are desirable as this translates to a better resolution of the 3D model created. The images obtained are saved in the digital imaging and communication in medicine (DICOM) format which is then processed to create 2D images. Segmentation of the region of interest and creation of a 3D virtual model using DICOM to Standard Triangle Language or Standard Tessellation Language (STL) conversion programs as MIMICS™, Inprint™ (Materialise, Leuven Belgium), 3D Doctor (MA, USA), 3D Slicer, Invesalious, or any equivalent DICOM to 3D model converter program is the next step. The 3D virtual model is exported as an STL file which is then imported

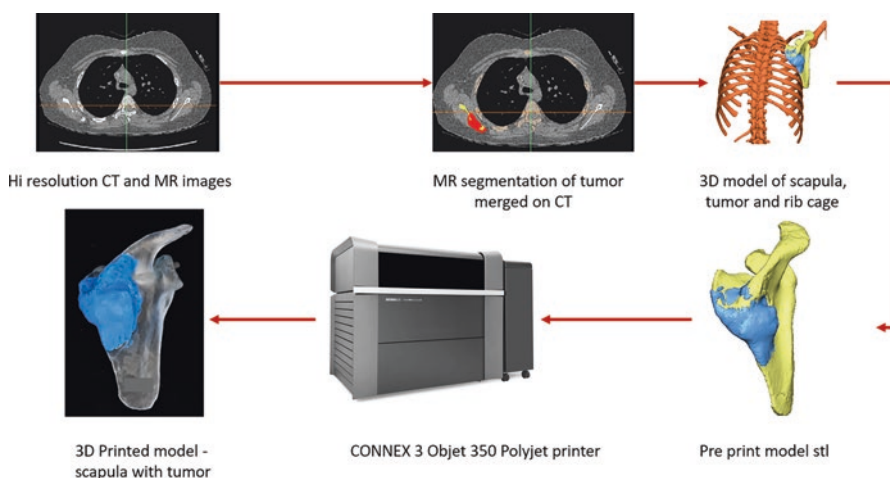


Fig. 1 Process flow for 3D printing patient-specific anatomic models from 2D DICOM images

into computer assisted design (CAD) programs such as Geomagic Freeform™ (3D Systems, Rock Hill, SC), 3Matics™ (Materialise Leuven, Belgium), mesh mixer, or similar programs. These programs are used to remove any anatomy that is not required to be printed while retaining details about specific structures to be printed. Non-anatomic components for structural integrity of the model are added at this time point and the STL files are exported to the printers for printing. During the manufacturing phase the STL file is then transmitted to the 3D printer which then uses this to generate a set of commands called the G-code which determines how the physical structure of the 3D model is produced by the printer [3]. Production of the physical model occurs by a process of layered printing, usually starting with a support structure or scaffolding upon which the 3D printed model is built. Once printing is completed, this base is removed. Depending on the fabrication technique used, multiple materials of differing textures and properties can be used to create structures of varying complexities [4]. In orthopedics, much of the printed materials come from additive manufacturing powder bed fusion printers [5]. Additional information on the 3D printing process can be found in Chap. 4.

The last three decades have seen rapid improvements in design and technology. Besides stereolithography (SLA), other 3D-printing technologies which have been developed include digital light processing (DLP), fused deposition modeling (FDM), selective laser sintering (SLS), selective laser melting (SLM), electronic beam melting (EBM), laminated object manufacturing (LOM), binder jetting (BJ), and material jetting (MJ) (Fig. 2). Of these, SLM and EBM have been found particularly useful in orthopedics. Polyjet technology has the ability to combine

Fig. 2 3D printer GE ARCAM EBM printer (powder bed fusion of metals with electron beam energy)



Table 1 Non-implantable materials and 3D printing processes

Process name	Materials	Energy used	Color	Hard/ flexible	Resolution	Post-processing	Biocompatible materials	Sterilization
Fused deposition modeling (FDM)	Thermoplastic spools, polylactic acid, ABS, polycarbonate, nylon, ULTEM	Heat	Single color	Hard	High	Breakaway supports	ABS M1, ULTEM 9085, polycarbonate, polylactic acid Polycaprolactone, PEG	ULTEM 9085 Autoclave
PolyJet™	Liquid resin	UV	Multicolor	Both	High	Waxy supports removed with high pressure waterjet and lye bath	MED 610	Sterrad®
Stereolithography apparatus (SLA)	Liquid resin	UV	Single color 3D systems 2 colors by over curing	Both	High	Secondary curing needed, breakaway supports	Dental SG Surgical Guide	Autoclave Sterrad®
Selective laser melting/sintering (SLM)	Powder bed	LASER	Single color	Hard	High	Postprocessing	Polyamide, nylon	Sterrad®
Binder jet	Powder bed	Chemical with cyanoacrylate jet	Multicolor	Hard	Low	Secondary process	Not biocompatible	Not biocompatible

Table 2 Implantable materials and 3D printing processes (non-biodegradable)

Process name	Materials	Energy used	Resolution	Post-processing	Region of implantation	Sterilization	Bone growth in lattice structures
Electron Beam Melting™ (EBM)	Ti alloys, Co Cr	Electron beam	High	Powder and supports removal by machining	Extremities, hip, spinal cages	Autoclave	Yes
Direct Metal Laser Sintering™ (DMLS)	Ti alloys, Co Cr	Laser	Ti alloys, Co Cr	Powder and supports removal by machining	Spinal cages	Autoclave	Yes
Laser sintering	PEEK (polyether ether ketone)	Laser	High	Powder and supports removal by machining	Spinal cages	Autoclave	Yes

materials to produce parts with intermittent physical and mechanical properties as color and duraform and also build parts with rigid and flexible materials. The process can also produce a single model with multiple materials and properties.

The field of materials for 3D printing is also advancing very rapidly and newer materials are being introduced by every manufacturer. The process of choosing the appropriate printing material for any model/implant to be produced depends on the end use of the model/implant. Tables 1 and 2 show the materials currently available in the 3D-printing arena for orthopedic applications. These include making 3D-printed patient-specific models, non-implantable surgical guides that come in contact with skin, mucosa, and blood as well as implants that remain in the body long term. Most of the materials are supplied by the original equipment manufacturers of the 3D printers and can be used only on the specific printer. Therefore, the manufacturing facility is limited with respect to material options depending on the equipment and technology resources available.

3 Applications of 3D Printing Technology in Pediatric Orthopedics

Since its advent in the 1980s, the development of 3D printing technology has provided opportunities to advance the management of disease conditions in pediatric orthopedics. The last decade has seen a rapid rise in the use of 3D printing

technology in orthopedics as evidenced by a more than tenfold increase in publications based on 3D printing technology in orthopedics [6]. From deformity correction to oncology and production of prosthetics, 3D printing is rapidly changing the face of orthopedic treatment options. The ability to generate precise anatomical models, patient-specific surgical templates, instruments, and implants, as well as custom prosthetics and orthotics are just some of the methods where 3D printing is currently being utilized in pediatric orthopedic surgery [7]. More recently, bioengineering methods are being combined with 3D printing to create tissue engineered biomaterials that may revolutionize treatment options in musculoskeletal oncology and in the management of congenital and acquired skeletal deficiencies. The remainder of the chapter will summarize the current literature regarding the applications of 3D printing in pediatric orthopedic surgery.

3.1 Treatment Planning

A systematic review looking at the advantages and disadvantages of 3D printing in surgery found the production of anatomic models to be the commonest use of 3D printing [8]. Via a process called rapid prototyping, the use of preoperative anatomic models has been utilized across pediatric orthopedic subspecialty areas including limb reconstruction, oncology, and spine surgery [9–11]. By allowing the surgeon to better visualize and delineate certain anatomic structures, 3D printed models enhance the process of creating a preoperative plan. The surgeon can develop patient-specific detailed surgical plans for both the approach and the hardware placement. This has translated to improved accuracy in surgical procedures as well as reduced intraoperative time and better treatment outcomes. For example, it has been found to be beneficial in the management of pediatric pelvis and spinal conditions, providing better insight in the preoperative planning stage, providing a continuous reference during surgery, improving safety of the procedure, and shortening surgery duration [12]. In deformity correction surgery, these anatomically accurate models of complex bone deformities can be produced from processed CT scan images [13]. Hand-held mobile scanners have also been developed which can create 3D models of limbs including the entire soft tissue envelope which can then be utilized for computer based surgical planning and hardware design [14]. In serving as planning tools, these models are useful in determining appropriate location for placement of trans-osseous wires and half pins as well as permitting trial correction and preoperative assessment of correction of the deformity [13]. This “virtual surgical procedure” has the dual advantage of improving the precision and accuracy of the actual surgical procedure as well as providing a teaching tool for surgeons-in-training. Within the safety of a simulation lab, it also enables potential problems in the course of surgery to be anticipated. The surgeon can plan strategies to overcome or completely avoid these obstacles intraoperatively. In musculoskeletal oncology, 3D printing from reconstructed CT and MRI images has proven to be valuable in determining the optimal surgical resection plan that strikes a delicate balance

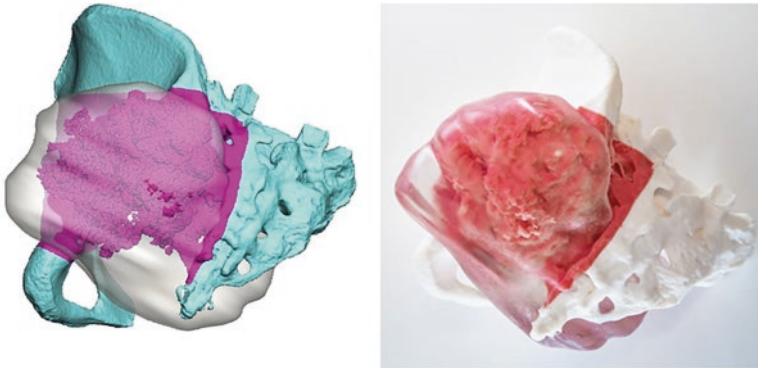


Fig. 3 Left pelvis chondrosarcoma model with resection plan—bony pelvis model derived from the CT and soft tissue tumor model from the MR image data

between wide tissue resection and sparing adjacent tissue [15]. Figure 3 shows a model derived by combining CT and MR scans of a patient with a chondrosarcoma of the left hip with a resection plan used in preoperative planning. This model is also useful for patient and family education and as a reference model during surgery. Composite 3D printed models created by overlaying MRI and CT data of a patient give the surgeon a better understanding of the pathologic anatomy and the spatial relationship of the lesion to the neighboring vital structures such as vessels and nerves.

3.2 Education

3D printing technology has been used both in the training of health care workers and in the education of patients. With the use of these anatomical models, physicians can better illustrate pathology and planned surgical interventions to patients and parents to enhance their understanding of the issues. It can therefore play a key role in the process of obtaining informed consent in conditions like Blount's disease, Perthes disease, and physeal bars [16].

Prior to the advent of 3D printing technology in modern orthopedics, hands-on training in areas like complex limb deformity correction surgery was only possible based on the availability of real-life cases or using theoretical approaches with archived two-dimensional X-ray images and clinical photos. Creation of anatomical models to serve as educational aids can now be achieved, thus enhancing training and education of healthcare providers. For example, in the treatment of clubfeet, it has been used to create models which are used to train healthcare providers in manipulation techniques as well as providing a better appreciation of pathologic anatomy [17].

3.3 *Patient-Specific Implants (PSI) and Instrumentation*

In addition to anatomical modeling, 3D printing can be used to create unique surgical instruments and implants. This can be especially helpful in cases that have unusual anatomy or presentation where standard “off the shelf” items have an imperfect fit. The surgeon can avoid the need to modify existing instruments or implants during surgery which can cause damage or weaken them in the process. By designing custom instruments or implants, 3D printing can potentially streamline the amount of inventory that needs to be stored in the operating room. 3D printing also increases the access to these instruments and implants in areas of the world that are resource challenged. Expensive implants or instruments that are not normally available can be 3D printed as an alternative in these countries. 3D printed PSI have gained importance due to their better fit and performance over their generic counterparts. The ability to control design and mechanical properties of the implant and optimization to the clinical scenario requirements, depending on the region of implantation is the key to the success of PSI. Traditionally used metals such as Titanium and its alloys, Tantalum and Stainless steel and Chrome cobalt are many times heavier and have a higher elastic modulus compared to bone. This discrepancy reduces mechanical forces transmitted to the bone and results in stress shielding leading to aseptic loosening and early loss of the implant [18, 19]. 3D printing with no manufacturing design constraints gives the unique ability to create an implant with the combination of lattice structures and smooth surfaces appropriately. The lattice structures reduce weight of the implant and alter the mechanical properties close to the region of implantation [20]. The resultant functionally graded implant specifications enable bone growth within the lattice structures for better stability and create smooth surfaces where friction between the joint surfaces is a concern [21, 22]. Mechanical properties as elastic modulus of the lattice structures can be altered by the thickness of the struts and the voids in the lattice structure. Moreover, the ability to enhance osseointegration and osseointegration of porous metallic implants by altering their biological, chemical, and physical characteristics, by surface modifications makes PSI better candidates. Metal 3D printing technologies such as electron beam melting (EBM) and direct metal laser sintering (DMLS) are the processes that are used to create patient-specific metallic implants. Other non-resorbable implants as spinal cages are 3D printed on laser sintering with polyether ether ketone (PEEK) or poly ether ketone ketone (PEKK).

3D printing has found a role in the intraoperative management of some musculoskeletal conditions. In a cadaveric study by Birnbaum et al., pedicle screw fixation in the lumbar spine was determined to be more accurate and faster using 3D printed templates created from CT scan images of the lumbar vertebrae. This was in comparison to conventional techniques of fluoroscopy and CT scan as well as other means of computer assisted spine surgery with navigation systems for pedicle screw fixation [23]. Spine models have become a definitive part of the surgical planning armamentarium in scoliosis surgery as they depict the complex 3D curve of the spine as seen in Fig. 4. CAD/CAM workflow for 3D printing spine braces has been well established and is being used currently in the clinical scenario as an option [24].



Fig. 4 Spine—a 3D printed scoliosis model showing anterior view on the left and posterior view on the right

Patient-specific models have also been utilized to plan corrective osteotomies in the management of complex limb deformities like intra-articular deformities and rotational forearm deformities. This application is particularly valuable in unilateral deformities since the contralateral normal limb can serve as a design template. In this process, synthetic templates are created and placed in the osteotomy gap, thus restoring the normal anatomy of the deformed bone. Patient-specific instrumentation can then be designed and 3D printed to precisely match the deformities and the planned osteotomy site. Specially designed implants used to hold the corrected position complete the potentially comprehensive 3D printed management using this technique [25, 26]. The reported advantages of this process are decreased surgery and anesthesia time, reduced risk of structural damage to the bone as well as reduced exposure to intraoperative ionizing radiation. Patient-specific 3D printed external fixators have also been designed for use in the management of long bone fractures [27]. These fixators have been deemed to be more accurate and user-friendly, being less reliant on surgeon expertise. Their major drawback is the prolonged fabrication waiting time which can be as much as 20 h preventing its use in an acute trauma setting. Similarly, 3D printed dynamizers have been designed and incorporated into standard external fixator struts. These have proven useful in accelerating bone healing in a large animal reverse dynamization fracture model [28].

More recently, 3D printing technology has been applied to the management of bone defects through the use of bio-engineered bone scaffolds [29–32]. Although they can be created as bespoke grafts specific to each patient, these materials are also attractive because they can be produced as versatile, universal grafts to fill bone defects without the added morbidity of donor site issues in traditional bone grafting techniques (Fig. 5). They can also be printed as multi-material constructs to create multifunctional grafts [32].

With the development of 3D cell-printing technology and the advances made in tissue engineering, the potential possibilities seem endless. Work is already being done to incorporate stem cells and growth factors as well as endothelial cells which enables the creation of vascular-primed constructs that show better osteointegration in their host sites [33, 34].

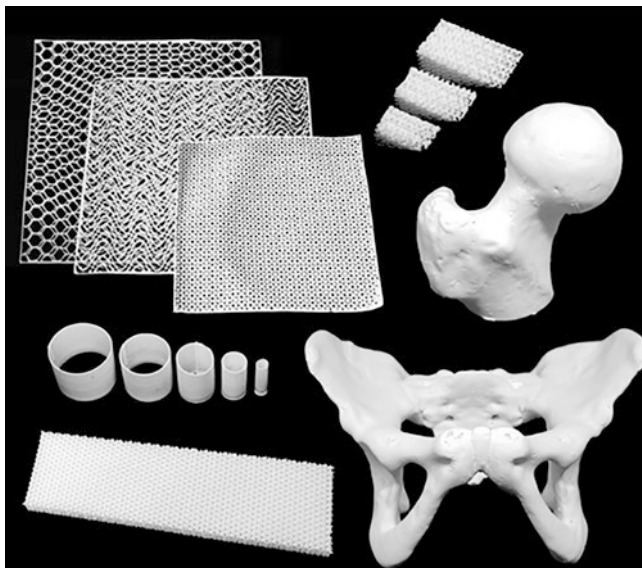


Fig. 5 Examples of 3D printed hyperelastic bone showing off the shelf or patient matched forms. (Images provided courtesy of Dimension Inx)

3.4 Rehabilitation

3D printing technology has been used in the production of custom splints and braces as well as in the production of prosthetic limbs. The function of traditional prosthetic limbs for upper limb deficiencies has been driven by advances in robotic engineering. Consequently, prosthetic upper limbs for pediatric patients were considered almost impractical due to the weight, the cost, and the need for frequent size changes in a growing child. However, it is now possible to create 3D printed prosthetic devices for the upper limb in children [35] (Fig. 6). Available open source designs (<https://enablingthefuture.org/upper-limb-prosthetics/>, <https://3dprint.nih.gov/>) can be used to custom design and print an affordable patient-specific hand prosthesis.

These devices are lighter than standard available prosthetic limbs and they can be easily customized, replaced, or upgraded as the child grows. The light-weight nature of these new devices allows for improved mobility in children and consequently, much better functional abilities [36]. One of the major attractions is that these functional limbs can be produced for as little as \$300 in comparison to costs ranging from \$4000 to \$50,000 for the traditional body powered and externally powered prosthetic limbs [37, 38].

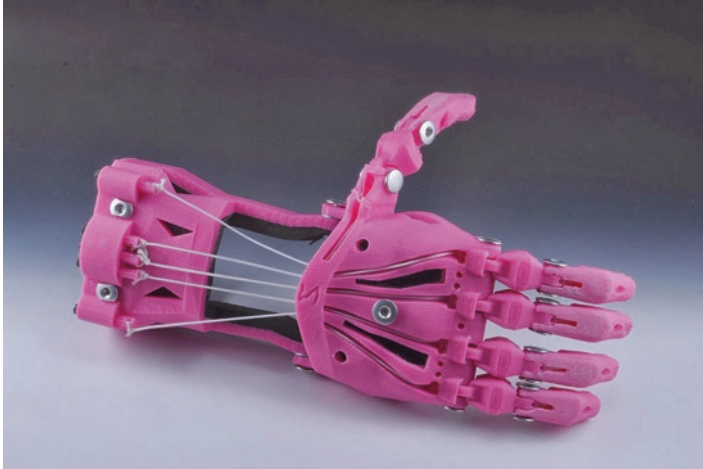


Fig. 6 3D Printed hand prosthesis <https://enablingthefuture.org/current-design-files/cyborg-beast-hand/>

4 Limitations of 3D Printing Technology in Pediatric Orthopedics

With medical grade 3D printers priced as much as \$40,000, the high initial costs of setting up a medical 3D printing service remain one of the most important limitations in its applicability [23]. This is especially relevant in resource-poor settings. Some authorities believe however that once the barrier of the initial investment is overcome, the technology has the potential to be a cost-effective addition to the armamentarium of modern medicine. Some studies show a reduction in production costs to as little as 10% of the cost of some standard instruments [39]. Further obstacles for 3D printed technology include: (1) the need for a preparatory CT scan which causes additional exposure to ionizing radiation for pediatric patients and (2) the time it takes to produce patient-specific materials [14]. This production time delay remains a substantial issue with the clinical applicability of 3D printing technology. The time scale from image capture, through data processing and the generation of a digital model has been reduced significantly to minutes but actual printing time continues to be a process requiring as much as 20 h or more in some instances. This currently makes the technology prohibitive in an emergency setting. As the technology continues to evolve, it is hoped that this process will become quicker.

Another shortcoming of 3D printed patient-specific instrumentation is that a much bigger surgical exposure is sometimes required in order to accommodate precise positioning of the 3D printed instrument [40]. This in turn may lead to an increase in the incidence of wound complications, such as delayed healing or infection.

5 Quality Control and Quality Assurance of 3D-Printed Patient-Specific Devices

3D printing lends itself well to creation of highly precise patient-specific models, implants, and devices. The final product is a culmination of several stages of design and manufacturing processes beginning with patient-specific imaging. It is therefore imperative that quality control and quality assurance processes are maintained throughout the process to deliver the right product for the particular patient and clinical needs. With imaging, a slice thickness of more than 1.25 mm can compromise the surface rendition precision of the models [41]. Segmentation is manual and establishing and maintaining intra- and inter-operator differences to acceptable levels is key to producing good meaningful parts. On the manufacturing side, regular equipment maintenance and choice of the right material for the application is of the utmost importance. Lastly, the importance of physician, biomedical engineers, and 3D printing and material composition experts' coordination throughout the process to deliver meaningful quality models/implants that are useful to end user the surgeon and the patient cannot be overemphasized.

6 Future of 3D Printing Technology in Pediatric Orthopedics

With recent advances allowing the design of 3D printed scaffolds incorporating living cells, growth factors, and extracellular matrix in a process called 3D bioprinting, the possibility of creating more complex tissue continues to increase. This will potentially have far reaching effects in the management of congenital and acquired skeletal deficiencies. This design process is based on the concepts of biomimicry and biologic self-assembly [42, 43]. It is facilitated by using bio-inks which are a combination of a printed scaffold or matrix material (typically a hydrogel), with embedded living cells. The matrix material may be naturally occurring, synthetic, or a combination of both [44]. Gelatin is a common example of a naturally occurring material, while polyethylene glycol is an example of a synthetic matrix. The cells may be primary cells, adult stem cells, or induced pluripotent stem cells [30]. The ideal bio-ink is printable, inert, nontoxic, stable and of the desired mechanical integrity [42]. Challenges still exist with the issue of cellular damage during the printing process and maintaining porosity of the scaffold following instillation of the hydrogel-based printing ink [45]. The role of 3D bioprinting in the repair of articular cartilage and in the management of bone defects is currently being investigated as the search for the ideal bio-ink continues [46].

Managing bone defects in the pediatric population is a challenge. The pediatric bone is thinner and retains the potential for growth, which must be considered when planning treatment. Advances in bone tissue engineering have been made in reconstruction of the pediatric craniofacial skeletal. Composite scaffolds comprising polylactic polymer, collagen matrix, and nonceramic hydroxyapatite seeded with

autologous bone marrow cells have shown good osteointegration properties in the reconstruction of pediatric cranial defects [47]. Despite extensive research in this area, clinical translation of this technology remains a challenge. Several scientific, ethical, and technological factors account for this. Some of these factors include control of scaffold degradation, vascularization of the scaffold, improvements in the mechanical properties of scaffolds as well as the ethical considerations involved with using mesenchymal stem cells and the potential teratogenicity of using bio-printed cells [48]. The use of highly specific biomimetic construct microarchitecture and smart hydrogels capable of modifying properties like increased bioactivity, stiffness, and degradation are some of the future trends proposed to tackle some of these challenges [49, 50].

There has been some interest in the role of 3D printing technology in the management of musculoskeletal infections. In the past, there was difficulty in achieving high concentrations of disease specific drugs at a desired location. However, this problem can be overcome by direct local administration of the drugs. This concept has proven effective in the management of chronic osteomyelitis [51, 52]. 3D printing technology using poly DL-lactide nano-hydroxyapatite has been proposed as a technique to create scaffolds that can act as drug delivery systems in some musculoskeletal infection models [53]. There is optimism that these models can also be utilized as local drug delivery systems in chemotherapy and radiation treatment of cancer patients.

With the process of rapid prototyping, 3D printing enables implant and instrument manufacturers to test devices before commercialization of the final product. It is conceivable that the use of this technology can support remote location medical care, particularly in the developing world. Case specific implants and instruments can be 3D printed on site rather than coping with the logistic problems of transporting a large inventory of these hardware [3].

3D printing technology research is being conducted to design methods that speed up the healing of bone in fracture models as well as create an environment for more rapid consolidation of regenerated bone in distraction osteogenesis. Customized 3D printed strut modifications for external fixators which allow for controlled micro-motion have been investigated in large animal fracture models [28]. Their use is currently under investigation to determine their effect on healing of regenerated bone during distraction osteogenesis.

7 Conclusion

3D printing is changing the face of pediatric orthopedics. With a reduction in the size and cost of 3D printers, it is becoming more accessible for use around the world. Its applications in diagnosis, patient education and consenting, treatment planning, treatment execution, rehabilitation as well as training of healthcare workers continue to push the limits for excellence in this area of surgery. With improvements in technology and decreasing costs, it is expected that most of the limitations

will be overcome with time. With the recent developments in 3D printing using biomaterials, there is growing optimism that someday, evaluating the safety of new drugs and possibly new medical devices would be less reliant on animal testing. While this remains an attractive feature of this technology, there are growing calls for legal regulation of this emerging field of regenerative medicine and indeed, ethical concerns need to be addressed especially since it is new technology and the risks have not been fully evaluated [54, 55].

References

1. Ponseti IV. History of orthopedic surgery. *Iowa Orthop J*. 1991;11:59–64.
2. Whitaker M. The history of 3D printing in healthcare. *Bull R Coll Surg Engl*. 2014;96(7):228–9.
3. Skelley NW, Smith MJ, Ma R, Cook JL. Three-dimensional printing technology in orthopaedics. *J Am Acad Orthop Surg*. 2019;27(24):918–25.
4. Hasan O, Atif M, Jessar MM, Hashmi P. Application of 3D printing in orthopaedic surgery. A new affordable horizon for cost-conscious care. *J Pak Med Assoc*. 2019;69(1):s46–50.
5. Trauner KB. The emerging role of 3D printing in arthroplasty and orthopedics. *J Arthroplast*. 2018;33(8):2352–4.
6. Vaishya R, Patralekh MK, Vaish A, Agarwal AK, Vijay V. Publication trends and knowledge mapping in 3D printing in orthopaedics. *J Clin Orthop Trauma*. 2018;9(3):194–201.
7. Malik HH, Darwood ARJ, Shaunak S, Kulatilake P, El-Hilly AA, Mulki O, et al. Three-dimensional printing in surgery: a review of current surgical applications. *J Surg Res*. 2015;199(2):512–22.
8. Martelli N, Serrano C, Van Den Brink H, Pineau J, Prognon P, Borget I, et al. Advantages and disadvantages of 3-dimensional printing in surgery: a systematic review. *Surgery (United States)*. 2016;159(6):1485–500.
9. Tam MD, Laycock SD, Bell D, Chojnowski A. 3-D printout of a DICOM file to aid surgical planning in a 6 year old patient with a large scapular osteochondroma complicating congenital diaphyseal aclasia. *J Radiol Case Rep*. 2012;6(1):31–7.
10. Esses SJ, Berman P, Bloom AI, Sosna J. Clinical applications of physical 3D models derived from MDCT data and created by rapid prototyping. *Am J Roentgenol*. 2011;196(6):W683–8.
11. Mao K, Wang Y, Xiao S, Liu Z, Zhang Y, Zhang X, et al. Clinical application of computer-designed polystyrene models in complex severe spinal deformities: a pilot study. *Eur Spine J*. 2010;19:797–802.
12. Guarino J, Tennyson S, McCain G, Bond L, Shea K, King H. Rapid prototyping technology for surgeries of the pediatric spine and pelvis: benefits analysis. *J Pediatr Orthop*. 2007;27(8):955–60.
13. Burzyńska K, Morasiewicz P, Filipiak J. The use of 3D printing technology in the ilizarov method treatment: pilot study. *Adv Clin Exp Med*. 2016;25(6):1157–63.
14. Iobst CA. New technologies in pediatric deformity correction. *Orthop Clin North Am*. 2019;50(1):77–85.
15. Sternheim A, Gortzak Y, Kolander Y, Dadia S. 3D printing in orthopedic oncology. In: Dipaola M, Wodajo FM, editors. *3D printing in orthopaedic surgery* [Internet]. St. Louis: Mica Haley; 2019. p. 179–94. <https://www.sciencedirect.com/science/article/pii/B9780323581189000154>.
16. Starosolski ZA, Kan JH, Rosenfeld SD, Krishnamurthy R, Annapragada A. Application of 3-D printing (rapid prototyping) for creating physical models of pediatric orthopedic disorders. *Pediatr Radiol*. 2014;44(2):216–21.
17. Windisch G, Salaberger D, Rosmarin W, Kastner J, Exner GU, Haldi-Brändle V, et al. A model for clubfoot based on micro-CT data. *J Anat*. 2007;210(6):761–6.

18. Park J, Lakes RS. *Biomaterials: an introduction: third edition*. 6th ed. New York: Springer-Verlag; 2007. p. 1–16.
19. Heinel P, Müller L, Körner C, Singer RF, Müller FA. Cellular Ti-6Al-4V structures with interconnected macro porosity for bone implants fabricated by selective electron beam melting. *Acta Biomater*. 2008;4(5):1536–44.
20. Parthasarathy J, Starly B, Raman S, Christensen A. Mechanical evaluation of porous titanium (Ti6Al4V) structures with electron beam melting (EBM). *J Mech Behav Biomed Mater*. 2010;3(3):249–59.
21. Parthasarathy J, Starly B, Raman S. A design for the additive manufacture of functionally graded porous structures with tailored mechanical properties for biomedical applications. *J Manuf Process*. 2011;13(2):160–70.
22. Wong KC. 3D-printed patient-specific applications in orthopedics. *Orthop Res Rev*. 2016;8:57–66.
23. Birnbaum K, Schkommodau E, Decker N, Prescher A, Klapper U, Radermacher K. Computer-assisted orthopedic surgery with individual templates and comparison to conventional operation method. *Spine (Phila Pa 1976)*. 2001;26(4):365–70.
24. Weiss H-R, Tournavitis N, Nan X, Borysov M, Paul L. Workflow of CAD/CAM scoliosis brace adjustment in preparation using 3D printing. *Open Med Inform J*. 2017;11:44–51.
25. de Muinck Keizer RJO, Lechner KM, Mulders MAM, Schep NWL, Eygendaal D, Goslings JC. Three-dimensional virtual planning of corrective osteotomies of distal radius malunions: a systematic review and meta-analysis. *Strateg Trauma Limb Reconstr*. 2017;12(2):77–89.
26. Zheng P, Yao Q, Xu P, Wang L. Application of computer-aided design and 3D-printed navigation template in locking compression pediatric hip plate TM placement for pediatric hip disease. *Int J Comput Assist Radiol Surg*. 2017;12(5):865–71.
27. Qiao F, Li D, Jin Z, Gao Y, Zhou T, He J, et al. Application of 3D printed customized external fixator in fracture reduction. *Injury*. 2015;46(6):1150–5.
28. Glatt V, Samchukov ML, Cherkashin AM, Iobst CA. Reverse dynamization accelerates bone-healing in a large-animal osteotomy model. *J Bone Joint Surg Am*. 2021;103(3):257–63.
29. Jakus AE, Geisendorfer NR, Lewis PL, Shah RN. 3D-printing porosity: a new approach to creating elevated porosity materials and structures. *Acta Biomater*. 2018;72:94–109.
30. Jakus AE, Rutz AL, Shah RN. Advancing the field of 3D biomaterial printing. *Biomed Mater*. 2016;11(1):014102.
31. Jakus AE, Secor EB, Rutz AL, Jordan SW, Hersam MC, Shah RN. Three-dimensional printing of high-content graphene scaffolds for electronic and biomedical applications. *ACS Nano*. 2015;9(4):4636–48.
32. Jakus AE, Shah RN. Multi and mixed 3D-printing of graphene-hydroxyapatite hybrid materials for complex tissue engineering. *J Biomed Mater Res Part A*. 2017;105A(1):274–83.
33. Frohlich M, Grayson W, Wan L, Marolt D, Drobnic M, Vunjak-NG. Tissue engineered bone grafts: biological requirements, tissue culture and clinical relevance. *Curr Stem Cell Res Ther*. 2008;3(4):254–64.
34. Liu X, Jakus AE, Kural M, Qian H, Engler A, Ghaedi M, et al. Vascularization of natural and synthetic bone scaffolds. *Cell Transplant*. 2018;27(8):1269–80.
35. Tanaka KS, Lightdale-Miric N. Advances in 3D-printed pediatric prostheses for upper extremity differences. *J Bone Joint Surg Am*. 2016;98(15):1320–6.
36. Haumont T, Rahman T, Sample W, King MM, Church C, Henley J, et al. Wilmington robotic exoskeleton: a novel device to maintain arm improvement in muscular disease. *J Pediatr Orthop*. 2011;31(5):e44–9.
37. Gretsck KF, Lather HD, Peddada KV, Deeken CR, Wall LB, Goldfarb CA. Development of novel 3D-printed robotic prosthetic for transradial amputees. *Prosthetics Orthot Int*. 2016;40(3):400–3.
38. Resnik L, Meucci MR, Lieberman-Klinger S, Fantini C, Kelty DL, Disla R, et al. Advanced upper limb prosthetic devices: implications for upper limb prosthetic rehabilitation. *Arch Phys Med Rehabil*. 2012;93(4):710–7.

39. Rankin TM, Giovinco NA, Cucher DJ, Watts G, Hurwitz B, Armstrong DG. Three-dimensional printing surgical instruments: are we there yet? *J Surg Res.* 2014;189(2):193–7.
40. Hoekstra H, Rosseels W, Sermon A, Nijs S. Corrective limb osteotomy using patient specific 3D-printed guides: a technical note. *Injury.* 2016;47(10):2375–80.
41. Way TW, Chan HP, Goodsitt MM, Sahiner B, Hadjiiski LM, Zhou C, et al. Effect of CT scanning parameters on volumetric measurements of pulmonary nodules by 3D active contour segmentation: a phantom study. *Phys Med Biol.* 2008;53(5):1295–312.
42. Dhawan A, Kennedy PM, Rizk EB, Ozbolat IT. Three-dimensional bioprinting for bone and cartilage restoration in orthopaedic surgery. *J Am Acad Orthop Surg.* 2019;27(5):e215–26.
43. Bishop ES, Mostafa S, Pakvasa M, Luu HH, Lee MJ, Wolf JM, et al. 3-D bioprinting technologies in tissue engineering and regenerative medicine: current and future trends. *Genes Dis.* 2017;4(4):185–95.
44. Rutz AL, Hyland KE, Jakus AE, Burghardt WR, Shah RN. A multimaterial bioink method for 3D printing tunable, cell-compatible hydrogels. *Adv Mater.* 2015;27(9):1607–14.
45. Lee HJ, Koo YW, Yeo M, Kim SH, Kim GH. Recent cell printing systems for tissue engineering. *Int J Bioprinting.* 2017;3(1):1–15.
46. Larsen C, Stapleton E, Sgaglione J, Sgaglione M, Goldstein T, Sgaglione N, et al. Three-dimensional bioprinting in orthopaedics. *JBJS Rev.* 2020;8(4):e0204.
47. Velardi F, Amante PR, Caniglia M, De Rossi G, Gaglini P, Isacchi G, et al. Osteogenesis induced by autologous bone marrow cells transplant in the pediatric skull. *Childs Nerv Syst.* 2006;22(9):1158–66.
48. Turnbull G, Clarke J, Picard F, Riches P, Jia L, Han F, et al. 3D bioactive composite scaffolds for bone tissue engineering. *Bioact Mater.* 2018;3(3):278–314.
49. Xia LW, Xie R, Ju XJ, Wang W, Chen Q, Chu LY. Nano-structured smart hydrogels with rapid response and high elasticity. *Nat Commun.* 2013;4:2226.
50. An J, Teoh JEM, Suntornnond R, Chua CK. Design and 3D printing of scaffolds and tissues. *Engineering.* 2015;1(2):261–8.
51. McNally MA, Ferguson JY, Lau ACK, Diefenbeck M, Scarborough M, Ramsden AJ, et al. Single-stage treatment of chronic osteomyelitis with a new absorbable, gentamicin-loaded, calcium sulphate/hydroxyapatite biocomposite: a prospective series of 100 cases. *Bone Joint J.* 2016;98-B(9):1289–96.
52. Hashmi MA, Norman P, Saleh M. The management of chronic osteomyelitis using the Lautenbach method. *J Bone Joint Surg Ser B.* 2004;86-B(2):269–75.
53. Dong J, Zhang S, Liu H, Liu Y, Du Y, Li X. Novel alternative therapy for spinal tuberculosis during surgery: reconstructing with anti-tuberculosis bioactivity implants. *Expert Opin Drug Deliv.* 2014;11(3):299–305.
54. Vermeulen N, Haddow G, Seymour T, Faulkner-Jones A, Shu W. 3D bioprint me: a socioethical view of bioprinting human organs and tissues. *J Med Ethics.* 2017;43(9):618–24.
55. Bauer H-K, Heller M, Fink M, Maresch D, Gartner J, Gassner UM, et al. Social and legal frame conditions for 3D (and) bioprinting in medicine [Gesellschaftliche und rechtliche Rahmenbedingungen für 3-D-druck und bioprinting in der medizin]. *Int J Comput Dent.* 2016;19(4):293–9.

Bone Grafting in the Regenerative Reconstruction of Critical-Size Long Bone Segmental Defects



Xiaowen Xu and Jie Song

Abbreviations

3D printing	Three-dimensional printing
ACS	Absorbable collagen sponge
ADSC	Adipose-derived stem cell
BMP	Bone morphogenetic protein
BMSC	Bone marrow-derived stromal cell
CAD	Computer-assisted design
CaP	Calcium phosphate
CT	Computer tomography
DBM	Demineralized bone matrix
ECM	Extracellular matrix
FDA	Food and Drug Administration
FGF23	Fibroblast growth factor 23
HA	Hyaluronic acid
hAFSC	Human amniotic fluid-derived stem cell
HAp	Hydroxyapatite
HDB	Heterogeneous deproteinized bone
Ihh	Indian hedgehog
LBSD	Long bone segmental defect
MSC	Mesenchymal stem cell
mSSC	Mouse skeletal stem cell
OVX	Ovariectomy
PCL	Polycaprolactone
PEG	Poly(ethylene glycol)
PEGDA	Poly(ethylene glycol) diacrylate
PELGA	Poly(lactic- <i>co</i> -glycolic acid)- <i>b</i> -poly(ethylene glycol)- <i>b</i> -poly(lactic- <i>co</i> -glycolic acid)
PGA	Poly(glycolic acid)

X. Xu · J. Song (✉)

Department of Orthopedics and Physical Rehabilitation, University of Massachusetts Medical School, Worcester, MA, USA

e-mail: Jie.Song@umassmed.edu

© Springer Nature Switzerland AG 2022

F. P. S. Guastaldi, B. Mahadik (eds.), *Bone Tissue Engineering*,
https://doi.org/10.1007/978-3-030-92014-2_8

165

PLGA	Poly(lactic- <i>co</i> -glycolic acid)
PLA	Poly(lactic acid)
PLA-DX-PEG	Poly D,L-lactic acid- <i>p</i> -dioxanone-polyethylene glycol block copolymer
PVA	Poly(vinyl alcohol)
rAAV	Recombinant adeno-associated virus
RANKL	Receptor activator of nuclear factor κ B ligand
rhBMP-2	Recombinant human bone morphogenetic protein-2
rhBMP-2/7	Recombinant human bone morphogenetic protein-2/7 heterodimer
rt	Room temperature
TCP	Tricalcium phosphate
TEP	Tissue-engineered periosteum
VEGF	Vascular endothelial growth factor
WSF	Wistar skin fibroblast
β -TCP	β -Tricalcium phosphate
μ -CT	Micro-computed tomography

1 Introduction

Long bone segmental defects (LBSD) resulting from high-energy traumas or tumor resections remain a major, unresolved clinical challenge in orthopedic care. To salvage the limb in the case of segmental bone loss, a rational strategy is to fill the defect with a suitable bone graft [1]. Since Vittorio Putti systematically outlined the principles of bone grafting in the early twentieth century, researchers and surgeons have continued to gain basic science understanding of and develop new toolkits for bone grafting to improve the clinical outcomes [2]. Nowadays, it is estimated that over two million bone grafting procedures are performed annually worldwide, making bone the second most transplanted tissue next to blood. For the regenerative reconstruction of critical-size LBSD, the gold standard autografting is often impractical due to either the lack of sufficient volume of autografts or potential nonunion due to the premature resorption of cancellous autografts [3]. Meanwhile, devitalized allogenic bone grafts, the leading choice for arthroplasty and spinal surgery, are known for notoriously high failure rates (>50%) for long bone grafting due to poor graft fixation and inadequate vascularization/osteointegration, limiting their clinical uses (<10% in long bone grafting) [4]. Consequently, synthetic bone graft alternatives have long been sought after [5]. Current clinically used synthetic bone graft substitutes (e.g. brittle bioceramics, weak collagen sponges/gel foams, or their coarse combinations), however, suffer from poor surgical handling characteristics and inadequate in vivo performances. Synthetic composite bone graft substitutes composed of hydrogels or conventional degradable polylactides and osteoconductive minerals have been exploited to guide the regenerative reconstruction of LBSD with varying successes. More recently, amphiphilic degradable polymer-mineral composites have been designed to improve the structural integration with the

hydrophilic minerals (e.g. overcoming the brittleness and weak interface of conventional degradable polymer-mineral composites [6]) and consistencies of their *in vivo* performances. Finally, although adjuvant use of osteoinductive human recombinant bone morphogenetic protein-2 (rhBMP-2) [7–10] is effective in augmenting graft healing/osteointegration, reviews of its clinical use have revealed severe local/systemic complications [11] associated with the high clinical doses of rhBMP-2 (milligram scale) typically used in combination with collagen sponge carriers (e.g. Infuse®) or conventional synthetic bone graft substitutes reported in literature. Overall, there is a critical need for more effective long bone grafting technologies to salvage limbs following traumatic long bone injuries or tumor resections.

This chapter discusses recent strategies in augmenting the performance of structural allografts and the development of novel synthetic bone graft substitutes, including those fabricated by the increasingly accessible three-dimensional (3D) printing technology, for scaffold-guided long bone regeneration in the past two decades. To both serve as temporary structural supports and to promote bone regeneration, bone grafts should exhibit adequate osteoconductivity and osteoinductivity and promote osteointegration. These characteristics refer to the ability of a bone graft to support stem/skeletal progenitor cell attachment/invasion, to promote the differentiation of stem/progenitor cells into bone-forming cell lineage, and to template the formation of new bone that fully integrate with the surrounding host bone, respectively. We will highlight key examples of each scaffolding material type, including synthetic periosteal membranes, demineralized bone matrices, metallic mesh cages, bioceramics, naturally occurring biopolymers and polysaccharides, synthetic polymeric hydrogels, and synthetic degradable polymers and their mineral composites, discussing their respective pros and cons for guiding the regenerative reconstruction of critical-size LBSD from these perspectives. Whenever possible, we will contrast the regenerative outcome of LBSD achieved by these bone grafting technologies with clinically used control grafts (e.g. autografts or collagen sponge absorbed with rhBMP-2) or healthy long bone controls. Restoration of the mechanical integrity is valued as an important indication of functional regeneration of the LBSD and will be presented along with quantitation of new bone to the extent possible.

2 Autografts for LBSD Treatments

Autologous bone graft is retrieved from another anatomic site of the patient's own skeleton. The non-weight bearing and regenerative iliac crest is the most frequently used donor site, while the proximal tibial, distal radius as well as greater trochanter are other options [12]. With its natural osteoconductivity and osteoinductivity, autografts can be integrated with the host bone faster and more completely, thus are considered as the gold standard and a benchmark in evaluating the performance of other bone grafts [13]. One of the earlier studies on autografts for LBSD repair compared the performance of iliac crest autografts and cortical (ulna) autografts

with demineralized bone matrix control in the reconstruction of 1-cm segmental defects in rabbit ulna. It showed that the ulna autografts resulted in higher union rate and superior mechanical strength of the repaired long bone than the iliac crest autograft while performing comparably to the demineralized bone matrix control [14]. It should be noted that there was no specific attempt to preserve or remove the periosteum at the defect site in this study, thus the relative regenerative contributions of the periosteum versus those of the autografts cannot be determined. This study outcome highlights the concern over the faster resorption of autologous cancellous bone grafts that could translate into poor union rate for long bone reconstruction. Indeed, although cancellous autografts can be more readily harvested from the patient's ilia, ribs, and fibulae, their intrinsically poor structural integrity/strength and rapid resorption characteristics greatly limit their applications for the reconstruction of load bearing LBSD [15]. Meanwhile, despite the excellent performance of the cortical autograft in LBSD repair, its limited availability is a key limiting factor for its practical clinical applications.

3 Structural Allografts for LBSD Treatments

Unlike autografts, allografts are harvested from a donor, often a cadaver [16], thus are more readily available. Allografts, both cancellous and cortical bone grafts, can be processed and machined for a wide range of customized uses [17]. To mitigate the adverse immunological rejections and disease transmission risks [18], structural allografts need to undergo rigorous decellularization (e.g. chemical treatment, irradiation, repeated lysing, and/or freeze-thaw cycles) and sterilization processes [19]. Although these processes effectively improve the safety and reduce immunological rejections of allografts, they also inevitably compromise the structural integrity and the osteointegrative property of the allograft due to the loss of key skeletal progenitors and vascular cells and factors residing in the periosteal and intramedullary niches. Indeed, poor structural integrity, nonunion, and inadequate vascularization are leading causes of allograft failures for LBSD treatments. A retrospective study on allograft fractures revealed that ~18% of traumatic long bone injury patients experienced structural allograft failures in the first 3 years, while ~46% of the allografts ultimately failed [20].

To improve structural allograft vascularization and osteointegration with host bone, Schwarz and colleagues used a gene therapy approach to deliver signals promoting bone remodeling and vascularization to the devitalized allograft surface [21]. Using gene expression analyses, they first revealed substantial decrease in the expression of genes encoding receptor activator of nuclear factor κ B ligand (RANKL) and vascular endothelial growth factor (VEGF) during allograft healing. They then immobilized via freeze-dry coating of the respective viral vectors, recombinant adeno-associated virus (rAAV)-RANKL and rAAV-VEGF, on the cortical surface of the processed cortical allograft placed within a 4-mm murine femoral segmental defect. They demonstrated that the resulting expressions of the VEGF

and RANKL signals were sufficient to rejuvenate the processed cortical bone allograft, resulting in complete union by 4 weeks and full restoration of the mechanical strength [21].

To restore the periosteum cellular niche lost during trauma and destroyed in allograft processing, Zhang and colleagues engineered biomimetic tissue-engineered periosteum (TEP) [22]. The TEP was fabricated layer-by-layer comprising polycaprolactone, collagen, and hydroxyapatite (HAp) composite nanofiber sheets embedded with bone marrow stromal cells (BMSCs) [23]. When applied to the surface of a processed cortical allograft to heal a 4-mm mouse femoral segmental defect, the TEP promoted the formation of periosteal bone at the donor site, resulting in total bony callus formation comparable to that in the autogenic femoral graft control group by 6 weeks (Fig. 1). It should be noted, however, although the TEP greatly strengthened the biomechanical integrity of the grafted defect by 6 weeks, the allograft was not fully remodeled by then. The TEP recapitulated the periosteal bone healing process as shown by the donor-dependent bone and cartilage regeneration. Compared with the nanofiber sheets lacking donor BMSC, the use of the biomimetic cellularized TEP significantly improved the osseointegration at the periosteal defect site (Fig. 1).

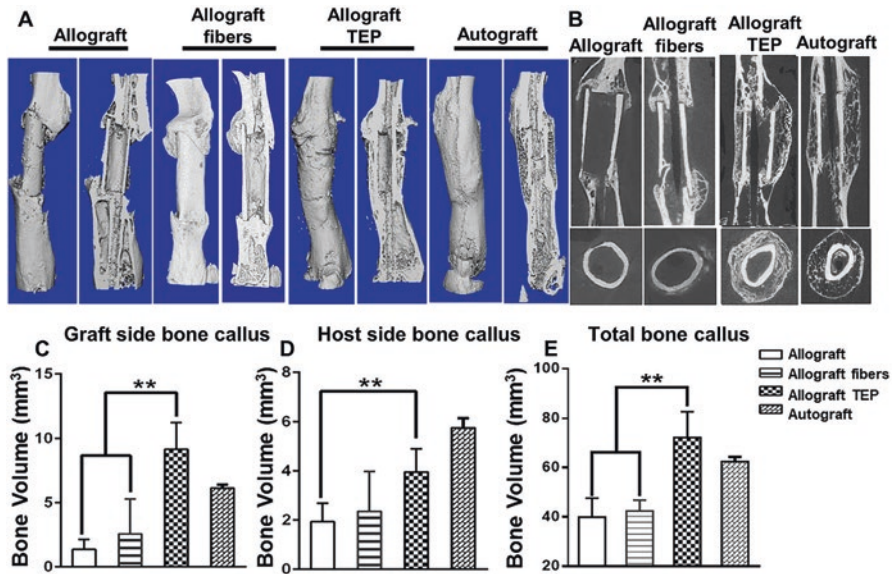


Fig. 1 TEP restored donor site periosteal callus formation and enhanced donor allograft incorporation in repair of a 4 mm mouse femoral segmental bone defect. Representative micro-CT 3D images of autograft and allograft with or without TEP treatment 6 weeks post-surgery (A). Longitudinal and cross-sectional micro-CT 2D slice views illustrate organized multilayered periosteal bone formation in TEP treated sample as opposed to the other groups (B). Volumetric micro-CT analyses of new bone in donor (C), host (D), and total callus (E) ($n = 6, p < 0.05$). (Reproduced from [22] with permission from Elsevier)

To facilitate more convenient delivery of exogenous cells or cell sheets around devitalized structural allografts, we developed a self-wrapping degradable shape memory composite fibrous mesh consisting of poly(lactide-*co*-glycolide)-*b*-poly(ethylene glycol)-*b*-poly(lactide-*co*-glycolide) (PELGA) and osteoconductive mineral HAp [24]. The thermoplastic shape memory composites can be programmed with an allograft-wrapping “permanent” shape in warm water, deformed into a flat sheet at room temperature (rt) to facilitate the transfer of stem cell sheet formed on and released from poly(*N*-isopropylacrylamide) surfaces (Nunc UpCell™), and allowed to undergo instantaneous shape recovery to wrap around a rat femur allograft upon body-temperature saline rinse (Fig. 2). The unique hydration-induced stiffening behavior, driven by PEG crystallization and microphase separation of the amphiphilic PELGA [25], ensured the stable wrapping of the shape recovered membrane around the allograft. Combined with its tunable degradation and ability to support the proliferation and osteogenesis of BMSCs and periosteum-derived cells [24], this shape memory composite has great potential as smart degradable synthetic periosteal membrane to deliver pro-healing cellular components and/or signaling molecules to facilitate LBSD repair. The minimal effective cellular/biochemical signals to be restored to the allograft surface [26] as well as appropriate *in vivo* degradation rate of the synthetic membrane for LBSD repair remain determined.

4 Demineralized Bone Matrix (DBM) for LBSD Treatments

Besides full structural allografts, demineralized bone matrix (DBM) can be processed from allograft and used in guided bone regeneration. DBM is the mixture of type I collagen matrix and osteoinductive, non-collagenous proteins and growth factors obtained from natural bone grafts following acid or calcium ion-chelator treatments for mineral removal. DBM is attractive for surgical uses due to its processing flexibility (as gels, flexible strips, malleable putty, or injectable bone paste) and its porosity and osteoinductivity desired for osteointegration [19]. Because of its inferior mechanical strength, however, DBM is most commonly used for filling

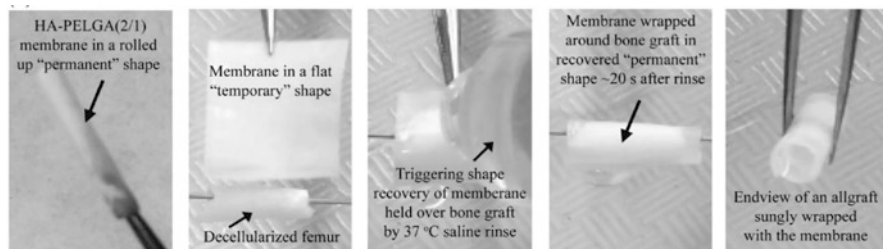


Fig. 2 Permanent shape programming, temporary shape fixing, and shape recovery of electrospun HA-PELGA membrane for self-wrapping around a devitalized rat femoral bone graft. (Reproduced with permission from Fig. 4b of [24]. Copyright 2017 John Wiley and Sons)

bone defects in non-weight-bearing regions. But there are some reported uses of DBM-based scaffolds for critical-size LBSD. For instance, DBM scaffolds with or without seeded allogenic BMSCs were used to treat critical-size radial segmental defects in ovariectomized (OVX) rabbits. Whereas DBM alone failed to promote new bone formation in the osteoporotic rabbit by 3 months, the DBM seeded with BMSCs resulted in significant increase in new bone formation within the radial defect, although new bone remodeling and integration with host bone remained inadequate by 3 months [27]. Partially demineralized allografts were also attempted for the repair of critical-size tibial segmental defects in normal rabbits, but they were found inferior to ceramic grafts pre-cellularized with autologous mesenchymal stem cells (MSCs) [28].

To facilitate more convenient surgical delivery and better fitting of the weak DBM in weight-bearing LBSD, an auxiliary device such as a titanium mesh cage can be used. Cylindrical titanium mesh cages were approved by the United States Food and Drug Administration (FDA) in the 1990s for delivering weak cancellous bone grafts or DBM for spine fusion and other selected skeletal reconstructions [29, 30]. They have also been used for the clinical management of large segmental long bone defects. In a two-patient case report, the cylindrical titanium mesh cages packed with cancellous bone graft and DBM putty, stabilized with statically locked intramedullary nails, were used to treat traumatic open tibial fractures (with 85-mm and 95-mm long segmental bone defects, respectively) [31]. At 1-year and 9-month follow-ups, both patients achieved excellent limb alignment, stability, and fully bridging bony healing radiographically. The hollow and fenestrated osteoconductive titanium cage reduced the risk for stress shielding while helping maintain the form and continuity of the weak DBM putty delivered to the defect. A more recent 17-case multi-center report used cylindrical titanium mesh cages in combination with autologous graft/allogenic cancellous bone chips and DBM to restore the LBSD in the tibia, femur, radius, and humerus (with average segmental defect size of 8.4 cm) [32]. The mean time to follow-up was 55 months (12–126 months). Overall, 16 (94%) of the patients achieved radiological filling of their bony defect and united to the native bone ends proximally and distally, resulting in a functioning limb.

Currently, there are several commercially available DBM-based products. Although a growing number of studies have presented encouraging outcomes of the use of DBM-based products in treating critical-size LBSD [33], higher quality/better controlled clinical studies are still needed to establish their unequivocal efficacy and advantages in critical-size LBSD treatments.

5 Synthetic Bone Graft Substitutes for LBSD Treatments

The limitations of autografts and allografts have motivated the development of viable synthetic alternatives for LBSD treatments. Recent advances in controlled polymerization/bioconjugation chemistry, biotherapeutics, and the popularization

of computational modeling and computer-assisted design (CAD) tools and 3D scaffold fabrication techniques (e.g. freeze-casting, 3D printing, bioprinting) have allowed for the development of synthetic bone grafts that exhibit structural, mechanical, and degradative characteristics well-suited for scaffold-guided bone regeneration. Here we discuss recent applications of 3D synthetic scaffolds based on designer titanium mesh cages, bioceramics, naturally occurring or synthetic hydrogels, and degradable synthetic polymers or their composites for the treatment of LBSD.

5.1 *Titanium Mesh Cages*

Although titanium mesh cage implants were approved for the reinforcement of deficient bone in 1990s by the FDA and subsequently used in combination with weak cancellous bone chips and DBM for spine fusion [34] and guided segmental bone regeneration [35], the cage design was recently optimized by Duda and colleagues to provide local mechanical stimulus to improve segmental long bone regeneration [36]. Two mechanically distinct titanium mesh scaffolds were designed using finite element techniques in a honeycomb-like configuration to minimize stress shielding while ensuring resistance against mechanical failure. Scaffold stiffness was altered through small changes in the strut diameter only. Honeycombs were aligned to form three differently oriented channels to guide the bone regeneration. The 3D additive manufactured (laser sintered) titanium mesh cages were packed with autologous cancellous bone retrieved from the sheep iliac crest and implanted into 4-cm tibial segmental defects in sheep. To verify that local scaffold stiffness could enhance healing, defects were stabilized with either a common locking compression plate that allowed dynamic loading of the critical-size defect or a rigid custom-made plate that mechanically shielded the defect. The 6-month follow-up showed that the titanium mesh cage with lower stress shielding led to earlier defect bridging, increased endochondral bone formation and advanced bony regeneration within the critical-size defect. These findings support that rational mechanobiological optimization of 3D auxiliary titanium mesh cages can significantly enhance the critical-sized LBSD reconstruction outcome when used in combination with weaker bone grafts.

5.2 *Bioceramics*

Bioresorbable ceramics, such as amorphous and crystalline calcium phosphates (CaP), calcium apatites, and bioactive glass have long been used in bone and dental repair and tissue engineering due to their osteoconductivity, similarity to the mineral compositions of calcified tissues, and their ability to absorb a wide range of protein factors owing to their pH-dependent surface zeta potentials [37]. Bioceramics of varying aqueous solubilities (e.g. amorphous CaP, beta tricalcium phosphate/ β -TCP vs. crystalline HAp) can be used in defined ratios to achieve targeted in vivo

resorption rate [38]. Owing to the high strength yet low fracture toughness of most bioceramics, they are often combined with compliant polymers to achieve improved toughness for use as bone tissue engineering scaffolds. Being slightly basic, many of these bioceramics also help buffer the acidic degradation products of synthetic degradable polymers such as polylactides, thereby mitigating the local inflammatory responses to the degrading scaffold.

Kasten and colleagues used the high-surface calcium-deficient hydroxyapatite (CDHA) scaffold in combination with allogenic platelet-rich-plasma (PRP) and/or MSCs for the regenerative repair of 15-mm rabbit critical-size segmental ulna defect [39]. The periosteum around the adjacent bone, 5 mm away from each side of the segmental defect, was removed. The bone defect was filled with the CDHA scaffold with/without allogenic PRP, MSCs, or both. Compared to the CDHA only groups, the CDHA + PRP and CDHA + MSC groups promoted better bone formation as evidenced by radiography and histology at 16-weeks post-implantation. However, the synergistic delivery of PRP and MSCs via the CDHA scaffold did not lead to statistically significant further improvement in new bone formation, and a substantial amount of the CDHA scaffolds remained un-resorbed by 16 weeks in all groups. Non-destructive 4-point bending test of the new bone at 16 weeks showed that while all scaffold-treated group resulted in higher stiffness compared to untreated control, none of them restored the mechanical integrity beyond those of cancellous bone. Indeed, slow-resorbing HAp scaffolds have been shown by others to persist even after 7 years in patients [40]. It is possible that a ceramic scaffold with faster *in vivo* resorption may expedite the graft incorporation.

Porous ceramic scaffolds composed of 80% β -TCP and 20% HAp impregnated with osteogenically induced autologous MSCs and plasma-derived fibrin were used for repairing critical-size 1-cm rabbit tibial segmental defects stabilized by k-wires and external fixators. The periosteum surrounding the defect was removed. The cellularized tissue-engineered porous ceramic scaffold was shown to outperform partially demineralized allograft controls by achieving faster union and higher compressive strength by 3 months [28]. The regeneration outcome was not compared to autograft controls or unoperated tibial controls.

Bioglass, mainly consisting of calcium, phosphorus and silicon dioxide, is known for its ability to template the surface deposition of carbonated hydroxyapatite upon contact with simulated body fluid *in vitro* or upon implantation *in vivo*. By varying the composition of bioglass, its resorption rate can be altered. Bioglass has been shown to promote the adhesion, proliferation, and differentiation of osteoprogenitor cells into osteoblasts, thus accelerating new bone formation and osteointegration [41]. For *in vivo* applications, bioglass is often combined with other materials or therapeutic proteins to enhance their biological performance. For example, Tolli and colleagues loaded reindeer bone protein extract on bioglass carrier for the regenerative repair of a 8-mm rat critical-size femur segmental defect [42]. Compared to the untreated defect or the control treated with only bioglass, the bioglass + bone protein extract groups (with 10 mg or more) significantly enhanced new bone formations at 8 weeks post-implantation as shown by bone mineral density quantitation by peripheral computer tomography (CT). The bioglass loaded

with 15-mg bone protein extract was found to enhance the bone torsional stiffness when compared with less protein extract loadings, although the observed improvement was statistically insignificant. Besides the repair of critical-size LBSD, bio-glass composites were also employed to heal non-critical tibia defects [43].

5.3 *Naturally Occurring Biopolymers and Their Bioceramic Composites*

Collagen and Collagen/Bioceramic Composites

Collagens are ubiquitous extracellular matrix (ECM) proteins in native tissues. In bone, type I collagen provides elasticity of the calcified tissue and serves as the protein template for both bone mineralization and numerous non-collagenous protein attachment. Thus, collagen has long been used as a rational bone tissue engineering component, especially for therapeutic protein delivery. Most commonly used absorbable collagen sponges (ACS) for the delivery of rhBMP-2 [7–10, 44], for instance, can be prepared from purified bovine or porcine collagen [45]. Major limitations of ACS for critical-size LBSD treatment include its poor mechanical strength complicating its surgical handling and in vivo stability (tendency for breakage) and its suboptimal BMP-2 release kinetics responsible for the supraphysiological loading doses required (e.g. milligram scale via INFUSE® for human uses). Indeed, safety reviews have revealed severe local (e.g. ectopic bone formation) and systemic complications [11, 46] associated with the high clinical doses of rhBMP-2 used in combination with ACS carriers and have led to safety warnings issued by the FDA. To improve the mechanical strength and therapeutics release profiles of ACS, collagen is often combined with osteoconductive bioceramics for bone tissue engineering applications [47].

Collagen membranes have also been combined with bioceramic scaffolds to improve their osteointegration for traumatic long bone injury repair. Guda and colleagues applied permeable collagen membrane to a porous HAp scaffold for the regenerative repair of a critical-size, 10-mm rabbit ulna segmental defect [48]. Compared to the scaffold-only group, the collagen membrane-wrapped group increased regenerated bone volume (e.g. 59% and 27% greater at 4 and 8 weeks, respectively) as quantified by the micro-CT (μ -CT) analysis. Flexural testing of the rabbit radius–ulna complex after 8 weeks revealed that both the collagen-wrapped group and the autograft control showed significantly stronger flexural strength than the untreated defect group, but the HAp scaffold group did not, consistent with the increased interfacial bone ingrowth and periosteal remodeling observed in the collagen-wrapped group. The improved outcomes were attributed to the collagen wrap's promotion of periosteal callus ossification while preventing fibrous tissue infiltration. It should be noted that the porous HAp scaffold remained largely unresorbed by 8 weeks. Longer-term graft remodeling and osteointegration was not reported. It is of interest to determine whether the delivery of exogenous anabolic

factors and/or the choice of faster resorbing bioceramics could further expedite the healing.

Gelatin, the hydrolyzed collagen fragments, have also been used for the delivery of rhBMP-2 for LBSD repair. Tabata and colleagues crosslinked gelatin hydrogel with glutaraldehyde for BMP-2 delivery to 20-mm, critical-size segmental defects in rabbit ulna [49]. High-water content (~98%) gelatin hydrogels incorporating 17- μ g rhBMP-2 exhibited significantly higher osteoinductivity than free rhBMP-2, resulting in significantly higher bone mineral density within the defect at 6 weeks post-surgery. However, the degree of mechanical restoration of the repaired defect was not evaluated. This study also showed that gelatin hydrogel itself was not osteoinductive but could serve as a good delivery vehicle for rhBMP-2.

Polysaccharide Hydrogels and Their Composites

Hydrogels can be prepared by naturally occurring polysaccharides (e.g. hyaluronic acid, alginate, and chitosan) or synthetically modified polysaccharides (e.g. PEGylated or methacrylated), enabling cytocompatible encapsulation and local release of a wide range of biotherapeutics (e.g. cells, proteins, growth factors) and structural additives (e.g. bone minerals) [50]. These hydrogels have been used for critical-size LBSD reconstruction.

Hyaluronic acid (HA) or hyaluronan is a glycosaminoglycan found in various tissues, especially in joint and bone, that binds to specific cell surface receptors and matrix proteins and provides lubrication to the synovial membranes in the joint capsule. It is the only non-sulfated glycosaminoglycan that consists of repeating units of *N*-acetyl-D-glucosamine and D-glucuronic acid and is degraded by hyaluronidases. HA has been widely investigated, often upon covalent crosslinking, for the delivery of biotherapeutics (e.g. via electrostatic binding of cationic protein/growth factors) and as a structural template for bone and cartilage tissue engineering [51]. As the crosslinked hydrophilic polysaccharide gel or powder gel is intrinsically weak, HA is often integrated with other structural components (e.g. bioceramics, collagen/gelatin, chitosan) for guided long bone regeneration. Lee and colleagues delivered rhBMP-2 via injectable, butanediol diglycidyl ether-crosslinked HA powder gel/ β -TCP microsphere composites to repair 5-mm rat fibular LBSD [52]. Unlike the β -TCP/HA only group that did not lead to detectable new bone formation by 9 weeks, the injected composite with 10- μ g rhBMP-2 resulted in robust bony callus formation bridging over the defect at 9 weeks post-surgery [52]. However, no biomechanical test was conducted to evaluate the degree of mechanical restoration of the LBSD. These results show that whereas HA by itself is not sufficient to template long bone regeneration, it served as a good rhBMP-2 delivery vehicle. It should be noted that the 10- μ g dose of rhBMP-2 delivered in this rodent study was quite high, which would scale to tens of milligrams in human that are known for causing undesired systemic and local side effects.

Alginate, isolated from seaweeds, is a linear copolymer with homopolymeric blocks of (1-4)-linked β -D-mannuronate and its C-5 epimer α -L-guluronate. It has

been employed to encapsulate cells and deliver growth factors for decades including for bone regeneration [53]. Alginate 3D hydrogels or microspheres can be formed by ionic crosslinking of the linear polysaccharide with divalent calcium ions in the presence of therapeutic cargos (e.g. rhBMP-2) and be injected to fill irregularly shaped tissue defects. The 3D network of ionically crosslinked alginate gel would eventually fall apart *in vivo* (e.g. due to the dynamic exchange of the divalent cation crosslinkers with monovalent cations like Na^+ in the tissue environment), although the linear polysaccharide chains are not inherently degradable under physiological conditions [54]. As alginate microspheres/hydrogels lack mechanical strength and cell-adhesiveness, their use for LBSD regeneration often involves secondary containment and/or requires chemical modification with integrin-binding peptides. For instance, Guldberg and colleagues conjugated arginine-glycine-aspartic acid (RGD) to alginate via carbodiimide chemistry and Ca^{2+} -crosslinked the RGD-modified alginate with/without 5- μg rhBMP-2, and delivered them to a challenging 8-mm rat femoral segmental defect in an electrospun poly(ϵ -caprolactone) (PCL) fibrous mesh tube with/without perforated surfaces [55]. In the absence of rhBMP-2, no bridging of the defect was accomplished by 12 weeks in the mesh tube alone or mesh tube + alginate groups (Fig. 3, top), supporting that alginate was largely bio-inert. However, with the 5- μg rhBMP-2 delivered, bony callus completely bridged over the defect by 12 weeks in both mesh + alginate + BMP-2 and perforated mesh + alginate + BMP-2 groups, with the latter achieving earlier osteointegration (Fig. 3, bottom) and the full restoration of torsional integrity to the level of intact bone by 12 weeks [55]. μCT -based angiography analyses showed that the presence of perforations in the fibrous mesh tube did not improve vascular invasion. The exact mechanism for the accelerated bone formation and defect bridging in the perforated mesh group, including potential impact of altered rhBMP-2 release kinetics, remains fully elucidated. Interestingly, this group also compared the *in vivo* performance of the non-perforated mesh + alginate hybrid carrier with the conventional collagen sponge carrier for BMP-2 delivery using the same rat LBSD model and showed that at the 1- μg rhBMP-2 loading dose, the hybrid delivery system yielded greater connectivity by week 4 and 2.5-fold greater bone volume by week 12 [56].

Alginate or RGD-modified alginate have also been used to deliver DNA encoding BMP [57], multiple anabolic protein factors [58], or the combination of BMP-2 and mechanical stimulation [59] to improve LBSD repair outcomes. To accelerate the degradation of alginate in these *in vivo* applications, Mooney and colleagues used gamma irradiation to lower the molecular weight of the polysaccharide chains prior to implantation and showed that the irradiated alginate scaffolds were degraded faster and facilitated cellular infiltration *in vivo* [60]. They also used sodium periodate to partially oxidize alginate to expedite its degradation [61]. Guldberg and colleagues prepared oxidized-irradiated alginate hydrogels that even more readily degraded *in vivo* and accelerated the release of rhBMP-2 for the repair of the challenging 8-mm, critical-size rat femoral segmental defects [62]. With the delivery of 2 μg of rhBMP-2, bridging bony callus was observed in both oxidized-irradiated alginate and irradiated alginate groups. At 12 weeks post-surgery, histology showed that oxidized-irradiated alginate was degraded to a greater extent and had more

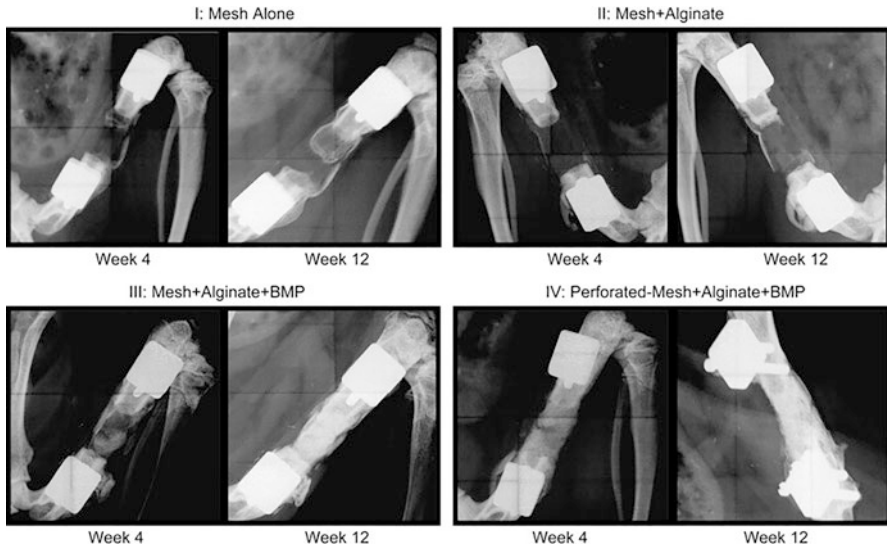


Fig. 3 Representative radiographs at 4 and 12 weeks. Defects in Groups I and II demonstrated small amount of bone formation and did not bridge, even after 12 weeks. At week 4, defects in Groups III samples were infiltrated with considerable bony tissue, while Group IV samples exhibited the most robust mineralization. All samples in Groups III and IV were bridged with densely packed bone at week 12. (Reproduced from [55] with permission from Elsevier)

mature bone penetration within the hydrogel scaffold. Biomechanical strengths of the repaired LBSD at 12 weeks were similar for both groups, with full functional restoration of torsional stiffness achieved. Without examining the mechanical property of the regenerated bone at an earlier time point, it is unclear whether the faster degradation of oxidized-irradiated alginate and more rapid release of rhBMP-2 translated into expedited functional healing of the LBSD.

Chitosan, obtained from the base hydrolysis of exoskeletons of crustaceans, is a linear polysaccharide composed of randomly distributed β -linked D-glucosamine and N-acetyl-D-glucosamine; it is also the primary component of exoskeleton of insects and the cell walls of some bacteria and fungi. Chitosan has been explored for many biomedical applications due to its biocompatibility, biodegradability, as well as antimicrobial properties [63]. Chitosan is appealing for scaffold-guided bone regeneration due to the ease of fabricating porous chitosan scaffolds [64]. Chitosan powder was shown to expedite long bone fracture healing in dogs in an early study [65]. Chitosan has also been combined with other grafting materials or osteogenic growth factors for critical-size LBSD repair. For instance, chitosan gel-DBM powder mixture was used for treating 15-mm, rabbit radial segmental defects, with bony bridging observed by 12 weeks, although the mechanical property restoration was not evaluated [66]. Chitosan hydrogel/TCP composite loaded with an exceptionally high dose of 150- μ g rhBMP-2 was used for the repair of 15-mm, rabbit radius segmental defects, which resulted in incomplete regeneration at 8 weeks along with

observed composite leakage from the defect [67]. These outcomes highlight the general challenges associated with the relatively weak polysaccharide hydrogels including chitosan for LBSD regeneration and calls for further formulation optimizations for such applications.

To facilitate neo-osteogenesis and expedite regeneration of the defects in a dose-dependent manner, Yang and colleagues photo-crosslinked chitosan-lactide-fibrinogen (CLF) hydrogels incorporated with BMP-2 for treating a 6-mm, critical-size segmental defect in rat femur [68]. Unlike the CLF hydrogel alone or the group containing a low dose of rhBMP-2 (0.5 μg) that led to very little bone formation, the CLF hydrogels containing 5- μg rhBMP-2 promoted bridging bony callus formation at 4 weeks post-implantation. No biomechanical test was conducted to evaluate the degree of mechanical restoration of the LBSD in this study. This study also revealed that CFL hydrogel by itself did not promote osteogenesis. Instead, it served as a reasonable rhBMP-2 delivery system. Finally, the use of chitosan-based scaffold for the repair of infected LBSD is worthy of further investigation given the antimicrobial properties of chitosan.

5.4 Synthetic Polymeric Materials and Their Bioceramic Composites

Unlike natural polymeric materials that vary greatly in compositions and molecular weights depending on their sources as well as isolation and processing conditions, synthetic polymers can be designed and synthesized with more precise compositions, molecular architectures, controlled charge distributions, cytocompatible covalent crosslinking, dynamic non-covalent crosslinking, tunable degradative properties, and salient functional groups for modulating cellular interactions [69–72]. Here we discuss the use of poly(ethylene glycol) (PEG)-based hydrogels, conventional degradable polylactide-based composites as well as multi-functional amphiphilic degradable composites for critical-size LBSD regeneration.

Poly(Ethylene Glycol) (PEG) Hydrogels

PEG, also known as Macrogol, is a polyether consisting of repeated ethylene glycol units. It can be prepared either by anionic polymerization of ethylene oxide with any hydroxyl initiators (e.g. water, ethylene glycol, or any diols) or through ring-opening polymerization of epoxyethane. PEG is non-biodegradable, yet it is also low-fouling and easily excretable. For tissue engineering applications, PEG has been explored for both biotherapeutics encapsulation/delivery and as synthetic tissue scaffolds

[73]. For the latter application, however, chemical modifications of PEG with cell adhesive signals or blending with other structural additives known to promote cell adhesion and bone matrix deposition are often required to overcome the low-fouling nature of PEG.

Olmsted-Davis and colleagues delivered 20 million allogenic Wistar skin fibroblast (WSF) cells transduced with an adenovirus expressing BMP-2 via injectable poly(ethylene glycol) diacrylate (PEGDA) hydrogel microspheres to repair a 5-mm, critical-size segmental defect in rat femur [74]. The injectable PEGDA hydrogel was designed as a bioinert barrier mitigating the immune responses to the encapsulated allogenic, BMP-2 expressing WSF cells. It was shown that the continuous secretion of BMP-2 by these cells (with in vitro assay suggesting 96-ng/day BMP-2 production at the cell encapsulation dose applied) led to bony callus formation bridging over the defect within 3 weeks, which was continuously remodeled into more mature bone over 12 weeks. Although torsion test also suggested that the torsional strength and stiffness approached those of the intact controls by 12 weeks, the limited sample size of $n = 3$ combined with a relatively large standard deviation in the experimental group prevented a solid conclusion from being drawn. Notably, the size of the bony callus remained abnormally large even after 12 weeks, which was attributed to the non-degradable hydrogel impeding adequate remodeling and tissue integration. In addition, the long-term survival of the encapsulated genetically engineered cells as well the local and systemic safety of this approach remains to be addressed.

Garcia and colleagues functionalized 4-armed PEG-maleimide with a pro-osteogenic $\alpha 2\beta 1$ integrin-specific hexapeptide (GFOGER) and crosslinked them, in the presence or absence of varying doses of rhBMP-2, with a peptide crosslinker sensitive to the cleavage by matrix metalloproteinase (MMP) [75]. These MMP-degradable, GFOGER-modified PEG hydrogels were examined for their ability to repair a 2.5-mm, critical-size segmental defect in mouse radius. In the absence of encapsulated rhBMP-2, the GFOGER-functionalized PEG hydrogel templated substantial new bone formation within the defect, albeit non-bridging, by 8 weeks post-surgery, supporting the osteoinductivity of the GFOGER-functionalized PEG hydrogel. This observation was in stark contrast to the lack of new bone formation in the defects treated with the control PEG hydrogel functionalized with the more commonly used cell adhesive RGD peptide. When encapsulated with a low dose of 30-ng of rhBMP-2, the MMP-degradable, GFOGER-modified PEG hydrogels underwent rapid degradation and sustain-released of BMP-2 in vivo, resulting in new bone fully bridging the critical-sized ulna defect by 8 weeks and restoring its maximal torque to that the level of intact radii (Fig. 4). Notably, this outcome was superior to that achieved with the same dose of rhBMP-2 delivered via the collagen control, which failed to fully bridge the defect by 8 weeks. This scaffold has the potential to improve both the safety and the efficacy of the BMP therapeutics.

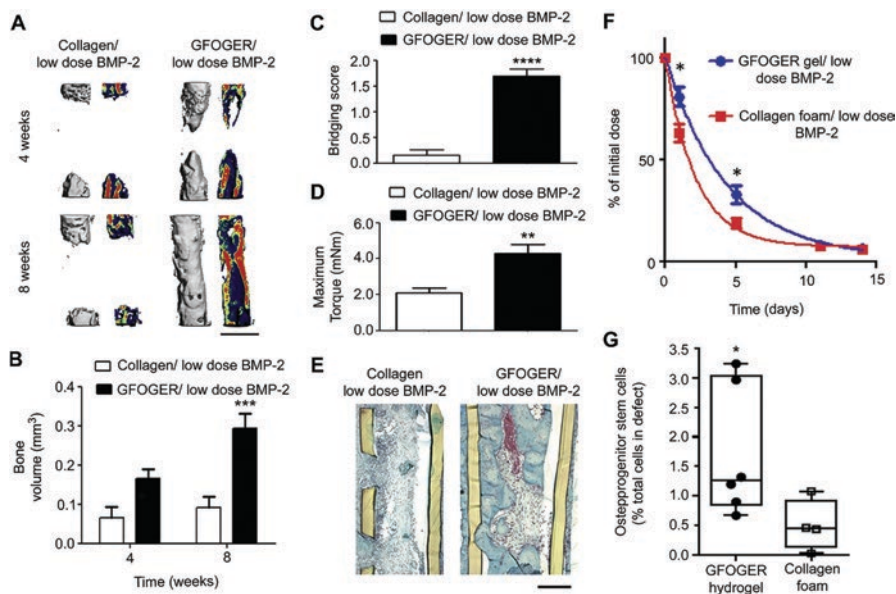


Fig. 4 BMP-2 delivery from GFOGER-functionalized gels improves bone regeneration compared to collagen foams. (A) 3D micro-CT reconstructions of radii (left) and mineral density sagittal sections (right), scale bar 1 mm. (B) micro-CT measures of bone volume in radial defects. (C) Bridging score at 8 weeks post-implantation $n = 13$. (D) Maximum torque values for 8-week radial samples subjected to torsion mechanical testing to failure $n = 5-9$. (E) Sections of 8-week radial samples stained with Safranin-O/Fast Green, scale bar 200 μm . (F) Retention of infrared dye-labeled BMP-2 at implanted defect site in vivo $n = 6$. (G) Quantification of CD45⁻/CD90⁺ osteoprogenitor cells present in defect 7 days post-implantation, $n = 4-6$. * $p < 0.05$, *** $p < 0.001$, and **** $p < 0.0001$ compared to collagen foam/low dose BMP-2. (Reproduced from [75] with permission from Elsevier)

Poly lactides and Composites

Numerous degradable synthetic polymers, including polyesters [76] (e.g. poly(propylene fumarate) [77], polylactides), polyamides [78] and polyamino acids [79], have been pursued for scaffold-guided tissue repair over the past a few decades [80]. Of them, the most investigated for in vivo uses are polylactides. Poly(lactic acid) (PLA), poly(D,L-lactic-co-glycolic acid) (PLGA), PCL and their copolymers have been approved by the FDA for many medical applications including orthopedics [81]. These polymers can be readily prepared using scalable ring-opening (co)polymerization of lactide, glycolide, and/or ϵ -caprolactone. They can be solvent cast into films, electrospun into fibrous meshes, thermal-extruded into filaments, and rapid prototyped/3D printed into macroporous 3D scaffolds tailored for specific tissue defects. These polymers generally support cellular adhesion and degrade into natural metabolites such as lactic acid. For guided bone regeneration, these polymers are often combined with osteoconductive minerals to achieve improved mechanical strength, facilitate absorption and delivery for osteogenic

protein therapeutics, and mitigate inflammatory response to their acidic degradation products.

Conventional Poly lactide-Mineral Composites

In an earlier study, Kirker-Head and colleagues delivered rhBMP-2 and autologous blood via PLGA microparticles to 25-mm segmental defects in sheep femora [82]. Unlike the PLGA and blood only groups that failed to induce sufficient new bone formation, the adjuvant delivery of 2- and 4-mg rhBMP-2 with PLGA and autologous blood significantly enhanced new bone formation, with new bone content approaching that of the intact femur at 16 weeks post-implantation while the recanalization of intramedullary canal nearly completed by 1 year. The PLGA was resorbed by ~4 months after implantation. Since no biomechanical test was conducted, the restoration of mechanical integrity, however, could not be evaluated. It was noted that the weak and brittle PLGA tended to fragment during the implantation, underscoring a weakness in the handling characteristics of such conventional degradable polymers. Zhang et al. examined porous PLA/DBM composite [83] for the repair of 12-mm rabbit radius segmental defects and observed radiographic healing approaching that of the autograft control. The study, however, lacked quantitative evaluations of new bone formation or assessment of mechanical integrity of the repaired LBSD. Kokubo and colleagues implanted PLGA-coated gelatin sponges impregnated with 0.4 mg/mL of rhBMP-2 in 25-mm segmental defects in dog tibiae [84]. Whereas the defect treated with the composite scaffold alone resulted in nonunion at 16 weeks, all defects treated with the scaffold along with rhBMP-2 resulted in radiographic union by 8 weeks. Restoration of the torsional integrity to the level at or beyond that of intact tibiae was achieved at 32 weeks, with all biomechanical parameters examined comparable to that of the intact tibia at 2 years.

Reichert and colleagues showed that 3D printed PCL/TCP composites, in the absence of any exogenous therapeutics, performed far inferior to autologous cancellous bone grafts for the repair of LBSD [85]. However, they showed that when the 3D printed macroporous PCL/ β TCP composite scaffold was used to deliver rhBMP-7 to 3-cm critical-size segmental defect in sheep tibia [86], those incorporating 1.75 or 3.5 mg rhBMP-7 resulted in bridging bony callus by 3 months, restoring torsional strength to the level achieved by autologous cancellous bone grafting. Although the scaffold did not fully degrade even after 12 months [87], the mechanical restoration in the PCL/ β TCP/3.5-mg rhBMP-7 group exceeded that of the autologous cancellous bone graft at 12 months. It should be noted that the milligrams of rhBMP-2 and rhBMP-7 delivered by the conventional poly lactide-based scaffolds in these large animal studies are similar to the high human clinical doses that are known for causing adverse local and systemic side effects.

Amphiphilic Polylactides and Mineral Composites

Integrating hydrophilic polymer blocks such as PEG within the hydrophobic PLA, PLGA, and PCL is an effective way to modulate their physical (e.g. enhanced aqueous wettability; improved structural blending with biominerals), mechanical, and degradative (e.g. expedited hydrolytic degradation) properties [88]. A number of amphiphilic polylactides and mineral composites have been applied for the treatment of LBSD. Kaito and colleagues prepared porous amphiphilic copolymer PLA-PEG/HAp composite bearing 5 or 20 μg of rhBMP-2 to repair a 1.5-cm, critical-size segmental defects in rabbit radius [89]. Bony callus bridged over the defect by 8 weeks with both BMP-2 doses delivered, although the composite graft still remained by 8 weeks and it was unclear how the mechanical integrity of the bridged defect compared with that of the intact controls. Yasuda and colleagues developed a PLA-PEG/ β TCP paste to deliver varying doses of rhBMP-2 to the surface of structural allograft for the repair of 8-mm, critical-size segmental bone defects in rat femur [90]. By 12 weeks, with 10- and 20- μg rhBMP-2, bony callus bridged over the allograft and the host bone, with the 10- μg rhBMP-2 group restoring the bending strength of the treated defect to those of the intact controls. It is unclear, however, whether the deep-frozen structural allografts used in this study were adequately decellularized. In addition, the host periosteum retained during the creation of the segmental defect may have also contributed to the healing. Yoenda and colleagues prepared composite blocks consisting of a copolymer of PLA with randomly inserted *p*-dioxanone and PEG (PLA-DX-PEG) and porous β -TCP to deliver 50 μg of rhBMP-2 to a 1.5-cm critical-size segmental defect in rabbit femur [91]. Bony union was achieved by 8 weeks, resulting in the restoration of its bending stiffness to 40% of the intact control. The new bone was continuously remodeled, culminating in full resorption of the composite scaffold and the restoration of the natural anatomy and mechanical integrity of the regenerated femur by 6 months.

We have shown that by engineering appropriate block lengths and ratio of amphiphilic block copolymers PLA-PEG-PLA (PELA) and PLGA-PEG-PLGA (PELGA), well integrated polymer-HAp composites exhibiting shape memory behavior, controlled *in vivo* degradation, and unique hydration-induced stiffening could be prepared [24, 25, 92–94]. The hydrophobic PLA and PLGA blocks provide tunable degradability, while the center hydrophilic PEG block ensures excellent bonding with osteoconductive HAp, resulting in composites with improved elasticity and aqueous wettability [24, 92, 95]. These amphiphilic composites stiffen upon hydration as a result of microphase separation and PEG crystallization and exhibit thermal-responsive shape memory properties that enable facile temporary shape programming at room temperature and rapid shape recovery at body temperature [92]. The well-distributed HAp maximized the osteoconductivity and osteoinductivity of the composite, promoting osteochondral lineage commitment of BMSCs in unstimulated culture and supporting more potent osteogenesis upon *in vitro* induction (by 2–3 orders of magnitude) compared to conventional degradable polymer-HAp composites [95]. The HAp also enabled stable encapsulation/sustained release of BMP protein therapeutics on both electrospun composite meshes [93] and 3D

composite grafts [94] to guide the regeneration of critical-size femoral segmental defects in rodents.

For instance, we 3D printed macroporous 25%HAp-PELGA(8/1) grafts (25 wt% HA; lactide-to-glycolide ratio of 8/1 within the PLGA blocks) designed for critical-size, 5-mm rat femoral segmental defects [94]. The grafts were compressed into shorter cylinders at rt and conveniently placed within the 5-mm rat LBSD (periosteum from adjacent bone was circumferentially removed), which underwent instantaneous shape recovery, swelling, and stiffening at body temperature, resulting in stable graft fixation. By contrast, resorbable collagen sponge control lost its shape upon wetting, making its surgical placement into the defect tedious. Pull-out test measuring the force required to dislodge hydrated HA-PELGA graft vs. collagen sponge from the defect confirmed superior fixation of HA-PELGA (by >2 orders of magnitude). When a single dose of 400-ng rhBMP-2/7 heterodimer (~13- μ g when scaled to 60-kg human as opposed to the typical mg-scale clinical rhBMP-2 doses) was loaded on the 25%HA-PELGA(8/1) graft, bony callus fully bridged the LBSD by 4 weeks, with the new bone rapidly remodeled into mature bone and recanalized in 8–12 weeks (Fig. 5a). Continued increases in bone volume (BV) and bone mineral density (BMD) were confirmed by μ CT quantification over time (Fig. 5b). Femoral histology confirmed active new bone remodeling by coordinated osteoclast (tartrate-resistant acid phosphatase/TRAP, red) and osteoblast (alkaline phosphatase/ALP, blue) activities at 4 weeks and the timely resorption of the graft by 12 weeks (Fig. 5c). Full restoration of torsional strength of the regenerated femurs to that of intact control femurs was achieved by 16 weeks (Fig. 5d). Finally, no ectopic bone formation was detected in the HA-PELGA/BMP-treated LBSD, contrasting extensive ectopic bone formation observed in the collagen/BMP control group. This study demonstrated that osteoconductive HA-degradable amphiphilic polymer composites can be engineered as smart-fitting synthetic bone graft to achieve improved surgical handling and expedited functional regeneration of LBSD with a safer dose of BMP therapeutics (>100 times lower than typically required with collagen carriers).

6 Potentials of Complex Bioprinted Cell-Laden Hydrogel/Mineral Composite Scaffolds

Compared to thermal extrusion-based 3D printing, 3D bioprinting enables the integration of temperature-sensitive biofactors and cells within a polymeric hydrogel and/or mineral-based tissue engineering scaffold in a spatially defined manner for both soft and hard tissue regeneration [96]. Naturally occurring biopolymer-based hydrogels such as alginate, gelatin, collagen, hyaluronic acid, chitosan, and decellularized extracellular matrices as well as synthetic polymeric hydrogels such as PEG (meth)acrylates and Pluronics have all been exploited as bioinks to deliver therapeutic cells and/or biofactors during 3D bioprinting. For example, Atala and

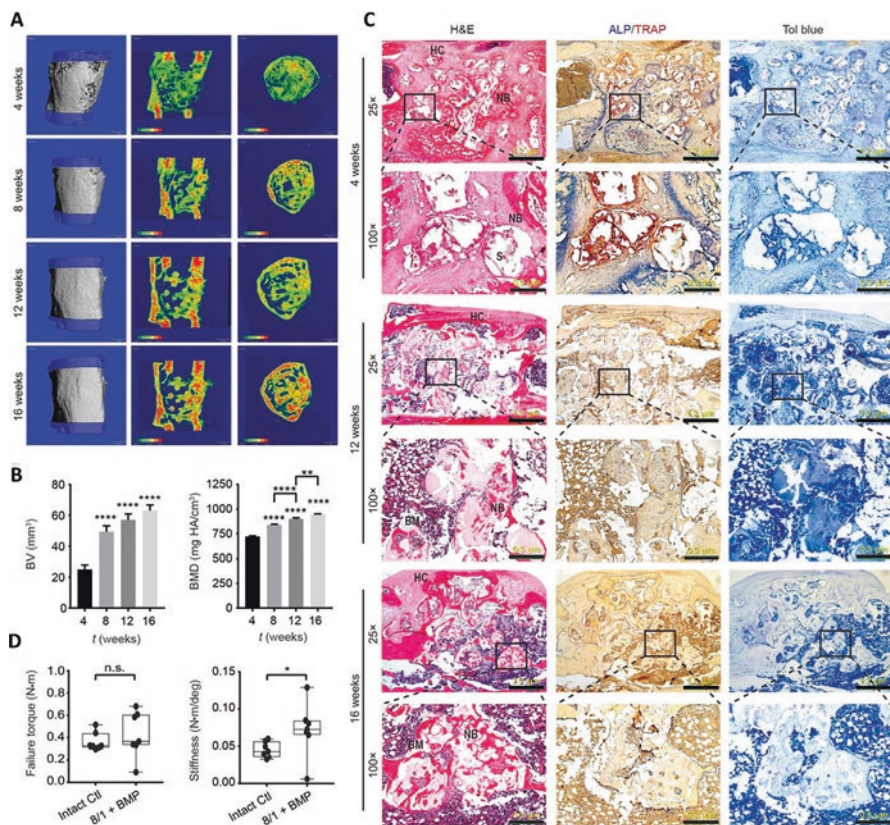


Fig. 5 Accelerated healing of 5-mm rat femoral segmental defects by 25% HA-PELGA(8/1) grafts preabsorbed with 400-ng rhBMP-2/7. (A) 3D μ CT images and BMD color maps (center sagittal and axial slices) of the ROI showing maturing regenerated bone within the defect over time. Global thresholding was applied to exclude bone densities below 518.2 mg HA/cm³ (HA-PELGA graft invisible at this threshold). (B) Longitudinal μ CT quantification of BV and BMD ($n \geq 12$) within the ROI over time. Statistical significance over the 4-week data or as indicated by brackets indicated as follows: ** $p < 0.01$, **** $p < 0.0001$. One-way ANOVA with Tukey's post hoc test. Data are presented as means \pm SEM. The global lower threshold of 518.2 mg HA/cm³ was applied for all quantifications. (C) Histological micrographs of H&E-, ALP/TRAP-, and Tol blue-stained sections of explanted graft-filled femurs over time. Scale bars, 1.2 mm (25 \times magnification) and 300 μ m (100 \times magnification). Boxed regions shown at higher magnification in bottom rows. HC healing callus, S scaffold, NB new bone, BM bone marrow. (D) Boxplots of failure torque and stiffness of intact (control, Ctl) versus regenerated femur (8/1 + BMP) 16 weeks after being treated with HA-PELGA(8/1) grafts preloaded with 400-ng rhBMP-2/7 ($n = 7$). * $p < 0.05$, n.s.: $p > 0.05$, Wilcoxon–Mann–Whitney rank sum test. (Reprinted from [94] with permission from AAAS)

colleagues 3D bioprinted complex tissue-engineered constructs comprising of human amniotic fluid-derived stem cell (hAFSC)-laden hydrogels (gelatin, hyaluronic acid, fibrinogen, and glycerol) and the sacrificial Pluronic F-127 hydrogel, which were reinforced by thermal printed PCL support [97]. These cell-laden

scaffolds were successfully applied for the regeneration of rodent mandibular and calvarial bone defects. Keriquel and colleagues used laser-assisted bioprinting to seed MSCs in collagen/nano-HAp discs in a spatially controlled manner prior to their implantation to treat mouse calvarial bone defects [98]. It was shown that the degree of new bone regeneration was highly dependent on the spatial arrangement of the cells printed, with mature bone formed throughout the defects in 2 months when cells were bioprinted at the center of the discs while no significant bone formation when cells were printed onto the periphery of the discs [98].

More recently, proof-of-concept intravital bioprinting technologies have been developed to explore the feasibility of noninvasive *in vivo* 3D bioprinting of synthetic tissue constructs. Urciuolo et al. [99] utilized bio-orthogonal two-photon cycloaddition to crosslink photo-sensitive gelatin or 4-arm PEG derivatives by near infrared irradiation. *De novo* formation of myofibers by donor-muscle-derived stem cells delivered by the intravital 3D bioprinting was demonstrated in mice. Chen et al. [100] developed digital photopolymerization-based 3D bioprinting where near infrared is modulated into customized patterns by a digital micromirror device and dynamically projected for inducing polymerization of subcutaneously injected bio-ink in a spatially defined manner.

These new technological developments will likely have a positive impact on the regenerative reconstruction of LBSD, an area that has not yet seen a significant use of bioprinting. For instance, bioprinting may enable the delivery of therapeutic factors and progenitor cells tailored to overcome the limited regenerative potentials of older patients or those suffering from metabolic conditions in a spatially defined manner to conventional bone grafts. It still remains to be seen, however, whether intravital 3D bioprinting may be successfully translated for more deeply embedded calcified tissue regeneration such as the scaffold-guided LBSD regenerative repair.

7 Conclusions and Future Perspectives

Bone grafting technologies play a crucial role in the regenerative repair of LBSD. Recent advances in the understanding of cellular and molecular events governing the tissue integration of allogenic bone grafts have inspired the development of novel biomaterials to facilitate the delivery of key signaling molecules and progenitor cells to the periosteal surface of devitalized structural allografts. Successes in promoting vascularization along with osteogenesis of structural allografts using these approaches will likely be instrumental in improving their long-term success rate in the regenerative reconstruction of LBSD. Meanwhile, there has been exciting new developments of synthetic bone graft substitutes in the past two decades, ranging from novel auxiliary metallic cage design to environmentally responsive drug release carriers and self-fitting shape memory polymeric bone grafts. Enabling technologies such as controlled polymerizations, high-fidelity bioconjugation chemistries, and 3D printing (both thermal extrusion and bioprinting) have enabled the design of synthetic bone grafts with controlled porosities, degradation profiles,

mechanical properties, as well as spatially defined presentation of biochemical signals and progenitor cells. Animal studies rigorously evaluating the efficacy and safety of these novel grafting technologies against proper controls will be essential for their iterative optimizations and eventual clinical translations. The use of critical-size LBSD models and adequate sample sizes in the study design, assessment of mechanical restoration of regenerated bone (vs. those achieved by current clinical standards and healthy controls), and determination of the long-term safety of both biomaterials and biotherapeutics should be implemented to allow meaningful comparisons of competing technologies.

Acknowledgements This work is supported by an Alex Lemonade Stand Foundation Innovation Grant and a BRIDGE Award from the University of Massachusetts Medical School.

Conflict of Interests The authors declare there is no conflict of interests.

References

1. Bauer TW, Muschler GF. Bone graft materials: an overview of the basic science. *Clin Orthop Relat Res.* 2000;371:10–27.
2. Urist MR. 23 Physiologic basis of bone-graft surgery, with special reference to the theory of induction. *Clin Orthop Relat Res.* 1953;1:207–16.
3. Mauffrey C, Barlow BT, Smith W. Management of segmental bone defects. *J Am Acad Orthop Surg.* 2015;23(3):143–53.
4. Bostrom MPG, Seigerman DA. The clinical use of allografts, demineralized bone matrices, synthetic bone graft substitutes and osteoinductive growth factors: a survey study. *HSS J.* 2005;1(1):9–18.
5. Zhang M, Matinlinna JP, Tsoi JKH, Liu W, Cui X, Lu WW, Pan H. Recent developments in biomaterials for long-bone segmental defect reconstruction: a narrative overview. *J Orthop Transl.* 2019;22:26–33.
6. Supová M. Problem of hydroxyapatite dispersion in polymer matrices: a review. *J Mater Sci Mater Med.* 2009;20:1201–13.
7. Geiger M, Li RH, Friess W. Collagen sponges for bone regeneration with rhBMP-2. *Adv Drug Deliv Rev.* 2003;55(12):1613–29.
8. McKay WF, Peckham SM, Badura JM. A comprehensive clinical review of recombinant human bone morphogenetic protein-2 (INFUSE (R) bone graft). *Int Orthop.* 2007;31(6):729–34.
9. Glatt V, Bartnikowski N, Quirk N, Schuetz M, Evans C. Reverse dynamization: influence of fixator stiffness on the mode and efficiency of large-bone-defect healing at different doses of rhBMP-2. *J Bone Joint Surg Am.* 2016;98(8):677–87.
10. Makhni MC, Caldwell J-ME, Saifi C, Fischer CR, Lehman RA, Lenke LG, Lee FY. Tissue engineering advances in spine surgery. *Regen Med.* 2016;11(2):211–22.
11. Zara JN, Siu RK, Zhang X, Shen J, Ngo R, Lee M, Li W, Chiang M, Chung J, Kwak J, Wu BM, Ting K, Soo C. High doses of bone morphogenetic protein 2 induce structurally abnormal bone and inflammation in vivo. *Tissue Eng Part A.* 2011;17(9–10):1389–99.
12. Baldwin P, Li DJ, Auston DA, Mir HS, Yoon RS, Koval KJ. Autograft, allograft, and bone graft substitutes: clinical evidence and indications for use in the setting of orthopaedic trauma surgery. *J Orthop Trauma.* 2019;33(4):203–13.
13. van de Vijfeijken SE, Münker TJ, Spijker R, Karssemakers LH, Vandertop WP, Becking AG, Ubbink DT, Becking A, Dubois L, Karssemakers L. Autologous bone is inferior to alloplastic

- cranioplasties: safety of autograft and allograft materials for cranioplasties, a systematic review. *World Neurosurg.* 2018;117(443–452):e8.
14. Hopp SG, Dahners LE, Gilbert JA. A study of the mechanical strength of long bone defects treated with various bone autograft substitutes: an experimental investigation in the rabbit. *J Orthop Res.* 1989;7(4):579–84.
 15. Lauthe O, Soubeyrand M, Babinet A, Dumaine V, Anract P, Biau D. The indications and donor-site morbidity of tibial cortical strut autografts in the management of defects in long bones. *Bone Joint J.* 2018;100(5):667–74.
 16. Buser Z, Brodke DS, Youssef JA, Rometsch E, Park J-B, Yoon ST, Wang JC, Meisel H-J. Allograft versus demineralized bone matrix in instrumented and noninstrumented lumbar fusion: a systematic review. *Global Spine J.* 2018;8(4):396–412.
 17. Mankin HJ, Fogelson FS, Thrasher AZ, Jaffer F. Massive resection and allograft transplantation in the treatment of malignant bone tumors. *N Engl J Med.* 1976;294(23):1247–55.
 18. Samsell B, Softic D, Qin X, McLean J, Sohoni P, Gonzales K, Moore MA. Preservation of allograft bone using a glycerol solution: a compilation of original preclinical research. *Biomater Res.* 2019;23(1):5.
 19. Boyce T, Edwards J, Scarborough N. Allograft bone: the influence of processing on safety and performance. *Orthop Clin.* 1999;30(4):571–81.
 20. Sorger JJ, Hornicek FJ, Zavatta M, Menzner JP, Gebhardt MC, Tomford WW, Mankin HJ. Allograft fractures revisited. *Clin Orthop Relat Res.* 2001;382:66–74.
 21. Ito H, Koefoed M, Tiyyapatanaputi P, Gromov K, Goater JJ, Carmouche J, Zhang X, Rubery PT, Rabinowitz J, Samulski RJ. Remodeling of cortical bone allografts mediated by adherent rAAV-RANKL and VEGF gene therapy. *Nat Med.* 2005;11(3):291–7.
 22. Zhang X, Awad HA, O'Keefe RJ, Guldberg RE, Schwarz EM. A perspective: engineering periosteum for structural bone graft healing. *Clin Orthop Relat Res.* 2008;466(8):1777–87.
 23. Wang T, Zhai Y, Nuzzo M, Yang X, Yang Y, Zhang X. Layer-by-layer nanofiber-enabled engineering of biomimetic periosteum for bone repair and reconstruction. *Biomaterials.* 2018;182:279–88.
 24. Zhang B, Fillion TM, Kutikov AB, Song J. Facile stem cell delivery to bone grafts enabled by smart shape recovery and stiffening of degradable synthetic periosteal membranes. *Adv Funct Mater.* 2017;27(5):1604784.
 25. Zhang B, DeBartolo JE, Song J. Shape recovery with concomitant mechanical strengthening of amphiphilic shape memory polymers in warm water. *ACS Appl Mater Interfaces.* 2017;9(5):4450–6.
 26. Chang H, Knothe Tate ML. Concise review: the periosteum: tapping into a reservoir of clinically useful progenitor cells. *Stem Cells Transl Med.* 2012;1(6):480–91.
 27. Wang ZX, Chen C, Zhou Q, Wang XS, Zhou G, Liu W, Zhang Z-Y, Cao Y, Zhang WJ. The treatment efficacy of bone tissue engineering strategy for repairing segmental bone defects under osteoporotic conditions. *Tissue Eng Part A.* 2015;21(17–18):2346–55.
 28. Ng MH, Duski S, Tan KK, Yusof MR, Low KC, Mohamed Rose I, Mohamed Z, Bin Saim A, Idrus RBH. Repair of segmental load-bearing bone defect by autologous mesenchymal stem cells and plasma-derived fibrin impregnated ceramic block results in early recovery of limb function. *Biomed Res Int.* 2014;2014:345910.
 29. Hertlein H, Mittlmeier T, Piltz S, Schürmann M, Kauschke T, Lob G. Spinal stabilization for patients with metastatic lesions of the spine using a titanium spacer. *Eur Spine J.* 1992;1(2):131–6.
 30. Hollowell JP, Vollmer DG, Wilson CR, Pintar FA, Yoganandan N. Biomechanical analysis of thoracolumbar interbody constructs: how important is the endplate? *Spine (Phila Pa 1976).* 1996;21(9):1032–6.
 31. Cobos JA, Lindsey RW, Gugala Z. The cylindrical titanium mesh cage for treatment of a long bone segmental defect: description of a new technique and report of two cases. *J Orthop Trauma.* 2000;14(1):54–9.

32. Attias N, Thabet A, Prabhakar G, Dollahite J, Gehlert R, DeCoster T. Management of extra-articular segmental defects in long bone using a titanium mesh cage as an adjunct to other methods of fixation: a multicentre report of 17 cases. *Bone Joint J.* 2018;100(4):646–51.
33. Drosos GI, Touzopoulos P, Ververidis A, Tilkeridis K, Kazakos K. Use of demineralized bone matrix in the extremities. *World J Orthop.* 2015;6(2):269–77.
34. Grob D, Daehn S, Mannion AF. Titanium mesh cages (TMC) in spine surgery. *Eur Spine J.* 2005;14(3):211–21.
35. Attias N, Lindsey RW. Management of large segmental tibial defects using a cylindrical mesh cage. *Clin Orthop Relat Res.* 2006;450:259–66.
36. Pobloth A-M, Checa S, Razi H, Petersen A, Weaver JC, Schmidt-Bleek K, Windolf M, Tatai AÁ, Roth CP, Schaser K-D. Mechanobiologically optimized 3D titanium-mesh scaffolds enhance bone regeneration in critical segmental defects in sheep. *Sci Transl Med.* 2018;10(423):eaam8828.
37. Chung W-J, Kwon K-Y, Song J, Lee S-W. Evolutionary screening of collagen-like peptides that nucleate hydroxyapatite crystals. *Langmuir.* 2011;27(12):7620–8.
38. Nancollas GH, Henneman ZJ. Calcium oxalate: calcium phosphate transformations. *Urol Res.* 2010;38(4):277–80.
39. Kasten P, Vogel J, Geiger F, Niemeyer P, Luginbühl R, Szalay K. The effect of platelet-rich plasma on healing in critical-size long-bone defects. *Biomaterials.* 2008;29(29):3983–92.
40. Marcacci M, Kon E, Moukhachev V, Lavroukov A, Kutepov S, Quarto R, Mastrogiacomo M, Cancedda R. Stem cells associated with macroporous bioceramics for long bone repair: 6-to 7-year outcome of a pilot clinical study. *Tissue Eng.* 2007;13(5):947–55.
41. Patel KD, Buitrago JO, Parthiban SP, Lee J-H, Singh RK, Knowles JC, Kim H-W. Combined effects of nanoroughness and ions produced by electrodeposition of mesoporous bioglass nanoparticle for bone regeneration. *ACS Appl Bio Mater.* 2019;2(11):5190–203.
42. Tölli H, Kujala S, Levenon K, Jämsä T, Jalovaara P. Bioglass as a carrier for reindeer bone protein extract in the healing of rat femur defect. *J Mater Sci Mater Med.* 2010;21(5):1677–84.
43. Gabbai-Armelin PR, Wilian Kido H, Fernandes KR, Fortulan CA, Muniz Renno AC. Effects of bio-inspired bioglass/collagen/magnesium composites on bone repair. *J Biomater Appl.* 2019;34(2):261–72.
44. Bougioukli S, Jain A, Sugiyama O, Tinsley BA, Tang AH, Tan MH, Adams DJ, Kostenuik PJ, Lieberman JR. Combination therapy with BMP-2 and a systemic RANKL inhibitor enhances bone healing in a mouse critical-sized femoral defect. *Bone.* 2016;84:93–103.
45. Friess W, Uludag H, Foskett S, Biron R, Sargeant C. Characterization of absorbable collagen sponges as recombinant human bone morphogenetic protein-2 carriers. *Int J Pharm.* 1999;185(1):51–60.
46. Lissenberg-Thunnissen SN, de Gorter DJJ, Sier CFM, Schipper IB. Use and efficacy of bone morphogenetic proteins in fracture healing. *Int Orthop.* 2011;35(9):1271–80.
47. Kuttappan S, Mathew D, Nair MB. Biomimetic composite scaffolds containing bioceramics and collagen/gelatin for bone tissue engineering—a mini review. *Int J Biol Macromol.* 2016;93:1390–401.
48. Guda T, Walker JA, Singleton BM, Hernandez JW, Son J-S, Kim S-G, Oh DS, Appleford MR, Ong JL, Wenke JC. Guided bone regeneration in long-bone defects with a structural hydroxyapatite graft and collagen membrane. *Tissue Eng Part A.* 2012;19(17–18):1879–88.
49. Yamamoto M, Takahashi Y, Tabata Y. Enhanced bone regeneration at a segmental bone defect by controlled release of bone morphogenetic protein-2 from a biodegradable hydrogel. *Tissue Eng.* 2006;12(5):1305–11.
50. Mano JF, Silva GA, Azevedo HS, Malafaya PB, Sousa RA, Silva SS, Boesel LF, Oliveira JM, Santos TC, Marques AP, Neves NM, Reis RL. Natural origin biodegradable systems in tissue engineering and regenerative medicine: present status and some moving trends. *J R Soc Interface.* 2007;4(17):999–1030.
51. Collins MN, Birkinshaw C. Hyaluronic acid based scaffolds for tissue engineering—a review. *Carbohydr Polym.* 2013;92(2):1262–79.

52. Han SH, Jung SH, Lee JH. Preparation of beta-tricalcium phosphate microsphere-hyaluronic acid-based powder gel composite as a carrier for rhBMP-2 injection and evaluation using long bone segmental defect model. *J Biomater Sci Polym Ed.* 2019;30(8):679–93.
53. Gibbs DM, Black CR, Dawson JI, Oreffo RO. A review of hydrogel use in fracture healing and bone regeneration. *J Tissue Eng Regen Med.* 2016;10(3):187–98.
54. Shoichet MS, Li RH, White ML, Winn SR. Stability of hydrogels used in cell encapsulation: an in vitro comparison of alginate and agarose. *Biotechnol Bioeng.* 1996;50(4):374–81.
55. Kolambkar YM, Dupont KM, Boerckel JD, Huebsch N, Mooney DJ, Hutmacher DW, Guldberg RE. An alginate-based hybrid system for growth factor delivery in the functional repair of large bone defects. *Biomaterials.* 2011;32(1):65–74.
56. Boerckel JD, Kolambkar YM, Dupont KM, Uhrig BA, Phelps EA, Stevens HY, García AJ, Guldberg RE. Effects of protein dose and delivery system on BMP-mediated bone regeneration. *Biomaterials.* 2011;32(22):5241–51.
57. Krebs MD, Salter E, Chen E, Sutter KA, Alsberg E. Calcium phosphate-DNA nanoparticle gene delivery from alginate hydrogels induces in vivo osteogenesis. *J Biomed Mater Res A.* 2010;92(3):1131–8.
58. Oest ME, Dupont KM, Kong HJ, Mooney DJ, Guldberg RE. Quantitative assessment of scaffold and growth factor-mediated repair of critically sized bone defects. *J Orthop Res.* 2007;25(7):941–50.
59. Boerckel JD, Dupont KM, Kolambkar YM, Lin AS, Guldberg RE. In vivo model for evaluating the effects of mechanical stimulation on tissue-engineered bone repair. *J Biomech Eng.* 2009;131(8):084502.
60. Alsberg E, Kong H, Hirano Y, Smith M, Albeiruti A, Mooney D. Regulating bone formation via controlled scaffold degradation. *J Dent Res.* 2003;82(11):903–8.
61. Boonthekul T, Kong H-J, Mooney DJ. Controlling alginate gel degradation utilizing partial oxidation and bimodal molecular weight distribution. *Biomaterials.* 2005;26(15):2455–65.
62. Priddy LB, Chaudhuri O, Stevens HY, Krishnan L, Uhrig BA, Willett NJ, Guldberg RE. Oxidized alginate hydrogels for bone morphogenetic protein-2 delivery in long bone defects. *Acta Biomater.* 2014;10(10):4390–9.
63. Oryan A, Alidadi S, Bigham-Sadegh A, Moshiri A. Effectiveness of tissue engineered based platelet gel embedded chitosan scaffold on experimentally induced critical sized segmental bone defect model in rat. *Injury.* 2017;48(7):1466–74.
64. LogithKumar R, KeshavNarayan A, Dhivya S, Chawla A, Saravanan S, Selvamurugan N. A review of chitosan and its derivatives in bone tissue engineering. *Carbohydr Polym.* 2016;151:172–88.
65. Khanal D, Minami S, Rakshit S, Chandrakrachang S, Stevens W. Management of fracture with chitosan in dogs. *Indian Vet J.* 2000;77(12):1085–90.
66. Shuang F, Hou S, Zhao Y, Zhong H, Xue C, Zhu J, Bu G, Cao Z. Characterization of an injectable chitosan-demineralized bone matrix hybrid for healing critical-size long-bone defects in a rabbit model. *Eur Rev Med Pharmacol Sci.* 2014;18:740–52.
67. Luca L, Rougemont AL, Walpoth BH, Boure L, Tami A, Anderson JM, Jordan O, Gurny R. Injectable rhBMP-2-loaded chitosan hydrogel composite: osteoinduction at ectopic site and in segmental long bone defect. *J Biomed Mater Res A.* 2011;96(1):66–74.
68. Kim S, Bedigrew K, Guda T, Maloney WJ, Park S, Wenke JC, Yang YP. Novel osteoinductive photo-cross-linkable chitosan-lactide-fibrinogen hydrogels enhance bone regeneration in critical size segmental bone defects. *Acta Biomater.* 2014;10(12):5021–33.
69. Huang H, Tan Y, Ayers DC, Song J. Anionic and zwitterionic residues modulate stiffness of photo-cross-linked hydrogels and cellular behavior of encapsulated chondrocytes. *ACS Biomater Sci Eng.* 2018;4(5):1843–51.
70. Tan Y, Huang H, Ayers DC, Song J. Modulating viscoelasticity, stiffness, and degradation of synthetic cellular niches via stoichiometric tuning of covalent versus dynamic noncovalent cross-linking. *ACS Cent Sci.* 2018;4(8):971–81.

71. Madl CM, Heilshorn SC. Engineering hydrogel microenvironments to recapitulate the stem cell niche. *Annu Rev Biomed Eng.* 2018;20:21–47.
72. Xu X, Jerca FA, Jerca VV, Hoogenboom R. Covalent poly (2-isopropenyl-2-oxazoline) hydrogels with ultrahigh mechanical strength and toughness through secondary terpyridine metal-coordination crosslinks. *Adv Funct Mater.* 2019;29(48):1904886.
73. Hubbell JA. Synthetic biodegradable polymers for tissue engineering and drug delivery. *Curr Opin Solid State Mater Sci.* 1998;3(3):246–51.
74. Sonnet C, Simpson CL, Olabisi RM, Sullivan K, Lazard Z, Gugala Z, Peroni JF, Weh JM, Davis AR, West JL. Rapid healing of femoral defects in rats with low dose sustained BMP2 expression from PEGDA hydrogel microspheres. *J Orthop Res.* 2013;31(10):1597–604.
75. Shekaran A, García JR, Clark AY, Kavanaugh TE, Lin AS, Guldberg RE, García AJ. Bone regeneration using an alpha 2 beta 1 integrin-specific hydrogel as a BMP-2 delivery vehicle. *Biomaterials.* 2014;35(21):5453–61.
76. Webb AR, Yang J, Ameer GA. Biodegradable polyester elastomers in tissue engineering. *Expert Opin Biol Ther.* 2004;4(6):801–12.
77. Lee K-W, Wang S, Lu L, Jabbari E, Currier BL, Yaszemski MJ. Fabrication and characterization of poly (propylene fumarate) scaffolds with controlled pore structures using 3-dimensional printing and injection molding. *Tissue Eng.* 2006;12(10):2801–11.
78. Wada K, Yu W, Elazizi M, Barakat S, Ouimet MA, Rosario-Meléndez R, Fiorellini JP, Graves DT, Uhrich KE. Locally delivered salicylic acid from a poly(anhydride-ester): impact on diabetic bone regeneration. *J Control Release.* 2013;171(1):33–7.
79. Yan L, Jiang D-m. Study of bone-like hydroxyapatite/polyamino acid composite materials for their biological properties and effects on the reconstruction of long bone defects. *Drug Des Devel Ther.* 2015;9:6497.
80. Ye H, Zhang K, Kai D, Li Z, Loh XJ. Polyester elastomers for soft tissue engineering. *Chem Soc Rev.* 2018;47(12):4545–80.
81. Narayanan G, Vernekar VN, Kuyinu EL, Laurencin CT. Poly (lactic acid)-based biomaterials for orthopaedic regenerative engineering. *Adv Drug Deliv Rev.* 2016;107:247–76.
82. Kirker-Head CA, Gerhart TN, Armstrong R, Schelling SH, Carmel LA. Healing bone using recombinant human bone morphogenetic protein 2 and copolymer. *Clin Orthop Relat Res.* 1998;349:205–17.
83. Zhang Y, Wang J, Wang J, Niu X, Liu J, Gao L, Zhai X, Chu K. Preparation of porous PLA/DBM composite biomaterials and experimental research of repair rabbit radius segmental bone defect. *Cell Tissue Bank.* 2015;16(4):615–22.
84. Kokubo S, Mochizuki M, Fukushima S, Ito T, Nozaki K, Iwai T, Takahashi K, Yokota S, Miyata K, Sasaki N. Long-term stability of bone tissues induced by an osteoinductive biomaterial, recombinant human bone morphogenetic protein-2 and a biodegradable carrier. *Biomaterials.* 2004;25(10):1795–803.
85. Reichert JC, Wullschleger ME, Cipitria A, Lienau J, Cheng TK, Schütz MA, Duda GN, Nöth U, Eulert J, Hutmacher DW. Custom-made composite scaffolds for segmental defect repair in long bones. *Int Orthop.* 2011;35(8):1229–36.
86. Reichert JC, Cipitria A, Epari DR, Saifzadeh S, Krishnakanth P, Berner A, Woodruff MA, Schell H, Mehta M, Schuetz MA, Duda GN, Hutmacher DW. A tissue engineering solution for segmental defect regeneration in load-bearing long bones. *Sci Transl Med.* 2012;4(141):141ra93.
87. Reichert JC, Cipitria A, Epari DR, Saifzadeh S, Krishnakanth P, Berner A, Woodruff MA, Schell H, Mehta M, Schuetz MA. A tissue engineering solution for segmental defect regeneration in load-bearing long bones. *Sci Transl Med.* 2012;4(141):141ra93.
88. Kutikov AB, Song J. Biodegradable PEG-based amphiphilic block copolymers for tissue engineering applications. *ACS Biomater Sci Eng.* 2015;1(7):463–80.
89. Kaito T, Myoui A, Takaoka K, Saito N, Nishikawa M, Tamai N, Ohgushi H, Yoshikawa H. Potentiation of the activity of bone morphogenetic protein-2 in bone regeneration by a PLA-PEG/hydroxyapatite composite. *Biomaterials.* 2005;26(1):73–9.

90. Yasuda H, Yano K, Wakitani S, Matsumoto T, Nakamura H, Takaoka K. Repair of critical long bone defects using frozen bone allografts coated with an rhBMP-2-retaining paste. *J Orthop Sci.* 2012;17(3):299–307.
91. Yoneda M, Terai H, Imai Y, Okada T, Nozaki K, Inoue H, Miyamoto S, Takaoka K. Repair of an intercalated long bone defect with a synthetic biodegradable bone-inducing implant. *Biomaterials.* 2005;26(25):5145–52.
92. Kutikov AB, Gurijala A, Song J. Rapid prototyping amphiphilic polymer/hydroxyapatite composite scaffolds with hydration-induced self-fixation behavior. *Tissue Eng Part C Methods.* 2015;21(3):229–41.
93. Kutikov AB, Skelly JD, Ayers DC, Song J. Templated repair of long bone defects in rats with bioactive spiral-wrapped electrospun amphiphilic polymer/hydroxyapatite scaffolds. *ACS Appl Mater Interfaces.* 2015;7(8):4890–901.
94. Zhang B, Skelly JD, Maalouf JR, Ayers DC, Song J. Multifunctional scaffolds for facile implantation, spontaneous fixation, and accelerated long bone regeneration in rodents. *Sci Transl Med.* 2019;11(502):eaa7411.
95. Kutikov A, Song J. An amphiphilic degradable polymer/hydroxyapatite composite with enhanced handling characteristics promotes osteogenic gene expression in bone marrow stromal cells. *Acta Biomater.* 2013;9(9):8354–64.
96. Koons GL, Mikos AG. Progress in three-dimensional printing with growth factors. *J Control Release.* 2019;295:50–9.
97. Kang H-W, Lee SJ, Ko IK, Kengla C, Yoo JJ, Atala A. A 3D bioprinting system to produce human-scale tissue constructs with structural integrity. *Nat Biotechnol.* 2016;34(3):312–9.
98. Keriquel V, Oliveira H, Rémy M, Ziane S, Delmond S, Rousseau B, Rey S, Catros S, Amédée J, Guillemot F. In situ printing of mesenchymal stromal cells, by laser-assisted bioprinting, for in vivo bone regeneration applications. *Sci Rep.* 2017;7(1):1–10.
99. Urciuolo A, Poli I, Brandolino L, Raffa P, Scattolini V, Laterza C, Giobbe GG, Zambaiti E, Selmin G, Magnussen M. Intravital three-dimensional bioprinting. *Nat Biomed Eng.* 2020;4(9):901–15.
100. Chen Y, Zhang J, Liu X, Wang S, Tao J, Huang Y, Wu W, Li Y, Zhou K, Wei X. Noninvasive in vivo 3D bioprinting. *Sci Adv.* 2020;6(23):eaba7406.

3D Bioprinting and Nanotechnology for Bone Tissue Engineering



Robert Choe, Erfan Jabari, Bhushan Mahadik, and John Fisher

1 Introduction

On the nanoscale, bone tissue is a composite of organic and inorganic constituents (Fig. 1) [1]. The organic phase, which makes up 30% of bone, consists of a variety of structural proteins and polysaccharides. Its main constituents are collagen fibrils that have diameters between 35 and 60 nm and can be up to 1 μm in length [2]. The remaining 10% of the organic phase consists of noncollagenous proteins that include osteocalcin, osteonectin, bone sialoprotein, bone phosphoproteins, and small proteoglycans. Additionally, these fibrils are organized with a periodicity of 67 and 40 nm gaps and are mineralized with hydroxyapatite crystals. Making up the remaining 70% of bone, the inorganic phase functions as an ion reservoir for Ca, P, Na, and Mg and provides stiffness and strength of bone in the form of apatite, carbonate, acid phosphate, and brushite. As the main component of the inorganic phase, hydroxyapatite is an anisotropic and extremely stiff inorganic component that lies in the collagen gaps [3]. This unique combination between the two phases has allowed the bone to achieve an ideal mechanical strength and architecture to support de novo bone formation.

Most bone tissue engineering (BTE) research to date has focused on mimicking the mechanical properties of the native tissue and induction of new tissue ingrowth [4]. Numerous biomaterials have been utilized to match the stiffness of bone and support bone formation. However, most have failed to integrate completely with the host tissue due to several factors that have limited bone restoration capabilities [5]. While attempts have been made to mimic the macro and microstructure of bone using porous scaffolds, these fabrication methods have not been able to fully recapitulate the complex cortical and trabecular architecture of native bone. As a result, nanostructured scaffolds based on nanomaterials have been explored to better mimic

R. Choe · E. Jabari · B. Mahadik · J. Fisher (✉)

Fischell Department of Bioengineering, University of Maryland, College Park, MD, USA

e-mail: bhushanpmahadik@gmail.com; jpfisher@umd.edu

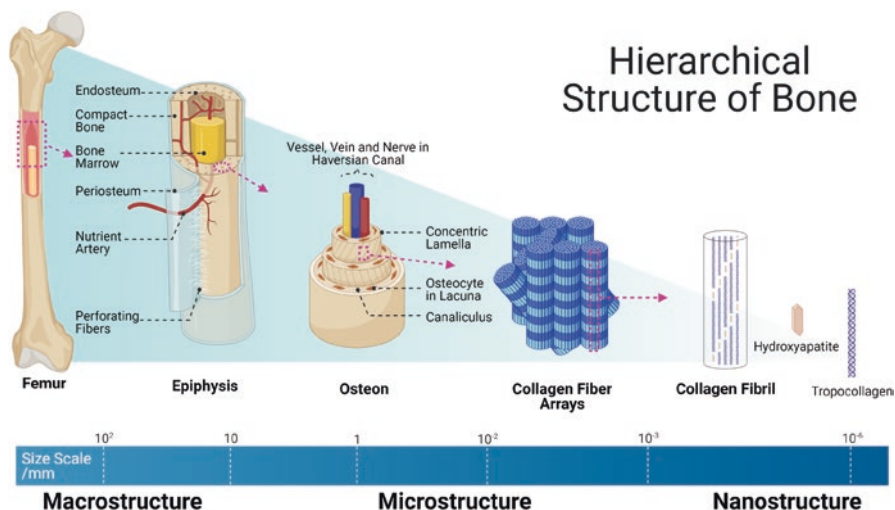


Fig. 1 Bone tissue is a complex structure consisting of organic and inorganic phases down to the nanoscale. Making up 30% of bone, the organic phase consists of a variety of structural proteins and polysaccharides. The collagen fibrils are the main constituents of the organic phase with ranging between 35 and 60 nm in diameter and up to 1 μm in length. The inorganic phase makes up the remaining 70% of bone and functions as an ion reservoir for Ca, P, Na, and Mg. Additionally, this phase provides stiffness and strength mainly in the form of hydroxyapatite. (Created with [Biorender.com](https://www.biorender.com))

the natural bone extracellular matrix (ECM) [6]. The nanotechnology utilized in these constructs has demonstrated added benefits in stimulating functional tissue due to improved cellular- and protein-level interactions [7] and has provided new avenues to engineer scaffolds with better bioactivity, cytotoxicity, and mechanical properties suitable for bone regeneration.

The purpose of this chapter is to highlight the current developments in BTE with regard to 3D bioprinting and nanotechnology. We will first introduce how 3D bioprinting has been applied in BTE and then examine various nanomaterials that have been utilized for bone regeneration. The combined application of 3D bioprinting and nanotechnology will be discussed in each section.

2 Overview of 3D Bioprinting in Bone Tissue Engineering

Additive manufacturing methods have become a more attractive approach for BTE due to their ability to replicate complex macroscale geometries using patient defect-specific scanning techniques [8]. Another advantage of these techniques is their ability to produce constructs with consistent microscale geometry, which eliminates sample to sample variability that has critical implications for future clinical translation. Additive manufacturing techniques have been available since the 1980s and

have been increasingly utilized in the tissue engineering field to fabricate bone constructs [9].

The three main 3D bioprinting strategies that have been utilized in BTE are stereolithography (SLA), extrusion printing, and inkjet printing [10]. Stereolithography, which utilizes ultraviolet (UV) light beam focused on a bed of liquid photopolymer to print layer-by-layer, is a prevalent 3D printing strategy utilized to create anatomical models to preplan orthopedic and craniofacial surgeries. While many others have utilized this strategy to manufacture biodegradable scaffolds for several decades, numerous challenges associated with SLA printing still remain, such as overcoming the toxic effects of the residual photoinitiators and the negative impact of UV light on cells [11]. In contrast, extrusion printing utilizes pneumatic or mechanical force to extrude the bioink. Due to the ability to print high viscosity bioinks and print high cell densities, extrusion-based printing still remains an attractive printing strategy for BTE [4]. However, distortion of the cell structure post-printing and low resolution of the final printed constructs remain key challenges in building upon extrusion-based printing [12]. The last printing strategy available for BTE involves inkjet printing, which utilizes thermal, piezoelectric, or electromagnetic means to deposit droplets of bioink. While this methodology provides great advantages of high speed, availability, and relatively low cost, there are major challenges involving the lack of precise droplet size and placement and its requirement for low viscosity bioinks with less than ideal mechanical properties for BTE [13]. Earlier studies involving inkjet printers used this strategy as a means to achieve indirect fabrication of the bone scaffold [14]. Nonetheless, more research needs to be done to optimize the printing parameters of inkjet printing for BTE.

All three bioprinting techniques have demonstrated promise in manufacturing BTE scaffolds. Each printing strategy offers advantages and disadvantages in terms of accessibility, cost, and resolution. Therefore, the selection of a particular bioprinting option mostly depends on the specific needs of the user. Chapter “Additive Manufacturing Technologies for Bone Tissue Engineering” provides additional details on various additive manufacturing technologies.

3 Nanomaterials in Bone Tissue Engineering

Extensive research in BTE has revealed that there are numerous physical and biological requirements in designing an ideal bone implant. Since the native bone ECM possess structures that extend down to the nanoscale, nanomaterials have been investigated to help replicate these nanostructures within the bone microenvironment and better control cell behavior. Nanomaterials possess at least one dimension that is less than 100 nm, and they have numerous advantageous traits that their micro-sized counterparts do not possess. These properties range from specific surface characteristics to superior mechanical, electrical, optical, and/or magnetic properties that are oftentimes absent in micro-sized counterparts [5]. When nanomaterials are incorporated into scaffolds, the surfaces obtain nanoscale roughness

and specific surface chemistries, wettability, and surface energies that can mimic the bone ECM [5]. Nanomaterials have demonstrated better osteoblast cell adhesion and proliferation than standard materials [7]. While the underlying mechanisms of cell response on the nanostructures are still being investigated, the unique surface topography provided by these materials plays a large role in modulating bone healing [15]. More specifically, the nanotopography introduced by the nanomaterials have been shown to affect cell adhesion, proliferation, and differentiation behavior and matrix organization [16]. Mechanistically, cell fate is influenced by changes to the surface texture, geometry, spatial position, and height of the scaffold, because these changes all affect the clustering of integrins responsible for signal transduction, development of focal adhesions, and cytoskeletal structure [17]. Additionally, nanostructures further promote protein adsorption to aid the process of cell adhesion on biomaterials [18]. These proteins ultimately help regulate cell attachment and initiate signal transduction within cells to further influence cell migration, proliferation, differentiation, and ultimately tissue formation [19].

In general, nanomaterials are subdivided into nanoparticles, nanofibers, and nanocomposites. Nanoparticles, which are particles with a size less than 100 nm in all three dimensions, have been explored to improve bone healing and provide cellular cues for osteogenesis. Nanoparticles have demonstrated the ability to enhance bone regeneration, prevent infection, and improve the outcome of implant osseointegration [20, 21]. These particles have been commonly utilized as delivery agents for bioactive molecules, cell labeling agents to monitor and target sites of interest, and supplements to improve the overall performance of bone scaffolds [5]. Nanofibers, where only two dimensions are less than 100 nm, are fibers that mimic

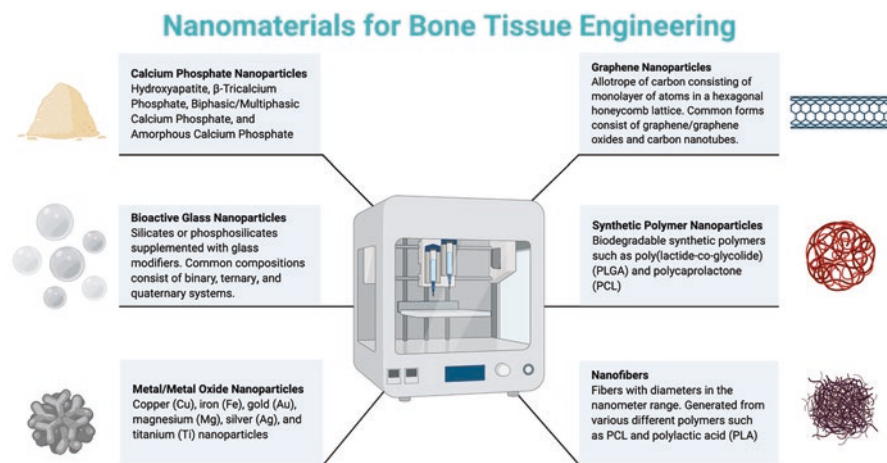


Fig. 2 Various nanomaterials have been utilized for BTE to date, which include calcium phosphates, bioactive glass, metal nanoparticles, graphene, nanofibers, and synthetic polymer nanoparticles. Recent scaffold strategies involving these nanomaterials have tried to enhance a biomaterial response to meet the mechanical and physiological demands of the host bone tissue. (Created with [Biorender.com](https://biorender.com))

the nanofibrous nature of the native ECM and provide the topographical layout to aid cell attachment [18]. Lastly, nanocomposites are composite scaffolds that utilize various combinations of nanomaterials, since bone engineering strategies utilizing only one material have not been able to fulfill the requirements of an ideal bone scaffold. Figure 2 overviews nanomaterials that have been used in BTE to date. More recent strategies have attempted to tailor a biomaterial response that can meet the mechanical and physiological demands of the host tissue capitalizing on the beneficial properties of multiple materials. The properties of specific nanomaterials in BTE and how each are incorporated into bone bioprinting will be discussed in the following subsections.

3.1 Calcium Phosphate Nanoparticles

Calcium phosphates have been extensively utilized in BTE. Table 1 summarizes current bone bioprinting studies utilizing calcium phosphate nanoparticles to date. Being composed of calcium and phosphorus ions, these minerals have demonstrated the ability to regulate the bone remodeling process by influencing osteoblast and osteoclast differentiation [48, 49]. Additionally, controlling the surface properties and porosity of calcium phosphates have also been shown to influence protein absorption, cell adhesion, and bone mineralization [50]. Depending on the type of calcium phosphate, the bioactivity will vary due to different rates of ion release, solubility, stability, and mechanical strength [51]. As the osteoconductivity and osteoinductivity of calcium phosphates are influenced by physical and chemical properties, numerous types of the mineral have been investigated for BTE applications.

Hydroxyapatite ($\text{Ca}_{10}(\text{PO}_4)_6\text{OH}_2$ or HAp) is a very common form of calcium phosphate used in BTE applications. HAp crystals make up the inorganic phase of bone, which forms needle-like 20–60 nm crystals and can be harvested from bone [52]. Various studies have established that HAp is the most stable calcium phosphate with low solubility in physiological conditions [53]. Additionally, HAp has demonstrated good biocompatibility since it does not induce an inflammatory reaction when utilized clinically [54]. The surface of HAp particles can serve as nucleating site for bone minerals in body fluids [55]. While HAp is inherently osteoconductive, additional ions such as fluoride, chloride, and carbonate ions have been incorporated to make these minerals more osteoinductive [56, 57]. Numerous studies have demonstrated the potential for HAp to improve *in vivo* bone regeneration through increased mesenchymal stem cell proliferation, due to better osteoblast adhesion, and enhanced differentiation [58].

More recent studies have demonstrated that nanohydroxyapatite (nHAp) enhances the performance of engineered scaffolds with respect to its microscale counterpart. Since the morphology of nHAp inherently leads to a greater surface area compared to micro-HAp, these nanoparticles can be densely packed as the scaffolds are fabricated [59], which significantly improves the mechanical

Table 1 Bone bioprinting with calcium phosphate nanoparticles

Study type	Calcium phosphate type	Additional constituents	Printing method	Observations	References
In vitro	Amorphous calcium phosphate	rhBMP-2	Extrusion (cryogenic 3D printing)	<ul style="list-style-type: none"> – Improved cell viability – Increased attachment, proliferation, and differentiation 	Wang et al. [22]
In vitro	β -TCP	Silver nanoparticles (AgNP)	Extrusion	<ul style="list-style-type: none"> – Constructs displayed well-defined morphology and mechanical properties suitable for bone implants – Incorporating AgNPs helped improve mechanical properties, biocompatibility, and bactericidal activity 	Correia et al. [23]
In vitro In vivo (rabbit)	β -TCP		Robocasting	<ul style="list-style-type: none"> – No immunogenicity – Increased bone formation 	Tovar et al. [24]
In vitro In vivo (rat)	β -TCP	<ul style="list-style-type: none"> – 2D black phosphorus (BP) nanosheets – P24 peptide – Doxorubicin (DOX) 	Extrusion (cryogenic 3D printing)	<ul style="list-style-type: none"> – Nanocomposites hierarchically porous and mechanically strong – Observed prompt tumor ablation and long-term suppression of tumor recurrence – BP nanosheets could control the long-term toxicity of released DOX 	Wang et al. [25]
In vitro	β -TCP	Silver nanoparticle-graphene oxide nanocomposite (Ag@GO)	Extrusion	<ul style="list-style-type: none"> – Presented excellent antibacterial activity – Accelerated osteogenic differentiation and increased osteogenic gene expression 	Zhang et al. [26]
In vitro In vivo (rabbit)	Biphasic calcium phosphate (BCP)	Platelet-rich fibrin (PRF)	Extrusion	<ul style="list-style-type: none"> – Sustained release of bioactive factors – Improve biocompatibility and bioactivity – Induced greater bone formation than BCP/PVA scaffolds 	Song et al. [27]

Study type	Calcium phosphate type	Additional constituents	Printing method	Observations	References
In vitro	Citrate-HAp	Minocycline	Fused deposition modeling	<ul style="list-style-type: none"> – Uniform macroporosity, adequate wettability and excellent compressive strength – Citrate-HA stimulated adhesion, proliferation and differentiation – Antimicrobial 	Martin et al. [28]
In vitro	Mineral-substituted HAp (Mg-HAp)		Extrusion	<ul style="list-style-type: none"> – Scaffolds smoother than HAp scaffolds – More acidic conditions due to Mg ion release – Higher cell attachment, proliferation, and increased osteogenic gene expression 	Chen et al. [29]
In vitro In vivo (rabbit)	Mineral-substituted HAp (Sr-HAp)		Extrusion	<ul style="list-style-type: none"> – Enhanced cell adhesion, proliferation and ALP activity 	Luo et al. [30]
In vitro	nHAp	Compatibilized MgF ₂ (cMgF ₂) nanoparticle	Extrusion	<ul style="list-style-type: none"> – Stimulated more bone formation – Enhanced mechanical and biological properties – Improved osteogenic differentiation and stimulated mineralization 	Bas et al. [31]
In vitro	nHAp	Core-shell PLGA/TGF-β1 nanospheres	SLA	<ul style="list-style-type: none"> – Fabricated highly interconnected osteochondral scaffold with hierarchical structure and spatiotemporal bioactive factor gradients – Improved hMSC adhesion, proliferation, and directed osteochondral differentiation 	Castro et al. [32]

(continued)

Table 1 (continued)

Study type	Calcium phosphate type	Additional constituents	Printing method	Observations	References
In vitro	nHAp	Chitosan/sodium hyaluronate (CS/SH) coating	Extrusion	<ul style="list-style-type: none"> - Decreased swelling ratio - Increased compressive strength - Slow degradation - Successful loading and release of growth factors 	Chen et al. [33]
In vitro In vivo (rabbit)	nHAp	<ul style="list-style-type: none"> - Vancomycin - Levofloxacin 	Fused deposition modeling	<ul style="list-style-type: none"> - Ability to load and release vancomycin and levofloxacin for antibacterial effect - Demonstrate osteogenic and osteoconductive potential 	Chen et al. [34]
In vitro	nHAp		Extrusion	<ul style="list-style-type: none"> - Higher elastic moduli - Improved mechanical properties - More bioactive 	Demirtas et al. [35]
In vitro In vivo (rabbit)	nHAp	rhBMP-2/chitosan nano-sustained release carrier	Extrusion	<ul style="list-style-type: none"> - Exhibited early burst and controlled release of rhBMP-2 - Biocompatible and induced osteogenic effect - Successful bone repair in rabbit mandible 	Deng et al. [36]
In vitro	nHAp	Bioactive glass	Thermal inkjet printing	<ul style="list-style-type: none"> - HAp scaffolds more effective for cell viability, increased compressive modulus, and hMSC osteogenesis than bioactive glass scaffolds 	Gao et al. [37]
In vitro	nHAp	Carbon nanotubes (CNT)	Extrusion	<ul style="list-style-type: none"> - CNT scaffold with 2 wt% offers the best combination of mechanical properties and electrical conductivity - Scaffold demonstrated typical HAp bioactivity and cell adhesion/proliferation behavior 	Goncalves et al. [38]

Study type	Calcium phosphate type	Additional constituents	Printing method	Observations	References
In vitro	nHAp		Extrusion	<ul style="list-style-type: none"> - Adequate mechanic strength and elastic behavior - Flow properties similar to native blood vessels - Enhanced hMSC adhesion, proliferation, and differentiation 	Holmes et al. [39]
In vitro	nHAp		Extrusion with thermally induced phase separation (TIPS)	<ul style="list-style-type: none"> - Fabricated a large-dimension nanofibrous scaffold with defined architecture - Enhanced fibronectin absorption, hMSC adhesion, and osteogenic differentiation 	Prasophum et al. [40]
In vitro In vivo (rabbit)	nHAp		Extrusion	<ul style="list-style-type: none"> - Observed uniform sonocoated nHAp layer of 200–300 nm - Stimulation of new bone tissue formation 	Rogowska-Tyiman et al. [41]
In vitro	nHAp	<ul style="list-style-type: none"> - MgO nanoparticle - O₂ and N₂ plasma treatment 	Extrusion	<ul style="list-style-type: none"> - Enhanced adhesion, proliferation, and differentiation of preosteoblast cells - Plasma treatment also affected behavior of cells due to changes in surface morphology/chemistry 	Roh et al. [42]
In vitro	nHAp		Extrusion	<ul style="list-style-type: none"> - Fabricated scaffolds with well-defined layers with interconnected pores - Scaffolds exhibited a controlled HAp gradient 	Trachtenberg et al. [43]

(continued)

Table 1 (continued)

Study type	Calcium phosphate type	Additional constituents	Printing method	Observations	References
In vitro In vivo (rat)	nHAp	Atstrin	Extrusion	<ul style="list-style-type: none"> – Scaffold exhibits precise structure – Sustained release of atstrin – Minimal cytotoxicity and supports cell adhesion – Enhanced bone regeneration 	Wang et al. [44]
In vitro	nHAp (modified with dopamine and hexamethylenediamine)		Extrusion	<ul style="list-style-type: none"> – Robust mechanical properties – Good biocompatibility – Support proliferation and osteogenic differentiation 	Yang et al. [45]
In vitro	nHAp		Extrusion	<ul style="list-style-type: none"> – Increased ALP activity and mineralization – Improved preosteoblast proliferation and differentiation 	Yu et al. [46]
In vitro	nHAp	TGF- β 1 PLGA nanoparticle	SLA	<ul style="list-style-type: none"> – Promoted osteogenic and chondrogenic differentiation – Enhanced osteogenic and chondrogenic gene expression 	Zhou et al. [47]

properties of the scaffold [60]. Additionally, the increased surface area of nHAp drastically improves protein adsorption capabilities compared to larger HAp particles [61]. Synthesized nHAp can be fabricated as rods, fibers, or particulates due to the different modes of synthesis [62, 63]. Since nHAp is very similar to native bone in terms of size and chemistry, it has firmly established itself as a favorable material for BTE.

Research has demonstrated that nanohydroxyapatite can be successfully incorporated into bone bioprinting strategies. The most prevalent approach involves adding nHAp to synthetic polymer such as polycaprolactone (PCL) [39]. While some groups resorted to coating the scaffold surface with nHAp post-printing, others have successfully mixed the nHAp particles directly into the bioink formulation for extrusion printing. Trachtenberg et al. utilized an extrusion-based printing strategy to develop poly(propylene fumarate) (PPF) scaffolds with a mineral gradient within the scaffold (Fig. 3) [43]. In order to improve the dispersion of the nHAp particles within the scaffold, a surfactant was added to the print formulation without compromising the compressive strength overall. The printed PPF composite scaffolds with nHAp nanoparticles consisted of well-defined layers with interconnected pores that could potentially serve as mechanically robust bone implants. Few groups have proceeded on to functionalize scaffolds with even more constituents to create complex

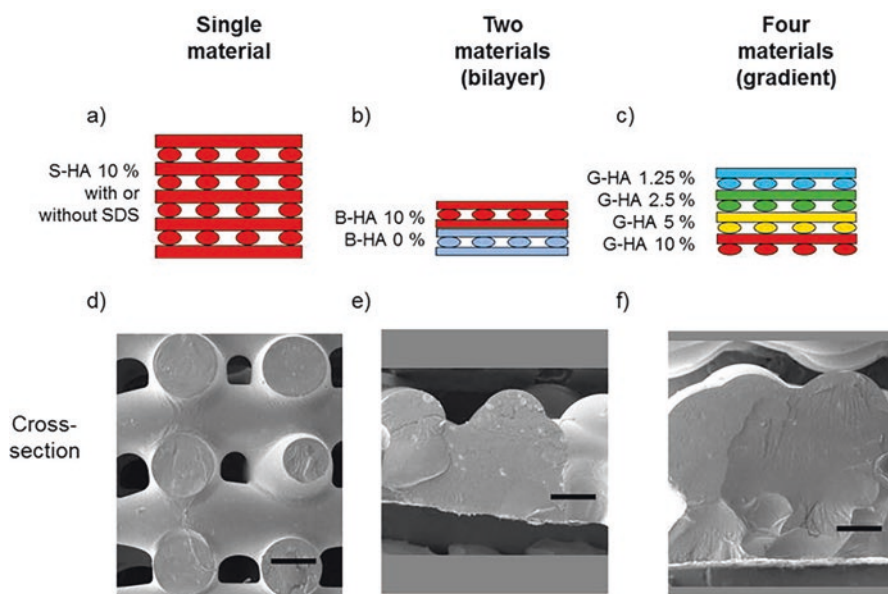


Fig. 3 Schematic of printed scaffolds. (a) PPF-HA (10 wt%) scaffold with or without SDS. (b) PPF-HA bilayer scaffold containing PPF and PPF-HA (10 wt%). (c) PPF-HA gradient scaffold containing layers of 1.25, 2.5, 5, and 10 wt% HA. Respective SEM cross-sections of (d) a PPF-HA scaffold with or without SDS, (e) a PPF-HA bilayer scaffold, and (f) a PPF-HA gradient scaffold. Pore interconnectivity is lost with the addition of multiple materials. Scale bars in (d–f) represent 0.5 mm. (Reprinted by permission of the publisher (Taylor & Francis Ltd.) [43])

multiphase scaffolds. Deng et al. recently fabricated poly(lactic-*co*-glycolic) acid (PLGA)/nHAp/chitosan (CS)/rhBMP-2 scaffolds with an extrusion printer [36]. CS nanospheres encapsulating rhBMP-2 were embedded within a CS hydrogel to prepare a nano-sustained release carrier, which was then co-printed with PLGA/nHA bioink to create the composite scaffold. The scaffold complex demonstrated an effective controlled burst release of rhBMP-2 that further aided in osteogenesis within mandibular bone defects. Others have loaded antibiotics within these composite scaffolds to introduce an antibacterial effect with good results [28].

Some groups have explored the use of hydrogel incorporated with nHAp for bone bioprinting. Wang et al. 3D printed alginate/nHAp scaffolds incorporated with atsttrin, which is a progranulin-derived engineered protein that exerts an antagonistic effect on proinflammatory TNF- α [44]. This composite scaffold was able to demonstrate sustained release of the atsttrin that enhanced the bone regeneration within a mouse calvarial defect. Another group successfully printed chitosan/nHAp scaffolds that had superior cell proliferation and differentiation capabilities compared to alginate-based scaffolds [35]. However, hydrogels are still challenging to use as a bone scaffold due to inadequate mechanical properties. In order to enhance the mechanical and bioactive properties of hydrogel scaffolds, Chen et al. extrusion printed with a bioink formulation consisting of 60% nHAp particles and 40% gelatin/hyaluronate hydrogel [33]. These scaffolds were lyophilized and then coated with multiple layers of chitosan and sodium hyaluronate, which significantly helped improve the compressive strength and ability to load growth factors onto the scaffold surface.

Tricalcium phosphate ($\text{Ca}_3(\text{PO}_4)_2$ or TCP) is another common calcium phosphate utilized in bone regeneration other than HAp [51]. While two phases of TCP exist, β -TCP is generally used in bone regeneration due to its more stable structure and higher biodegradation rate [64]. Additionally, β -TCP degrades faster and is more highly soluble than HAp, which leads to a higher resorption rate and increase biocompatibility [65]. β -TCP also promotes proliferation of osteoprogenitor cells due to its inherent nanoporous structure that enables excellent biomineralization and cell adhesion [66]. Therefore, numerous groups have utilized β -TCP as the main additive for bone bioprinting. Tovar et al. successfully robocasted 100% β -TCP scaffolds that were biocompatible, resorbable, and could anisotropically regenerate bone within a rabbit model [24]. Additionally, Wang et al. fabricated a complex β -TCP/PLGA scaffold with a novel cryogenic 3D printer involving water-in-oil polyester emulsion inks with multiple functional agents—2D black phosphorus nanosheets, doxorubicin hydrochloride, and BMP-2-like osteogenic peptide (P24) [25]. The group was able to print hierarchically porous and mechanically strong scaffolds that can be potentially applied for large defect repair.

Lastly, calcium phosphates with variable compositions have also been utilized during bone bioprinting. To capitalize on the beneficial properties of both nHAp and β -TCP, some groups have utilized biphasic calcium phosphate within bone-engineered scaffolds. Biphasic or multiphasic calcium phosphates are homogeneously mixed at the submicron level to make the separation of each constituent difficult [67]. Song et al. used low-temperature robocasting to fabricate a 3D printed

ceramic scaffold composed of nano-biphasic calcium phosphate, polyvinyl alcohol, and platelet-rich fibrin [27]. Without the addition of toxic chemicals during the printing process, the group demonstrated that these composite scaffold could be printed with the desired internal and external architecture while enhancing bone defect repair with the incorporated bioactive factors. Also possessing intermediate properties, amorphous calcium phosphate ($\text{Ca}_3(\text{PO}_4)_2 \cdot n\text{H}_2\text{O}$) is a less-ordered, transition phase calcium phosphate that serves as a precursor state that precedes biological apatite formation [68]. Since the mineral in natural bone is composed of poorly crystalline, highly substituted apatite nanocrystals interspersed within a collagen matrix, one potential bone regenerative strategy is to deposit a less ordered mineral phase to mimic the biomineralization process [55]. Wang et al. demonstrated that PLA scaffolds loaded with amorphous calcium phosphate nanoparticles with rhBMP-2 could improve cell viability, attachment, proliferation, and differentiation for BTE applications [22].

3.2 *Bioactive Glass Nanoparticles*

Bioactive glass nanoparticles (BGNP) are another class of ceramic nanoparticles that are commonly used in bone regeneration due to their high bioactivity and great bone bonding properties [69]. BGNPs are generally comprised of silicates or phosphosilicates supplemented with distinct proportions of glass modifiers like sodium oxide (Na_2O) and calcium oxide (CaO) [69]. The common compositions of BGNPs are binary (e.g., $\text{SiO}_2\text{-CaO}$), ternary (e.g., $\text{SiO}_2\text{-CaO-P}_2\text{O}_5$), or quaternary systems (e.g., $\text{SiO}_2\text{-CaO-P}_2\text{O}_5\text{-Na}_2\text{O}$), which in turn affects the porous structure and surface area of the BGNPs [70–72]. Most BGNPs possess a spherical morphology, but non-spherical BGNPs have also been generated in the form of pineal or rod shapes [73, 74]. Some reports have indicated that spherical nanoparticles may be taken up by the cell more quickly and efficiently than non-spherical nanoparticles [75]. However, non-spherical nanoparticles present a more biomimetic morphology analogous to the natural HAp structural units, which can ultimately improve the mechanical properties and biomineralization capability more ideal for bone scaffolds [76].

Decreasing the dimensions of the bioactive glass particles down to the nanoscale increases the specific surface area, pore size, and ion exchange capabilities compared to bioactive glass microparticles [77]. In effect, BGNPs are able to generate a calcium phosphate layer more quickly due to improved exposure to the bioactive elements. Ajita et al. highlighted how nanoscale bioactive glass particles could affect the proliferative behavior in mouse MSCs [78]. The group demonstrated that all BGNPs administered at 20 mg/mL showed no cytotoxic effect, but the cells treated with smallest nanoparticles (37 nm) experienced the greatest increase in cell proliferation. The faster ion release rate and the increased surface area improve protein adsorption, which in turn promote cell adhesion, proliferation, and differentiation. Some studies have indicated that calcium silicate exhibits better

Table 2 Bone bioprinting with bioactive glass nanoparticles

Study type	Calcium phosphate	Additional constituents	Printing method	Observations	References
In vitro	Bioactive glass (SiO ₂ -CaO-P ₂ O ₅ with weight ratio 80:15:5)	Poly(citrate-siloxane) (PCS)	Extrusion	<ul style="list-style-type: none"> -Scaffolds with BG-PCS presented superior elasticity and superior compressive strength -Controlled release of Si and Ca ions and enhanced biomineralization -Promoted cell attachment, proliferation, and enhanced osteogenic differentiation 	Chen et al. [80]
In vitro In vivo (mouse)	Bioactive glass (SiO ₂ -CaO-P ₂ O ₅ with weight ratio 70:25:2.5)	CuFeSe ₂ nanocrystals (CFS)	Extrusion	<ul style="list-style-type: none"> -Varying the concentration of the CF crystals and laser power density helped regulate photothermal performance of scaffold -BG-CFS scaffolds could stimulate osteogenic gene expression and new bone formation 	Dang et al. [81]
In vitro	Bioactive glass (bioglass 45S5 or SiO ₂ -CaO-Na ₂ O-P ₂ O ₅ with weight ratio 45:24.5:24.5:6)	nHAp	Thermal inkjet printing	<ul style="list-style-type: none"> -HAp scaffolds more effective for cell viability, increased compressive modulus, and hMSC osteogenesis than bioactive glass scaffolds 	Gao et al. [82]
In vitro	Bioactive glass (SiO ₂ -B ₂ O ₃ -CaO-Na ₂ O-P ₂ O ₅ -MgO-SrO with weight ratio 47.12:6.73:6.77:22.66:1.72:5:10)	Wood-based nanocellulose (CNF)	Extrusion	<ul style="list-style-type: none"> -Cells less viable and proliferative in BG bioinks -Constant increase in ALP activity observed in all hydrogels -hBMSC tolerated bioprinting process better than Saos-2 cells 	Ojansivu et al. [83]

Study type	Calcium phosphate	Additional constituents	Printing method	Observations	References
In vitro In vivo (mouse)	Bioactive glass (SiO ₂ -CaO-P ₂ O ₅ with weight ratio 80:15:5)	Mesoporous silica nanosphere (MSN) - Isoniazid - Rifampin	Extrusion	<ul style="list-style-type: none"> - Scaffolds demonstrated prolonged drug release - Displayed good osteogenic potential 	Zhu et al. [84]
In vitro	Laponite®		Extrusion	<ul style="list-style-type: none"> - Improved stability at physiological conditions - No change in mechanical stiffness - Improved bioactivity, hMSC proliferation, and differentiation 	Carrow et al. [85]
In vitro Ex vivo (chick chorioallantoic membrane)	Laponite®		Extrusion	<ul style="list-style-type: none"> - Scaffold displayed enhanced shape retention and interconnected porosity - Improves hBMSC viability, attachment, proliferation, and differentiation - Scaffold supports cell growth and retention/delivery of growth factors 	Cidonio et al. [86]
In vitro Ex vivo (chick chorioallantoic membrane)	Laponite®		Extrusion	<ul style="list-style-type: none"> - Significant potential in printing fidelity, tailorable swelling characteristics, and enhanced shape retention - Laponite increased cell-laden bioink functionality - Absorption/release properties depended on Laponite incorporation 	Cidonio et al. [87]
In vitro Ex vivo (chick chorioallantoic membrane) In vivo (mouse)	Laponite®	- BMP-2 - VEGF	Extrusion	<ul style="list-style-type: none"> - Demonstrated elevated viability and functionality in vitro, ex vivo, and in vivo 	Cidonio et al. [88]

(continued)

Table 2 (continued)

Study type	Calcium phosphate	Additional constituents	Printing method	Observations	References
In vitro In vivo (rat)	Laponite®		Extrusion	<ul style="list-style-type: none"> – Demonstrated improved proliferation and differentiation than PEG-clay scaffolds – Scaffold possesses excellent osteogenic potential 	Zhai et al. [89]
In vitro	Polydopamine-modified calcium silicate (CaO-SiO ₂ -Al ₂ O ₃ -ZnO with weight ratio 65:25:5:5)		Extrusion	<ul style="list-style-type: none"> – PDACS/PCL experienced more cell attachment and proliferation due to improved hydrophilicity – Scaffolds showed increased osteogenic and angiogenic potential 	Chen et al. [79]

biodegradation and osteoconductivity than calcium phosphate, which has led to research adding these powders into the 3D bioprinting process [79].

Various bioactive glass nanoparticles have been explored for bone bioprinting. Table 2 summarizes current bone bioprinting studies utilizing bioactive glass nanoparticles to date. Carrow et al. extrusion-printed bioactive nanocomposites by incorporating 2D nanosilicates into a co-polymer (PEOT/PBT) scaffold [85]. The inclusion of nanosilicates improved the stability and bioactivity of the scaffold under physiological conditions without compromising the mechanical stiffness of the printed scaffold. Laponite nanoclay, a type of nanosilicate similar to hectorite, was also utilized in several different hydrogel nanocomposites to demonstrate improved printability and mechanical stability of the printed constructs, without compromising cell viability and distribution [86–89]. Current research has demonstrated that these nanoparticles possess a versatile ability to functionalize additional components onto their surface. Luo et al. integrated the adhesion peptide (RGD sequence) onto mesoporous silica nanoparticles to dually functionalize bone forming peptide-1 [90]. This dual-peptide-loaded alginate hydrogel system promoted the sequential differentiation of hMSCs. Some groups have also succeeded in functionalizing photothermal or photoluminescent components onto these nanoparticles, opening up the possibility of utilizing them for bioimaging, tumor therapy, and bone regeneration applications [80, 81]. Lastly, few groups have begun to develop ternary nanocomposites with additional biopolymers to supplement more bioactivity, mechanical advantages, and cell attachment potential within the printed construct [83, 91].

3.3 *Metal and Metal Oxide Nanoparticles*

Metals have been widely explored as a material to replace bone tissue, primarily because of their strong mechanical properties to withstand physiological forces experienced by bone. While most research into the area has utilized metals as the major implant component, recent studies have demonstrated the potential of utilizing metal nanoparticles to enhance the bioactivity of the implants.

Titanium-Based Nanoparticles

Titanium and its alloys are some of the most explored metals to date due to their ideal mechanical properties, resistance to corrosion, and no cytotoxic effect when implanted in the body [92]. Therefore, titanium-based implants are often utilized to repair critical-sized bone defects [93]. Some studies have begun to investigate composite scaffolds that incorporate titanium nanoparticles for bone regeneration. Rasoulianboroujeni et al. recently printed a nanocomposite scaffold, comprised of PLGA and TiO₂ nanoparticles with an extrusion printer [94]. Incorporation of the nanoparticles improved the compressive modulus of the scaffolds, enhanced the

wettability of the scaffold surface, and increased osteogenic proliferation and mineralization. Another group fabricated a hybrid polymer (Ormocomp[®]) scaffold doped with barium titanite (BaTiO₃) nanoparticles via two photon lithography [95]. Preliminary in vitro testing demonstrated enhanced cell differentiation due to the refined architecture generated and the piezoelectric cues from this printing strategy.

Magnesium-Based Nanoparticles

Magnesium has been explored in bone bioprinting since it is biocompatible, regulates the density and structure of bone apatite, and mediates cell–ECM interactions [96]. Roh et al. utilized magnesium oxide (MgO) nanoparticles as a bioink additive during extrusion printing [42]. A composite scaffold comprised of PCL, HAp, and MGO contributed to enhanced adhesion, proliferation, and differentiation of cells within the scaffold. Another group developed a ternary nanocomposite consisting of PCL, nHA powder, and compatibilized magnesium fluoride nanoparticle (cMgF₂) fillers with enhanced mechanical and biological properties through extrusion printing [31]. The incorporation of cMgF₂ nanoparticles particularly led to significant improvements in the mechanical properties within the scaffolds, enhanced osteogenic differentiation, and stimulated mineralization.

Metal Nanoparticles with Antimicrobial Properties

Chronic implant-related bone infections are a major problem in orthopedic and trauma-related surgery with serious consequences that can affect the final prognosis of bone implants [97]. As a result, silver nanoparticles (AgNP) with antimicrobial properties have been incorporated into 3D printed bone scaffolds. Jia et al. demonstrated that the addition of silver nanoparticles on titanium alloy meshes helped reduce bacterial biofilm buildup, especially in combination with antibiotic therapy [98]. Silver nanoparticles have also been incorporated into extrusion printed ceramic/polymer scaffolds, further establishing their potential to enhance biocompatibility, mechanical properties, and osteogenic activity [26, 99]. Besides AgNPs, several other metal nanoparticles with antimicrobial properties have been investigated with bone bioprinting. Zou et al. recently incorporated copper-loaded-ZIF-8 nanoparticles within PLGA scaffolds through extrusion printing and found that these scaffolds possessed enhanced antibacterial and osteoconductive properties [100]. Additionally, 3D printed zirconia ceramic hip joints with a coating of ZnO nanoparticles also demonstrated antibacterial properties while maintaining the benefits of precise structure and wear resistance [101].

Iron-Based Nanoparticles

Iron oxide (Fe_2O_3) nanoparticles, being in the ferrimagnetic class of magnetic materials, have various preclinical and therapeutic uses [102]. On top of retaining the bioactivity of nanomaterials, magnetic iron nanoparticles are able to directionally aggregate and localize under a constant magnetic field. Consequently, iron oxide nanoparticles can couple to the cell surface and control cell functions such as MSC differentiation [103]. Huang et al. developed a novel diphasic magnetic nanocomposite scaffold utilizing low-temperature deposition manufacturing [104]. These scaffolds demonstrated good biocompatibility and mechanical properties, while also promoting cell differentiation. Another group incorporated presynthesized iron oxide nanoparticles into polyamide scaffolds fabricated on a selective laser sintering (SLS) printer [105]. These nanoparticles demonstrated the ability to heat up rapidly in response to an applied AC magnetic field, offering a potential avenue to remotely induce controlled gene expression within cells on these scaffolds. At the very least, iron oxide nanoparticles possess osteogenic and radiopaque properties that can be used to develop biodegradable and radiographically detectable bone implants that can aid in diagnostics and bone healing [106].

Gold-Based Nanoparticles

One nanoparticle that has not been fully utilized in bone bioprinting are gold nanoparticles (AuNPs), which have become a promising tool in nanomedicine due to their nanoscale dimensions, ease of preparation, high surface area, and functionalization capability [107]. Therefore, some groups have investigated how AuNPs can promote osteogenic differentiation in stem cells. Choi et al. demonstrated that chitosan-conjugated AuNPs increase the calcium content and osteogenic gene expression at non-toxic concentration through the Wnt/ β -catenin signaling pathway. The particle size also appears to play a role in MSC differentiation, as 30 and 40 nm AuNPs were taken up by the MSCs, the most and consequently demonstrated the highest cell differentiation rates [108]. Some groups have explored functionalizing AuNPs to influence the MSC behavior. Li et al. functionalized gold nanoparticles with various chemical groups to find that amino-functionalized AuNPs exhibited increased ALP expression and matrix mineralization [109]. AuNPs can also serve as a suitable protein or peptide delivery mechanism, as Schwab et al. were able to assess the impact of surface immobilized BMP-2 on the Smad signaling pathway with these particles [110]. The group utilized nanolithography to create a precisely spaced, tunable gold nanoparticle array embedded with single BMP-2 molecules. Compared to the control condition consisting of soluble BMP-2, the AuNP-immobilized BMP-2 demonstrated a prolonged and elevated intracellular signal transduction that could help upregulate the TGF β superfamily growth factors to further stimulate bone regeneration.

3.4 Graphene Nanomaterials

Graphene is a novel nanomaterial that has potential applications for BTE. With exceptional conductivity and physiochemical and mechanical properties, these thin carbon sheets with large surface area can significantly improve the properties of the composite at minute concentrations. Graphene has an aromatic configuration that been reported to promote cell attachment, growth, proliferation, and differentiation [111]. Choe et al. utilized an extrusion printer to fabricate alginate/graphene oxide (GO) composites to improve the printability, structural stability, and osteogenic potential of scaffolds [112]. This bioink formulation demonstrated high printability and stability and was able to maintain high cell viability and stimulate osteogenic differentiation. Another study printed polylactic acid (PLA) scaffolds incorporated with GO using fused deposition modeling (FDM) printer [113]. The addition of GO increased the surface roughness, hydrophilicity, and mechanical properties of the PLA/GO scaffolds. Additionally, the PLA/GO scaffolds proved to be more biocompatible and promoted cell proliferation and mineralization more efficiently than pure PLA scaffolds.

Some researchers have also incorporated carbon nanotubes (CNT) into bone tissue regeneration. CNTs are a variation of a single graphene sheet that is rolled up into a hollow cylindrical nanostructure and are commonly divided into either single-walled carbon nanotubes (SWCNT) or multi-walled carbon nanotubes (MWCNT) [114]. SWCNTs are formed from a single tubular graphene while MWCNTs consist of multiple concentric tubular graphene layers. Their unique nanoscale cylindrical shape makes them capable delivery agents for various biomolecules and drugs [115]. CNTs offer great strength, elasticity and fatigue resistance that can help reinforce composite scaffolds for bone regeneration [116]. With enhanced mechanical properties, CNTs are able to create a strong bond on composite scaffolds that facilitates load transfer and strengthens the scaffold matrix [117]. Additionally, CNTs are more conducive to protein adsorption and cell attachment due to their high specific surface area resulting from their highly porous structure [118, 119]. This porous interlinked nanostructure is favorable for nutrient transport throughout the bone matrix. CNTs can also influence cell morphology and promote osteogenesis with modifications to their surface chemistry and affinity for cell-binding proteins [120].

Recent studies have examined how CNTs can be incorporated into the bioprinting process. Huang et al. fabricated a porous PCL/MWCNT composite scaffold utilizing an extrusion printer (Fig. 4) [121]. The addition of the MWCNT improved protein adsorption, mechanical and biological properties of the scaffolds, indicating that these composite scaffolds can be a viable candidate for bone tissue regeneration. Another group similarly developed a three-phase nanocomposite scaffold with nHAp, CNTs, and PCL via extrusion printing [38]. They also found that the composite scaffolds demonstrated typical bioactivity, good cell adhesion, and

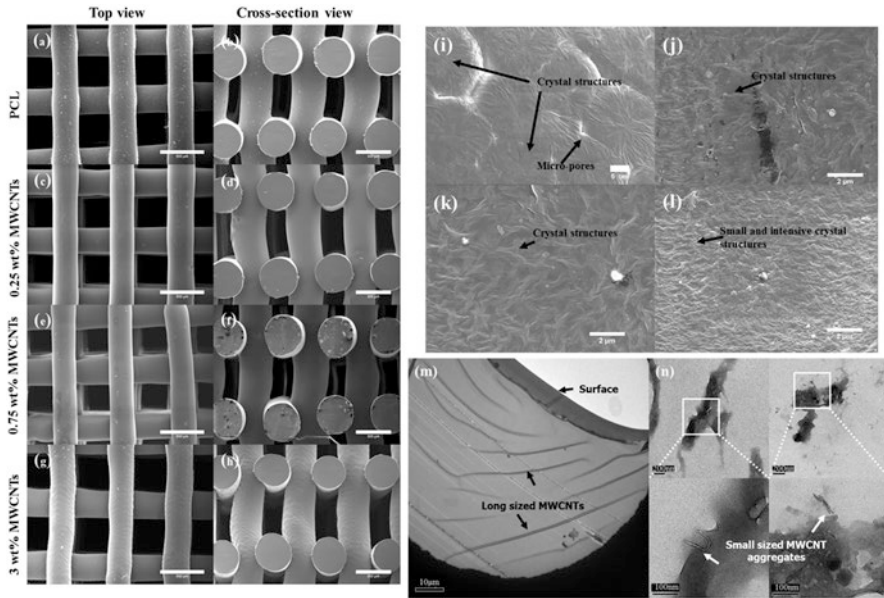


Fig. 4 SEM images of (a) top view and (b) cross-section view of PCL scaffold, (c) top view and (d) cross-section view of PCL/MWCNT 0.25 wt% scaffold, (e) top view and (f) cross-section view of PCL/MWCNT 0.75 wt% scaffold, and (g) top view and (h) cross-section view of PCL/MWCNTs 3 wt% scaffold; High-magnification SEM images showing spherulites in the PCL matrix and boundaries between crystal structures in the filament surface of (i) PCL, (j) 0.25 wt%, (k) 0.75 wt%, and (l) 3 wt% PCL/MWCNT composite scaffolds; TEM images showing (m) the alignment and migration of long-length MWCNTs, (n) the agglomeration of short-length MWCNTs in PCL/MWCNT 3 wt% [121]

proliferation with added mechanical performance and electrical conductivity from CNT. These graphene-based nanocomposites show promise as they help improve the mechanical properties and cytocompatibility within scaffolds. However, more work is being done to effectively synthesize these novel CNT-based nanocomposites. Liu et al. were able to effectively print PPF scaffolds with negatively charged CNT/ssDNA nanocomplexes through stereolithography [122]. Their rapid and homogenous functionalization process helped coat the scaffold surface to promote adhesion, proliferation, and differentiation of the cells. Another group explored incorporating carbon nanotubes within a hydrogel [123]. Utilizing a polyion complex composed of poly(sodium *p*-styrene sulfonate) and poly(3-(methacryloylamino) propyl triethylammonium), a tough hydrogel with MWCNT was formulated to manufacture 3D scaffolds via extrusion printing. These composite scaffolds demonstrated biocompatibility and facilitated osteogenic differentiation, suggesting that hydrogels with CNTs can be used to enhance the efficiency of bone repair.

3.5 *Synthetic Polymer Nanoparticles*

Biodegradable synthetic polymers have been among the most investigated polymers due to good biocompatibility, mechanical properties, and rates of degradation that are comparable to the bone turnover rate [124]. Synthetic polymer nanoparticles have garnered much interest as a drug delivery mechanism because they have controlled degradability and have shown the potential to deliver small molecules, nucleic acids, and proteins [125, 126]. These nanoparticles are superior to conventional drug delivery mechanisms because they are more readily available, can undergo controlled release over a longer duration of time, and minimize undesirable effects such as toxicity and immunogenicity [127].

Past research has demonstrated that PLGA nanoparticles can maintain a sustained release of BMP-2 to support bone healing in vivo [128]. Kim et al. investigated the performance of a 3D-printed calcium phosphate scaffold coated with a layer of PLGA nanoparticles loaded with BMP-2 [129]. The group was able to achieve a uniform distribution of the nanoparticles and a gradual release of BMP-2. Additionally, higher de novo bone formation was observed in vivo. However, there are limited studies that have directly incorporated the polymer nanoparticles into the 3D printing process. Another study fabricated novel biphasic nanocomposite scaffolds for osteochondral regeneration that incorporated nHAp and TGF- β 1-loaded PLGA nanoparticles through stereolithography [32]. These scaffolds demonstrated that a biomimetic graded construct could be printed with hydrogels and offers a strategy to develop an implant for orthopedic application.

3.6 *Nanofibers*

Nanofibers are a valuable tool in tissue engineering for their ability to simulate the physical and biochemical environment of the natural bone ECM. Several strategies have been utilized to produce nanofibers, including phase separation and self-assembly [130, 131]. The most ubiquitous fabrication method to produce nanofibers is electrospinning, which controls the extrusion of the polymer fibers through the use of an electric field [132]. Yao et al. recently fabricated 3D nanofibrous scaffolds utilizing solely electrospinning [133]. The group demonstrated that PCL/PLA nanofibrous scaffolds, with respect to neat PCL scaffolds, possessed greater mechanical properties while enhancing cell viability of hMSCs and osteogenic differentiation in vitro and in vivo. The improved performance of the copolymer nanofibrous scaffold was noted to be attributed to the higher mechanical stiffness and bioactivity introduced by PLA itself. However, since the densely packed nanofibers lead to a distinctly smaller pore space, tissue ingrowth can be negatively affected within these scaffolds [134]. Additionally, the mechanical performance of nanofibrous scaffolds are poorer in comparison to other tissue-engineered constructs due to their large surface area-to-volume ratios and high porosities [135].

An alternative strategy is to incorporate both electrospinning and extrusion printing into the scaffold fabrication process. Since extrusion printed scaffolds often suffer from low print resolution, nanofibers have been infused into the 3D printed scaffold to introduce nanoscale features within the overall construct [136]. Vasquez-Vasquez et al. were able to show that incorporating a PLA nanofiber coating on a PLA scaffold promoted bioactivity, cell attachment, and proliferation when compared to neat PLA scaffolds [137]. Even though both the scaffold and nanofibers were synthesized with the same polymer, the nanotopographical changes introduced by the nanofibers enhanced the overall performance of the tissue construct. Nanofibers can also be functionalized with various bioactive molecules through encapsulation or surface immobilization. Li et al. examined the performance of bioactive glass short nanofibers functionalized with BMP-2 on 3D-printed PCL scaffolds [135]. Immobilizing BMP-2 onto the scaffold surface through nanofibers allowed enhanced osteogenic gene expression of bone marrow MSCs, further demonstrating that expanded applications that can be incorporated into a BTE approach of combining 3D printing and electrospinning.

Few studies have directly incorporated nanofibers directly into the bioink before the printing process. Thermoplastic polymer printing has limitations due to high temperature and pressure that can interfere with the integrity of the print [138]. Therefore, hydrogels have offered a low-temperature printing strategy that bypasses some of the issues associated with synthetic polymer printing. Abouzeid et al. recently demonstrated that alginate/PVA hydrogels can be prepared with bifunctional cellulose nanofibers with reactive carboxyl and aldehyde groups [139]. The 3D printed scaffold was able to demonstrate the ability to mineralize. However, there is still more work to be done to print a hydrogel construct that can withstand physiological load while maintaining precise control over fiber diameter and morphology due to the intrinsic effect of material properties on printing precision and overall scaffold mechanics.

4 Future Outlook and Conclusions

Nanotechnology has provided tissue engineers the ability to mimic native bone ECM and improve the bone regeneration process. Numerous nanomaterials have demonstrated immense potential in bone bioprinting applications since they present nanoscale cues that can positively impact osteogenic attachment and differentiation. Additionally, various nanocomposites have displayed improved mechanical and biological properties in bioprinted bone scaffolds. Many of the scaffolds incorporated with nanoparticles have displayed the capacity to better mimic the complex properties of the natural bone environment that can promote cellular attachment, ingrowth, and bone formation. However, there are still questions regarding the interactions between the nanosurface topography and the osteal defects into which these enhanced scaffolds are introduced. Furthermore, new design strategies and fabrication methods will need to be expanded upon experimentally to be ultimately tailored

for complex bone defect repair treatment in the clinic. Also, large animal model studies that confirm that these scaffolds support vascularization and bone formation in clinically sized defects are still needed. Tissue engineers will need to examine the nanomaterials within structures that best support bone regeneration in a controlled manner. Ultimately, future research will need to overcome current challenges of bone regeneration and expand the multifunctional capabilities of nanomaterials for BTE.

References

1. Li X, Wang L, Fan Y, Feng Q, Cui FZ, Watari F. Nanostructured scaffolds for bone tissue engineering. *J Biomed Mater Res A*. 2013;101(8):2424–35.
2. Lopes D, Martins-Cruz C, Oliveira MB, Mano JF. Bone physiology as inspiration for tissue regenerative therapies. *Biomaterials*. 2018;185:240–75.
3. Nair AK, Gautieri A, Chang SW, Buehler MJ. Molecular mechanics of mineralized collagen fibrils in bone. *Nat Commun*. 2013;4:1724.
4. Gerdes S, Mostafavi A, Ramesh S, Memic A, Rivero IV, Rao P, Tamayol A. Process-structure-quality relationships of three-dimensional printed poly(Caprolactone)-hydroxyapatite scaffolds. *Tissue Eng Part A*. 2020;26(5–6):279–91.
5. Griffin MF, Kalaskar DM, Seifalian A, Butler PE. An update on the application of nanotechnology in bone tissue engineering. *Open Orthop J*. 2016;10:836–48.
6. Sun L, Stout DA, Webster TJ. The nano-effect: improving the long-term prognosis for musculoskeletal implants. *J Long-Term Eff Med Implants*. 2012;22(3):195–209.
7. Gong T, Xie J, Liao J, Zhang T, Lin S, Lin Y. Nanomaterials and bone regeneration. *Bone Res*. 2015;3:15029.
8. Moreno Madrid AP, Vrech SM, Sanchez MA, Rodriguez AP. Advances in additive manufacturing for bone tissue engineering scaffolds. *Mater Sci Eng C Mater Biol Appl*. 2019;100:631–44.
9. Tang D, Tare RS, Yang LY, Williams DF, Ou KL, Oreffo RO. Biofabrication of bone tissue: approaches, challenges and translation for bone regeneration. *Biomaterials*. 2016;83:363–82.
10. Midha S, Dalela M, Sybil D, Patra P, Mohanty S. Advances in three-dimensional bioprinting of bone: progress and challenges. *J Tissue Eng Regen Med*. 2019;13(6):925–45.
11. Rider P, Kacarevic ZP, Alkildani S, Retnasingh S, Schnettler R, Barbeck M. Additive manufacturing for guided bone regeneration: a perspective for alveolar ridge augmentation. *Int J Mol Sci*. 2018;19(11):3308.
12. Nyberg E, Rindone A, Dorafshar A, Grayson WL. Comparison of 3D-printed poly- ϵ -caprolactone scaffolds functionalized with tricalcium phosphate, hydroxyapatite, Bio-Oss, or decellularized bone matrix. *Tissue Eng A*. 2016;23(11–12):503–14.
13. Ashammakhi N, Hasan A, Kaarela O, Byambaa B, Sheikhi A, Gaharwar AK, Khademhosseini A. Advancing frontiers in bone bioprinting. *Adv Healthc Mater*. 2019;8(7):e1801048.
14. Lee JY, Choi B, Wu B, Lee M. Customized biomimetic scaffolds created by indirect three-dimensional printing for tissue engineering. *Biofabrication*. 2013;5(4):045003.
15. Huang J, Gräter SV, Corbellini F, Rinck S, Bock E, Kemkemer R, Kessler H, Ding J, Spatz JP. Impact of order and disorder in RGD nanopatterns on cell adhesion. *Nano Lett*. 2009;9(3):1111–6.
16. Ahn EH, Kim Y, Kshitiz, An SS, Afzal J, Lee S, Kwak M, Suh KY, Kim DH, Levchenko A. Spatial control of adult stem cell fate using nanotopographic cues. *Biomaterials*. 2014;35(8):2401–10.

17. Guilak F, Cohen DM, Estes BT, Gimble JM, Liedtke W, Chen CS. Control of stem cell fate by physical interactions with the extracellular matrix. *Cell Stem Cell*. 2009;5(1):17–26.
18. Chen G, Lv Y. Immobilization and application of electrospun nanofiber scaffold-based growth factor in bone tissue engineering. *Curr Pharm Des*. 2015;21(15):1967–78.
19. Nyberg E, Holmes C, Witham T, Grayson WL. Growth factor-eluting technologies for bone tissue engineering. *Drug Deliv Transl Res*. 2016;6(2):184–94.
20. Walmsley GG, McArdle A, Tevlin R, Momeni A, Atashroo D, Hu MS, Feroze AH, Wong VW, Lorenz PH, Longaker MT, Wan DC. Nanotechnology in bone tissue engineering. *Nanomedicine*. 2015;11(5):1253–63.
21. Uskokovic V, Desai TA. Nanoparticulate drug delivery platforms for advancing bone infection therapies. *Expert Opin Drug Deliv*. 2014;11(12):1899–912.
22. Wang C, Zhao Q, Wang M. Cryogenic 3D printing for producing hierarchical porous and rhBMP-2-loaded Ca-P/PLLA nanocomposite scaffolds for bone tissue engineering. *Biofabrication*. 2017;9(2):025031.
23. Correia TR, Figueira DR, de Sa KD, Miguel SP, Fradique RG, Mendonca AG, Correia IJ. 3D printed scaffolds with bactericidal activity aimed for bone tissue regeneration. *Int J Biol Macromol*. 2016;93(Pt B):1432–45.
24. Tovar N, Witek L, Atria P, Sobieraj M, Bowers M, Lopez CD, Cronstein BN, Coelho PG. Form and functional repair of long bone using 3D-printed bioactive scaffolds. *J Tissue Eng Regen Med*. 2018;12(9):1986–99.
25. Wang C, Ye X, Zhao Y, Bai L, He Z, Tong Q, Xie X, Zhu H, Cai D, Zhou Y, Lu B, Wei Y, Mei L, Xie D, Wang M. Cryogenic 3D printing of porous scaffolds for in situ delivery of 2D black phosphorus nanosheets, doxorubicin hydrochloride and osteogenic peptide for treating tumor resection-induced bone defects. *Biofabrication*. 2020;12(3):035004.
26. Zhang Y, Zhai D, Xu M, Yao Q, Zhu H, Chang J, Wu C. 3D-printed bioceramic scaffolds with antibacterial and osteogenic activity. *Biofabrication*. 2017;9(2):025037.
27. Song Y, Lin K, He S, Wang C, Zhang S, Li D, Wang J, Cao T, Bi L, Pei G. Nano-biphasic calcium phosphate/polyvinyl alcohol composites with enhanced bioactivity for bone repair via low-temperature three-dimensional printing and loading with platelet-rich fibrin. *Int J Nanomedicine*. 2018;13:505–23.
28. Martin V, Ribeiro IA, Alves MM, Goncalves L, Claudio RA, Grenho L, Fernandes MH, Gomes P, Santos CF, Bettencourt AF. Engineering a multifunctional 3D-printed PLA-collagen-minocycline-nanoHydroxyapatite scaffold with combined antimicrobial and osteogenic effects for bone regeneration. *Mater Sci Eng C Mater Biol Appl*. 2019;101:15–26.
29. Chen S, Shi Y, Zhang X, Ma J. Biomimetic synthesis of Mg-substituted hydroxyapatite nanocomposites and three-dimensional printing of composite scaffolds for bone regeneration. *J Biomed Mater Res A*. 2019;107(11):2512–21.
30. Luo Y, Chen S, Shi Y, Ma J. 3D printing of strontium-doped hydroxyapatite based composite scaffolds for repairing critical-sized rabbit calvarial defects. *Biomed Mater*. 2018;13(6):065004.
31. Bas O, Hansske F, Lim J, Ravichandran A, Kemnitz E, Teoh SH, Hutmacher DW, Borner HG. Tuning mechanical reinforcement and bioactivity of 3D printed ternary nanocomposites by interfacial peptide-polymer conjugates. *Biofabrication*. 2019;11(3):035028.
32. Castro NJ, O'Brien J, Zhang LG. Integrating biologically inspired nanomaterials and table-top stereolithography for 3D printed biomimetic osteochondral scaffolds. *Nanoscale*. 2015;7(33):14010–22.
33. Chen S, Shi Y, Luo Y, Ma J. Layer-by-layer coated porous 3D printed hydroxyapatite composite scaffolds for controlled drug delivery. *Colloids Surf B Biointerfaces*. 2019;179:121–7.
34. Chen X, Gao C, Jiang J, Wu Y, Zhu P, Chen G. 3D printed porous PLA/nHA composite scaffolds with enhanced osteogenesis and osteoconductivity in vivo for bone regeneration. *Biomed Mater*. 2019;14(6):065003.
35. Demirtas TT, Irmak G, Gumusderelioglu M. A bioprintable form of chitosan hydrogel for bone tissue engineering. *Biofabrication*. 2017;9(3):035003.

36. Deng N, Sun J, Li Y, Chen L, Chen C, Wu Y, Wang Z, Li L. Experimental study of rhBMP-2 chitosan nano-sustained release carrier-loaded PLGA/nHA scaffolds to construct mandibular tissue-engineered bone. *Arch Oral Biol*. 2019;102:16–25.
37. Gao C, Deng Y, Feng P, Mao Z, Li P, Yang B, Deng J, Cao Y, Shuai C, Peng S. Current progress in bioactive ceramic scaffolds for bone repair and regeneration. *Int J Mol Sci*. 2014;15(3):4714–32.
38. Goncalves EM, Oliveira FJ, Silva RF, Neto MA, Fernandes MH, Amaral M, Vallet-Regi M, Vila M. Three-dimensional printed PCL-hydroxyapatite scaffolds filled with CNTs for bone cell growth stimulation. *J Biomed Mater Res B Appl Biomater*. 2016;104(6):1210–9.
39. Holmes B, Bulusu K, Plesniak M, Zhang LG. A synergistic approach to the design, fabrication and evaluation of 3D printed micro and nano featured scaffolds for vascularized bone tissue repair. *Nanotechnology*. 2016;27(6):064001.
40. Prasopthum A, Shakesheff KM, Yang J. Direct three-dimensional printing of polymeric scaffolds with nanofibrous topography. *Biofabrication*. 2018;10(2):025002.
41. Rogowska-Tylman J, Locs J, Salma I, Wozniak B, Pilmane M, Zalite V, Wojnarowicz J, Kedzierska-Sar A, Chudoba T, Szlczak K, Chlanda A, Swieszkowski W, Gedanken A, Lojkowski W. In vivo and in vitro study of a novel nanohydroxyapatite sonocoated scaffolds for enhanced bone regeneration. *Mater Sci Eng C Mater Biol Appl*. 2019;99:669–84.
42. Roh HS, Lee CM, Hwang YH, Kook MS, Yang SW, Lee D, Kim BH. Addition of MgO nanoparticles and plasma surface treatment of three-dimensional printed polycaprolactone/hydroxyapatite scaffolds for improving bone regeneration. *Mater Sci Eng C Mater Biol Appl*. 2017;74:525–35.
43. Trachtenberg JE, Placone JK, Smith BT, Fisher JP, Mikos AG. Extrusion-based 3D printing of poly(propylene fumarate) scaffolds with hydroxyapatite gradients. *J Biomater Sci Polym Ed*. 2017;28(6):532–54.
44. Wang Q, Xia Q, Wu Y, Zhang X, Wen F, Chen X, Zhang S, Heng BC, He Y, Ouyang HW. 3D-printed Atsstrin-incorporated alginate/hydroxyapatite scaffold promotes bone defect regeneration with TNF/TNFR signaling involvement. *Adv Healthc Mater*. 2015;4(11):1701–8.
45. Yang WF, Long L, Wang R, Chen D, Duan S, Xu FJ. Surface-modified hydroxyapatite nanoparticle-reinforced polylactides for three-dimensional printed bone tissue engineering scaffolds. *J Biomed Nanotechnol*. 2018;14(2):294–303.
46. Yu J, Xu Y, Li S, Seifert GV, Becker ML. Three-dimensional printing of nano hydroxyapatite/poly(ester urea) composite scaffolds with enhanced bioactivity. *Biomacromolecules*. 2017;18(12):4171–83.
47. Zhou X, Esworthy T, Lee SJ, Miao S, Cui H, Plesiniak M, Fenniri H, Webster T, Rao RD, Zhang LG. 3D printed scaffolds with hierarchical biomimetic structure for osteochondral regeneration. *Nanomedicine*. 2019;19:58–70.
48. Ciapetti G, Di Pompo G, Avnet S, Martini D, Diez-Escudero A, Montufar EB, Ginebra MP, Baldini N. Osteoclast differentiation from human blood precursors on biomimetic calcium-phosphate substrates. *Acta Biomater*. 2017;50:102–13.
49. Muller P, Bulnheim U, Diener A, Luthen F, Teller M, Klinkenberg ED, Neumann HG, Nebe B, Liebold A, Steinhoff G, Rychly J. Calcium phosphate surfaces promote osteogenic differentiation of mesenchymal stem cells. *J Cell Mol Med*. 2008;12(1):281–91.
50. Samavedi S, Whittington AR, Goldstein AS. Calcium phosphate ceramics in bone tissue engineering: a review of properties and their influence on cell behavior. *Acta Biomater*. 2013;9(9):8037–45.
51. Jeong J, Kim JH, Shim JH, Hwang NS, Heo CY. Bioactive calcium phosphate materials and applications in bone regeneration. *Biomater Res*. 2019;23:4.
52. Yoshikawa H, Myoui A. Bone tissue engineering with porous hydroxyapatite ceramics. *J Artif Organs*. 2005;8(3):131–6.
53. Ramselaar MMA, Driessens FCM, Kalk W, De Wijn JR, Van Mullem PJ. Biodegradation of four calcium phosphate ceramics; in vivo rates and tissue interactions. *J Mater Sci Mater Med*. 1991;2(2):63–70.

54. Ramesh N, Moratti SC, Dias GJ. Hydroxyapatite-polymer biocomposites for bone regeneration: a review of current trends. *J Biomed Mater Res B Appl Biomater*. 2018;106(5):2046–57.
55. Li Y, Liu C. Nanomaterial-based bone regeneration. *Nanoscale*. 2017;9(15):4862–74.
56. Hong Z, Zhang P, Liu A, Chen L, Chen X, Jing X. Composites of poly(lactide-co-glycolide) and the surface modified carbonated hydroxyapatite nanoparticles. *J Biomed Mater Res A*. 2007;81(3):515–22.
57. LeGeros RZ. Properties of osteoconductive biomaterials: calcium phosphates. *Clin Orthop Relat Res*. 2002;395:81–98.
58. Sethu SN, Namashivayam S, Devendran S, Nagarajan S, Tsai WB, Narashiman S, Ramachandran M, Ambigapathi M. Nanoceramics on osteoblast proliferation and differentiation in bone tissue engineering. *Int J Biol Macromol*. 2017;98:67–74.
59. Suchanek W, Yoshimura M. Processing and properties of hydroxyapatite-based biomaterials for use as hard tissue replacement implants. *J Mater Res*. 1998;13(1):94–117.
60. Prakasam M, Locs J, Salma-Ancane K, Loca D, Largeteau A, Berzina-Cimdina L. Fabrication, properties and applications of dense hydroxyapatite: a review. *J Funct Biomater*. 2015;6(4):1099–140.
61. Wijerathne HMCS, Yan D, Zeng B, Xie Y, Hu H, Wickramaratne MN, Han Y. Effect of nano-hydroxyapatite on protein adsorption and cell adhesion of poly(lactic acid)/nano-hydroxyapatite composite microspheres. *SN Appl Sci*. 2020;2(4):722.
62. Wang X, Li Y, Wei J, de Groot K. Development of biomimetic nano-hydroxyapatite/poly(hexamethylene adipamide) composites. *Biomaterials*. 2002;23(24):4787–91.
63. Aydin E, Planell JA, Hasirci V. Hydroxyapatite nanorod-reinforced biodegradable poly(L-lactic acid) composites for bone plate applications. *J Mater Sci Mater Med*. 2011;22(11):2413–27.
64. Horch HH, Sader R, Pautke C, Neff A, Deppe H, Kolk A. Synthetic, pure-phase beta-tricalcium phosphate ceramic granules (Cerasorb) for bone regeneration in the reconstructive surgery of the jaws. *Int J Oral Maxillofac Surg*. 2006;35(8):708–13.
65. Yamada S, Heymann D, Bouler JM, Daculsi G. Osteoclastic resorption of calcium phosphate ceramics with different hydroxyapatite/beta-tricalcium phosphate ratios. *Biomaterials*. 1997;18(15):1037–41.
66. Kamitakahara M, Ohtsuki C, Miyazaki T. Review paper: behavior of ceramic biomaterials derived from tricalcium phosphate in physiological condition. *J Biomater Appl*. 2008;23(3):197–212.
67. Dorozhkin SV. Biphasic, triphasic and multiphasic calcium orthophosphates. *Acta Biomater*. 2012;8(3):963–77.
68. Combes C, Rey C. Amorphous calcium phosphates: synthesis, properties and uses in biomaterials. *Acta Biomater*. 2010;6(9):3362–78.
69. Leite AJ, Mano JF. Biomedical applications of natural-based polymers combined with bioactive glass nanoparticles. *J Mater Chem B*. 2017;5(24):4555–68.
70. Saravanapavan P, Jones JR, Pryce RS, Hench LL. Bioactivity of gel-glass powders in the CaO-SiO₂ system: a comparison with ternary (CaO-P₂O₅-SiO₂) and quaternary glasses (SiO₂-CaO-P₂O₅-Na₂O). *J Biomed Mater Res A*. 2003;66(1):110–9.
71. Saravanapavan P, Jones JR, Verrier S, Beilby R, Shirliff VJ, Hench LL, Polak JM. Binary CaO-SiO₂ gel-glasses for biomedical applications. *Biomed Mater Eng*. 2004;14(4):467–86.
72. Wang X, Li W. Biodegradable mesoporous bioactive glass nanospheres for drug delivery and bone tissue regeneration. *Nanotechnology*. 2016;27(22):225102.
73. Liang Q, Hu Q, Miao G, Yuan B, Chen X. A facile synthesis of novel mesoporous bioactive glass nanoparticles with various morphologies and tunable mesostructure by sacrificial liquid template method. *Mater Lett*. 2015;148:45–9.
74. Li Y, Chen X, Ning C, Yuan B, Hu Q. Facile synthesis of mesoporous bioactive glasses with controlled shapes. *Mater Lett*. 2015;161:605–8.
75. Geng Y, Dalhaimer P, Cai S, Tsai R, Tewari M, Minko T, Discher DE. Shape effects of filaments versus spherical particles in flow and drug delivery. *Nat Nanotechnol*. 2007;2(4):249–55.

76. Cui F-Z, Li Y, Ge J. Self-assembly of mineralized collagen composites. *Mater Sci Eng R Rep.* 2007;57(1):1–27.
77. Rocton N, Oudadesse H, Mosbahi S, Bunetel L, Pellen-Mussi P, Lefeuvre B. Study of nano bioactive glass for use as bone biomaterial comparison with micro bioactive glass behaviour. *IOP Conf Ser Mater Sci Eng.* 2019;628:012005.
78. Ajita J, Saravanan S, Selvamurugan N. Effect of size of bioactive glass nanoparticles on mesenchymal stem cell proliferation for dental and orthopedic applications. *Mater Sci Eng C Mater Biol Appl.* 2015;53:142–9.
79. Chen YW, Shen YF, Ho CC, Yu J, Wu YA, Wang K, Shih CT, Shie MY. Osteogenic and angiogenic potentials of the cell-laden hydrogel/mussel-inspired calcium silicate complex hierarchical porous scaffold fabricated by 3D bioprinting. *Mater Sci Eng C Mater Biol Appl.* 2018;91:679–87.
80. Chen M, Zhao F, Li Y, Wang M, Chen X, Lei B. 3D-printed photoluminescent bioactive scaffolds with biomimetic elastomeric surface for enhanced bone tissue engineering. *Mater Sci Eng C Mater Biol Appl.* 2020;106:110153.
81. Dang W, Li T, Li B, Ma H, Zhai D, Wang X, Chang J, Xiao Y, Wang J, Wu C. A bifunctional scaffold with CuFeSe₂ nanocrystals for tumor therapy and bone reconstruction. *Biomaterials.* 2018;160:92–106.
82. Gao G, Schilling AF, Yonezawa T, Wang J, Dai G, Cui X. Bioactive nanoparticles stimulate bone tissue formation in bioprinted three-dimensional scaffold and human mesenchymal stem cells. *Biotechnol J.* 2014;9(10):1304–11.
83. Ojansivu M, Rashad A, Ahlinder A, Massera J, Mishra A, Syverud K, Finne-Wistrand A, Miettinen S, Mustafa K. Wood-based nanocellulose and bioactive glass modified gelatin-alginate bioinks for 3D bioprinting of bone cells. *Biofabrication.* 2019;11(3):035010.
84. Zhu M, Li K, Zhu Y, Zhang J, Ye X. 3D-printed hierarchical scaffold for localized isoniazid/rifampin drug delivery and osteoarticular tuberculosis therapy. *Acta Biomater.* 2015;16:145–55.
85. Carrow JK, Di Luca A, Dolatshahi-Pirouz A, Moroni L, Gaharwar AK. 3D-printed bioactive scaffolds from nanosilicates and PEOT/PBT for bone tissue engineering. *Regen Biomater.* 2019;6(1):29–37.
86. Cidonio G, Alcalá-Orozco CR, Lim KS, Glinka M, Mutreja I, Kim YH, Dawson JI, Woodfield TB, Oreffo ROC. Osteogenic and angiogenic tissue formation in high fidelity nanocomposite Laponite-gelatin bioinks. *Biofabrication.* 2019;11(3):035027.
87. Cidonio G, Cooke M, Glinka M, Dawson JI, Grover L, Oreffo ROC. Printing bone in a gel: using nanocomposite bioink to print functionalised bone scaffolds. *Mater Today Bio.* 2019;4:100028.
88. Cidonio G, Glinka M, Kim YH, Kanczler JM, Lanham SA, Ahlfeld T, Lode A, Dawson JI, Gelinsky M, Oreffo ROC. Nanoclay-based 3D printed scaffolds promote vascular ingrowth ex vivo and generate bone mineral tissue in vitro and in vivo. *Biofabrication.* 2020;12(3):035010.
89. Zhai X, Ruan C, Ma Y, Cheng D, Wu M, Liu W, Zhao X, Pan H, Lu WW. 3D-bioprinted osteoblast-laden nanocomposite hydrogel constructs with induced microenvironments promote cell viability, differentiation, and osteogenesis both in vitro and in vivo. *Adv Sci (Weinh).* 2018;5(3):1700550.
90. Luo Z, Zhang S, Pan J, Shi R, Liu H, Lyu Y, Han X, Li Y, Yang Y, Xu Z, Sui Y, Luo E, Zhang Y, Wei S. Time-responsive osteogenic niche of stem cells: a sequentially triggered, dual-peptide loaded, alginate hybrid system for promoting cell activity and osteo-differentiation. *Biomaterials.* 2018;163:25–42.
91. Zhang Y, Yu W, Ba Z, Cui S, Wei J, Li H. 3D-printed scaffolds of mesoporous bioglass/gliadin/polycaprolactone ternary composite for enhancement of compressive strength, degradability, cell responses and new bone tissue ingrowth. *Int J Nanomedicine.* 2018;13:5433–47.

92. Ottria L, Lauritano D, Andreasi Bassi M, Palmieri A, Candotto V, Tagliabue A, Tettamanti L. Mechanical, chemical and biological aspects of titanium and titanium alloys in implant dentistry. *J Biol Regul Homeost Agents*. 2018;32(2 Suppl. 1):81–90.
93. Yang J, Chen HJ, Zhu XD, Vaidya S, Xiang Z, Fan YJ, Zhang XD. Enhanced repair of a critical-sized segmental bone defect in rabbit femur by surface microstructured porous titanium. *J Mater Sci Mater Med*. 2014;25(7):1747–56.
94. Rasoulianboroujeni M, Fahimpour F, Shah P, Khoshroo K, Tahriri M, Eslami H, Yadegari A, Dashtimoghadam E, Tayebi L. Development of 3D-printed PLGA/TiO₂ nanocomposite scaffolds for bone tissue engineering applications. *Mater Sci Eng C Mater Biol Appl*. 2019;96:105–13.
95. Marino A, Barsotti J, de Vito G, Filippeschi C, Mazzolai B, Piazza V, Labardi M, Mattoli V, Ciofani G. Two-photon lithography of 3D nanocomposite piezoelectric scaffolds for cell stimulation. *ACS Appl Mater Interfaces*. 2015;7(46):25574–9.
96. Nabyouni M, Bruckner T, Zhou H, Gbureck U, Bhaduri SB. Magnesium-based bioceramics in orthopedic applications. *Acta Biomater*. 2018;66:23–43.
97. Seebach E, Kubatzky KF. Chronic implant-related bone infections-can immune modulation be a therapeutic strategy? *Front Immunol*. 2019;10:1724.
98. Jia Z, Xiu P, Xiong P, Zhou W, Cheng Y, Wei S, Zheng Y, Xi T, Cai H, Liu Z, Wang C, Zhang W, Li Z. Additively manufactured macroporous titanium with silver-releasing micro-/nanoporous surface for multipurpose infection control and bone repair - a proof of concept. *ACS Appl Mater Interfaces*. 2016;8(42):28495–510.
99. Deng L, Deng Y, Xie K. AgNPs-decorated 3D printed PEEK implant for infection control and bone repair. *Colloids Surf B Biointerfaces*. 2017;160:483–92.
100. Zou F, Jiang J, Lv F, Xia X, Ma X. Preparation of antibacterial and osteoconductive 3D-printed PLGA/Cu(I)@ZIF-8 nanocomposite scaffolds for infected bone repair. *J Nanobiotechnol*. 2020;18(1):39.
101. Zhu Y, Liu K, Deng J, Ye J, Ai F, Ouyang H, Wu T, Jia J, Cheng X, Wang X. 3D printed zirconia ceramic hip joint with precise structure and broad-spectrum antibacterial properties. *Int J Nanomedicine*. 2019;14:5977–87.
102. Dadfar SM, Roemhild K, Drude NI, von Stillfried S, Knuchel R, Kiessling F, Lammers T. Iron oxide nanoparticles: diagnostic, therapeutic and theranostic applications. *Adv Drug Deliv Rev*. 2019;138:302–25.
103. Shimizu K, Ito A, Yoshida T, Yamada Y, Ueda M, Honda H. Bone tissue engineering with human mesenchymal stem cell sheets constructed using magnetite nanoparticles and magnetic force. *J Biomed Mater Res B Appl Biomater*. 2007;82(2):471–80.
104. Huang J, Liu W, Liang Y, Li L, Duan L, Chen J, Zhu F, Lai Y, Zhu W, You W, Jia Z, Xiong J, Wang D. Preparation and biocompatibility of diphasic magnetic nanocomposite scaffold. *Mater Sci Eng C Mater Biol Appl*. 2018;87:70–7.
105. Jackson RJ, Patrick PS, Page K, Powell MJ, Lythgoe MF, Miodownik MA, Parkin IP, Carmalt CJ, Kalber TL, Bear JC. Chemically treated 3D printed polymer scaffolds for biomineral formation. *ACS Omega*. 2018;3(4):4342–51.
106. Chang WJ, Pan YH, Tzeng JJ, Wu TL, Fong TH, Feng SW, Huang HM. Development and testing of X-ray imaging-enhanced poly-L-Lactide bone screws. *PLoS One*. 2015;10(10):e0140354.
107. Vial S, Reis RL, Oliveira J. Recent advances using gold nanoparticles as a promising multimodal tool for tissue engineering and regenerative medicine. *Curr Opin Solid State Mater Sci*. 2017;21(2):92–112.
108. Ko WK, Heo DN, Moon HJ, Lee SJ, Bae MS, Lee JB, Sun IC, Jeon HB, Park HK, Kwon IK. The effect of gold nanoparticle size on osteogenic differentiation of adipose-derived stem cells. *J Colloid Interface Sci*. 2015;438:68–76.
109. Li JJ, Kawazoe N, Chen G. Gold nanoparticles with different charge and moiety induce differential cell response on mesenchymal stem cell osteogenesis. *Biomaterials*. 2015;54:226–36.

110. Schwab EH, Pohl TL, Haraszti T, Schwaerzer GK, Hiepen C, Spatz JP, Knaus P, Cavalcanti-Adam EA. Nanoscale control of surface immobilized BMP-2: toward a quantitative assessment of BMP-mediated signaling events. *Nano Lett.* 2015;15(3):1526–34.
111. Ryoo SR, Kim YK, Kim MH, Min DH. Behaviors of NIH-3T3 fibroblasts on graphene/carbon nanotubes: proliferation, focal adhesion, and gene transfection studies. *ACS Nano.* 2010;4(11):6587–98.
112. Choe G, Oh S, Seok JM, Park SA, Lee JY. Graphene oxide/alginate composites as novel bioinks for three-dimensional mesenchymal stem cell printing and bone regeneration applications. *Nanoscale.* 2019;11(48):23275–85.
113. Belaid H, Nagarajan S, Teyssier C, Barou C, Bares J, Balme S, Garay H, Huon V, Cornu D, Cavailles V, Bechelany M. Development of new biocompatible 3D printed graphene oxide-based scaffolds. *Mater Sci Eng C Mater Biol Appl.* 2020;110:110595.
114. Pei B, Wang W, Dunne N, Li X. Applications of carbon nanotubes in bone tissue regeneration and engineering: superiority, concerns, current advancements, and prospects. *Nanomaterials (Basel).* 2019;9(10):1501.
115. Shao W, Paul A, Zhao B, Lee C, Rodes L, Prakash S. Carbon nanotube lipid drug approach for targeted delivery of a chemotherapy drug in a human breast cancer xenograft animal model. *Biomaterials.* 2013;34(38):10109–19.
116. Munir K, Wen C, Li Y. Carbon nanotubes and graphene as nanoreinforcements in metallic biomaterials: a review. *Adv Biosyst.* 2019;3:e1800212.
117. Gerasimenko A, Ichkitidze L, Podgaetskii V, Selishchev S. Biomedical applications of promising nanomaterials with carbon nanotubes. *Biomed Eng.* 2015;48:310–4.
118. Khalid P, Suman V. Carbon nanotube-hydroxyapatite composite for bone tissue engineering and their interaction with mouse fibroblast L929 in vitro. *J Bionanosci.* 2017;11:233–40.
119. Tutak W, Chowalla M, Sesti F. The chemical and physical characteristics of single-walled carbon nanotube film impact on osteoblastic cell response. *Nanotechnology.* 2010;21(31):315102.
120. Zhang F, Weidmann A, Nebe JB, Burkel E. Osteoblast cell response to surface-modified carbon nanotubes. *Mater Sci Eng C.* 2012;32(5):1057–61.
121. Huang B, Vyas C, Roberts I, Poutrel QA, Chiang WH, Blaker JJ, Huang Z, Bartolo P. Fabrication and characterisation of 3D printed MWCNT composite porous scaffolds for bone regeneration. *Mater Sci Eng C Mater Biol Appl.* 2019;98:266–78.
122. Liu X, George MN, Park S, Miller Ii AL, Gaihre B, Li L, Waletzki BE, Terzc A, Yaszemski MJ, Lu L. 3D-printed scaffolds with carbon nanotubes for bone tissue engineering: fast and homogeneous one-step functionalization. *Acta Biomater.* 2020;111:129.
123. Cui H, Yu Y, Li X, Sun Z, Ruan J, Wu Z, Qian J, Yin J. Direct 3D printing of a tough hydrogel incorporated with carbon nanotubes for bone regeneration. *J Mater Chem B.* 2019;7(45):7207–17.
124. Donnalaja F, Jacchetti E, Soncini M, Raimondi MT. Natural and synthetic polymers for bone scaffolds optimization. *Polymers.* 2020;12(4):905.
125. Sonaje K, Italia JL, Sharma G, Bhardwaj V, Tikoo K, Kumar MNVR. Development of biodegradable nanoparticles for Oral delivery of Ellagic acid and evaluation of their antioxidant efficacy against cyclosporine A-induced nephrotoxicity in rats. *Pharm Res.* 2007;24(5):899–908.
126. Jain A, Jain A, Gulbake A, Shilpi S, Hurkat P, Jain SK. Peptide and protein delivery using new drug delivery systems. *Crit Rev Ther Drug Carrier Syst.* 2013;30(4):293–329.
127. Rai R, Alwani S, Badea I. Polymeric nanoparticles in gene therapy: new avenues of design and optimization for delivery applications. *Polymers.* 2019;11(4):745.
128. Hassan AH, Hosny KM, Murshid ZA, Alhadlaq A, Alyamani A, Naguib G. Depot injectable biodegradable nanoparticles loaded with recombinant human bone morphogenetic protein-2: preparation, characterization, and in vivo evaluation. *Drug Des Devel Ther.* 2015;9:3599–606.
129. Kim BS, Yang SS, Kim CS. Incorporation of BMP-2 nanoparticles on the surface of a 3D-printed hydroxyapatite scaffold using an epsilon-polycaprolactone polymer emulsion coating method for bone tissue engineering. *Colloids Surf B Biointerfaces.* 2018;170:421–9.

130. Liu S, He Z, Xu G, Xiao X. Fabrication of polycaprolactone nanofibrous scaffolds by facile phase separation approach. *Mater Sci Eng C Mater Biol Appl.* 2014;44:201–8.
131. Xu H, Cao B, George A, Mao C. Self-assembly and mineralization of genetically modifiable biological nanofibers driven by beta-structure formation. *Biomacromolecules.* 2011;12(6):2193–9.
132. Guo Z, Xu J, Ding S, Li H, Zhou C, Li L. In vitro evaluation of random and aligned polycaprolactone/gelatin fibers via electrospinning for bone tissue engineering. *J Biomater Sci Polym Ed.* 2015;26(15):989–1001.
133. Yao Q, Cosme JG, Xu T, Miszuk JM, Picciani PH, Fong H, Sun H. Three dimensional electrospun PCL/PLA blend nanofibrous scaffolds with significantly improved stem cells osteogenic differentiation and cranial bone formation. *Biomaterials.* 2017;115:115–27.
134. Sisson K, Zhang C, Farach-Carson MC, Chase DB, Rabolt JF. Fiber diameters control osteoblastic cell migration and differentiation in electrospun gelatin. *J Biomed Mater Res A.* 2010;94(4):1312–20.
135. Li R, McCarthy A, Zhang YS, Xie J. Decorating 3D printed scaffolds with electrospun nanofiber segments for tissue engineering. *Adv Biosyst.* 2019;3(12):1900137.
136. Mendoza-Buenrostro C, Lara H, Rodriguez C. Hybrid fabrication of a 3D printed geometry embedded with PCL nanofibers for tissue engineering applications. *Proc Eng.* 2015;110:128–34.
137. Vazquez-Vazquez FC, Chanes-Cuevas OA, Masuoka D, Alatorre JA, Chavarria-Bolaños D, Vega-Baudrit JR, Serrano-Bello J, Alvarez-Perez MA. Biocompatibility of developing 3D-printed tubular scaffold coated with nanofibers for bone applications. *J Nanomater.* 2019;2019:6105818.
138. Placone JK, Mahadik B, Fisher JP. Addressing present pitfalls in 3D printing for tissue engineering to enhance future potential. *APL Bioeng.* 2020;4(1):010901.
139. Abouzeid RE, Khiari R, Salama A, Diab M, Beneventi D, Dufresne A. In situ mineralization of nano-hydroxyapatite on bifunctional cellulose nanofiber/polyvinyl alcohol/sodium alginate hydrogel using 3D printing. *Int J Biol Macromol.* 2020;160:538–47.

Bioreactors and Scale-Up in Bone Tissue Engineering



Shannon Theresa McLoughlin, Bhushan Mahadik, and John Fisher

1 Introduction

Tissue engineering strategies for bone defect repair typically consist of cells, scaffolds, and bioactive signals that, when combined, produce a regenerative bone template that degrades within the host over time and stimulates the body to produce new, functional bone tissue to take its place [1]. For strategies utilizing cell-based approaches, scaffolds are seeded with cells and pre-cultured in vitro to allow for cell proliferation and osteogenic differentiation prior to implantation [2]. However, traditional static culture technique has proven an inefficient method for culture of three-dimensional (3D) scaffolds. Static culture provides sufficient nutrients and oxygen to cells on outer surfaces of these scaffolds, but cells within the center of the scaffold rely on diffusive transport of nutrients. Consequently, a nutrient gradient forms within the scaffolds, resulting in cell death toward the center. These limitations restrict the production of regenerative bone tissue engineering (BTE) scaffolds of clinically relevant sizes, demonstrating these effects in constructs as small as 10 mm^3 [3, 4]. The difficulties associated with static culture conditions are ameliorated through the use of bioreactor culture. These systems provide dynamic culture environments in which media is constantly mixed and convectively transported to cells throughout the scaffold [2].

S. T. McLoughlin · B. Mahadik · J. Fisher (✉)

Fischell Department of Bioengineering, University of Maryland, College Park, MD, USA

Center for Engineering Complex Tissues, University of Maryland, College Park, MD, USA

e-mail: bhushanmahadik@gmail.com; jpfisher@umd.edu

© Springer Nature Switzerland AG 2022

F. P. S. Guastaldi, B. Mahadik (eds.), *Bone Tissue Engineering*,

https://doi.org/10.1007/978-3-030-92014-2_10

225

Although bone is a regenerative tissue that often heals without surgical intervention, defects of critical size do not spontaneously heal over time. Critical size bone defects, which were previously discussed in chapters “3D Printing for Oral and Maxillofacial Regeneration” and “Bone Grafting in the Regenerative Reconstruction of Critical-Size Long Bone Segmental Defects”, are on the scale of 2.5 cm, and their geometry varies with anatomical location [5]. When generating tissue engineering constructs to repair these large defects, bioreactor culture is often required to increase the nutrient transport throughout the scaffold via convective flow. Transporting media and oxygen through convective mechanisms allows cells within the entire construct to readily receive necessary nutrients during the culture period, leading to greater cell survival and more homogenous tissue formation. This same effect is related to bone tissue development and maintenance in vivo. Lack of appropriate vasculature limits new tissue formation in the body to sizes of 100–200 μm , which is the diffusion limit of oxygen in highly cellular tissues [6]. However, the presence of vasculature, which is further discussed in chapter “Strategies for 3D Printing of Vascularized Bone”, within these tissues allows for the transport of the growth factors necessary to instruct bone regeneration, such as bone morphogenic protein (BMP) and vascular endothelial growth factor (VEGF) [6, 7]. Bioreactor culture not only improves the transport of nutrients and oxygen from surrounding media but also has a positive impact on the formation of vascular-like networks within these constructs. These systems also have the potential to culture BTE constructs in a manner that replicates the in vivo environment of bone. Due to the nature of bone acting as a supportive tissue within the body, forces of tension and compression are constantly applied. Because these forces heavily regulate bone metabolism, their application is included within several bioreactor systems to generate more functional bone-like structures.

Advantages of Bioreactor Culture:

1. *Homogenous cell seeding:* Even cell seeding is essential in the formation of well-organized tissue within the scaffold [8]. Two dimensional cell seeding involves deposition of cell solution directly onto the scaffold and incubation for a period of time in static culture. Although this seeding method is relatively popular, it results in uneven matrix deposition in 3D bone tissue applications, typically on the periphery of the scaffolds, leading to nutrient gradients and cell death [8]. Perfusion bioreactor systems are used to combat this issue because they deliver cells and nutrients throughout BTE constructs [4, 9].
2. *Increased cell proliferation:* Along with consistent cell distribution, bioreactor culture increases cell proliferation on scaffolds as well. Convection mechanisms of transport lead to improved delivery of nutrients and oxygen, as well as better waste removal processes that are linked to greater cell survival and proliferation.
3. *Application of mechanical loading and fluid shear stress:* In order to more closely mimic the in vivo environment of bone, bioreactor systems are utilized to generate mechanical loading conditions and application of shear stress [2, 8]. The bone matrix is subjected to mechanical forces of cyclic loading while per-

forming everyday functions. This loading cycle on the bone matrix then transmits forces to cells within the tissue via fluid shear through channels called canaliculi [8]. These forces trigger bone cells to activate the bone remodeling process in order to maintain the necessary mechanical strength that bone provides in the body [2]. Also, research suggests that application of fluid shear stress to mesenchymal stem cells (MSCs), the most heavily utilized stem cell source in BTE applications, increases their osteoblastic differentiation [10]. Both compression and magnetic force bioreactor systems recreate the cyclic loading conditions that bone experiences. Several bioreactor systems apply fluid shear directly to cells within cultured scaffolds, including spinner flasks and perfusion systems.

4. *Vascularization*: Bioreactors are utilized to improve in vitro culture processes prior to scaffold implantation to produce more mature and complex tissue constructs [2]. One important aspect of generating these mature tissues in vitro includes scaffold vascularization, which will be discussed further in chapter “Strategies for 3D Printing of Vascularized Bone”. Bone vasculature provides the matrix with the necessary nutrients and oxygen it needs to maintain normal physiological functions, such as development, regeneration, and remodeling, and serves as a mechanism for waste removal [7]. Many vascularization strategies are available, but when combining a vascularization strategy with bioreactor culture, more highly organized and functional bone tissue substitutes can be generated. Both rotating wall vessels and perfusion systems have been utilized to produce preliminary vascular networks within tissue constructs, however there is still significant growth and optimization necessary to improve vascularization strategies [11].
5. *Biomanufacturing*: Bioreactor systems allow for the generation and maintenance of clinically relevant volumes of engineered bone on the centimeter scale. This provides a clear advantage over traditional static culture techniques that can only produce constructs on the millimeter scale. These systems also enhance and expedite the production process through minimization of necessary culture times and monitoring. Because culture processes often produce variable results, bioreactors standardize these processes and allow for the generation of multiple patient-specific grafts in parallel, so as to ensure that patients receive the most effective graft.
6. *Clinical translation*: To enhance the clinical potential for tissue engineering constructs, in vitro culture steps must be optimized to achieve maximum rate of production and automation, while minimizing risk of infection and necessary manual labor [2]. Bioreactor culture allows for cell seeding, proliferation, differentiation, and tissue maturation to occur within the same closed vessel, minimizing transfers of the cells and scaffolds during in vitro culture, and therefore minimizing contamination risks [2]. Its potential for automation, combined with increased nutrient delivery, and tissue maturation allows for the generation of BTE constructs of clinically relevant sizes by overcoming the size limitations that static culture conditions produce. These systems significantly augment the capacities of BTE scaffolds to serve as functional replacements for diseased or defective bone tissue in clinical scenarios.

Table 1 Summary of commercially available bioreactor systems and their respective uses

Bioreactor system	Company	Uses	Refs.
OsteoGen: Perfusion Bioreactor	BISS TGT	Provides media perfusion to bone constructs	[12]
CartiGen: Compression Bioreactor	BISS TGT	Oscillatory stress and perfusion to cartilage constructs	[12]
ZRP Cultivation System	ZellWerk	Ex vivo expansion of human blood and tissue-derived cells	[12]
TEB1000 Bioreactor	Ebers Medical	Culture of tissue engineering constructs under flow; eliminates need for external equipment	[12]
TISXell Biaxial Bioreactor	QuinTech Life Sciences	Growth and maturation of cells on 3D bone tissue engineering constructs; uniaxial, biaxial, and swing modes	[12, 13]
3DCulturePro	Bose	Perfusion of 3D cell culture constructs	[14]
Quasi Vivo	Lonza	Perfusion of interconnected or co-culture monolayer cultures	[15]
WAVE Bioreactor	Cytiva	Orbital shaker for cell expansion	[16]
Flexcell Tension System	Flexcell	Cyclic or static strain applied to in vitro cultured cells	[17]
Flexcell Compression System	Flexcell	Uses piston to apply compressive force to tissue samples	[18]
Streamer	Flexcell	Regulates laminar, pulsatile, or oscillating flow in cell cultures	[19]

2 Bioreactor Systems

Some commercially available bioreactor systems and their uses are presented in Table 1. Several bioreactor designs will be discussed in this chapter. These systems and a summary of their results are presented in Table 2

2.1 Spinner Flasks

Rationale and design: Spinner flask systems consist of a three-armed flask, magnetic stir bar, and scaffolds that are suspended in media via wires, needles, or thread [4]. A schematic of a spinner flask system is pictured in Fig. 1a. Typical stirring speeds are set between 30 and 50 rpm, so as to ensure dynamic mixing of media, but not to cause significant damage to cells seeded on the scaffolds [16, 18]. The rationale behind the use of spinner flasks for in vitro culture is that the dynamic mixing

Table 2 Summary of bioreactor systems, cell lines, and principal findings

Bioreactor system	Cell source	Principal finding	Refs.
Spinner Flask	Rat BM-MSCs	Upregulation of alkaline phosphatase (ALP), osteocalcin (OC), & calcium deposition; peripheral mineralization	[16]
	hMSCs	Peripheral mineralization	[17]
	hMSCs	Increased proliferation, ALP activity, & mineralized matrix	[18]
	hMSCs	CFD analysis, 300 rpm resulted in more homogenous mineralization	[19]
	Mouse-derived MSCs	Increased proliferation	[20]
Rotating Wall Vessel	Rat BM-MSCs	ALP activity, (OC) secretion, & calcium deposition lowest in RWV	[16]
	Rat osteoblast	Increased ALP activity, osteopontin (OPN), OC, & BMP-4; decreased proliferation; increased osteoprotegerin (OPG) & interleukin 6 (IL-6)	[21]
	Rat BM-MSCs	Inhibited proliferation and osteogenic differentiation under microgravity	[22]
	Human BM-MSCs	Runx2, ALP, collagen I, & osteonectin (ON) expression suppressed under microgravity, expression of adipogenic markers upregulated	[23]
	Human BM-MSCs	Bioinformatics study, microgravity downregulates osteogenic & chondrogenic genes & upregulates adipogenic genes	[24]
	Osteoblast	Varied ratios of LTW/HTW microcarriers resulted in more homogenous cell distribution	[25, 26]
	Fetal human osteoblast	Optimized fill volume and rotational speed resulted in greatest cell proliferation	[27]
Perfusion	hMSCs	Bioreactor culture of anatomically correct TMJs resulted in more homogenous cell distribution & matrix formation	[28]
	hMSCs	Increased viability, proliferation, & ALP activity; increased OC, OPN, & BMP-2 expression	[29]
	hMSCs	BMP-2 & OPN increase with increasing shear; increased proliferation, mineral deposition & OPN expression	[30]
	hMSCs	Increased bone area & host tissue integration in vivo	[31]
	hASCs	More homogenous cell distribution & collagen deposition; 8% increase in new bone area after 5 week culture	[32]
	hMSCs	Optimal flow rate exists in between 400 and 800 $\mu\text{m/s}$	[3]
	hMSCs	Transverse flow results in greatest MSC differentiation; parallel flow results in greater proliferation	[33]
	hMSCs	Unidirectional flow results in greater osteogenic gene expression near outlet region; alternating flow mitigated these differences	[34]

(continued)

Table 2 (continued)

Bioreactor system	Cell source	Principal finding	Refs.
Mechanical Force	Rabbit osteoprogenitor	Mechanically loaded samples showed increased collagen I& IX deposition & ECM calcification	[35]
Perfusion-compression	Human bone cells	Highest level of ALP activity in perfusion-compression cultures	[36]
	hMSCs	Perfusion culture increased proliferation; compression-perfusion increased OCN & Runx2 expression	[37]
Zetos	N/A	Mechanical loading decreases levels of cellular apoptosis	[38]
	N/A	Compressive forces increase trabecular thickness & compressive moduli	[39, 40]
Compression only	hMSCs	Physiological strain of 0.22% results in upregulation of ALP activity, ON expression, & collagen I deposition	[41]
Magnetic force	hMSCs	Mechanical stimulation of cells results in greater mineralization & collagen deposition	[42, 43]

of media allows for convective transport of nutrients and oxygen to cells throughout the entire scaffold, which increases cell viability and proliferation [4, 16, 18]. Furthermore, the dynamic environment results in the application of fluid shear forces to cells seeded on the scaffolds, particularly on the peripheral regions, which also enhances osteogenic differentiation and bone extracellular matrix (ECM) deposition [17, 18, 44]. Also, spinner flasks are utilized as a means of cell seeding, which increases cellularity in comparison to static culture and other mechanisms of dynamic seeding [20].

Applications: Several studies have investigated the effectiveness of spinner flasks for dynamic culture in BTE compared to other systems, such as rotating wall vessels (RWV), perfusion cartridges, and static culture. Sikavitsas et al. compared spinner flask culture to both RWV and static culture conditions of poly(lactic-co-glycolic acid) (PLGA) scaffolds seeded with rat bone marrow-derived MSCs [16]. In contrast with static conditions, scaffolds cultured in spinner flasks demonstrated increased cellularity, as well as an upregulation in markers of osteogenic differentiation, demonstrating the positive effect of the dynamic mixing environment on the culture of BTE constructs. However, both Sikavitsas et al. and Meinel et al. observed that mineralization occurs mostly on the outer periphery of these constructs, whereas other systems produce more homogenous mineral deposition [16, 17]. These studies demonstrate that spinner flask systems generate an uneven distribution of shear stress to cells within 3D scaffolds, resulting in uneven bone tissue development. Kim et al. sought to investigate how manipulation of scaffold design can eliminate this uneven tissue formation. By generating silk scaffolds with macroscale pores, more homogenous ECM deposition and mineralization was observed [18]. However, the use of larger scale pores resulted in mechanical properties that are less than desirable for BTE applications. This highlights the need for optimization strategies

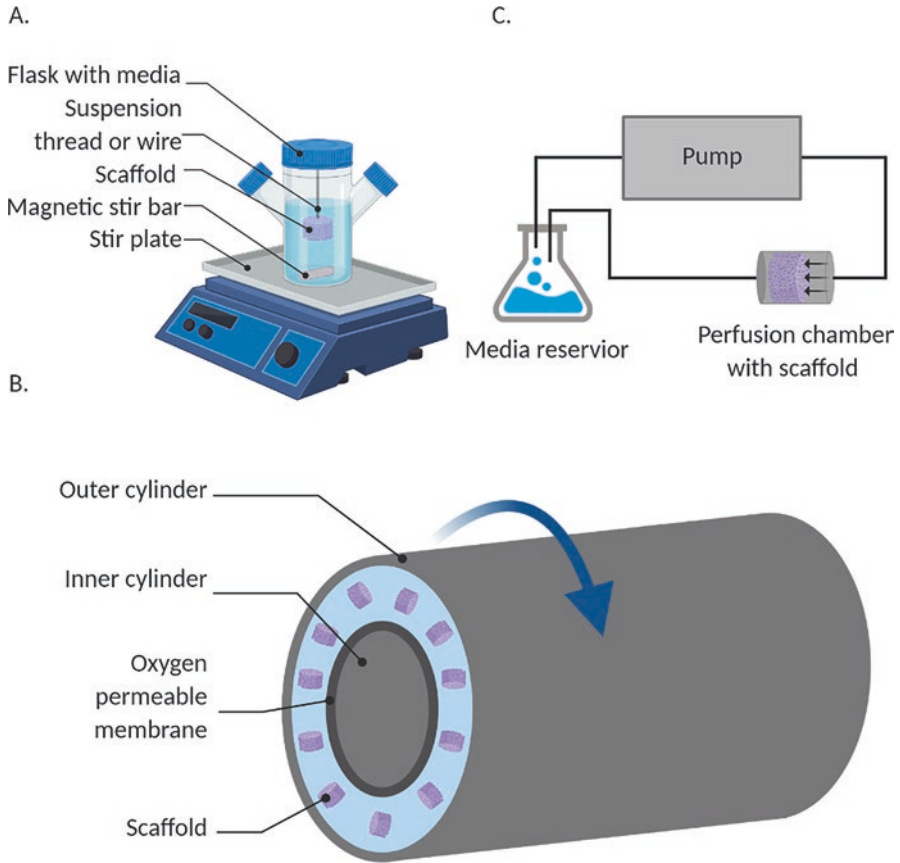


Fig. 1 Schematics of bioreactor systems. (a) Spinner flask. (b) Rotating wall vessel (arrow depicts rotation of outer cylinder) [2]. (c) Perfusion system. Perfusion chamber design varies with scaffold geometry. (Created with [BioRender.com](https://www.biorender.com))

of both scaffold design and culture conditions to balance desired tissue strength and homogenous tissue formation.

One available strategy for understanding, predicting, and optimizing nutrient transport across 3D scaffolds is computational fluid dynamics (CFD) analysis. In the case of spinner flask culture systems, various stir bar rotation speeds have been examined to determine velocity fields and shear rates within the culture vessel, providing greater insight about processing parameters that yield homogenous bone tissue formation. Most CFD analyses in spinner flask systems have been conducted to investigate optimal environments for culture of articular cartilage tissue. However, Melke et al. predicted and examined the localization of mineral deposits within silk fibroin scaffolds seeded with human bone marrow-derived MSCs as a function of wall shear stress generated by different stir bar speeds [19]. This analysis demonstrated that with increasing stirring speeds, mineral deposits were more

homogeneously distributed. Although this modeling approach is a useful tool for optimization of culture parameters, cell culture experiments conducted in parallel observing cell viability as a function of shear stress generated could provide greater insight on producing more homogenous bone tissue constructs.

These systems have also been examined as a means of dynamic cell seeding for tissue engineering constructs [20, 45]. Griffon et al. investigated a variety of dynamic seeding mechanisms, including spinner flasks, perfusion bioreactors, and orbital shakers for seeding of mouse-derived MSCs on a variety of scaffold materials. Spinner flasks demonstrated the greatest levels of DNA and cellularity in comparison to other culture methods [20]. However, other groups have seen greater success in cell seeding with perfusion bioreactors in comparison to spinner flask systems [45].

Limitations: A major restriction is the size of the constructs that can be successfully cultured using these systems. This is due to a difficult and delicate balance between convective transport via stirring and the resultant shear stress. In order to increase nutrient transport, stirring speeds are increased, which applies more shear stress to cells on the outer edges of scaffolds [4]. As these scaffolds are cultured over time, this results in greater matrix and mineral deposition on the periphery of scaffolds, creating a sharp nutrient gradient and inefficient waste removal [16, 17] on the inner portions of scaffolds, leading to necrosis [4]. The resulting non-homogeneous distribution of the deposited bone matrix severely impacts the mechanical integrity of these constructs. Because of these associated issues, culture of clinically relevant volumes of bone tissue is not currently possible using this method. The capacity of spinner flask systems to increase osteogenic differentiation and homogeneous bone matrix formation in bone tissue constructs seems promising, but significant optimization of both computational analyses and cell culture experiments needs to be conducted in order to enhance these systems' capabilities.

2.2 Rotating Wall Vessels

Rationale and design: The rotating wall vessel (RWV) bioreactor system, which is represented in the schematic in Fig. 1b, consists of two concentric cylinders, with a rotating outer cylinder and stationary inner cylinder, which contains an oxygen-permeable membrane for gas exchange [2, 4]. Media and scaffolds are present in the space between the two cylinders. RWV bioreactors create a microgravity environment in which scaffolds are in a constant state of "free fall" by balancing drag forces, centrifugal forces, and net gravitational forces [4, 8]. This design results in lower shear stresses and turbulence with increased nutrient delivery [8]. Several variations of these systems exist, including slow turning lateral vessels (STLV) and high-aspect ratio vessels (HARV). STLV systems allow for greater control over oxygen supply, pH, and temperature of the culture vessel, and HARV systems have reduced speeds and improved gas exchange [4].

Applications: One application of RWV bioreactors is to simulate the effects of “weightlessness” on the culture of bone-forming cells. The interest in studying these effects stems from observations of bone loss due to space travel, leading researchers to believe that lack of mechanical stimulation of the tissue in microgravity environments alters bone metabolic processes. Rucci et al. utilized a RWV to culture rat osteoblast-like cells that formed organoids to observe the impact of weightlessness on osteoblastic phenotype [21]. In comparison to cells cultured in a traditional static environment, RWV-cultured cells displayed upregulations in markers indicative of osteoclastic phenotypes, demonstrating that this environment can result in greater bone resorption. Similar studies evaluated the impact of microgravity on osteogenic differentiation of rat and human bone marrow-derived MSCs. Decreased proliferation and osteoblastic differentiation were observed [22], as well as upregulations in markers associated with adipogenic differentiation [23, 24]. These studies provide great insight into the underlying mechanisms of bone loss that result from microgravity environments.

To determine the efficacy of RWV to culture constructs for BTE applications, Sikavitsas et al. compared the use of RWV systems to spinner flask and static conditions for the culture of rat MSCs on PLGA scaffolds [16]. Cell proliferation and osteogenic differentiation were significantly lower in RWV than other culture conditions, leading researchers to believe that scaffold collisions with the culture vessel were detrimental to these processes. To overcome the issues associated with scaffold-wall collisions, Botchwey et al. and Yu et al. investigated the use of lighter than water (LTW) and heavier than water (HTW) PLGA microcarriers to culture osteoblast-like cells [25, 26]. The purpose of these studies was to manipulate the densities of these scaffolds to obtain greater control over scaffold movement within the vessels, therefore optimizing culture parameters to lead to increased osteogenesis. By varying the ratios of HTW and LTW microspheres, they were able to achieve a more homogenous cell distribution and upregulation in osteogenic markers in RWV systems [26]. Another optimization study conducted by Varley et al. investigated ideal operating parameters of both single and dual axis rotational reaction vessels on fetal human osteoblast proliferation on collagen-glycosaminoglycan (GAG) scaffolds [27]. By determining optimal media fill volume and rotational speed of both RWV systems, cell proliferation increased significantly in comparison to static controls. Even though this optimization strategy improved cell growth on the scaffolds within RWV structures, the researchers suggested that developing a variation of the RWV structure including perfusion could significantly enhance *in vitro* culture [27].

Limitations: Although some RWV systems demonstrate upregulation in osteogenic markers, they are not significantly different from static cultures. The microgravity environment results in low shear applications to cells within the scaffolds, which was initially hypothesized to lead to greater cell survival [8]. These vessels provide a mechanism to understand the impact of weightlessness on bone tissue formation, but they remain relatively ineffective for culturing regenerative BTE constructs. Scaffold collisions with the outer vessel walls also lead to decreased cell survival and disruption of bone tissue formation [2, 16]. To combat this, a variation

was designed in which scaffolds are fixed on the outer wall, which was demonstrated to increase cell proliferation, ECM deposition, and mineralization [2]. Another variation that was developed by Zhang et al. combined perfusion and biaxial rotation (BXR) within the same culture vessel, which led to increased proliferation and upregulation of osteogenic markers in comparison to spinner flasks, RWV, and perfusion systems [46]. Although these results are promising, researchers are turning to other dynamic culture systems due to the lack of efficacy observed in RWV systems.

2.3 Perfusion Systems

Rationale and design: Perfusion-based systems typically consist of a media reservoir, pump, and a perfusion cartridge which contains the scaffold, represented in Fig. 1c [2]. Scaffolds are press-fit to the bioreactor cartridges to allow media to perfuse directly through scaffold pores, rather than around the scaffold [2]. Two main design types for perfusion cartridges include packed and fluidized beds. Packed beds are typically used for microparticle-based scaffolds or scaffolds consisting of one piece [8]. Fluidized bed designs are mainly used for microparticle or particulate based biomaterials, which are mobilized due to the fluid flow of dynamic culture [8]. However, numerous perfusion bioreactor designs exist because their design is reliant on scaffold architecture. Media is perfused directly through scaffold pores in perfusion systems, resulting in more uniform cell seeding, osteogenic differentiation, and bone matrix production [8]. The efficiency of these systems is co-dependent on optimal scaffold properties, such as porosity [2, 47]. Because of the exciting potential that these systems have to improve the generation of bone-like tissue in vitro, several groups have also applied these systems to produce constructs of clinically relevant size, which will be discussed later in this chapter.

Applications: Because of the need to create scaffold-specific perfusion cartridges, several designs have been investigated in the context of BTE. One design that has been utilized is the tubular perfusion system (TPS) bioreactor [29–31]. Developed by Yeatts et al., this system was used to culture hMSCs in alginate beads to test the growth and differentiation of the cells within the system, as well as the effects of flow rate on these processes. Perfusion culture increased viability, proliferation, and osteogenic differentiation of hMSCs within the scaffolds [29]. The same group then investigated the effects of dynamic culture and application of shear on osteogenic differentiation and proliferation of hMSCs as a function of radial position within the same scaffolds. Over the course of the culture period, increases in DNA and osteogenic marker expression levels were observed in dynamically cultured scaffolds, whereas statically cultured scaffolds suffered from greater levels of cell death, specifically in larger scale constructs [30]. This demonstrates the capability of bioreactor culture to mitigate nutrient and oxygen diffusion limitations associated with static culture. The TPS system was used again by Yeatts et al. to culture hMSCs on electrospun nanofibrous PLGA/poly(ϵ -caprolactone) (PCL)

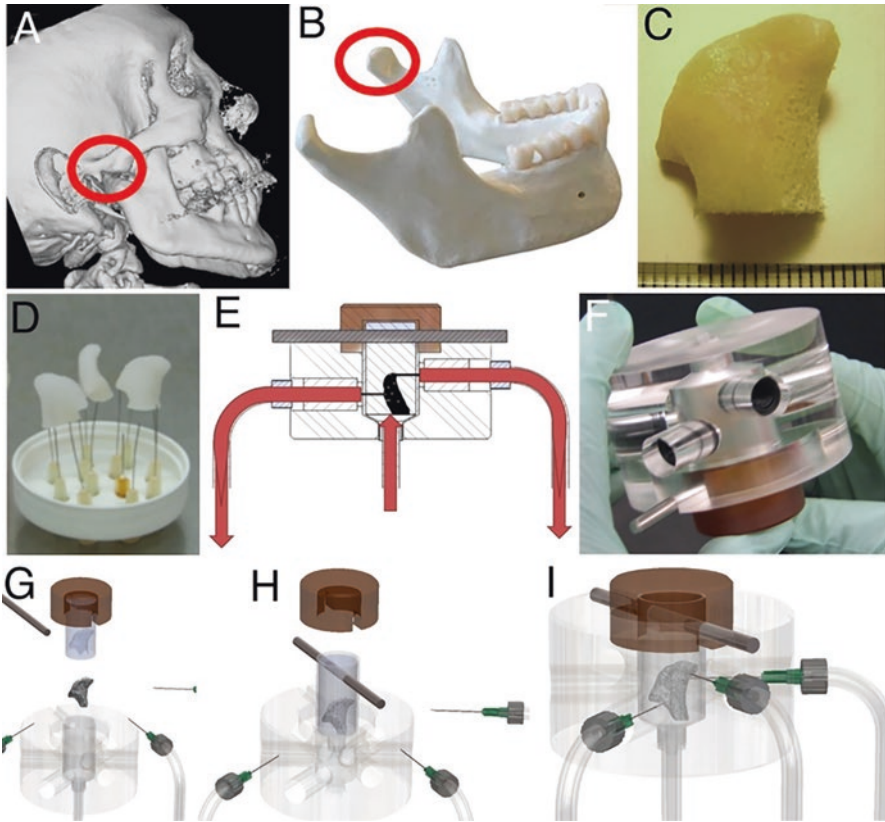


Fig. 2 Tissue engineering of anatomically shaped bone grafts. (a, b) Clinical CT imaging techniques were used to generate 3D models of TMJ. (c) Resulting machined decellularized bone scaffold. (d) Resulting scaffolds from different CT scans. (e) Culture schematic and (f) photograph of bioreactor utilized to culture TMJ constructs. (g–i) Assembly process of bioreactor. (Image adapted from [28])

scaffolds to understand the impact of dynamic culture on *in vivo* bone formation [31]. Bioreactor-cultured scaffolds exhibited the greatest increase in new bone area and better integration with host tissue, which demonstrates the positive effects of *in vitro* dynamic culture on bone tissue healing *in vivo*.

To demonstrate the capability of perfusion systems to produce complex anatomical structures of bone tissue, Grayson et al. developed a bioreactor system specifically to culture temporomandibular joints (TMJ) from decellularized bovine bone scaffolds and hMSCs [28]. As shown in Fig. 2, anatomical geometry was obtained via computed tomography (CT) imaging, which was then used to generate the polydimethylsiloxane (PDMS) fitting mechanism for the perfusion cartridge and the computer numerical control (CNC) milled scaffolds [28]. Static conditions resulted in the formation of bone matrix and mineralization primarily on the periphery of the scaffolds, while bioreactor culture groups exhibited a more even

distribution of matrix formation and greater cell proliferation [28]. This not only validates the advantages of bioreactor culture over static conditions, but also the flexibility of these systems to culture anatomically accurate bone grafts.

Frölich et al. compared static and perfusion culture conditions in control and osteogenic media using human adipose-derived stem cells (hASCs)-seeded decellularized bone scaffolds [32]. Although increases in mineralization and ECM deposition were observed, they were not statistically different from static controls, potentially due to low fluid shear rates [32]. Results such as this highlight the need for flow rate optimization studies to maximize the effectiveness of in vitro culture.

Grayson et al. conducted a flow rate optimization study to determine the impact of this parameter on osteogenic differentiation of hMSCs on decellularized bovine bone plug scaffolds in a perfusion bioreactor [3]. Flow rates and their corresponding interstitial fluid flow were determined via mathematical modeling. By observing cell and ECM distribution and gene expression, they were able to determine an optimal range of flow rates that enhanced the process of bone formation in the system. Another variation of flow optimization studies was conducted by Kim et al. by investigating the effects of parallel and transverse media flow through scaffold pores. By culturing hMSCs on polyethylene terephthalate (PET) scaffolds, it was demonstrated that transverse flow conditions increased the rate of MSC differentiation toward an osteoblastic lineage, whereas parallel flow allowed them to maintain greater proliferative potential [33]. Direction of perfusion was also investigated for its effects on osteogenic differentiation of hMSCs in alginate bead scaffolds, as a function of scaffold position within a TPS bioreactor. Nguyen et al. hypothesized that cells within these scaffolds at the inlet and outlet regions of the perfusion bioreactor experience different biochemical cues that guide osteogenic differentiation due to their differences in position [34]. Greater levels of osteogenic marker expression were observed toward the outlet region under unidirectional flow. Alternating the flow direction after 24 h mitigated these differences. The culmination of these results demonstrates the significant effort required to optimize perfusion systems in order to foster homogenous bone tissue formation.

Limitations: Although these systems show great promise for the culture of regenerative BTE constructs, several limitations exist. First, these systems are prone to leakage and contamination due to ill-fitting connections within the system. Significant optimization of processing parameters is also necessary. Ideal perfusion flow rates are necessary to determine, so as to aid in the process of osteogenic differentiation, but not to cause significant cell death within the scaffold. Bioreactor and scaffold designs must also be tuned in order to maximize the effects of the in vitro culture process. However, the use of CFD analyses allows for significant optimization within these areas prior to experimentation. Combining these analyses with perfusion bioreactor systems provides more standardized methods for producing clinically relevant volumes of bone tissue. Because perfusion systems overcome the issues associated with other bioreactor systems and static culture, these bioreactors and their derivatives present the most potential for use in clinical scenarios.

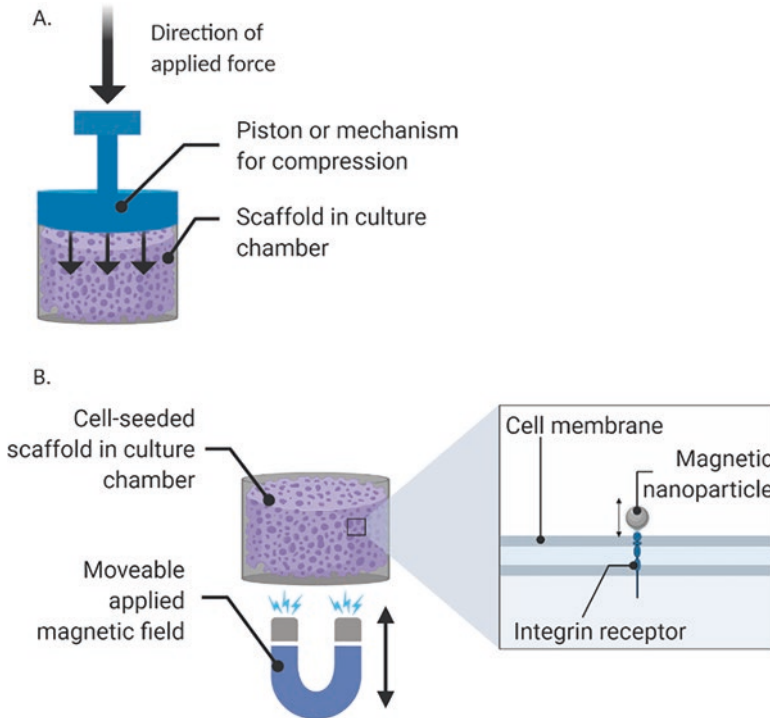


Fig. 3 Schematics of mechanical force bioreactor systems. (a) Compression bioreactor—arrows indicate direction of force applied to the system & the scaffold. (b) Magnetic force bioreactor—arrows indicate direction of movement of magnetic field and nanoparticle. (Created with Biorender.com)

2.4 Mechanical Force Systems

Rationale and design: The objective of mechanical force bioreactor systems is to more accurately mimic the mechanical loading forces, such as tension and compression, in the *in vivo* bone microenvironment. These forces are a result of regular physical movements such as walking, running, or jumping and are instrumental in guiding bone growth, remodeling, and other metabolic processes [4, 8]. Several designs have been investigated in the context of BTE, but the most common includes the application of compressive forces, which is often used in combination with perfusion. The synergistic relationship between fluid perfusion and compressive forces both mimics natural loading conditions of bone, while also recreating the *in vivo* microenvironment of interstitial canalicular flow in response to those loading conditions. These systems are typically composed of similar elements as traditional perfusion systems, but culture chambers include mechanisms for compressive force application, such as a piston driven by pneumatic pressure. Using compression systems to apply physiologically relevant loads in cyclic loading conditions increases

cellularity, matrix production, and osteogenic gene expression [8]. Another variation is the magnetic force bioreactor (MFBs), in which magnetic nanoparticles are attached to the cell membrane and force is applied via a magnetic field [4]. This system allows for forces to be applied directly to the cell membrane, rather than to the scaffold and then transmitted to cells. Because other systems require an external mechanism for forces of compression, this damages scaffold integrity and increases risk of infection. These are the limitations that magnetic force bioreactors seek to address. Both compression and magnetic force systems are represented in Fig. 3.

Applications: Matziolis et al. developed a compression-based system to simulate the in vivo fracture healing environment and investigate cell response [35]. The upper membrane of the system, driven by pneumatic pressure, applied compressive forces that mimic the cyclic loading cycle experienced by bone. Mechanically loaded scaffolds demonstrated an increase in ECM deposition and calcification, validating that the application of compressive forces aids in the process of bone tissue formation [35].

The application of compressive forces has been demonstrated to upregulate osteogenesis, but several groups investigated the use of compression-perfusion culture systems to more accurately replicate the in vivo fluid microenvironment of bone [36, 37]. Both Bölgen et al. and Jagodinski et al. conducted studies comparing perfusion, compression-perfusion, and static conditions. Although both dynamic environments resulted in homogenous tissue formation, markers of osteogenesis were significantly upregulated in compression-perfusion cultures, demonstrating the potential for these combined systems to enhance the process of bone tissue development.

One mechanical loading bioreactor system that has been investigated extensively for its use in culturing bone explants is the Zetos system [38–40, 48, 49]. Developed by Davies et al., this system has been utilized to culture human, bovine, and ovine trabecular bone explants to determine the effect of mechanical loading on cell and tissue response. Mann et al. investigated how mechanical loading simulating a jumping exercise impacted cellular apoptosis and bone formation in human trabecular bone. Their study established that mechanical stimulation decreased levels of apoptosis, whereas unloaded conditions resulted in decreased osteocyte viability and increased apoptotic behavior [38]. This same system was employed to investigate its effects on the mechanical properties of bovine bone, demonstrating that cyclic compression increases the thickness of trabeculae and compressive modulus [39, 40]. Endres et al. investigated several loading conditions for their effects on bovine bone stiffness and osteoid deposition, finding that stiffness increases with applied strain, but also depends on the amount of matrix deposited [49]. Overall, these studies demonstrate that viable bone explants are better maintained under loading conditions, but the system has yet to be applied to engineered bone tissue.

Previous studies reported various levels of loading conditions, all of which seemed to have a positive impact on bone formation or mechanical properties of the engineered or explanted constructs. However, Ravichandran et al. sought to investigate how physiologically relevant strains impact early osteogenesis on constructs in a compression bioreactor [41]. This study demonstrated that physiological loading

conditions caused an upregulation in osteogenic markers and ECM calcification earlier in the culture period than other strain levels and static controls. This presents a potential benefit for future clinical translation because culture times can be reduced due to the increased rate of bone tissue formation.

Another variation of mechanical loading bioreactors are MFBs. These systems apply different mechanical forces directly to cell membranes via membrane-attached magnetic nanoparticles [4]. The magnitude of the force applied changes based on the strength of the magnetic field. In comparison to other mechanical conditioning bioreactor systems, this system has several advantages, such as lesser risk of infection, precise control over applied force, no necessary optimization of scaffold parameters, and a scalable system [4]. Several groups have investigated the use of these bioreactors in BTE [42, 43]. Kanczler et al. targeted membrane potassium channels and integrin receptors to assess how loading on these targeted proteins affects osteogenesis and chondrogenesis in hMSCs. Markers of both processes were significantly upregulated when these proteins were mechanically stimulated. [42] Henstock et al. targeted the same membrane proteins in hMSCs and injected these mechanically conditioned cells into a chick fetal femur model for endochondral bone formation [43]. Mechanically stimulated cells mineralized the injection site better than unlabeled controls. The culmination of these results demonstrates the potential for MFBs to enhance bone regeneration by stimulating specific membrane proteins. However, it has yet to be investigated how they compare to other well-established systems.

Limitations: One major limitation associated with the design of mechanical force bioreactors is that the mechanisms that apply compressive forces enter the sterile bioreactor environment, which leads to potential contamination [4]. While mechanical conditioning has been demonstrated to increase the mechanical properties of BTE constructs, the scaffold material must withstand the forces applied over the culture period without rapid degradation in order to maintain relevance for clinical applications. It is therefore necessary to optimize scaffold material properties and fabrication strategy in order to ensure compatibility with these systems. Optimization of scaffold properties and operating conditions is challenging, but the use of finite element analysis and computational modeling aids in this process in silico prior to experimentation [50–52].

3 Biomanufacturing and Scale-Up

One of the greatest challenges is translating bioreactor technologies to a clinical setting. Several factors influence their translational capacity, but the most prevalent is their potential to generate clinically relevant volumes of bone. Although dynamic culture enhances osteogenesis and cell survival within scaffolds, the scale at which they are typically produced is that of a small in vivo animal model. Several groups have recently demonstrated that these systems can maintain clinically relevant volumes of bone for larger animal studies or human-sized defects, and they are

Table 3 Summary of scale-up bioreactor systems and dimensions of scaffolds successfully cultured

Scale-up bioreactor system	Scaffolds cultured	Refs.
Perfusion	(P[LLA- <i>co</i> -CL]) porous scaffolds 10.5 mm & 25 mm in diameter	[60]
Bidirectional continuous perfusion bioreactor	Starch/PCL fiber meshes 42 mm diameter	[53]
TPS	200 cm ³ of alginate beads in the shape of superior half of human femur	[54]
Direct perfusion	10 cm ³ of β -TCP implanted subcutaneously in nude mice	[55, 56]
	30 mm of β -TCP implanted in goat tibial defects	[57]
In vivo	AG or SG materials implanted to repair defects 15–19 mm length & 5–6 mm height	[58, 59]

summarized in Table 3. Most of these systems consist of perfusion bioreactors, but several groups have also investigated the use of in vivo bioreactors. In vivo bioreactors consist of a polymethyl methacrylate (PMMA) chamber filled with autograft or synthetic bone substitutes that are implanted into the rib periosteum to allow for ingrowth of vasculature and tissue development. The tissue developed in this chamber is then resected and used to repair a defect site within the same animal model.

Because perfusion systems demonstrated the most potential for BTE applications, these systems have also been applied in the scale-up movement for clinical relevance. Gardel et al. designed a perfusion-based system called the bidirectional continuous perfusion bioreactor (BCPB), in which the scaffold chamber consists of a center tube with perforations that the scaffold surrounds [53]. Using this system, researchers maintained the culture of a 42-mm thick scaffold containing goat bone marrow-derived MSCs. Similarly, Kleinhans et al. used another perfusion system to culture hMSCs on large-scale poly(L-lactide-*co*-caprolactone) (P[LLA-*co*-CL]) porous scaffolds [60]. Comparing static and dynamic seeding of cells, bioreactor-cultured constructs demonstrated more homogenous cell distributions, as well as an upregulation of markers of osteogenesis. These studies validate the feasibility in culturing large-scale constructs and inducing bone tissue formation through the use of bioreactor culture.

To confirm the possibility of culturing BTE constructs mimicking anatomical geometry and size of the greater half of a human femur, Nguyen et al. utilized a larger scale TPS bioreactor to culture hMSC-laden alginate beads, creating a volume of 200 cm³ of bone-like tissue, shown in Fig. 4 [54]. Cell viability was successfully maintained throughout the entire tissue. Although osteogenic marker expression was upregulated toward outer portions of the construct, the researchers hypothesized that this could lead to the development of cortical and cancellous bone tissue within the femur, more closely mimicking the structure of native bone. This study establishes both the scalability and the exciting potential of dynamic culture systems to maintain clinically relevant volumes and geometries of BTE constructs.

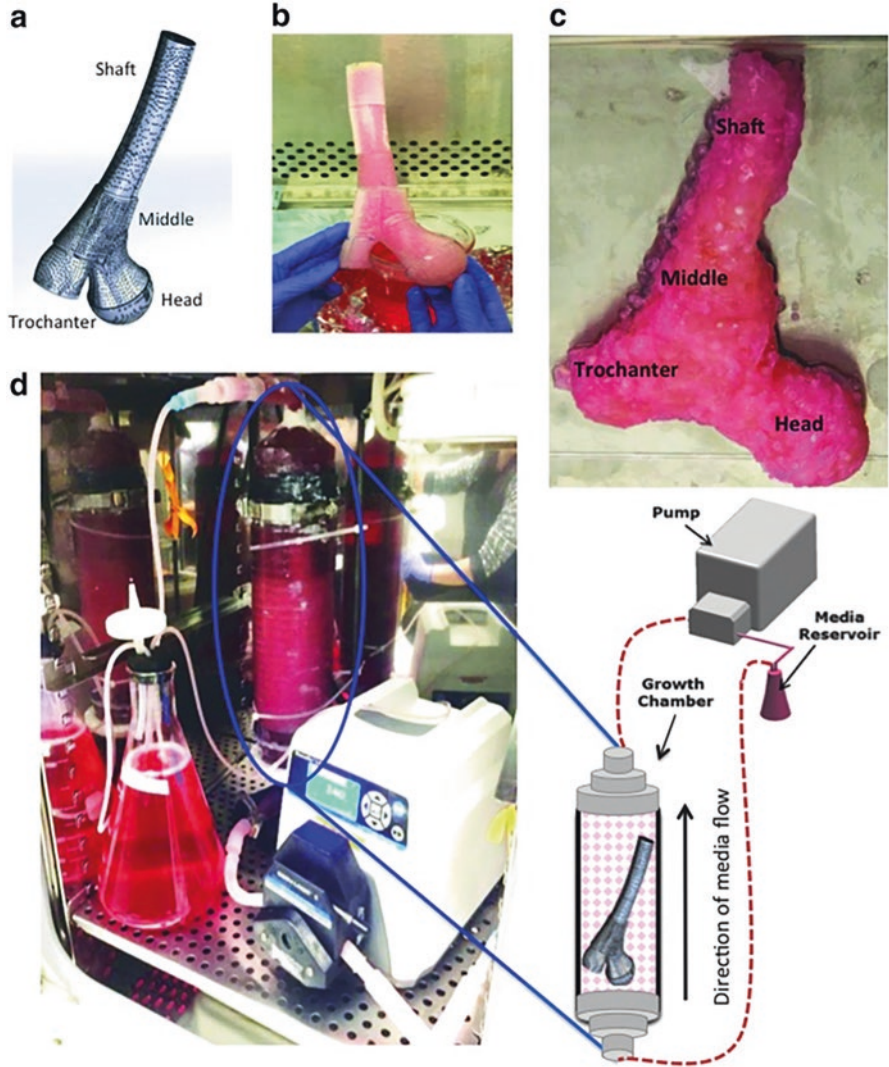


Fig. 4 Design, fabrication, and culture of human femur graft. (a) 3D CAD model of superior half of human femur. (b) 3D printed mold containing cell-laden alginate beads. (c) Aggregated construct. (d) Image of large scale TPS bioreactor setup. (Image adapted from [54])

Several *in vivo* studies have been conducted utilizing large-scale engineered bone tissue constructs cultured in dynamic conditions. Janssen et al. adapted a direct perfusion bioreactor system to culture goat bone marrow-derived MSCs or hMSCs on β -TCP scaffolds with an online monitoring system of oxygen consumption [55, 56]. Although no concrete differences were observed between static and dynamically cultured constructs *in vivo*, the addition of online monitoring capabilities

increases the clinical relevance by reducing the possibility of infection, minimizing transfers, and reducing the necessary monitoring procedures. To demonstrate the ability of these systems to be used in larger in vivo models, Wang et al. developed a perfusion-based system to culture goat bone marrow-derived MSCs on β -TCP scaffolds for goat tibial defects [57]. Constructs cultured dynamically exhibited greater mineral deposition and host tissue integration in vivo. While these results show promise for the use of dynamically cultured constructs in vivo, further research is needed to understand exactly how these culture environments influence bone tissue formation.

Another bioreactor design for the generation of large-scale BTE constructs is the in vivo bioreactor. Tatara et al. utilized this design to compare autograft and synthetic materials and their potential to regenerate mandibles in sheep models [58, 59]. Although these materials exhibited significantly lower bone densities than native mandibles when evaluated after resection, this study revealed the feasibility of this approach to generate vascularized bone tissue substitutes. The group also used 3D printed bioreactors of the same design to culture similar materials [61]. Using 3D printing to fabricate bioreactors allows for the culture and maintenance of patient-specific grafts, further increasing clinical translation potential. These strategies utilize common clinical imaging techniques, such as CT or MRI, to obtain scans of the patient defect, which can be reconstructed into 3D models that are compatible with printing software.

These studies validate the potential for bioreactor platforms to produce larger scale constructs of both clinically relevant size and shape. Although several in vivo studies have been conducted, further research is needed to understand the relationship between dynamic culture and bone regeneration. There are also several other factors that need to be optimized before these technologies are able to be utilized as new clinical standards of care.

4 Future Considerations for Clinical Translation

Bioreactor systems are utilized to overcome the issues associated with static culture of three-dimensional constructs. However, several improvements need to be made to increase their relevance to clinical applications.

4.1 Culture of Patient-Specific Grafts

Generation of patient-specific grafts from synthetic materials and readily available cells would mitigate the need for harvesting autologous tissue. Because these defects often require complex geometrical structures, it is necessary to find methods to successfully generate and culture these constructs. Traditional clinical imaging techniques can be utilized to generate 3D models of the defect site and additive

manufacturing technologies can be used to fabricate both synthetic grafts and bioreactors for dynamic culture. Costa et al. utilized additive manufacturing technologies to fabricate scaffolds and a perfusion bioreactor chamber for ovine tibia defects [62]. After conducting computational studies to optimize fluid flow rate in these bioreactors, scaffolds were seeded and cultured with primary human osteoblasts, resulting in relatively high cell viability [62]. Although this shows promise for the use of 3D printing technologies as a means of fabrication of bioreactors, further research is needed to confirm the potential of enhancing osteogenesis within these systems in comparison to static culture. Not only would 3D-printed bioreactors allow for the generation of patient specific grafts, but they would also enhance the process of biomanufacturing such scaffolds due to the ease with which these systems could be fabricated. This would be beneficial for the production of multiple patient-specific grafts at one time because the culture of 3D constructs varies significantly based on processing parameters and cell behavior. Generating multiple grafts at one time would allow for the “best” graft to be implanted [63]. However, optimizing processing parameters and cell seeding could further improve bioreactor systems.

4.2 Automation and Monitoring

Another crucial step toward clinical translation for these bioreactor systems is the inclusion of monitoring systems and automation of processes such as cell seeding and culture. Current research strategies rely heavily on manual labor and the technique of researchers. However, in order for these systems to be implemented on a large biomanufacturing scale, the level of manual labor and manipulation of tissue engineered constructs must be reduced in order to decrease variability. First, these systems should be implemented for cell seeding, rather than relying on manual seeding methods. Also, online and in situ monitoring of culture environment would reduce manual labor. Several groups have investigated the use of oxygen monitoring systems within culture vessels to monitor tissue culture without having to manipulate the constructs [55, 56]. These systems can be further improved by introducing feedback monitoring loops of quantitative markers for osteogenesis [63]. The generation of imaging-compatible bioreactor systems to monitor the growth and development of tissue engineered bone has also been investigated [63]. In addition to quantifying growth, online monitoring systems should be designed for easy manipulation without significant technical training. Automating these processes and designing user-friendly interfaces would optimize the potential for clinical translation and significantly reduce the variability associated with traditional tissue culture techniques.

4.3 Optimization

The greatest challenge that researchers face in translating bioreactor systems to clinical scenarios involves the process of optimization. Although bioreactors have been investigated extensively in the context of BTE, each specific design requires optimization of processing parameters so as to generate the most functional tissue constructs. From the cell type to flow rates and culture times, there are several variables that need to be optimized and standardized in order to make these systems more clinically relevant. For this reason, computational fluid dynamic studies within specific culture vessels should be conducted prior to experimentation. This will allow for the most ideal generation of synthetic bone grafts. Although these systems show great promise, significant research is needed in establishing a standardized use of bioreactors before they can be translated to the clinics.

References

1. Amini AR, Laurencin CT, Nukavarapu SP. Bone tissue engineering: recent advances and challenges. *Crit Rev Biomed Eng.* 2012;40:363. <https://doi.org/10.1615/CritRevBiomedEng.v40.i5.10>.
2. Yeatts AB, Fisher JP. Bone tissue engineering bioreactors: dynamic culture and the influence of shear stress. *Bone.* 2011;48:171. <https://doi.org/10.1016/j.bone.2010.09.138>.
3. Grayson WL, et al. Optimizing the medium perfusion rate in bone tissue engineering bioreactors. *Biotechnol Bioeng.* 2011;108:1151. <https://doi.org/10.1002/bit.23024>.
4. El Haj AJ, Cartmell SH. Bioreactors for bone tissue engineering. *Proc Inst Mech Eng H J Eng Med.* 2010;224:1523. <https://doi.org/10.1243/09544119JEIM802>.
5. Kim YS, Majid M, Melchiorri AJ, Mikos AG. Applications of decellularized extracellular matrix in bone and cartilage tissue engineering. *Bioeng Transl Med.* 2019;4:83. <https://doi.org/10.1002/btm2.10110>.
6. Rouwkema J, Koopman BFJM, Blitterswijk CAV, Dhert WJA, Malda J. Supply of nutrients to cells in engineered tissues. *Biotechnol Genet Eng Rev.* 2010;26:163. <https://doi.org/10.5661/bger-26-163>.
7. Filipowska J, Tomaszewski KA, Niedźwiedzki Ł, Walocha JA, Niedźwiedzki T. The role of vasculature in bone development, regeneration and proper systemic functioning. *Angiogenesis.* 2017;20:291. <https://doi.org/10.1007/s10456-017-9541-1>.
8. Carpentier B, Layrolle P, Legallais C. Bioreactors for bone tissue engineering. *Int J Artif Organs.* 2011;34:259. <https://doi.org/10.5301/IJAO.2011.6333>.
9. Martin Y, Vermette P. Bioreactors for tissue mass culture: design, characterization, and recent advances. *Biomaterials.* 2005;26:7481. <https://doi.org/10.1016/j.biomaterials.2005.05.057>.
10. Yourek G, McCormick SM, Mao JJ, Reilly GC. Shear stress induces osteogenic differentiation of human mesenchymal stem cells. *Regen Med.* 2010;5:713. <https://doi.org/10.2217/rme.10.60>.
11. Lovett M, Lee K, Edwards A, Kaplan DL. Vascularization strategies for tissue engineering. *Tissue Eng Part B Rev.* 2009;15:353. <https://doi.org/10.1089/ten.teb.2009.0085>.
12. Hansmann J, Groeber F, Kahlig A, Kleinhans C, Walles H. Bioreactors in tissue engineering-principles, applications and commercial constraints. *Biotechnol J.* 2013;8:298. <https://doi.org/10.1002/biot.201200162>.
13. Hutmacher DW, et al. Bioreactor for growing cell or tissue cultures. U.S. Patent Application Publication; 2006.

14. Ahmed S, Chauhan VM, Ghaemmaghami AM, Aylott JW. New generation of bioreactors that advance extracellular matrix modelling and tissue engineering. *Biotechnol Lett.* 2019;41:1. <https://doi.org/10.1007/s10529-018-2611-7>.
15. Buesch S, Schroeder J, Bunger M, D'Souza T, Stosik M. A novel in vitro liver cell culture flow system allowing long-term metabolism and hepatotoxicity studies. *Appl Vit Toxicol.* 2018; 4:232. <https://doi.org/10.1089/aivt.2018.0009>
16. Kim HJ, et al. Bone regeneration on macroporous aqueous-derived silk 3-D scaffolds. *Macromol Biosci.* 2007;7:643. <https://doi.org/10.1002/mabi.200700030>.
17. Melke J, Zhao F, Rietbergen B, Ito K, Hofmann S. Localisation of mineralised tissue in a complex spinner flask environment correlates with predicted wall shear stress level localisation. *Eur Cells Mater.* 2018;36:57. <https://doi.org/10.22203/eCM.v036a05>.
18. Griffon DJ, Abulencia JP, Ragetly GR, Fredericks LP, Chaieb S. A comparative study of seeding techniques and three-dimensional matrices for mesenchymal cell attachment. *J Tissue Eng Regen Med.* 2011;5:169. <https://doi.org/10.1002/term.302>.
19. Rucci N, Migliaccio S, Zani BM, Taranta A, Teti A. Characterization of the osteoblast-like cell phenotype under microgravity conditions in the NASA-approved rotating wall vessel bioreactor (RWV). *J Cell Biochem.* 2002;85:167. <https://doi.org/10.1002/jcb.10120>.
20. Sikavitsas VI, Bancroft GN, Mikos AG. Formation of three-dimensional cell/polymer constructs for bone tissue engineering in a spinner flask and a rotating wall vessel bioreactor. *J Biomed Mater Res.* 2002;62:136. <https://doi.org/10.1002/jbm.10150>.
21. Meinel L, et al. Bone tissue engineering using human mesenchymal stem cells: effects of scaffold material and medium flow. *Ann Biomed Eng.* 2004;32:112. <https://doi.org/10.1023/B:ABME.0000007796.48329.b4>.
22. Gomes ME, Sikavitsas VI, Behravesh E, Reis RL, Mikos AG. Effect of flow perfusion on the osteogenic differentiation of bone marrow stromal cells cultured on starch-based three-dimensional scaffolds. *J Biomed Mater Res A.* 2003;67:87. <https://doi.org/10.1002/jbm.a.10075>. PMID: 14517865
23. Chen X, et al. Mechanical stretch-induced osteogenic differentiation of human jaw bone marrow mesenchymal stem cells (hJBMMSCs) via inhibition of the NF- κ B pathway. *Cell Death Dis.* 2018; 9:207. <https://doi.org/10.1038/s41419-018-0279-5>.
24. Nettelhoff L, et al. Influence of mechanical compression on human periodontal ligament fibroblasts and osteoblasts. *Clin Oral Investig.* 2016; 20:621. <https://doi.org/10.1007/s00784-015-1542-0>.
25. Chen J, et al. Chromium oxide nanoparticle impaired osteogenesis and cellular response to mechanical stimulus. *Int J Nanomedicine.* 2021; 16:6157. <https://doi.org/10.2147/IJN.S317430>.
26. Dai ZQ, Wang R, Ling SK, Wan YM, Li YH. Simulated microgravity inhibits the proliferation and osteogenesis of rat bone marrow mesenchymal stem cells. *Cell Prolif.* 2007;40:671. <https://doi.org/10.1111/j.1365-2184.2007.00461.x>.
27. Zayzafoon M, Gathings WE, McDonald JM. Modeled microgravity inhibits osteogenic differentiation of human mesenchymal stem cells and increases adipogenesis. *Endocrinology.* 2004;145:2421. <https://doi.org/10.1210/en.2003-1156>.
28. Sheyn D, Pelled G, Netanel D, Domany E, Gazit D. The effect of simulated microgravity on human mesenchymal stem cells cultured in an osteogenic differentiation system: a bioinformatics study. *Tissue Eng Part A.* 2010;16:3403. <https://doi.org/10.1089/ten.tea.2009.0834>.
29. Botchwey EA, Pollack SR, Levine EM, Laurencin CT. Bone tissue engineering in a rotating bioreactor using a microcarrier matrix system. *J Biomed Mater Res.* 2001;55:242. [https://doi.org/10.1002/1097-4636\(200105\)55:2<242::AID-JBM1011>3.0.CO;2-D](https://doi.org/10.1002/1097-4636(200105)55:2<242::AID-JBM1011>3.0.CO;2-D).
30. Yu X, Botchwey EA, Levine EM, Pollack SR, Laurencin CT. Bioreactor-based bone tissue engineering: the influence of dynamic flow on osteoblast phenotypic expression and matrix mineralization. *Proc Natl Acad Sci U S A.* 2004;101:11203. <https://doi.org/10.1073/pnas.0402532101>.
31. Varley MC, Markaki AE, Brooks RA. Effect of rotation on scaffold motion and cell growth in rotating bioreactors. *Tissue Eng A.* 2017;23:522. <https://doi.org/10.1089/ten.tea.2016.0357>.

32. Grayson WL, et al. Engineering anatomically shaped human bone grafts. *Proc Natl Acad Sci U S A*. 2010;107:3299. <https://doi.org/10.1073/pnas.0905439106>.
33. Yeatts AB, Fisher JP. Tubular perfusion system for the long-term dynamic culture of human mesenchymal stem cells. *Tissue Eng Part C Methods*. 2011;17:337. <https://doi.org/10.1089/ten.tec.2010.0172>.
34. Yeatts AB, Geibel EM, Fears FF, Fisher JP. Human mesenchymal stem cell position within scaffolds influences cell fate during dynamic culture. *Biotechnol Bioeng*. 2012;109:2381. <https://doi.org/10.1002/bit.24497>.
35. Yeatts AB, et al. In vivo bone regeneration using tubular perfusion system bioreactor cultured nanofibrous scaffolds. *Tissue Eng Part A*. 2014;20:139. <https://doi.org/10.1089/ten.tea.2013.0168>.
36. Fröhlich M, et al. Bone grafts engineered from human adipose-derived stem cells in perfusion bioreactor culture. *Tissue Eng Part A*. 2010;16:179. <https://doi.org/10.1089/ten.tea.2009.0164>.
37. Kim J, Ma T. Perfusion regulation of hMSC microenvironment and osteogenic differentiation in 3D scaffold. *Biotechnol Bioeng*. 2012;109:252. <https://doi.org/10.1002/bit.23290>.
38. Nguyen BNB, Ko H, Fisher JP. Tunable osteogenic differentiation of hMPCs in tubular perfusion system bioreactor. *Biotechnol Bioeng*. 2016;113:10805. <https://doi.org/10.1002/bit.25929>.
39. Matziolis G, et al. Simulation of cell differentiation in fracture healing: mechanically loaded composite scaffolds in a novel bioreactor system. *Tissue Eng*. 2006;12:201. <https://doi.org/10.1089/ten.2006.12.201>.
40. Bölgen N, et al. Three-dimensional ingrowth of bone cells within biodegradable cryogel scaffolds in bioreactors at different regimes. *Tissue Eng Part A*. 2008;14:1743. <https://doi.org/10.1089/ten.tea.2007.0277>.
41. Jagodzinski M, et al. Influence of perfusion and cyclic compression on proliferation and differentiation of bone marrow stromal cells in 3-dimensional culture. *J Biomech*. 2008;41:1885. <https://doi.org/10.1016/j.jbiomech.2008.04.001>.
42. Mann V, Huber C, Kogianni G, Jones D, Noble B. The influence of mechanical stimulation on osteocyte apoptosis and bone viability in human trabecular bone. *J Musculoskelet Neuronal Interact*. 2006;6:408.
43. David V, et al. Ex vivo bone formation in bovine trabecular bone cultured in a dynamic 3D bioreactor is enhanced by compressive mechanical strain. *Tissue Eng Part A*. 2008;14:117. <https://doi.org/10.1089/ten.a.2007.0051>.
44. Vivanco J, et al. Apparent elastic modulus of ex vivo trabecular bovine bone increases with dynamic loading. *Proc Inst Mech Eng Part H J Eng Med*. 2013;227:904. <https://doi.org/10.1177/0954411913486855>.
45. Ravichandran A, et al. In vitro cyclic compressive loads potentiate early osteogenic events in engineered bone tissue. *J Biomed Mater Res B Appl Biomater*. 2017;105:2366. <https://doi.org/10.1002/jbm.b.33772>.
46. Kanczler JM, et al. Controlled differentiation of human bone marrow stromal cells using magnetic nanoparticle technology. *Tissue Eng Part A*. 2010;16:3241. <https://doi.org/10.1089/ten.tea.2009.0638>.
47. Henstock JR, Rotherham M, Rashidi H, Shakesheff KM, El Haj AJ. Remotely activated mechanotransduction via magnetic nanoparticles promotes mineralization synergistically with bone morphogenetic protein 2: applications for injectable cell therapy. *Stem Cells Transl Med*. 2014;3:1363. <https://doi.org/10.5966/sctm.2014-0017>.
48. Wang TW, Wu HC, Wang HY, Lin FH, Sun JS. Regulation of adult human mesenchymal stem cells into osteogenic and chondrogenic lineages by different bioreactor systems. *J Biomed Mater Res A*. 2009;88:935. <https://doi.org/10.1002/jbm.a.31914>.
49. Wendt D, Marsano A, Jakob M, Heberer M, Martin I. Oscillating perfusion of cell suspensions through three-dimensional scaffolds enhances cell seeding efficiency and uniformity. *Biotechnol Bioeng*. 2003;84:205. <https://doi.org/10.1002/bit.10759>.

50. Zhang ZY, et al. A comparison of bioreactors for culture of fetal mesenchymal stem cells for bone tissue engineering. *Biomaterials*. 2010;31:8684. <https://doi.org/10.1016/j.biomaterials.2010.07.097>.
51. Gomes ME, Reis RL, Mikos AG. Bone tissue engineering constructs based on starch scaffolds and bone marrow cells cultured in a flow perfusion bioreactor. In: *Materials Science Forum*; 2006.
52. Davies CM, et al. Mechanically loaded ex vivo bone culture system 'Zetos': systems and culture preparation. *Eur Cells Mater*. 2006;11:57. <https://doi.org/10.22203/eCM.v011a07>.
53. Endres S, Kratz M, Wunsch S, Jones DB. Zetos: a culture loading system for trabecular bone. Investigation of different loading signal intensities on bovine bone cylinders. *J Musculoskeletal Neuronal Interact*. 2009;9:173.
54. Wood MA, et al. Correlating cell morphology and osteoid mineralization relative to strain profile for bone tissue engineering applications. *J R Soc Interface*. 2008;5:899. <https://doi.org/10.1098/rsif.2007.1265>.
55. Baas E, Kuiper JH, Yang Y, Wood MA, El Haj AJ. In vitro bone growth responds to local mechanical strain in three-dimensional polymer scaffolds. *J Biomech*. 2010;43:733. <https://doi.org/10.1016/j.jbiomech.2009.10.016>.
56. Birmingham E, Niebur GL, McNamara LM, McHugh PE. An experimental and computational investigation of bone formation in mechanically loaded trabecular bone explants. *Ann Biomed Eng*. 2016;44:1191. <https://doi.org/10.1007/s10439-015-1378-4>.
57. Gardel LS, Correia-Gomes C, Serra LA, Gomes ME, Reis RL. A novel bidirectional continuous perfusion bioreactor for the culture of large-sized bone tissue-engineered constructs. *J Biomed Mater Res B Appl Biomater*. 2013;101:1377. <https://doi.org/10.1002/jbm.b.32955>.
58. Nguyen BNB, Ko H, Moriarty RA, Etheridge JM, Fisher JP. Dynamic bioreactor culture of high volume engineered bone tissue. *Tissue Eng Part A*. 2016;22:263. <https://doi.org/10.1089/ten.tea.2015.0395>.
59. Janssen FW, Oostru J, Van Oorschot A, Van Blitterswijk CA. A perfusion bioreactor system capable of producing clinically relevant volumes of tissue-engineered bone: in vivo bone formation showing proof of concept. *Biomaterials*. 2006;27:315. <https://doi.org/10.1016/j.biomaterials.2005.07.044>.
60. Janssen FW, et al. Human tissue-engineered bone produced in clinically relevant amounts using a semi-automated perfusion bioreactor system: a preliminary study. *J Tissue Eng Regen Med*. 2010;4:12. <https://doi.org/10.1002/term.197>.
61. Wang C, et al. Repair of segmental bone-defect of goat's tibia using a dynamic perfusion culture tissue engineering bone. *J Biomed Mater Res A*. 2010;92:1145. <https://doi.org/10.1002/jbm.a.32347>.
62. Tataru AM, et al. Autologously generated tissue-engineered bone flaps for reconstruction of large mandibular defects in an ovine model. *Tissue Eng Part A*. 2015;21:1520. <https://doi.org/10.1089/ten.tea.2014.0426>.
63. Tataru AM, et al. Reconstruction of large mandibular defects using autologous tissues generated from in vivo bioreactors. *Acta Biomater*. 2016;45:72. <https://doi.org/10.1016/j.actbio.2016.09.013>.
64. Kleinhans C, et al. A perfusion bioreactor system efficiently generates cell-loaded bone substitute materials for addressing critical size bone defects. *Biotechnol J*. 2015;10:1727. <https://doi.org/10.1002/biot.201400813>.
65. Tataru AM, et al. Biomaterials-aided mandibular reconstruction using in vivo bioreactors. *Proc Natl Acad Sci U S A*. 2019;116:6954. <https://doi.org/10.1073/pnas.1819246116>.
66. Costa PF, et al. Biofabrication of customized bone grafts by combination of additive manufacturing and bioreactor knowhow. *Biofabrication*. 2014;6:035006. <https://doi.org/10.1088/1758-5082/6/3/035006>.
67. Salter E, et al. Bone tissue engineering bioreactors: a role in the clinic? *Tissue Eng Part B Rev*. 2012;18:62–75.

Strategies for 3D Printing of Vascularized Bone



Favour Obuseh, Christina Jones, and Eric M. Brey

1 Introduction

The fields of tissue engineering and regenerative medicine seek to combine concepts from medicine, biology, materials science, engineering, and other related fields to develop strategies for replacing damaged or diseased tissues and organs. While progress has been made in engineering tissues that exhibit successful functional outcomes in small animal models, the growth of tissues to the relevant size and complexity required for clinical application is limited. This is due, in part, to the requirement of coordinating tissue formation with the assembly of a complex, functional vasculature, a frontier yet to be fully realized. The fabrication of three-dimensional blood vessels designed to meet the structural and functional requirements of a given tissue has the potential to revolutionize the field of tissue engineering.

In general, cells are located within 100–300 μm of a capillary. The vasculature functions to distribute oxygen, cells, and nutrients enable tissue–tissue communication and remove wastes. In the absence of vascularization, tissues are generally limited to less than a few millimeters in thickness. Attempts to engineer larger tissues may result in central necrosis due to the lack of sufficient oxygen or other nutrients within the tissue. Developing methods for growing tissues and organs of size relevant to clinical application requires control over the growth of vasculature that meets the specific metabolic demands of a tissue. While tissue engineers have shown an ability to grow capillary networks or large vessels separately, building extensive, functional vascular system is one of the most sought-after advances in the field of tissue engineering [1].

F. Obuseh · C. Jones · E. M. Brey (✉)

Department of Biomedical Engineering and Chemical Engineering, Institute of Regenerative Medicine, The University of Texas at San Antonio, San Antonio, TX, USA

e-mail: eric.brey@utsa.edu

© Springer Nature Switzerland AG 2022

F. P. S. Guastaldi, B. Mahadik (eds.), *Bone Tissue Engineering*,
https://doi.org/10.1007/978-3-030-92014-2_11

249

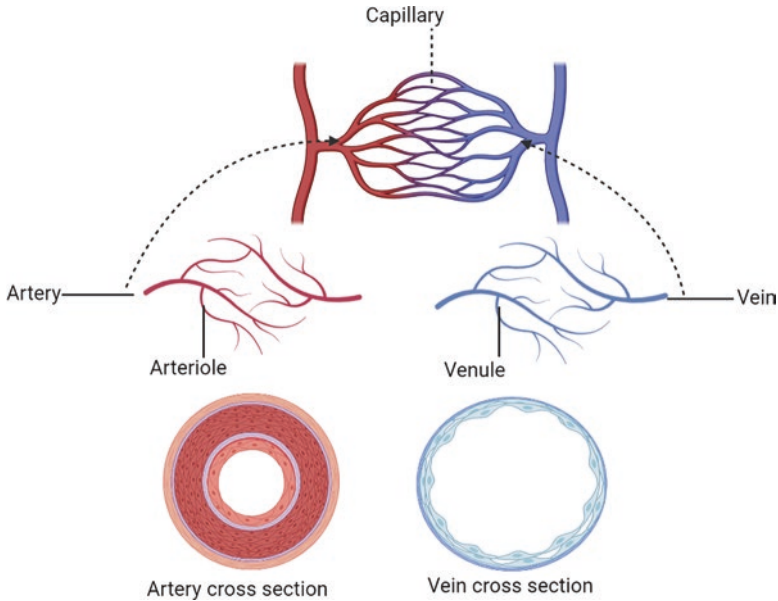


Fig. 1 Hierarchical structure and organization of vessels. (Image created with [BioRender.com](https://www.bio-render.com/))

Vascular architecture is complex, consisting of vessels of various size, thicknesses, composition, mechanical properties, and permeability. Blood vessels branch from aorta (≈ 1 cm in diameter) into pipelines with decreasing diameters which ultimately feed into dense, small capillaries (5–10 μm in diameter) [2]. Vessels can be generally divided into categories of arteries, veins, and capillaries (Fig. 1). While each class of vessels varies dramatically in size, arteries generally consist of a muscular wall and carry oxygenated blood, while veins carry deoxygenated blood and are generally thinner and less elastic. Capillaries are thin-walled consisting of an intima and basement membrane. Mural cells, or pericytes, are present intermittently on the surface and the inner diameter is small enough that only a single red blood cell can pass through at a time. These differing characteristics of blood vessels allow the vasculature to meet the specific demands of each tissue and organ to maintain appropriate function [2].

Bone is highly vascularized and critically dependent on a properly functioning vasculature. During skeletal development, vascularization and mineralization occur in a coordinated process. In addition to supporting proper function, bone tissue also depends on the microvasculature to regulate homeostasis and regeneration following injury. In bone tissue engineering (BTE), the focus is often on repairing and generating volumes of mineralized bone tissue based on the use osteoconductive scaffolds, osteoinductive growth factors, and osteogenic precursor cells [3]. Even with successful mineralized tissue growth, however, implanted materials with little to no vasculature are not likely to integrate with host tissue resulting in graft necrosis and failure. Multiple levels of vascular integration are required to provide

complete blood flow throughout a large volume scaffold. Larger vessels are required for providing convective blood flow throughout the tissue while microvascular networks are required for oxygenation and nutrient exchange [3].

Autologous bone graft is widely accepted as the gold standard for bone defect repair [4]. The success of bone graft results, in part, from the presence of a preexisting vascular network that can either be connected directly (microsurgical anastomosis) or indirectly (vascular ingrowth) with the host blood supply. This allows for the rapid establishment of flow in the new tissue and, in most cases, functional integration. To ultimately replace autologous bone grafts, tissue engineers need to develop methods to design and build vasculature with the complex three-dimensional structure present in autologous tissues.

2 Vascularization of Engineered Tissues

There are two primary mechanisms by which vessels form: angiogenesis and vasculogenesis. Angiogenesis is the formation of new blood vessels from existing vascular networks, while vasculogenesis is the assembly of new vessels from progenitor cells. Initially, many tissue engineering strategies focused on stimulating angiogenesis through the controlled delivery of growth factors. Growth factors are biological macromolecules that can conduct cell signaling and influence cell growth, differentiation, and migration. Strategies typically employ a controlled release system, with current results indicating that controlled delivery of multiple factors can result in more complex, stable, and functional vasculature. This is likely due to the importance of distinct growth factors at various stages of vascularization. A number of growth factors contribute to angiogenesis, including proteins from the vascular endothelial growth factor (VEGF), platelet-derived growth factor (PDGF), insulin growth factor, fibroblast growth factor (FGF), angiopoietin (Ang), and transforming growth factor families (TGF). VEGF is critical for the initiation of angiogenesis, inducing endothelial cell proliferation, migration, and new vessel formation [5]. PDGF/TGF are involved in recruiting and differentiation of mural cells critical for vessel maturation. VEGF/PDGF [6], FGF/PDGF [7], VEGF/Ang2 and PDGF/Ang1 [7] have been shown to improve vascularization above single-factor delivery alone, with outcome dependent on the sequence of delivery.

While progress has been made with these systems, the rate of vessels ingrowth, even under the best conditions, is unlikely to be successful when attempting to vascularize large tissues for clinical use. Another approach for promoting vascularization involves seeding scaffolds with endothelial cells prior to implantation. The goal is to enhance vascularization following implantation either via direct organization of the endothelial cells into new vasculature, or through the release of soluble factors that induce angiogenesis. The latter effect enables the use of other cells, including mesenchymal stem cells, which release a more potent mix of soluble factors. The endothelial cells may also be grown within the biomaterials prior to implantation under conditions that support the spontaneous assembly of a primitive vascular

network system. These networks can then inosculate with host vessels rapidly establishing flow within the scaffolds. While this approach has been shown to increase vascularization in scaffolds used for musculoskeletal applications, the overall impact on bone tissue engineering remains limited [8, 9]. The networks are limited in complexity, consisting only of smaller vessels, and usually take relatively long periods of time, from days to weeks to establish vascular networks. Due to these challenges, the impact of vascularization strategies has been limited regarding the development of engineered tissues.

2.1 Role of Bioreactors in Vascularization

Bioreactors are designed to provide an environment that enables tissue development under closely monitored and controlled conditions (e.g., pH, temperature, gas concentration, nutrient supply, waste removal) [10]. In addition, bioreactors can be designed to support tissue growth prior to the establishment of an extensive vascular network. The high degree of reproducibility, control and automation of bioreactors is critical for the potential clinical translation of engineered tissues. While the primary emphasis has been on improving the delivery of nutrients to the constructs in the bioreactor system, there have been breakthroughs in attaining vessel formation. For example, a perfusion bioreactor system employed was used to promote angiogenic cell migration and anastomosis in preformed microchannels [11]. See chapter “Bioreactors and Scale-Up in Bone Tissue Engineering” for in-depth review of bioreactors in BTE.

2.2 Scaffold Properties

Three-dimensional printing has the potential to allow unprecedented control over the cell and scaffold architecture. The ability to control the porosity and structure of biomaterials can allow for designing materials that mimic the native structure of bone [12], improving nutrient transport into the scaffold [13] or enhancing vascularized tissue growth within the construct [14]. In general, porosity allows cellular migration, facilitates vessel growth, and provides surfaces for cellular adhesion. However, increasing porosity typically compromises mechanical strength. Identifying optimal conditions to support vascularized tissue growth requires in-depth investigation of the relationship between scaffold architecture and tissue response.

A challenge with the design of engineered systems is the broad range of conditions in the design space that could be explored: including material features such as pore size features (e.g., mean diameter, distribution), porosity, interconnectivity, etc. It is neither practical nor efficient to explore these conditions experimentally. Computational systems allow for rapid investigation of a broad range of conditions.

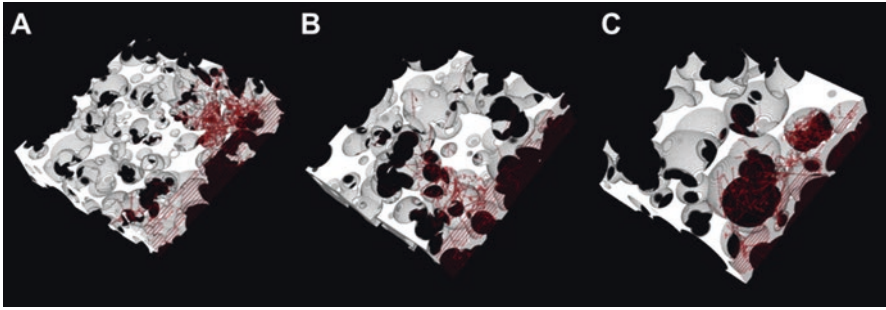


Fig. 2 Agent-based modeling of angiogenesis in porous scaffolds 3D renderings of heterogeneous scaffold vascularization after 6 weeks for different pore sizes of (a) 150, (b) 275, and (c) 400 μm . Overall scaffold porosity is 80% in all pore sizes, and pore size distribution is 75 μm . (Reproduced with permission from [15] LN.4902811426681)

Agent-based model systems have been used to systematically investigate the effect of pore structure on angiogenesis into porous biomaterials (Fig. 2) [2]. The simulation results allowed for the identification specific scaffold features that support rapid and extensive angiogenesis. Complex designs can be created and more rapidly scaled using 3D printing.

2.3 3D Bioprinting of Vascular Networks

Biofabrication or 3D bioprinting involves the use of bioinks to control the spatial distribution of cells. This enables the formation of specific structures and close proximity for cell–cell signaling essential for coordination of angiogenesis and osteogenesis [16]. Selecting materials for use as the bioink can be challenging. It is imperative to select biocompatible materials that provide physical and chemical support for regulation and survival of cells both during the printing process and after formation. The materials much meet the mechanical stiffness required for osteogenesis and mechanical strength require following application. In addition, the bioink must be printable, able to be extruded and maintain the printed structures. In designing a bioink, all of these properties, the mechanical, rheological, biodegradability, biocompatibility, and bioactivity must be taken into account, particularly taking into consideration the specific application [17].

Hydrogels are often used as bioinks based on their relatively lower viscosity and support for cell function following printing. Synthetic hydrogels often have good mechanical properties and easily tunable properties, but often lack some of the intrinsic bioactivity of natural materials. Natural hydrogels provide a structure and composition of the native environment; however, they typically lack the ability to produce lasting constructs due to poor mechanical qualities. Attempts have been made to combine hydrogels with the bioactivity and osteogenic capabilities of bio-ceramics to create composite bioinks [18]. Natural bioinks may need to be modified

so they can be cross-linked or stabilized during or immediately after printing to control the final shape, structure, and architecture of the designed construct.

Alginate is a commonly used bioink due to its biocompatibility and the ease at which it is crosslinked under conditions favorable for cell viability and function [19]. Other natural polymers used include gelatin, fibrinogen, silk, hyaluronic acid, and agarose. Commonly used artificial polymers include poly(ethylene) glycol (PEG), polycaprolactone (PCL), and poly(lactic-*co*-glycolic acid) (PLGA). The generation of polymer inks may require melting the polymer or dissolving the polymer in a solvent to provide the rheological properties required for printing. The use of these inks has been explored in other chapters and reviews [20, 21].

Another common bioink used for bone applications is gelatin (denatured collagen I) or a methacrylated gelatin (GelMa). Gelatin can be derived from bones, tendons, or skins of animals via acidic or basic hydrolysis. Combined with the ability to form hydrogels at lower temperatures in a concentration-dependent manner gelatin's biocompatibility, biodegradability, low antigenicity, inclusion of intrinsic Arg-Gly-Asp (RGD) motifs, ease of processing, and low cost make it popular for biomedical applications [22]. The addition of the methacrylate groups allows for more rapid crosslinking via free radical polymerization, facilitating the printing process. Due to its stability, ease of printing, and bioactivity, GelMa has received significant attention for printing in tissue engineering applications [23].

Bioinks are critical for 3D printing and the resultant tissue development and remodeling processes. When designed and implemented appropriately, materials used in bioinks may recreate the structure or biological properties of extracellular matrixes. In addition, bioinks of biodegradable polymers allow for scaffold design with controlled degradation and/or release of factors which may optimize localized vessel formation. Before examining approaches to develop 3D printed scaffolds for applications to bone regeneration, a brief overview is given on some applications for designing complex vasculature networks. Note that 3D printing is discussed in greater detail in chapters "Additive Manufacturing Technologies for Bone Tissue Engineering" and "Bioreactors and Scale-Up in Bone Tissue Engineering".

With regard to designing perfusable 3D vascular networks, Miller et al. printed a 3D carbohydrate framework which was covered by thin layer of poly(D-lactide-*co*-glycolide) (PDLGA) and loaded it with cell-laden prepolymers. The carbohydrate framework was then dissolved, leaving behind vascular networks. The vascular networks/channels formed support diffusion of nutrients and cell survival [24].

An aqueous ink composed of Pluronic F127 has been used to print structures which can be easily printed and removed under mild conditions. Vascular-like structures were generated by printing this "fugitive ink" within a GelMa matrix and then removing the ink leaving hollow network structures within the matrix. These printed systems (Fig. 3) were perfusable and could be seeded with HUVECS [16].

Synthetic and natural food dyes have been used as a source of biocompatible photo-absorbers and combined with stereolithographic techniques to produce complex vascular architectures within photocrosslinkable hydrogels [25]. These structures ranging from vascular networks derived were designed with mathematical space filling models and ultimately supported perfusion within the hydrogels.

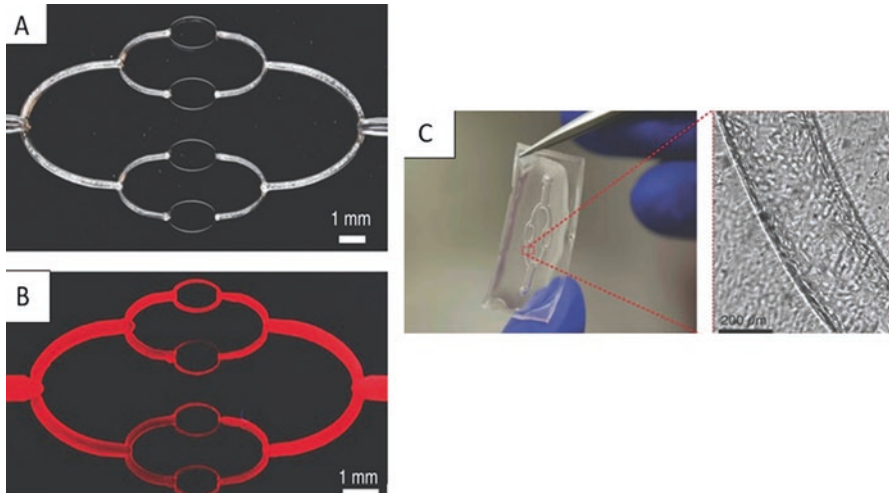


Fig. 3 (a) Printed vascular structure with open channels. (b) Perfused channels. (c) Channels with seeded HUVECs. (Reprinted with permission from [16])

Printing of “thick vascularized tissues” was accomplished using two inks which separately allowed printing of cellular and vascular patterns. Fibrinogen combined with gelatin were used as the ink for patterning cells while Pluronic inks were used to print vascular structures that would be ultimately removed to generate channels [26]. Constructing the “thick vascularized tissues” with 3D perfusion chips, resulted from print cell-laden and fugitive ink patterns within a perfusion chip printed using silicone inks. The silicone ink was printed on a glass substrate allowing creation of a customized environment for tissue formation [26]. After the inks were printed a matrix of gelatin was cast, surrounding the printed structures. The Pluronic F-127 ink, which was printed to embed a vascular network structure was removed by cooling the construct to 4 °C [26]. This resultant interconnected channels would be seeded with HUVECs and perfused [26].

The printing of Pluronic F-127 ink as a sacrificial ink was also used in a technique termed sacrificial writing into functional tissue (SWIFT) [27]. Using this technique, organoids were generated, placed in a mold, and then compacted via centrifugation to form a dense cellular structure [27]. The sacrificial ink was then patterned within the structure. Removal of the pattern yielded perfusable channels in the form of single or branching conduits [27]. HUVECs were loaded into the channels to generate an endothelial-cell lining [27].

3 3D Printing for Generating Vascularized Bone

Vascularized bone systems can be used as a tool to study tissue behavior in healthy and pathologic states, screen new therapies, and provide replacement tissues. In the following sections, we will briefly discuss advances that have been made using printing techniques to generate vascularized bone for a broad range of applications.

3.1 Lab-on-a-Chip and 3D Models

Lab-on-a-chip or micro total systems are designed to provide systems for high throughput and automation of standard laboratory processes. These systems could be used to study basic tissue processes, to evaluate disease states, or to screen new therapeutics. The incorporation of microvascular networks in these systems provides a more accurate tissue model and can enable physiologic mechanisms of transport. ECs have been introduced into microtissue systems under conditions that result in the ECs self-organizing into networks that, in some cases, have perfusable lumens.

Using this approach, HUVECs were seeded in fibrin gels and co-cultured with human lung fibroblasts (HLFs) which were placed in the middle region of the microfluidic chip with three parallel fluidic channels separated by precisely spaced micro-posts. Culture medium was subsequently introduced into the outside channels to support the development of vasculature. Through paracrine signaling, the fibroblasts were critical to the resultant network formation. This network inosculated with the side channels resulting in a perfusable network in 4–7 days [28].

Another microfluidic platform was developed that enabled culture of ECs in physiologic architectures and co-cultured with smooth muscle cells, allowing for the study of vascular wall permeability (Fig. 4). The platform allows for connection to various pumps and fluid handling systems to simulate blood pressure and flow. Fluorescent molecules were introduced to the engineered vessels, and its flow, distribution, transport across the vascular walls were analyzed [29].

An organoid model of angiogenic sprouting was developed where vessels sprouted from preformed vessels which were encapsulated within a 3D extracellular matrix [30]. In the setup, an endothelial layer was formed by seeding endothelial

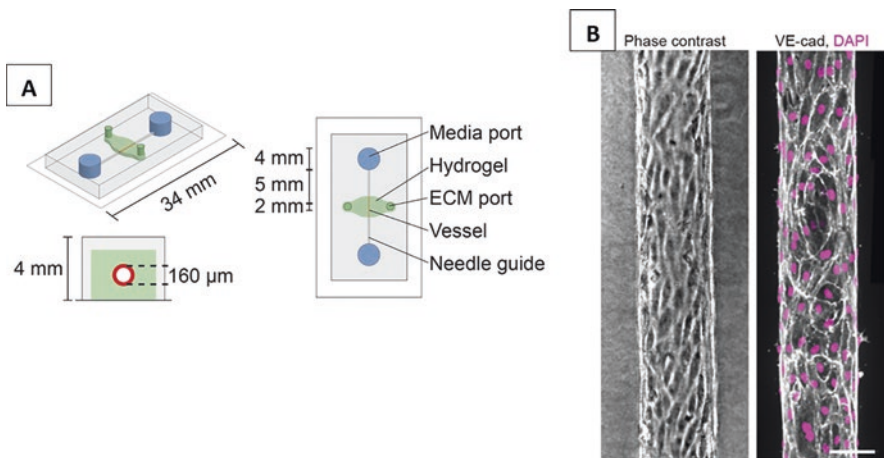


Fig. 4 (a) Overview of the microfluidic device showing the different components and dimensions. (b) Phase contrast image of the engineered blood vessel formed in the hydrogel of the device. (Reprinted with permission from [29])

cells in a cylindrical channel which was fully surrounded by a collagen matrix. A gradient of angiogenic factors resulted from a distal source channel. Angiogenic sprouts formed in response to a distinct angiogenic cocktail exhibiting hallmark structural features of *in vivo* angiogenesis [30]. The sprouts created bridges between preformed channels resulting in a perfusable system.

In a similar approach, a three-dimensional cellular spheroid with a perfusable vascular network was formed within a microfluidic device. The spheroid was prepared by coculturing human umbilical vein endothelial cells (HUVECs) and human lung fibroblasts (Fig. 5). The spheroids were loaded into a fibrin-collagen gel, before being introduced to the microfluidic device. Angiogenic sprouts were induced from microchannels seeded with endothelial cells in channels of the microfluidic device. The sprouts formed networks and reached the central spheroid. After 18 days of culture perfusion was established with flow from the channels [31].

Controlled study of processes that influence the cell localization, adhesion and extravasation from tumors to distal tissues are essential to understanding fundamental mechanisms of cancer metastasis. Bone models can provide insight into metastatic disease, particularly into diseases like breast cancer which have a high propensity to invade the stroma of large bones. Over 70% of advanced breast cancer patients have skeletal metastases. An *in vitro* model of vascularized bone can be used to study how microenvironmental factors influence metastasis [32].

In order to investigate the metastatic disease, a nanostructured bone extracellular matrix was printed using a photo-cross-linkable ink consisting of GelMa, polyethylene glycol diacrylate (PEGDA), and nanohydroxyapatite (nHA). The ink contained clusters of cancer cells, human fetal osteoblasts (hFOBS), and human umbilical vein endothelial cells which were placed in the printed structure to

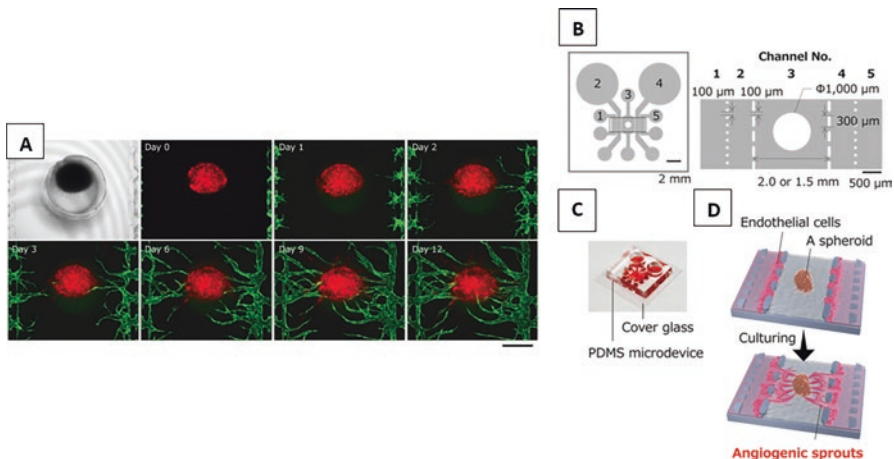


Fig. 5 Angiogenic sprouts of green fluorescent protein-HUVECs from microchannels anastomosed with red fluorescent protein-HUVECs in a spheroid. (a) Sequential images of channel 3. RFP-HUVECs in the spheroid, GFP-HUVECs cultured in microchannels. Both bright-field and fluorescent micrographs are shown for day 0 and sprouting and anastomosis were monitored for 12 days (b–d). Scale bar 500 μm . (Reprinted with permission from [31])

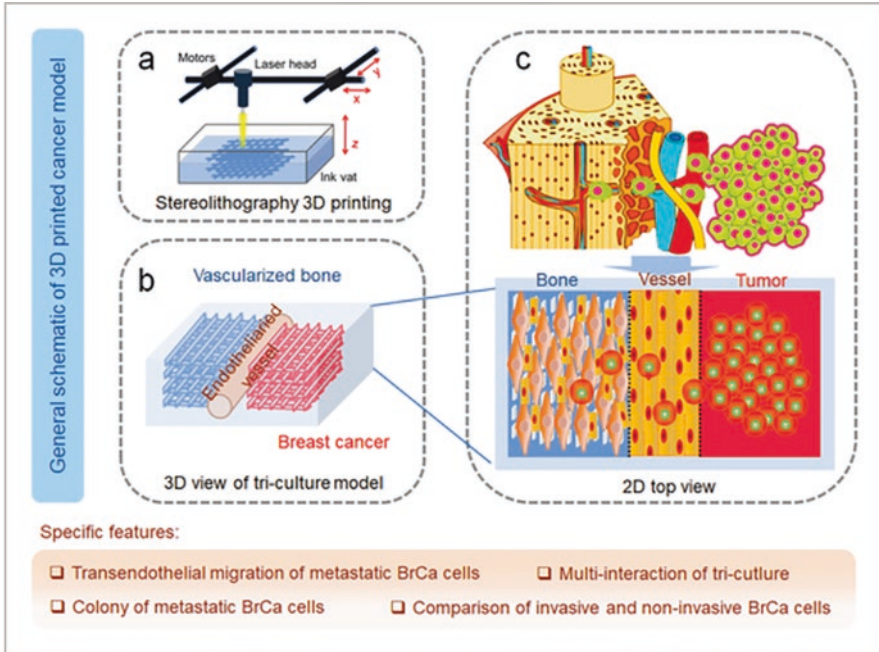


Fig. 6 3D vascular model of cancer metastases to bone. (a) Visual overview of the 3D printing process of the BrCa bone model. (b) 3D view of the triculture model including the breast cancer cells, endothelial cells, and human fetal osteoblasts (hFOBS). (c) 2D representation of the in vivo invasion of MDA-MB-231 cells into bone and 2D view of the triculture model. The localized niche has three neighboring regions, consisting of micro-vascularized bone, an endothelial vessel, and BrCa cells. (Reprinted with permission from [33])

provide a triculture model of a vascularized bone tumor. The construct as seen in Fig. 6, allowed for a substantial infiltration of the hFOBS by the cancer cells via trans-endothelial migration. It was observed that the endothelial cell proliferation increased prior to the presence of invasive cancer cells, while the proliferation rate of the invasive cancer cells increased in the presence of the osteoblasts. After the invasive cancer cells colonized the bone matrix, endothelial cells' expression of CD31 was upregulated, whereas OPN and OCN (osteogenic markers) expression were downregulated [33]. While used to study tumors, these studies provide insight into the critical communication between endothelial cells and bone cells.

3.2 Tissue Engineered Bone

While the advances described above are exciting and innovating, they specifically target the design of small volume model tissues with a focus on microvessel interactions. Printing large volumes of vascularized bone tissue requires an extensive and

more complex vasculature. As described previously, agent-based model systems can be used to guide the design of scaffold architecture to enhance vascularization. These computational environments were used to aid in the development of a toolbox for modular scaffold design that predicted the effects of polymer architecture on vessel invasion and bone formation. The computational tools guided the printing of polypropylene fumarate (PPF) scaffolds that supported vascularization after implantation [34, 35]. Cell culture studies have established critical interactions during co-culture of mesenchymal stem cells (MSCs) with endothelial cells. Prevascularization of these printed PPF scaffolds through EC/MSC co-culture further accelerated establishment of a functional vasculature within the scaffolds post implantation [36].

Endothelial cell/MSC interactions were further explored in a 3D printed gelatin nanohydroxyapatite (gel-nHA) structures. Following printing, human MSCs were seeded on the scaffold and allowed to undergo osteogenic differentiation for 2 weeks followed by seeding with human umbilical vein endothelial cells (HUVECs) which assembled into tubule structures [37]. While the cells were not printed at the same time as the construct, this approach combined the use of cells and a printed hydrogel-ceramic structure to generate a model of bone containing a microvascular network-like structure within it.

In attempts to facilitate osteogenesis, 3D printing was used to explore a silicate ($\text{Ca}_7\text{MgSi}_4\text{O}_{16}$) bio-ceramic mixed with sodium alginate and pluronic-127 acid. Two cylindrical scaffolds were printed, one with a hollow core (BRT-H) and a solid structure (BRT). HUVECs and MSCs were seeded onto the scaffolds, resulting in increased expression of actin-related proteins, including those involved in lamellipodia formation, cell migration, and network formation. The scaffolds were seeded with cells and implanted subcutaneously in nude mice. Blood vessels were observed within the lumen of the hollow pipes after 4 weeks. With the addition of recombinant human bone morphogenetic protein-2 (rhBMP-2), the scaffold facilitated vascularized bone regeneration and enhanced healing a segmental bone defect model. The BRT-H scaffolds exhibited improved healing over the solid scaffolds, possibly due to the greater surface area to volume ratio and inner region that facilitated tissue ingrowth (Fig. 7) [38].

The previously described methods attempted to induce vascularization following implantation and did not exploit the ability to use 3D printing to explicitly design vascular structures. To create a biomimetic scaffold, a vascular networks pattern consisting of a central vascular channel (2 mm diameter) with six branch channels (1 mm in diameter) with 0.45-mm spacing were printed into a beta-tricalcium phosphate (TCP) scaffold. HUVECs adhered to the surfaces of the scaffolds and the space provided by the vascular channels enabled the formation of lumen-like structures. A femoral vascular bundle (artery/vein pair) was placed within the central vascular channel during implantation, increasing vascularization within the scaffold in vivo. The scaffold containing the bundle and supplemented with recombinant bone morphogenetic protein-2 (rhBMP-2) exhibited increased vascularization and osteogenesis (Fig. 8) [39].

A 3D bioprinted vascularized bone model consisting of alternating polylactide (PLA) layers, and a cell-laden gelatin methacrylate (GelMA) hydrogel core, was

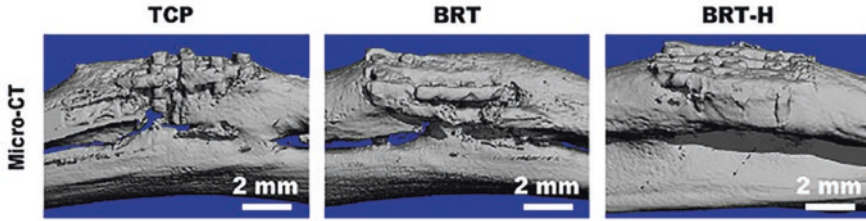


Fig. 7 Micro CT images of increased bone regeneration in a segmental bone defect with implantation of BRT-H scaffolds observed after 12 weeks. The hollow scaffold (BRT-H) performed better when compared with the solid scaffold and a control tricalcium phosphate (TCP) scaffold. (Reprinted with permission from [38] LN-4916780135691)

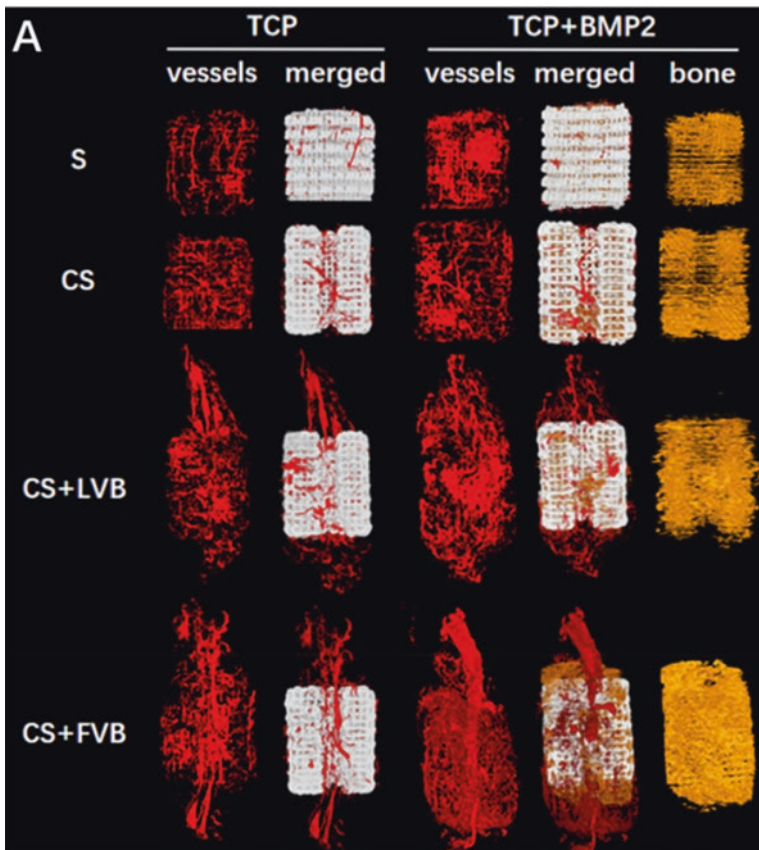


Fig. 8 Representative of micro-CT images of tricalcium phosphate (TCP) scaffold compared to TCP scaffolds with bone morphogenetic protein showing increased angiogenesis and osteogenesis within scaffolds implanted in rabbit vastus medialis pocket 4 weeks after implantation. The CS + FVB group refers to channeled scaffolds with an unligated vascular bundle (VB), the CS + LVB group is channeled scaffolds with ligated VB, the CS group is channeled scaffolds without any ligated/unligated VB, and the S group is conventional scaffolds without any prefabricated vascular channels. (LN-4916830272428 reprinted with permission from [39])

generated using fused deposition modeling (FDM) and stereo lithography (SLA). The architecture was designed to mimic bone structure by including vascular channels, haversian systems, and a central vascular core. The construct consisted of printed PLA seeded with hMSCs to spread on the entire scaffold in accordance with native bone microstructure. The soft (pore regions of the printed PLA) were filled with gelatin methacrylate (GelMa) hydrogels containing HUVECs and MSCs. Bioactive peptide regions of BMP-2 and vascular endothelial growth factor (VEGF) peptides were immobilized in the construct to promote osteogenesis (PLA region) and angiogenesis (GelMa region). Perfusion culture of the constructs in a bioreactor system designed to recapitulate the convective flow found *in vivo* resulted in a construct containing differentiated osteoblasts with organized microvessel networks surrounding the central core. The encapsulation of hMSCs and HUVECs (1:1 ratio) in the GelMa hydrogel resulted in the formation of network structures. This approach provides a platform for obtaining a hierarchically biomimetic construct with regions of osteogenesis and angiogenesis [40].

Another approach to 3D printed vasculature for bone applications considered the initial phase of bone injury when there is hematoma formation and a local hypoxic milieu. Large pores are needed to enable hematoma invasion and formation throughout the scaffold and to support nutrient transport. However, relatively smaller pores support cell attachment and communication. 3D printing was used to design a hierarchical organization approach with over five levels of scale from 1 μm to 20 mm. Combined with a modular design approach, a model scaffold was fabricated from PLA that supported cell survival, proliferation, and osteogenic differentiation [41].

These previous methods printed structures prior to implantation. Laser-assisted bioprinting (LAB) has been investigated for direct printing of endothelial cell patterns *in situ*. A mouse calvaria bone defect was filled with collagen containing mesenchymal stem cells (MSCs), apical papilla stem cells, and VEGF and then HUVECs patterned onto the structures. When compared to random seeding, the patterned cells performed better in controlling the position and the architecture of the defect revascularization (Fig. 9) [42]. *In situ* bioprinting provides a new method for approaching tissue engineering applications. However, challenges exist with regard to the complexity of structures that can be achieved and the practicality of the approach.

An issue with current vascular strategies is the tendency to focus on small vessels. Printing strategies also enable the ability to print more complex macrovascular structures. Vascular networks on the order of 1 mm in diameter with three vertical branches leading into nine additional branches were designed to enhance nutrient transport in a large volume tissue-engineered constructs. When connected to inlet and outlet flow in bioreactor system, these printed structures increased cell viability in the core of the scaffold [43]. While these systems were not investigated *in vivo*, this concept points to the critical ability of 3D printing to enable design of more complex vasculature which includes high convection vessels that will be needed for engineering large volume tissues.

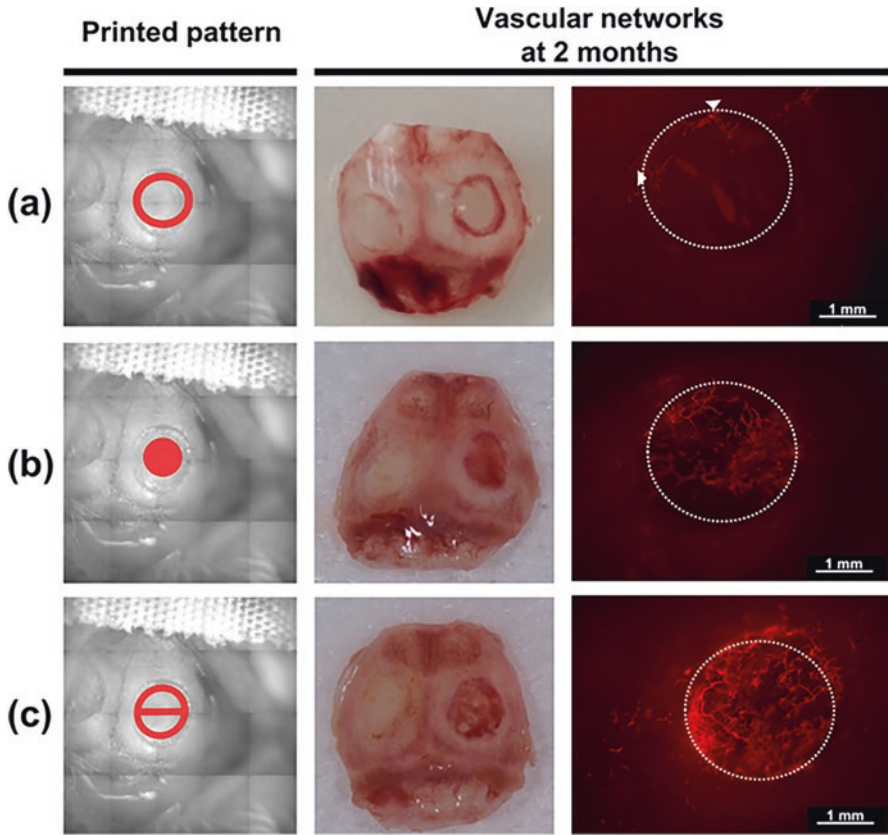


Fig. 9 Laser-assisted bioprinting of endothelial cells in a calvaria bone defect. RFP-labeled HUVECs were printed and imaged at 2 months. The following patterns (a) “ring” pattern, (b) “disc” pattern, (c) “crossed circle” pattern were printed. The left column shows schematic representations of each initial printed pattern design. The middle column shows the calvaria at 2 months. The right column shows fluorescence microscopy images of RFP-labeled HUVECs vascular networks 2 months post-printing. White circles indicate the initial size of the defect. (Reproduced with permission from [17])

4 Challenges and Future Directions in Bone Tissue Engineering

The studies described in this chapter show the substantial potential for 3D printing to enable vascularization of bone for tissue engineering applications. While excitement over these advances is high, several significant challenges remain.

As with any cell-based strategy, a viable source of endothelial cells needs to be identified. Many of the studies described used HUVECs as a model system. However, demonstrating 3D printing using cells that can be used in the targeted patient population is critical.

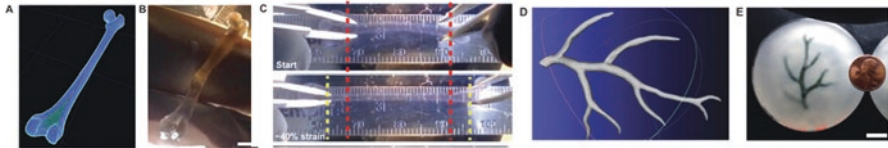


Fig. 10 Printing of biologically relevant structures using freeform reversible embedding of suspended hydrogels (FRESH) printing technique. (a) A model of a human femur from 3D CT imaging data is scaled down and processed into machine code for FRESH printing. (b) The femur model printed in alginate. (c) Response of FRESH printed femur to mechanical stress. (d) A model of a section of a human right coronary arterial tree from 3D MRI is processed at full scale into machine code for FRESH printing. (e) Arterial tree printed in a gelatin slurry. (Reprinted with permission from [44])

In addition to cell sourcing, a more complex vascular structure needs to be generated within the scaffolds. A significant limitation in 3D printing is the complex, hierarchical structure of vascular networks. Current printing systems cannot simultaneously print both μm -level capillaries and mm-sized blood vessels. This limits the development of large grafts for BTE. While technical advances in printing continue to be made, current strategies likely will rely on a combination of printing larger structures while simultaneously inducing self-assembly for smaller microvascular networks. Fortunately, a number of exciting new advances enable the design of complex 3D vascular structures [44]. The strategies are designed to allow a complex shape and hierarchical organization of cells that is persistent following implantation (Fig. 10). The integration of these techniques with bone tissue engineering strategies will further enhance the field.

Finally, it is important to develop methods that consider the critical step of host integration following implantation. This could include exploiting the body as an *in vivo* bioreactor to further enhance vascularization and integration [45]. This technique has been used clinically [46] and has recently been coordinated with 3D printing strategies to generate bone for reconstruction of large defects [47]. It is also possible that integrating the printing strategies with stimuli responsive materials may enable “four-dimensional system” where the printed construct can exhibit dynamic changes based on internal or external stimuli [48].

References

1. Yang G, et al. Vascularization in tissue engineering: fundamentals and state-of-art. *Prog Biomed Eng.* 2020;2(1):012002.
2. Calderon GA, et al. Tubulogenesis of co-cultured human iPS-derived endothelial cells and human mesenchymal stem cells in fibrin and gelatin methacrylate gels. *Biomater Sci.* 2017;5(8):1652–60.
3. Pape HC, Evans A, Kobbe P. Autologous bone graft: properties and techniques. *J Orthop Trauma.* 2010;24:S36–40.

4. Song HHG, et al. Vascular tissue engineering: progress, challenges, and clinical promise. *Cell Stem Cell*. 2018;22(3):340–54.
5. Greenhalgh DG. The role of growth factors in wound healing. *J Trauma Acute Care Surg*. 1996;41(1):159–67.
6. Chen RR, et al. Spatio-temporal VEGF and PDGF delivery patterns blood vessel formation and maturation. *Pharm Res*. 2007;24(2):258–64.
7. Brudno Y, et al. Enhancing microvascular formation and vessel maturation through temporal control over multiple pro-angiogenic and pro-maturation factors. *Biomaterials*. 2013;34(36):9201–9.
8. Roux BM, et al. Induced pluripotent stem cell-derived endothelial networks accelerate vascularization but not bone regeneration. *Tissue Eng Part A*. 2021;27:940–61.
9. Pilia M, et al. Transplantation and perfusion of microvascular fragments in a rodent model of volumetric muscle loss injury. *Eur Cell Mater*. 2014;28:11–23; discussion 23–4.
10. Martin I, Wendt D, Heberer M. The role of bioreactors in tissue engineering. *Trends Biotechnol*. 2004;22(2):80–6.
11. Takahashi H, et al. The use of anisotropic cell sheets to control orientation during the self-organization of 3D muscle tissue. *Biomaterials*. 2013;34(30):7372–80.
12. Vanderburgh JP, et al. Fabrication of trabecular bone-templated tissue-engineered constructs by 3D inkjet printing. *Adv Healthc Mater*. 2017;6(22)
13. Zhang L, et al. Tailored mechanical response and mass transport characteristic of selective laser melted porous metallic biomaterials for bone scaffolds. *Acta Biomater*. 2020;112:298–315.
14. Chiu YC, et al. The role of pore size on vascularization and tissue remodeling in PEG hydrogels. *Biomaterials*. 2011;32(26):6045–51.
15. Mehdizadeh H, et al. Three-dimensional modeling of angiogenesis in porous biomaterial scaffolds. *Biomaterials*. 2013;34(12):2875–87.
16. Kolesky DB, et al. 3D bioprinting of vascularized, heterogeneous cell-laden tissue constructs. *Adv Mater*. 2014;26(19):3124–30.
17. Gungor-Ozkerim PS, et al. Bioinks for 3D bioprinting: an overview. *Biomater Sci*. 2018;6(5):915–46.
18. Pahlevanzadeh F, et al. Recent trends in three-dimensional bioinks based on alginate for biomedical applications. *Materials (Basel)*. 2020;13(18):3980.
19. Van Belleghem S, et al. Hybrid 3D printing of synthetic and cell-laden bioinks for shape retaining soft tissue grafts. *Adv Funct Mater*. 2020;30(3):1907145.
20. GhavamiNejad A, et al. Crosslinking strategies for 3D bioprinting of polymeric hydrogels. *Small*. 2020;16(35):e2002931.
21. Abaci A, Guvendiren M. Designing decellularized extracellular matrix-based bioinks for 3D bioprinting. *Adv Healthc Mater*. 2020;9:e2000734.
22. Elzoghby AO. Gelatin-based nanoparticles as drug and gene delivery systems: reviewing three decades of research. *J Control Release*. 2013;172(3):1075–91.
23. Nichol JW, et al. Cell-laden microengineered gelatin methacrylate hydrogels. *Biomaterials*. 2010;31(21):5536–44.
24. Miller JS, et al. Rapid casting of patterned vascular networks for perfusable engineered three-dimensional tissues. *Nat Mater*. 2012;11(9):768–74.
25. Grigoryan B, et al. Multivascular networks and functional intravascular topologies within bio-compatible hydrogels. *Science*. 2019;364(6439):458–64.
26. Kolesky DB, et al. Three-dimensional bioprinting of thick vascularized tissues. *Proc Natl Acad Sci*. 2016;113(12):3179–84.
27. Skylar-Scott MA, et al. Biomufacturing of organ-specific tissues with high cellular density and embedded vascular channels. *Sci Adv*. 2019;5(9):eaaw2459.
28. Whisler JA, Chen MB, Kamm RD. Control of perfusable microvascular network morphology using a multiculture microfluidic system. *Tissue Eng Part C Methods*. 2014;20(7):543–52.
29. Polacheck WJ, et al. Microfabricated blood vessels for modeling the vascular transport barrier. *Nat Protoc*. 2019;14(5):1425–54.

30. Nguyen D-HT, et al. Biomimetic model to reconstitute angiogenic sprouting morphogenesis in vitro. *Proc Natl Acad Sci U S A*. 2013;110(17):6712–7.
31. Nashimoto Y, et al. Integrating perfusable vascular networks with a three-dimensional tissue in a microfluidic device. *Integr Biol*. 2017;9(6):506–18.
32. Cui X, et al. A microfluidic device for isolation and characterization of transendothelial migrating cancer cells. *Biomicrofluidics*. 2017;11(1):014105.
33. Cui H, et al. Engineering a novel 3D printed vascularized tissue model for investigating breast cancer metastasis to bone. *Adv Healthc Mater*. 2020;9(15):1900924.
34. Wang MO, et al. Evaluating 3D-printed biomaterials as scaffolds for vascularized bone tissue engineering. *Adv Mater*. 2015;27(1):138–44.
35. Bayrak ES, et al. Agent-based modeling of osteogenic differentiation of mesenchymal stem cells in porous biomaterials. *Annu Int Conf IEEE Eng Med Biol Soc*. 2014;2014:2924–7.
36. Mishra R, et al. Effect of prevascularization on in vivo vascularization of poly(propylene fumarate)/fibrin scaffolds. *Biomaterials*. 2016;77:255–66.
37. Chiesa I, et al. Endothelial cells support osteogenesis in an in vitro vascularized bone model developed by 3D bioprinting. *Biofabrication*. 2020;12(2):025013.
38. Zhang W, et al. 3D-printed scaffolds with synergistic effect of hollow-pipe structure and bioactive ions for vascularized bone regeneration. *Biomaterials*. 2017;135:85–95.
39. Zhou M, et al. Bioinspired channeled, rhBMP-2-coated β -TCP scaffolds with embedded autologous vascular bundles for increased vascularization and osteogenesis of prefabricated tissue-engineered bone. *Mater Sci Eng C*. 2021;118:111389.
40. Cui H, et al. Hierarchical fabrication of engineered vascularized bone biphasic constructs via dual 3D bioprinting: integrating regional bioactive factors into architectural design. *Adv Healthc Mater*. 2016;5(17):2174–81.
41. Söhling N, et al. 3D-printing of hierarchically designed and osteoconductive bone tissue engineering scaffolds. *Materials (Basel, Switzerland)*. 2020;13(8):1836.
42. Kérouédan O, et al. In situ prevascularization designed by laser-assisted bioprinting: effect on bone regeneration. *Biofabrication*. 2019;11(4):045002.
43. Ball O, et al. 3D printed vascular networks enhance viability in high-volume perfusion bioreactor. *Ann Biomed Eng*. 2016;44(12):3435–45.
44. Hinton TJ, et al. Three-dimensional printing of complex biological structures by freeform reversible embedding of suspended hydrogels. *Sci Adv*. 2015;1(9):e1500758.
45. Akar B, et al. Large animal models of an in vivo bioreactor for engineering vascularized bone. *Tissue Eng Part B Rev*. 2018;24(4):317–25.
46. Cheng MH, et al. Mandible augmentation for osseointegrated implants using tissue engineering strategies. *Plast Reconstr Surg*. 2006;118(1):1e–4e.
47. Tatara AM, et al. Biomaterials-aided mandibular reconstruction using in vivo bioreactors. *Proc Natl Acad Sci U S A*. 2019;116(14):6954–63.
48. Morouço P, Lattanzi W, Alves N. Four-dimensional bioprinting as a new era for tissue engineering and regenerative medicine. *Front Bioeng Biotechnol*. 2017;5:61.

Development of Additive Manufacturing-Based Medical Products for Clinical Translation and Marketing



Johnny Lam, Brian J. Kwee, Laura M. Ricles, and Kyung E. Sung

1 Introduction

Tissue engineering (TE) and regenerative medicine is a continually evolving field of research that is poised to introduce many innovative technologies for treating serious or life-threatening diseases or complex health conditions. Tissue engineers aim to combine scaffolds, cells, and biologically active moieties as a means to restore, maintain, improve, or replace tissue functions [1]. The use of a scaffold provides structural support for healing tissues and serves to act as templates for complex cell–cell and cell–scaffold interactions toward maximizing tissue regeneration [2]. Despite its promise and its relative maturity as a research discipline, tissue engineering has only gained more traction recently as a translational technology due to advances in suitable manufacturing capabilities engendered by additive manufacturing [3].

Additive manufacturing (AM) is defined as a class of manufacturing processes for the construction of three-dimensional (3D) objects, typically layer-by-layer, using computer-aided design (CAD) [4] and is a rapidly evolving technology used for building medical products (which may include scaffold components of cell–scaffold constructs). The use of CAD allows for the design and creation of complex physiologically relevant structures based on patient-specific anatomical data that can be built as a single piece without the need for retooling [5]. Additionally, CAD and computer-aided manufacturing (CAM) offer unprecedented precision, resolution, and reproducibility while also allowing for the modulation of various construct features that include but are not limited to porosity, size, and geometric design [6]. AM techniques encompass different methodologies that have varying suitability for

J. Lam (✉) · B. J. Kwee · L. M. Ricles · K. E. Sung
Division of Cellular and Gene Therapies, Office of Tissues and Advanced Therapies, Center for Biologics Evaluation and Research, U.S. Food and Drug Administration (FDA), Silver Spring, MD, USA
e-mail: johnny.lam@fda.hhs.gov

TE scaffold fabrication depending on the design requirements of the AM product's intended use [7–9]. Within the context of TE, AM can be used to fabricate implants for both hard and soft tissues. The increased utilization of AM technologies for the production of such medical products has spurred efforts in regulatory science toward understanding and applying the best approach for assessing their safety and efficacy. Indeed, the use of AM may introduce additional or unique technical or regulatory considerations depending on the product type.

This chapter provides a resource for researchers seeking to utilize AM for the development of medical products for translation and is broadly organized into three sections. AM technologies are also discussed in greater detail in Chap. 4. The first section presents a cursory overview of AM techniques and a brief survey of AM applications in TE with a small focus on bone TE. The second section discusses technical considerations that may be taken into account during the design and manufacturing process as well as AM product testing. Following this section is a regulatory considerations discussion related to AM-based medical products.

2 Additive Manufacturing Overview

2.1 Additive Manufacturing Technologies for Medical Products in Regenerative Medicine

Although broad, AM techniques can be largely classified by their fabrication principle into several categories which include stereolithography, fused-deposition modeling, selective laser sintering, and three-dimensional (3D) printing [10, 11]. In addition to these conventional AM approaches, there are several other more specialized techniques that have been developed to achieve certain resolution or compatibility requirements for TE applications. These different AM techniques commonly leverage 3D model medical imaging data for scaffold development through the use of CAD/CAM software where most CAD software converts model data into a standard tessellation language file to digitalize instructions for layer-by-layer AM fabrication. The following subsections will provide brief overviews of basic principles for select AM techniques that have particular utility in TE applications. Table 1 at the end of this section summarizes the discussed AM techniques.

Stereolithography

Stereolithography (SLA) is an AM technique that employs an ultraviolet (UV) light source to selectively polymerize photosensitive polymers in a format that polymerizes single layers at a time [12]. The SLA vat polymerization process begins with the immersion of a fabrication platform into a photosensitive polymer liquid. A UV light or laser is used to selectively polymerize a single layer of polymer according

Table 1 Summary of advanced manufacturing technologies

Technology		Summary	Printed materials
Stereolithography		Utilizes ultraviolet light to polymerize liquid polymers	Photocrosslinkable polymers
Selective laser sintering		Sintering of powdered materials with a high-powered energy source	Powdered thermoplastics, metals, and ceramics
Bind jet printing		Liquid binder is used to cross-link powdered material	Powdered polymers and ceramics
Fusion deposition modeling (FDM)/ fused filament fabrication (FFF)		Melt extrusion of polymer filaments through heated nozzle	Thermoplastic polymers
Melt electrospin writing		Applies voltage across melted polymer to form ultrafine filaments	Thermoplastic polymers with high viscosity and low conductivity
Bioprinting	Extrusion-based bioprinting	Bioinks are extruded through nozzle by pneumatic or mechanical forces	Shear-thinning polymers with or without biologics
	Inkjet bioprinting	Utilizes thermal or acoustic forces to eject bioink droplets onto substrate	Biological materials with or without polymeric materials
	Laser-assisted bioprinting (LAB)	Utilizes laser-induced forward transfer to propel bioink onto substrate	Biological materials with or without polymeric materials

to a desired digital design where only points of the polymer layer exposed to light are polymerized. Following the polymerization of one layer, the software-controlled fabrication platform is lowered a defined distance (i.e., the layer thickness) to allow a recoat bar to deposit a uniform layer of fresh, non-polymerized polymer resin for patterning. The laser-guided polymerization of the subsequent layers is performed with a slight percentage overlap with the previously built layer to avoid delamination between adjacent layers. This process is repeated until the 3D object to be built is completed. After the 3D object is completely formed, it is subjected to several post-processing steps to remove non-polymerized resin and to fully cure the construct. Post-processing steps help to improve polymerization of resins between layers and to remove surface irregularities.

SLA as a technique became useful in TE following the development of photocurable polymers with good cytocompatibility. The introduction of photocurable cytocompatible polymers derived from natural or synthetic materials have since enabled the use of SLA for fabricating cell-encapsulated or cell-seeded scaffolds for TE applications. Indeed, SLA offers some of the highest resolutions achievable with AM techniques. More specialized versions of SLA have been developed to improve

manufacturing efficiency (i.e., digital light processing SLA) and resolution (i.e., microSLA (μ SLA)) where sub-micro SLA processes such as two-photon μ SLA can achieve resolutions down to 100 nm.

Despite its utility in scaffold fabrication, SLA possesses several disadvantages. These include structure distortion due to polymer shrinkage during fabrication and post-processing, the need for auxiliary support when constructing complex geometries, and problems with combining different components for multi-material constructs [13].

Selective Laser Sintering and Powder-Based Printing

Selective laser sintering (SLS) belongs to a class of AM techniques based on the sintering of materials using a high-powered energy source (e.g., carbon dioxide laser or electron beam) [14]. The build medium for SLS generally includes thermoplastics, metals, and ceramics in powder form. SLS is amenable to materials that can be processed in powder form and do not decompose when exposed to high energies during sintering. During SLS fabrication, a high-powered laser beam is used to fuse particles within the printing chamber, to form a single layer of a user-specified CAD model following a layer-by-layer approach [15].

The quality of SLS builds, which includes mechanical properties and variation in size specifications, is dependent on a number of parameters such as build orientation, scanning speed, laser intensity, laser diameter, powder particle size, and thermal properties of the material [16]. By modulating these parameters, SLS has been used to produce scaffolds with tailored properties for TE applications. Initial efforts to use SLS for regenerative medicine produced scaffolds with mechanical properties that fall within the lower range of trabecular bone [17]. SLS offers a solvent-free method for the fabrication of complex geometries without support structures and can achieve resolutions between 50 and 1000 μ m. However, the technique also possesses several inherent disadvantages. Particularly, SLS scaffolds composed from thermoplastic polymers are prone to laser-induced degradation and shrinkage or warping after fabrication. Scaffolds built using SLS are also more brittle with increased surface roughness when compared to constructs produced using other AM modalities due to internal structural porosity and poor control of surface topography. Finally, the large-scale commercial translation of SLS for biomedical applications may prove difficult as the cost of processing powder materials for sintering can be prohibitively high.

Binder jet printing, or binder jetting, shares similarities with SLS in that it offers a method to selectively bind powder materials on a powder bed as its mode of operation [18]. As a technique with a high production rate that can operate at low cost, binder jetting has been explored in TE applications using a number of different natural and synthetic polymer or ceramic materials [19, 20]. The type of material used will govern the type of liquid binder, organic or water-based, required for 3D printing. The quality of scaffolds produced using this method is affected by a number of manufacturing parameters such as powder packing density, powder

flowability, particle size, binder selection, binder drop volume, binder saturation, powder wettability, and post processing steps [18, 21]. Of the materials available for binder jetting, 3D printed ceramic materials commonly used for bone TE such as hydroxyapatite or calcium phosphates typically require post processing steps (e.g., sintering) to complete particle binding and improve inherently weak mechanical properties [22]. Such sintering steps for finishing 3D printed ceramic parts can cause significant shrinkage that adversely influence scaffold mechanical properties and prevents the incorporation of thermosensitive biomolecules.

Fused Deposition Modeling or Fused Filament Fabrication and Extrusion-Based Printing

Fused deposition modeling (FDM), or fused filament fabrication (FFF), is a form of melt extrusion AM that was originally invented for rapid prototyping in industrial applications [10, 23]. The technique is founded on the melt extrusion of polymer filaments through a heated nozzle where the deposition of the extruded polymer layers follows Cartesian coordinates according to a computer-controlled robot. In addition to conventional Cartesian printers, other more advanced FDM/FFF printers have been developed to operate using polar coordinates or a robotic arm with higher (i.e., six compared to three) degrees of freedom [24, 25]. FDM/FFF printers represent one of the more popular types of AM adopted for scaffold or device fabrication due to their relatively low cost and high efficiency [8]. Additionally, FDM/FFF AM platforms offer advantages in terms of short-cycle time, high-dimensional precision/accuracy, scalability, ease of use, and integration with various CAD software [26].

The quality of FDM/FFF builds depends on a number of factors that include but are not limited to the anisotropy in mechanical properties due to print orientation, heat retention in the polymer material after construction that causes warping, and construct irregularities (in the case of discontinuous scaffolds) due to polymer stringing or dribbling caused by movement of the extruder head [27–29]. Measures may be taken to mitigate some of these drawbacks, such as better control over the temperature of the FDM/FFF setup (i.e., the fabrication platform and chamber) to minimize warping due to differential cooling [30, 31]. In addition to quality, the resolution achievable with FDM/FFF, with fiber diameters ranging in the tens to hundreds of microns [8], is mainly determined by the rheological and viscoelastic properties of the base thermoplastic material. Although FDM/FFF is largely limited to thermoplastic polymers that are amenable to being processed in filament or pellet form, the selection of such materials is large and range from engineering materials (e.g., polyamides like nylon, polycarbonates, polyethylene terephthalate glycols) to high-performance thermoplastics (i.e., polyetheretherketone and polyetherimide). FDM/FFF compatible polyesters such as polycaprolactone or polylactide can support the seeding of cells for the fabrication of TE constructs with enhanced bioactivity [32–34].

Extrusion-Based Bioprinting and Other Bioprinting Techniques

In addition to conventional AM process categories, the term “bioprinting” has recently emerged to describe a subset of AM techniques that employs cells, growth factors, and cytocompatible materials, known as “bioinks,” to create living tissue constructs [35]. The bioprinting techniques are generally more amenable to producing cell-laden scaffolds for soft TE and include extrusion-based, inkjet, and laser-assisted bioprinting. In addition to cell-laden bioinks, where cells are encapsulated in cytocompatible materials, cell aggregate-based bioinks are increasingly used to create scaffold-free tissue fabrication [35]. While various materials are compatible with this technique, shear-thinning polymeric materials that can be physically, chemically, or photo-crosslinked are often used to formulate bioinks given their cytocompatibility [36, 37]. Materials are extruded via pneumatic or mechanical (i.e., piston or screw) mechanisms that permit the deposition of high cell densities. However, the shear stresses exerted on cells during extrusion can result in cell-laden scaffolds with lower viabilities when compared to those produced by inkjet bioprinting.

Inkjet bioprinting, also referred to as drop-on-demand bioprinting, employs thermal or acoustic forces to form liquid bioink droplets for ejection onto a substrate to build a construct. Thermal inkjet bioprinters operate by applying heat to printheads to create air pressure pulses that force the ejection of droplets from the printhead nozzle for printing. Temperature ranges used for this technique can reach upwards of 200–300 °C but do not adversely affect cell viability due to the short duration of bioink exposure to heating [38]. Unlike thermal inkjet printers, acoustic inkjet printers utilize a vibrating piezoelectric crystal to generate acoustic waves for bioink droplet formation. Each of these methods have their own unique advantages and disadvantages for cell bioprinting [38].

Laser-assisted bioprinting (LAB), another method commonly used for bioprinting, relies on laser-induced forward transfer for the printing of biological materials (i.e., peptides, nucleic acids, and cells) [39]. LAB offers an advantageous and rapid method for the bioprinting of high cell densities without the need for printing through a nozzle. However, LAB functions best when working with bioinks with fast gelation kinetics and when working with single cells types or materials.

Bioprinting is a rapidly growing area of research in AM with significant potential. The reader is referred to a deeper exploration of bioprinting approaches and techniques by Murphy et al. [38] and Vijayavenkataraman et al. [40].

Table 2 Representative companies and respective commercial printers that have been used for BTE in peer-reviewed publications

Company	Printer	Technology	Representative result	Reference
3D Systems, USA (est. 1986)	250/40	Stereolithography (SLA)	Prototyping of a diethyl fumarate/poly(propylene fumarate) (PPF) scaffold	[42]
	Sinterstation 2500	Selective laser sintering (SLS)	Scaffolds consisting of PLG alone or PLA/ β -tricalcium phosphate composite scaffolds were sintered	[43]
ZCorporation, USA (acquired by 3D Systems) (est. 1986)	Zprinter310	3D printing (3DP)	Printing of hydroxyapatite (HA) and poly(vinyl) alcohol scaffold	[44]
Electro Optical Systems, Germany (est. 1989)	EOSINT-M270	Selective laser melting	Titanium printed scaffolds demonstrated bone formation in rabbit femur injury model	[45]
GeSiM, Germany (est. 1995)	BioScaffolder	Extrusion, inkjet, melt electrospin	Printed VEGF-loaded calcium phosphate cement scaffolds with alginate-gellan gum blend	[46]
EnvisionTEC, Germany (est. 2002)	Perfactory	Stereolithography (SLA)	Studied relationship between architecture of 3D printed PPF scaffolds with resulting vascularization in vivo in rats	[47]
	Bioplotter	Extrusion bioprinting and FDM	Bone marrow-MSCs printed in hydrogels showed no difference in viability compared to unprinted cells in the same hydrogels	[48]
Organovo, USA (est. 2007)	NovoGen MMX BioPrinter	Extrusion bioprinting	Bioprinting of perfusable gelatin-methacryloyl scaffold embedded with silicate nanoplates, HUVECs, MSCs, and VEGF	[49]
RegenHU, Switzerland (est. 2007)	3D Discovery	Extrusion bioprinting and FDM	MSCs in irradiated alginate with RGD modification were printed alongside PCL printed fibers for enhanced scaffold stiffness	[50]

(continued)

Table 2 (continued)

Company	Printer	Technology	Representative result	Reference
Cyfuse Biomedical, Japan (est. 2010)	Regenova	Kenzan method	Scaffold-free constructs made from adipose-derived MSCs were used to treat femoral defects in pigs	[51]
Seraph Robotics, USA (est. 2012)	Fab@Home	Extrusion bioprinting	Printing of chitosan or chitosan-HA composite gels embedded with MC3T3-E1 osteoblast cells	[52]
Rokit, South Korea (est. 2012)	3Dison Pro	Extrusion bioprinting and FDM	Incorporation of Ti into PLA-printed scaffolds enhanced mechanical properties and in vitro osteogenesis with MC3T3 cells	[53]
Regenovo Biotech, China (est. 2013)	Bioarchitect	Extrusion bioprinting	Printing of magnesium (Mg)-HA, chitosan, and gelatin composite scaffolds	[54]
Sunp Biotech, China (est. 2014)	ALHA-BP11	Extrusion bioprinting	Calcium-phosphate (Ca-P) printed scaffolds showed greater vascularization in beagle skull model compared to gas-foamed Ca-P scaffolds	[55]
Cellink, USA (est. 2016)	INKREDIBLE	Extrusion bioprinting	Characterization of printed HA scaffolds of varying infill density	[56]

2.2 Commercial Landscape of AM Applications in Bone Tissue Engineering

For researchers and academics in the field of bone TE, the commercial AM landscape includes numerous companies that sell printers for fabricating 3D tissues and scaffolds (refer to [41] for comprehensive list of bioprinting companies); only a subset of these printers, however, have been utilized in peer-reviewed publications for printing bone or bone-like scaffolds for tissue engineering (Table 2). Printers from older and more established 3D printing companies, such as 3DSystems, have been used by researchers to fabricate polymer, ceramic, and metal scaffolds with traditional forms of AM, such as stereolithography and selective laser sintering [42–44]. More recently, several printers and companies have emerged that focus on bioprinting; most of these printers utilize extrusion bioprinting technology with or without fusion deposition modeling (FDM) of thermoplastics. Two of the first

commercially available bioprinters, the Bioscaffolder from GeSiM and 3D-BioPlotter from EnvisionTec, have provided researchers the ability to incorporate hydrogel materials into their printed scaffolds [46, 48]. Since the release of these bioprinters, companies across Europe, United States, and Asia, such as RegenHU, Seraph Robotics, and Rokit, have released their own extrusion and FDM bioprinters that have been utilized by researchers worldwide [50, 52, 53]. One bioprinting company, Cyfuse Biomedical, offers a unique bioprinter that prints with the Kenzan method, which forms scaffold-free tissue constructs from cell spheroids [51]. When trying to differentiate among the different types of bioprinters available, researchers may refer to the specifications of each available printer (described in detail in [41]) to decide which best matches their research applications.

Several bioprinting companies also offer custom-made bioinks for bone tissue engineering with their commercial bioprinters. Of the companies that have been utilized in peer-reviewed publications, RegenHU and Rokit offer bioinks specific to BTE, consisting of calcium phosphate pastes and/or polycaprolactone (PCL) [57, 58]. Other bioprinting companies, such as Aether and Allevi, also offer unique, bone-specific bioinks consisting of poly(ethylene glycol) diacrylate, poly(L-lactide-co-glycolide) (PLG), PCL, alginate, and/or hydroxyapatite (HA) [59, 60]. One

Table 3 Representative peer-reviewed publications utilizing custom or modified printers for BTE

Technology	Printer details	Major result	Reference
Extrusion bioprinting	Custom extrusion printer with four independent heads	Print of vascular channels (Pluornic F127 and thrombin) lined with HUVECs in 1 cm ³ scaffold (fibrinogen and gelatin) embedded with fibroblasts and MSCs with osteogenic differentiation	[64]
Extrusion bioprinting and FDM	Multi-head tissue/organ building system (MtoBS) with six dispensing heads to print hydrogels or thermoplastics	Printing of two alginate bioinks consisting of osteoblasts or chondrocytes on a PCL printed framework	[65]
Extrusion bioprinting and FDM	Integrated tissue and organ printing (ITOP) consists of multiple dispensing heads for hydrogels and thermoplastics	Printed mandible and calvarial bone structures with microchannels consisting of PCL as structural scaffold and mixture of fibrinogen, HA, and glycerol as cell-laden hydrogel	[66]
Inkjet bioprinting	Custom piezoelectric inject printer that forms 2D patterns of growth factor	Muscle-derived stem cells cultured on fibrin substrate showed selective osteogenic differentiation in areas with printed BMP-2	[67]
Inkjet bioprinting	Modified Hewlett-Packard deskjet thermal inkjet printer combined with UV lamp	Human bone marrow-derived MSCs in poly(ethyleneglycol)dimethacrylate were co-printed with nanoparticles of bioactive glass and HA	[68]
Laser-assisted bioprinting	Custom laser-assisted workstation with a Nd:YAG crystal laser	In situ printing of MSCs associated with collagen and nano-HA to treat calvaria defect in mice	[69]

bioprinting company, Dimension Inx, has focused on selling unique 3D-Print bioinks to distributors that have been demonstrated to produce scaffolds of unique electronic and mechanical properties [61–63].

Several key advancements in the field of bone 3D printing have been made with customized bioprinters created by specific research groups that are currently not commercially available (Table 3). These groups have designed and built their own custom extrusion and FDM bioprinters to demonstrate bioprinting of vascularized, osteogenic tissue of 1 cm³ size [64], mechanically enhanced scaffolds with osteoblasts and chondrocytes bioprinted in distinct regions [65], and cell-laden bone constructs of clinically relevant size, shape, and structural integrity [66]. As these groups continue to advance their bioprinting technologies, there may be a similar emergence of companies that sell or utilize these custom-made printers to offer unique bone printing services in the future.

Several additive manufacturing and medical device companies have focused on providing 3D printed products or services as treatments for patients with bone injury or disease. Numerous 3D printed titanium devices, such as Johnson and Johnson's CONDUIT™ (formerly made by Emerging Implant Technologies GmbH) [70] and Osseus Fusion System's ARIES Lumbar Interbodies, have been FDA cleared as intervertebral fusion devices that mediate bone ingrowth when combined with autologous or allograft bone grafts [71, 72]. Other 3D printed titanium bone fusion devices have also been FDA cleared for treating other types of bone injuries in the absence of additional bone grafts, such as Si-Bone's iFuse-3D implant for sacroiliac fusion [73] and Additive Orthopedics' Lattice Locking Plates for alignment, stabilization, and fusion of fractures, osteotomies, and arthrodesis of small bones [74]. In addition to these titanium printed products, other companies are currently pursuing technologies and regulatory clearance to provide services for printing ceramic bone replacements. Particle 3D, a start up in Denmark, is developing their company to print 3D bone replacements out of tricalcium phosphate and fatty acids [75, 76]. Xilloc from the Netherlands is collaborating with Next21 from Japan to print calcium phosphate printed bone tissue based on CT scans of patients [77]. A survey of the US regulatory landscape of AM medical products was also recently performed by the FDA and shows an increasing trend in the number of AM medical products being reviewed [78].

3 Technical Considerations for Additive Manufacturing of Medical Products

When it comes to medical product development for clinical applications, both biological considerations (such as tissue, structural, and metabolic requirements) and technical considerations (including design, materials, manufacturing, and properties of the scaffold) are important. Given the breadth of materials available and the wide range of AM technologies to select from, the understanding and defining of

design requirements early on based on how the product will be used will facilitate successful clinical translation of AM products. The following subsections of this portion of the chapter will cover two major aspects of technical considerations associated with AM processes for fabricating medical products: design and manufacturing factors, and product testing factors. Many of the considerations covered in this chapter are explained more in detail in the FDA guidance “Technical Considerations for Additive Manufactured Medical Devices” [79]. Due to their diversity and complexity, it is important to note that AM products that include biological materials (e.g., cells) have additional considerations that will not be covered in depth in this chapter.

3.1 Design and Manufacturing Considerations for AM Medical Products

The design and manufacturing process for an AM product can be generally captured by a process flowchart that comprises several distinct phases (Fig. 1). Briefly, AM product development begins with the design process where model geometry dimensions are either determined from predetermined specifications or using patient-matched dimensions derived from medical imaging. The next phase consists of material control, which includes the control of scaffold materials and bioinks, and software workflow, both of which may be developed concurrently. For instance, digitally processed modeling data for 3D printing can occur while simultaneously selecting materials and ensuring their quality for printing. Following AM fabrication, the build is then subjected to post-processing prior to testing and characterization of the final product. Manufacturing experience and quantitative knowledge of the product are mainly acquired through test builds, worst-case builds, or verification and validation activities. Effectively documenting and characterizing the parameters and output specifications of each process step are critical to understanding how design parameters interact with one another in influencing product

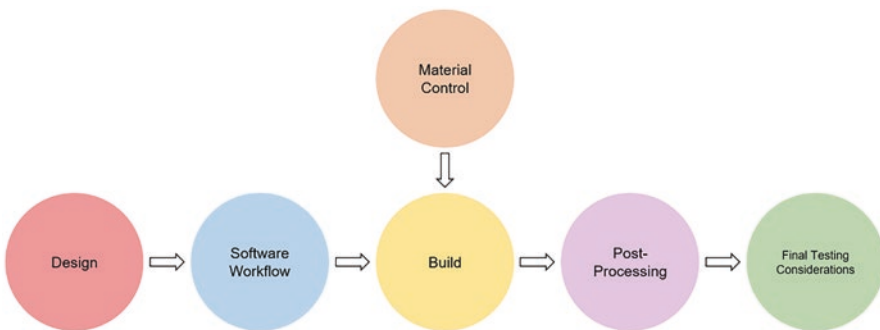


Fig. 1 AM process flowchart

function. This will also be helpful for identifying the root cause of defects acquired during manufacturing.

Similar to traditional manufacturing methods, understanding design requirements helps to guide AM processes to reliably and consistently produce an AM products. Therefore, the early identification of key design parameters is important for developing a consistent manufacturing process and implementing effective controls to ensure quality throughout all phases of design and manufacturing. One potentially useful case study is presented by Morrison et al. [80].

Scaffold Design Considerations

The first phase of an AM process mostly begins with scaffold design. When determining quantitative design targets for an AM scaffold, it is important to consider clinical user needs as part of the design phase of the manufacturing process. Generally defined as qualitative requirements deemed necessary for the treatment of a target disease or illness, the “user needs” provide a blueprint for identifying scaffold attributes to be translated into quantifiable and distinct specifications [81]. User needs can be outlined in accordance to the proposed clinical indication for the use of the scaffold to be fabricated. It may prove helpful to determine quantitative design targets for the desired feature sizes based on the clinical user needs of the envisioned final product in order to guide the selection of a suitable AM technique. Choosing an AM technology that can consistently achieve the minimum desired feature size of the final product with the given manufacturing tolerances of the machine is key for establishing a robust process. This is important as innovative AM technologies may introduce unique variability into the manufacturing process.

AM technologies are particularly amenable to the fabrication of patient-matched (PM) designs, which brings about unique manufacturing considerations [82, 83]. PM designs can be created by scaling standard-sized template design models using one or several anatomic references, or by leveraging anatomic features in their entirety from patient imaging data. In most cases, PM scaffolds are produced within a predefined specification range or performance envelope, which describes the minimum and maximum limits for clinically relevant specifications based on user needs. Once defined, PM designs may be further modified in response to additional clinical needs. While technical considerations for standard-sized scaffolds are also applicable to PM scaffolds, the following considerations may also be:

1. **Imaging effects:** Although most AM products are created from medical imaging data, not every product will require the same level of imaging fidelity for achieving the desired function. The fit, and therefore, adequacy of a PM scaffold is primarily determined by the minimum feature resolution used for matching, the image processing algorithm that may cause dimensional deviations from the reference anatomy, the propensity of the imaged anatomic structures for deformation, and the clarity of matched anatomic landmarks. It is important to assess these imaging effects on scaffold function.

2. Design model interactions: For PM scaffolds that are made through modification of a standard-sized template model, the modeling manipulation software used to make modifications can be built with internal checks to prevent users from exceeding pre-established specifications. To help with ensuring an effective workflow toward optimization of scaffold properties, it is important for modeling manipulation software to document the design iteration that is being altered by the end user. Such manipulation software for creating PM designs should only be used for scaffolds and accessories for which it is validated.
3. Complex design files: While PM scaffold designs offer the advantage of being tailored to fit the needs of certain patient subsets, the file conversion steps needed each time a unique PM scaffold is built pose a risk of conversion errors. Therefore, software validated for data integrity during file conversions offers potential for greatest process consistency.

Software Workflow

As previously mentioned, AM processes interface heavily with software. Hence, it is important to verify that the critical specifications (e.g., scaffold dimensions, geometry, critical features) and performance criteria of AM products are not adversely affected by software conversion or compatibility issues. Such software-related effects on final product properties produced using an AM process should be validated as part of the software workflow. To ensure a consistent manufacturing process, final versions of the CAD files used for printing can be stored in standardized formats and made available for referencing as part of a document control system.

The software workflow phase largely involves the computational steps necessary to prepare a digital product model for AM fabrication. These preparatory steps include optimizing build volume placement, adding supporting structures (if necessary), slicing the digital model, and creating build paths. With regard to build volume, the orientation, placement, and packing density (i.e., distance between components) of the product will inevitably influence final product properties and anisotropy. Additionally, most if not all AM machines inherently have some heterogeneity in print function throughout various areas of the build volume [84]. This heterogeneity is unique to AM machines and even between AM machines of the same model.

Due to the layer-by-layer process, the AM fabrication of a medical product may necessitate the addition of support structures into the build depending on the technology used and the complexity of the printed structure [85, 86]. When support structures are needed, it is often good practice to analyze geometric and structural requirements of the builds to optimize the selection of support materials. These include a consideration of structural overhangs, high aspect ratio features protruding from the main scaffold body, internal voids or porosity, and thin features. Following construction of a build with support structures, support materials may be removed using physical or chemical processes. It is important to ensure that processes for the removal of support structures will not leave artifacts that will affect

the quality of the final scaffold. Unlike the selection of support structures, the selection of a layer thickness for build model slicing is more or less needed for all layer-by-layer AM technologies. Choosing an optimal layer thickness for printing will necessitate careful consideration of the technical characteristics of the employed AM machine and the physical properties of the raw build materials.

In addition to the aforementioned software workflow considerations, the software-programmed build path for an AM built object can significantly impact the quality of the finished construct. The effects of build path on the final scaffold properties are highly dependent on the AM technology used [87]. For example, an optimized build path for FDM/FFF processes will take into account the cooling time required for extruded polymer melts to minimize heterogeneity in scaffold features and anisotropy. The effect of differences in build path on scaffold performance is important to evaluate and minimize. Given that the discussion of software workflow standardization and validation are outside the scope of this chapter, more information may be found in the FDA guidance “Technical Considerations for Additive Manufactured Medical Devices” [79].

Material Controls

The selection of materials and establishment of material controls may be performed in parallel with software workflow optimization. Choosing a base material for medical product fabrication first necessitates an understanding of the user needs of the final product. Toward this goal, the selection of raw materials can begin by defining broad targets for scaffold or final product mechanical function, mass transport, and surface chemistry based on the properties of the target tissue to be engineered. One useful guideline for determining such target scaffold properties was proposed by Hollister [88]; accordingly, general targets for mechanical function, mass transport, and surface chemistry may be narrowed down based on tissue types that can be broadly categorized into soft versus hard and vascular versus avascular. Generally, hard tissues require elastic mechanical properties with high moduli, whereas soft tissues are typically more viscoelastic. The desired mass transport properties for vascularized tissues are higher permeability and higher diffusivity when compared

Table 4 Examples of raw material controls depending on the material type used for AM

Material type	Specification(s)
Solid	Particle size and distribution; rheological properties; filament diameter and filament diametric tolerance
Fluid	Viscosity; viscoelasticity; pot life
Aqueous polymer or monomer mixture	Composition; water content; molecular weight; molecular formula; chemical structure; molecular weight distribution; glass transition temperatures; melting temperatures; crystallization point temperatures; purity information (i.e., ratio of monomer mixtures, impurities, etc.)
Metal, metal alloy, or ceramic	Chemical composition; purity

to avascular tissues. As another example, the desired surface characteristics for vascularized hard tissues like bone would ideally be osteoinductive or osteoconductive to facilitate osteogenic differentiation of host progenitor cells [8].

Starting materials can have a significant impact on the quality of the final build as they may undergo physical or chemical change during fabrication depending on the AM technique. To ensure the consistency of the fabricated scaffold or final product, specifications for raw materials and methods for material qualification may be established in accordance with the chosen AM modality. Such specifications will also be dependent on the type of materials used for AM as outlined in Table 4.

Some AM technologies, such as powder bed fusion or vat polymerization stereolithography, allow for raw materials like unsintered powders or uncured resins to be reused. While efficient, materials for reuse are likely to be exposed to intense conditions that render them different from virgin materials. Studies can be conducted to assess the effects of reusing raw materials on the properties of final scaffolds in material reuse protocols.

In addition to the specifications defined as a part of material controls, it may become necessary to characterize all material chemistry changes to be expected during the fabrication of a medical product when using a particular AM technology. This is due to the iterative processes involved in AM that cyclically expose materials to extreme temperatures or energy with the potential to yield undesirable material chemistries during fabrication. Depending on their starting materials, additional material chemistry testing or characterization can be performed if polymers are used in order to ensure that by-products that are known or thought to be unsafe to human are not formed.

Post-processing

Post-processing steps, which include physical or chemical methods for the removal of residues from the construct, heat treatments, and final machining, can be performed as finishing steps for an AM product. In some cases, a tissue-engineered construct, particularly a cell-laden construct, may need to be matured in a custom bioreactor as a post-processing step. Post-processing processes are necessary to achieve the intended function of the final product; however, the processes have the potential to significantly impact final material properties and performance of the product. Given the many types of post-processing methods available depending on the AM technology, it is important to document all methods used to finish their products and analyze how post-processing influences their final product performance for its intended use. For products with complex internal structures, methods can be used to assess and verify the fidelity of internal structures after post-processing steps have been performed.

Manufacturing Consistency

Due to the nature of AM, the quality (including mechanical properties) of a medical product fabricated using AM may vary between different AM machines of the same model even when the same input parameters, process steps, and raw materials are used. Hence, it becomes essential to understand the variability associated with each input parameter and characterize the effects of this variability on product quality in order to separate the variability due to the machine and the variability due to the input. It is important to verify the quality of products fabricated in a single build cycle, between multiple build cycles, and between AM machines especially if the prespecified requirements of a product can only be verified using destructive testing. The software workflow, including all software packages, operates most consistently when validated for its intended use with respect to AM product fabrication.

It is important that AM parameters (such as laser beam energy density, deposition velocity, humidity, or scanning speed) that have significant potential to affect the build environment, design output, and subsequent product performance are identified and evaluated. Characterizing the level of variability associated with each manufacturing parameter and parameter interactions during the AM process will help to understand how well parameters can be controlled during manufacturing. In characterizing the effects of AM variability on design output and product performance, it is most effective when parameters are controlled to be within defined acceptable variations. Uniformity of prints may also be considered since AM products are typically anisotropic and may not be uniformly load-bearing. Characterization of mechanical properties of the product along its dimensions and characterization of the build environment may prove useful for evaluating build consistency. Fixing a range of build parameters may also help to improve manufacturing process consistency.

Fabricated samples that are representative of a feature or a set of features of a scaffold, also referred to as test coupons, can be used for verification activities. The advantage of using test coupons lays with the ability to simulate worst-case conditions in the AM process as well as for identifying worst-case orientations or locations within a build volume. Test coupons are also suitable for both destructive (e.g., mechanical testing) and non-destructive evaluation (e.g., ultrasound, computed tomography, dye penetration, microscopy) techniques. The test coupons should be representative of the final AM product.

3.2 Testing of AM Medical Products

Performance Testing

Aside from design and manufacturing considerations, another important technical aspect to consider for AM products is their performance testing and characterization. Generally, product testing is performed with appropriate methods to verify and

validate functional requirements of the AM product. The amount of testing information or data needed to support the clinical use of a product will depend on the product type and its intended use, risk profile, and novelty. The type of testing needed will also depend heavily on important factors such as whether the product will be implanted, whether the scaffold will be load-bearing, and whether the scaffold dimensions are standard-sized or patient-matched. Depending on the type of product (e.g., bone scaffold, joint replacements, osteochondral scaffolds), performance testing may include material property testing or mechanical testing for characterization of yield strength, creep, viscoelasticity, fatigue, moduli, and other relevant properties. Performance testing is ideally conducted on the final version of products that have been subjected to all post-processing, cleaning, and sterilization steps in order to accurately characterize product properties for its intended use. An effective performance testing program also considers worst-case combinations of product features, dimensions, and build orientations. If test coupons or surrogates are used in lieu of the final product for testing, it is critical to have sufficient scientific rationale supported by data to demonstrate how the test coupons or surrogates are representative of the final product.

Effective performance testing of medical products produced using AM technologies also uniquely considers the effects of build orientation on final mechanical properties due to potential variations in how anisotropy is introduced during fabrication. Depending on the AM methodology, build orientation and build location effects within a build volume can vary significantly in how they influence final product properties [89]. These differences in orientation effects between different AM technologies largely arise from how strongly and in which direction the layers are bound during the layer-by-layer printing process. Build location effects stem from how the AM printed materials absorb energy from or dissipate heat to neighboring scaffold components during fabrication and are especially prevalent for powder bed fusion AM methods. As such, a baseline study evaluating the selected AM machine and technology interacts with a chosen material for scaffold fabrication may prove useful in determining orientation and build location effects during performance testing. *In silico* methods can also be considered in addition to performance testing to assess and refine design validation processes via the modeling of mechanical response to various stresses.

Manufacturing Material Residual Testing

AM fabricated medical products offer the advantage of being complex in geometry and may comprise intricate features such as internal porosity, honeycomb structures, channels, voids, or cavities that are uniquely created by AM methods. Despite the advantages associated with such intricate geometric features, the enhanced surface area and difficult-to-access internal features also increase the difficulty in removing excess manufacturing or sterilant residuals during scaffold cleaning. The presence of manufacturing material residuals may adversely impact the performance of a product. As such, it is important to use documented testing procedures

and data to show that the cleaning and residual removal processes adequately remove residuals to the extent where they do not negatively affect product quality. Such testing may necessitate the use of destructive methods depending on the accessibility of complex geometries or trapped internal volumes in the product.

Biocompatibility Testing

Certain AM products may also be evaluated within the framework of a risk management process for biocompatibility. Biocompatibility testing of a medical product is performed to assess the risk of a harmful biological response to the product due to chemical toxicity or adverse reactions to physical characteristics of the product or its manufacturing and processing. A testing plan may be developed to appropriately address the knowledge gaps posed by the potential biological impact of the AM product given the type and duration of biological contact. As biocompatibility testing is largely outside the scope of this chapter, more specific information can be found in the FDA guidance entitled “Use of International Standard ISO 10993-1, Biological evaluation of medical devices – Part 1: Evaluation and testing within a risk management process” [90].

3.3 Cell–Scaffold TE Products

Unlike AM medical products that comprise only a scaffold, cell–scaffold TE products are inherently complex and often involve multilayered product development considerations [91]. Cell–scaffold TE products present unique manufacturing and characterization challenges since these TE products often combine metabolically active cellular components with scaffolds to yield complex three-dimensional constructs. As such, the final attributes of cell–scaffold TE products are not only dependent on the characteristics of the individual components that the product comprises, but also must factor in the effects of product assembly and subsequent cell–material interactions. Indeed, cell–scaffold TE products are frequently designed to remodel or degrade *in vitro* and/or *in vivo* which can further complicate functional testing of these products. The packaging, shipping, and stability (or shelf-life) of cell–scaffold TE products may also prove challenging.

As with other medical products, the safety and efficacy of cell–scaffold TE products should be supported with data obtained from appropriate *in vitro* and *in vivo* preclinical testing. Many of the important tests for the individual components, such as sterility, mycoplasma, pyrogenicity/endotoxin, scaffold properties, adventitious agent testing, cell viability, identity, and purity, are applicable for the combined product as well. Due to their multifaceted nature, many cell–scaffold TE products do not have established preclinical testing paradigms and cannot rely on precedence for testing considerations. Given the potential difficulties in fully characterizing complex TE products, their testing may necessitate the development of new

scientific techniques to be performed at relevant stages of product development. The preclinical testing program for cell–scaffold TE products may combine testing performed on individual components prior to product assembly with relevant testing that is performed after product assembly.

4 Regulatory Considerations for Additive Manufacturing-Based Medical Products

Given its versatility, AM can be employed to fabricate a wide breadth of different products that span multiple product types. As such, AM products can be regulated as medical devices, biologics, drugs, or combination products. The formal definitions are as follows:

- Device (21 USC 321[h]): “An instrument, apparatus, implement, machine, contrivance, implant, in vitro reagent, or other similar or related article, including any component, part, or accessory, which is: (1) recognized in the official National Formulary, or the US Pharmacopeia, or any supplement to them, (2) intended for use in the diagnosis of disease or other conditions, or in the cure, mitigation, treatment, or prevention of disease, in man or other animals, or (3) intended to affect the structure or any function of the body of man or other animals, and which does not achieve its primary intended purposes through chemical action within or on the body of man or other animals and which is not dependent upon being metabolized for the achievement of its primary intended purposes.”
- Biological Product (42 USC 262[i](1)): “A virus, therapeutic serum, toxin, antitoxin, vaccine, blood, blood component or derivative, allergenic product, protein (except any chemically synthesized polypeptide) or analogous product, or arsphenamine or derivative of arsphenamine (or any other trivalent organic arsenic compound), applicable to the prevention, treatment, or cure of a disease or condition of human beings.”
- Drug (21 USC 321[g][1]): “(A) Articles recognized in the official US Pharmacopeia, official Homeopathic Pharmacopeia of the United States, or official National Formulary, or any supplement to any of them; and (B) articles intended for use in the diagnosis, cure, mitigation, treatment, or prevention of disease in man or other animals; and (C) articles (other than food) intended to affect the structure of any function of the body of man or other animals; and (D) articles intended for use as a component of any articles specified in clause (A), (B), or (C).”
- Combination Product (21 CFR 3.2[e]): “(1) A product composed of two or more regulated components, that is, drug-device, biologic-device, drug-biologic, or drug-device-biologic, that are physically, chemically, or otherwise combined or mixed and produced as a single entity; (2) two or more separate products packaged together in a single package or as a unit and composed of drug and device

products, device and biological products, or biological and drug products; (3) a drug, device, or biological product packaged separately that according to its investigational plan or proposed labeling is intended for use only with an approved individually specified drug, device, or biological product where both are required to achieve the intended use, indication, or effect and where upon approval of the proposed product the labeling of the approved product would need to be changed, for example, to reflect a change in intended use, dosage form, strength, route of administration, or significant change in dose; or (4) any investigational drug, device, or biological product packaged separately that according to its proposed labeling is for use only with another individually specified investigational drug, device, or biological product where both are required to achieve the intended use, indication, or effect.”

Medical products are subject to different regulatory pathways depending on whether the product meets the formal definition of a drug, biological product, device, or combination product [92]. Such regulatory pathways include (1) the New Drug Application (NDA) for drugs [93]; (2) the Biologics License Application (BLA) for biologics [93]; and (3) the Premarket Approval (PMA) [94], Humanitarian Device Exemption (HDE) [95], 510(k) premarket notification clearance mechanism [96], and De Novo classification process [97] for medical devices. NDAs and BLAs are applications for licensure under the safety and effectiveness requirements of the FD&C Act. Biologics are further subject to the approval standards set forth in the PHS Act that requires demonstration that the product is safe, pure, and potent. For a medical device, the appropriate regulatory pathway and classification depend heavily on the associated risks; Class I includes devices with the lowest risk and Class III includes devices with the highest risk. A PMA is an application for the approval of most Class III medical devices; to gain PMA approval, there must be a reasonable assurance of safety and effectiveness [94]. The premarket notification, or 510(k), clearance process applies to devices that are “substantially equivalent” to a medical device already on the market [98]. The de novo process provides a pathway to Class I or Class II classification for medical devices for which there is no legally marketed device to enable a demonstration of “substantial equivalence” but for which regulatory controls provide a reasonable assurance of safety and effectiveness [97].

When clinical investigation is needed to evaluate the safety and efficacy of an investigational product before marketing approval, an Investigational New Drug (IND) application [99] is required for drugs and biologics, and an Investigational Device Exemptions (IDE) [100] is generally required for devices. More specific information regarding such approval mechanisms may be found in the referenced guidance included in this section of the chapter.

The FDA has programs to help innovators and medical product developers. Some of these resources are specific to the area of additive manufacturing. FDA resources that are relevant to additive manufacturing products are shown in Table 5.

Table 5 FDA resources relevant to additive manufacturing of devices and biologics

Web resource	Link
3D Printing of Medical Devices	https://www.fda.gov/3dprinting
Technical Considerations for Additive Manufactured Devices: Guidance for Industry and FDA Staff	https://www.fda.gov/media/97633/download
Additive Manufacturing of Medical Products	https://www.fda.gov/medical-devices/cdrh-research-programs/additive-manufacturing-medical-products
Formal Meetings Between the FDA and Sponsors or Applicants of PDUFA Products: Guidance for Industry	https://www.fda.gov/media/109951/download
Requests for Feedback and Meetings for Medical Device Submissions: The Q-Submission Program: Guidance for Industry and FDA Staff	https://www.fda.gov/media/114034/download
Center for Devices and Radiological Health (CDRH) Learn	https://www.fda.gov/training-and-continuing-education/cdrh-learn
Office of Tissues and Advanced Therapies (OTAT) Learn	https://www.fda.gov/vaccines-blood-biologics/news-events-biologics/otat-learn
CDRH's Division of Industry and Consumer Education (DICE)	Email: DICE@fda.hhs.gov
Center for Biologics Evaluation and Research (CBER)'s Manufacturer's Assistance and Technical Training Branch (MATTB)	Email: industry.biologics@fda.gov

5 Conclusions

Regenerative medicine and AM offer a means to introduce many innovative products for application in tissue engineering and for manufacturing products with potential for clinical translation and commercialization. As AM processes are adapted for production, the early consideration of technical aspects as applicable can significantly facilitate the development of safe and effective products. Developers can interact with the FDA through various channels described in FDA resources to ensure adequate testing toward the manufacture of a safe and effective product. The interactions between product developers and regulators, along with interdisciplinary research, support and foster innovation in AM technology.

Acknowledgments We thank Drs. Bao-Ngoc Nguyen and Matthew Klinker for their technical review of this chapter.

Disclaimer The authors do not endorse or recommend any commercial products or services listed in this chapter. The views and opinions of authors stated in this chapter do not necessarily state or reflect those of the U.S. Government, and they may not be used for advertising or product endorsement purposes.

References

1. Langer R, Vacanti JP. Tissue engineering. *Science*. 1993;260(5110):920–6.
2. Landers R, Hubner U, Schmelzeisen R, et al. Rapid prototyping of scaffolds derived from thermoreversible hydrogels and tailored for applications in tissue engineering. *Biomaterials*. 2002;23(23):4437–47.
3. Langer R, Vacanti J. Advances in tissue engineering. *J Pediatr Surg*. 2016;51(1):8–12.
4. ASTM/ISO. ASTM52900-15 standard terminology for additive manufacturing—general principles—terminology, vol 3(4). West Conshohocken: ASTM International; 2015. p. 5.
5. Bidra AS, Taylor TD, Agar JR. Computer-aided technology for fabricating complete dentures: systematic review of historical background, current status, and future perspectives. *J Prosthet Dent*. 2013;109(6):361–6.
6. Chen J, Ahmad R, Suenaga H, et al. Shape optimization for additive manufacturing of removable partial dentures—a new paradigm for prosthetic CAD/CAM. *PLoS One*. 2015;10(7):e0132552.
7. Li J, Wu C, Chu PK, et al. 3D printing of hydrogels: rational design strategies and emerging biomedical applications. *Mater Sci Eng R Rep*. 2020;140:100543.
8. Madrid APM, Vrech SM, Sanchez MA, et al. Advances in additive manufacturing for bone tissue engineering scaffolds. *Mater Sci Eng C*. 2019;100:631–44.
9. Tappa K, Jammalamadaka U. Novel biomaterials used in medical 3D printing techniques. *J Funct Biomater*. 2018;9(1):17.
10. Mota C, Puppi D, Chiellini F, et al. Additive manufacturing techniques for the production of tissue engineering constructs. *J Tissue Eng Regen Med*. 2015;9(3):174–90.
11. Youssef A, Hollister SJ, Dalton PD. Additive manufacturing of polymer melts for implantable medical devices and scaffolds. *Biofabrication*. 2017;9(1):012002.
12. Skoog SA, Goering PL, Narayan RJ. Stereolithography in tissue engineering. *J Mater Sci Mater Med*. 2014;25(3):845–56.
13. Konstantinou G, Kakkava E, Hagelüken L, et al. Additive micro-manufacturing of crack-free PDCs by two-photon polymerization of a single, low-shrinkage preceramic resin. *Addit Manuf*. 2020;35:101343.
14. Shirazi SF, Gharekhani S, Mehrali M, et al. A review on powder-based additive manufacturing for tissue engineering: selective laser sintering and inkjet 3D printing. *Sci Technol Adv Mater*. 2015;16(3):033502.
15. Mazzoli A. Selective laser sintering in biomedical engineering. *Med Biol Eng Comput*. 2013;51(3):245–56.
16. Pereira T, Silva M, Oliveira M, et al. Effect of process parameters on the properties of selective laser sintered poly(3-hydroxybutyrate) scaffolds for bone tissue engineering: this paper analyzes how laser scan spacing and powder layer thickness affect the morphology and mechanical properties of SLS-made scaffolds by using a volume energy density function. *Virtual Phys Prototyp*. 2012;7(4):275–85.
17. Williams JM, Adewunmi A, Schek RM, et al. Bone tissue engineering using polycaprolactone scaffolds fabricated via selective laser sintering. *Biomaterials*. 2005;26(23):4817–27.
18. Moon J, Grau JE, Knezevic V, et al. Ink-jet printing of binders for ceramic components. *J Am Ceram Soc*. 2002;85(4):755–62.
19. Yeong WY, Chua CK, Leong KF, et al. Rapid prototyping in tissue engineering: challenges and potential. *Trends Biotechnol*. 2004;22(12):643–52.
20. Butscher A, Böhner M, Hofmann S, et al. Structural and material approaches to bone tissue engineering in powder-based three-dimensional printing. *Acta Biomater*. 2011;7(3):907–20.
21. Chen H, Zhao YF. Process parameters optimization for improving surface quality and manufacturing accuracy of binder jetting additive manufacturing process. *Rapid Prototyp J*. 2016;22:527–38.

22. Shanjani Y, De Croos JN, Pilliar RM, et al. Solid freeform fabrication and characterization of porous calcium polyphosphate structures for tissue engineering purposes. *J Biomed Mater Res B Appl Biomater.* 2010;93(2):510–9.
23. Brenken B, Barocio E, Favaloro A, et al. Fused filament fabrication of fiber-reinforced polymers: a review. *Addit Manuf.* 2018;21:1–16.
24. Faria C, Fonseca J, Bicho E. FIBR3DEmul—an open-access simulation solution for 3D printing processes of FDM machines with 3+ actuated axes. *Int J Adv Manuf Technol.* 2020;106(7–8):3609–23.
25. Brooks BJ, Arif KM, Dirven S, et al. Robot-assisted 3D printing of biopolymer thin shells. *Int J Adv Manuf Technol.* 2017;89(1–4):957–68.
26. Boparai KS, Singh R, Singh H, "Development of rapid tooling using fused deposition modeling: a review", *Rapid Prototyping Journal.* 2016;22(2):281–299.
27. Ahn S, Montero M, Odell D, et al., "Anisotropic material properties of fused deposition modeling ABS", *Rapid Prototyping Journal.* 2002;8(4):248–257.
28. Raut S, Jatti VS, Khedkar NK, et al. Investigation of the effect of built orientation on mechanical properties and total cost of FDM parts. *Procedia Mater Sci.* 2014;6:1625–30.
29. Popescu D, Zapciu A, Amza C, et al. FDM process parameters influence over the mechanical properties of polymer specimens: a review. *Polym Testing.* 2018;69:157–66.
30. Kim E, Shin YJ, Ahn SH, "The effects of moisture and temperature on the mechanical properties of additive manufacturing components: fused deposition modeling", *Rapid Prototyping Journal.* 2016;22(6):887–894.
31. Yang C, Tian X, Li D, et al. Influence of thermal processing conditions in 3D printing on the crystallinity and mechanical properties of PEEK material. *J Mater Process Technol.* 2017;248:1–7.
32. Teixeira BN, Aprile P, Mendonca RH, et al. Evaluation of bone marrow stem cell response to PLA scaffolds manufactured by 3D printing and coated with polydopamine and type I collagen. *J Biomed Mater Res B Appl Biomater.* 2019;107(1):37–49.
33. Jensen J, Kraft DC, Lysdahl H, et al. Functionalization of polycaprolactone scaffolds with hyaluronic acid and beta-TCP facilitates migration and osteogenic differentiation of human dental pulp stem cells in vitro. *Tissue Eng Part A.* 2015;21(3–4):729–39.
34. Reichert JC, Heymer A, Berner A, et al. Fabrication of polycaprolactone collagen hydrogel constructs seeded with mesenchymal stem cells for bone regeneration. *Biomed Mater.* 2009;4(6):065001.
35. Gungor-Ozkerim PS, Inci I, Zhang YS, et al. Bioinks for 3D bioprinting: an overview. *Biomater Sci.* 2018;6(5):915–46.
36. Guvendiren M, Lu HD, Burdick JA. Shear-thinning hydrogels for biomedical applications. *Soft Matter.* 2012;8(2):260–72.
37. Chen MH, Wang LL, Chung JJ, et al. Methods to assess shear-thinning hydrogels for application as injectable biomaterials. *ACS Biomater Sci Eng.* 2017;3(12):3146–60.
38. Murphy SV, Atala A. 3D bioprinting of tissues and organs. *Nat Biotechnol.* 2014;32(8):773–85.
39. Guillotin B, Ali M, Ducom A, et al. Laser-assisted bioprinting for tissue engineering. In: *Biofabrication.* Amsterdam: Elsevier; 2013. p. 95–118.
40. Vijayavenkataraman S, Yan WC, Lu WF, et al. 3D bioprinting of tissues and organs for regenerative medicine. *Adv Drug Deliv Rev.* 2018;132:296–332.
41. Choudhury D, Anand S, Naing MW. The arrival of commercial bioprinters—towards 3D bioprinting revolution. *Int J Bioprint.* 2018;4(2):139.
42. Cooke MN, Fisher JP, Dean D, et al. Use of stereolithography to manufacture critical-sized 3D biodegradable scaffolds for bone ingrowth. *J Biomed Mater Res B Appl Biomater.* 2003;64(2):65–9.
43. Simpson RL, Wiria FE, Amis AA, et al. Development of a 95/5 poly (L-lactide-co-glycolide)/hydroxylapatite and β -tricalcium phosphate scaffold as bone replacement material via selective laser sintering. *J Biomed Mater Res Part B Appl Biomater.* 2008;84(1):17–25.

44. Cox SC, Thornby JA, Gibbons GJ, et al. 3D printing of porous hydroxyapatite scaffolds intended for use in bone tissue engineering applications. *Mater Sci Eng C*. 2015;47:237–47.
45. Pattanayak DK, Fukuda A, Matsushita T, et al. Bioactive Ti metal analogous to human cancellous bone: fabrication by selective laser melting and chemical treatments. *Acta Biomater*. 2011;7(3):1398–406.
46. Ahlfeld T, Akkineni AR, Förster Y, et al. Design and fabrication of complex scaffolds for bone defect healing: combined 3D plotting of a calcium phosphate cement and a growth factor-loaded hydrogel. *Ann Biomed Eng*. 2017;45(1):224–36.
47. Wang MO, Vorwald CE, Dreher ML, et al. Evaluating 3D-printed biomaterials as scaffolds for vascularized bone tissue engineering. *Adv Mater*. 2015;27(1):138–44.
48. Fedorovich NE, De Wijn JR, Verbout AJ, et al. Three-dimensional fiber deposition of cell-laden, viable, patterned constructs for bone tissue printing. *Tissue Eng Part A*. 2008;14(1):127–33.
49. Byambaa B, Annabi N, Yue K, et al. Bioprinted osteogenic and vasculogenic patterns for engineering 3D bone tissue. *Adv Healthcare Mater*. 2017;6(16):1700015.
50. Daly AC, Cunniffe GM, Sathy BN, et al. 3D bioprinting of developmentally inspired templates for whole bone organ engineering. *Adv Healthcare Mater*. 2016;5(18):2353–62.
51. Yamasaki A, Kunitomi Y, Murata D, et al. Osteochondral regeneration using constructs of mesenchymal stem cells made by bio three-dimensional printing in mini-pigs. *J Orthop Res*. 2019;37(6):1398–408.
52. Demirtaş TT, Irmak G, Gümüşderelioğlu M. A bioprintable form of chitosan hydrogel for bone tissue engineering. *Biofabrication*. 2017;9(3):035003.
53. Lee J, Lee H, Cheon K-H, et al. Fabrication of poly (lactic acid)/Ti composite scaffolds with enhanced mechanical properties and biocompatibility via fused filament fabrication (FFF)-based 3D printing. *Addit Manuf*. 2019;30:100883.
54. Chen S, Shi Y, Zhang X, et al. Biomimetic synthesis of Mg-substituted hydroxyapatite nanocomposites and three-dimensional printing of composite scaffolds for bone regeneration. *J Biomed Mater Res Part A*. 2019;107(11):2512–21.
55. Zhang B, Sun H, Wu L, et al. 3D printing of calcium phosphate bioceramic with tailored biodegradation rate for skull bone tissue reconstruction. *Bio-Design Manuf*. 2019;2(3):161–71.
56. Roopavath UK, Malferrari S, Van Haver A, et al. Optimization of extrusion based ceramic 3D printing process for complex bony designs. *Mater Des*. 2019;162:263–70.
57. OSTEOINK calcium phosphate material for 3D tissue printing. 2020. <https://www.regenhu.com/biomaterials#osteoink>.
58. INVIVO@Bioinks Series. 2020. <https://rokithealthcare.com/bioinks/#1548111415858-782441e3-96dd>.
59. Advanced Ink, SynthBone UV. 2020. <https://discoveraether.com/advanced-ink/>.
60. Cells and bioinks of bone. 2020. <https://www.allevi3d.com/cells-bioinks/>.
61. Patented 3D-Painting Materials Design & Manufacturing System. 2020. <https://www.dimensionix.com/publications>.
62. Jakus AE, Secor EB, Rutz AL, et al. Three-dimensional printing of high-content graphene scaffolds for electronic and biomedical applications. *ACS Nano*. 2015;9(4):4636–48.
63. Jakus AE, Rutz AL, Jordan SW, et al. Hyperelastic “bone”: a highly versatile, growth factor-free, osteoregenerative, scalable, and surgically friendly biomaterial. *Sci Transl Med*. 2016;8(358):358ra127.
64. Kolesky DB, Homan KA, Sklyar-Scott MA, et al. Three-dimensional bioprinting of thick vascularized tissues. *Proc Natl Acad Sci*. 2016;113(12):3179–84.
65. Shim J-H, Lee J-S, Kim JY, et al. Bioprinting of a mechanically enhanced three-dimensional dual cell-laden construct for osteochondral tissue engineering using a multi-head tissue/organ building system. *J Micromech Microeng*. 2012;22(8):085014.
66. Kang H-W, Lee SJ, Ko IK, et al. A 3D bioprinting system to produce human-scale tissue constructs with structural integrity. *Nat Biotechnol*. 2016;34(3):312.

67. Phillippi JA, Miller E, Weiss L, et al. Microenvironments engineered by inkjet bioprinting spatially direct adult stem cells toward muscle- and bone-like subpopulations. *Stem Cells*. 2008;26(1):127–34.
68. Gao G, Schilling AF, Yonezawa T, et al. Bioactive nanoparticles stimulate bone tissue formation in bioprinted three-dimensional scaffold and human mesenchymal stem cells. *Biotechnol J*. 2014;9(10):1304–11.
69. Keriquel V, Oliveira H, Rémy M, et al. In situ printing of mesenchymal stromal cells, by laser-assisted bioprinting, for in vivo bone regeneration applications. *Sci Rep*. 2017;7(1):1–10.
70. CONDUIT Interbody Platform; EIT Cellular Titanium. 2020. <https://www.jnjmedicaldevices.com/en-US/product/conduit-interbody-platform-eit-cellular-titanium>.
71. 510(k) summary: EIT Cellular Titanium Lumbar Cage LLIF. 2020. https://www.accessdata.fda.gov/cdrh_docs/pdf18/K181644.pdf.
72. 510(k) summary: Aries Lumbar Interbodies. 2020. https://www.accessdata.fda.gov/cdrh_docs/pdf18/K181347.pdf.
73. 510(k) summary: iFure Implant System. 2020. https://www.accessdata.fda.gov/cdrh_docs/pdf19/K190230.pdf.
74. 510(k) summary: Additive ORThopaedics Locking Lattice Plate. 2020. https://www.accessdata.fda.gov/cdrh_docs/pdf17/K170214.pdf.
75. 3D printing ceramic structures. 2020. <https://particle3d.com/technology/>.
76. Jensen MB, Slots C, Ditzel N, et al. Composites of fatty acids and ceramic powders are versatile biomaterials for personalized implants and controlled release of pharmaceuticals. *Bioprinting*. 2018;10:e00027.
77. CT-bone: real bone from the 3D Printer. 2020. <https://www.xilloc.com/ct-bone/>.
78. Ricles LM, Coburn JC, Di Prima M, et al. Regulating 3D-printed medical products. *Sci Transl Med*. 2018;10(461):eaan6521
79. U.S. FDA. Technical considerations for additive manufactured medical devices. 2017. <https://www.fda.gov/media/97633/download>.
80. Morrison RJ, Kashlan KN, Flanagan CL, et al. Regulatory considerations in the design and manufacturing of implantable 3D-printed medical devices. *Clin Transl Sci*. 2015;8(5):594–600.
81. U.S. FDA. Design control guidance for medical device manufacturers; 1997.
82. Salmi M, Paloheimo K-S, Tuomi J, et al. Accuracy of medical models made by additive manufacturing (rapid manufacturing). *J Craniomaxillofac Surg*. 2013;41(7):603–9.
83. Salmi M, Tuomi J, Paloheimo K, et al., "Patient-specific reconstruction with 3D modeling and DMLS additive manufacturing", *Rapid Prototyping Journal*. 2012;18(3):209-214.
84. Kok Y, Tan XP, Wang P, et al. Anisotropy and heterogeneity of microstructure and mechanical properties in metal additive manufacturing: a critical review. *Mater Des*. 2018;139:565–86.
85. Strano G, Hao L, Everson R, et al. A new approach to the design and optimisation of support structures in additive manufacturing. *Int J Adv Manuf Technol*. 2013;66(9–12):1247–54.
86. Mirzendehtel AM, Suresh K. Support structure constrained topology optimization for additive manufacturing. *Comput Aided Des*. 2016;81:1–13.
87. Cheng B, Shrestha S, Chou K. Stress and deformation evaluations of scanning strategy effect in selective laser melting. *Addit Manuf*. 2016;12:240–51.
88. Hollister SJ. Scaffold design and manufacturing: from concept to clinic. *Adv Mater*. 2009;21(32–33):3330–42.
89. Farzadi A, Solati-Hashjin M, Asadi-Eydivand M, et al. Effect of layer thickness and printing orientation on mechanical properties and dimensional accuracy of 3D printed porous samples for bone tissue engineering. *PLoS One*. 2014;9(9):e108252.
90. U.S. FDA. Use of international standard ISO 10993-1. Biological evaluation of medical devices—part 1: evaluation and testing within a risk management process. 2016. <https://www.fda.gov/media/85865/download>.
91. Yong C, Kaplan DS, Gray A, et al. Overview of the US Food and Drug Administration regulatory process, principles of regenerative medicine. Amsterdam: Elsevier; 2019. p. 1345–65.

92. U.S. FDA. Classification of products as drugs and devices & additional product classification issues: guidance for industry and FDA staff. 2011. <https://www.fda.gov/media/80384/download>.
93. U.S. FDA. Providing clinical evidence of effectiveness for human drugs and biological products. 1998. <https://www.fda.gov/media/71655/download>.
94. U.S. FDA. Premarket Approval (PMA). 2019. <https://www.fda.gov/medical-devices/premarket-submissions/premarket-approval-pma>.
95. U.S. FDA. Humanitarian Device Exemption (HDE) Program: guidance for Industry and Food and Drug Administration Staff. 2019. <https://www.fda.gov/media/74307/download>.
96. U.S. FDA. The 510(k) program: evaluating substantial equivalence in premarket notifications [510(k)]: guidance for Industry and Food and Drug Administration Staff. 2014. <https://www.fda.gov/media/82395/download>.
97. U.S. FDA. De novo classification process (evaluation of automatic class III designation): guidance for Industry and Food and Drug Administration Staff. 2017. <https://www.fda.gov/media/72674/download>.
98. U.S. FDA. Premarket Notification 510(k). 2020. <https://www.fda.gov/medical-devices/premarket-submissions/premarket-notification-510k>.
99. U.S. FDA. Investigational New Drug (IND) Application. 2020. <https://www.fda.gov/drugs/types-applications/investigational-new-drug-ind-application#Laws,%20Regulations,%20Policies%20and%20Procedures>.
100. U.S. FDA. Investigational device exemptions (IDEs) for early feasibility medical device clinical studies, including certain first in human (FIH) studies. 2013. <https://www.fda.gov/media/81784/download>.

Future Direction and Challenges



Nina Tandon and Sarindr Bhumiratana

1 Introduction

A key tenet of reconstructive surgery is that “when a part of a person is lost, it should be replaced in kind, bone for bone...” [1]. From a bone reconstruction perspective, however, our ability to put this principle into practice has historically been limited, since our only supplies of human bone must be donated, either from ourselves autologously or from cadavers. The emergence of tissue engineering has therefore been greeted with excitement at the possibility of making surgeons’ ideal a reality.

This book has provided a comprehensive overview of the technical challenges for creation of patient-specific, clinically relevant-sized tissue-engineered bone for clinical applications. However, as the future directions of tissue engineering grow clearer and the possibilities grow increasingly profound, it is important not to lose sight of the key activities that are required to ensure that the scientific discoveries described here eventually evolve into practical solutions that in turn provide improved clinical outcomes.

The term *clinical translation* has been coined to denote the process of turning observations in the laboratory, clinic, and community into interventions that improve the health of individuals and the public. The goal of clinical translation is to translate (or move) basic science discoveries quickly and efficiently into practice, or in the parlance of the field “from bench to bedside.”

Major considerations for clinical translation fall into three categories: economic, regulatory, and manufacturing. A major, cross-cutting theme, which we call the “translational mindset,” involves simplification of the technology to facilitate not only regulatory approval but also clinical adoption. Successful migration through translation therefore requires an interdisciplinary approach with significant

N. Tandon (✉) · S. Bhumiratana
EpiBone Inc, New York, NY, USA
e-mail: nina@epibone.com

foresight into downstream activities. Successful solutions must be not only approachable to regulators, but also manufacturable, scalable, usable by clinicians, and beneficial to both patients' real-world outcomes and ideally economic cost. With application of the principles outlined in this chapter, we hope to make the dream of a regenerative approach to bone reconstruction approachable and practical.

2 Overview of Translational Development

The thrill of scientific discovery has often been described by an elusive moment of so-called *eureka* when creative insight sheds light on a future possibility. From the perspective of bone tissue engineering, several of these “aha moments” have converged to point us toward a future in which regenerative approaches to bone healing may eventually become the future standard of care. Basic bone biology research has revealed bone as a tissue that is a self-renewing, self-healing, composite material which undergoes constant remodeling in the body. Advances in biomaterials research have revealed the possibility for 3D cell culture in scaffolds replicating key aspects of the bone cellular microenvironment. Advances in digital fabrication have facilitated the recreation of complex anatomical geometry, and advances in bioreactor development have facilitated directed differentiation of stem cells inside *ex vivo* environments toward mature tissues. These “aha moments,” which have occurred in academic labs throughout the world, are an amazing testament to the painstaking labor and ingenuity of countless scientists and engineers in academia. However, from a clinical perspective, they represent merely the starting line of a long marathon race toward translational development.

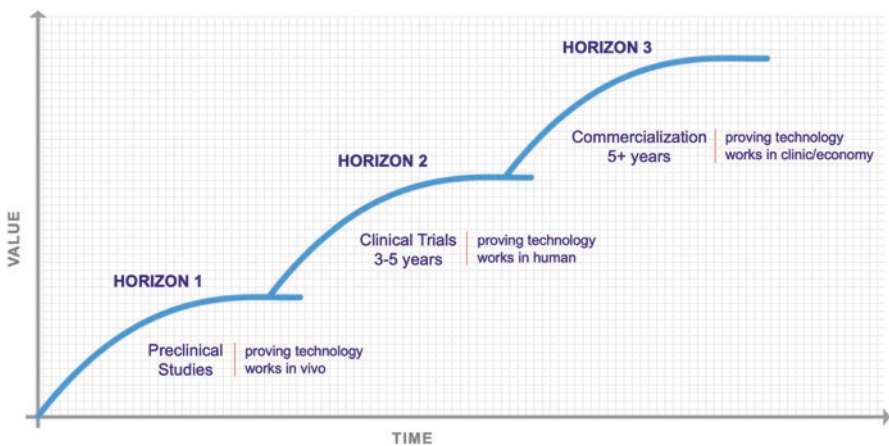


Fig. 1 The three horizons of clinical translation (i.e., preclinical studies, clinical trials, and commercialization)

Successful translation is characterized by three key (and overlapping) stages of value creation as the technology achieves validation and risks of failure are addressed (see Fig. 1). Each stage, or “horizon,” as we call it, differs with respect to key activities and barriers to success. The first stage involves *in vitro* and *in vivo* studies to reveal the underlying mechanisms of how a prospective technology works biologically. The second stage involves human clinical studies proving safety and efficacy of the technology as a requisite before regulatory approval. The third stage involves manufacturing scale-up and subsequent commercialization. The timeline for development can be quite expensive and take many years; new drug approvals in the United States take an average of 12 years and cost approximately \$1 billion, respectively, from preclinical testing to approval, accounting for the cost of failed trials [2].

For tissue-engineered bone to mature into clinical practice, a handoff must occur between the academic labs often performing activities in earlier phases of development to the industry partners usually responsible for commercialization. And in parallel, a shift in mindset must also occur from the earlier stages’ emphasis on novelty toward the simplification required for practical implementation within the community via clinical trials, manufacturing scale-up, and commercialization.

In an academic mindset, for example, the hallmark of successful innovation is to be as distinct as possible from all other innovations. However, since introduction of new materials into the body introduces risks associated with biocompatibility, success from a regulatory perspective may inversely hinge upon being as similar as possible to previously approved products (so-called predicate devices).

Furthermore, from a clinical adoption perspective, it is widely known that the healthcare industry at large, and especially surgery, can be conservative with regard to uptake of evidence-based surgical procedures due to the training required to use novel instrumentation and/or methods, and the associated risk of reduced outcomes. Here, too, compatibility with existing instruments and similarity to existing methods can be advantages.

Finally, once a product is approved, it needs to integrate into an extremely complex modern healthcare industry with multiple stakeholders with distinct requirements. The end user may be the patient, but the key decision maker is often the surgeon, and the payer is the government or private insurer (with patients often bearing significant cost, as well). Future engineered bone products must therefore confer a benefit—and avoid an inconvenience—to each of those groups.

In our view, the considerations relating to the second and third horizons outlined above lead us to conclude that successful translation of a new technology such as bioengineered bone must tread the narrow path of retaining tight focus on its core innovation while staying as conventional as possible with all other aspects of its production and use. If the core innovation centers on the driving goals of personalization and biological replacement, for example, the goal should be to situate that product as neatly as possible into existing systems of regulation, manufacturing, and medical care—rather than trying to reinvent whole systems at once. Introduction of biological complexity (e.g., via cellular reprogramming, drug delivery methods, or novel biomaterials) should be avoided unless necessary. Surgical instrumentation

and fixation hardware should minimize deviation from tried-and-true surgical practice. And costs should be minimized wherever possible.

The complex reality of translation can appear daunting, or even distasteful, to innovators with dreams of transforming medical care. Fortunately, the academy-industry jump is easier now than it used to be, and as the boundary between academy and industry becomes more porous, and the stigma for academics being involved in translational research has eased, the movement of experts among stages of development is more fluid. With a translational mindset, interdisciplinary attitude, and forward-looking strategy, it becomes increasingly possible to preserve the value of the core innovation while clearing other extraneous obstacles from its way.

3 Economic Considerations and Challenges

Science has a long history of inspiring innovation and thus being a driver of business enterprise. The chemical industry of the late nineteenth and early twentieth century, and the pharmaceutical industry of the post-World War II period, stemmed directly from contemporary advances in science [3]. However, the nature of the connection between science and business has begun to change in important ways as large biopharma and medical device players have pulled away from riskier research and universities, and their spin-offs have become central figures not just in the intellectual pursuit of science, but also in the business of science in the earlier, riskier stages.

Successful translation of tissue-engineered bone grafts “from bench to bedside” requires setting forth a roadmap across five key areas of economic development and eventual sale: market size/indication, physician adoption, economic viability, intellectual property, and funding. As described earlier, a “translational mindset” must retain a view toward the entire translation journey even at the earliest stages of planning. Product approval is often the central focus in the early stages of translation, and rightly so, but it is still essential to have a plan for launch and sale even at the outset.

As stated earlier, in addition to building the five areas of economic development into the business plan, it is also essential to take all stakeholders into account—including regulators, payers, physicians, and patients—considering their roles and needs at each step of the process, ensuring a benefit and avoiding inconvenience to each of those groups.

3.1 Market Size

Developers of innovative bone grafting solutions will encounter a tradeoff between market size and regulatory-acceptable indication (*see Sect. 4 below for more details*). On the one hand, it is ideal to set as broad as an indication as possible, so

as to be applicable to a wide range of indications. However, setting a very broad indication might draw skepticism from regulators, because different parts of the body and different diseases may be perceived as possessing different risks.

A company with infinite resources could design and test its technology for a host of indications (such as growing bone to implant anywhere in the body), but realistically a small biotech firm has to choose its use case very carefully—even if it is producing a platform technology.

Making this choice wisely means carefully balancing the considerations of approvability and market size. The optimal choice has a good chance of approval and a significant market size. In weighing the market size, developers should ask how many people suffer from the particular injury or illness that your product would remedy, how many of them actually need the therapy that they would provide, and whether there exists a robust large-animal model to validate the use case preclinically. Given that regulators require animal studies to be specific to the product's use case, these questions should be considered even before proof-of-concept animal studies are performed. When considering different use cases, it is also important to keep in mind that the product may be used by different sets of doctors (such as an orthopedist, an ENT, or a neurosurgeon) with different preferences and risk tolerances.

3.2 Physician Adoption

A common criticism of innovative products that lack user-friendliness is that they “look like they were designed by an engineer.” For innovators involved in the earliest stages of development, it can indeed be fascinating to tinker with the possibilities in the solution space. Why make choices that limit power and flexibility? But a big mistake of many early startups is to design a product—and make a business plan—without enough input from the stakeholders who are key users of the technology. A therapy is essentially a tool for a physician to use, and as such it is critical to consider how a physician will use it—not only in terms of ergonomics but all human factors associated with the surgical workflow, such as training, surgical planning, instrumentation hardware, surgical guides, and timing.

The essential principle that should be applied here, again in a “translational mindset,” is to innovate only on the core technology, avoiding changing too much of the surrounding use system or physician workflow. If physicians have to adjust their workflow to use a new product, they will not use it, because no surgeon wants to risk diminishing their outcomes while learning a new process.

In practice, for example, in craniofacial repair physicians typically take a CT scan to plan surgery and routinely generate 3D printed models as part of surgical planning. Companies developing anatomically precise bone grafts should therefore aim to leverage these scans whenever possible rather than introducing additional steps or imaging modalities into physician workflow. Further downstream, when designing the implantation process, successful strategies should simplify

instrumentation that physicians might have to train on and integrate with products, such as fixation hardware, that surgeons normally use to hold a graft in place. Involving surgeons directly in the design process early on can obviate the need for expensive workarounds at a later date.

3.3 *Economic Viability*

When considering economic viability of tissue-engineered bone grafts, differing cost drivers relate to each horizon of development. In Horizons 1 and 2 of Fig. 1, risk/reward economics dominate the considerations for total cost of getting a product approved, and for Horizon 3, unit cost economics apply once a product is approved. Finally, upon commercialization, reimbursement economics must also be taken into account.

During Horizon 1 (preclinical studies), a key activity is mapping the manufacturing process to GMP, with a focus on minimizing risk and associated costs of seeking approval. During this stage, it is critical to maximize use of the library of materials that are well known and acceptable to the FDA and to do this from the beginning of the translation process so as to minimize cost of approval. This principle applies to the finest level of detail. Every material that comes in contact with the product should contain no leachables and no contamination that could lead to unfavorable outcomes. Even the tubing in the bioreactor should ideally have been used in other, established products. While choosing these materials, costs should be considered so that the unit cost of production will not be overwhelming downstream upon commercialization.

It may be obvious to most entrepreneurs that reducing the costs of production through scalable manufacturing and commercialization is critical to creating a profitable product. For the living, patient-specific engineered grafts described in this book, a necessary bar for economic viability stems from unit cost economics (*see Sect. 5 below for more details*). Hands-on activities such as cell culture media changes should be replaced wherever possible with automated processes. Bulk purchasing and batch processing must also be implemented to maximize efficiency of reagents and expensive quality control processes. And supply risks must be considered so that developers are not reliant on single suppliers of any key materials.

For all the importance of de-risking approval that covers only part of the risk equation. A key principle for considering the full spectrum of economic risk is that an approvable product is not necessarily a reimbursable product. It is critical, therefore, to make sure that clinical trial comparators are selected wisely to maximize enrollment in trials (thus reducing time). Comparators should also be suited to prove the relevant outcomes that will matter to payers, such as shorter surgical/recovery time, prevented surgeries, etc., so as to achieve reimbursement. If a product's clinical benefit is deemed not to provide enough of an incremental benefit above standard of care to justify its price tag, the product is less likely to get on any payer's formulary.

3.4 *Intellectual Property*

In the academic mindset, intellectual property (IP) provides a critical asset to the university and its researchers, and the mark of a successful patent is often tied to the broadness of the patent claims. In the translational mindset, however, the mark of a stellar IP portfolio is more complicated, and it hinges on two factors: blocking and freedom to operate, supported by trade secrets and company know-how.

Freedom to operate (FTO) is essentially the ability of a company to develop, make, and market products without legal liabilities to third parties (e.g., other patent holders). Essentially, FTO means that a developer's process and product does not infringe on the IP of any other companies. When performing an FTO analysis, search criteria should include assignees, licenses, and international classification codes. By searching assignees, you can identify the patents that a company and its subsidiaries own. In order to assess demand for a given technology, searching for license agreements will also give a sense of how beneficial a market is; if there are many licensing opportunities, the technology is likely in demand. It is important to note that FTO must cover not only the core technology but the translation, as well: manufacturing, transportation/delivery, and scalability of the product.

A blocking patent is a patent that prevents another party from producing a product (even if it is patented). [4] The purpose of a blocking patent is not only to protect the patent owner's invention against copycats but also to prevent competitors from putting rival products on the market that might cannibalize revenue from the original patent holder.

Beyond the mechanical aspects of FTO and blocking patents, it is especially important to consider that IP is a company's currency for attracting investment. Investors want to see solid FTO and blocking patents. To make all of this work smoothly, it is important for developers to invest early in high-quality patent law counsel.

Finally, it is important to consider that patents are only one pillar of intellectual property and that trade secrets and know-how can be equally valuable to companies. A proprietary recipe for cell culture media, for example, may be more valuable to a company when held as a trade secret so as to avoid publication of the ingredients and expiration of patent protection. Furthermore, given the high degree of specialization required for engineering bone, know-how achieved via training of employees is also an important company asset that prevents others from copying processes.

3.5 *Funding*

One of the biggest challenges in financing translational medicine is the gap in feasibility and funding between government-grant funded basic science and creating a product that generates a positive cash flow. Since developers during Horizons 1 and 2 are not generating cash via sale of product, and many products fail to fully fund

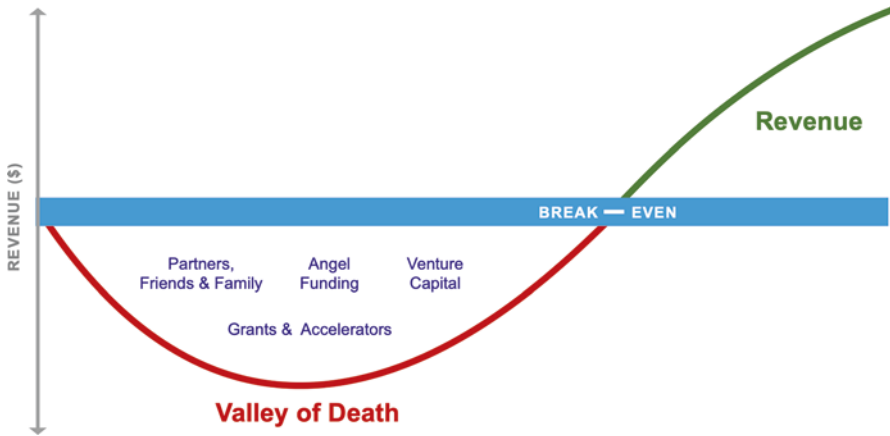


Fig. 2 The so-called valley of death and sources of capital corresponding to maturity of the business. (Graphic adapted from SBA)

their development programs, this gap is colloquially called “the valley of death” (see Fig. 2).

A critical problem to solve to cross the valley of death is the chicken and egg problem of getting first funding. A startup company needs data to get funding and funding to get data. Solving the chicken/egg problem is also essential to de-risking to entice investors. A range of funding sources corresponding to increasing levels of maturity of the product (and inversely to level of risk) are available. At the earliest stages of development, government-funded grants from programs such as the Small Business Innovation and Research (SBIR) program are available in the USA. These grants are excellent sources of non-dilutive capital and also serve as a vetting of the technology for private investors, since grants are highly competitive to achieve and are subject to rigorous peer review. Subsequent sources of capital may be friends and family, followed by angel investors and angel groups, then venture capital (VC) firms as the technology continues to be de-risked. VCs make a return on investment—and ideally make an exit—when the startup is merged into or acquired by an established company or via an offering on public stock exchanges (i.e., initial public offering or IPO). Strategic alliances with and/or investment from established players can also increase a developer’s chance of success.

Given the high cost and long timelines of preclinical and clinical studies, the valley of death has proven difficult to cross, but there are strategies to do so. Economic viability in the earlier phases of translational development hinges on the forward-looking risk/reward horizon in which the totality of the future cost required to fund development of this product is weighed against the projected financial return.

4 Regulatory Considerations and Challenges

As the economic strategy defines the commercial success of the product, clinical and regulatory strategy defines the map toward commercialization. In order to have a head start in setting the regulatory direction of the product, it is highly recommended that the innovator enters into a conversation with the regulatory agency early in the product development to define the product type and its regulatory requirement. In this section, we recommend three clinical and regulatory considerations that every innovator should contemplate as part of their product translation.

4.1 Consideration of Product Benefit Based on Regulatory Pathway Requirement

Bone grafts generated with 3D printing are categorized by regulators as one of three product types based on product composition: a device, a drug–device, or a biologic–device combination. Under the US FDA, each product type is designated to a lead regulatory agency based on the primary mode of action: devices fall under the purview of the Center for Devices and Radiological Health (CDRH), drugs of the Center for Drug Evaluation and Research (CDER), and biologics of the Center for Biologics Evaluation and Research (CBER). For example, an inert polymeric scaffold would be considered a device and regulated under CDRH, whereas a polymeric scaffold which elutes drugs or small molecules to induce osteointegration would likely be considered a drug–device combination and be regulated under CDER. Similarly, a polymeric scaffold with attached functional growth factor such as BMP-2 would be considered a biologic–device combination and regulated under CBER.

The product type and its associated regulatory pathway have profound implications for development time and cost. A pure device is regulated under the 510 K or PMA regulatory pathway, while the drug–device or biologic–device combinations

Table 1 Summary of premarket requirements of each product type [5]

	Device	Drugs	Biologics
Submission	<ul style="list-style-type: none"> • 510(k) • PMA 	NDA through IDE	BLA through IND
Clinical trial	<ul style="list-style-type: none"> • 510(k)—No • PMA—Yes, with some exceptions 	Yes	Yes
Standard of evidence	<ul style="list-style-type: none"> • 510(k)—Substantial equivalence • PMA—Reasonable assurance that the device is safe and effective for its intended use(s) 	Substantial evidence of effectiveness and adequate tests of safety	Safe, pure, and potent
Compliance with CGMPs	Yes	Yes	Yes

are required to follow NDA and BLA regulatory pathways, respectively. Table 1 summarizes the premarket requirement for each type of product. The drugs and biologics pathway presents much steeper hurdles of evidence, time, and cost. For devices, the approval process in the United States takes an average of 7 years from preclinical testing to approval [2]. In contrast, drug and biologic developers must conduct three clinical trials which take a much longer time from preclinical testing to approval [2]. As a result, the development costs for drugs and biologics can likewise run ten times higher than those for devices. Pursuing development of a drug–device or biologic–device combination, in turn, is a tough sell for investors accustomed to a shorter, less costly, less scientifically rigorous path. Therefore, the innovators must ensure that the inclusion of the drug or biologic component provides significant clinical and commercial benefit to the product before embarking on this more strenuous journey.

4.2 Consideration of Product Indication Based on Regulatory Viewpoint

The product developer will learn that the meaning of “indication” in the eye of the regulatory agency may be different than in the clinical and business viewpoints, and this has crucial implications for development. Consider, for example, that the adult human skeleton is made up of more than 200 bones, many of which are similar and some of which have their own unique function. Long bones provide support, store minerals and fat, and serve as a location for hematopoiesis, while the main function of cranium is to exclusively protect the brain.

From the clinical and commercial viewpoints, bone is independent from where it is located in the body. As a result, clinicians harvest bone from a less important and more abundant location as an autograft to replace or repair a defect in a more important region. For example, both iliac crest bone graft and split cranium can be used to repair facial deformity. On the other hand, the regulatory agency may define bone in part by its location. The agency may view 3D printed bone grafts placed in two locations as the same or different depending on the surrounding environment and its function. For example, a 3D printed bone scaffold or a tissue-engineered bone graft that is successfully used to reconstruct long bone may still require a new preclinical and clinical study if the developer wants to use the same product to repair cranium. This is because long bone and cranium have different environments and exhibit different safety profiles. Long bone provides bodily support and is adjacent to ligament and muscles, while cranium provides brain protection and is adjacent to skin and dura mater. Depending on the locations of the bone to be repaired, the regulatory agency may define indication based on their view of safety and function.

In addition to its location of placement in the body, a product’s indication may also be defined by the particular disease it treats. For example, a product might have the potential to treat either mandibular non-union fracture or radiated and

tumorectomy bone void. Since one of these indications exhibits a harsher environment for bone repair, regulators may not consider both indications to be the same. Because different parts of the body and different diseases may entail distinctive risks, the solution is to find a middle ground and potentially produce products to cover multiple bone locations or indications of similar risk profile. Therefore, product developers should spend extra effort in defining the product market and indication.

The solutions to some of these inherent tensions must be determined through collaborating with the regulatory agency, which should begin as early in the development as possible. There are more than 200 bones in the body, yet it is impossible to conduct 200 clinical trials. Even for the smaller number of bones in the head and face, it is essential to define how many clinical trials will be required to approve an indication that covers the whole head and face. This is currently an open question that the FDA and product developers will have to work together to solve to successfully and economically drive new innovations to help patients in need.

4.3 Consideration of Clinical Trial Design Based on Clinical Goals

With an indication pinpointed, the product developer must develop a solid clinical plan to gain approval for that indication on a feasible budget and timeline. Furthermore, the outcome of the clinical trial will dictate product market penetration. The clinical plan should center on two key components: comparator as well as study size and length.

Comparator: Choosing the right indication is only half the story. It is also crucial to choose the right comparator for your product. Choosing a highly desirable comparator will make it easier to recruit patients, because the control arm is appealing. But to compete with the gold standard and prove the bare minimum—that your product is not inferior—will require a significantly larger study size. In contrast, an unattractive comparator (such as inert material) will make it easier to prove a therapeutic advantage. However, the outcome of the study will likely not be attractive to clinicians to use your product.

It is also important to keep in mind that the product may offer additional benefit beyond the site of repair. For example, although autograft is a gold standard and is known to be successful for bone reconstruction, the use of autograft causes major pain at the donor site. Historically, regulators traditionally do not consider factors beyond the study location—yet their approval decisions hinge on calculations of risk and benefits. Therefore, it may be advantageous to the developer to be creative in capturing the full benefit of the product and design a study that allows measurement of this additional benefit relative to the selected comparators.

Length/size of study: The unique nature of tissue-engineered products also creates ambiguity around the optimal length and size of trials. For example,

tissue-engineered products may offer regenerative properties by continuing to develop and remodel after implantation, which may take several years to complete. Although it is ideal for the regulatory agency to see data with large numbers of patients for lengthy periods, the developer will likely desire smaller, shorter trials.

The solution here lies in the balance of adequate study length with sufficient safety and efficacy profiles. The FDA has, in fact, been making concerted efforts to be more open and cooperative with companies in this regard. To find a middle ground between competing interests, it is important for developers to take advantage of this opportunity and work with the FDA closely and early on, paying particular attention toward understanding regulators' concerns and priorities.

5 Manufacturing Considerations and Challenges

Historically, the small molecules that defined drugs could easily win sufficient patent protection with composition of matter patents, irrespective of the underlying chemical processes of manufacture, and in turn, regulators have not given their manufacturing process much scrutiny. However, for biologics such as protein immunotherapy, which are sensitive to the conditions in which they are produced, purified, and stored, minor differences in manufacturing processes or cell lines can alter or destroy the desired proteins. Furthermore, biologics are more difficult to chemically characterize and manufacture than small molecule drugs, and so for biologics, such as protein immunotherapy, the FDA does indeed scrutinize the product's underlying manufacturing processes. In the case where tissue-engineered products are a subset of biologics, the regulation centers largely on manufacturing. *In essence, the process is the product.* The essential thinking on manufacturing, including materials and processes, should take place early in the product development to avoid potential manufacturing risks such as inability to scale or failure to release the product under required specifications.

Manufacturing considerations lead to particular implications for products made through 3D printing. 3D printing has been developed as a tool to simplify manufacturing of complex structure. With the advancement of virtual surgical planning (VSP), 3D fabrication can be used to generate an anatomically matched bone graft quickly with great precision. Since the route of administration of tissue-engineered bone graft is implantation, the manufacturing of the products—whether a device or combination product—requires a highly regulated facility and process under Current Good Manufacturing Practice (CGMP). The CGMP guidance ensures that: (1) there is good documentation and record keeping, (2) there is assurance of the cleanliness and sanitation of the product, (3) the process is validated and reproducible, (4) the procedures are well monitored and consistent across the manufacturing process, and (5) the product meets specifications.

This section covers four elements that the developer of a tissue-engineered bone product with 3D printing must consider.

5.1 *Quality Control*

Defining the core manufacturing process to stand the tests of time and regulatory scrutiny means spelling out each step of the process thoroughly in sequence. To pass muster, these steps will have to be followed in precise order and with high precision. The quality control process must be set up to show what each step accomplished and ensure that the measurements cover both the quality and the safety of the product.

Scaffolds generated from 3D printing must exactly match the shape and contour designed from VSP, as precision is essential for the anatomy of the patient. Because 3D printed materials may expand or contract during printing or post processing, great consideration must be taken to design methods to determine that the 3D printed scaffold exhibits the correct shape and dimension upon implantation.

When cells are utilized in tissue-engineered bone product, additional quality control measurements must be established. To confirm that the cells are of the correct type, techniques such as flow cytometry and gene expression profiling can be used. For products that utilize more mature or differentiated cells, protein content measurement or gene expression markers could be used to ensure that the product meets the desired quality.

Lastly, the current regulation requires that every batch of product must pass required safety measurements which include mycoplasma, endotoxin, and sterility testing. The product developers must consider the method of sampling and must perform testing process to validate. Since 3D printed tissue-engineered bone products will exhibit the exact defect shape, sampling from the product may not be ideal. Surrogates or extra piece of tissue from the same manufacturing batch may be needed to perform these safety tests. The developer must carefully design a sampling process that is practical and still represents the product batch.

5.2 *Quality Attributes*

From the manufacturing perspective, tissue-engineered bone product developers should balance quality attributes and manufacturability of the product. 3D printing may be a double-edged sword when it comes to design flexibility. As the product architecture resolution increases, so do the time and equipment advancement needed. Therefore, designing a product that perfectly matches the native bone architecture may not always be the optimal solution. The developer must consider which quality attributes are sufficient based on a product's mechanism of action and testing optimization.

Defining a product's properties based on today's 3D printing technology can likewise be risky, as 3D printing will likely continue to develop at a faster pace than the other biological components of tissue-engineered bone. The risk of relying on current 3D printing capabilities when defining a process is that the product then becomes bound to those constraints even as the technology evolves. Instead,

developers should define the core product quality attributes, keeping in mind that the 3D printing technology will evolve to support the fabrication of the product to meet the desired attributes.

Since biological products exhibit high variability, another challenge is to correlate efficacy and potency. As the product is being developed and tested in both the preclinical and clinical stages, collecting ample data on a range of measures that go beyond the obvious will be a key to eventual success in defining potency. Consider, for example, that a cell producing half as much protein may well still have the potency it requires. It is important to think about the definition of potential potency for the product early in the development, even though the FDA does not require a definition until phase III clinical trials.

5.3 Scalability

The key to scalability is simplicity. The more complex a product fabrication process is, the exponentially greater challenge there is to scale the production. A plan for scalable manufacturing should center on utilizing other existing technologies to support the manufacturing. For example, a 3D printing product may rely greatly on post processing technique. Developers should always consider utilizing simple and potentially scalable techniques. Cleaning a 3D printed structure by brushing the deep pores within the scaffold, for instance is less scalable than using harsh agitation or high pressure washing. Automation will definitely come into play to support scalable manufacturing as the product continues to develop into later stages. Avoiding complex fabrication processes will greatly facilitate the translation of the product at commercialization.

5.4 Logistics

A final, crucial piece of managing risk through a sound manufacturing plan centers on supply risks. Because materials are defined into the process, which in turn defines the product, it is extremely difficult to change materials if the original material is unique and becomes scarce in the future. For example, if a developer selects a boutique polymer for its product, and there is a stock shortage or the supplier goes out of business, the product and the company will be at great risk. The core lesson here is to stay with the mainstream supply that is widely available. If boutique products or suppliers cannot be avoided, the developers must institute a risk mitigation plan, such as performing extensive study to validate a potential replacement early on in development.

6 Summary

Translation of tissue-engineered bone products using 3D printing requires understanding of patients' unmet needs, the product's ecosystem, regulatory requirements, and manufacturing knowledge. Successful translation of a new technology must tread the narrow path of retaining tight focus on its core innovation while staying as conventional as possible with all other aspects of its production and use. If innovators make themselves aware of potential challenges and adopt a translational mindset, interdisciplinary attitude, and forward-looking strategy, they can increase their chance of success, ultimately helping patients.

Acknowledgments The authors would like to acknowledge the assistance of Grace Rubenstein with the manuscript and NOLA Marketing LLC with figures.

References

1. Kalaska DM, Butler PE, Ghali S. Textbook of plastic and reconstructive surgery. London: UCL Press; 2016.
2. Van Norman GA. Drugs, devices, and the FDA: part 1: an overview of approval processes for drugs. *J Am Coll Cardiol Basic Transl Science*. 2016;1(3):170–9.
3. Pisano GP. The evolution of science-based business: innovating how we innovate. Harvard Business School Working Paper 10-062; 2010.
4. USLegal.com (n.d). Blocking patent law and legal definition. <https://definitions.uslegal.com/blocking-patent/>.
5. Dabrowska A, Green VR. Medical product regulation: drugs, biologics, and devices. Congressional Research Service Reports; 28 Jan 2019. <https://fas.org/sgp/crs/misc/IF11083.pdf>.

Index

A

- Absorbable collagen sponges (ACS), 174
- Active remodeling, 19
- Additive manufacturing (AM), 71, 267
 - advantages, 85, 282
 - binder jetting, 79
 - biocompatible polymers, 85
 - bioprinting, 272
 - bone tissue engineering, 72
 - CAD/CAM software, 268
 - cell–scaffold TE products, 284
 - complex design files, 279
 - composition, 73
 - computational models, 73
 - design and manufacturing process, 277, 282
 - design model interactions, 279
 - design requirements, 268
 - directed energy deposition, 77
 - DLP, 74
 - fabrication, 277
 - FDA resources, 287
 - FDM/FFF, 271
 - formal definitions, 285
 - layer-by-layer process, 279
 - limitations, 85
 - material extrusion, 83
 - material jetting, 81
 - materials, 280, 281
 - and medical device, 276
 - medical products, 268, 276, 283
 - open-source software, 73
 - parameters, 282
 - performance testing, 283
 - porosity, 72
 - post-processing steps, 281
 - powder bed fusion, 75
 - products, 278
 - scaffold design, 278
 - sheet lamination, 82
 - SLA, 268, 269
 - SLS, 270
 - software-related effects, 279
 - software workflow considerations, 280
 - software workflow phase, 279
 - STL, 73
 - TE applications, 268
 - techniques, 72, 85–87
 - technologies, 71, 97, 276, 278
 - 3D modeling software, 71
 - 3D printed objects, 71
 - 3D printed structures, 73
 - 3D printing companies, 274
 - 3D structure, 72
 - 3D tissues and scaffolds, 274
 - type, 280
 - vat photopolymerization techniques, 75
- Adipose derived stem cells (ADSCs), 126, 127
- Advanced manufacturing technologies, 269
- Agent-based model systems, 253
- Alginate, 254
- Allografts, 40
- Alveolar bone defects, 101
- Anatomically shaped frameworks, 7
- Angiogenesis, 59, 95, 251
- Angiogenic sprouts, 257
- Anterior cruciate ligament (ACL), 124
- Anti-resorptive therapies, 25
- Appendicular skeleton, 17
- Arthroscopic knee surgery, 122
- Articular cartilage, 17
- Autografts, 39, 44, 50

- Autologous bone graft, 251
- Autologous chondrocyte implantation (ACI), 127, 128
- B**
- Basic multicellular unit (BMU), 25
- β -TCP scaffold, 50
- Bilateral alveolar clefts, 9
- Binder jet printing, 270
- Binder jetting (BJ), 79, 151
 - advantage, 79
 - AM techniques, 79
 - hydroxyapatite and calcium phosphates, 80
 - metals, 79
 - polymers, 80
 - schematic diagram, 80
- Bioactive glass nanoparticles (BGNP), 205–209
- Bioactive glass particles, 205
- Bioactive synthetic biomaterials, 93
- Bioceramics, 50, 51
- Biocompatibility testing, 284
- Biocompatible polymers, 85
- Biodegradable synthetic polymers, 214
- Bioengineering principles, 7
- Biofabrication, 253
- Bio-inks, 84, 85, 160, 254
- Biological products, 306
- Biomaterial implants
 - advantages, 60
 - biocompatibility, 41
 - bone regeneration, 43
 - degradation and bioresorption, 43
 - design criteria, 41
 - design strategies, 40
 - disadvantages, 60
 - fabrication methods, 41
 - mechanical properties, 42
 - pore size and orientation, 42, 43
 - repairs, 37
 - scaffold, 54
- Biomaterials, 97, 133, 154, 162
- Bioprinting, 58, 85, 160, 195, 272, 275
- Bioreactors, 227, 252
 - cell proliferation, 226
 - cell seeding, 226
 - fluid shear stress, 227
 - functional bone-like structures, 226
 - mechanical loading, 226
 - regenerative tissue, 226
 - static culture, 225
 - systems, 228, 242, 243
 - tissue engineering, 225
 - vascularization, 227
- Bone, 250
 - appendicular skeleton, 26
 - composite material, 13
 - organic fraction, 20
 - scarless healing, 26
 - structural characteristics, 13
- Bone biology research, 294
- Bone bioprinting, 198–202, 206–208
- Bone-cartilage interface, 136
- Bone cells
 - apoptosis, 16
 - characteristics, 15
 - macrostructure, 16–19
 - M-CSF, 15
 - mesenchymal stem cell, 15
 - microstructure, 19–20
 - osteoblasts, 15
 - osteoclast, 15
 - osteocyte, 16
 - RANKL, 15
 - response to stimuli, 16
 - types, 15
 - ultrastructure, 20–21
- Bone development
 - calcified cartilage matrix, 22
 - chondrocytes, 24
 - endochondral ossification, 22
 - growth plate, 22
 - intramembranous ossification, 21
 - osteocytes, 22
 - proliferative cells, 23
 - resting zone, 23
- Bone elongation, 24
- Bone grafting, 8
 - allografts, 40
 - autografts, 39
 - disadvantages, 40
 - failure, 5
 - gold standard, 39
 - solutions, 296
 - xenografts, 40
- Bone growth, 56
- Bone healing, 14
 - BMP-induced healing, 31
 - bone injuries, 31
 - bone structure and function, 31
 - causative factors influencing healing, 31
 - cell-type requirements, 29
 - critical size defects, 31
 - cytokines, 29
 - endochondral bone formation, 29
 - hierarchical organization, 14
 - intramembranous and endochondral healing, 29

- intramembranous and endochondral ossification, 27
 - mechanical load, 26
 - mechanical strength, 31
 - monocyte/macrophages, eosinophils, 29
 - progenitor cells, 27
 - provisional stability, 28
 - recruited mesenchyme, 29
 - secondary, 28
 - segmental defects, 38
 - signaling pathways, 31
 - traditional endochondral development pathways, 30
 - types, 27
 - VEGF signaling, 29
 - Wnt signaling, 30
 - Bone implant materials, 45–46
 - Bone injury
 - healing cascade, 38, 39
 - types, 37
 - Bone loss, 8
 - Bone marrow, 18
 - Bone marrow derived stem cells (BMSCs), 126, 127
 - Bone matrix, 226
 - Bone mineral density (BMD), 183
 - Bone modeling
 - anabolic therapies, 26
 - bone mass, 25
 - bone surface, 25
 - radial growth, 25
 - Bone morphogenetic proteins (BMPs), 55, 102, 226
 - Bone regeneration, 27, 30, 43, 58, 94, 95, 99
 - Bone remodeling
 - activation signal, 24
 - anti-resorptive therapies, 25
 - BMU, 25
 - bone healing/regeneration, 14
 - collagenous matrix, 25
 - cortical and cancellous bone tissue, 24
 - definition, 13
 - factors, 25
 - osteoblasts and osteoclasts, 25
 - replacements, 24
 - Bone repair
 - biomaterial properties, 41
 - growth factors (*see* Growth factors)
 - Bone structure, 31
 - Bone 3D printing, 276
 - Bone tissue, 193, 194
 - Bone tissue engineering (BTE), 85, 193, 225, 250
 - abrasion chondroplasty, 126
 - allograft implants, 129
 - articular/hyaline cartilage, 121–123
 - biomaterials, 193
 - calcium phosphates, 197, 204
 - cartilage defects, 121
 - cartilage tissue engineering, 132, 133, 136, 138–140, 142, 143
 - clinical need, 8
 - developments, 194
 - fabrication methods, 193
 - hydrogel, 204
 - hydroxyapatite, 197
 - microfracture, 124
 - mouse calvarial defect, 204
 - nanocomposites, 197
 - nanohydroxyapatite, 197, 203
 - nanomaterials, 195–197
 - nanosilicates, 209
 - nanotechnology, 194
 - nanotopography, 196
 - osteochondral defects, 121
 - osteochondral drilling, 125
 - PPF, 203
 - printed scaffolds, 203
 - properties, 195
 - refinements, 7
 - restoration, 121, 123, 127, 140
 - scaffold, 127, 130, 133, 134, 136
 - SLA printing, 195
 - TCP, 204
 - 3D bioprinting, 195
 - 3D printing, 132, 133, 136, 138–140, 142, 143
 - Bone volume (BV), 183
 - Bony autografts, 6
 - Bony reconstruction, 5
- C**
- Cadaveric and bovine-derived grafts, 5
 - Calcified cartilage cores, 24
 - Calcium-deficient hydroxyapatite (CDHA), 173
 - Calcium phosphate nanoparticles, 198–202
 - Callus remodeling, 31
 - Callus tissue inflammatory cells, 28
 - Canaliculi, 19
 - Capillaries, 250
 - Carbon nanotubes (CNT), 212
 - Cartilage formation, 38
 - Cell-based bone tissue engineering studies, 9
 - Cell death, 53
 - Cell localization, 257
 - Cell seeding, 226

- Cellular proliferation, 100
 - Cement line, 19
 - Center for Drug Evaluation and Research (CDER), 301
 - Centers for Disease Control and Prevention, 8
 - Chitosan, 48, 177
 - Chitosan-lactide-fibrinogen (CLF), 178
 - Chondral defects, 122, 123
 - Chondrocytes, 122
 - Chondroplasty, 123
 - Chronic implant-related bone infections, 210
 - Clinical adoption perspective, 295
 - Clinical translation, 227, 293
 - biomaterials research, 294
 - commercialization, 295
 - creative insight, 294
 - development, 294
 - Collagen, 48
 - Collagen-based scaffolds, 54
 - Collagen fibrils, 20
 - Collagen molecules, 21
 - Composite skin products, 1
 - Computational fluid dynamics (CFD)
 - analysis, 231
 - Computer-aided design (CAD), 71, 150
 - Computer-aided manufacturing (CAM), 109, 267
 - Computer assisted design (CAD)
 - programs, 151
 - Computer-assisted planning, 94
 - Computerized tomography (CT), 149, 150, 173
 - Convection mechanisms, 226
 - Cortical bone, 16, 17
 - Cranial healing, 31
 - Craniofacial defects, 37
 - Craniomaxillofacial injuries, 37
 - Critical size defects, 31, 172
 - Custom 3D-printed scaffolds, 110
 - Cylindrical structures, 19
 - Cytokines, 59
- D**
- Decellularized dermal matrices, 4
 - Decellularized tissues, 106
 - Dedifferentiated fat cells (DFAT), 100
 - Degradation/aging, 23
 - Delivery system, 58
 - DeminerIALIZED bone matrix (DBM), 170, 171
 - De Novo classification process, 286
 - Dental stem cells, 101
 - Dentin matrix acidic phosphoprotein 1 (DMP-1), 21
- Dentoalveolar defect, 2
 - Digital imaging and communication in medicine (DICOM), 150
 - Digital light processing (DLP), 151
 - Digital mirror device (DMD), 74
 - Directed energy deposition, 77
 - Direct metal laser sintering (DMLS), 156
 - Donor sites, 5
 - Drop-on-demand bioprinting, 272
- E**
- Economic strategy, 301
 - Elastic modulus, 156
 - Electron beam melting (EBM), 151, 156
 - Electrospinning, 47, 215
 - Embryonic stem cells (ESCs), 53
 - Emerging technologies, 93
 - Endochondral bone formation, 29
 - Endochondral bone regeneration, 30
 - Endochondral ossification, 22, 38
 - Endothelial cell/MSC interactions, 259
 - Endothelial progenitors, 29
 - Endothelial vessel formation, 55
 - Epiphyseal growth plate, 23
 - Epiphyses region, 17
 - Extracellular matrix (ECM), 106, 174, 230
 - Extrusion-based bioprinting, 85
 - Extrusion method, 51
- F**
- Feedback monitoring, 243
 - FGF signaling, 57
 - Fibril aggregation, 20
 - Fibroblast growth factors (FGF), 55, 57
 - Fibula free flap, 5
 - The Food and Drug Administration, 8
 - Formation-based modeling, 25
 - Fracture healing, 28
 - Freedom to operate (FTO), 299
 - Fused deposition modeling (FDM), 83, 151, 271
 - Fused deposition printing, 51
 - Fused filament fabrication (FFF), 271
 - Fusion deposition modeling (FDM), 274
- G**
- Gelatin, 95, 175
 - Gel-based biomaterials, 95
 - Genes, 16
 - Geomagic Freeform™, 151
 - Glycine–proline–hydroxyproline, 20

- Good manufacturing practice (CGMP), 304
Graphene, 212
Growth factors, 101, 102
 applications, 58, 59
 BMPs, 55, 57
 critically sized defects, 55
 FGF, 57
 functions, 56
 IGF, 57
 PDGF, 57
 polypeptides, 55
 protein therapy/gene therapy, 55
 PRP, 58
 recombinant growth factors, 58
 TGF- β , 57
 types, 55
 VEGF, 57
Growth plate, 17
- H**
Hemi-osteons, 19
Heterogeneity, 19
Heterotopic ossification, 57
Human adipose-derived stem cells
 (hASCs), 236
Human amniotic fluid-derived stem cell
 (hAFSC), 184
Hyaluronan, 175
Hyaluronic acid (HA), 175
Hydrogels, 133, 166, 172, 253
Hydroxyapatite, 197
Hydroxyapatite and bioactive ceramics, 50, 51
Hypertrophied chondrocytes, 24
Hypertrophy, 29
- I**
Iliac crest, 39
Immune-sensitive smart scaffolds, 7
Immunomodulation, 95
 angiogenesis, 95
 biocompatibility, 97
 bone regeneration, 97
 gel-based biomaterials, 95
 macrophage, 95
Individual trabeculae, 16
Induced pluripotent stem cells (iPSCs), 53
Injury progenitor cells, 26
Inkjet bioprinting, 272
Insulin-like growth factors (IGFs), 55, 57
Intellectual property (IP), 299
International Cartilage Repair Society
 (ICRS), 140
Intramembranous and endochondral bone
 formation, 30
Intramembranous bone healing, 31
Intramembranous ossification, 21, 26, 38
Intrinsic multicellular process, 13
Intrinsic toughening mechanism, 20
In vivo bioreactor, 108
In vivo studies, 50, 58
Iron oxide (Fe₂O₃) nanoparticles, 211
- L**
Lab-on-a-chip or micro total systems, 256
Lactic acid, 180
Lacunar/canalicular network, 19
Laminated object manufacturing (LOM), 151
Laponite nanoclay, 209
Laser-assisted bioprinting (LAB), 185, 272
Logistics, 306
Long bone, 17, 18
Long bone segmental defect (LBSD)
 amphiphilic poly lactides, 182, 183
 arthroplasty, 166
 autografts, 167, 168
 bioceramics, 172, 173
 bioprinted cell-laden hydrogel/mineral
 composite scaffolds, 183, 185
 bone grafting procedures, 166
 collagen/bioceramic composites, 174, 175
 collagens, 174, 175
 composites, 175–178, 180
 conventional polylactide-mineral
 composites, 181
 demineralized bone matrix (DBM),
 170, 171
 mineral composites, 182, 183
 orthopedic care, 166
 poly(ethylene glycol) (PEG) hydrogels,
 178, 179
 polylactides, 180
 polysaccharide hydrogels, 175–178
 regenerative outcome, 167
 regenerative reconstruction, 166
 spinal surgery, 166
 stem/progenitor cells, 167
 structural allografts, 168, 170
 synthetic bone grafts, 172
 3D printing technology, 167
 titanium mesh cage, 172
Lysyl oxidase-mediated reaction, 20

M

Magnesium, 50
 Magnetic force bioreactor (MFBs), 238, 227, 237, 239
 Magnetic resonance imaging (MRI), 149, 150
 Magnetic resonance observation of cartilage repair tissue (MOCART), 138
 Mandibular marginal resection defect, 2
 Manufacturing process, 305
 Material extrusion, 83
 Material jetting (MJ), 81, 82, 151
 Maxillofacial bone, 94
 Maxillofacial bone regeneration, 94
 Maxillofacial regeneration, 94, 96, 99, 110, 112
 large jawbone defects, 95
 management and regeneration, 93
 mandible, 94
 3D architecture and functional dynamics, 94
 titanium-based reconstruction plates, 95
 Mechanical force bioreactor systems, 237
 Mechanical load, 26
 Mechanical loading bioreactor system, 238
 Medical products, 286
 Mesenchymal-angiogenic response phase, 28
 Mesenchymal progenitor cells, 29
 Mesenchymal stem cells (MSCs), 53, 54, 122, 261
 Metallic biomaterials, 79
 Metal oxide nanoparticles
 AuNPs, 211
 CNTs, 212, 213
 component, 209
 graphene, 212
 iron oxide nanoparticles, 211
 magnesium, 210
 mechanical properties, 209
 MWCNT, 212
 nanoparticle, 211
 PLGA nanoparticles, 214
 PLGA scaffolds, 210
 silver nanoparticles, 210
 synthetic polymers, 214
 titanium, 209
 Metal scaffolds, 49, 50
 Metaphysis, 18
 Micro-CT (μ -CT) analysis, 174
 Microfracture, 124
 Microvascular surgery, 93
 Mineralized collagen, 44, 48, 49, 52
 Modulus-matched biomaterials, 42
 MSC migration, 53
 Multi-component systems, 8

N

Nanofibers, 214
 Nanoscale, 193
 Nanostructured bone extracellular matrix, 257
 Nanotechnology, 215
 Natural polymeric scaffolds
 bone repair, 48
 chitosan, 48
 collagen, 48
 disadvantages, 48
 elements, 48
 endogenous production, 48
 heal bone defects, 48
 osteoclastogenesis, 49
 pathogenic impurities, 48
 pore sizes and orientations, 49
 posterolateral fusions, 49
 Near infrared (NIR) irradiation, 185
 Nickel-titanium (Nitinol), 50
 Non-collagenous proteins, 20
 Nonenzymatically mediated crosslinks, 20

O

Optimizing processing parameters, 243
 Oral and maxillofacial surgery (OMFS), 109
 Orbital floor tumor, 2
 Organ bioprinting, 54
 Osseo-immunomodulation, 95
 Osseointegration, 42
 Osteoarthritis, 122
 Osteoblasts, 52
 Osteoblast specific alterations, 31
 Osteochondral allograft (OCA)
 transplantation, 129
 Osteochondral autograft transfer (OATS), 128–130
 Osteochondral defects management, 5
 Osteoclast, 15
 Osteoclastogenesis, 58
 Osteoconductivity, 72
 Osteocytes, 16, 19, 52
 Osteogenesis, 95, 259
 Osteogenic cell differentiation, 43
 Osteogenic differentiation, 58
 Osteolysis, 20
 Osteons, 19
 Ovariectomized (OVX), 171
 Overexposure, 75

P

Patient-specific implants (PSI), 142, 156, 157
 Patient-specific instrumentation, 157, 159

- Pediatric orthopedics
 biologic self-assembly, 160
 biomimetic construct
 microarchitecture, 161
 biomimicry, 160
 bone tissue engineering, 160
 chronic osteomyelitis, 161
 congenital and acquired skeletal
 deficiencies, 160
 development, 153
 education, 155
 field of materials, 153
 GE ARCAM EBM printer, 151
 implantable materials, 153
 instrumentation, 156, 157
 limitations, 159
 musculoskeletal conditions, 149
 musculoskeletal infections, 161
 non-implantable materials, 152
 patient evaluation, 149
 patient-specific implants (PSI), 156, 157
 quality assurance, 160
 quality control, 160
 rehabilitation, 158
 treatment planning, 154, 155
- PEG hydrogels, 47
- Perfusion-based systems, 234
- Perfusion bioreactor systems, 226
- Perfusion systems, 227
- Pericytes, 53
- Perilacunar space, 20
- Periosteum, 16
- Persistent inflammation, 42
- PHB scaffolds, 47
- Physiological/pharmacological stressors, 19
- Physiological stressors, 14
- Placental stem cells, 53
- Platelet-derived growth factor (PDGF), 55, 57
- Platelet-rich fibrin (PRF), 4
- Platelet-rich-plasma (PRP), 4, 58, 101,
 103, 173
- Pluronic F-127 ink, 255
- Poly(caprolactone)(PCL), 47
- Poly(D,L-lactic-co-glycolic acid) (PLGA), 180
- Polyether ether ketone (PEEK), 156
- Poly ether ketone ketone (PEKK), 156
- Polyethylene glycol (PEG), 47
- Poly(ethylene glycol) (PEG) hydrogels,
 178, 179
- Poly(lactic acid) (PLA), 47, 133, 180
- Poly(lactide-co-glycolide) (PLGA), 47, 133
- Polyactides, 180
- Polymerization printing, 51
- Poly(methyl-methacrylate) (PMMA), 47
- Poly(propylene fumarate) (PPF), 203, 259
- Porcine mandibular defects, 105
- Pore size, 38
- Post-menopausal osteoporosis, 19
- Powder bed fusion, 75, 77
 biomedical field, 76
 commercial devices, 75
 3D structures, 77
- Preclinical large animals, 104
- Primary mineralization, 20
- Pro-inflammatory, 38
- Pro-inflammatory cytokines, 136
- Pro-inflammatory immune response, 55
- Pro-inflammatory phenotype, 43
- Pure poly(ϵ -caprolactone) (PCL), 77
- R**
- Radial bone growth, 26
- Radiographs, 27
- RANKL signaling, 31
- Rapid prototyping, 150, 154, 161
- Rayleigh–Plateau instability, 81
- Receptor activator of nuclear factor κ B ligand
 (RANKL), 15, 168
- Recombinant human BMP-2 (rhBMP-2), 56
- Recombinant human bone morphogenetic
 protein-2 carried on an acellular
 collagen sponge (rhBMP-2/ACS), 7
- Red marrow, 18
- Regenerative medicine, 249, 287
- Relative stability, 27
- Revolutionized the healthcare system, 109
- Rotating wall vessel (RWV)
 application, 233
 bioreactor designs, 234
 bioreactor system, 232
 BTE applications, 233
 compression-based system, 238
 hMSCs, 236
 mechanical loading bioreactors, 239
 microgravity environment, 233
 optimization, 236
 perfusion culture, 234
 perfusion systems, 235
- S**
- Scaffold-guided bone regeneration, 172, 177
- Scaffolds
 autografts, 44
 bone regeneration, 44
 hydroxyapatite and ceramics, 50, 51
 materials, 44

- Scaffolds (*cont.*)
 metallic, 49, 50
 natural polymers, 48–49
 synthetic polymers, 46–47
 3D printed/cast, 44
- Scalability, 306
- Science, 296
- Secondary Haversian systems, 14
- Secondary mineralization, 20
- Secondary osteons, 19
- Selective laser melting (SLM), 151
- Selective laser sintering (SLS), 51, 151, 270
- Sheet lamination, 82
 AM techniques, 83
 pressure and temperature, 83
- Single-walled carbon nanotubes (SWCNT), 212
- Skeletal Biology Research Center, 105
- Skeletal tissue engineering, 14
- Slicer software, 72
- Small Business Innovation and Research (SBIR) program, 300
- Smart biomaterial scaffolds, 6
- Soft and hard tissue defects, 1, 2
- Soft tissue coverage flap, 5
- Spinal fusions, 37
- Spinner flasks, 228
 application, 230
 CFD analyses, 231
 limitation, 232
 spinner and flasks, 228
- Standard Tessellation Language (STL), 150
- Standard Triangle Language, 150
- Stem cells, 100, 102
 bioprinting, 54
 cell death, 53
 cell line, 53
 encapsulation, 53
 hydrogels, 54
 immune cells, 52
 implant materials, 53
 mesenchymal, 53
 placental, 53
 types, 53
 wound healing cascade, 54, 55
- Stereolithography (SLA), 71, 73, 109, 151, 195, 268
 bone regeneration, 75
 bone tissue engineering applications, 75
 DLP, 74, 75
 top-down approach, 74
- Surgical instrumentation, 295
- Synthetic and natural food dyes, 254
- Synthetic bone grafts, 166, 167, 185
- Synthetic bone substitutes, 5
- Synthetic degradable polymers, 167, 173
- Synthetic polymeric scaffolds
 advantage, 46, 47
 bone tissue engineering, 47
 exotic methods, 47
 gas-foaming, 46
 man-made polymers, 46
 PMMA, 47
 porous scaffold architectures, 46
 3D printing, 47
- Systemic anti-inflammatory agents, 29
- T**
- Thermoplastic polymer printing, 215
- Thick vascularized tissues, 255
- Three-dimensional (3D) biofabrication
 technique, 113
- Three-dimensional (3D) bioprinting, 194
- Three-dimensional (3D) bone tissue
 applications, 226
- Three-dimensional (3D) cellular spheroid, 257
- Three-dimensional (3D) defects, 1
- Three-dimensional (3D) microstructure, 94
- Three-dimensional (3D) printed
 bioreactors, 242
- Three-dimensional (3D) printed customized
 bone, 111
- Three-dimensional (3D) printed polymers, 52
- Three-dimensional (3D) printed scaffolds, 59
- Three-dimensional (3D) printed
 vasculature, 261
- Three-dimensional (3D) printing, 41, 72, 109, 113, 252, 259, 262, 301
 additive manufacturing, 51
 being bioactive titanium scaffolds, 52
 bone regeneration, 52
 categories, 51
 growth factors, 52
 materials, 52
 process, 110
 regular inkjet printing, 51
 strategies, 263
 technologies, 94, 95, 109, 110, 112, 243
 user-created design, 51
- Three-dimensional (3D) scaffolds, 47
- Tissue engineering (TE), 225, 249, 267
 applications, 77
 composite hard and soft tissue defects, 9
 fundamental requirements, 5
 goals, 1
 rapid expansion, 4
 skin grafting techniques, 1
 solutions, 1

Tissue-engineered bone, 8, 295
Tissue-engineered bone grafts, 296, 298
Tissue-engineered bone product, 305
Tissue-engineered products, 303
Tissue-engineered skin substitutes, 1
Titanium, 49, 51
Trabecular bone, 16, 17
Tracheostomy, 1
Traditional clinical imaging techniques, 242
Traditional endochondral development pathways, 30
Traditional static culture technique, 225
Traditional tissue culture techniques, 243
Transforming growth factor beta (TGF- β), 55, 57
Translating bioreactor systems, 244
Translational feasibility, 9
Translational medicine, 299
Translational mindset, 297
Tricalcium phosphate (TCP), 50, 204

U

Ultra- and nanostructural levels, 14
Umbilical cord blood multilineage cells, 53

V

Vascular architecture, 250
Vascular endothelial growth factor (VEGF), 31, 55, 57, 168, 251
Vascularization, 112, 227, 252
 biocompatible materials, 253

 bioink, 254
 engineered systems, 252
 microchannels, 252
 and mineralization, 250
 OPN and OCN, 258
 silicone ink, 255
 3D extracellular matrix, 256
 3D printing, 254
Vascularized bone model, 261
Vascularized bone systems, 255
 angiogenic sprouting, 256
 applications, 255
 HUVECs, 256
 microfluidic platform, 256
Vascularized bone tissue, 258
Vascularized scapular free flap, 5
Vascularized tissue growth, 252
Vasculature, 100, 249
Virtual surgical planning (VSP), 304

W

Wistar skin fibroblast (WSF) cells, 179
Wnt signaling, 30

Y

Young's modulus, 42, 49
Yucatan minipig model, 106

Z

Zirconia-yttria ceramics, 51